Hashemite Kingdom of Jordan

Jordan Journal of Biological Sciences

An International Peer-Reviewed Scientific Journal

Financed by the Scientific Research and Innovation Support Fund

This title is indexed in Scopus

http://jjbs.hu.edu.jo/

المجلة الأردنية للعلوم الحياتية
Jordan Journal of Biological Sciences (JJBS)
http://jjbs.hu.edu.jo

Jordan Journal of Biological Sciences (JJBS) (ISSN: 1995–6673 (Print); 2307-7166 (Online)): An International Peer- Reviewed Open Access Research Journal financed by the Scientific Research and Innovation Support Fund, Ministry of Higher Education and Scientific Research, Jordan and published quarterly by the Deanship of Scientific Research , The Hashemite University, Jordan.

Submission Address
Professor Atoum, Manar F
The Hashemite Universit y
P.O. Box 330127, Zarqa, 13115, Jordan
Phone: +962-5-3903333 ext.4147
E-Mail: jjbs@hu.edu.jo

المجلة الاردنية للعلوم الحياتية
Jordan Journal of Biological Sciences (JJBS)
http://jjbs.hu.edu.jo

International Advisory Board (Arranged alphabetically)

Instructions to Authors

Scopes

Study areas include cell biology, genomics, microbiology, immunology, molecular biology, biochemistry, embryology, immunogenetics, cell and tissue culture, molecular ecology, genetic engineering and biological engineering, bioremediation and biodegradation, bioinformatics, biotechnology regulations, gene therapy, organismal biology, microbial and environmental biotechnology, marine sciences. The JJBS welcomes the submission of manuscript that meets the general criteria of significance and academic excellence. All articles published in JJBS are peer-reviewed. Papers will be published approximately one to two months after acceptance.

Type of Papers

The journal publishes high-quality original scientific papers, short communications, correspondence and case studies. Review articles are usually by invitation only. However, Review articles of current interest and high standard will be considered.

Submission of Manuscript

Manuscript, or the essence of their content, must be previously unpublished and should not be under simultaneous consideration by another journal. The authors should also declare if any similar work has been submitted to or published by another journal. They should also declare that it has not been submitted/ published elsewhere in the same form, in English or in any other language, without the written consent of the Publisher. The authors should also declare that the paper is the original work of the author(s) and not copied (in whole or in part) from any other work. All papers will be automatically checked for duplicate publication and plagiarism. If detected, appropriate action will be taken in accordance with International Ethical Guideline. By virtue of the submitted manuscript, the corresponding author acknowledges that all the co-authors have seen and approved the final version of the manuscript. The corresponding author should provide all co-authors with information regarding the manuscript, and obtain their approval before submitting any revisions. Electronic submission of manuscripts is strongly recommended, provided that the text, tables and figures are included in a single Microsoft Word file. Submit manuscript as e-mail attachment to the Editorial Office at: JJBS@hu.edu.jo. After submission, a manuscript number will be communicated to the corresponding author within 48 hours.

Peer-review Process

It is requested to submit, with the manuscript, the names, addresses and e-mail addresses of at least 4 potential reviewers. It is the sole right of the editor to decide whether or not the suggested reviewers to be used. The reviewers' comments will be sent to authors within 6-8 weeks after submission.
Manuscripts and figures for review will not be returned to authors whether the editorial decision is to accept, revise, or reject. All Case Reports and Short Communication must include at least one table and/ or one figure.

Preparation of Manuscript

The manuscript should be written in English with simple lay out. The text should be prepared in single column format. Bold face, italics, subscripts, superscripts etc. can be used. Pages should be numbered consecutively, beginning with the title page and continuing through the last page of typewritten material.

The text can be divided into numbered sections with brief headings. Starting from introduction with section 1. Subsections should be numbered (for example 2.1 (then 2.1.1, 2.1.2, 2.2, etc.), up to three levels. Manuscripts in general should be organized in the following manner:

Title Page

The title page should contain a brief title, correct first name, middle initial and family name of each author and name and address of the department(s) and institution(s) from where the research was carried out for each author. The title should be without any abbreviations and it should enlighten the contents of the paper. All affiliations should be provided with a lower-case superscript number just after the author's name and in front of the appropriate address.
The name of the corresponding author should be indicated along with telephone and fax numbers (with country and area code) along with full postal address and e-mail address.

Abstract

The abstract should be concise and informative. It should not exceed **350 words** in length for full manuscript and Review article and **150 words** in case of Case Report and/ or Short Communication. It should briefly describe the purpose of the work, techniques and methods used, major findings with important data and conclusions. No references should be cited in this part. Generally non-standard abbreviations should not be used, if necessary they should be clearly defined in the abstract, at first use.

Keywords

Immediately after the abstract, **about 4-8 keywords** should be given. Use of abbreviations should be avoided, only standard abbreviations, well known in the established area may be used, if appropriate. These keywords will be used for indexing.

Abbreviations

Non-standard abbreviations should be listed and full form of each abbreviation should be given in parentheses at first use in the text.

Introduction

Provide a factual background, clearly defined problem, proposed solution, a brief literature survey and the scope and justification of the work done.

Materials and Methods

Give adequate information to allow the experiment to be reproduced. Already published methods should be mentioned with references. Significant modifications of published methods and new methods should be described in detail. Capitalize trade names and include the manufacturer's name and address. Subheading should be used.

Results

Results should be clearly described in a concise manner. Results for different parameters should be described under subheadings or in separate paragraph. Results should be explained, but largely without referring to the literature. Table or figure numbers should be mentioned in parentheses for better understanding.

Discussion

The discussion should not repeat the results, but provide detailed interpretation of data. This should interpret the significance of the findings of the work. Citations should be given in support of the findings. The results and discussion part can also be described as separate, if appropriate. The Results and Discussion sections can include subheadings, and when appropriate, both sections can be combined

Conclusions

This should briefly state the major findings of the study.

Acknowledgment

A brief acknowledgment section may be given after the conclusion section just before the references. The acknowledgment of people who provided assistance in manuscript preparation, funding for research, etc. should be listed in this section.

Tables and Figures

Tables and figures should be presented as per their appearance in the text. It is suggested that the discussion about the tables and figures should appear in the text before the appearance of the respective tables and figures. No tables or figures should be given without discussion or reference inside the text.

Tables should be explanatory enough to be understandable without any text reference. Double spacing should be maintained throughout the table, including table headings and footnotes. Table headings should be placed above the table. Footnotes should be placed below the table with superscript lowercase letters. Each table should be on a separate page, numbered consecutively in Arabic numerals.

Each figure should have a caption. The caption should be concise and typed separately, not on the figure area. Figures should be self-explanatory. Information presented in the figure should not be repeated in the table. All symbols and abbreviations used in the illustrations should be defined clearly. Figure legends should be given below the figures.

References

References should be listed alphabetically at the end of the manuscript. Every reference referred in the text must be also present in the reference list and vice versa. In the text, a reference identified by means of an author's name should be followed by the year of publication in parentheses (e.g.(Brown,2009)). For two authors, both authors' names followed by the year of publication (e.g.(Nelson and Brown, 2007)). When there are more than two authors, only the first author's name followed by "*et al*." and the year of publication (e.g. (Abu-Elteen *et al*., 2010)). When two or more works of an author has been published during the same year, the reference should be identified by the letters "a", "b", "c", etc., placed after the year of publication. This should be followed both in the text and reference list. e.g., Hilly, (2002a, 2002b); Hilly, and Nelson, (2004). Articles in preparation or submitted for publication, unpublished observations, personal communications, etc. should not be included in the reference list but should only be mentioned in the article text (e.g., Shtyawy,A., University of Jordan, personal communication). Journal titles should be abbreviated according to the system adopted in Biological Abstract and Index Medicus, if not included in Biological Abstract or Index Medicus journal title should be given in full. The author is responsible for the sccuracy and completeness of the references and for their correct textual citation. Failure to do so may result in the paper being withdraw from the evaluation process. Example of correct reference form is given as follows:-

Reference to a journal publication:

Bloch BK. 2002. Econazole nitrate in the treatment of *Candida vaginitis*. *S Afr Med J.* , **58**:314-323.

Ogunseitan OA and Ndoye IL. 2006. Protein method for investigating mercuric reductase gene expression in aquatic environments. *Appl Environ Microbiol*., **64**: 695-702.

Hilly MO, Adams MN and Nelson SC. 2009. Potential fly-ash utilization in agriculture. *Progress in Natural Sci.*, **19**: 1173-1186.

Reference to a book:

Brown WY and White SR.1985. **The Elements of Style**, third ed. MacMillan, New York.

Reference to a chapter in an edited book:

Mettam GR and Adams LB. 2010. How to prepare an electronic version of your article. In: Jones BS and Smith RZ (Eds.), **Introduction to the Electronic Age**. Kluwer Academic Publishers, Netherlands, pp. 281–304.

Conferences and Meetings:

Embabi NS. 1990. Environmental aspects of distribution of mangrove in the United Arab Emirates. Proceedings of the First ASWAS Conference. University of the United Arab Emirates. Al-Ain, United Arab Emirates.

Theses and Dissertations:

El-Labadi SN. 2002. Intestinal digenetic trematodes of some marine fishes from the Gulf of Aqaba. MSc dissertation, The Hashemite University, Zarqa, Jordan.

Nomenclature and Units

Internationally accepted rules and the international system of units (SI) should be used. If other units are mentioned, please give their equivalent in SI.

For biological nomenclature, the conventions of the *International Code of Botanical Nomenclature, the International Code of Nomenclature of Bacteria,* and the *International Code of Zoological Nomenclature* should be followed.
Scientific names of all biological creatures (crops, plants, insects, birds, mammals, etc.) should be mentioned in parentheses at first use of their English term.

Chemical nomenclature, as laid down in the *International Union of Pure and Applied Chemistry* and the official recommendations of the *IUPAC-IUB Combined Commission on Biochemical Nomenclature* should be followed. All biocides and other organic compounds must be identified by their Geneva names when first used in the text. Active ingredients of all formulations should be likewise identified.

Math formulae

All equations referred to in the text should be numbered serially at the right-hand side in parentheses. Meaning of all symbols should be given immediately after the equation at first use. Instead of root signs fractional powers should be used. Subscripts and superscripts should be presented clearly. Variables should be presented in italics. Greek letters and non-Roman symbols should be described in the margin at their first use.

To avoid any misunderstanding zero (0) and the letter O, and one (1) and the letter l should be clearly differentiated. For simple fractions use of the solidus (/) instead of a horizontal line is recommended. Levels of statistical significance such as: $^{*}P < 0.05$, $^{**}P < 0.01$ and $^{***}P < 0.001$ do not require any further explanation.

Copyright

Submission of a manuscript clearly indicates that: the study has not been published before or is not under consideration for publication elsewhere (except as an abstract or as part of a published lecture or academic thesis); its publication is permitted by all authors and after accepted for publication it will not be submitted for publication anywhere else, in English or in any other language, without the written approval of the copyright-holder. The journal may consider manuscripts that are translations of articles originally published in another language. In this case, the consent of the journal in which the article was originally published must be obtained and the fact that the article has already been published must be made clear on submission and stated in the abstract. It is compulsory for the authors to ensure that no material submitted as part of a manuscript infringes existing copyrights, or the rights of a third party.

Ethical Consent

All manuscripts reporting the results of experimental investigation involving human subjects should include a statement confirming that each subject or subject's guardian obtains an informed consent, after the approval of the experimental protocol by a local human ethics committee or IRB. When reporting experiments on animals, authors should indicate whether the institutional and national guide for the care and use of laboratory animals was followed.

Plagiarism

The JJBS hold no responsibility for plagiarism. If a published paper is found later to be extensively plagiarized and is found to be a duplicate or redundant publication, a note of retraction will be published, and copies of the correspondence will be sent to the authors' head of institute.

Galley Proofs

The Editorial Office will send proofs of the manuscript to the corresponding author as an e-mail attachment for final proof reading and it will be the responsibility of the corresponding author to return the galley proof materials appropriately corrected within the stipulated time. Authors will be asked to check any typographical or minor clerical errors in the manuscript at this stage. No other major alteration in the manuscript is allowed. After publication authors can freely access the full text of the article as well as can download and print the PDF file.

Publication Charges

There are no page charges for publication in Jordan Journal of Biological Sciences, except for color illustrations,

Reprints

Ten (10) reprints are provided to corresponding author free of charge within two weeks after the printed journal date. For orders of more reprints, a reprint order form and prices will be sent with article proofs, which should be returned directly to the Editor for processing.

Disclaimer

Articles, communication, or editorials published by JJBS represent the sole opinions of the authors. The publisher shoulders no responsibility or liability what so ever for the use or misuse of the information published by JJBS.

Indexing

JJBS is indexed and abstracted by:

DOAJ (Directory of Open Access Journals)	CABI
Google Scholar	EBSCO
Journal Seek	CAS (Chemical Abstract Service)
HINARI	ETH- Citations
Index Copernicus	Open J-Gat
NDL Japanese Periodicals Index	SCImago
SCIRUS	Clarivate Analytics (Zoological Abstract)
OAJSE	Scopus
ISC (Islamic World Science Citation Center)	AGORA (United Nation's FAO database)
Directory of Research Journal Indexing (DRJI)	SHERPA/RoMEO (UK)
Ulrich's	

المجلة الأردنية للعلوم الحياتية
Jordan Journal of Biological Sciences (JJBS)
ISSN 1995- 6673 (Print), 2307- 7166 (Online)
http://jjbs.hu.edu.jo

The Hashemite University

Deanship of Scientific Research

TRANSFER OF COPYRIGHT AGREEMENT

Journal publishers and authors share a common interest in the protection of copyright: authors principally because they want their creative works to be protected from plagiarism and other unlawful uses, publishers because they need to protect their work and investment in the production, marketing and distribution of the published version of the article. In order to do so effectively, publishers request a formal written transfer of copyright from the author(s) for each article published. Publishers and authors are also concerned that the integrity of the official record of publication of an article (once refereed and published) be maintained, and in order to protect that reference value and validation process, we ask that authors recognize that distribution (including through the Internet/WWW or other on-line means) of the authoritative version of the article as published is best administered by the Publisher.

To avoid any delay in the publication of your article, please read the terms of this agreement, sign in the space provided and return the complete form to us at the address below as quickly as possible.

Article entitled:----------

Corresponding author: ----------

To be published in the journal: Jordan Journal of Biological Sciences (JJBS)

I hereby assign to the Hashemite University the copyright in the manuscript identified above and any supplemental tables, illustrations or other information submitted therewith (the "article") in all forms and media (whether now known or hereafter developed), throughout the world, in all languages, for the full term of copyright and all extensions and renewals thereof, effective when and if the article is accepted for publication. This transfer includes the right to adapt the presentation of the article for use in conjunction with computer systems and programs, including reproduction or publication in machine-readable form and incorporation in electronic retrieval systems.
Authors retain or are hereby granted (without the need to obtain further permission) rights to use the article for traditional scholarship communications, for teaching, and for distribution within their institution.

☐ **I am the sole author of the manuscript**

☐ **I am signing on behalf of all co-authors of the manuscript**

☐ **The article is a 'work made for hire' and I am signing as an authorized representative of the employing company/institution**

Please mark one or more of the above boxes (as appropriate) and then sign and date the document in black ink.

Signed:_____ **Name printed:** _____
Title and Company (if employer representative) : _____
Date: _____

Data Protection: By submitting this form you are consenting that the personal information provided herein may be used by the Hashemite University and its affiliated institutions worldwide to contact you concerning the publishing of your article.

Please return the completed and signed original of this form by mail or fax, or a scanned copy of the signed original by e-mail, retaining a copy for your files, to:

Hashemite University
Jordan Journal of Biological Sciences
Zarqa 13115 Jordan
Fax: +962 5 3903338
Email: jjbs@hu.edu.jo

EDITORIAL PREFACE

Jordan Journal of Biological Sciences (JJBS) is a refereed, quarterly international journal financed by the Scientific Research and Innovation Support Fund, Ministry of Higher Education and Scientific Research in cooperation with the Hashemite University, Jordan. JJBS celebrated its 12th commencement this past January, 2020. JJBS was founded in 2008 to create a peer-reviewed journal that publishes high-quality research articles, reviews and short communications on novel and innovative aspects of a wide variety of biological sciences such as cell biology, developmental biology, structural biology, microbiology, entomology, molecular biology, biochemistry, medical biotechnology, biodiversity, ecology, marine biology, plant and animal biology, plant and animal physiology, genomics and bioinformatics.

We have watched the growth and success of JJBS over the years. JJBS has published 11 volumes, 45 issues and 479 articles. JJBS has been indexed by SCOPUS, CABI's Full-Text Repository, EBSCO, Clarivate Analytics- Zoological Record and recently has been included in the UGC India approved journals. JJBS Cite Score has improved from 0.18 in 2015 to 0.7 in 2019 (Last updated on 1 March, 2021) and with Scimago Institution Ranking (SJR) 0.18 (Q3) in 2019.

A group of highly valuable scholars have agreed to serve on the editorial board and this places JJBS in a position of most authoritative on biological sciences. I am honored to have six eminent associate editors from various countries. I am also delighted with our group of international advisory board members coming from 15 countries worldwide for their continuous support of JJBS. With our editorial board's cumulative experience in various fields of biological sciences, this journal brings a substantial representation of biological sciences in different disciplines. Without the service and dedication of our editorial; associate editorial and international advisory board members, JJBS would have never existed.

In the coming year, we hope that JJBS will be indexed in Clarivate Analytics and MEDLINE (the U.S. National Library of Medicine database) and others. As you read throughout this volume of JJBS, I would like to remind you that the success of our journal depends on the number of quality articles submitted for review. Accordingly, I would like to request your participation and colleagues by submitting quality manuscripts for review. One of the great benefits we can provide to our prospective authors, regardless of acceptance of their manuscripts or not, is the feedback of our review process. JJBS provides authors with high quality, helpful reviews to improve their manuscripts.

Finally, JJBS would not have succeeded without the collaboration of authors and referees. Their work is greatly appreciated. Furthermore, my thanks are also extended to The Hashemite University and the Scientific Research and Innovation Support Fund, Ministry of Higher Education and Scientific Research for their continuous financial and administrative support to JJBS.

Professor Atoum, Manar F.
March, 2021

JJBS

Volume 14, Number 5,December 2021
ISSN 1995-6673

Jordan Journal of Biological Sciences

CONTENTS

Original Articles

881 - 887 Antioxidant and antibacterial activities of *Coix lacryma-jobi* seed and root oil potential for meningitis treatment
Diky Setya Diningrat , Novita Sari Harahap , Marsal Risfandi , Zulfahri , Ayu Nirmala Sari , Kusdianti

889 - 897 Further studies on evaluation of the toxicity potential of *Terminalia catappa* Lin. Combretaceae leaf extract: effects on the histology, liver enzymes, and haematology profile of albino rats
Chika B. Ikele , Elijah Okwuonu and Anya N. Ijem

899 - 903 Green Synthesis of Silver Nanoparticles using Neem and Collagen of Fish Scales as a Reducing and Stabilizer Agents
Mustafa Mudhafar , Ismail Zainol, H.A. Alsailawi and C. N. Aiza Jaafar

905 - 910 Antioxidant effect of Beta-D-glucan-polysaccharide fractionate of *Auricularia polytricha* on Hyperglycaemia-Induced Kidney Dysfunction in Experimental Diabetic Nephropathy
Agbor C A and Anyanwu G E

911 - 918 Effect of Stress on Ontogeny of Humoral Immunity in Catla
Purandara Ballyaya Abhiman, Md. Abdullah-Al Mamun , Manjulesh Pai, Shamima Nasren, Sanjay Singh Rathore and Kalkuli Mariappa Shankar

919 - 923 Covid-19: Viral Pathogenesis and The Host Immune Response
Nasiru Usman Adabara, Sherifat Ozavize Enejiyon , Faruk Adamu Kuta, Ayanwale Oluwatobi Abraham and Samia Alkhalil

925 - 931 The Role of Calcium Ions to Improve Activity of Chitinase Isolated from *Vibrio* sp.
Noor Harini, Ya Xi Han, and Johan Sukweenadhi

933 - 937 Callus-mediated Somatic Embryogenesis and Plant Regeneration in *Vanda tricolor* Lindl. var. Pallida
Popy Hartatie Hardjo , Wina Dian Savitri, Ida Bagus Made Artadana, Sulistyo Emantoko Dwi Putra, Elizabeth Pio Parac and Asad Jan

939 - 944 Growth and Productivity of Four Cassava Cultivars on Several Levels of Mixed Fertilizers
Sri Wahyuningsih, Febria Cahya Indriani, Joko Restuono1, Kartika Noerwijati ,Abdullah Taufiq, Yuliantoro Baliadi, Rohmad Budiono, Nguyen Van Minh and Peeyush Soni

945 - 951 Utilization of "Uwi" Plant (*Dioscorea* sp.) as a Renewable Bioenergy Resource
Wuryantoro Wuryantoro , Praptiningsih Gamawati Adinurani,Ratna Mustika Wardhani, Sutrisno Sutrisno, Bohari Mohammad Yamin and Syukri Muhammad Nur

953 - 958 Metabolite Profiling of Black Rice (*Oryza sativa* L.) Following *Xanthomonas oryzae* pv. *Oryzae* Infection
Ema Nur Hidayah, Febri Adi Susanto, Tri Joko, Yekti Asih Purwestri, Tri Rini Nuringtyas, Manar Fayiz Mousa Atoum, and Asad Jan

959 - 964 Evaluation of Efficiency of *Echinodorus palaefolius* (J.F. Macbr.) Involved in the *Clarias gariepinus* (Burchell, 1822) Culture for Water Quality Recovery and Fish Growth Support
Hany Handajani, Ganjar Adhywirawan, Soni Andriawan, Dony Prasetyo and Boy Ronald Mavuso

965 - 968 Effect of Bioagent-added Organo-mineral Nitrogen Fertilizer on Total Nitrogen, pH, and Chrome Content in Lowland Paddy
Rija Sudirja , Indra Oktavianus Lubis, Nadia Nuraniya Kamaluddin, Santi Rosniawaty

968 - 974 The Effect of Bathing Length Time to Axillary Temperature and Dry Heat Loss on Newborns; A Comparative Analysis
Hotma Sauhur Hutagaol

975 - 981 Identification of Consumers' Motives in Buying Organic Luwak Coffee in terms of Agri-Touirism
Yosini Deliana , Lucyana Trimo, Sri Fatimah, Mai Fernando N and Mohamad Djali

983 - 989 Combination of Hyaluronic Acid with Advance-Platelet Rich Fibrin to Reduce Chronic Inflammation: a study in IL-6 and Granulation Index
Ronald W. Kartika, Idrus Alwi, Mirta Hediyati Reksodiputro, *Em Yunir, Sarwono Waspadji, Suzzana Immanuel,Todung Silalahi, Saleha Sungkar, Jusuf Rachmat, Saptawati Bardosono, Franciscus D. Suyatna*

991 - 997 Value Chain Model for Straw Mushroom (*Volvariella volvacea*) Agribusiness Performance in Karawang, Indonesia
Suhaeni, Winda Rianti and Yuyun Umaidah

999 - 1008 Integrative survey for ant diversity: exhaustive deployment of several ant collection methods in Biological Education and Research Forest of Universitas Andalas, Indonesia
Henny Herwina , Rijal Satria, Yaherwandi, Yositaka Sakamaki, Mairawita, Diyona Putri, Ahmad Efendi, Yusuke Kusuhata, Muhammad N. Janra

1009 - 1014 Combined Test of Jatropha Biodiesel Based on Altitude Towards Arbuscular Mycorrhizal Fungi (AMF) Combination with Cultivars and Cytokinins
R. Budiasih, Kovertina Rakhmi Indriana, Reni Nurhayatini, Roni Assafaat Hadi, Noertjahyani, Karyana K.S.

1015 - 1020 Effect of Mangosteen Peel Extract (Garcinia mangostana l.) with Supplemental Zinc and Copper on Performance and Egg Quality of Sentul Laying Chicken
Tuti Widjastuti , Lovita Adriani, Indrawati Yuda Asmara, Iwan Setiawan, Abun, Leni Nurlaeni

1021 - 1024 Improving Blood Protein and Albumin Level Using Dried Probiotic Yogurt in Broiler Chicken
Lovita Adriani , Andi Mushawwir, Chitra Kumalasari, Leni Nurlaeni Ronny Lesmana, Urip Rosani

1025 - 1029 Physiological Analysis of Orchid Chlorophyll against *Odontoglossum ringspot virus* Infection
Mahfut, Irni Yuni Minarni, Sri Wahyuningsih, Tundjung Tripeni Handayani

1031 - 1034 Morphological Identification of Mycorrhizal Fungi Isolated from Native Orchid in Indonesia
Mahfut

1035 - 1043 Transcriptional Impact of E-cadherin Loss on Embryonic Stem Cells
Hani Alotaibi

1045 - 1050 Mathematical evaluation of chromosomal anomalies induced by xylol in *Vicia faba* L. regarding application time and concentration
Ali Özdemir and Canan Özdemir

JJBS

Volume 14, Number 5,December 2021
ISSN 1995-6673
Pages 881 – 887

Jordan Journal of Biological Sciences

Antioxidant and antibacterial activities of *Coix lacryma-jobi* seed and root oil potential for meningitis treatment

Diky Setya Diningrat [1,*] , Novita Sari Harahap [2] , Marsal Risfandi [3] , Zulfahri [4] , Ayu Nirmala Sari [5] , Kusdianti [6]

[1] *Department Biology, Faculty Mathematics and Natural Sciences Universitas Negeri Medan, Indonesia;* [2,3,4] *Departement Sport Sciences, Faculty Sport Sciences, Universitas Negeri Medan, Indonesia;*[5] *Department Biology, Faculty Science and Technology UIN Ar Raniry, Banda Aceh, Indonesia;*[6] *Department Biology, Faculty Education of Mathematics and Natural Sciences Universitas Pendidikan Indonesia, Bandung, Indonesia*

Received: April 19, 2020; Revised: Nov 21, 2020; Accepted: Dec 5, 2020

Abstract

Bacterial meningitis is a dreaded infectious disease in the human pulmonary system caused by bacterial invasion and promoting inflammation. Hanjeli (*Coix lacryma-jobi*) seed and root oil have antioxidant, anti-inflammatory, and antibacterial properties that can be used in the treatment of bacterial meningitis. The study aims to investigate the potential of oil from *C. lacryma-jobi* seed and root part for bacterial meningitis treatment. The phytochemical screening was performed using standard protocols. Antibacterial activity and minimum inhibitory concentration (MIC) were conducted by the disc diffusion and two-fold dilution method. The preliminary phytochemical screening of *C. lacryma-jobi* shows that essential oil of root and seed part contains steroids, carotenoids, tannins, alkaloid salts, reducing compounds, flavonoid, anthracenoid, coumarin derivatives, cardenoid, anthocyanins, and saponins. The determination of total phenolic, tannin contents, and antioxidant in essential oil from the root was significantly higher ($p < 0.05$) than the seed part. The *C. lacryma-jobi* oil from both parts expressed the highest antimicrobial activity against *Streptococcus pneumoniae* and *Klebsiella pneumoniae*. Additionally, the lowest minimum inhibitory concentration (12.5–50 mg/mL) was observed against selected bacteria of meningitis. It is concluded that oil from *C. lacryma-jobi* root and seed parts contains compounds that might be used in the bacterial meningitis treatment.

Keywords: *Coix lacryma-jobi*; antioxidant; antibacterial; essential oil; bacterial meningitis; phytochemical; DPPH; minimum inhibitory concentration

1. Introduction

Hanjeli (*Coix lacryma-jobi*) is one of the Poaceae family (Chhabra and Gupta, 2015; Patel et al., 2017). Hanjeli may be indigenous and unfamiliar cereal grains grown in Sumatra, Indonesia. Hanjeli is reported to have higher carbohydrates, protein, fat and dietary fiber than rice and corn (Chhabra and Gupta, 2015; Rajesh, 2016). Additionally, other phytochemical components are also reported in Hanjeli, such as calcium, phosphorus, iron, niacin, thiamine, and riboflavin (Rajesh, 2016; Qu et al., 2014).

In addition, *Coix lacryma-jobi* is used as nourishing food in traditional Chinese medicine and has proven to reduce the risk of cancer (Kuo et al., 2002; Wang et al., 2016). In recent years, an adlay seed oil emulsion has been approved as an antineoplastic therapy by the Chinese Ministry of Public Health, in particular for lung cancer (Wang et al., 2016; Zhang et al., 2014).

The preliminary phytochemical screening of the Hanjeli essential oil indicated the presence of alkaloids, carbohydrates, saponins, glycosides, flavonoids, phenols, tannins, and steroids, whereas the seed and root essential oil contained glycosides, flavonoids, phenols, and steroids, which revealed higher antimicrobial activity (Al-Shuneigat et al., 2015; Diningrat et al., 2020; Zhang et al., 2014). However, the lowest minimum inhibitory concentration was observed against *Escherichia coli, Pseudomonas aeruginosa, Klebsiella pneumoniae, Streptococcus pneumoniae*, and *Streptococcus feaecalis*, which were selected as bacteria of meningitis.

Bacterial meningitis is a severe infectious disease of the membranes lining the brain resulting in high mortality and morbidity throughout the world (El Bashir et al., 2003). An annual Islamic pilgrimage to Mecca, known as the Hajj and Umra, attracts more than a million pilgrims from many countries worldwide, including Indonesia, which is the biggest Moslem country, and this has been associated with the outbreak of bacterial meningitis disease (Al-Gosha'ah et al, 2014; De Gans et al., 2002; Yezli et al., 2016). The first reported international outbreak of bacterial meningitis following the Hajj occurred in 1987 (van de Beek et al., 2012; Yezli et al., 2016). This epidemic emphasized the potentially high risk of transmission during the pilgrimage and in their home countries (Al-Gosha'ah et al, 2014; van de Beek et al., 2012; van de Beek et al., 2016), such as Indonesia.

In the last decades, the epidemiology and treatment strategies for community-acquired bacterial meningitis

* Corresponding author e-mail: dikysd@unimed.ac.id.

have significantly changed (van de Beek et al., 2012; van de Beek et al., 2016). Firstly, the introduction of conjugate vaccines has substantially reduced the burden of bacterial meningitis (De Gans et al., 2002; van de Beek et al., 2016). As a result, community-acquired bacterial meningitis has become a disease that currently affects more adults than infants, with its specific complications and treatment options (van de Beek et al., 2012; Al-Lahham et al., 2018). The second important development is the increasing rate of reduced susceptibility to common antimicrobial agents among strains of *Streptococcus pneumoniae (pneumococcus)* and *Neisseria meningitidis (meningococcus)*. There is a large difference in the resistance rates, and the empiric antibiotic treatment needs to be adjusted according to regional epidemiology (Al-Lahham et al., 2018; De Gans et al., 2002). Finally, several adjunctive treatments have been tested in randomized controlled trials, often with conflicting results (van de Beek et al., 2016).

Therefore, this study aimed to determine phytochemical compounds contained in the essential oil extracted from the root and seed of *C. lacryma-jobi*, related to its antioxidant and antibacterial. This study also aimed to determine the antibacterial activity of essential oil from the seed and root of *Coix* against bacterial meningitis. This study suggests the potential of *C. lacryma-jobi* essential oil for bacterial meningitis treatment, which would be beneficial because meningitis affects many Hajj pilgrims from Indonesia.

2. Materials and Methods

2.1. Collection, identification, and processing of plant samples

The seeds and roots of *C. lacryma-jobi* were collected from Pamah Village Area, Semelir District, Langkat District North Sumatra 20773, Indonesia and submitted in the Herbarium Bandungense, Bandung Institute of Technology in Indonesia, Bandung (3749/II.CO2.2/PL/2019). Firstly, the seeds and roots were naturally dried for seven days to remove the water contents. After it was kept in an air-tight container with necessary markings for identification, it was stored in a cool, dark, and dry place for further investigation (Diningrat et al., 2020).

2.2. Oil extraction

Oil extraction of *C. lacryma-jobi* was performed by steam distillation. The essential oil from (seeds and root part of *C.lacryma-jobis*) was obtained by steam distillation using a Clevenger apparatus. Batches of 100 g of homogenized plant materials were mixed with 3 L of distilled water in a 5 L round-bottomed flask and heated using a heating mantle. The vapor of the essential oil was condensed and collected. Fractions of essential oil were collected every hour within 4 hours. The extracts were evaporated at room temperature to concentrate the samples, which were then stored in the refrigerator prior to the analysis (Al-Shuneigat et al., 2015; Benkeblia, 2004; Diningrat et al., 2020; Tepe et al., 2005).

2.3. Preliminary antioxidant screening

Comprehensive antioxidant screening of the essential oils was performed as preliminary phytochemical screening by following the procedures as described in the previous study (Aiyegoro and Okoh, 2010; Diningrat et al., 2020; Gowri and Vasantha, 2010; Igbinosa et al., 2009; Valgas et al., 2007).

2.3.1. Determination of total phenolic content

The reaction mixture consisted of 1 mL of essential oil, 1 mL of FCR (Folin Ciocalteu Reagent) 2N, and 3 mL of a 20% sodium carbonate solution. This mixture was placed at room temperature for 40 mins, and the absorbance was then measured (spectrophotometer Agilent 8453) at 760 nm. Distilled water was used as a blank in this measurement. A standard curve was plotted using tannic acid (1-5 µg/mL). Tests were performed in triplicate. The total phenolic content of the extract was calculated using the formula:

$$T_{PT} = \frac{C_{Tube}}{C_i} \times D$$

Where T_{PT} is the total phenolic content of the extract expressed as tannic acid equivalent (mg TAE)/g, C_{Tube} is the concentration (mg/mL) in the test tube, D is the dilution factor, and C_i is the concentration in mg/mL in the stock solution (Igbinosa et al., 2009; Tan and Lim, 2015).

2.3.2. Determination of tannin content

Polyvinyl polypyrrolidone (PVPP) can precipitate tannins by the formation of a complex; 100 mg of PVPP can complex 2 mg of total phenolics. 1 mL of essential oil (0.50 mg/mL) was added to the quantity of PVPP to complex the total phenolics present in the essential oil (and determined as described above). The mixture was vortexed, stored at 4°C for 15 min, and then centrifuged at 3000 g for 10 min. The supernatant contains phenolic compounds other than tannins (which have been precipitated by PVPP). A test tube was performed for total phenolics. After 40 minutes, it was centrifuged, and the absorbance of the supernatant was measured at 760 nm. The total phenolic content of the supernatant was calculated by the above formula. Tannin content was determined as the difference between the first value of total phenolics (containing tannins) and the second value of total phenolics (in the absence of tannins) (Valgas et al., 2007; Tan and Lim, 2015).

2.3.3. Determination of flavonoid content

100 µL of essential oil (10 mg/mL) in methanol was mixed with 100 µL of 20% antioxidant activity and adjusted to 5 mL with methanol. After 40 minutes, the absorbance was recorded at 415 nm (with a spectrophotometer Agilent 8453). Blank consisted of 100 µL of extract, a drop of acetic acid and adjusted to 5 mL with methanol. The absorbance of Quercetin (0.10 mg/mL), used as a reference compound, was measured under the same conditions. The tests were performed in triplicate. The flavonoids content expressed as quercetin equivalent (QE) was calculated using the following formula:

$$T_{Flav} = \frac{A \cdot m_0}{A_0 \cdot m}$$

T_{Flav} is the flavonoid content of essential oil in mg QE/mg; A is the absorbance of the extract; A_0 is the absorbance of Quercetin; m is the mass of the extract in mg, and m_0 is the mass of Quercetin in mg (Aiyegoro and Okoh, 2010; Tan and Lim, 2015).

2.3.4. Determination of flavonol content

The flavonol content was determined using Quercetin as a reference compound. The dosage was based on the formation of a complex with maximum absorption at 440 nm. 1 mL of essential oil was mixed with 1 mL of aluminum trichloride (20 mg/mL) and 3 mL of sodium acetate (50 mg/mL). The absorption was measured after 2 h 30 min. The absorbance of Quercetin (0.025 mg/mL in methanol) was measured under the same condition. The tests were performed in triplicate. The content of flavonols in the essential oil (expressed as quercetin equivalent, QE) was calculated using the same formula with the determination of flavonoids (above) (Aiyegoro and Okoh, 2010; Tan and Lim, 2015).

2.3.5. Antioxidant activities

The antioxidant activity by 1,1-diphenyl-2-picrylhydrazyl (DPPH) test was evaluated using the method described by Kim et al. (2003). The essential oil was prepared with an initial concentration of 21 mg/mL in dimethyl sulfoxide (DMSO). The concentration range of extracts or standard (Quercetin) was prepared by successive dilution using a microplate technique. The absorbance of residual DPPH in each well was measured at 490 nm (with a spectrophotometer BIO-RAD Model 680) after incubation at 37°C for 30 min. The antioxidant activity of a sample (calculated by the following formula) was given as the percentage of reduced DPPH:

$$I\% = \frac{A_0 - A_s}{A_0} \times 100$$

Where I is the percentage of inhibition, A_0 is the absorbance of the control, A_s is the absorbance of the sample (Tan and Lim, 2015).

2.4. Antibacterial activity

The antimicrobial screening was performed by the disc diffusion method against selected bacterial meningitis (Table 1) collected as pure cultures from the Department of Microbiology, Adam Malik Hospital, Medan, Indonesia. Standard disc of Ciprofloxacin (5 µg/disc) and blank discs (impregnated with solvents followed by evaporation) were used as the positive and negative control, respectively. The antimicrobial activity of the test agents was determined by measuring the diameter of the zone of inhibition expressed in mm (Al-Shuneigat et al., 2015; Diningrat et al., 2020; Restuati and Diningrat, 2018).

2.5. Determination of MIC

The MIC of the essential oil was determined by a two-fold dilution method. Subjected bacterial strains were grown in Nutrient Agar (HiMedia) until they reached the exponential phase. *C. lacryma-jobi* seed and root essential oil with different dilutions were given concentrations of 50, 25, 12.5, 6.25, 3.14, 1.56, and 0.78 mg/ mL, respectively. Thereafter, 0.5 mL essential of each concentration was added into separate test tubes containing 0.5 mL nutrient broth with the bacterial suspension at a final concentration of 1 mL in each tube and incubated at 37°C for 24 h. As a negative control, 7% of 0.5 mL chloroform was added with 0.5 mL liquid broth of bacteria. After incubation, 100 µL of culture from each tube was transferred and spread over the Mueller-Hinton agar (HiMedia) plate and incubated (Binder, Germany) at 37°C overnight for the bacterial count (Diningrat et al., 2020; Klančnik et al., 2020).

2.6. Statistical analysis

In the antioxidant and antibacterial activity test, the experimental data were calculated as mean ± SEM, evaluated by unpaired One-way ANOVA. Test values of $p < 0.01$ were considered statistically significant (Diningrat et al., 2020; Restuati and Diningrat, 2018).

3. Results

3.1. Preliminary phytochemical screening

The essential oil from the root and seed part of *C. lacryma-jobi* contained steroids, carotenoïds, tannins, alkaloid salts, reducing compounds, flavonoid, anthracenoid, coumarin derivatives, cardenoid, anthocyanins, saponins, while alkaloids and coumarins were absent (Table 1).

Table 1. Phytochemical composition of *C. lacryma-jobi* root and seed oil

Chemical groups	Essential oil	
	Root	Seed
Steroids	+	+
Carotenoïds	+	+
Alkaloid bases	-	-
Coumarins	-	-
Tannins	+	+
Alkaloid salts	+	+
Reducing compounds	+	+
Flavonoid	+	+
Anthracenoid	+	+
Coumarin derivatives	+	+
Cardenoid	+	+
Anthocyanins	+	+
Saponins	+	+

+: indicates the presence of phytochemical compounds; -: indicates the absence of a phytochemical compound

3.2. Antioxidant activity and phenolic content

DPPH scavenging activities of all the extracts depends on the concentration (Table 2). However, the highest DPPH scavenging activity was shown by the essential oil extract from seeds (9.58 ± 0.12 µg/mL, IC_{50}). Both essential oils showed a weak activity compared to those of Quercetin (4.60 ± 0.08 µg/mL, IC_{50}), which was a reference antioxidant. The total phenolic, tannin, flavonoid, and flavonol contents of the two essential oils were determined in this study (Table 2). The concentration of phenolic compounds, tannins, and flavonoids was higher in the essential oil from seeds than that of the roots. For the flavonol content, essential oil from the roots (0.28

± 0.01 mg QE/g) was richer than essential oil from the seeds (0.24 ± 0.01 mg QE/g).

Table 2. Phenolic content and scavenging activity by the DPPH test of *C. lacryma-jobi* root and seed oil

	Total phenolic mg TAE/g	Tannins mg TAE/g	Flavonoids mg QE/g	Flavonols mg QE/g	Antioxidant activity against DPPH IC50 (µg/ml)
Root essential oil	236.00 ±0.63[a]	124.80 ±0.75[a]	18.98 ±0.16 [a]	0.28 ±0.01[a]	33.81±0.57[a,b]
Seed essential oil	357.90 ±0.80	193.74 ±0.90	21.47 ±0.10	0.24 ±0.01	9.58±0.12[b]
Quercetin					4.50±0.12

TAE, Tannic Acid Equivalent; QE, Quercetin Equivalent; values are mean ±SEM (n = 3); a, $p<0.05$ against seed; b, $p<0.05$ against quercetin

3.3. Determination of antibacterial activity

The essential oil from the root of C. lacryma-jobi showed a wide range of antibacterial activity against Escherichia coli, Pseudomonas aeruginosa, Klebsiella pneumoniae, Streptococcus pneumoniae, and Streptococcus feaecalis at a concentration of 800 µg/mL, whereas the range of inhibition zone was within 20–30 mm (Table 3).

However, when essential oil from the seeds of *C. lacryma-jobi* was subjected to antibacterial screening at 800 µg/disc, it showed antibacterial activity against *E. coli, P. aeruginosa, K. pneumoniae, S. pneumoniae,* and *S. feaecalis* with the zone of inhibition ranging from 20 to 32 mm, whereas the remaining tested microorganisms were found to be resistant at the same concentration (Table 3).

Table 3. Antibacterial activity by disc diffusion assay (mm)

Bacterial meningitis isolates		Zone of inhibition in diameter		
		Root Essential Oil	Seed Essential Oil	Ciprofloxacin
Gram-negative bacteria	*Escherichia coli*	21	21	40
	Pseudomonas aeruginosa	26	20	31
	Klebsiella pneumoniae	30	32	40
Gram-positive bacteria	*Streptococus pneumoniae*	28	21	34
	Streptococus feaecalis	24	20	31

3.4. Determination of MIC

The inhibition of microorganism's growth at the lowest concentration of plant extract is known as MIC. In the MIC test, the essential oil of *C. lacryma-jobi* root was capable of inhibiting all types of Gram-positive and Gram-negative (*E. coli, P. aeruginosa, K. pneumoniae, S. pneumoniae, S. feaecalis*) meningitis bacterials at the concentration of 12.5–50 mg/mL (Table 4). In contrast, *E. coli, P. aeruginosa, K. pneumoniae, S. pneumoniae, S. feaecalis* were inhibited at the concentration of 25–50 mg/mL in the essential oil from *C. lacryma-jobi* seed (Table 5).

Table 4. MIC of *C. lacryma-jobi* root essential oil against selected bacteria of meningitis.

Bacterial meningitis isolates		MIC of root essential oil (mg/mL)						
		50	25	12.5	6.25	3.14	1.56	0.78
Gram-negative bacteria	*Escherichia coli*	0	0	0	29	106	166	222
	Pseudomonas aeruginosa	0	0	0	8	23	46	102
	Klebsiella pneumoniae	0	0	0	4	7	16	46
Gram-positive bacteria	*Streptococus pneumoniae*	0	0	0	7	20	48	96
	Streptococus feaecalis	0	0	0	6	16	27	66

Values are represented as the number of colonies.

Table 5. MIC of *C. lacryma-jobi* seed essential oil against selected bacteria of meningitis.

Bacterial meningitis isolates		MIC of seed essential oil (mg/mL)						
		50	25	12.5	6.25	3.14	1.56	0.78
Gram-negative bacteria	*Escherichia coli*	0	0	13	35	87	137	202
	Pseudomonas aeruginosa	0	0	7	16	41	92	137
	Klebsiella pneumoniae	0	0	6	10	23	47	106
Gram-positive bacteria	*Streptococus pneumoniae*	0	0	11	25	53	85	136
	Streptococus feaecalis	0	0	6	19	63	89	136

Values are represented as the number of colonies.

4. Discussion

Neisseria meningitidis, Streptococcus pneumoniae, Haemophilus influenzae, Pseudomonas aeruginosa, Klebsiella pneumoniae, Streptococcus feaecalis, and Escherichia coli are the leading causes of bacterial meningitis infections worldwide (Al-Gosha'ah et al, 2014; Paireau et al., 2016; van de Beek et al., 2016; Yezli et al., 2016). Bacterial meningitis causes inflammation of the meninges, which leads to a sudden onset of fever, headache, stiff neck, nausea, vomiting, and altered mental status, and can rapidly result in death (Paireau et al., 2016; van de Beek et al., 2016). The relative contribution of these pathogens to the incidence of bacterial meningitis varies over time, by location, and by characteristics such as the age of patients. Although vaccination programs have been implemented in many countries, including Indonesia, and have had a considerable impact on the disease, more than 1.2 million cases of bacterial meningitis are estimated to occur each year (El Bashir et al., 2003; Paireau et al., 2016; van de Beek et al., 2016; Yezli et al., 2016).

Phytochemical analysis of the *Coix lacryma-jobi* oil from root and seed part revealed the presence of steroids, carotenoids, tannins, alkaloid salts, reducing compounds, flavonoid, anthracenoid, coumarin derivatives, cardenoid, anthocyanins, saponins (Table 1). These phytochemical compounds are known to be biologically active, which enhances the antimicrobial activities of plants. In addition, alkaloids are also known to have antimicrobial, anti-inflammatory, anti-asthmatic, and anti-anaphylactic properties (Diningrat et al., 2018; Diningrat et al., 2020; Diningrat and Marwani, 2018).

The presence of flavonoids in *C. lacryma-jobi* oil is essential because they have been reported to exhibit antimicrobial, anti-inflammatory, anti-angiogenic, analgesic, anti-allergic, cytostatic, antioxidant, antitrypanosomal, and antileishmanial properties (Diningrat et al., 2020; Sari et al., 2018). Saponins and tannins were also reported in this study. Saponins were responsible for numerous pharmacological properties and were known to induce inhibitory effects on inflammation (Benkeblia, 2004; Tepe et al., 2005). Moreover, tannins exerted antimicrobial activities by iron deprivation, hydrogen bonding, or specific interactions with vital proteins, such as enzymes in microbial cells (Devi et al., 2015; Wang et al., 2016).

Steroidal compounds were also present in *Coix lacryma-jobi* oil, and they have drawn much interest due to their relationship with compounds such as sex hormones (Qu et al., 2014). Anthracenoid has a role as a free radical binding agent (Rajesh, 2016). Coumarin derivatives (4-hydroxycoumarin compounds) are oral anticoagulants (OA) that prevent vitamin K from acting as a cofactor in the hepatic synthesis (Chhabra and Gupta, 2015). Cardenoid, carotenoid, and anthocyanin might be responsible for antioxidants and anti-cancer (Rajesh, 2016; Qu et al., 2014). *Coix lacryma-jobi* oil was very potential as an agent that can be used for the treatment of bacterial meningitis based on its phytochemical compounds.

According to the observed antioxidant potential of *Coix lacryma-jobi* oil from roots and seeds and the potent DPPH radical, OH^- radical, $O2^-$ radical, NO^- scavenging activities, the results demonstrated that the oil possessed high phenol contents, antioxidant and nitric oxide scavenging abilities. In other words, the plants contained certain compounds that were potential antioxidants (Table 2). It is assumed that this oil is able to prevent lipid peroxidation, and it is further suggested that the extract was a potential therapeutic agent for the control of oxidative and non-oxidative damage caused by reactive oxygen and nitrogen species (Devi et al., 2015; Kuo et al., 2002; Wang et al., 2016). Since reactive oxygen species are thought to be associated with the pathogenesis of bacterial infections and inflammatory diseases (Rajesh, 2016), the observed inhibitory potential might partially explain the beneficial effects of *Coix lacryma-jobi* oil in treating bacterial meningitis disease.

Plant oil has been long used in pharmaceuticals, alternative medicine, and natural therapies (Benkeblia, 2004; Tepe et al., 2005). *Coix lacryma-jobi* oil is a potential source of novel antimicrobial compounds, especially against bacterial pathogens (Diningrat et al., 2020). In vitro studies in this study showed that the oil inhibited some bacterial meningitis growth, but their effectiveness was classified strong (Table 3). Several compounds, such as steroids, carotenoids, tannins, alkaloid salts, reducing compounds, flavonoid, anthracenoid, coumarin derivatives, cardenoid, anthocyanins, and saponins (Table 1) were identified in the composition of the obtained *Coix lacryma-jobi* oil. Many components of *Coix lacryma-jobi* oil were characterized by Diningrat et al. (2020) using GC-MS, and all of these compounds had antibacterial effects.

The results indicated that *Coix lacryma-jobi* oil with concentrations of 6.25 and 12.5 mg/ml prevented the growth of *Escherichia coli, Pseudomonas aeruginosa, Klebsiella pneumoniae, Streptococcus pneumoniae,* and *Streptococcus feaecalis.* Furthermore, a study by Diningrat et al. (2020) investigated *Coix lacryma-jobi* oil and reported a significant effect on the standard *E. coli, S. aureus,* and *B. subitlis*. In this study, the antimicrobial effect of *N. Sativa* oil extract was investigated in the laboratory against bacteria causing bacterial meningitis. The results showed that the antimicrobial effect of *Coix lacryma-jobi* oil from roots and seeds was comparable with antibiotics, such as Ciprofloxacin.

The activity of *Coix lacryma-jobi* oil from roots and seeds against both Gram-positive and Gram-negative selected bacteria of meningitis is an indication of the broad spectrum of activity, so it can be used as sources of antibiotic substances for drug development in the control of these bacterial meningitis infections (van de Beek et al., 2016; Al-Lahham et al., 2018; Diningrat et al., 2020). The essential oil of *C. lacryma-jobi* roots and seeds showed a wide range of antimicrobial activity against Gram-positive and Gram-negative bacterial meningitis. Finally, our results showed that *Coix lacryma-jobi* oil-induced antimicrobial activity against a broad range of bacteria in bacterial meningitis. From this study, it can be concluded that the *Coix lacryma-jobi* oil from roots and seeds possesses antibacterial activity for bacterial meningitis treatment. Furthermore, our results support the use of the plants in traditional medicine and suggest that *Coix lacryma-jobi* oil possesses compounds with good antibacterial properties. Thus, it can be used as an antibacterial supplement in developing countries towards the development of a new therapeutic agent. However, additional in vivo studies and clinical trials would be needed to justify and further evaluate its potentials as an antibacterial agent for topical or oral applications.

5. Conclusions

Based on the observation of the antioxidant and antibacterial potential of the investigated oil from *Coix lacryma-jobi* roots and seeds, it can be concluded that this oil is able to prevent bacterial meningitis and becomes a potential therapeutic agent for bacterial meningitis treatment. The results also suggest that oil extracted from *Coix lacryma-jobi* roots and seeds can be used in bacterial meningitis treatment as a natural antioxidant and antibacterial. The antioxidants and antibacterial present in the *Coix lacryma-jobi* oil may function by combining with the pharmaceutical components. However, it is important to further investigate the in vivo potentials of the *Coix lacryma-jobi* oil and also isolate the active components, which can ultimately lead to their application in the pharmaceutical formulations industry as antioxidant and antibacterial agents for bacterial meningitis treatment.

6. Conflict of interest statement

All authors stated that they have no conflict of interest in the results of this study.

Acknowledgments

The authors thank the Biology Department, Faculty of Mathematics and Natural Science, Universitas Negeri Medan, LPPM Universitas Negeri Medan (KDBK-BOPTN Grant), DRPM Kemenristekdikti Republic of Indonesia (Grant No. 36/UN33.8/PL.DRPM/2019).

References

Aiyegoro, O. A., and Okoh, A. I. 2010. Preliminary phytochemical screening and in vitro antioxidant activities of the aqueous extract of Helichrysum longifolium DC. *BMC complementary and alternative medicine*, ***10*(1)**, 21. https://doi.org/10.1186/1472-6882-10-21

Al-Gosha'ah, F. A., Al-Baker, S. M., & Al-Hetar, K. Y. 2014. Bacteriocin Typing of Staphylococcus aureus Isolated from Different Sources in Ibb City, Yemen. *Jordan J. of Biological Sciences*, ***147*(1570)**,1-5.

https://platform.almanhal.com/Files/2/56256

Al-Lahham, A., Qayyas, J. A., and van der Linden, M. 2018. The Impact of the 7-Valent Pneumococcal Conjugate Vaccine on Nasopharyngeal Carriage of Streptococcus pneumoniae in Infants of Ajlun Governorate in Jordan. *Jordan J. of Biological Sciences*, ***11*(2).** 155-162.

http://jjbs.hu.edu.jo/files/v11n2/Paper%20Number%206.pdf

Al-Shuneigat, J. M., Al-Tarawneh, I. N., Al-Qudah, M. A., Al-Sarayreh, S. A., Al-Saraireh, Y. M., and Alsharafa, K. Y. 2015. The chemical composition and the antibacterial properties of Ruta graveolens L. essential oil grown in Northern Jordan. *Jordan J. of Biological Sciences*, ***147*(3427),** 1-5. https://platform.almanhal.com/Files/2/88303

Benkeblia, N. 2004. Antimicrobial activity of essential oil extracts of various onions (Allium cepa) and garlic (Allium sativum). *LWT-food science and technology*, ***37*(2)**, 263-268. https://doi.org/10.1016/j.lwt.2003.09.001

Chhabra, D., and Gupta, R. K. 2015. Formulation and phytochemical evaluation of nutritional product containing Job's tears (Coix lachryma-Jobi L.). *J. of Pharmacognosy and Phytochemistry*, ***4*(3)**, 291-298. http://www.phytojournal.com/archives/2015/vol4issue3/PartD/4-3-51-740.pdf

De Gans, J., and Van de Beek, D. 2002. Dexamethasone in adults with bacterial meningitis. *N. Engl. J. of Medicine*, ***347*(20)**, 1549-1556. https:// /doi.org/10.1056/NEJMoa021334

Devi, K. S., Damayanti, M., and Singh, D. V. N. R. 2015. Analysis of kidney stones by PXRD and evaluation of the antiurolithic potential of Coix lacryma jobi. *International J. of Scientific and Res. Publications*. **5(3),** 303-319 http://citeseerx.ist.psu.edu/viewdoc/download?doi=10.1.1.734.8669&rep=rep1&type=pdf#page=319

Diningrat, D. S., and Marwani, E. (2018). De novo transcriptome profiling of buasbuas (Premna pubescens. Blume). *Biotechnology*, ***17*(2),** 75-85.

DOI:10.3923/biotech.2018.75.85

Diningrat, D. S., Restuati, M., Kusdianti, K., Sari, A. N., and Marwani, E. 2018. Analysis of Ethanol Extract of Buasbuas (Premna Pubescens) Stalk Using Gas Chromatography Mass Spectrophotometer (GCMS). *Elkawnie*, ***4*(1)**, 1-12. http://dx.doi.org/10.22373/ekw.v4i1.3075

Diningrat, D. S., Risfandi, M., Harahap, N. S., Sari, A. N., and Siregar, H. K. (2020). Phytochemical Screening and Antibacterial Activity Coix lacryma-jobi Oil. *J. of Plant Biotechnology*, ***47*(1)**, 100-106. https://doi.org/10.5010/JPB.2020.47.1.100

El Bashir, H., Laundy, M., and Booy, R. 2003. Diagnosis and treatment of bacterial meningitis. *Archives of dis. in child.*, ***88*(7)**, 615-620. http://dx.doi.org/10.1136/adc.88.7.615

Gowri, S. S., & Vasantha, K. 2010. Phytochemical screening and antibacterial activity of Syzygium cumini (L.) (Myrtaceae) leaves extracts. *Int J Pharm Tech Res*, ***2*(2)**, 1569-1573. http://www.academia.edu/download/31144347/PT_95__1569-1573_.pdf.

Igbinosa, O. O., Igbinosa, E. O., and Aiyegoro, O. A. 2009. Antimicrobial activity and phytochemical screening of stem bark extracts from Jatropha curcas (Linn). *African j. of pharm. and pharmacology*, ***3*(2)**, 058-062.

https://doi.org/10.5897/AJPP.9000049

Klančnik, A., Piskernik, S., Jeršek, B., and Možina, S. S. 2010. Evaluation of diffusion and dilution methods to determine the antibacterial activity of plant extracts. *J. of microbiological methods*, ***81*(2)**, 121-126.

https://doi.org/10.1016/j.mimet.2010.02.004

Kuo, C. C., Chiang, W., Liu, G. P., Chien, Y. L., Chang, J. Y., Lee, C. K., and Kuo, Y. H. 2002. 2, 2 '-Diphenyl-1-picrylhydrazyl radical-scavenging active components from adlay (Coix lachryma-jobi L. Var. ma-yuen Stapf) hulls. *J. of Agricultural and Food Chemistry*, ***50*(21)**, 5850-5855.https://doi.org/10.1021/jf020391w

Paireau, J., Chen, A., Broutin, H., Grenfell, B., and Basta, N. E. 2016. Seasonal dynamics of bacterial meningitis: a time-series analysis. *The Lancet glob. health*, ***4*(6)**, e370-e377. https://doi.org/10.1016/S2214-109X(16)30064-X

Patel, B., Patel, G., Shah, S., and Parmar, S. 2017. A Review: Coix lacryma jobi L. *Res. J. of Pharmacognosy and Phytochemistry*, ***9*(4)**, 248-252. DOI:10.5958/0975-4385.2017.00046.2

Qu, D., He, J., Liu, C., Zhou, J., and Chen, Y. 2014. Triterpene-loaded microemulsion using Coix lacryma-jobi seed extract as oil phase for enhanced antitumor efficacy: preparation and in vivo evaluation. *International j. of nanomed.*, ***9*,** 109-119. doi: 10.2147/IJN.S54796

Rajesh, K S, Ishwara, B K, and Vaman, R 2016. Preliminary phtocemical investigation and anti-venom activity of Coix lacrymajobi root extract against daboia Rajesh venom-induced myonecrosis. *Asian J Pharm Clin Res*, ***9*(1)**, 319-321. https://innovareacademics.in/journals/index.php/ajpcr/article/view/9165.

Restuati, M., and Diningrat, D. S. 2018. Antimicrobial profile of Premna pubescens. blume and Centella asiatica extracts against bacteria and fungi pathogens. *International J. of Pharmacology*, ***14*(02),** 272-275. DOI: 10.3923/ijp.2018.271.275

Sari, A. N., Kusdianti, K., and Diningrat, D. S. 2018. The Potency of Natural Antioxidant in The Rind Extract of Jamblang (Syzigium cumini (L.) Skeels) using DPPH Method. *J. BIOS LOGOS*, ***8*(1)**. 20-25 https://doi.org/10.35799/jbl.8.1.2018.20593

Tan, J. B. L., & Lim, Y. Y. (2015). Critical analysis of current methods for assessing the in vitro antioxidant and antibacterial activity of plant extracts. *Food chemistry*, *172*, 814-822. https://doi.org/10.1016/j.foodchem.2014.09.141

Tepe, B., Daferera, D., Sokmen, A., Sokmen, M., and Polissiou, M. 2005. Antimicrobial and antioxidant activities of the essential oil and various extracts of Salvia tomentosa Miller (Lamiaceae). *Food chemistry*, ***90*(3)**, 333-340.

https://doi.org/10.1016/j.foodchem.2003.09.013

Valgas, C., Souza, S. M. D., Smânia, E. F., and Smânia Jr, A. 2007. Screening methods to determine antibacterial activity of natural products. *Brazilian J. of Microbiology*, *38*(2), 369-380. http://dx.doi.org/10.1590/S1517-83822007000200034

van de Beek, D., Brouwer, M. C., Thwaites, G. E., and Tunkel, A. R. 2012. Advances in treatment of bacterial meningitis. *The Lancet*, ***380*(9854),** 1693-1702.https://doi.org/10.1016/S0140-6736(12)61186-6

van de Beek, D., Cabellos, C., Dzupova, O., Esposito, S., Klein, M., Kloek, A. T., ... and Pfister, H. W. 2016. ESCMID guideline: diagnosis and treatment of acute bacterial meningitis. *Clinical microbiology and infection*, ***22*,** S37-S62. https://doi.org/10.1016/j.cmi.2016.01.007

Wang, L., Chen, C., Su, A., Zhang, Y., Yuan, J., and Ju, X. 2016. Structural characterization of phenolic compounds and antioxidant activity of the phenolic-rich fraction from defatted adlay (Coix lachryma-jobi L. var. ma-yuen Stapf) seed meal. *Food chemistry*, ***196***,509-517. https://doi.org/10.1016/j.foodchem.2015.09.083

Yezli, S., Assiri, A. M., Alhakeem, R. F., Turkistani, A. M., and Alotaibi, B. 2016. Meningococcal disease during the Hajj and Umrah mass gatherings. *International J. of Infectious Diseases*, ***47***, 60-64. https://doi.org/10.1016/j.ijid.2016.04.007

Zhang, W., Wen, T., and Qiu, G. 2014. Isolation and antimicrobial activity of endophytic fungi in Coix lacryma-jobi kernels. *Guizhou Agricultural Sciences*, ***42*(10)**, 152-157.https://www.cabdirect.org/cabdirect/abstract/20153090154.

JJBS

Volume 14, Number 5 ,December 2021
ISSN 1995-6673
Pages 889 – 897

Jordan Journal of Biological Sciences

Further studies on evaluation of the toxicity potential of *Terminalia catappa* Lin. Combretaceae leaf extract: effects on the histology, liver enzymes, and haematology profile of albino rats

Chika B. Ikele* , Elijah Okwuonu and Anya N. Ijem

Department of Zoology and Environmental Biology, University of Nigeria, Nsukka, Enugu State, Nigeria

Received: March 21, 2020; Revised: Dec 12, 2020; Accepted: Dec 21, 2020

Abstract

There is a global utilization of *Terminalia catappa* as a medicinal plant. In this study, the effect of aqueous leaf extract of *Terminalia catappa* (ALETA) on the haematological profile, liver function enzymes, and histology of some organs in albino rats was examined. Seventy-two healthy albino rats were randomly distributed into four groups (A-D) in 6 rats per triplicate. The normal control received 1ml/kg of deionized water while groups B-D received 150, 300, and 450 mg/kg ALETA, respectively for 21 days. Minor cytoplasm vacuolation, focal necrosis, and dilated sinusoids were observed in the liver tissue. The kidney showed minor degenerative changes characterized by few shrunk glomeruli while no tissue damage was observed in the heart tissue and minor passive congestion was observed in the pyloric stomach. The packed cell volume (PCV), red blood cell (RBC), haemoglobin (HB), neutrophils (N), eosinophils (E), monocytes (M), lymphocytes (L), and means cell haemoglobin (MCH) responded significantly ($p<0.05$) to treatment dosage. Meanwhile, the increased aspartate aminotransfarase (AST), alanine aminotransfarase (ALT), acid phosphatase (ACP) and alkaline phosphatase (ALP) were an indication of compromised liver function by the ALETA. There is a need for safety assessment, regulation, and intake of *Terminalia catappa* as a medicinal herb.

Keyword: *Terminalia catappa*, histopathology, haematology, liver enzymes, *Rattus norvegicus*

1. Introduction

Globally, fruit nutriments have beneficial health therapeutic and economic benefits (Venkatalakshmi and Brindha 2016). Indian almond seed, *Terminalia catappa*Linn (family Combretaceae) is a plant species with good records of medicinal importance associated with its chemical constituents. In Nigeria, the most popularly used plant parts are commonly referred to as 'fruit' by some local folks. The seeds and leaf of the plant mostly contribute to a high percentage of waste in the environment without being utilized more effectively for the benefit of society. Indian almond is popularly used as a herbal treatment for management of diabetes mellitus (Divya et al, 2018, Biswas et al, 2011, Koffi et al, 2011, Nagappa et al, 2003,). It is also used as analgesic (Mohale et al, 2008), for the alleviation of inflammation (Lin et al, 1997), etc. Most often, the fruit parts (kernel endocarp and fleshy mesocarp) of *T. catappa* are consumed roasted, raw, and sundried. Other plant parts such as the roots, barks, and leaf are used in the treatment of different ailments such as malaria (Mudi and Muhammed, 2009), respiratory disorders (asthma) (Raj et al, 2013), hypertension (Odugbemi, 2008), and as an antiretroviral (Alka et al, 2016). They possess therapeutic components that increase the potential use similar to conventional drugs. Several studies have reported that *T. catappa*can exert a multitude of effects such as anticancer (Shanehbandi et al, 2019; Lee et al, 2019) antimetastatic (Yang et al, 2010, Chu et al, 2007), antioxidant (Kumar et al, 2018, Krishnaveni et al, 2014), antimicrobial (Kumar et al, 2018), antidiabetic (Koffi et al, 2011, Ahmed et al, 2005, Lin et al, 1997), aphrodisiac (Ratnasooriya and Dharmasiri, 2000), antinociceptive (Ratnasooriya et al, 2002), and hepatoprotective (Kinoshita et al, 2007.

Globally, there is an increase in the intake of medicinal plants (mostly self-prescribed by consumers) without complying with World Health Organization (WHO) recommendations and guidelines. It is worthy of note that increased utilization of medicinal plants necessitated the WHO to provide the recommended intake per time to avoid negative/or side effects (WHO, 2004, WHO, 1998). Most plant materials can be taken indiscriminately or wrongly prescribed as prophylaxis against diseases. The safety regulation of global phytopharmaceutical products is paramount, essential, and implemented to avoid toxicity or adverse effects on the human body. In Nigeria, most herbal drugs are produced and consumed indiscriminately by local folks irrespective of strict regulations. However, despite the extensive use of herbs, there is a need to add to knowledge scientific proof validating their safety, efficacy, and usage. Histopathological assessment is a marker considered as a useful indicator for assessing the abnormal health effects of environmental materials on the living system (Arsad et al., 2014). Possibilities of organ toxicity

* Corresponding author e-mail: chika.ikele@unn.edu.ng.

(nephrotoxicity, hepatotoxic, etc.) cannot be overruled on the unpredictable intake of plant products. Blood regulation at a normal range elicits homeostatic mechanism, and changes in the blood parameters. Liver enzymes are an indicator of the deleterious effect of chemical products. Moreover, the therapeutic uses of aqueous leaf extract of *T. catappa* (ALETA) have been scientifically supported by effects in malaria (Mudi and Muhammed, 2009), respiratory disorders (asthma) (Raj et al, 2013), and hypertension (Odugbemi, 2008), However, there is a need to promote more information on the histological, hematological, and liver enzyme alterations mediated by this plant extract. In this study, albino rats, *Rattus norvegicus* have been used to obtain such information.

2. Materials and Methods

2.1. Experimental Animal

Seventy-two healthy male albino Wistar rats weighing between 150-200g were used for the study. The animals were procured from the animal rearing facility of the Department of Zoology and Environmental Biology, University of Nigeria, Nsukka, and housed in well-ventilated cages. Animals were acclimatized for two weeks and fed with standard pellets (Top Feeds, Plc Nigeria) with access to water *ad libitum* and maintained at different standard laboratory conditions, temperature (25±2°C), humidity (50±5%), and 12 hours light and dark cycle. This study was carried out following ethical guidelines for animal welfare by the Faculty of Biological Sciences, University of Nigeria, Nsukka.

2.2. Plant material and preparation

Whole plant leaf (4kg) of *Terminalia catappa* were obtained from the Botanical garden of Plants Science and Biotechnology, University of Nigeria. The leaf was authenticated by a plant taxonomist in the Herbarium of Plant Science and Biotechnology Department (Voucher Number: UNH/027-University of Nigeria Herbarium/027). The leaf was separated from the stem and washed thoroughly with distilled water to remove debris. The dried pulverized leaf (1,486 g) was concentrated in 3.5 litres of deionized water for 18 hours. The mixture was filtered using a muslin cloth and further filtered with Whatmann No 1 filter paper. The mixture was evaporated to dryness LEICA RM 2125 RTS rotary microtone. 204.18g of the extract was obtained after evaporation with a percentage yield of 13.74% (McCloud, 2010). The extract was stored in a refrigerator for later use.

2.3. Experimental Design

The experimental animals were randomly distributed into four groups of six rats per triplicate. Group 1 served as control and was orally administered normal deionized water at a dose of 1ml/kg body weight. Group 2, 3, and 4 were administered with aqueous leaf extract of *Terminalia catappa* (ALETA) at 150, 300, and 450mg/kg, respectively by oral gavage for 3 weeks. The dosages administered were obtained after zero mortality record of the acute toxicity test following the protocol of Lorke (1983). Meanwhile, the animals were immobilized using chloroform to obtain 3 tissues (liver, heart, and kidney) from 3 rats per group for histological examinations at the end of the experiment which lasted for three weeks.

2.4. Phytochemical Screening of the Plant Material

The analysis of the extract (flavonoids, tannins, saponins, alkaloids, steroids) was done following the standard methods of Trease and Evans, (2002).

2.5. Histological Examination

The histological analyses of the tissues (liver, kidney, and heart) were done according to the method of Akilandeswarietal, 2010).

2.6. Haematological Parameters

The blood haematocrit was determined by stuffing capillary tube with blood and centrifuged in a microheamatocrit (Hawksley England) at 14,000 Xg rpm for 5 minutes, and the percentage of the erythrocyte layers was evaluated and read using a heamatocrit reader (Wintrobe, 1967). The erythrocytes and leucocyte count were determined manually utilizing heamocytometer under X40 magnification. The concentration of haemoglobin in the blood was estimated using spectrophotometry combined with cyanmethaemoglobin method using Drabkins reagents (Wintrobe, 1967). The erythrocytes, packed cell volume, and haemoglobin were used in estimating the erythrocytes derivatives such as mean cell volume (MCV in fentolitres), mean cell haemoglobin (MCH in picogram) and mean cell haemoglobin concentration (MCHC in grams decilitre). Blood smears were obtained and stained with a may-Grunwald-Giemsa solution for accurate determination of differential leucocyte subpopulations.

2.7. Biochemical Parameters

Plasma levels of aspartate aminotransferase (AST) and Alanine aminotransferase (ALT) were assayed following the protocol of Reitman and Frankel, (1957). Acid and alkaline phosphatase enzymatic activity was determined following the protocol of Babson and Read (1959) and Bergmeyer, (1974), respectively.

2.8. Data analysis

The haematology and liver enzyme data were analyzed for significant differences ($p<0.05$) using analysis of variance (ANOVA). Also, differences between means were partitioned using the Duncan Multiple Range test (DNMRT). All analyses were done using Statistical Package for Social Sciences windows version 20.0 (IBM Corporation, Armonk, USA).

3. Phytochemicals

The phytochemical components of the aqueous leaf extract of *Terminalia catappa* were shown in Table 1. Meanwhile, the presence of alkaloids, terpenoids, saponins, tannins, and flavonoids was observed. The concentrations of the chemical constituents were similar.

Table 1. Phytochemical constituents of aqueous leaf extract of *Terminalia catappa*

Phytochemical constituents	Bioavailability	Concentration (%)
Tannins	+	0.32±0.00
Saponins	+	0.48±0.01
Alkaloids	+	0.37±0.00
Steroids	-	0.03±0.00
Flavonoids	++	1.68±0.14

-, absent +, present ++ moderately present

3.1. Histological Changes in some tissues of Albino Rats Exposed to Aqueous Leaf Extracts of Terminalia catappa

The histological patterns of the normal liver revealed clearly defined parenchyma cells, central veins, sinusoids, and kupfer cells. Cytoplasmic vacuolations and kupfer cell hyperplasia were observed in the liver of albino rats exposed to 150mg/kg ALETA. The enlarged sinusoid was filled with mixed infilterate. The clogged sinusoid observed in the liver of albino rats exposed to 300mg/kg impeded the functions of the kupfer cells and allowed spent erythrocyte to build up in the blood instead of being removed, (Plate 1A). Further observations such as the influx of mononuclear cells in the dilated sinusoid were obvious, while the kupfer cells lined at the basement of the sinusoid phagocytized and removed spent erythrocytes and other particulate debris from circulating in the blood vessel of the liver tissue (Plate 1D). Moreso, cytoplasmic vacuolation associated with cells adaptively altered to resist further degeneration was observed. This also reflected a cellular adaptation beneficial to the host.

The histological patterns of the kidney shown in (Plate 2A) revealed normal renal corpuscles with intact glomerulus and epithelial cells linked to the tubules and connected with a tight junction that prevents waste products and other potentially harmful substances from passing between the cells and reaching the bloodstream. Some of the glomeruli structure appeared shrunk and vacuolated with discrete clear or translucent spaces observed in the kidney of albio rat administered 150mg/kg (Plate 2B) and 300mg/kg ALETA (Plate 2C), respectively. Renal corpuscles were also intact in the group treated with 450mg/kg ALETA (Plate 2D).

The histological patterns of the normal heart of albino rats showed prominent branching in the cardiac muscle fibre (Plate 3A). Myocardial fibre variations and blood vessels were observed in the heart of the albino rats exposed to 150mg/kg of ALETA (Plate 3B), while at 300mg/kg (Plate 3C) and 450mg/kg ALETA (Plate 3D), heart architecture showed normal branching of anastomosing intercalated disc with each other in a network pattern.

The stomach histological section of the normal control revealed intact muscularis mucosa and lamina propria of the stomach architecture (Plate 4A). Hemorrhage was observed in the fundic region of the stomach. Meanwhile, hemorrhage was observed in the blood vessels of the stomach following 150mg/kg ALETA administration (Plate 4B). More so, at 300mg/kg and 450mg/kg ALETA (Plate 4C, and D), vascular congestion and degeneration of the inner circular layer such as degenerated muscularis mucosa were similarly observed, respectively.

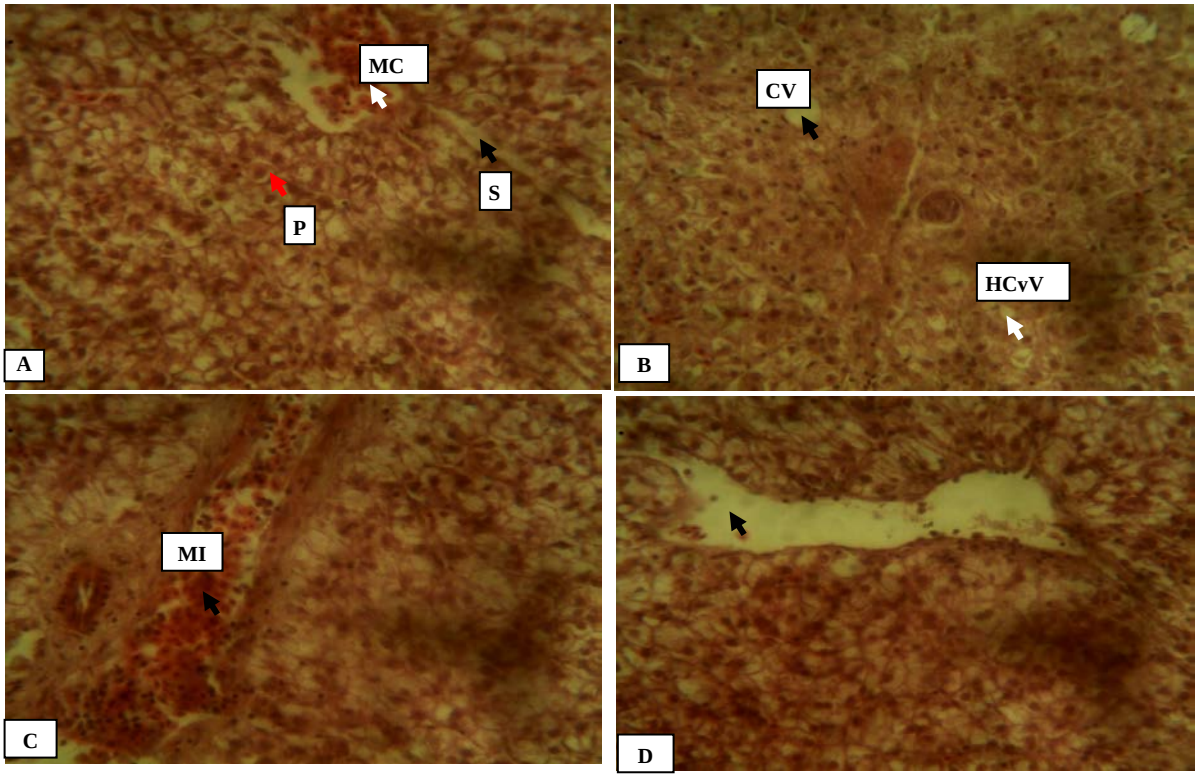

Plate 1: Photomicrograph of liver **(A)**. normal parenchymal cells (PC) (red arrow), intact sinusoids (black arrow) and central vein infilterated with mononuclear cells (MC) (white arrow). **Plate B**. 150mg/kg of ALETA showing central vein (CV, black arrow), hepatocyte cytoplasmic vacuolation (HCyV, white arrow). **Plate C:** 300mg/kg of ALETA showing mixed infilterate (MI) in the sinusoid (black arrow). **Plate D**: 450mg/kg of ALETA showing enlarged sinusoids with few mononuclear cells (black arrow). H&E. mag. 400X.

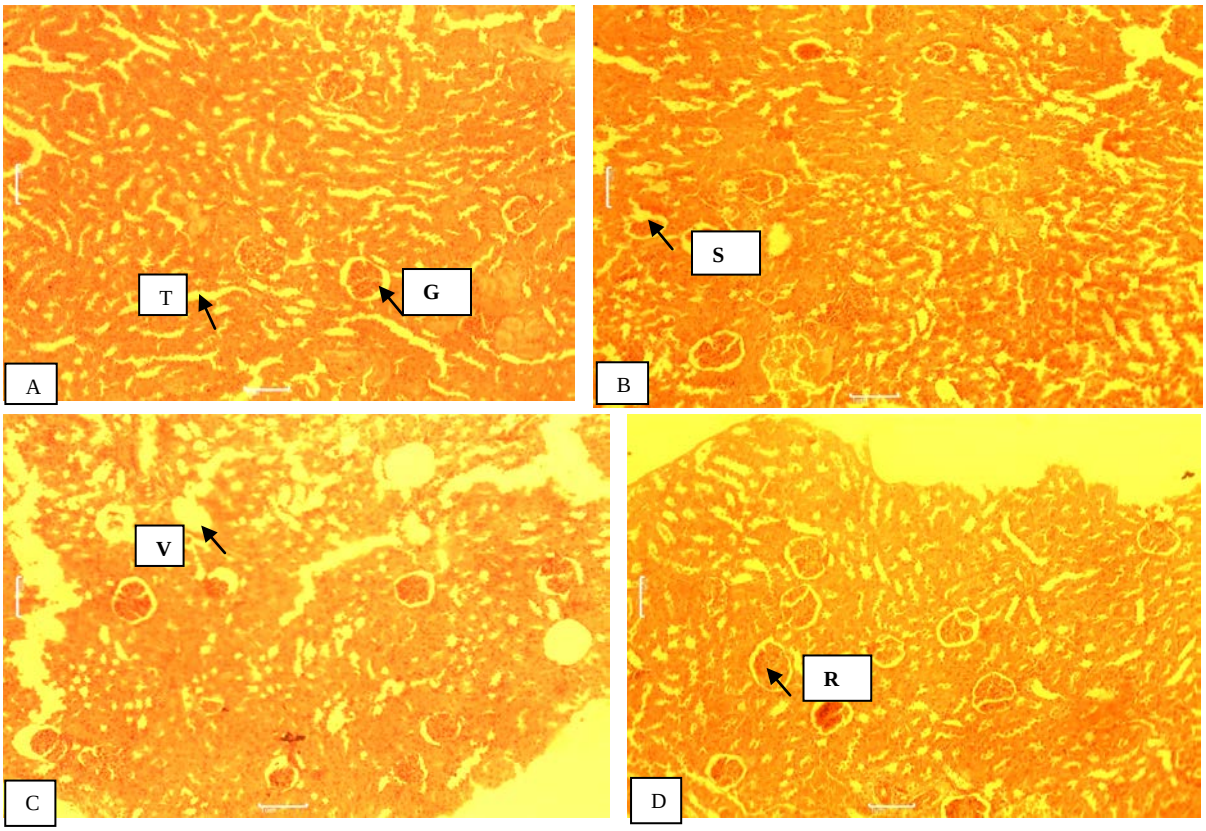

Plate 2: Photomicrograph of kidney of albino rats **A**: Normal group showing, normal renal corpuscles with intact glomerulus (GL) and tubules (T) lined with epithelial cells connected to each other in the kidney cortex. **B:** 150mg/kg of ALETA showing shrinkage of the glomeruli (SG black arrow). **C:**300mg/kg ALETA showing kidney vacuolation (V black arrow) was observed. **D:** 450mg/kg ALETA, with intact renal corpuscules (RC). H&E. mag. 100X.

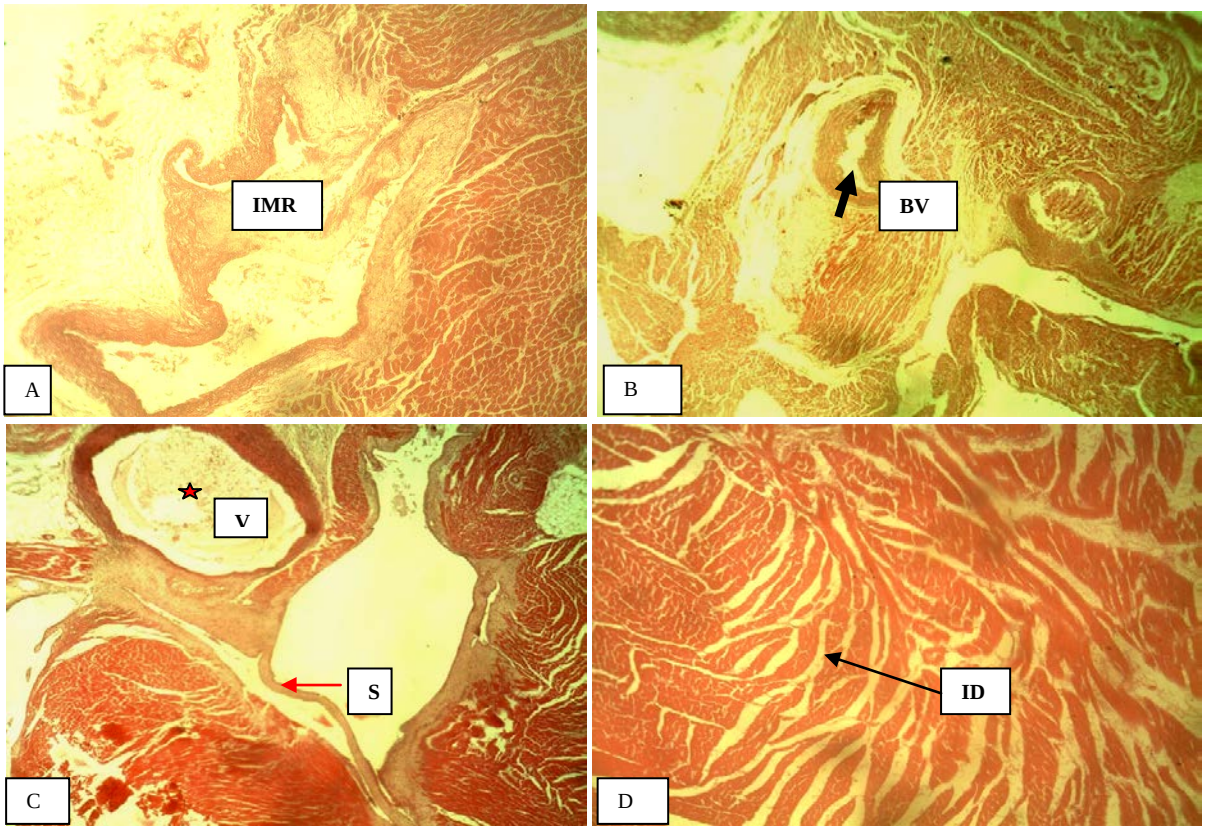

Plate 3: Photomicrograph of heart of albino rats showed **A.** intact region of myocardial fibre (IMR (yellow arrow) with no variations in fibre sizes. **B**. 150mg/kg of ALETA showing no myocardial fibre variation and intact blood vessels (BV black arrow). **Plate C**. 300mg/kg of ALETA showing normal heart architecture, intact valve (red star), and septum (red arrow). **Plate D**. 450mg/kg of ALETA showing rominent cardiac region of the heart with intact intercalated disc (ID). H&E. mag. 100X.

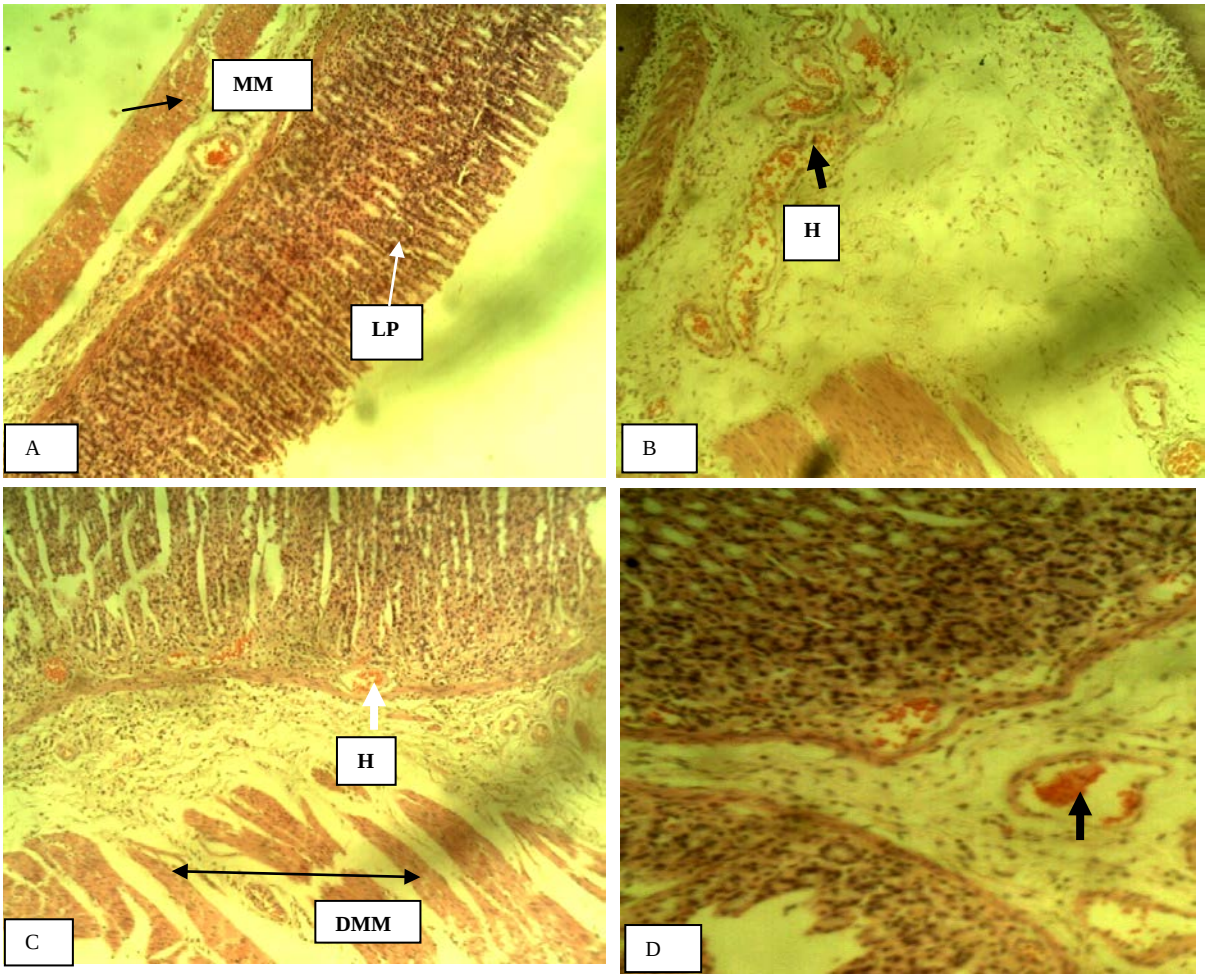

Plate 4. Photomicrograph of stomach of albino rats **A.** Normal group with intact stomach architecture characterized by muscularis mucosa (MM black arrow) and lamina propria (LP) (white arrow). **B**. 150mg/kg of ALETA with revealed hemorrhage (black arrow) mainly in blood vessels which occurred on the mucosal region of the stomach. **C:** 300mg/kg of ALETA with degenerated muscularis mucosa (DMM black arrow), minor hemorrhage (white arrow), blood vessel congestion and degeneration of the inner circular layer. **D**. 450 mg/kg of ALETA with revealed thickness of the muscularis mucosa, minor vascular congestion (black arrow) H&E. mag. 100X.

3.2. Effects of Terminaliacatappaon Haematological Parameters of animals

The haematological parameters PCV, RBC, HB, and WBC were affected by *T. catappa* treatment. The response of these parameters was mainly dose-dependent. The duration of treatment significantly affected RBC ($F = 8.149$, $p < 0.0001$). PCV was not different between the groups except on week 2 where PCV was significantly higher in 450mg/kg extract group compared to others. Hb concentration was similarly different between the groups. Those treated with 450mg/kg extract had the highest Hb level. WBC was not different between the groups and did not change significantly for the duration of treatment with *T. catappa* (Table 1). White blood cell differential to *T. catappa* responses are summarized in Table 2. No consistent response of neutrophil, eosinophil, and monocytes to the extract treatment was observed, irrespective of the concentrations used. Lymphocytes, however, appeared to increase in concentration with increasing doses of extract. The concentration of lymphocyte at 450mg/kg and 300mg/kg was significantly higher compared to control on weeks 2 and 3. The red blood cell derivatives, MCV, MCH, and MCHC responded minimally to *T. catappa* treatment. Overall, only MCV ($F = 3.857$, $p = 0.018$) and MCH ($F = 5.869$, $p = 0.003$) were significantly affected by the duration of treatment, while only MCH ($F = 3.232$, $p = 0.035$) was affected significantly by the extract. A significant increase in MCH relative to control, was observed on week 2 at 450mg/kg extract (Table 3).

Table 2. Haematological changes in animals treated with *Terminalia catappa*

Parameter	Concentration. (mg/kg)	Duration (week)			
		0	1	2	3
PCV(%)	Control	24.67±1.15^{a2}	26.67±1.53^{a2}	19.00±2.00^{b1}	27.66±2.52^{a2}
	150	24.33±5.51^{a1}	22.00±2.65^{a1}	21.66±3.51^{b1}	23.00±3.61^{a1}
	300	26.67±4.93^{a1}	27.67±2.89^{a1}	20.33±1.53^{b1}	22.33±4.73^{a1}
	450	27.33±6.11^{a1}	27.00±1.73^{a1}	31.66±2.52^{a1}	29.33±4.51^{a1}
RBC($X10^6$)	Control	118.0±7.55^{a1}	121.0±4.36^{a1}	104.6±15.5^{a1}	120.6±12.1^{a1}
	150	83.33±1.53^{b1}	120.6±9.6^{a2}	96.00±11.0^{a1}	84.00±5.57^{b1}
	300	97.00±7.00^{b1}	131.3±15.5^{a2}	98.33±5.51^{a1}	94.33±16.2^{b1}
	450	134.0±11.1^{a1}	124.3±6.81^{a1}	135.3±7.09^{b1}	131.3±7.02^{a1}
HB(g/dl)	Control	8.233±0.40^{ab2}	8.867±0.51^{a2}	6.333±0.65^{b1}	9.220±0.84^{ab2}
	150	8.100±1.82^{ab1}	7.333±0.91^{a1}	7.200±1.15^{a1}	6.566±0.81^{b1}
	300	7.000±0.30^{b12}	9.233±0.92^{a2}	6.767±0.50^{a1}	7.433±1.53^{b12}
	450	16.57±0.80^{a1}	8.967±0.58^{a1}	10.57±0.81^{a1}	11.20±1.55^{a1}
WBC ($\times10^3$)	Control	14733.33±2362.90^{a2}	11266.66±1040.83^{a2}	14766.66±750.56^{a2}	9800.00±1228.82^{a1}
	150	1400.00±3019.93^{a1}	14533.33±3744.77^{a1}	12633.33±1755.94^{a1}	14100.00±854.40^{a1}
	300	1340.00±3019.93^{a1}	12900.00±624.50^{a1}	12300.00±1228.82^{a1}	15000.00±4293.02^{a1}
	450	11666.66±378.60^{a1}	12166.66±4539.0^{a1}	13000.00±1900.00^{a1}	13800.00±1400.00^{a1}

Values as mean ± standard deviation. Values with different alphabet superscript along a column were significantly different, while values with different numeric superscript across a row were significantly different ($p < 0.05$).

Table 3. White blood cell differential (%) of animals treated with *Terminalia catappa* extract

Parameters	Conc. (mg/kg)	Duration (week)			
		0	1	2	3
Neutrophil	Control	66.67±3.79^{b3}	18.67±2.08^{a1}	43.00±4.00^{a2}	14.67±1.53^{ab1}
	150	71.67±4.73^{ab3}	23.00±2.00^{a1}	42.00±3.40^{a2}	22.67±4.04^{a1}
	300	71.67±3.79^{ab3}	18.33±2.08^{a12}	26.33±4.51^{b2}	16.00±5.30^{ab1}
	450	77.67±1.53^{a3}	19.67±4.62^{a2}	11.00±1.00^{c1}	11.00±1.00^{a1}
Eosinophil	Control	2.000±1.13^{a1}	1.333±0.58^{a1}	0.000±0.00^{b1}	1.667±1.53^{a1}
	150	1.667±0.58^{a1}	0.667±0,58^{a1}	0.000±0.00^{b1}	1.000±1.000^{a1}
	300	2.000±1.00^{a1}	1.00±1.00^{a1}	2.000±1.00^{a1}	0.667±1.15^{a1}
	450	0.00±0.00^{a1}	6.667±0.58^{a1}	0.000±0.00^{b1}	0.667±1.15^{a1}
Monocytes	Control	7.67±2.52^{a1}	6.667±2.53^{a1}	11.33±1.53^{ab1}	8.667±2.89^{a1}
	150	6.67±2.31^{a1}	6.000±2.65^{a1}	14.00±3.00^{a1}	11.000±4.36^{a1}
	300	7.00±2.00^{a1}	7.667±2.89^{a1}	7.000±2.00^{b1}	11.333±2.52^{a1}
	450	3.67±3.06^{a1}	6.000±1.73^{a1}	7.000±1.00^{b1}	7.333±1.53^{a1}
Lymphocytes	Control	23.00±4.00^{a1}	60.67±25.81^{a2}	45.67±3.21^{c12}	75.000±2.00^{ab2}
	150	20.00±2.00^{a1}	70.33±1.53^{a3}	44.00±1.73^{c2}	69.33±6.11^{b3}
	300	19.33±1.15^{a1}	73.000±1.00^{a2}	64.67±5.03^{b2}	72.00±4.60^{ab2}
	450	18.67±1.53^{a1}	73.67±6.66^{a2}	82.000±1.73^{a2}	81.00±0.00^{a2}

Values as mean ± standard deviation. Values with different alphabet superscript along a column were significantly different, while values with different numeric superscript across a row were significantly different ($p < 0.05$).

Table 4. Red blood cell derivatives of animals treated with *Terminalia catappa*

Parameter	Conc. (mg/kg)	Duration (week)			
		0	1	2	3
MCV (fl $cell^{-1}$)	Control	2.093±0.08^{a2}	2.20±0.06^{a2}	1.83±0.17^{b1}	2.29±0.02^{a2}
	150	2.919± 0.06^{a1}	1.84±0.33^{a1}	2.25±0.12a1	2.76±0.06^{a1}
	300	2.771±0.06^{a1}	2.11±0.50^{a1}	2.07±0.11^{ab1}	2.36±0.13^{a1}
	450	2.073±0.06^{a1}	2.17±0.16^{a1}	2.34±0.08^{b1}	2.23±0.30^{a1}
	Control	0.6985±0.03^{a2}	0.73±0.021^{a2}	0.61±0.06^{b1}	0.76±0.01^{a2}
MCH(pg $cell^{-1}$)	150	0.972±0.22^{a2}	0.61±0.011^{a1}	0.75±0.04^{a12}	0.78±0.05^{a12}
	300	0.723±0.03^{a12}	0.70±0.018^{a1}	0.69±0.03^{ab1}	0.78±0.04^{a2}
	450	0.789±0.02^{a1}	0.72±0053^{a1}	0.78±0.03^{a1}	0.86±0.16^{a1}
	Control	33.38±0.07^{a1}	33.25±0.07^{a1}	33.34±0.19^{a1}	33.32±0.01^{a1}
MCHC g/dl)	150	33.30±0.07^{a1}	33.32±0.16^{a1}	33.24±0.08^{a1}	29.26±7.06^{a1}
	300	26.95±5.71^{a1}	33.38±0.01^{a1}	33.28±0.19^{a1}	33.31±0.23^{a1}
	450	40.35±11.4^{a1}	33.21±0.01^{a1}	33.37±0.12^{a1}	39.05±10.18^{a1}

Values as mean ± standard deviation. Values with different alphabet superscript along a column were significantly different, while values with different numeric superscript across a row were significantly different ($p < 0.05$).

3.3. Effects of Terminalia catappa on Biochemicalparameters of animals

The changes in the liver enzyme of albino rats exposed to ALETA are shown in Table 5. The level of AST, ALT, ALP, and ACP in the ALETA exposed rats did not differ significantly ($p>0.05$) at the end of the experiment. Overall, all the biochemical parameters investigated were not affected significantly by the extract.

Table 5. Changes in the liver enzymes of animals treated with *Terminalia catappa*

Parameter	Conc. (mg/kg)	Duration (week) 1	2	3
AST (U/L)	Control	43.67 ±4.16^{c1}	36.67±1.16^{b1}	39.00±3.00^{a1}
	150	71.33±3.51^{a1}	70.67±3.06^{a1}	73.00±10.58^{a1}
	300	60.00±6.25^{b1}	76.33±11.15^{a1}	72.67±6.11^{a1}
	450	63.33±2.89^{ab1}	74.67±6.03^{a1}	62.33±7.37^{a1}
ALT (U/L)	Control	42.00±3.61^{b1}	42.67±9.29^{b1}	41.67±5.51^{a1}
	150	60.67±5,86^{a1}	61.00±3.61^{ab1}	61.33±9.45^{a1}
	300	75.67±6.03^{a1}	72.00±9.64^{a1}	59.67±6.11^{a1}
	450	61.00±10.15^{a1}	49.33±5.69^{b1}	65.33±15.18^{a1}
ACP (U/L)	Control	20.59±0.72^{a1}	22.99±0.64^{a1}	23.36±2.68^{a1}
	150	24.28±1.66^{a1}	30.64±4.87^{a1}	24.43±3.33^{a1}
	300	24.00±3.04^{a1}	28.42±0.82^{a1}	24.54±2.07^{a1}
	450	21.29±1.12^{a1}	25.75±3.15^{a1}	27.68±3.17^{a1}
ALP (U/L)	Control	24.31±18.15^{a1}	38.28±1.54^{b1}	33.73±2.08^{a1}
	150	40.44±7.69^{a1}	43.22±4.64^{a1}	36.63±5.08^{a1}
	300	37.08±1.90^{a1}	45.21±4.66^{a2}	33.54±1,15^{a1}
	450	37.76±4.14^{a1}	33.01±2.39^{b1}	35.65±2.16 ^{a1}

Values as mean ± standard deviation. Values with different alphabet superscript along a column were significantly different, while values with different numeric superscript across a row were significantly different ($p < 0.05$).

4. Discussion

Physiological and nutritional observations (Azrul *et al*., 2013) have shown that *Terminalia catappa* has the potential to induce primary toxicity in rats. The phytochemical constituents (alkaloids, flavonoids etc.) of the ALETA reported in the current study are in consonance with those observed by previous investigators (Divya et al, 2018, Divya and Vijya-Anand, 2014). The histopathology alterations in the liver against highest dosage of ALETA presented minor clear liver alterations such as Kupfer cell hyperplasia, cytoplasmic vacuolation, necrosis, and sinusoid enlargement. However, the observations in the kidney suggested that ALETA had a renal protective ability to prevent kidney dysfunction by accelerating regeneration. Alade *et al* (2009) opined that 4g/kg *Baulinia monandra* leaf extract caused focal prominent tubular epithelial necrosis in the kidney. Further studies reported widened glomeruli of the kidney exposed to 1000mg/kg *Cassia fistula*. This coincided with the changes in the kidney of rats exposed to 150, 300, and 450mg/kg ALETA observed with shrinkage of glomeruli, discrete clear or translucent space associated with vacuolations was reported in the present study. No damage was observed in the heart histology. This was due to possible cardioprotective potentials of ALETA administered between 150 to 450mg/kg in the study. Observed vascular and minor lesions, in the fundic stomach of albino rats exposed to different dosages of the ALETA, were due to intoxication of the extracts.

Blood parameters are used to ascertain the physiological effects of foreign compounds, including medicinal plants. The current study revealed significant activity of the plant extract on RBC, PCV, HB, N, E, M, L, MCH, and MCHC, does not affect erythropoiesis and osmotic fragility of the red blood cells. The white blood cells (WBC) are the first line of defense which responds to infectious agents, inflammatory process, or tissue injury. The increased WBC level in the blood cells of wistar rats observed in the current study was due to stimulation of production of leucocytes by *Terminalia catappa* as immune booster. On the contrary, Ezekiel et al, (2019) reported decreased WBC level in wistar rats exposed to *Termialia catappa* leaf extract. More so, there were no significant changes observed in the neutrophils, lymphocytes, and monocytes in *Terminalia catappa* leaf extract-treated animals. The Hb levels made *T. catappa* a positive herb for blood building. 450mg/kg *T catappa* decreased packed cell volume and erythrocyte count in albino rats (Ezekiel et al, 2019, Aimola et al, 2011). No significant change in the PCV was observed in*T.catappa* decoctions administered albino rats (Ibegbulem et al 2011). The increased MCHC values have been reported to be one of the conditions that precipitated disease conditions such as sickling Ibegbulem et al (2011). Erythrocytes derivatives were not altered after administration of *T. catappa* to albino rats (Ezekiel et al, 2019).

Liver enzymes are consistently utilized as an index of liver diagnosis, investigation of disease, and safety assessment of herbal plants (Madu and Nadro, 2017). The ALETA dosages caused liver damage with increased AST and ALT concentrations in the serum. *Terminalia catappa* plant extracts affected the level of aminotransferase enzymes (AST and ALT) in the serum supported by the limited degree of altered liver enzyme which indicated amelioration of hepatotoxic in the animal (Lin, 1997). Meanwhile, a two to four folds increase of liver enzymes raised concerns as an indication of potential hepatic injury Arjariya et al, (2013). The mechanism of action of the plant extracts prevented the intracellular release of enzyme and its membrane. Arjariya et al (2013) reported that the transaminases (AST and ALT) are well-known enzymes used as biomarkers predicting possible liver toxicity. This coincided with our present findings of elevated liver enzymes AST, ALT, ACP, ALP on chronic ingestion of ALETA. These observations may indicate that chronic ingestion of ALETA may result in potential hepatic injury/or compromised liver function.

5. Conclusion

The aqueous leaf extract of *Termialia catappa* has shown a significant effect on the tissues in the major body organs of rats that were investigated, with no toxicological effects observed in the heart of the animal. Therefore, the use of *Terminalia catappa* leaf as prophylaxis, nutriment, anti-inflammatory, etc., should be adopted with caution if

it must be used, and serious review on the administration must be emphasized.

Acknowledgment

We acknowledge the Department of Zoology and Environmental Biology for their assistance in providing laboratory work space.

Authors Contributions

Chika B. Ikele (CBI). Designed the experiment, supervised the research, conducted and monitored the experiment, interpreted histological tissues, and proofread the manuscript. Elijah Okwuonu(EO), analyzed the research data. Nnachi A. Ijem (NAI) proofread the manuscript.

Data Availability

Research Data are not shared.

Conflict of interest

The authors declare no conflict of interests.

References

Ahmed SM, Vrushabendra SBM, Gopkumar RD and Chandrashekara VM. 2005. Anti-diabetic activity of *Terminalia catappa*Lin- leaf extracts in alloxan-induced diabetic rats. Iranian *J Pharm Therap*, **4**(1):36-39.http://ijpt.iums.ac.ir

Aimola S, Inuwa H, Mamman A, Habila N, Agbaji A and Omoniwa D. 2011. *Terminalia catappa* extract enhances erythropoiesis in adult Balb C Mice. *JMol Bio Res*, **1** : 40-46. Doi :10.5539/jmbr.v1n1p40

Akilandeswari S, Senthamarai R, Valarmarthi R, Shanthi S and Prema S. 2010. Screening of gastric antiulcer activity of *Sidaacuta* burm. *Int J Pharmtech Res*, **2**:1644-1648.

AladeGO, Akanmu MA, Obuotor EM, Osasan SA and Omobuwajo AN. 2009. Acute and oral subacute toxicity of methanolic extract of *Bauhinia monandra* leaf in rats. *Afri JPharm Pharmacol*,**3**: 354-358.

http://www.academicjournals.org/ajpp
Alka D. Raman D. and Yogesh KS. 2016. Exploration of phytochemicals found in *Terminalia sp* and their antiretroviral activities. PHARMACOGREV, **10**: 73-83. Doi:10.4103/0973-7847.194048

Anand AV, Natarajan DP and Kotti PP. 2014. An updated review of *Terminalia catappa*PHARMACOGREV, **9**: 93 – 98. Doi:10.4103/0973-7847.162103.

Arjariya S, Nema N and Tiwari S. 2013. Investigate the toxicological effect on aqueous extract of *Terminalia catappa*Lin in rat. *Int J Res Dev Pharm Life Sci*,**2**: 596 – 601.

Azrul LM, Adeemi MA, Ahmad WM and Effendy AW. 2013. Determination of toxicological effects of *Termianliacatappa*leaf on Sprague-Dawley white rats in short period. *IntJ Toxicol Applied Pharmacol*, **3**: 44 – 47.

Babson AL and Read AP. 1959. A colorimetric method for the determination of acidphosphatase enzyme. *Am J ClinPath*, 32: 89 – 91

Bergmeyer HU. 1974. **Methods of Enzymatic Analysis**, 2nd edition. Academic Press, New York.

Biswas M, Kar B, Bhattachyra S, Suresh-Kumar RB, Ghosh AK, Haldar PK. 2011. Antihyperglycemic activity and antioxidant role of *Terminalia arjuna* leaf in streptozotocin-induced diabetic rats. Pharma Biol, **49:** 335-340.
https://doi.org/10.3109/13880209.2010.515755

Chu SC, Yang SF, Liu SJ, Kuw WH, Chang YZ and Hsei YS. 2007. Invitro and in vivo antimetastatic effects of *Terminalia catappa* L. leaf on lung cells. Food Chem Toxicol, **45**:1197-1201. Doi:10.1016/j.fct.2006.12.028

Divya N and Vijya-Anand A. 2014. Phytochemical investigation and in vitro anti-diabetic activity of *Terminalia catappa*leaf. Int J Phyto Pharm, **4**:132-134.

Divya N, Rengarajan, RL, Ramalingam, Elsayed, FA, Abdulaziz, AA, Abeer H, Manikandan R and Vijaya-Anand, A. 2018. Phytotherapeutic efficacy of the medicinal plant *Terminaliacatappa* L. Saudi J Biol Sci, 26: 985-988.. https:doi.org/10.1016/j.sjbs.2018.12.010

Ezekiel EB, Esther OAand Asuquo EA. 2019. Changes in heamatological parameters and possible adverse reactions of *Terminalia catappa*leaf extract in wister rats. *J Nurs Health Sci*, **8**:80-86. www.iosrjournals.org.

Ibegbulem CO, Eyong EU. and Essien ET. (2011). Biochemical effects of drinking *Terminalia catappa*Lin. decoction in Wistar rats *Afri J Biochem Res***5**: 237 – 243.

Kinoshita S and Aniya Y. 2007. Antioxidant and hepatoprotective actions of medicinal herb, *Terminalia catappa* L. from Okinawa Island and its tannin corilagin, *Phytomedi*, **14**: 755-762. Doi.org/10.1016/j.phymed.2006.12.012.

Koffi N, Bra Yvette F and Noel Z. 2011. Effect of aqueous extract of *Terminalia catappa*leaf on the glycaemia of rabbits. *J Appl Pharmaceutical Sci*; **1**: 59 – 64. www.japsonline.com

Krishnaveni M. 2014. In vitro antioxidant activity of *Terminalia catappa* nuts. *Asian J Pharmaceutic Clin Res*, 7(4): 33-35.

Kumar V, Sharma N, Sourirajan A, Khosla KP and Dev K. 2018. Comparative evaluation of antimicrobial and antioxidant potential of ethanolic extract and its fraction of bark and leaf of *Terminalia arjuna* from North-Western Himalayas India. *J Trad Compl Med*, **8**: 100-106. Doi:10.24896/eijppr.2016615

Lee CJ, Yang SF, Wang PH, Su CW, Hsu HF, Tsai, HT et al. 2019. Antimetastatic effects of *Terminalia catappa* leaf extracts on cervical cancer through the inhibitation of matrix metalloprotein-9 and MAPK pathway. *Environ Toxicolo***34**:60-66.https://doi.org/10.1002/tox.22657

Lin C, Chen Y, Lin J and Ujiie T. 1997. "Evaluation of the Antioxidant and Hepatoprotective Activity of *Terminalia catappa*," *Am J Chinese Med*, 25:53-161. doi:10.1142/S0192415X97000172

Lorke D. 1983. A new approach to practical acute toxicity testing. *ArchToxicolo*, **54**: 275–287.

Madu JO and Nadro M. 2017. Evaluation of the Toxicological effects of *Senecio aureus* extract on the liver and hematological parameters in wistar rats. Jordan J Bio Sci, **10:** 29-32

Mccloud TG. 2010. High throughput extraction of plant, marine and fungal specimens for preservation of biologically active molecules. *Molecules*, **15**:4526– 4563.
doi:10.3390/molecules15074526.

Mohale DS, Dewani AP, Chandewar AV, Khadse CD, Tripathi ASand AgrawalSS. 2009. Brief review on medicinal potentials of *Terminalia catappa*. *J Herb Med Toxicol*,**3**: 7 – 11.ISSN:0973-4643

Mudi S and Muhammed A. 2009. Antimalaria activity of ethanolic extracts of leaf of *Terminalia catappa* L. combretaceae (Indian almond). *Bayero J Pure Appl Sci*, **2**: 14-18.

Nagappa AN, Thakurdesai NV, Raob JS. 2003. Antidiabetic activity of *Terminalia catappa*Lin fruits. J Ethnopharmacol , **88:**45-50

Odugbemi T. 2008. **A Text Book of Medicinal Plant From Nigeria**. University of Lagos Press, Yaba, Lagos.

Raj K, Mandeedn S, Nitesh G, Manoj K, Indu B and Shailendra NG. 2013. Prevalence of food intolerance in bronchial asthma in India. *India J Allergy, Asthma Immunolo*, **27**: 121-128. Doi:10.4103/0972-6691.124394

Ratnasooriya WD and Dharmasiri MG. 2000. Effects of *Terminalia catappa* seeds on sexual behavior and fertility of male rats. *Asian J Adrology*, 2(3):213 –219.doi:

Reitman S and Frankel S. 1957. A colorimetric method for the determination of serum glutamic oxaloacetic and glutamic transaminases. *Am J Clin Path*, **28**: 56 - 63.

Shanehbandi D, Zariedar H, Asadi M et al. 2019. Anti cancer impacts of *Terminalia catappa* extract on SN 480 Colorectal Neoplasm cell line. *J Gastrointes Cancer*, 10: 1-7.doi:10.1007/s12029-019-00349-z.

Trease G and Evans SM. 2002. **Pharmacognosy** 15th ed. London. Bailer Tindal. Pp23-67.

Venkatalakshmi P and Brindha P. 2016. Antimicrobial activity of aqueous extracts of different parts of *Terminalia catappa* L. *Int. J. Curr. Microbiol App. Sci*, 5(12): 493-498.

WHO (1998). Regulatory situation of herbal medicines a Worldwide Review. http;//www.who.int/medicineddocs/. Accessed, 20th April, 2020.

Wintrobe, P. K. (1967). **Clinical Haematology**. Williams and Wilkins, Lippincott

World Health Organization Dept. of Essential Drugs and medicine policy (2004). WHO guideline on safety monitoring of herbal medicines in pharmacovigilance systems, Geneva; WHO publishers, P18. http://www.who.int/iris/handle/10665/43034. Accessed 24th October, 2019

Yang SF, Cha MK, Hseih YS, Yang JS, Zauras AI and Hsei YH. (2010). Antimetastatic effects of *Terminalia catappa* L. on oral cancer via a donor regulation of metastasis-associated proteases. *Food Chem Toxicol*, 48(4):1052-1058. Doi:10.1016/j.fct.2010.01.019

JJBS

Volume 14, Number 5 ,December 2021
ISSN 1995-6673
Pages 899 – 903

Jordan Journal of Biological Sciences

Green Synthesis of Silver Nanoparticles using Neem and Collagen of Fish Scales as a Reducing and Stabilizer Agents

Mustafa Mudhafar[1,2,*] , Ismail Zainol[2], H.A. Alsailawi[1] and C. N. Aiza Jaafar[3]

[1]*Department of Anesthesia and Intensive Care Techniques, Faculty of AL, Tuff Collage, Karbala, 56001, Iraq*

[2]*Department of Chemistry, Faculty of Science and Mathematics, Universiti Pendidikan Sultan Idris, Proton City, 35900 Tanjung Malim, Perak, Malaysia,*[3]*Department of Mechanical and Manufacturing Engineering, Faculty of Engineering, Universiti Putra Malaysia, 43000 Serdang Selangor, Malaysia.* [4]*Department of Biology, Faculty of Science and Mathematics, Universiti Pendidikan Sultan Idris, Proton City, 35900 Tanjung Malim, Perak, Malaysia.*

Received: March 16, 2020; Revised: Dec 2, 2020; Accepted: Dec 21, 2020

Abstract

This study was conducted to synthesize and characterize silver nanoparticles (AgNPs) using a rapid green synthesis approach. Antibacterial properties of AgNPs were evaluated. Extract of Melia Dubia (Neem) and collagen produced from the fish scales were used as reducing and stabilizer agents respectively. Uv-Vis Spectroscopy, Scanning Electron Microscopy (SEM), Energy-Dispersive X-Ray Spectroscopy (EDX), Fourier-Transform Infrared Spectroscopy (FTIR), and Dynamic Light Scattering (DLS) were used to characterize the synthesized AgNPs. Evaluation of the synthesized AgNP's antibacterial activity was conducted, with Staphylococcus Aureus (S. aureus) as Gram-positive and Escherichia Coli (E. coli) as the negative bacteria. The peak of absorbance for the synthesized AgNPs was at 454 nm, indicating conformed AgNPs. SEM image showed semi-evenly distributed rod shapes. The EDX data revealed presence of the metallic silver. Meanwhile, FTIR analysis indicated presence of C2H2, C=O, N-H groups. DLS showed an average size of 437.6 nm. XRD showed calculation for particle size using $d = K\lambda/\beta\cos\theta$. Average size of AgNPs was 141.81 ± 5 nm. AgNPs also displayed tangible antibacterial activity towards the S. aureus and pathogenic E. coli. AgNPS were successfully synthesized and evaluated for their antibacterial properties. The outcomes being the multifaceted biological activities alongside application of biocompatible green nanoparticles, is discoverable in the field of Nanomedicine.

Keywords: Silver nanoparticles, Fish Scales Collagen (FsCol), Melia Dubia (neem), Antibacterial

1. Introduction

AgNPs are common nanoparticles, vastly used in cleaning agents, commercial industry, food storage, healthcare products, packing and textile coating. Their antimicrobial property against bacteria, fungi, and viruses, makes them suitable for several environmental applications besides being used extensively in products specific to biomedical purposes such as topical creams, antiseptic sprays, and wound dressings. This is due to their capability in disabling a microorganism's enzymatic activities by disrupting the membrane of the pathogenic organisms (Haghighi et al., 2017; Pugazhendhi et al., 2018).

Many techniques were introduced to synthesise AgNPs, such as thermal decomposition, chemical reduction of silver ions (Ag+), pyrolysis microwave irradiation, electrochemical methods, and laser ablations (Beyene et al., 2017; Sundarrajan et al.,2019). Among all, the most traditional way to synthesize AgNPs is via chemical reduction technique. The agents commonly used lessen the chemical are sodium borohydride and sodium citrate (Ojo et al., 2017). Traditional chemical synthesis stipulates the necessity to have metal precursor, reducing agents and capping/stabilizing agents to prevent vigorous spreading of the nanoparticles (Chowdhury et al., 2015). The traditional ways are claimed to be more effective in controlling distribution and reproducibility of the nanoparticle size as they require greater input of energy alongside presence of toxic chemicals. Under certain circumstances, it may require occurrence of controlled pressure and temperature. This may lead to higher cost and environmental contamination.

"Green chemistry" was introduced as an economically feasible option and is known to be a biogenic way to synthesize metallic nanoparticles and AgNPs (Ahmed et al., 2019). This approach is known to be a biogenic synthesis of the metallic nanoparticles. This approach is reputable for its simplicity, environmental-friendliness, cost-effectiveness and scale-up efficiency. The procedure is carried out at room temperature and pressure, within aqueous ambiance, without organic solvents (Sportelli et al., 2018). It is also conducted via biological systems, which includes algae, bacteria, plants, fungi, diatoms, and yeast. The simplicity of the biogenic way made it possible for plant extracts to be used to eradicate the procedure of sustaining cell cultures. Metallic nanoparticles that are based on plant-mediated synthesis are also less biohazardous (Mudhafar et al., 2020).

Recently, plant extracts have gained much interest. They are commonly used as agents to reduce and cap

* Corresponding author e-mail: Almosawy2014@gmail.com.

metallic nanoparticles mainly due to their advantageous potentials which include fast, simple, economically feasible green technique, and environmentally-friendly nature (Ajitha et al., 2016). The phytochemicals of the plants play the role of tough reducing agent, resulting in development of capped nanoparticles. This signifies that plant extract is a one-step natural capping and reducing agent, reducing not just the cost but the use of chemical reagents too (Govindarajan et al., 2017). In addition, chemical compounds are replaced with phytochemicals' surroundings, while organic solvents are replaced by aqueous surroundings (Jyoti et al., 2016). Today, distinct parts of plants, like its fruits, bran, bark, flowers, and leaf, are used in metallic nanoparticle synthesis (Shaik et al., 2018) as they possess medicinal value attributed to presence of amino acids, phenolic compounds, such as polyphenols, flavonoids, terpenoids, and vitamins (Mudhafar et al., 2019).

Neem is a part of the Melia genes belonging to the Meliaceae family. It is greatly distributed in India and Malaysia. The Indian neem have been extracted and used to produce nano-silver, showing good result when AgNO3 was used for anticancer activity. Kathiravan et al., (2014), have synthesized the AgNPs for anticancer. However, there has yet to be any report of AgNPs synthesis from neem leaves and its antimicrobial activity from neem extract.

Collagen is a known biocompatible polymer that is water-soluble, and synthetic, evidenced by its broad use for biomedical purposes. Among such purpose includes the use of nanoparticles' coating to enhance spreading of nanoparticles in an aqueous medium and their penetration into the mucus layer. Furthermore, collagen can guard nanoparticle against immune system clearance by avoiding the opsonization of nanoparticle in the blood, lessening the toxicity of nanoparticles, and increasing the lifetime of the nanomaterial within the circulation system (Sawadkar et al., 2019; Mudhafar et al., 2020). Additionally, collagen can also be used as a stabilizing agent (Tarannum et al., 2015). For the purpose of this study, Fish Collagen was used as safe stabilizing agent for AgNPs.

The AgNPs' biogenic synthesis was studied with the one-pot green protocol because of its advantageous traits. Meanwhile, the reducing agent used was from neem extracts. To enhance the capability of the green neem that synthesized the AgNPs, the nanoparticles were stabilized with collagen. Different analytical methods were conducted to characterize the AgNPs. The classification of the AgNPs' infusion of antimicrobial activity towards a few Gram-positive and Gram-negative pathogenic bacterial strain was conducted based on vitro evaluation. Outcome from a simple green protocol revealed that the commercial green neem extract led to successful development of plant-mediated AgNPs. Furthermore, the nanoparticles' antibacterial activity against varying strains of bacteria was shown at concentration. These support outcomes from the previous study, where biosynthesis of nanometals had strong antibacterial effects.

2. Materials and methods

2.1. Materials

$AgNO_3$ was obtained from Bendosen Company. Neem leaves were sourced locally from Perak, Malaysia. Collagen was extracted from fish scales and were produced in the Chemistry Department laboratory, UPSI, Perak, Malaysia. The broth and nutrient agar were bought from Merck.

2.2. Methods

2.2.1. Neem leaf preparation

Fresh neem leaves were collected from Perak. The leaves were cleaned several times to eradicate dust and fungi after which it was sun-dried for one week to completely remove moisture. The dried neem leaves were then crushed and converted to powder form. A total of 10g powder was extracted with 100 ml distilled water in a 250 ml conical flask. Subsequently, the powder was heated for 10 minutes, cooled and filtered to obtain a crude extract before being incubated at 4 °C.

2.2.2. Green synthesis of AgNPs

1 mM of $AgNO_3$ was dissolved in 90 ml distilled water and the solution formed was transferred into a 250ml conical flask. 10 ml of crude extract was then added into the conical flask and stirred thoroughly. Then, 0.1g of collagen was added into the conical flask and the mixture was again stirred thoroughly. UV-Vs Spectroscopy was then utilized to analyses development of AgNPs. The solution containing AgNPs was centrifuged for 10 minutes at a rate of 14000 rpm. Meanwhile, the supernatants were discarded, and the NP portion was sterilized in distilled water. This aforementioned step was repeated three times to eradicate unused biomaterial and impurity. The freeze-drying method was used to obtain dry particles for the purified sample of dry particles (Joseph et al., 2015).

2.2.3. Characterization of AgNPs

Absorbance between 200nm and 800 nm was conducted using the UV–Vis Spectroscopy Agilent Cary 60 UV Spectrophotometer. EDX, SEM, and DLS were performed respectively via Bruker X Flash 6110, Nova Nanosem 450.

2.2.4. Antibacterial activity

Paper disk diffusion test was employed to investigate antibacterial activities of *E. coli* and *S. aureus*. Nutrient agar media was used to cultivate bacteria. 10 µg of AgNPs was saturated in 1 ml of distilled water and tested against the bacteria. Neem were also examined. Next, a total of 10, 20, 40, and 80 µM/ml of AgNPs were dissolved in distilled water and poured onto a 6 mm disk filter [24]. Upon 24 hours incubation, inhibited zones were measured and the magnitude of antibacterial impacts on *S. aureus* and the *E. coli* were determined.

3. Results and Discussion

3.1. UV–Vis Spectroscopy

UV–Vis Spectroscopy was used to corroborate stability and development of AgNPs in a solution. Figure 1 displays the extinction spectra of AgNPs. As observed, the

absorption band of synthesized AgNPs was 454 nm. Many studies have documented absorbance of AgNPs, whereby peak of surface plasmon for AgNPs sized <100 nm was located between 400–450 nm (Rathod et al., 2016).

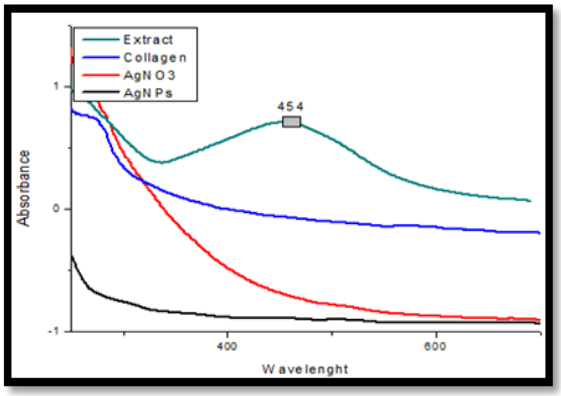

Figure 1. UV-Vis Spectroscopy of AgNPs , $AgNO_3$ and FsCol

3.2. SEM

SEM was utilised to classify the parts of synthesized AgNPs. SEM's image displays the AgNPs' constant spreading. It was discovered that the AgNPs had a rod-like shape with smooth morphology, almost the same shape as the AgNPs when using a microwave. Figure 2 displays SEM image such as that of the prepared powdered AgNPs. The magnification specification for SEM image was 100000x for 500 nm image size, which is a considerably big for AgNPs. Especially since the formation of AgNPs were considerably shorter compared to that mentioned in literature; that the size of the Silver Nanoparticles will decrease with increased formation time (Dehnavi et al., 2013).

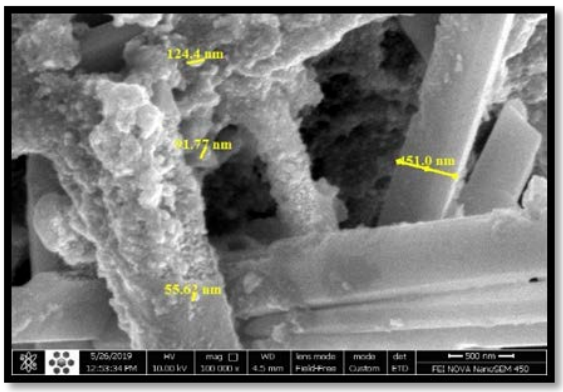

Figure 2. SEM for the morphology and measured of AgNPs

3.3. FTIR

FTIR was used to evaluate factional groups of fish collagen and neem leaves in comparison with factional groups of synthesized AgNPs. This is to gain insight on factional groups surrounding the silver nanoparticles. As shown in Figure 4, the FsCol reveals two major peaks, which are 3441 cm-1 for the NH (amide A) and 1646 cm-1 for CO stretching (amide I) (Hamidi et al., 2019). Peaks of the four miners were monitored at 1548 cm-1, 1466 cm-1, 1392 cm-1, and 1242 cm-1. 1548 cm-1-1466 cm-1 refers to the N-H bend coupled with C-N stretch (Amide II), and 1392 -1242 cm-1 refers to the N-H bending (Amide III) [23]. Neem leaves were characterized with two major peaks located at 3296 cm-1 and 1629 cm-1. The peak at 3296 cm-1 refers to the stretch of N–H and O–H due to the presence of water, alcohols, and phenols (polyphenols) in neem extract (Philip, 2010). Amide I was observed at 1629 cm-1, while miner peaks were observed at 2115 cm-1, 618 cm-1, 480 cm-1, and 333 cm-1. At 2115 cm-1, the bands appeared parallel to the present Alkyne group (C2H2) because of neem extract phytoconstituents (Mudhafar et al., 2019). At 618 cm-1, the band matched the C-H bonds in the phenolic rings while the band at 480 cm-1 were attributed to the existence of alkyl halides.

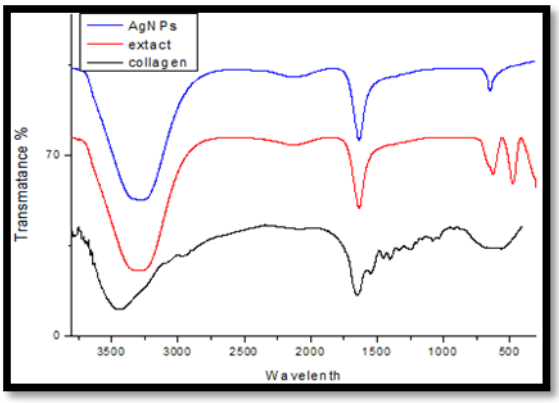

Figure 3. FTIR spectrum of FsCol, *M. Dubia*, and AgNPs

Among AgNPs, two major peaks were observed in the FTIR graph; 3315 cm-1 and 1641 cm-1. At 3315 cm-1, the band is referring to the stretch of O-H and N–H (amide A), while at 1641 cm-1, the band refers to the similar stretching of CO that belonging to amide I. Both these bands were observed in the fish collagen and neem extract. The band located at 2128 cm-1, refers to alkyne group (C_2H_2) from the neem extract phytoconstituents. At 1361 cm-1, the band corresponds to N-H bending (Amide III) from fish collagen. Two peaks at 608 cm-1 and 689 cm-1 indicates C-H bonds in phenolic rings. Table 1 shows all details for AgNPs, plant extract and FsCol (Singh et al., 2016: Mudhafar et al., 2021).

Table 1: Factional groups in AgNPs in FTIR

Factional groups	Wavenumber cm^{-1}		
	FsCOL	Plant extract	AgNPs
N-H (stretch)	3446 cm^{-1}	3296 cm^{-1}	3301 cm^{-1}
Alkyne group (C_2H_2)	--	2115 cm^{-1}	2140 cm^{-1}
C=O Stretching (amide I)	1646 cm^{-1}	1629 cm^{-1}	1668 cm^{-1}
N-H bends couple C-N stretch (Amide II) CN	1531 cm^{-1}		--
Amide III N-H bend	1348 cm^{-1}		1366 cm^{-1}
Amide III N-H bend	1242 cm^{-1}		1227 cm^{-1}
O-H	--	618 cm^{-1}	634 cm^{-1}
Alkyl halides	--	480 cm^{-1}	488 cm^{-1}

3.4. DLS

Zeta sizer shows the peak of AgNPs. Based on the pattern, the AgNPs synthesized through this technique had shown a 0.249 polydispersity index (PDI) with a Zeta average diameter of 437.6 nm. The size of the zeta sizer measures is slightly bigger than the size of the particle as measured in SEM micrographs due to DLS method which measures the hydrodynamic radius (Ahmed et al., 2017). In addition, DLS also measures attached surface proteins,

carbohydrates, and other cellular materials. However, they could not be kept in a vacuum under an electron beam as it can also be associated with the consistency of biosynthesis (Liu et al., 2019). The DLS graph of synthesized AgNPs showed two peaks, a strong peak at 480.7 nm with 98% intensity area and a weak peak at 5256 nm with 2% intensity area. Meanwhile, the Zeta average diameter was 437.6 nm, as shown in Figure 5.

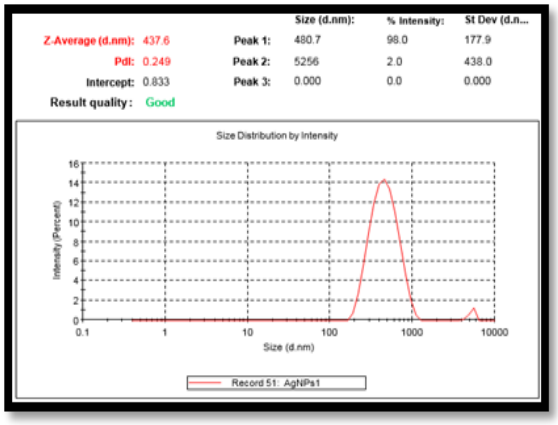

Figure 4. DLS analyses of AgNPs

3.5. Antibacterial activities

The AgNPs' antibacterial properties were recorded according to disk diffusion method. A ruler was used to measure the AgNPs' ability to prevent bacterial growth against both bacteria (Anandalakshmi et al., 2016). Distilled water was used for negative control, while ampicillin was used and tested against bacteria for positive control. Figure 5 shows the inhibition zones of *E. coli* and *S. aureus* bacteria. The distilled water inhibition appeared zero in both bacteria. The inhibition zones of the extract were 12.2 and 10.4 mm, in contrast to *E. coli* and *S. aureus*, respectively. The inhibition zones of ampicillin were 28.6 for *E. coli* and 22.1 for *S. aureus*. Many AgNPs' concentrations resulted in good inhibition zones against both bacteria. The inhibition zone increased with AgNPs concentration. Table 2 shows details of AgNPs inhibition and control.

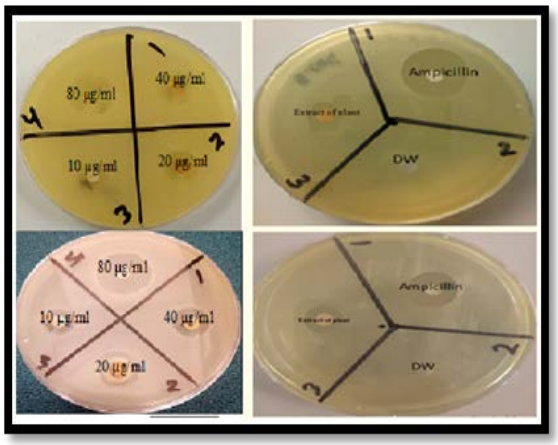

Figure 5. Antibacterial activities of A) AgNPs and control samples against *E. Coli* and B) AgNPs against *S. Aureus*

4. Conclusions

The characteristics of biosynthesis methods, such as safety, low cost, and environmental friendliness are deemed attractive by researchers. Green synthesis method was employed in this study to synthesize AgNPs from biological sources. Neem leaves were utilized as natural source. The use of UV–vis, FTIR, SEM, EDX, and DLS resulted in successful synthesis and categorization of AgNPs. The morphology and particle size were also investigated. These techniques revealed a rod shape with average sizes ranging from 150 nm to 430 nm. The antimicrobial characteristics of the synthesized AgNPs were also examined using the Gram-positive and Gram-negative bacteria. To which it was discovered that AgNPs was highly efficient as an agent for microbes and has great potential for use as antibacterial agent within the medical field.

Acknowledgement

This study was partially supported by grant no. FRGS 2019-0147-103-02

References

Ahmed, S., Ahmad, M., Swami, B. L., & Ikram, S. 2016. A review on plants extract mediated synthesis of silver nanoparticles for antimicrobial applications: a green expertise. *J adv Res*, ***7*(1):** 17-28.

Ahmed, S., Saifullah, Ahmad, M., Swami, B. L., & Ikram, S. 2016. Green synthesis of silver nanoparticles using Azadirachta indica aqueous leaf extract. *J Rad Res appl Sci*, ***9*(1)**: 1-7.

Ajitha, B., Reddy, Y. A. K., Reddy, P. S., Jeon, H. J., & Ahn, C. W. 2016. Role of capping agents in controlling silver nanoparticles size, antibacterial activity and potential application as optical hydrogen peroxide sensor. *RSC advances*, ***6*(42)**: 36171-36179.

Anandalakshmi, K., Venugobal, J., & Ramasamy, V. 2016. Characterization of silver nanoparticles by green synthesis method using Pedalium murex leaf extract and their antibacterial activity. *Appl Nanosci*, ***6*(3):** 399-408.

Beyene, H. D., Werkneh, A. A., Bezabh, H. K., & Ambaye, T. G. 2017. Synthesis paradigm and applications of silver nanoparticles (AgNPs), a review. *Sust Mat Technol*, ***13*:** 18-23.

Chowdhury, S., Yusof, F., Sulaiman, N., & Faruck, M. O. 2017. The Aggregation Study and Characterization of Silver Nanoparticles. *Solid State Phen*, **263:**165-169.

Dehnavi, A. S., Raisi, A., & Aroujalian, A. 2013. Control size and stability of colloidal silver nanoparticles with antibacterial activity prepared by a green synthesis method. *Synthesis and Reactivity in Inorganic, Metal-Organic, and Nano-Metal Chemistry*, ***43*(5)**: 543-551.

Govindarajan, M., Kadaikunnan, S., Alharbi, N. S., & Benelli, G. 2017. Single-step biological fabrication of colloidal silver nanoparticles using Hugonia mystax: larvicidal potential against Zika virus, dengue, and malaria vector mosquitoes. *Arti Cells, Nanomedicine, and biotechnol*, ***45*(7):** 1317-1325.

Haghighi Pak, Z., Karimi, N., & Abbaspour, H. 2017. Effects of Silver Nanoparticle Exposure on Growth, Physiological and biochemical Parameters of Dracocephalum moldavica L. *Plant Phys*, ***7*(4):** 2173-2183.

Hamidi, A., Yazdi, M. E. T., Amiri, M. S., Hosseini, H. A., & Darroudi, M. 2019. Biological synthesis of silver nanoparticles in Tribulus terrestris L. extract and evaluation of their photocatalyst, antibacterial, and cytotoxicity effects. *Res Chem Intermid*, ***45*(5)**: 2915-2925.

Joseph, S., & Mathew, B. 2015. Facile synthesis of silver nanoparticles and their application in dye degradation. *Mat Sci Eng, B*, ***195***: 90-97.

Jyoti, K., Baunthiyal, M., & Singh, A. 2016. Characterization of silver nanoparticles synthesized using Urtica dioica Linn. leaves and their synergistic effects with antibiotics. *J Rad Res Appl Sci*, ***9*(3)**: 217-227.

Kathiravan, V., Ravi, S., & Ashokkumar, S. 2014. Synthesis of silver nanoparticles from Melia dubia leaf extract and their in vitro anticancer activity. *Spectrochimica Acta Part A: Mol Biomol Spectroscopy*, ***130***:116-121.

Mudhafar M, Zainol I, Jaafar CNA, Alsailawi HA, Desa S. 2021. A review study on synthesis methods of Ag nanoparticles, considering a antibacterial property and cytotoxicity. *Int J Drug Delivery Technol*, **2**:635-48.

Liu, Y., Kim, S., Kim, Y. J., Perumalsamy, H., Lee, S., Hwang, E., & Yi, T. H. 2019. Green synthesis of gold nanoparticles using Euphrasia officinalisleaf extract to inhibit lipopolysaccharide-induced inflammation through NF-κB and JAK/STAT pathways in RAW 264.7 macrophages. *Int J Nanomed*, ***14***: 2945.

Mudhafar, M., & Alsailawi, H. A. 2019. An Expression Study Profile of Proinflammatory Cytokines in Asthma Patient. *J Asian Sci Res*, ***9*(12)**: 227-234.

Mudhafar, M., Zainol, I., Desa, S 2019. and Che Nor Aziza Jaafar. "review of Phytochemistry for Polyalithia **14**:119-147

Mudhafar, M., and Zainol, I. "Medical values, antimicrobial, and anti fungal activities of Polyalthia genus 2019." *Int J Pharml Res*, **11**: 91-96.

Mudhafar, M., Zainol, I., Jaafar, C. N., Alsailawi, H. A., Majhool, A. A., & Alsaady, M. 2020. Phytochemical Screening and Characterization of Meliadubia Leaves Extract for Antimicrobial Activity against Escherichia coli and Staphylococcus aureus. *Indian J Ecol*, ***47*(2)**: 493-496.

Mudhafar M, Zainol I, Alsailawi HA, Aiza Jaafar CN. 2021. Synthesis and characterization of fish scales of hydroxyapatite/collagen–silver nanoparticles composites for the applications of bone filler. *J Korean Ceramic Soc*. 12:1-1.

Ojo, O.A., Oyinloye, B.E., Ojo, A.B., Afolabi, O.B., Peters, O.A., Olaiya, O., Fadaka, A., Jonathan, J. and Osunlana, O., 2017. Green synthesis of silver nanoparticles (AgNPs) using Talinum triangulare (Jacq.) Willd. leaf extract and monitoring their antimicrobial activity. *J Bionanosci*, ***11*(4)**: 292-296.

Pugazhendhi, A., Prabakar, D., Jacob, J.M., Karuppusamy, I. and Saratale, R.G., 2018. Synthesis and characterization of silver nanoparticles using Gelidium amansii and its antimicrobial property against various pathogenic bacteria. *Microbial patho*, ***114***: 41-45.

Rathod, D., Golinska, P., Wypij, M., Dahm, H. and Rai, M., 2016. A new report of Nocardiopsis valliformis strain OT1 from alkaline Lonar crater of India and its use in synthesis of silver nanoparticles with special reference to evaluation of antibacterial activity and cytotoxicity. *Med Microbiol Immunol*, ***205*(5)**: 435-447.

Sawadkar, P., Sibbons, P., Ahmed, T., Bozec, L., & Mudera, V. 2019. Engineering of a functional tendon using collagen as a natural polymer. *ACS Biomat Sci Eng*, ***5*(10)**: 5218-5228.

Shaik, M.R., Khan, M., Kuniyil, M., Al-Warthan, A., Alkhathlan, H.Z., Siddiqui, M.R.H., Shaik, J.P., Ahamed, A., Mahmood, A., Khan, M. and Adil, S.F., 2018. Plant-extract-assisted green synthesis of silver nanoparticles using Origanum vulgare L. extract and their microbicidal activities. *Sustainability*, ***10*(4)**: 913.

Singh, Priyanka, Yeon J. Kim, Chao Wang, Ramya Mathiyalagan, and Deok C. Yang. "Weissella oryzae DC6-facilitated green synthesis of silver nanoparticles and their antimicrobial potential." *Art Cells, Nanomed Biotechnol*, 2016; 44: 1569-1575.

Sportelli, Maria C., Maurizio Clemente, Margherita Izzi, Annalisa Volpe, Antonio Ancona, Rosaria A. Picca, Gerardo Palazzo, and Nicola Cioffi. **"Exceptionally stable silver nanoparticles synthesized by laser ablation in alcoholic organic solvent A Physicochemical and engineering aspects** 2018; 559: 148-158.

Sripriya, Ramasamy, and Ramadhar Kumar. "A Novel Enzymatic Method for Preparation and Characterization of Collagen Film from Swim Bladder of Fish Rohu (Labeo rohita). *Food Nut Sci*, 2015; 6: 1468.

Sundarrajan, Priya, and Sangeetha Shetty. "Synthesis And Characterization Of Silver Nanoparticles Using Various Plant Extracts And Their Various Environmental Applications 2019; 5: 91.

Tarannum, Aafiya, Charuvaka Muvva, Ami Mehta, J. Raghava Rao, and N. Nishad Fathima. "Phosphonium based ionic liquids-stabilizing or destabilizing agents for collagen. *RSC Advances*, 2016; 6: 4022-4033.

JJBS

Volume 14, Number 5,December 2021
ISSN 1995-6673
Pages 905 – 910

Jordan Journal of Biological Sciences

Antioxidant effect of Beta-D-glucan-polysaccharide fractionate of *Auricularia polytricha* on Hyperglycaemia-Induced Kidney Dysfunction in Experimental Diabetic Nephropathy

Agbor C A [1,*] and Anyanwu G E[2]

[1] *Department of Anatomy, Faculty of Basic Medical Sciences, University of Calabar, Nigeria;* [2] *Department of Anatomy, Faculty of Basic Medical Sciences, University of Nigeria, Nigeria.*

Received: May18, 2020; Revised: Dec 2, 2020; Accepted: January 4, 2021

Abstract

β-D-Glucan polysaccharide is a major bioactive component fractionated from *Auricularia polytricha* (mushroom), an edible fungus used for both nutritional and therapeutic purposes. Local Nigerian men use *A. polytricha* to manage diabetes related complications without accepted experimentation to ascertain the role and mechanism of action of it fractionates. This study was intended to find out the effect of β-D-Glucan polysaccharide supplementation of hyperglycaemia-induces kidney dysfunction in diabetic Wistar rat. Experiment animals were divided into four groups and received treatment as follows; Group A (treated with normal saline and served as normal control), Group B, (diabetic control animals were treated with 65mg/kg.bw of streptozotocin (STZ)), Groups C and D, (placed on 120 mg/kg.bw and 200 mg/kg.bw of β-D-Glucan polysaccharide respectively after inducing diabetics). At termination, 24 hours urine was collected and analyzed for creatinine clearance and proteinuria, both kidneys were harvested and weighed, serum was collected by cardiac puncture and analysed for serum creatinine and oxidative stress markers (Superoxide Dismutase. Catalase and Malondialdehyde), while histopathological examination was done using routine Hematoxyline and Eosine technique with the help of light microscope. The result showed that hyperglycaemic ambience caused a significant increase in serum level of oxidative stress markers along with concomitant cytoarchitectural alterations of kidney tissue and a change in values of renal parameters (serum creatinine, proteinuria, and creatinine clearance) indicating kidney dysfunction in diabetic control animals. However, decrease in activities of oxidative stress markers, reversal of alterations in kidney microstructure, and the overall improvement in values of renal parameters were observed following administration of β-D-Glucan polysaccharide in a dose-dependent manner. The present study suggests that β-D-Glucan polysaccharide supplementation can ameliorate hyperglycaemia-induced nephrotoxicity in diabetic wistar rat model.

Keywords: β-D-Glucan polysaccharide, diabetic nephropathy, *Auricularia polytricha*, kidney, oxidative stress

1. Introduction

Diabetic nephropathy is one of the major complications associated with diabetes mellitus. It is characterized by accumulation of extracellular matrix in the glomerular and tubulointerstitial compartments of the kidney which may result in renal failure (Nangaku et al. 2004). Researchers have described cellular events during diabetic nephropathy to include generation of Reactive Oxygen Specie (ROS), channeling of glucose intermediates into metabolic pathways resulting in generation of advanced glycation product and the increase in expression of transforming growth factor. The result is hyperglycaemia-induced injury from excessive generation of ROS thereby causing an alteration in intraglomerular hemodynamics (Singh et al. 2008).

Both glomerular and tubulointerstitial injuries are involved in pathogenetic mechanisms of diabetic nephropathy. Diabetic kidney injury begins with hyperglycaemia which in turn creates a redox environment in the vasculature, nephron and surrounding interstitium causing dysfunction of virtually all types of kidney cells (Phillips et al. 2003). Tubulointerstitial injury develops after glomerular injury and correlates with alteration in renal parameters such as decreased Glomerular Filtration Rate (GFR), increase in proteinuria and decrease in creatinine clearance (Nangaku et al. 2004).

Oxidative stress caused by increased levels of ROS serve as an inducer and amplifier of signaling cellular events that occur in high glucose ambience (Ha and Lee, 2005; Brownlee, 1995). ROS is required in small amounts necessary to maintain cellular homeostasis, but sustained hyperglycaemia in diabetic conditions will cause a dramatic rise in ROS thereby damaging target organs (Lee et al. 2003). Mechanism of reactive oxygen specie generation involves, high oxygen concentration reduced to water, while part of it is transformed to O_2^- in the mitochondria (Brand, 2010). This is capable of causing cellular dysfunction, apoptosis and mutations (Nishikawa *et al*., 2000)

There has been a shift to herbal therapy with an increasing acceptance in recent times, even among the elite confirming that that herbal therapy is potent in

* Corresponding author e-mail: agbor_cyril@yahoo.com.

management ant treatment of several diseases (Anthony *et al*., 2006). Numerous animal and plant products have been reported to have medicinal properties (Bhatia et al., 2010). β-D-Glucan polysaccharide is a major bioactive constituent of *Auricularia polytricha* (mushroom), an edible fungus used globally for culinary and therapeutic purposes. β-glucans are glucose polymers polysaccharides linked together by a 1-3 linear β-glycosidic chain core and are found as a major constituent in the cell wall of fungus. They differ from each other by their length and branching structures (Stone and Clarke, 1992) and do not always exist in single form but as conjugate with other biomolecules such as amino acid, protein, lipid and nucleic acid residue. More so, its low molecular weight, chelating effect and chemical modification by biochemical intermediates makes them a strong source of exogenous antioxidant (Nie et al., 2011).

Local Nigerian men have used *A. polytricha* to manage complications in diabetic men without reliable experimentation to back up their claim. This study tried to find out the antioxidant effect of β-D-Glucan polysaccharide fractionate of *A. polytricha* on experimental diabetes nephropathy using Wistar rat model.

2. Materials And Methods

2.1. Collection of Mushroom

A. Polytricha was purchased from Etomi central market in Etung Local Government Area of Cross River State. It was then taken to Department of Biological Sciences, University of Nigeria for identification. The mushroom was dried under room temperature, powdered and then extracted with ethanol (Anyanwu and Agbor, 2020).

2.2. Fractionation of β-D-glucan polysaccharide

β-D-glucan polysaccharide was experimentally separated from *A. polytricha* using acetyl trimethyl ammonium bromide to form a precipitated complex with the acidic polysaccharide. It was further purified and structurally described through the use of a combination of fractional precipitation with acetic acid using ion-exchange chromatography. (Zhang et al. 2007)

2.3. Experimental Animals

Sixteen (16) adult male Wistar rats were weighed and grouped into four in clean cages with four rats in each. The rats were kept for two weeks of acclimatization in animal house, Department of Anatomy, Faculty of Basic Medical Sciences, University of Nigeria, Enugu Campus and allowed free access to available chow and water.

2.4. Experimental Design

The experimental grouping, treatment and dosage are shown in Table 1

Table 1. Experimental animals were divided into four (4) groups with 4 animals in each. Treatment received is as follows:

Group	Number of Animals	Treatment	Dose
A	4	Distilled water	3 mls
B	4	Streptozotocin (STZ)	65mg/kg.bw
C	4	STZ + β-D-glucan polysaccharide	120mg/kg.bw
D	4	STZ + β-D-glucan polysaccharide	200mg/kg.bw

2.5. Induction of Hyperglycaemia

Diabetes was induced by administration of 65 mg/kgbw of Streptozotocin (STZ) intraperitoneally after allowing the animals to fast for 12 hours, STZ was reconstituted in 0.5M of Sodium citrate before administration (Ugochukwu and Babady 2003).

2.6. Confirmation of Hyperglycaemia

Accu-Check glucometer (Roche diagnostic, Germany) was used to confirm diabetes 3 days after STZ administration, using blood samples from the tails of experimental animals. Blood glucose levels was checked before and after induction to confirm diabetic state (Anyanwu and Agbor, 2020).

2.7. Administration of Extract

After two weeks of sustained hyperglycaemia, β-D-glucan polysaccharide was administered via oral gastric intubation. to experimental groups (B, C and D) once daily. The experiment lasted for 2 weeks,

2.8. Collection of Tissues and Samples for Analysis

At termination, kidneys were harvested weighed together using an electronic weighing balance (Mettler Instrument AG, Switzerland) and suspended in buffered neutral formaldehyde for further processes with conventional histological techniques. Paraffin sections were cut at 5.0 microns using a Manual Rotary Microtome. Heamatoxylin and Eosin (H & E) stained sections were observed under a light microscope.

2.9. Evaluation of Oxidative Stress Markers

Oxidative stress markers were analyzed using blood obtained by cardiac puncture. Samples were transported to the laboratory for biochemical study. Oxidative stress marker kits (Sigma-Aldrich Products, Germany) was used to demonstrate for Superoxide Dismutase (SOD), Catalase and Malondialdehyde (MDA) (Anyanwu and Agbor, 2020).

2.10. Analysis for Renal Parameters

Urine was obtained from metabolic cages housing the experimental animals on the last day, before sacrifice. Creatinine auto-analyzer (Beckman Instrument Fullerton CA) was used to evaluate urine and serum creatinine levels while spectrophotometric assay was adopted in estimation of total protein (Sharma et al., 2001).

2.11. Statistical Analysis

Data obtained from this study was recorded and analyzed using one way analysis of variance (ANOVA) with SPSS program (version 20). Post-hoc test was conducted using Fischer's Least Significant Difference (LSD) to determine statistical significance among groups. Probability level of $P<0.05$ was considered significant.

3. Results

3.1. Weight of Kidney

As shown in Figure 1, a significantly ($p<0.05$) lower kidney weight (0.80±0.34 g) was observed in diabetic control (Group B) when compared to normal control (1.82±0.67 g). However, hyperglycaemic animals that received 120 mg/kg.bw and 200mg/kg.bw of β-D-glucan polysaccharide in Groups C and D respectively recorded kidney weights that were significantly ($p<0.05$) higher when compared to the diabetic control.

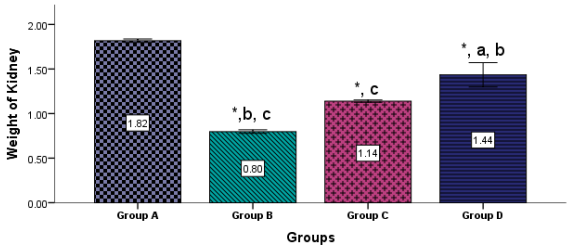

Fig 1: Comparison of Weight of Kidney in different experimental Groups
Values are expressed as mean ±SEM, n = 4.
* = significantly different from Group A at p<0.05
a = significantly different from Group B at p<0.05
b = significantly different from Group C at p<0.05
c = significantly different from Group D at p<0.05

3.2. Biochemical Analysis

High serum SOD, Catalase and Malondialdehyde (MDA) level were recorded by the diabetic control animals and these values were significantly ($p<0.05$) higher when compared to normal control group. However, all the diabetic animals treated with graded doses of β-D-glucan polysaccharide had significantly lower SOD, catalase and Melondialdehyde activities when compared with diabetic control (Figures 2, 3 and 4).

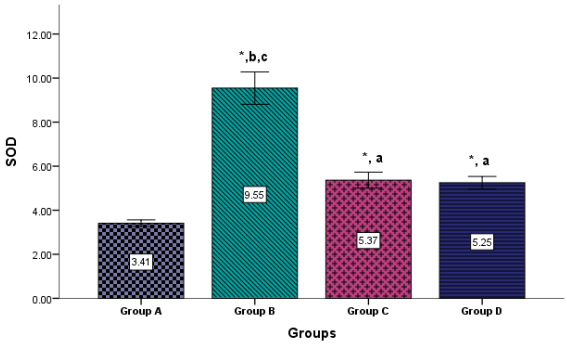

Fig 2: Comparison of SOD level in different experimental Groups
Values are expressed as mean ±SEM, n = 4.
* = significantly different from Group A at p<0.05
a = significantly different from Group B at p<0.05
b = significantly different from Group C at p<0.05
c = significantly different from Group D at p<0.05

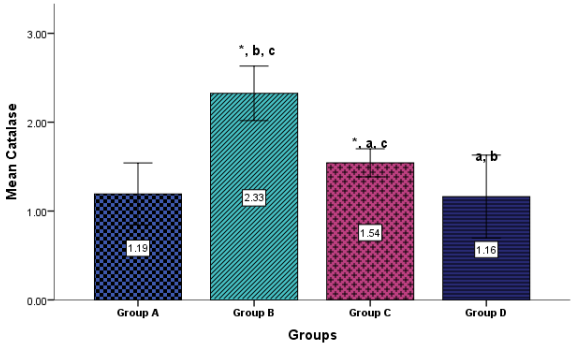

Fig 3: Comparison of Catalase level in different experimental Groups
Values are expressed as mean ±SEM, n = 4.
* = significantly different from Group A at p<0.05
a = significantly different from Group B at p<0.05
b = significantly different from Group C at p<0.05
c = significantly different from Group D at p<0.05

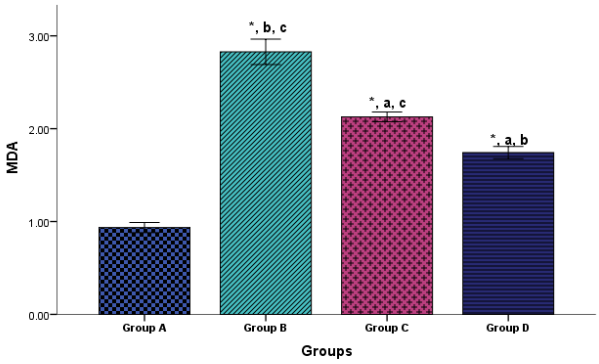

Fig 4: Comparison of MDA level in different experimental Groups
Values are expressed as mean ±SEM, n = 4.
* = significantly different from Group A at p<0.05
a = significantly different from Group B at p<0.05
b = significantly different from Group C at p<0.05
c = significantly different from Group D at p<0.05

3.3. Histopathological Examination

Fig. 4: Histopathological Examination of Kidney – X400

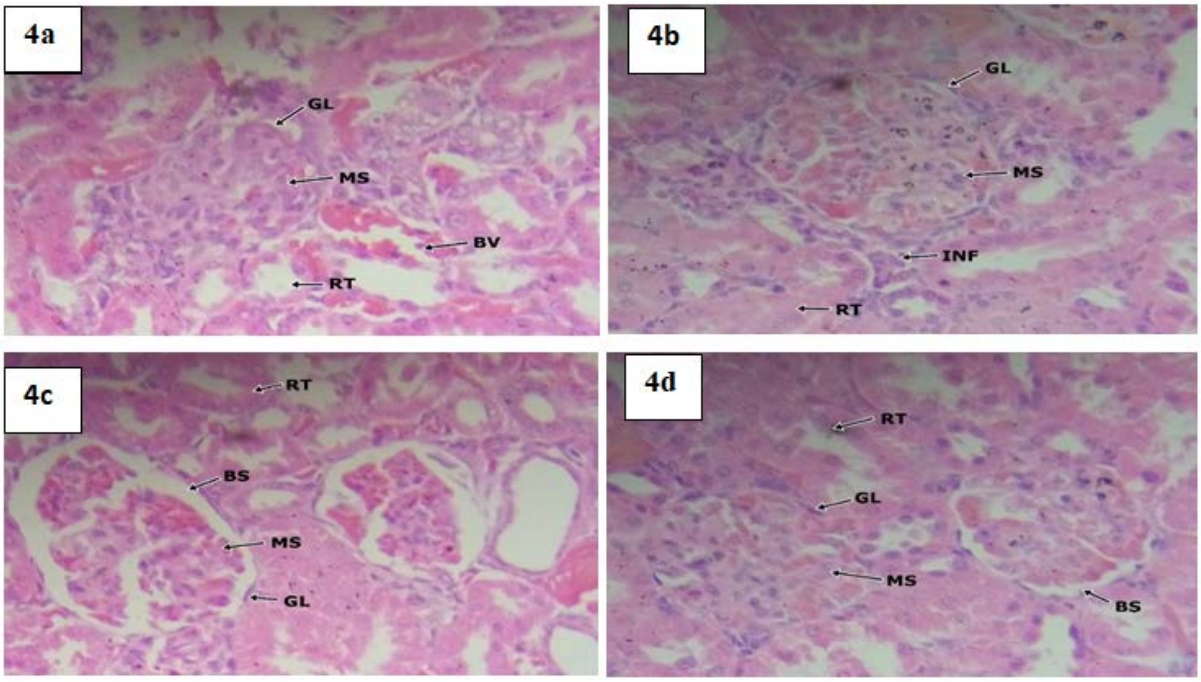

Key GL – Glomerulus MS – Mesangium RT – Renal tubuleBS – Bowman.s Space BV – Blood Vessel.

Figure 4. a) Section of the kidney in group A (Normal control) showing prominent renal tubules and glomeruli. The intervening stroma is scanty and consists of sparse interstitial cells and dilated blood vessels. The glomeruli and Bowman's space were seen intact. **b)** Section of the kidney of animals in Group B (Diabetic control) showing prominent renal tubules and glomeruli with diffused expansion and proliferation of mesangium, thickening of glomerular basement membrane and renal tubular hypertrophy. The intervening stroma consists of inflammatory infiltrates. The glomeruli are mildly swollen with a distorted Bowman's space. Extensive haemorrhage is seen within the mesangial matrix. **c**) Section of the kidney in group C (Diabetic animals placed on 120mg/kg.bw β-D-glucan polysaccharide) shows prominent renal tubules and glomeruli. The intervening stroma is scanty and consists of sparse interstitial cells and mild inflammatory infiltrates. The glomeruli are atrophic with an intact bowman space and a cellular mesangium. **d**) Section of the kidney in group D (Diabetic animals placed on 200mg/kg.bw β-D-glucan polysaccharide) shows prominent renal tubules and glomeruli. The intervening stroma is scanty and consists of sparse interstitial cells and mild inflammatory infiltrates. The glomeruli have intact Bowman's space and a cellular mesangium.

3.4. Renal Parameters

As shown in figures 6, 7 and 8, serum creatinine level (2.58±0.44 mg/dl) in diabetic control (Group B) was remarkably increased when compared to normal control (0.69±0.84), proteinuria in diabetic control group was also significantly higher when compared to normal control, whereas creatinine clearance in diabetic control group was significantly ($p<0.05$) lower when compared to normal control.

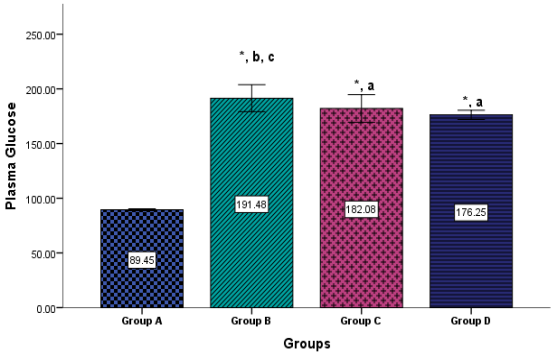

Fig 5: Comparison of Plasma glucose level in different experimental Groups
Values are expressed as mean ±SEM, n = 4.
* = significantly different from Group A at p<0.05
a = significantly different from Group B at p<0.05
b = significantly different from Group C at p<0.05
c = significantly different from Group D at p<0.05

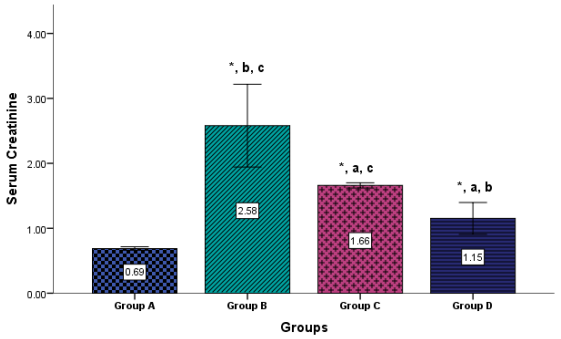

Fig 6: Comparison of Serum creatinine level in different experimental Groups
Values are expressed as mean ±SEM, n = 4.
* = significantly different from Group A at p<0.05
a = significantly different from Group B at p<0.05
b = significantly different from Group C at p<0.05
c = significantly different from Group D at p<0.05

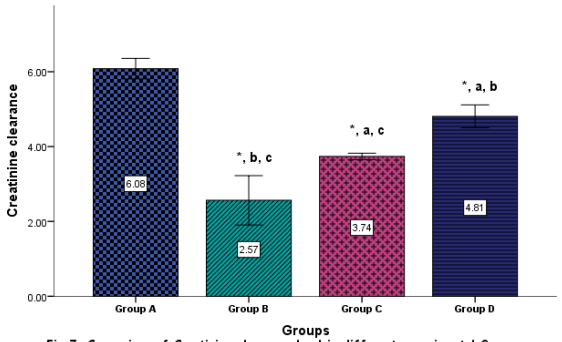

Fig 7: Comparison of Creatinine clearance level in different experimental Groups
Values are expressed as mean ±SEM, n = 4.
* = significantly different from Group A at p<0.05
a = significantly different from Group B at p<0.05
b = significantly different from Group C at p<0.05
c = significantly different from Group D at p<0.05

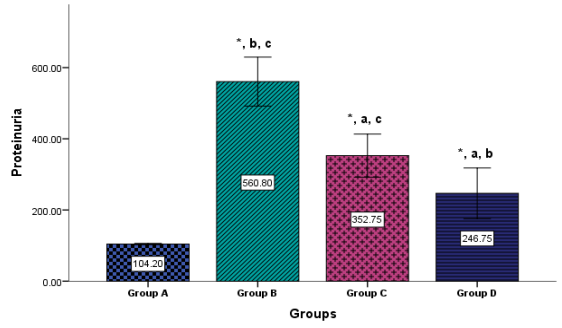

Fig 8: Comparison of Proteinuria level in different experimental Groups
Values are expressed as mean ±SEM, n = 4.
* = significantly different from Group A at p<0.05
a = significantly different from Group B at p<0.05
b = significantly different from Group C at p<0.05
c = significantly different from Group D at p<0.05

4. Discussion

This study has revealed that sustained hyperglycaemia within the tissue of the kidney can cause significant reduction in weight of organ. It has been demonstrated that weight of an organ depends, to a large extent, on the mass of various cells. According to Wolf (2004), hyperglycaemic injury affects all cell types in the kidney including mesangial, vascular endothelia interstitial and fibroblast cells at varying degrees. When compared to the diabetic control group, ten weeks of administration of β-D-glucan polysaccharide to diabetic rat may have caused the increase in kidney weight in a dose-dependent manner. Chang et al. (2011) have reported that *A. polytricha* (unfractionated fungi) is capable of inhibiting lipid peroxidation in body organs thereby restoring their weight. There are also confirmatory reports by Sherma *et al.* (2001).

The remarkably higher levels of serum SOD, Catalase and melondialdehyde in group B when compared to group A confirm high hyperglycaemic ambience within the renal tissue. It has been documented that β-D-glucan polysaccharide is a strong exogenous source of antioxidant that do not exist as a single form but forms conjugates with other vital bio-molecular elements like amino acid, protein, lipid and nucleic acid residue (Nie et al., 2011). The underlying mechanism could be that β-D-glucan polysaccharide has low molecular weight and more hydroxyl group terminals capable of accepting and eliminating free radicals and these are the most important structural feature that determines the antioxidant capacity of polysaccharides. Liu et al. (2010) reported that peptide moiety of polysaccharide has been found to have high free radical scavenging activity which is a possible reason for low levels of oxidative stress markers in diabetic animals treated with β-D-glucan polysaccharide.

As shown in figure 4, Group A presented a kidney section having prominent renal tubules with an intact glomeruli (figure 4a). Histological section of kidney in diabetic control (figure 4a) group reveals diffused expansion and proliferation of mesangium, thickening of glomerular basement membrane, renal tubular hypertrophy, scanty and sparse interstitial cells with inflammatory infiltrates, distorted Bowman's space and extensive hemorrhage within the mesangial matrix as a result of hyperglycaemic injury which affects all cell types in the kidney. Fioretto and Mauer (2007) reported that glomerular, tubule-interstitial and vascular changes constitute pathogenicity of diabetic nephropathy. In this study, glomerular changes are shown in mesangial cell proliferation and thickening of glomerular basement membrane, changes in the tubulointerstitial compartment included inflammatory infiltrate and tubular hypertrophy while the changes in vascular compartment were notices in the various degrees of hemorrhage within the mesangial matrix. Hyperglycaemia-induced injury results from excessive generation of ROS causing changes in intraglomerular hemodynamics.

Extensive experimental evidence (Aitken and Krausz 2001; Lenzi *et al.*, 1993;) have reported modification of nucleotide bases thereby causing alteration in DNA structure accompanied by deletion, cross linking and chromosomal rearrangement with its attendant consequences that ends in cellular damage.

Findings from this study also show that hyperglycaemia-induced alterations which are signs of kidney damage were minimized and reversed in a dose dependent manner following administration of β-D-Glucan polysaccharide as shown in figures 4c and 4d. Even though a comprehensive investigation into the mechanism of action of β-D-Glucan polysaccharide is still lacking, its low molecular weight and existence in conjugate forms may trigger an interaction with certain receptors that may result in some specific therapeutic signaling pathway to benefit host organ. β-D-Glucan polysaccharide have also been shown to possess lipid peroxidation inhibitory effect which make it capable of preventing damage of cell membrane. Renard et al (2001) reported similar findings.

Renal parameters obtained from the diabetic control group are indicators of renal dysfunction. Results obtained

from renal parameters in different experimental groups show a correlation between these parameters and hyperglycaemia-induced kidney injury. However, these values were reversed following β-D-Glucan polysaccharide administration. Improvement in these renal parameters following administration of β-D-glucan polysaccharide may have reflected the reversal in hyperglyaemia-induced distortion of glomerular, tubolointerstitial and vascular compartments in the kidney tissue.

In conclusion, the findings from this research revealed that β-D-Glucan polysaccharide fractionate of *A. polytricha* was capable of ameliorating hyperglycaemia-induced kidney damage in experimental diabetic nephropathy models. This research therefore suggest that β-D-Glucan polysaccharide may reduce the risk of kidney dysfunction in diabetic men.

Acknowledgment

I acknowledge the technical support from the Department of Histopathology, University of Calabar Teaching Hospital, Nigeria and Endocrinology Laboratory in the Department of Biochemistry, University of Calabar Nigeria.

Funding

This research had no external source of funding.

Competing Interest

All authors in this research are not by any means linked to any funding body, and so there was a complete absence of competing interest.

Authors' Contributions

All authors gave equal contribution to this research.

Ethical Clearance

Ethical clearance for this research was obtained from the Ethical Committee, Faculty of Basic Medical Sciences, University of Nigeria, Enugu Campus, Nigeria.

References

Aitken RJ and Krause C. 2001. Oxidative stress, DNA damage and the Y- chromosome. *Reproduction* **122**: 497-506.

Anthony BO, Oladipo AL, Adedoyin KL and Tajudin IA. 2006. Phytochemistry and spermatogenic potential of aqueous extracts of Cissus Populnear. *The Sci World J*, **6**:2140-2146.

Anyanwu GE and Agbor CA. 2020. Assessment of testicular histomorphometric parameters and reticular fibre density on testicular tissue of diabetic Wister rat placed on Auricularia Polytricha. Jordan J. Biol. Sci. 13(Supplementary): 709-714

Bhatia DK, Sharma AK, Pathania PC and Khauduri NC. 2010. Antifertility effect of crude extract of Adiantum Lunulatum on Reproductve-organs of male wister rats. *Int. J Biol Forum*, **2 (2):**88-93.

Brand MD. 2010. The sites and topology of mitochondrial superoxide production. *Exper Gerontol*, vol 45, No 7-8, pp. 466-472.

Brownlee M. 1995. Advanced protein glycosylation in diabetes and aging. *Annu. Rev. Med*.; 46:223–234.

Chang JS, Kim HJ, Bae JT, Park SH, Kim SE and Kim OM. 2011. Inhibition effects of *Auricularia auricula-judae* methanol extract on lipid peroxidation and liver damage in benzo(a)pyrene-treated mice. *J Korean Soc Food Sci Nut* **27**: 712–717.

Fioretto P, Mauer M. 2007. Histopathology of diabetic nephropathy. *Semin. Nephrol*. **27**:195–207.

Ha H, Lee HB. 2005. Reactive oxygen species amplify glucose signaling in renal cells cultured under high glucose and in diabetic nephropathy. *Nephrol*. 10:S7–S10.

Lee HB, Yu MI-RA, Yang Y, Jiang Z, Ha H. 2003. Reactive oxygen species-regulated signaling pathways in diabetic nephropathy. *J. Am. Soc. Nephrol*. **14**:S241–S245.

Lenzi A, Cualosso F, Gandini L, Lombardo F and Dondero F. 1993. Placebo controlled, double-blind, cross-over trial of glutathione therapy in male infertility. *Human Rep* **9**: 2044-2050.

Liu W, Wang H, Pang X, Yao W and Gao X. 2010. Characterization and antioxidant activity of two low-molecular-weight polysaccharides purified from the fruiting bodies of *Ganoderma lucidum* . *Int J of Biol Macromol*. **46(4):**451–457. doi: 10.1016/j.ijbiomac.2010.02.006.

Nangaku M. 2004. Mechanisms of tubulointerstitial injury in the kidney: final common pathways to end stage renal failure. *Int Med*. 43:9–17.

Nie S.-P., Xie M.-Y., 2011. A review on the isolation and structure of tea polysaccharides and their bioactivities. *Food Hydrocolloids*. **25(2):**144–149. doi: 10.1016/j.foodhyd.2010.04.010.

Nishikawa T, Edelstein D and Brownlee M. 2000. The missing link: a single unifying mechanism for diabetes complications. *The Kidney J*, 77, pp.526-530.

Phillips AO. 2003. The role of renal proximal tubular cells in diabetic nephropathy. *Curr Diabetes Rep*. **3**:491–496.

Renard CM. Baron A, Guyot S and Drilleau JF. 2001. Interactions between apple cell walls and native apple polyphenols: quantification and some consequences. *Int J Biol Macromol*. 29(2):115–125. doi: 10.1016/s0141-8130(01)00155-6

Sharma RK, Pasqualotto AE and Nelson DR. 2001. Relationship between seminal white blood cell count and oxidative stress in men treated at an infertility clinic. *J Androl*, **22**:575-583.

Singh DK, Winocour P, Farrington K. 2008. Mechanisms of disease: the hypoxic tubular hypothesis of diabetic nephropathy. *Nat. Clin. Pract. Nephrol*. 4:216–226.

Stone BA, Clarke AE. 1992. **Chemistry and biology of (1,3)-D-glucans**. Victoria, Australia.: *La Trobe University Press.*

Ugochukwu NH and Babady NE. 2003. Antihyperglycaemic effect of aqueous and ethanolic extracts of Gongronema latifolium leaves on glucose and glycogen metabolism in livers of normal and streptozotocin induced diabetic rats. *Life sci*, 73 (150): 1925-1938.

Wolf G. 2004. New insights into the pathophysiology of diabetic nephropathy: from hemodynamics to molecular pathology. *Eur. J. Clin. Investig*. **34**:785–796.

Zhang H, Wang ZY, Yang L, Yang X, Wang X and Zhang Z. 2007. *In vitro* antioxidant activities of sulfated derivatives of polysaccharides extracted from *Auricularia auricular*. *Int J of Mol Sci* **12**: 3288–3302.

JJBS

Volume 14, Number 5,December 2021
ISSN 1995-6673
Pages 911 – 918

Jordan Journal of Biological Sciences

Effect of Stress on Ontogeny of Humoral Immunity in Catla

Purandara Ballyaya Abhiman[1], Md. Abdullah-Al Mamun[1,2,*] , Manjulesh Pai[1], Shamima Nasren[1,3], Sanjay Singh Rathore[1] and Kalkuli Mariappa Shankar[1]

[1]*Laboratory of Aquatic Health Management, Department of Aquaculture, College of Fisheries, Mangalore-575002, Karnataka Veterinary Animal and Fisheries Science University, Karnataka, India.*[2]*Department of Fish Health Management, Sylhet Agricultural University, Sylhet-3100, Bangladesh.*[3]*Department of Fish Biology and Genetics, Sylhet Agricultural University, Sylhet-3100, Bangladesh.*

Received: May 9, 2020; Revised: Dec 22, 2020; Accepted: January 12, 2021

Abstract

The present study aimed to evaluate the crowding and handling stress with increased cortisol production, its effect on growth and ontogeny of humoral immunity in *Catla catla*. Fishes were stressed at different stocking densities (T_1, T_2, T_3 and T_4) in crowding stress and were monitored for various parameters including length, weight, serum cortisol and immunoglobulin. In comparison to low stocking density group T_1 (3000/ m^2), high stocking groups (T_2, T_3 and T_4) showed reduction in both average length and weight on 6th day onwards up to 40th day. The results of T_4 (18000/m^2) showed drastic reduction up to 12th day and died afterwards. Similarly, in handling stress fishes were stocked in six hapas at equal densities (3000/m^2) with different stress (HS_1, HS_2, HS_3, HS_4, HS_5 and HS_6) revealed a decrease in average length and weight in comparison to control throughout the study period. Serum cortisol levels were significantly elevated ($P<0.05$) in higher crowding and handing stress groups. The results of ELISA for crowding stress showed that immunoglobulins were detectable in the spawn from 3 days post hatching (DPH). The immunoglobulin levels decreased till 18 DPH in T_2, T_3 and T_4 groups, although the levels were significantly higher ($P<0.05$) in lower stocking density group (T_1). In response to handling, all the stressed groups showed significant decrease ($P<0.05$) in immunoglobulin production in comparison to control at 18 DPH onwards. A slow recovery was observed on 40th day, although the immunoglobulin levels in stressed groups were remained lesser than the control.

Keywords: Stress, Cortisol, Humoral, Immunoglobulin, ELISA, *Catla catla*

1. Introduction

The maintenance of good fish health is critical to profitable fish culture. Aqua cultural ecosystems are innately unstable, unnatural environments. In general, the greater the culture intensity, the greater is the environmental instability. Fishes are exposed to various stressors under natural and cultural conditions (Sharma *et al.*, 2016; Tengjaroenkul and Neeratanaphan, 2020). Alteration of water salinity, pH, hardness, alkalinity, dissolved solids, water level or current, inadequate nutrition and exposure to waterborne pathogens or toxicants are the common stressors for fish (Harper and Wolf, 2009, Lavanya *et al*., 2011). The procedural stressors include handling, crowding, netting, sorting, vaccine administration etc. Stressors may be acute or chronic and their impacts on fish are additive and cumulative at least for a short period. The extent of stress may vary with nature of stress and its duration and dependable upon age, sex, maturation stage, species and strain of the fish (Perumal *et al.,* 2015). Fish react to stress with a primary neuroendocrine response, represented by a rapid hyper secretion of catecholamines (adrenaline and noradrenaline) and corticosteroids (mainly cortisol) into the blood stream (Pickering, 1981). As a result of their high levels in the circulatory system, a wide range of secondary responses can be observed. The effects of these hormones at blood and tissue level include disturbance of the metabolic and hydro mineral balance. Tertiary responses include behavioral modifications, implications for fish growth and reproduction and increased susceptibility to diseases (Pickering *et al.,* 1982; Pankhurst *et al.,* 1997; Okpashi *et al.,* 2018).

A variety of biochemical measurements are used as indicators of stress in fish. Among the most frequently measured variables, there are levels of circulating corticosteroid hormones (mainly cortisol) and glucose, lactate, haemoglobin, proteins and haematocrit (Poli *et al.,* 2005). In addition, some components of innate immune system (e.g. lysozyme, haemolytic and haemagglutinating activity) and humoral factors such as IgM levels are used as indicators of immunocompetence in fish exposed to stress (Sunyer *et al.,* 1995; Tort *et al.,* 2004). The immune parameters including IgM are essential to measure the health status of fish and as markers for stress (Sahoo *et al*., 2005). The immune system in newly hatched larvae is not fully developed and they are exposed to a potentially pathogenically hostile environment (Breuil *et al.,* 1997). The immunoglobulins detected in the eggs, hatchlings and the spawns are of maternal origin. The maternal transfer of IgM has been documented in several teleost fish including, tilapia (*Oreochromis aureus*) (Avtalion and Mor, 1992; Takemura, 1993), channel catfish, (*Ictalurus punctatus*)

* Corresponding author e-mail: mamunff@gmail.com.

(Hayman and Lobb, 1993), chum salmon, (*Oncorhynchus keta*) (Fuda *et al.*, 1992) and coho salmon *Oncorhynchus kisutch* (Yousif *et al.*, 1995), Indian major carps (Bag *et al.*, 2009). Limited research has been carried out relating with growth and humoral immune parameters with husbandry stress on early developmental stages in Indian Major Carps, *Catla catla*, an aquaculture potential species. The present study was undertaken in an attempt to explain the mechanism of growth inhibition, cortisol indication and humoral immunity by crowding and handling stress.

2. Materials and methods

2.1. Seed collection and transportation

Two day post hatch spawn of the Indian major carp, catla (*Catla catla*) used in the present study was procured from the fish seed farm, State Department of Fisheries, Bhadra Reservoir Project (BRP), Shimoga, Karnataka, India in packed plastic bags containing 1/3rd water and 2/3rd oxygen.

2.2. Larval rearing

The larvae were reared in hapas suspended in the freshly manured water (cow dung 10,000kg/ha) of pretreated cement cisterns of size 25m^2 at the fish farm of College of Fisheries, Mangalore. The aquatic insects were eradicated by using Butox (0.04ml/m^2), one week after the manuring. Hatchlings were stocked at the rate of 1000/m^2. Larvae were fed on the naturally available planktons; in addition, they were fed daily with rice bran and groundnut oil cake at a ratio 1:1 at 10% of the body weight. The experimental protocol lasted for 40 days and temperature variation was in the range of 21 ºC to 26 ºC during the entire study period.

2.3. Stressing protocol

2.3.1. Crowding Stress

The hatchlings were individually stocked in the hapas at the densities of 3000, 6000, 12000 and 18000 per m^2 in triplicate. The samples for cortisol and IgM estimation were collected from the experimental hapas using a hand net, on 3rd, 6th, 12th, 18th, 24th, 30th and 40th day post hatching.

2.3.2. Handling Stress

Spawn were held in seven different hapas at equal stocking densities (3000/m^2). Fishes of the one hapa were maintained as control without any handling. Fishes of the other six hapa were stressed according to the method of Feist and Schreck (2001) with slight modifications by holding them out of water for 30 sec and releasing back to recover for a period for 15 min, were stressed again two times by holding them out of water for 15 sec after 15 and 30 min of the original stressing. Fishes were sampled after 15 min of the last stressor. Fishes were sampled on 3rd, 6th, 12th, 18th, 24th and 30th day post hatched. The length-weight parameters were measured for the handled group HS_1 (the group handled on 3rd day or 3DPH) and control group on the 3rd day. The group HS_2 was handled only on 6th day (when the larvae were 6DPH). The group HS_3 was handled on 12th day, both the previously stressed groups HS_1 and HS_2 were sampled. The group HS_4 was handled on the 18th day, the previously stressed groups HS_1, HS_2 and HS_3 were sampled. Similarly HS_5 and HS_6 were handled on 24th day and 30th day respectively. On 40th day no handling was done, only sampling was done for all previously stressed groups

In case of both the stressing protocols, a pool of 100-300 spawn and a pool of 5-30 fry fishes were used to prepare the cortisol and antibody extract solution. The number of individuals sampled decreased with increase in the fish body weight. Fish samples were collected from the experimental hapas using a hand net, immediately anesthetized, rinsed with distilled water and then with PBS (Phosphate Buffer Saline) (pH 7.4). Wet body weight and total length of the fish were recorded.

2.4. Preparation of fish extracts for antibody extraction

Spawn and fry extracts of both control and stressed groups were prepared according to the method of Breuil *et al*. (1997) with slight modification in rpm employed in centrifugation. The spawn and fry of catla were homogenized with three volumes of PBS pH 7.4; and the resultant homogenate was centrifuged at 12000 rpm for 15 min under 4º C. The supernatants were collected, centrifuged twice at 12000 rpm for 10 min, and pooled supernatants were stored at -40 º C with addition of Protease inhibitor cocktail (Sigma,USA) till use.

2.5. Determination of protein concentration

Protein concentration of tissue extracts of different samples of catla was determined according to Lowry *et al*. (1951) using protein estimation kit (Bangalore, Genei India Pvt. Ltd.)

2.6. Monoclonal Antibody production from the hybridoma clone C_6E_2

Hybridoma clones C_6E_2 raised against IgM of catla (Honnananda, 2008) were revived from the frozen state at -196 ºC by thawing at 37 ºC in the water bath. The cell suspension was suspended in 10 ml of serum (FBS) free RPMI cell culture medium. The cells were harvested by centrifuging at 1800 rpm. The supernatant was decanted and the cell pellet was re-suspended in 5 ml RPMI medium enriched with 15% FBS and distributed to 96 well tissue culture plate or 25 cm² flask according to the cell density. The plates/flasks were incubated at 37ºC in CO_2 incubator and subsequently transferred to 75 cm² flasks for production of monoclonal antibody (MAb).

2.6.1. Enzyme- linked Immunosorbent Assay (ELISA)

ELISA was carried out according to Furuta *et al.* (1995) with slight modifications. Microtitre plates were coated with tissue extract (100µl/well) diluted in carbonate-bicarbonate buffer (pH 9.6) to a concentration of 10µg/ml protein and incubated overnight at 4 ºC .Unbound proteins were removed by washing once with PBS-T20 (0.05% Tween-20 in PBS) subsequently with PBS with a 3 min interval. 300 µl of PBS-5% skimmed milk was added as a blocking reagent to each well and 2h at room temperature. The blocking was followed by washing with PBS-T20 and PBS. 100µl MAb was added to each well except to the antibody blank and incubated for 3h at room temperature. The excess MAb was poured off and the plate was washed twice with PBS-T20 and once with PBS alone. The plates were then incubated for 45min at room temperature by adding Rabbit anti mouse IgG peroxidase conjugate at 1:2000 dilution in 3% BSA-PBS (Bangalore, Genie Pvt. Ltd.), washed three times PBS-T20 and once

with PBS. The peroxidase activity was then measured by adding 100µl of a substrate solution containing tetramethylebenzidine and hydrogen peroxide (TMB/ H_2O_2) diluted in distilled water at a ratio 1:20. After incubation for 10 min in the dark at room temperature, the enzyme reaction was stopped by adding 50µl of 2N H_2SO_4 to each well and the optical density was measured at 450nm using a Microplate reader (Bio-Tek Instruments, Inc. USA).

2.7. Estimation of whole body cortisol levels

2.7.1. Preparation fish extracts for cortisol estimation

Spawn and fry extracts of both control and stressed groups were prepared as previously described, except that the centrifugation was carried out at 3000 rpm for 10min at 4º C. The supernatant was immediately analysed after processing.

2.7.2. Determination of Cortisol levels in stressed fish by competitive ELISA

Cortisol levels in the stressed (both crowding and handling) as well as control groups were measured using Cortisol Saliva Kit (Diagnostics Biochem Canada Inc.).Working solutions of the cortisol-HRP conjugate and wash buffer were prepared according to manufacturers' instructions. Each calibrator, control and stressed samples 50 µl were pipetted into strips of labelled microwells in duplicates. The conjugate working solution of 100 µl was dispensed into each well. The plate was then incubated on a plate shaker at 200 rpm for 45 min at room temperature. The wells were washed three times with 300 µl of diluted wash buffer per well and plate was tapped firmly against absorbent paper to ensure that it was dry. TMB substrate of 150 µl was pipetted into each well at timed intervals and incubated on a plate shaker for 15-20 min at room temperature. 50 µl of stopping solution was pipetted into each well and the plate was read on a Microplate reader (Bio-Tek Instruments, Inc. USA) at 450 nm within 20 min of addition of the stopping solution.

2.8. Statistical analysis

All data were expressed as mean ± SE (standard error). Differences in the cortisol and immunoglobulin levels between the treatments were analysed statistically through one-way analysis of variance (ANOVA) followed by Duncan's multiple range test by using SPSS software (20.0 version). The level of significance was chosen at $P<0.05$.

3. Results

3.1. Measurement of average length and weight

3.1.1. Crowding stress

The initial average length and weight of a sample of 3DPH larvae was measured before stocking. The mean length and weight were found to be 0.5 cm and 0.0015 g respectively (Table 1). Sampling was done for cortisol and IgM estimation was done on scheduled days up to 40th day. In comparison to low stocking density group T_1 (3000/ m^2), high stocking groups showed reduction in both average length and weight 6th day onwards up to 40th day. There has been slight variation observed among the groups T_1 (3000/ m^2) and T_2 (6000/ m^2). The results of T_4 (18000/m^2) showed drastic variation up to 12th day in comparison to all other groups. In comparison to groups T_1 and T_2 the reduction in the average length and weight in the group T_3 (12000/m^2) was observed throughout the study period up to the 40th day.

Table1. Average length and weight of catla subjected to crowding stress (CS)

Sampling days	T_1 (3000/ m^2)		T_2(6000/m^2)		T_3 (12000/m^2)		T_4 (18000/m^2)	
	L(cm)	W(g)	L(cm)	W(g)	L(cm)	W(g)	L(cm)	W(g)
3rd day	0.5±0.03	0.0015±0.0002	0.5±0.03	0.0015±0.0002	0.5±0.03	0.0015±0.0002	0.5±0.03	0.0015±0.0002
6th day	0.70±0.03	0.0030±0.0003	0.68±0.02	0.0025±0.0003	0.61±0.02	0.0019±0.0005	0.58±0.04	0.0016±0.0003
12th day	1.20±0.03	0.004±0.002	1.1±0.03	0.0038±0.0004	0.9±0.05	0.0035±0.0006	0.7±0.04	0.00280±0.0004
18th day	1.80±0.02	0.028±0.004	1.6±0.03	0.016±0.002	1.2±0.02	0.004±0.002	-	-
24th day	2.50±0.04	0.070±0.003	2.4±0.02	0.068±0.002	1.9±0.04	0.038±0.002	-	-
30th day	3.10±0.06	0.096±0.002	3.0±0.02	0.094±0.003	2.3±0.05	0.079±0.004	-	-
40th day	3.60±0.04	0.142±0.005	3.5±0.01	0.140±0.001	2.7±0.03	0.086±0.002	-	-

Values are expressed as mean ± SE

3.1.2. Handling stress

The initial average length and weight were measured for samples of control groups and different treatment groups. The initial mean length and weight were 0.5 cm and 0.0015 g respectively. The group HS_2 was handled only on 6th day (when the larvae were 6DPH), reduction in average length and weight of the previously stressed group HS_1 was noted on 6th day sampling. Similarly HS_3, HS_4, HS_5 and HS_6 were handled on 12, 18, 24 and 30 DPH respectively and showed reduced length and weight compared to the control groups at different sampling periods. On 40th day, no handling was done, only sampling was done for all previously stressed groups which showed reduced growth rate in comparison to control groups (Table 2).

Table 2. Average length and weight of catla subjected to handling stress (HS)

Sampling days	Control		HS_1		HS_2		HS_3		HS_4		HS_5		HS_6	
	L(cm)	W(g)	L(cm)	W(g)	L(cm)	W(g)	L(cm)	W(g)	L(cm)	W(g)	L(cm)	W(g)	L(cm)	W(g)
3rd day	0.5± 0.03	0.0015± 0.0002	0.5± 0.03	0.0015± 0.0005	-	-	-	-	-	-	-	-	-	-
6th day	0.8± 0.03	0.0030± 0.001	0.58± 0.04	0.0017± 0.001	0.7± 0.03	0.0028± 0.0006	-	-	-	-	-	-	-	-
12th day	1.3± 0.05	0.005± 0.001	0.9± 0.06	0.0034± 0.001	1.1± 0.06	0.0038± 0.0003	1.2± 0.09	0.004± 0.001	-	-	-	-	-	-
18th day	1.9± 0.04	0.036± 0.004	1.6± 0.03	0.014± 0.004	1.4± 0.05	0.009± 0.006	1.3± 0.03	0.005± 0.002	1.7± 0.04	0.02± 0.01	-	-	-	-
24th day	2.5± 0.04	0.072± 0.003	2.0± 0.08	0.048± 0.004	1.9± 0.04	0.034± 0.001	1.6± 0.04	0.018± 0.004	1.8± 0.05	0.028± 0.007	2.4± 0.09	0.064± 0.006	-	-
30th day	3.1± 0.06	0.098± 0.003	2.6± 0.04	0.080± 0.005	2.2± 0.03	0.06± 0.003	2.0± 0.05	0.052± 0.006	1.9± 0.05	0.036± 0.007	2.5± 0.05	0.072± 0.006	3.0± 0.05	0.092± 0.04
40th day	3.6± 0.04	0.142± 0.006	2.9± 0.04	0.092± 0.004	2.6± 0.02	0.078± 0.006	2.2± 0.03	0.060± 0.009	2.1± 0.02	0.056± 0.005	2.7± 0.03	0.084± 0.002	3.2± 0.06	0.102± 0.07

Values are expressed as mean ± SE

3.2. Cortisol response to crowding and handling in catla

3.2.1. Crowding stress

The data on effect of crowding stress are presented in the Fig 1. Cortisol was detectable in the four groups, namely T_1:3000/m^2; T_2:6000/m^2; T_3:12000/m^2 and T_4:18000/m^2. Significantly, lower level ($P<0.05$) of cortisol were detected in T_1 compared to T_2 and T_3 in 3DPH. Moreover, the significant increased levels of cortisol were noted in all the higher stocking groups at the respective sampling periods. The highest cortisol levels were found in T_3 at 18DPH (54.6 ng/ml) and then declined sharply up to 40DPH. In T_4, cortisol levels rose very sharply up to 12DPH, and all the fish in this group died thereafter.

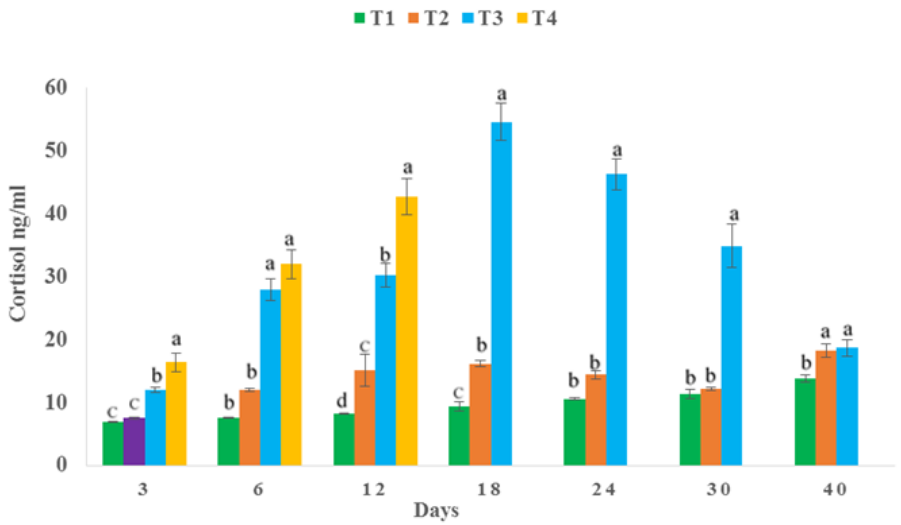

Figure 1. Cortisol levels (ng/ml) in response to crowding stress of catla. Different letters indicate significant differences ($P<0.05$) between groups (Mean ± SE).

3.2.2. Handling stress

The data on the cortisol response to handling stress of different age groups of spawn and fry of catla are presented in the Table 3.There was a sharp increase in cortisol levels in the early handled period (HS_1). There were significantly higher ($P<0.05$) cortisol levels in HS_2 and HS_1 groups compared to control. Similarly, cortisol levels were significantly elevated in different stressed groups (HS_3, HS_4, HS_5 and HS_6) in comparison to the control handled in different sampling periods. The highest cortisol level were detected in HS_6 stress group (100±7.10 ng/ml) at 40DPH. The cortisol level were returned to normal levels in HS_1, HS_2 and HS_3 with non-significant level with control group at 40DPH; however, values remained significantly higher in HS_4, HS_5 and HS_6 groups. The values in those groups were declining, indicating that they would return to normal level.

Table 3. Cortisol levels (ng/ml) in response to handling stress of catla.

Sampling days	Control	HS_1	HS_2	HS_3	HS_4	HS_5	HS_6
3rd day	7.1±0.84^{b}	46.2±2.80^{a}	-	-	-	-	-
6th day	8.0±0.52^{c}	31.3±1.70^{b}	54.6±2.86^{a}	-	-	-	-
12th day	8.8±0.84^{d}	23.8±2.34^{c}	38.2±1.15^{b}	64.5±3.52^{a}	-	-	-
18th day	9.1±0.88^{e}	19.2±2.28^{d}	32.4±2.18^{c}	48.6±2.88^{b}	86.2±4.62^{a}	-	-
24th day	10.4±1.21^{fe}	15.7±1.18^{ed}	25.8±1.65^{d}	39.6±3.32^{c}	62.4±5.20^{b}	90.1±5.37^{a}	-
30th day	11.5±0.95^{f}	14.9±0.97^{f}	19.3±1.70^{ef}	27.4±2.37^{df}	44.2±3.15^{c}	76.4±6.27^{b}	100±7.10^{a}
40th day	14.1±1.141^{d}	13.4±1.18^{d}	15.2±1.13^{d}	18.9±1.41^{d}	26.4±2.27^{c}	34.3±2.64^{b}	39.2±3.74^{a}

Values are expressed as mean ± SE in the rows with different superscripts differ significantly (P<0.05)

3.3. Measurement of Immunoglobulins through ELISA

3.3.1. Immunoglobulin levels in different crowding stress treatments during life stages of catla

The results of ELISA showed that immunoglobulins were detectable in the spawn from 3DPH onwards. The immunoglobulin levels decreased till 18DPH in T_2, T_3 and T_4 groups, although the levels were significantly higher (P<0.05) in lower stocking density group (T_1). An increment level of immunoglobulins from 18DPH to the end of the research period of 40DPH were detected. Moreover, the IgM level were remarkably down-regulated in higher stressed group fishes (T_3) in comparison to treatments of lower stocking densities T_2 and T_1 at that period. The IgM levels in different treatments during different life stages are shown in Fig. 2.

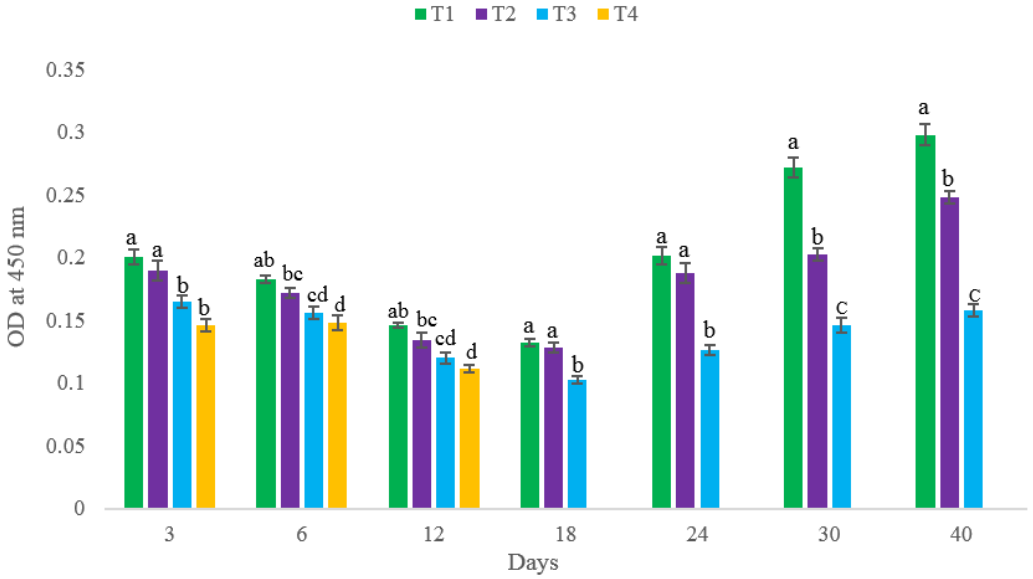

Figure 2. Immunoglobulin levels (OD) in different crowding stress of catla. Different letters indicate significant differences (P<0.05) between groups (Mean ± SE).

3.3.2. Immunoglobulin levels in different handling stress treatments during life stages of catla

The results of ELISA showed that immunoglobulins were detectable in the larvae from 3DPH. The immunoglobulin levels decreased till 18DPH. Significant elevated (P<0.05) levels of immunoglobulins were observed in the control group at early DPH compared to the groups of HS_1 and HS_2. The gradual increase was observed throughout the study period of 40th day for control groups. In response to handling, all the stressed groups have shown significant decrease (P<0.05) in antibody production in comparison to control 18DPH onwards. Other than group HS5, which was handled on 24th day, all the previously handled groups HS_1, HS_2, HS_3 and HS_4 showed significant reduction in immunoglobulin levels on 24th day. Similarly, on 30th day group HS_6 was handled out of water; all the previously stressed groups including HS_5 showed reduction in immunoglobulin levels. Observation on 40th day showed that there is slow recovery in all the previously stressed groups, but still the values remain significant lesser than the control. The IgM levels in different treatments during different life stages are shown in the Table 4

Table 4. Immunoglobulin levels (OD) in different handling stress of catla.

Sampling days	Control	HS_1	HS_2	HS_3	HS_4	HS_5	HS_6
3rd day	0.212±0.005[a]	0.182±0.005[b]	-	-	-	-	-
6th day	0.183±0.006[a]	0.146±0.006[b]	0.162±0.004[b]	-	-	-	-
12th day	0.159±0.007[a]	0.131±0.006[b]	0.136±0.007[b]	0.142±0.004b[a]	-	-	-
18th day	0.154±0.005[a]	0.123±0.005[b]	0.113±0.007[b]	0.109±0.003[b]	0.148±0.007[a]	-	-
24th day	0.225±0.004[a]	0..141±0.005[bc]	0.129±0.005[dc]	0.134±0.008[bc]	0.150±0.006[b]	0.218±0.005[a]	-
30th day	0.274±0.006[a]	0.153±0.008[c]	0.142±0.007[c]	0.146±0.005[c]	0.154±0.003[c]	0.160±0.006[c]	0.248±0.004[b]
40th day	0.325±0.005[a]	0.180±0.006[c]	0.167±0.005[c]	0.166±0.007[c]	0.164±0.0061[c]	0.174±0.004[c]	0.228±0.005[b]

Values are expressed as mean ± SE, in the rows with different superscripts differ significantly (P<0.05)

4. Discussion

Suppression of growth is often considered to be a good indicator of chronic stress. A variety of stressors challenges a fish at all times either in captivity or wild (Galhardo and Oliveira, 2009). In captivity, Nile tilapia, *O. niloticus* showed significant reduction (P<0.05) in the values of haemoglobin (Hb) and other blood parameters (Ugwem *et al.,* 2011). In captive condition of fish, overcrowding may be accompanied by additional stressors such as poor water quality, exposure to organic pollutants, and conspecific aggression and predation (Harper and Wolf, 2009).

High stocking density has been reported to cause decreased growth in salmonids (Vijayan and Leatherland, 1988) due to different factors such as decreased food consumption and social interactions (Wedemeyer, 1997) or decreased water quality (Pickering and Stewart, 1984). Moreover, high stocking density produces both hormonal and metabolic alterations (Leatherland and Cho, 1985; Schreck *et al.,* 1985) including a reduction in thyroid hormone activity (Vijayan and Leatherland, 1988). The high stocking density has been shown to exert adverse effects on growth, and there is a negative correlation between them in the fish culture (Andrews *et al.,* 1971; Refstie, 1982; Leatherland and Cho, 1985). The results of present study suggest that stocking density has a marked effect on growth of catla. There has been reduction in average length and weight, with increased cortisol levels in high density stressed groups in comparison to low stocking density groups, suggesting that stress induced growth suppression. Suppression of growth is often considered to be a good indicator of chronic stress (Pickering, 1990; Pankhurst and Van der Kraak, 1997; Barton and Iwama, 1991). Similarly, the present study showed reduction in average length and weight also in case of handling stress groups, with elevated levels of plasma cortisol in comparison to control. The present findings corroborated with results of Khan and Moseki (2018) reported significantly higher levels of shock proteins in both hepatopancreas and muscles of catla exposed with high light intensities. Moreover, as a consequence of stress due to intense light, a 12.5% of growth retardation was found in treated fish.

During earlier development, cortisol levels have shown a general pattern of relatively higher levels after fertilization followed by a decline until the time of hatching. It is believed that the cortisol is of maternal origin and that embryos are mobilizing the cortisol during early development (Paitz *et al.,* 2016). Typically, the first signs of cortical tissue in teleosts are observed before hatching (Chester Jones *et al.,* 1980), which was consistent with the findings of Stouthart *et al*. (1998) reported that upon handling (mechanical pressure during egg stage or netting during the larval stage) embryos and larvae increased their whole-body cortisol levels. In the present study conducted on catla spawn and fry, all the stressed groups showed sharp increase in cortisol levels in response to acute handling throughout the study period. In general, plasma cortisol levels rise at the beginning of high stocking density condition and decrease to initial values in a few days (Pickering and Stewart, 1984; Tort *et al.,* 2004), indicated the adaptation of the fish to the new situation. This effect has been described for different species, including coho salmon (Patino *et al.,* 1986) and Arctic charr *Salvelinus alpinus* (Jorgensen *et al.,* 1993). Vijayan *et al*. (1990) found high plasma cortisol values in brown trout held at high stocking density. However, in the present study, fish held at high stocking density showed significantly higher levels of plasma cortisol than those held at low density, suggesting the incapacity of these fish to reach adaptation under these conditions. A similar elevation of plasma cortisol with high rearing density has been described for Atlantic salmon, *Salmo salar* (Mazur and Iwama, 1993).

In the present study the IgM production in catla was observed from 3DPH for control and all the stressed groups. In the previous work by Lokesh (2009) in catla, the IgM production was reported from 21DPH onwards, the reason being the variability in the environmental conditions leading to the variability in the period of development of functional immunity. Indian major carp, catla showed lower non-specific immune values indicated its weak resistance compared with rohu, *Labeo rohita* (Sahoo *et al*., 2009). One degree fall of temperature from 28 °C resulted into

10.7 % mortality of larvae of catla (Sharma *et al*., 2016). The autologous production of IgM in channel catfish was first reported on 21st day (Petrie-Hanson and Ainsworth 1999). The subsequent work by Petrie-Hanson and Ainsworth (2001) reported the appearance of IgM on 7, 10, 14DPH. The first appearance of IgM in carp was reported from 2nd week post hatch (Koumans-van Diepen *et al.,* 1994). The present study has revealed that stress induces elevated plasma cortisol levels leading to growth suppression and reduction in IgM production as consequence of crowding stress and handling stress on ontogeny of catla, although the age at which humoral response is initiated is not affected by stress. Transportation stress demonstrated reduction in the IgM concentration and fry of catla were more sensitive to stress

than the fingerling (Ahmed and Shenoy, 2012). In a study by Saha *et al*. (2004) *in vitro* administration of cortisol was shown to reduce the number of IgM-secreting cells and IgM secretion in common carp.

In the present study, the results show that catla held at high stocking density appear to be experiencing stress, as indicated by the significant elevation in plasma cortisol. This crowding stress affected the immune activity. The fish showed no signs of disease but displayed symptoms of immunosuppression with reduced antibody or IgM production in the early stages of development. In case of crowding stress, low stoking density groups increase in the level of Immunoglobulins were detected on 24th day and gradually increased thereafter till the study period of 40th day (Fig. 2). On the other hand, in stressed groups the increase in antibody production was very slow compared to the non-stressed group. In response to handling stress, all the stressed groups have shown significant decrease in immunoglobulin production in comparison to control 18DPH onwards (Table 4). Observation on 40th day showed that there was a slow recovery in all the previously stressed groups, but still the values remain significantly lesser than the control, clearly explaining that handling stress induced suppression in the IgM production on ontogeny of catla, but not the ontogeny of humoral immune response.

5. Conclusion

In our investigation, both crowding and handling stress have resulted in elevated levels of plasma cortisol as a primary response in early developmental stages of catla. As a consequence of crowding and handling stress, elevated levels of plasma cortisol had a deleterious impact on growth of catla. Both crowding and handling stress induced immune suppression on ontogeny of catla linked with elevated levels of plasma cortisol. There is no effect as the onset of ontogeny of humoral immunity, but the strength of the responses decreases with increasing level of crowding as well as handling stress. Both crowding and handling stress need to be minimized for producing healthy catla fry.

Funding

This work was funded by the project # 8086, Department of Biotechnology (DBT), Government India.

Acknowledgments

All the authors are grateful to the DBT, India for financial supports. The 2nd and 4th authors are thankful to the Indian Council of Agricultural Research (ICAR) for sponsoring their Ph.D. and for the award of the Netaji Subhas International Fellowship 2015-2016.

Conflict of Interest

Authors have no conflict of interest to declare.

References

Ahmed I and Shenoy KB. 2012. Effect of transportation stress on the humoral immunity of catla fry and fingerlings. *J Acad Ind Res*., **1**: 401-403.

Andrews JW, Knight LH, Page JW, Matsuda Y and Brown EE. 1971. Interactions of stocking density and water turnover on growth and food conversion of channel catfish reared in intensively stocked tanks. *Prog Fish-Cult*., **33**: 197-203.

Avtalion RR and Mor A. 1992. Monomeric IgM is transferred from mother to egg in tilapias. *Isr J Aquacult*., **44**:93-98

Bag MR, Makesh M, Rajendran KV and Mukherjee SC. 2009. Characterization of IgM of Indian major carps and their cross-reactivity with anti-fish IgM antibodies. *Fish Shellfish Immunol*., **26**: 275-278.

Barton BA and Iwama GK. 1991. Physiological changes in fish from stress in aquaculture with emphasis on the response and effects of corticosteroids. *Rev Fish Dis*., **1**:3-26.

Breuil G, Vassiloglou B, Pepin JF and Romestand B. 1997. Ontogeny of IgM-bearing cells and changes in the immunoglobulin M-like protein level (IgM) during larval stages in sea bass (*Dicentrarchus labrax*). *Fish Shellfish Immunol*., **7**: 29-43.

Chester Jones I, Mosley W, Henderson IW and Garland HO. 1980. The interrenal gland in pisces. *General, comparative and clinical endocrinology of the adrenal cortex*, **3**:396-523.

Feist G and Schreck CB. 2001. Ontogeny of the stress response in Chinook salmon, *Oncorhynchus tshawytscha. Fish Physiol Biochem.*, **25**: 31–40.

Fuda H, Hara A, Ymazak IF and Kobayashi K. 1992. A peculiar immunoglobulin M (IgM) identified in eggs of chum salmon (*Oncorhynchus keta*). *Dev Comp Immunol*., **16**:415-423.

Furuta T, Trongv Anichnam, Zakaguchi J, Akaba Y and Ashi H. 1995. Indirect enzyme linked immunosorbant assay (ELISA) for the detection of antibody in serum of Japanese flounder. *Fisheries Sci*., **61**: 663-667.

Galhardo L and Oliveira RF. 2009. Psychological stress and welfare in fish. *Annu. Rev. Biomed. Sci*., **11**: 1-20.

Harper C and Wolf JC. 2009. Morphologic effects of the stress response in fish. *Ilar Journal*, **50**: 387-396.

Hayman JR and Lobb CJ. 1993. Immunoglobulin in the eggs of the channel catfish (*Ictalurus punctatus*). *Dev Comp Immunol*., **17**: 241-248.

Honnananda BR. 2008. Monoclonal antibodies for characterization and detection of immunoglobulins of Indian Major Carp, *Catla catla* (Hamilton). Ph.D thesis, submitted to the Karnataka Veterinary Animal and Fisheries Sciences University, Bidar, India.

Jorgensen EH, Christiansen JS and Jobling M. 1993. Effects of stocking density on food intake, growth performance and oxygen consumption in Arctic charr (*Salvelinus alpinus*). *Aquaculture* **110**: 191-204.

Khan NA and Moseki P. 2018. Investigating the role of heat shock proteins and melanophores during stress caused by high light intensity in Indian major carp, *Catla catla*. *Int. J. Pharm. Sci*., **9**: 5226-5233.

Koumans-van Diepen JCE, Taverne-Thiele JJ, Van Rens BTTM and Rombout JHWM. 1994. Immunocytochemical and flow cytometric analysis of B cells and plasma cells in carp (*Cyprinus carpio* L.); an ontogenetic study. *Fish Shellfish Immunol*., **4**: 19-28.

Lavanya S, Ramesh M, Kavitha C and Malarvizhi A. 2011. Hematological, biochemical and ionoregulatory responses of Indian major carp *Catla catla* during chronic sub-lethal exposure to inorganic arsenic. *Chemosphere*, **82:** 977-985.

Leatherland JF and Cho CY. 1985. Effect of rearing density on thyroid and interregnal gland activity and plasma and hepatic metabolite level in rainbow trout, Salmo gairdneri. *J Fish Biol*., 27: 583-592.

Lokesh J. 2009. Ontogeny of humoral immunity in Indian major carps – studies using monoclonal antibody based ELISA. M.F.Sc., thesis, submitted to the Karnataka Veterinary Animal and Fisheries Sciences University, Bidar, India

Lowry OH, Rosebrough NH, Farr AL and Randall RJ. 1951. Protein measurement with folin phenol reagent. *J Biol Chem*., **183**: 265-275.

Mazur CF and Iwama GK. 1993. Effect of handling and stocking density on haematocrit, plasma cortisol, and survival in wild and hatchery reared Chinook salmon (*Oncorhynchus tshawytscha*). *Aquaculture*, **112**: 291-299.

Okpashi VE, Ogugua VN, Ubani CS and Juliet NO. 2018. An evaluation of contaminant body burdens in selected fish species: associating toxicity to upgrade the hazard assessment. *Jordan J Biol Sci*., **11**:171-177.

Paitz RT, Bukhari SA and Bell AM. 2016. Stickleback embryos use ATP-binding cassette transporters as a buffer against exposure to maternally derived cortisol. *Proc R Soc Lond B Biol Sci*, **283**: 20152838p.

Pankhurst NW and Van Der Kraak G. 1997. Effects of stress on reproduction and growth of fish. In: Iwama, G.K., Pickering, A.D., Sumpter, J.P., Schreck, C.B. (Eds.), Fish stress and Health in Aquaculture. Cambridge University Press, UK. p. 73-93.

Patino R, Schreck CB, Banks JL and Zaugg WS. 1986. Effects of rearing conditions on the developmental physiology of smolting coho salmon. *Trans Am Fish Soc*., **115**: 828-837.

Perumal S, Thirunavukkarasu AR and Pachiappan P. 2015. Advances in marine and brackishwater aquaculture. Springer India.

Petrie-Hanson L and Ainsworth AJ. 2001. Ontogeny of channel catfish lymphoid organs. *Vet Immunol. Immunopathol*., 81: 113-127.

Petrie-Hanson L and Ainsworth AJ. 1999. Humoral immune responses of channel catfish (*Ictalurus punctatus*) fry and fingerlings exposed to *Edwardsiella ictaluri*. *Fish Shellfish Immunol*. **9**:579–589.

Pickering AD. 1981. Introduction: The concept of biological stress. In *Stress and Fish*, Pickering, A.D., (Ed.) Academic Press, London, p. 1-10

Pickering AD, Pottinger TG and Christie P. 1982. Recovery of the brown trout, *Salmo trutta* L., from acute handling stress: a time course of study. *J Fish Biol*., **20**: 229-244.

Pickering AD and Stewart A. 1984. Acclimation of the interrenal tissue of the brown trout, *Salmo trutta* L., to chronic crowding stress. *J Fish Biol*., 24: 731-740.

Pickering AD. 1990. Stress and the suppression of somatic growth in teleost fish. *Prog Clin Biol Res*., **342**: 473-479.

Poli BM, Parisi G, Scappini F and Zampacavallo G. 2005. Fish welfare and quality as affected by pre-slaughter and slaughter management. *Aquacul Int*., **13**: 29-49.

Refstie T. 1982. Preliminary results: difference between rainbow trout families in resistance against vibriosis and stress. *Dev Comp Immunol*., **2**: 205-209

Saha NR, Usami T and Suzuki Y. 2004. In vitro effects of steroid hormones on IgM-secreting cells and IgM secretion in common carp (*Cyprinus carpio*). *Fish Shellfish Immunol*., **17**: 149-158.

Sahoo PK, Kumari J and Mishra BK. 2005. Non-specific immune responses in juveniles of Indian major carps. *J Appl Ichthyol*., **21**: 151-155.

Schreck CB, Patino R, Pring CK, Winton JR and Holway JE. 1985. Effects of rearing density on indices of smoltification and perfomance of coho salmon, *Oncorhynchus kitsutch*. *Aquaculture*, **45**:345–358.

Sharma JG, Singh SP, Mittal P and Chakrabarti R. 2016. Impact of temperature gradient on the Indian major carp *Catla catla* larvae. *Proc Natl Acad Sci India Sect B Biol Sci.*, **86**: 269-273.

Stouthart AJHX, Lucassen ECHET, Van Strien FJC, Balm PHM, Lock RAC and Wendelaar Bonga SE. 1998. Stress responsiveness of the pituitary-interrenal axis during early life stages of common carp (*Cyprinus carpio*). *J Endocrinol*., **157**:127–137

Sunyer JO, Gomez E, Navarro V, Quesada H and Tort L. 1995. Physiological responses and depression of humoral components of the immune system in gilthead seabream (*Sparus aurata*) following daily acute stress. *Can J Fish Aquat Sci*., **52**: 2339-2346.

Takemura A. 1993. Changes in an immunoglobulin M (IgM)-like protein during larval stages in tilapia, *Oreochromis mossambicus*. *Aquaculture*, 115: 233-241.

Tengjaroenkul B and Neeratanaphan L. 2020. Acute effect of cadmium chloride on chromosomal abnormalities in the Nile tilapia fish In Vivo. *Jordan J Biol Sci*., **13**:127-132

Tort L, Balasch JC and Mackenzie S. 2004. Fish health challenge after stress. Indicators of immunocompetence. *Contrib Sci*., **2**: 443- 454.

Ugwem U, Ojo AG and Funkeye E. 2011. Haematological responses of Wild Nile Tilapia *Oreochromis niloticus* after acclimation to captivity. *Jordan J Biol Sci*., **4**: 225-230.

Vijayan MM, Ballantyne JS and Leatherland JF. 1990. High stocking density alters the energy metabolism of brook charr, *Salvelinus fontinalis. Aquaculture* **88**: 371–381.

Vijayan MM and Leatherland JF. 1988. Effect of stocking density on the growth and stress-response in brook charr, *Salvelinus fontinalis*. *Aquaculture*, **75**: 159–170.

Wedemeyer GA. 1997. Effects of rearing conditions on the health and physiological quality of fish in intensive culture. In: *Fish Stress and Health in Aquaculture* Iwama, G.K., Pickering, A.D., Sumpter, J.P.and Schrek, C.B. (Eds), Society for Experiment Biology, Seminar Series 62. Cambridge: Cambridge University Press, p. 35-72.

Yousif AN, Albright LJ and Evelyn TPT. 1995. Immunological evidence for the presence of an IgM-like immunoglobulin in the eggs of coho salmon *Oncorhynchus kisutch*. *Dis Aquat Org*., **23**:109-114.

JJBS

Volume 14, Number 5,December 2021
ISSN 1995-6673
Pages 919 – 923

Jordan Journal of Biological Sciences

Covid-19: Viral Pathogenesis and The Host Immune Response

Nasiru Usman Adabara[1], Sherifat Ozavize Enejiyon[1,*] , Faruk Adamu Kuta[1], Ayanwale Oluwatobi Abraham[1] and Samia Alkhalil[2]

[1] *Department of Microbiology, School of Life Sciences, Federal University of Technology Minna, Nigeria;* [2]*Department of Clinical Laboratory Sciences, College of Applied Medical Sciences, Shaqra University, Saudi Arabia.*

Received: Sep 9, 2020; Revised: Dec 7, 2020; Accepted: January 12, 2021

Abstract

COVID-19, a pandemic caused by a betacoronavirus known as SARS-CoV-2 (severe acute respiratory syndrome coronavirus-2) has recorded 18 354 342 number of cases and 696 147 deaths globally as of August 5, 2020. It was first recorded in Wuhan, China in 2019. The virus bears close resemblance to SARS-CoV-1 and MERS-CoV that have emerged and caused outbreaks of deadly human diseases. The main component of the virus responsible for the host range specific tropism and pathogenicity is the S-glycoprotein. The primary route of transmission of infection is through human to human via close contact, usually through spraying of droplets from sneeze or cough of an infected person. The incubation period for COVID-19 following viral infection is between 2 to 14 days. The target cells of SARS-CoV-2 are those cells that highly expressed ACE2 (angiotensin-converting enzyme 2). Viral receptor binds to the ACE2, to allow the virus entry into the cell via endosomal pathway. The host innate immune system detects the viral infection by using pattern recognition receptors which result in activation of downstream signalling cascade. Understanding the virulence factors contributing to pathology, host immune responses and strategies employed by the virus in bypassing host immune response is paramount in developing therapeutic options that can help to tackle the COVID-19 pandemics.

Keywords: COVID-19, coronavirus, receptors, immune response, pathogenesis.

1. Introduction

Corona Virus Disease 2019, abbreviated as COVID-19, is caused by a novel betacoronavirus, SARS-CoV-2 (severe acute respiratory syndrome coronavirus-2) (Kowalik *et al*., 2020). It is a newly emerging virus previously named 2019 novel coronavirus (2019-nCoV). The international committee on the taxonomy of viruses (ICTV) christened the new coronavirus as severe acute respiratory syndrome coronavirus 2 (SARS-CoV-2) on the 11th day of February, 2020 due to its close genetic relatedness to SARS-CoV that caused an outbreak in 2002/2003 (Wu *et al*., 2020; CSG-ICT, 2020). An outbreak of the disease was first recorded in Wuhan, Hubei Province of China in December 2019, from which it disseminated to other parts of China and every other country. It was later declared a pandemic in March 2020 by the World Health Organization (Cucinotta and Vanelli, 2020). Currently, more than 6 million people have been infected globally with over 369, 258 deaths (WHO, 2020). The newly emerging virus, SARS-CoV-2 is an enveloped, un-segmented, positive sensed single stranded-RNA virus found within the subfamily *"Coronavirinae"*, which includes viruses that infect humans and mammals. Three of these viruses known to cause human diseases have emerged during the last two decades and have caused widespread outbreaks of deadly human diseases. These highly pathogenic zoonotic coronaviruses include SARS coronavirus-1(SARS-CoV-1) which was first observed in 2002, Middle East respiratory syndrome coronavirus (MERS-CoV) first identified in 2012 and SAR-CoV-2 which was first reported towards the end of 2019 (Dorsten *et al*., 2003; Zaki *et al*., 2012; Wu *et al*., 2020).

The clinical manifestation, morbidity rate, mortality rate and the case fatality ratio have slowly emerged. However, there are still some confusion about the pathogenesis and the specific role of the host immune responses in combating the infection. A lot of conclusion is being drawn from cumulated data on the previous coronaviruses namely SARS-CoV-1 and MERS-CoV because of their close genetic relatedness to the novel SARS-CoV-2. This review examines issues related to SARS-CoV-2 pathogenesis as well as the specific role played by the host immunity during infection drawing insights from other published works on the outbreak of COVID-19.

2. Virulence Factors

The occurrence and course of clinical manifestation in COVID-19 depend on pathogen factors which include virus type, virulence factors, viral load, mutation, replication and viability of the virus *in vitro* (Tang *et al*., 2020). Meanwhile, host factors such as the age of an infected person and the presence of comorbidities have also been identified to affect the clinical outcome of the viral infection (Abduljalil and Abduljalil, 2020).

* Corresponding author e-mail: enejiyon.sherifat@futminna.edu.ng.

Coronaviruses are crown-like shaped, enveloped viruses of about 100 nm in diameter that are surrounded by spikes which protrude from the envelope. The virus genome is complemented by about 14 open reading frames (ORF). Each ORF encodes an array of proteins, accessory proteins, structural proteins and non-structural proteins that have important roles in virulence and propagation of the virus. The virus consists of four important structural proteins, membrane (M) glycoprotein, envelope (E) glycoprotein spike (S) glycoprotein and nucleocapsid (N) glycoprotein, as well as 16 nonstructural proteins (Fehr and Perlman, 2015; Kim *et al*., 2020).

Membrane and envelope glycoproteins are required for virus maturation, assembly, and replication. Together, they form the viral envelope as well as determine its shape. N-glycoprotein forms an enclosure around the virus RNA genome known as viral nucleocapsid while spike glycoprotein is the elemental determinant of pathogenicity and host tropism (Hulswit *et al*., 2016; Felsenstein *et al*., 2020).

S glycoprotein is a transmembrane protein found in the outer region of the virus with a molecular weight of 150 kDa. It enables the binding of viruses to host cells by forming homotrimers projecting on the surface of the virus to bind ACE2 found in cells of various organs including the kidney, liver and the lung (Fehr and Perlman, 2015). Furin-like protease of host cell split S protein into two subunits (S1 and S2). S1 subunit consists of two important domains; receptor binding domain (RBD) and N-terminal domain (NTD) (Wall *et al*., 2020). The RBD of the S glycoprotein has six critical amino acids that are responsible for binding to receptor ACE2 on host cells as well as the determination of virus cellular and host tropism (Andersen *et al*., 2020). On the other hand, the S2 functions in mediating the fusion between the virus and host cellular membrane (Guo *et al*., 2020).

Nonstructural proteins (nsps) carry out very essential roles in several processes in viruses as well as in the host cells; Nsp5 and Nsp3 encode proteases enzymes; chymotrypsin-like main protease and papain-like protease respectively. These enzymes help in the expression of cytokines, production and cleavage of viral amino acids polyprotein.

The virus demonstrates a high replication number (Anastassopoulou *et al*., 2020; Li *et al*., 2020) and it is more infectious probably as a result of acquisition of furin-cleavage site, which makes it spread very easily amongst people than the previous coronaviruses (Liu *et al*., 2020). The genome of SARS-CoV-2 consists of a sequence encoding amino acids PRRA and R within the original sequence of the S glycoprotein, generating a polybasic cleavage site (RRAR) for Furin protease at the junction of S1 and S2, leading to increase in the virus infectivity (Andersen *et al*., 2020; Liu *et al*., 2020). Combination of RBD and an insertion of cleavage site in genome of the virus have been reported to increase its infectivity in a study involving analysis of genomic sequences of SARS-CoV-2 (Wu *et al*., 2020).

SAR-COV-2 has been indicated to evolve into leucine (L) and serine (S) types from the analyses of 103 SARS-CoV-2 genomes, where the serine type might be the ancestral type and leucine type might spread rapidly and be more aggressive (Tang *et al*., 2020). It has been suggested that variations in genome of SARS-CoV-2 might provide a basis for multiple sources outbreak (Zhang *et al*., 2020; Ceraolo and Giorgi, 2020**)**.

3. Viral Recognition by the Immune System

Pathogenesis of coronavirus disease is still under research; the first site of infection with SARS-CoV-2 is airways epithelial cells. COVID-19 affects only the lungs in most patients as it is mainly a respiratory disease. The transmission of viral infection is primarily between humans through spraying droplets from cough or sneeze of an infected person in close contact with a susceptible person. The incubation period of COVID-19 is between 2 to 14 days, during which the virus can be spread (CDC, 2020). On the average, an infected person has the potential to infect at least two other people (Wu *et al*., 2020). Fever, cough, sore throat, fatigue and shortness of breath are the most common symptoms of the disease.

The functional receptor of SARS-CoV-2, angiotensin converting enzyme 2 (ACE2) plays a critical role in the pathogenesis of the virus. It provides the virus the opportunity of entry into human cells (Shereen *et al*., 2020; Lan *et al*., 2020). S glycoprotein of SARS-CoV-2 binds to ACE2. The binding domains of S-protein are present in 331 to 524 residues. Coding variants of ACE2 display high similarity in structural and binding affinity with the S glycoprotein of SARS-CoV-2. The cells of the host most commonly targeted by SARS-CoV-2 are those cells that highly expressed ACE2 and these include epithelial cells of oesophagus and ileum, alveolar cells, proximal tubule cells of kidney, myocardial cells and bladder urothelial cells (Chen *et al*., 2020; Zhou *et al*., 2020). Subsequent to the receptor binding, the virus gains entry into the cell through the endosomal pathway. The virus entry is mediated by S glycoprotein activated by the host cell type II transmembrane serine protease (TMPRSS2) present on the host cell surfaces (Ou *et al*., 2020). TMPRSS2 will clear the ACE2 and also activate S glycoproteins attached to the receptor by cleaving it into S1 and S2 subunit (Simmons *et al*., 2013; Rabi *et al*., 2020). S2 subunit facilitates the fusion of virus to the host cell membranes. Upon entry, the genomic material of the virus is released within the cytoplasm. The virus mRNA released into the cytoplasm is subjected to translation in the nuclei to produce replicase polyproteins (pp1a and pp1b) by ribosomal frame-shifting (Masters, 2006). The polyproteins are processed by protease enzymes encoded in Nsp3 and Nsp5. Subsequent cleavage of pp1a and pp1b into small proteins (Nsps1–Nsps11 and Nsps1–Nsps16 respectively) occurs. Viral RNA and nucleocapsid proteins interaction occur in the endoplasmic reticulum-Golgi complex compartment leading to the assemblage of the virion which can be liberated from the infected cell through exocytosis to infect adjacent cells (Hoffmann *et al*., 2020; Zhou *et al*., 2020).

4. Immune Effector cells and their Activation

With RNA viruses especially the coronaviruses, the human innate immune system uses the PRRs (pattern recognition receptors) such as TLR (toll-like receptors), RIG-I (retinoic acid inducible gene-I-like receptor), NLR (nucleotide-binding oligomerization domain like receptor), MDA5 (melanoma differentiation-associated protein 5

receptor) and other free small receptor molecules located in the cytoplasm to recognize coronavirus PAMPs (pathogen associated molecular patterns) in order to detect the viral infection (Li *et al*., 2020; Kumar *et al*., 2020). PAMPs in the form of viral genomic RNA comprising nucleic acids, carbohydrate moieties, glycoproteins, lipoproteins and/or the intermediates products of viral replication (dsRNA) are recognized by the PRR. Each of the PRRs can then induce various biological responses through the activation of adapter proteins. TLRs results in the translocation of NF-κB and IRF3 while RIG-I and MDA5 effect in the activation of IRF3 (Yi *et al*., 2020; Li *et al*., 2020).

Recognition events by PRRs lead to the activation of the downstream signaling cascade using specific signal adapter proteins to produce immune system effector cells followed by their translocation into the nuclei. NF-κB and IRF3 (transcription factors) promote the synthesis of type I interferons (IFNs) and other pro-inflammatory cytokines in the nuclei (de Witt *et al*., 2016). Type I IFN via the cell surface receptor; IFN-α receptor complex (IFNAR) subsequently activates the Janus kinase-signal transducer and activator of transcription (JAK-STAT) signaling pathway, where JAK1 and JAK2 kinases phosphorylate STAT 1 and 2. STAT1/2 produce a complex with IRF9 and together, enter the nucleus to begin the transcription of interferon-stimulated genes, which leads to the suppression of viral replication by limiting viral spread and promotion of phagocytosis of viral particles by macrophages (Bergmann and Silvermann, 2020; Prompetchara *et al*., 2020). However, excess expression of pro-inflammatory cytokines and chemokines such as IFN-γ, IFN-α, IL-33, IL-21, IL-18, IL-12, IL-6, IL-1β, TGFβ, TNF-α and MCP-1 from effector cells of immune system, result in hyper-inflammation which will ultimately lead to acute respiratory distress syndrome (ARDS) (Chen *et al*., 2010; Li *et al*., 2020).

T lymphocytes (CD4+) are promptly activated into T-helper (Th1) cells when fragmented viral structural protein particles are presented by the major histocompatibility complex or human leukocyte antigen (HLA) and then recognized by virus-specific cytotoxic T lymphocytes. CD4+ T promotes the production of virus specific antibody by activating T cell-dependent B cells. Activated B cells will produce two specific immunoglobulins (Ig); IgM that last for only 12 weeks and IgG that can last for longer period and also provide long lasting immunity (Rabi *et al*., 2020; Astuti and Ysrafil, 2020). Activated T-helper cells are able to stimulate CD8+, which are part of the effectors of T lymphocyte that are cytotoxic and can destroy coronaviruses infected cells. Pro-inflammatory cytokines including interleukins-12 and interferon-α are generated by T-helper cells via NF-kB signaling pathway. Generated cytokines induce inflammatory T cells, monocytes and neutrophils which induce inflammatory response (Zhou *et al*., 2020). These monocytes and T cells might move into blood circulation from where monocytes transformed into macrophages in tissues (Tang *et al*., 2020). Several cytokines including IL-6 in combination with dendritic cells (Nazinitsky and Rosenthal, 2010) trigger cytokine release syndrome (CRS) (Zhou *et al*., 2020). These responses allow the suppression of the viral infection inside the infected organs, clearance of the virus as well as the repair of the damaged tissues.

5. Virus Response to Host Immune System

Viral pathogenicity depends, in part, on the response of the virus against immune responses mounted by the host immune system. There are various strategies employed by coronaviruses in their response to the host immune system (Kikkert, 2020). Below are some of the specific mechanisms detected to play protective role in coronaviruses pathogenicity.

Viruses try to escape recognition by PRR in the cytosol through the formation of vesicle using some non-structural proteins by forming a capsule composed of protein and intracellular membrane around its genetic material. Viruses avoid recognition by MDA5 through the synthesis of RNA terminus crown to hide its 5' end thereby mimicking RNA terminus crown of human cells (Li *et al*., 2020; Petrosillo *et al*., 2020; Siddique and Mehra, 2020).

Apart from avoiding recognition by PRR which is important for the initiation of host immune response, coronaviruses employ mechanisms that directly disrupt host defenses. Evidence of interruption of some processes of protein synthesis within cells infected with coronaviruses has been provided (Gaete-Argel *et al*., 2019). Viruses employ proteases to disrupt regulatory processes such as interferon activation within the infected cells that are dependent on ubiquitin. SARSCoV-2 has been found to cause the alteration of ubiquitination and the degradation of RIG-I/MDA5/MAVS/TRAF3/IRF3/IRF7 pathways (Siu *et al*., 2009). Important pathways for host specific responses against viruses such as RIG I and IRF3/7 can be targeted and blocked by viral proteins in various ways; inhibition of mitochondrial antiviral signaling (MAVS) proteins synthesis, increase in stimulation of pro-inflammatory cytokines, NF-kB and necroptosis leading to inadequate synthesis of type 1 interferon and impairment of specific immune responses which will invariably result in hyper-inflammation, enhanced cellular death and cytokine storm (Li *et al*., 2020; Yi *et al*., 2020).

SARS-CoV-2 viral proteins target and inhibit various signaling proteins involved in the activation of TLRs/TRIF/MyD88/IkB/NF-kB/MAPK/AP-1 pathway thereby causing inhibition of the synthesis of pro-inflammatory cytokines (Conti *et al*., 2020). Nonstructural proteins are involved in blockage and inhibition of interferon pathway and NF-κB pathway while interferon-inducible mRNA nuclear export complex can be impeded by Orf6 (Dai *et al*., 2020; Gordon *et al*., 2020).

Coronavirus can combine with non-neutralizing antibodies to form immune complexes which often lead to a severe inflammation (Hohdatsu *et al*., 1998; Jaume *et al*., 2011). These complexes can bind to the Fc receptor of specific neutralizing antibodies thereby enabling SARS-CoV-2 to penetrate and multiply in target cells such as antigen-presenting cells and phagocytes. Maffia *et al.* (2019) reported that SARS-CoV-2 directly infects macrophages and T cells by attaching to CD209 receptor on macrophages thereby invading effector cells in vascular and cardiac tissues.

Impairment of protective immune responses by SARS-CoV-2 allows it to easily propagate and cause severe damage to infected cells in organs such as intestine and kidney where ACE2 are highly expressed. Pro-inflammatory cells such as granulocytes and macrophages

in the damaged cells induce inflammatory response in the lung (Shi *et al*., 2020).

6. Conclusion

COVID-19 caused by SARS-CoV-2 is still a pandemic affecting the lives of millions of people worldwide. SARS-CoV-2 propagates and replicate easily in target cells by actively disrupting host immune responses. It induces hyper-inflammation which often leads to cytokine storm or life threatening condition by recruiting uninfected cells to the focal point of infection and/or infecting effector cells of immune system.. Understanding the virulence factors contributing to pathology, host immune responses and strategies employed by the virus in bypassing host immune response is paramount in developing therapeutic options that can help to tackle the COVID-19 pandemics.

References

Abduljalil JM and Abduljalil BM. 2020. Epidemiology, genome, and clinical features of the pandemic SARS-CoV-2: a recent review. *New Microbe and New Infect*., **35(100672)**: 1-8.

Anastassopoulou C, Russo L, Tsakris A and Siettos C. 2020. Data-based analysis, modelling and forecasting of the novel coronavirus (2019- nCoV) outbreak. *PLoS One*., **15(3)**: e0230405.

Andersen KG, Rambaut A, Lipkin WI, Holmes EC and Garry RF. 2020. The proximal origin of SARS-CoV2. *Nat Med*., **26**: 450-452.

Astuti I and Ysrafil. 2020. Severe Acute Respiratory Syndrome Coronavirus 2 (SARSCoV-2): An overview of viral structure and host response. *Diabetes Metab Syndr*., **14(4)**: 407-412.

Bergmann CC and Silvermann RH. 2020. COVID-19: Coronavirus replication, pathogenesis, and therapeutic strategies. *Cleve Clin J Med*., **87(6)**: 321-327.

Center for Disease Control and Prevention (2020). "Symptoms of Novel Coronavirus (2019-nCoV)". Https://www.cdc.gov/coronavirus/2019-ncov/about/symptoms.html (May 24, 2020).

Ceraolo C and Giorgi FM. 2020. Genomic variance of the 2019-nCoV coronavirus. *J Med Virol*., **92(5)**: 522–528.

Chen L, Li X, Chen M, Feng Y and Xiong C. 2020. The ACE2 expression in human heart indicates new potential mechanism of heart injury among patients infected with SARS-CoV-2. *Cardiovas Res*., **116(6)**: 1097-1100.

Conti P, Ronconi G, Caraffa A, Gallenga C, Ross R, Frydas I *et al*. 2020. Induction of pro-inflammatory cytokines (IL-1 and IL-6) and lung inflammation by Coronavirus-19 (COVI-19 or SARS-CoV-2): anti-inflammatory strategies. *J Biol Regul Homeost Agents.*, **34(2)**: 327-331.

Coronaviridae Study Group of the International Committee on Taxonomy (CSG-ICT) of Virus. 2020. The species severe acute respiratory syndrome-related coronavirus: classifying 2019-nCoV and naming it SARS-CoV-2. *Nat Microbiol*., **5(4)**: 536-544.

Cucinotta D and Vanelli M. 2020. WHO declares COVID-19 a pandemic. *Acta Biomed*., **91(1)**: 157-160.

Dai W, Zhang B, Jiang XM, Su H, Li J, Zhao Y *et al*. 2020. Structure-based design of antiviral drug candidates targeting the SARS-CoV-2 main protease. *Science*., **368(6497)**: 1331-1335.

de Wit E, van Doremalen N, Falzarano D and Munster VJ. 2016. SARS and MERS: recent insights into emerging coronaviruses. *Nat Rev Microbiol*., **14(8)**: 523-534.

Drosten C, Gunther S, Preiser W, van der Werf S, Brodt HR, Becker S *et al*. 2003. Identification of a novel coronavirus in patients with severe acute respiratory syndrome. *N Engl J Med*., **348(20)**: 1967–1976.

Fehr AR and Perlman S. 2015. Coronaviruses: an overview of their replication and pathogenesis. *Method Mol Biol*., **1282**: 1–23.

Felsenstein S, Herbert JA, McNamara PS and Hedrich CM. 2020. COVID-19: immunology and treatment options. *Clin Immunol*., **215**: 108448.

Gaete-Argel A, Márquez CL, Barriga GP, Soto-Rifo R and Valiente-Echeverria F. 2019. Strategies for success. Viral infections and membraneless organelles. *Front Cell Infect Microbiol.*, **9**: 336.

Gordon DE, Jang GM, Bouhaddou M, Xu J, Obernier K, White KM *et al*. 2020. A SARS-CoV-2 protein interaction map reveals targets for drug repurposing. *Nature*, **583(7816)**: 459-468.

Guo YR, Cao QD, Hong ZS, Tan YY, Chen SD, Jin HJ *et al*. 2020. The origin, transmission and clinical therapies on coronavirus disease 2019 (COVID-19) outbreak–an update on the status. *Mil Med Res*., **7(1)**: 11.

Hoffmann M, Kleine-Weber H and Pohlmann S. 2020. A multibaic cleavage site in the spike protein of SARS-CoV-2 is essential for infection of human lung cells. *Mol cell*., **78(4)**: 779-784.

Hohdatsu T, Yamada M, Tominaga R, Makino K, Kida K and Koyama H. 1998. Antibody-dependent enhancement of feline infectious peritonitis virus infection in feline alveolar macrophages and human monocyte cell line U937 by serum of cats experimentally or naturally infected with feline coronavirus. *J Vet Med Sci*., **60(1)**: 49-55.

Hulswit RJ, de Haan CA and Bosch BJ. 2016. Coronavirus Spike Protein and Tropism Changes. *Adv Virus Res*., **96**: 29–57.

Jaume M, Yip MS, Cheung CY, Leung HL, Li PH, Kien F *et al*. 2011. Anti-severe acute respiratory syndrome coronavirus spike antibodies trigger infection of human immune cells via a pH- and cysteine protease-independent FcγR pathway. *J Virol*., **85(20)**: 10582–10597.

Kikkert M. 2020. Innate immune evasion by human respiratory RNA viruses. *J Innate Immunol*., **12(1)**: 4–20.

Kim YI, Kim SG, Kim SM, Kim EH, Park SJ, Yu KM *et al*. 2020. Infection and rapid transmission of SARS-CoV-2 in Ferrets. *Cell Host Microbe*., **27(5)**: 704-709.e2.

Kowalik MM, Trzonkowski P, Łasińska-Kowara M, Mital A, Smiatacz T and Jaguszewski M. 2020. COVID-19 - Toward a comprehensive understanding of the disease. *Cardio J*., **27(2)**: 99–114.

Kumar S, Nyodu R, Maurya VK and Saxena SK. 2020. Morphology, genome organization, replication, and pathogenesis of severe acute respiratory syndrome coronavirus 2 (SARS-CoV-2). Saxena SK (Eds.), Coronavirus Disease 2019 (COVID-19), **Medical Virology: from Pathogenesis to Disease Control**.

Lan J, Ge J, Yu J, Shan S, Zhou H, Fan S *et al*. 2020. Structure of the SARS-CoV-2 spike receptor binding domain bound to the ACE2 receptor. *Nature*., **581(7808)**: 215-220.

Li G, Fan Y, Lai Y, Han T, Li Z, Zhou P *et al*. 2020. Coronavirus infections and immune responses. *J Med Virol*., **92(4)**: 424-432.

Li Q, Guan X, Wu P, Wang X, Zhou L, Tong Y *et al*. 2020. Early transmission dynamics in Wuhan, China, of novel coronavirus-infected pneumonia. *New Engl J Med*., **382(13)**: 1199-1207.

Liu H, Wu C, Yang Y, Liu Y, Zhang P, Wang Y *et al*. 2020. Furin, a potential therapeutic target for COVID-19. *ChinaXiv*.

Maffia P and Guzik TJ. 2019. When, where, and how to target vascular inflammation in the post-CANTOS era?. *Eur Heart J*., **40(30)**: 2492-2494.

Masters PS. 2006. The molecular biology of coronaviruses. *Adv Virus Res*., **6**: 193-292.

Nazinitsky A and Rosenthal KS. 2010. Cytokine storms: systemic disasters of infectious diseases. *Infect Dis Clin Pract*., **18(3)**: 188–192.

Ou X, Liu Y, Lei X, Li P, Mi D, Ren L *et al*. 2020. Characterization of spike glycoprotein of SARS-CoV immune cross-reactivity with SARS-CoV. *Nat Commun*., **11(1)**: 1620.

Petrosillo N, Viceconte G, Ergonul O, Ippolito G and Petersen E. 2020. COVID-19, SARS and MERS: are they closely related?. *Clin Microbiol Infect*., **26(6)**: 729-734.

Prompetchara E, Ketloy C and Palaga T. 2020. Immune responses in COVID-19 and potential vaccines: Lessons learned from SARS and MERS epidemic. *Asian Pac J Allergy Immunol*., **38(1)**: 1-9.

Rabi FA, Al Zoubi MS, Kasasbeh GA, Salameh DM and Al-Nasser AD. 2020. SARS-CoV-2 and coronavirus disease 2019: what we know so far. *Pathogen*., **9(3)**: 231-235.

Shereen MA, Khan S, Kazmi A, Bashir N and Siddique R. 2020. COVID-19 infection: origin, transmission, and characteristics of human coronaviruses. *J Adv Res*., **24**: 91-98.

Shi Y, Wang Y, Shao C, Huang J, Gan J, Huang X *et al*. 2020. COVID-19 infection: the perspective on immune responses. *Cell Death Differ*., **27(5)**: 1451-54.

Siddiqi HK and Mehra MR. 2020. COVID-19 illness in native and immunosuppressed states: A clinical-therapeutic staging proposal. *J Heart Lung Transplant*., **39(5)**: 405–407.

Simmons G, Zmora P, Gierer S, Heurich A and Pöhlmann S. 2013. Proteolytic activation of the SARS coronavirus spike protein: cutting enzymes at the cutting edge of antiviral research. *Antiviral Res*., **100(3)**: 605-614.

Siu KL, Kok KH, Ng MH, Poon VKM, Yuen KY, Zheng BJ *et al*. 2009. Severe acute respiratory syndrome coronavirus M protein inhibits type I interferon production by impeding the formation of TRAF3.TANK.TBK1/IKKepsilon complex. *J Biol Chem*., **284(24)**: 16202-16209.

Tang X, Wu C, Li X, Song Y, Yao X, Wu X *et al*. 2020. On the origin and continuing evolution of SARS-CoV-2. *Natl Sci Rev*., nwaa036.

Walls AC, Park YJ, Tortorici MA, Wall A, McGuire AT and Veesler D. 2020. Structure, function, and antigenicity of the SARS-CoV-2 spike glycoprotein. *Cell*., **181(2)**: 281-292.

World Health Organization (WHO) (2020). "Naming the coronavirus disease (COVID-19) and the virus that causes it". https://www.who.int/emergencies/diseases/novel-coronavirus-2019/technical-guidance/naming-the-coronavirus-disease-(covid-2019)-and-the-virus-that-causes-it (May 24, 2020).

Wu A, Niu P, Wang L, Zhou H, Zhao X, Wang W *et al*. 2020. Mutations, recombination and insertion in the evolution of 2019-nCoV. *ChinaXiv*.

Wu F, Zhao S, Yu B, Chen YM, Wang W, Song ZG *et al*. 2020. A new coronavirus associated with human respiratory disease in China. *Nature*., **579(7798)**: 265-269.

Yi Y, Lagniton PNP, Ye S, Li E and Xu RH. 2020. COVID-19: what has been learned and to be learned about the novel coronavirus disease. *Int J Biol Sci*., **16(10)**: 1753–1766.

Zaki M, van Boheemen S, Bestebroer TM, Osterhaus AD and Fouchier RA. 2012. Isolation of a novel coronavirus from a man with pneumonia in Saudi Arabia. *N Engl J Med*., **367(19)**: 1814–1820.

Zhang L, Yang JR, Zhang Z and Lin Z. 2020. Genomic variations of SARSCoV-2 suggest multiple outbreak sources of transmission. *MedRxiv*., **PPR**: PPR114841.

Zhou G, Chen S and Chen S. 2020. Advances in COVID-19: the virus, the pathogenesis, and evidence-based control and therapeutic strategies. *Front Med*., **14(2)**: 117-125.

Zhou Y, Fu B, Zheng X, Wang D, Zhao C, Qi Y *et al*. 2020. Aberrant pathogenic GM-CSF+ T cells and inflammatory CD14+CD16+ monocytes in severe pulmonary syndrome patients of a new coronavirus. *bioRxiv*.

JJBS

Volume 14, Number 5,December 2021
ISSN 1995-6673
Pages 925 – 931

Jordan Journal of Biological Sciences

The Role of Calcium Ions to Improve Activity of Chitinase Isolated from *Vibrio* sp.

Noor Harini[1], Ya Xi Han[2], and Johan Sukweenadhi[3,*]

[1]*Department of Food Science and Technology, Faculty of Agriculture-Animal Science, University of Muhammadiyah Malang, Jl. Raya Tlogomas No 246, Malang 65114, Indonesia;* [2]*Graduate School of Biotechnology, College of Life Science, Kyung Hee University, Yongin-si, Gyeonggi-do, 17104, Republic of Korea;* [3]*Department of Bionutrition and Food Innovation, Faculty of Biotechnology, University of Surabaya, Jl. Ngagel Jaya Selatan No 169, Surabaya 60294, Indonesia.*

Received: May 15, 2021; Revised: June 18, 2021; Accepted: June22, 2021

Abstract

Chitinase (EC 3.2.1.14) plays a crucial role in chitin degradation, specifically by breaking down the 1→4 β-glycosidic bonds of N-acetyl-D-glucosamine (GlcNAc) to produce its mono- or oligomers. This study aims to study the characteristics of chitinase from *Vibrio* sp. (isolated from tiger shrimp in Indonesia) and to explore the role of calcium ions (Ca^{2+}) in increasing chitinase activity. The optimum condition for chitinase activities is pH 7.5, 45 ^{o}C of temperature, and 120 min of incubation time. The enzyme activity parameters such as K_m and V_{max} values were calculated by varying the concentration of Ca^{2+}, namely: 0 % ; 0.2 % ; 0.4 %; 0.6% ; 0.8 %. The final product of the chitinase reaction, which is the GlcNAc, is then used as a basis for measuring the enzyme activity based on the Somogyi-Nelson method. The results showed that chitinase isolated from *Vibrio* sp. has increasing activity with the addition of Ca^{2+}. Without the addition of Ca^{2+}, the K_m and V_{max} of chitinase were 7.781 µmol mL^{-1} and 0.066 µmol min^{-1}, respectively. The treatment of 0.4 % Ca^{2+} shows optimum activity with the K_m and V_{max} at 6.723 µmol mL^{-1} and 0.079 µmol min^{-1}, respectively. The results showed the potential use of Ca^{2+} as a chitinase activator to fulfill demands for energy-efficient and economically profitable chitinase usage.

Keywords: Eco-friendly waste management, Enzyme activity, Marine waste, Profitable chitinase, Utilization of Agro-industrial waste

1. Introduction

Chitinase is an enzyme that catalyzes the hydrolysis reaction of N-acetyl-D-glucosamine (GlcNAc) polymers. It can be used in the decomposition and re-utilization of chitin, one of the major marine waste problems (Atalla *et al.,* 2020). GlcNAc itself has been widely applied in the health sector, including reducing blood pressure and blood fat levels, suppressing cancer cell development, malignant tumors, and other inflammation, low-calorie sweeteners, cosmetics, biocontrol agents, and packaging materials (Awad *et al.*, 2014; Krolicka *et al.*, 2018; Rathore and Gupta, 2015; Van den Broek *et al.*, 2015; Veliz *et al.*, 2017). Thus, looking for the chitinase can be key to reduce the environmental hazards through eco-friendly waste management, and generate an added-value product which is important to the industry (Hamed *et al.,* 2015; Jahromi and Barzkar, 2018; Sadik *et al.*, 2021).

Chitinase is a chitinolytic enzyme in cell organisms and can be synthesized from various sources such as bacteria, fungi, and various other types of microorganisms. Chitinase synthesized by animals and plants has several functions, including helping the metabolic process and preventing infections, such as preventing the growth of fungi or bacteria that can damage the individual's tissues. Chitinase, which is produced by bacteria, has the function to degrade chitin into compounds that can fulfill the nutritional needs of these bacteria (Adrangi and Faramarzi, 2013). Recent chitinase isolated from several species of *Vibrio sp*. has optimum enzyme activity at pH 5 to pH 7 with incubation temperature at 45 ^{o}C to 50 ^{o}C (He *et al.*, 2020).

Vibrio sp. is a bacterium that is often found in prawns bred in brackish water or from the water itself (Felix *et al.*, 2011; Kharisma and Manan, 2012; Kusmarwati *et al.*, 2017). It can infect and cause diseases namely Vibriosis which can cause huge loss in shrimp culture. This disease is caused by bacteria *Vibrio* genera such as *V. harveyi, V. alginolyticus, V. parahaemolyticus,* and *V. penaeicida* (Utami, 2016). Some cofactors such as Na^{+}, Ca^{2+}, Mn^{2+}, Fe^{2+}, Fe^{3+}, Cu^{2+} and Zn^{2+} can function as chitinase activators (Jahromi and Barzkar, 2018). The presence of

* Corresponding author e-mail: sukwee@staff.ubaya.ac.id.

calcium ions in brackish water is normal due to efforts to regulate salinity conditions, which later relate to the *Vibrio* survivability, osmoregulation, and post-larval metabolic ability of shrimp (Taqwa *et al.*, 2014). Based on these problems, it is necessary to examine the effect of Ca^{2+} in addition to increasing chitinase activity. After finding the chitinase optimum parameter, chitinase activity with and without the addition of Ca^{2+} will be compared. This can be known through the measurement of K_m (Michaelis-Menten coefficient) and V_{max} (maximum V value). The study aims to determine the role of Ca^{2+} ions to increase isolated chitinase activity from *Vibrio* sp.

2. Materials and Method

2.1. Research materials

The research was conducted in the Laboratory of Parasites and Fish Diseases, Department of Aquaculture, Faculty of Fisheries; Biochemistry Laboratory, Biomolecular Laboratory, Microbiology Laboratory, Faculty of Mathematics and Natural Sciences, Brawijaya University, Malang; Agricultural Product Technology Laboratory, Agricultural Biotechnology Center, Science and Technology of Food Laboratory, University of Muhammadiyah Malang; and Bionutrition and Food Innovation Laboratory, Faculty of Biotechnology, University of Surabaya. The materials and tools used include a tool to characterize chitinase and test the enzyme activity. The *Vibrio* sp. used in this research was obtained from previous work (Zafran *et al.*, 2017) located at Provincial Fish Seed Center (*Balai Benih Ikan Provinsi*-BBIP), Gondol, Bali. The strain was isolated from tiger shrimp (*Penaues monodon* Fabricius, 1798), and the only one which is non-pathogenic was used in this research.

2.2. Preparation of Vibrio culture

The solid medium was made for the propagation of *Vibrio* bacteria in a petri dish (Pyrex 3160-100), wherein how to make it followed previous work by Zarkasi *et al.* (2019) with some modification. Nutrient composition so that TCBSA (Thiosulfate-citrate-bile salts-sucrose agar, Oxoid, United Kingdom) for 1 L was needed as much as 88 g so that for making solid medium as much as 20 mL it was needed TCBSA as much as 1.76 g and chitin (Oxoid, United Kingdom) as much as 0.4 g. Nutrients to be dissolved in distilled water to a volume of 20 mL, heated to boiling for 10 min then put 10 mL each into petri dish that has been sterilized in an autoclave (All-American 25×, USA) at 121 ^oC, pressure 1.5 atm for 15 min (1 atm = 101 325 Pa). Furthermore, it was desirable for cooling it down at room temperature (25 ^oC) to harden. In another way, a liquid medium was used for *Vibrio* growth medium on growth curves and enzyme production. The medium used for making liquid medium was TSB (Tryptone Soya Broth, Oxoid, United Kingdom). To make 100 mL of liquid TSB medium, 3 g TSB, 0.5 g NaCl (Oxoid, United Kingdom), and 2 g chitin were dissolved in 100 mL distilled water and then sterilized in an autoclave at 121 ^oC, 1.5 atm for 15 min.

2.3. Isolation of crude chitinase

Vibrio sp. cultures that had been rejuvenated for 2 d (day) were taken using a loop wire and suspended in 20 mL of the sterile liquid medium in 125 mL Erlenmeyer flask (Pyrex 4450-125) and placed in a shaking incubator at room temperature (25 ^oC) for 16 h (half logarithmic phase). The 20 mL inoculum solution was inoculated into 200 mL of sterile liquid medium and grown at room temperature (25 ^oC) on a shaking incubator (Bionics, BST/MIS-100B, India) at speeds of 125 rpm (1 rpm = 1/60 Hz) to 32 h (stationary phase). Then it was centrifuged at 4 ^oC for 10 min at 3 000 rpm (Denley BR401, United Kingdom) and the supernatant was immediately tested for its enzyme activity. The enzyme was purified by the saturated ammonium sulfate (Oxoid, United Kingdom) precipitation method followed by dialysis and Sephadex 75G (Oxoid, United Kingdom) column chromatography method. Each enzyme fractionation was tested for chitinase activity (Harini and Indranila, 2006).

2.4. Chitinase Activity Test

The chitinase activity was tested by using Somogyi-Nelson assay. As much as 1 mL of 30 mg L^{-1} N-acetyl-D-glucosamine (Sigma-Aldrich, Germany) standard solution was taken and added with 1 mL of the Somogyi-Nelson cooper reagent (Sigma-Aldrich, Germany). The mouth of the tube was covered with aluminum foil, then heated in boiling water for 10 min. The tube was cooled in ice water and added with 1 mL of arsenomolybdate reagent, shaken, and allowed to stand for several minutes until the foam disappeared. After that, the distilled water was added up to 10 mL in volume and then shaken and measured the absorbance in the wavelength range of 500 nm to 800 nm by UV-vis spectrophotometer (Shimadzu-1601A, Japan), which maximum wavelength (λ_{max}) was 750 nm (Shalaby *et al.*, 2019). The arsenomolybdate reagent was made of 25 g of ammonium molybdate (Sigma-Aldrich, Germany) dissolved in 450 mL distilled water, 21 mL of concentrated H_2SO_4 (JT Baker, United States), and 3 g of $Na_2HAsO_4.7H_2O$ (Sigma-Aldrich, Germany) dissolved in 25 mL of H_2O, mix then place in an incubator (Heraeus B5042, Germany) at 37 ^oC for 24 h to 48 h. The standard N-acetyl-glucosamine curves were prepared by testing several N-acetyl-glucosamine concentrations [10, 20, 30, 40, 50, and 60) mg L^{-1}] following exactly Somogyi-Nelson assay which written above.

A total of 1 mL of 2.5 % (w/v) chitin in 0.1 M phosphate buffer pH 7.5 was added to 1 mL of chitinase solution. Then the mixture was incubated at 45 ^oC and after 120 min of incubation time, it was centrifuged at 5 000 rpm for 10 min. The enzyme activity was stopped by heating it in boiling water for 15 min before it was mixed with the reagent. Furthermore, the supernatant obtained was taken

as much as 1 mL to be tested by Somogyi-Nelson assay. The solution was diluted with distilled water to a final volume of 10 mL and read the absorbance at λ_{max} with a phosphate buffer blank which was treated the same as the sample. Enzyme activity value was measured by the levels of N-acetyl-D-glucosamine obtained from the plot results against the standard curve of N-acetyl-D-glucosamine. The measurement of enzyme activity was done by converting the absorbance value to the concentration of N-acetyl-D-Glucosamine (Yang *et al.*, 2016) and calculating it following equation (1):

$$\text{Enzyme Activity} = \frac{[N-\text{Acetyl}-D-\text{Glucosamine}]\ x\ V}{\text{Mr}\ N-\text{Acetyl}-D-\text{Glucosamine}} x \frac{df}{E\ x\ t} \quad (1)$$

Note: V = total sample volume (mL), E = amount of crude enzyme (mL), t = incubation time (min), df = dilution factor, Enzyme Activity (unit) = µmol N-acetyl-D-glucosamine which is produced by each mL of the enzyme each one minute under certain conditions. The N-acetyl-D-glucosamine obtained was measured absorbance by the UV-Vis spectrophotometer at λ_{max} 750 nm.

2.5. Determination of the optimum pH, temperature and incubation time

The determination of the optimum pH of chitinase was carried out with a variation of pH 6; pH 6.5; pH 7.0; pH 7.5; pH 8; and pH 8.5. Each test tube was provided with 1 mL chitin 2 % (w/v) in a phosphate buffer with variation of pH 6; pH 6.5; pH 7.0; pH 7.5; pH 8; and pH 8.5. Then 0.5 mL of enzyme filtrate was added and incubated at 45 ^{o}C for 60 min. The solution was centrifuged at 5 000 rpm for 10 min, then the filtrate obtained was taken 1 mL and added 1 mL of Somogyi-Nelson reagents and shaken. The mouth of the tube was covered with aluminum foil and heated for 20 min in boiling water. After chilling, 2 mL of arsenomolybdate reagent was added, mixed, and allowed to stand for 4 min. Subsequently, the solution was diluted with distilled water to a volume of 10 mL and the absorption was read at the λ_{max}. Then the activity was determined, where the optimum pH was determined from the graph of the relationship between changes in pH of the enzyme activity.

Determination of the optimum temperature was done by the same procedure as the method used to determine the optimum pH, while the incubation temperature was varied at (30, 35, 40, 45, 50, 55) ^{o}C for 60 min at pH 7. Then the activity was determined based on the absorbance value of the molybdenum blue complexes which is equivalent to the amount of N-acetyl-D-glucosamine produced from the enzymatic reaction of chitinase. The optimum temperature was determined from a graph of the relationship between temperature changes and enzyme activity.

The optimum incubation time was determined by the same procedure as the method used to determine the optimum pH and temperature, while the incubation time variations were (30, 60, 90, 120, 150, 180) min, at 45 ^{o}C and pH 7. Then the activity was determined based on the absorbance value of the molybdenum blue complexes which is equivalent to the amount of N-acetyl-D-glucosamine produced from the enzymatic reaction of chitinase. The optimum incubation time was determined from a graph of the relationship between time changes to enzyme activity.

2.6. Effect of Ca2+ ions

Addition of Ca^{2+} ions to increase chitinase activity was done by checking the chitinase reaction with variations in Ca^{2+} concentration, as follows: (0; 0.2; 0.4; 0.6; 0.8) %. For each kind of treatment, K_m and V_{max} were measured. The enzyme activity and the K_m and V_{max} values were determined employing the linear regression from the graph of the relationship between V^{-1} and $[S]^{-1}$ (or called Lineweaver-Burk curve). Those enzyme reactions were done using the optimum parameter (pH, temperature, incubation time) which was first tested.

3. Results

3.1. Optimum Condition of Chitinase Activity

Based on sequential trials on each reaction parameter, such as pH, temperature, and incubation time, it is shown that chitinase from *Vibrio* sp. has optimum reaction condition at pH 7.5 (Figure 1A), the temperature of 45 ^{o}C (Figure 1B), and 120 min incubation time (Figure 1C).

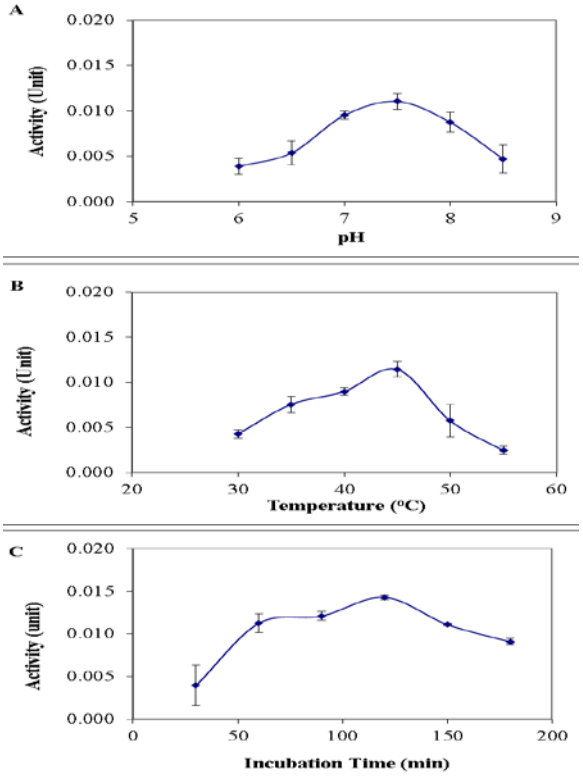

Figure 1. Optimum Condition Chitinase Activity at various pH (A), temperature (B), and incubation time (C).

3.2. Determination of Km and Vmax

In this study, the determination of K_m and V_{max} of chitinase were carried out with variations in substrate (chitin) concentration as follows: (1; 1.5; 2; 2.5; 3; 3.5) % (w/v). The relationship of enzyme activity to substrate concentration is shown in Figure 2. It shows that the greater concentration of chitin, the greater the speed of the enzymatic reaction to a point where an increase in substrate concentration does not significantly increase the reaction speed.

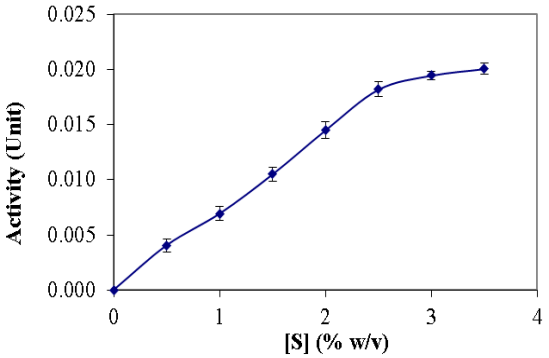

Figure 2. Relationship Curve of Chitinase Activity by Various Chitin Concentrations

Based on the Lineweaver-Burk curve shown in Figure 3 the values of K_m and V_{max} can be determined from the equation Y = aX + b. The value of V_{max}^{-1} is 15.145 and K_m V_{max}^{-1} is 117.84, so the V_{max} is 0.066 µmol min^{-1} and K_m is 7.781 µmol mL^{-1}.

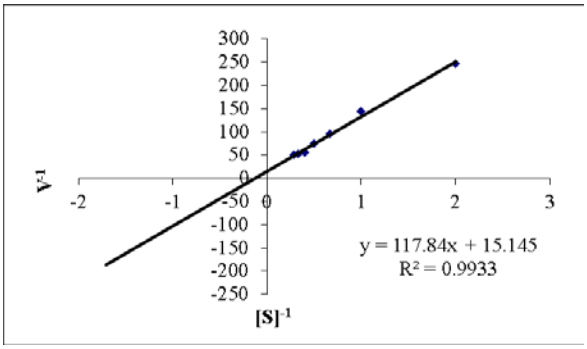

Figure 3. Lineweaver-Burk Curve of Chitinase Activity Isolated from *Vibrio sp.*

3.3. The Role of Calcium Ions on Chitinase Enzyme Activity

Figure 4. shows that Ca^{2+} increases enzyme activity until the addition of 0.4 % (w/v), whereas above 0.4 %, the enzyme activity starts to decline. The enzyme can be saturated with Ca^{2+} because the ability of the allosteric site to bind Ca^{2+} decreases. Thus, the addition of excess Ca^{2+} may cause denaturation on the enzyme which is characterized by decreased enzyme activity (Kumari *et al.*, 2010).

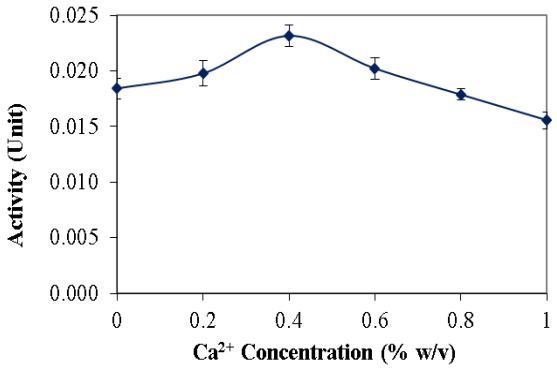

Figure 4. Chitinase Activity with the Addition of Ca^{2+}

The effect of chitinase activity in the presence of Ca^{2+} ions on various variations is shown in Figure 5. Changes in activity caused the price of K_m and V_{max} to change. The value of K_m obtained is 6.723 µmol mL^{-1} and V_{max} is 0.079 µmol min^{-1} (Figure 6).

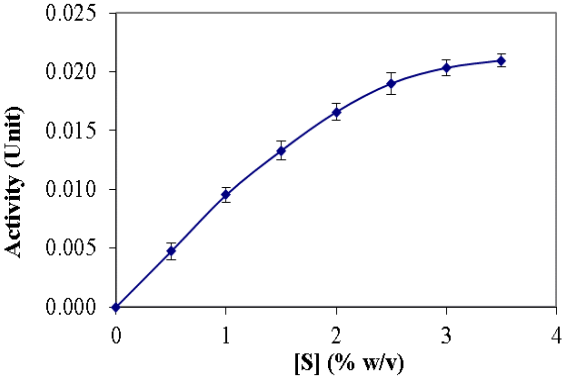

Figure 5. Chitinase Activity in the Various Concentration of the Substrate with Ca^{2+} Addition

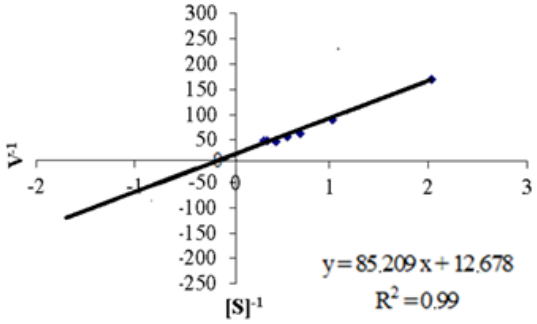

Figure 6. Lineweaver-Burk Curve Chitinase Activity by Addition of Ca^{2+}

4. Discussion

The optimization results of chitinase activity (Figure 1) are concurrent with the previously reported study of He *et al.* (2020), which showed optimum chitinase activity at pH 5 to pH 7 with incubation temperature at 45 °C to 50 °C. However, it quite a different condition compared to other

work of Nguyen and Nguyen (2020), which stated warm temperature (30 ^{o}C or 35 ^{o}C) and mildly alkaline pH (8.0) are the best conditions of chitinase from *V. parahaemolyticus*, one of the pathogenic species which infect shrimp.

One of the important things to know about the characteristics of an enzyme is the determination of K_m and V_{max}. The Michaelis-Menten constant (K_m) is a certain substrate concentration when the enzyme reaches half the maximum speed. Whereas Vmax is the maximum speed of an enzyme. To determine the value of K_m and V_{max}, measurement of enzyme activity was done at various concentrations of substrate, under optimum conditions (pH 7.5, temperature 45 ^{o}C, and 120 min incubation time). Thus, the K_m indicates the amount of substrate needed to obtain high chitinase activity as indicated by V_{max}, which is the fastest enzyme reaction achieved at the optimum concentration (Nakamura *et al.*, 2018). According to Robinson (2015), the speed of enzymatic reactions will increase with increasing substrate concentration until finally reaching a stationary point. After exceeding that point, although the substrate amount is increased, the increase of enzyme reaction speed is very small (almost constant), but will never reach the maximum condition. This condition limit is called the maximum speed (V_{max}) where the enzyme becomes saturated by its substrate, as shown in Figure 2.

The Michaelis-Menten equation for precisely determining K_m and V_{max} is quite difficult. For this reason, the Michaelis-Menten equation is transformed into the Lineweaver-Burk equation. The Lineweaver-Burk equation is the opposite of the Michaelis-Menten equation which can determine K_m and V_{max} precisely, as shown in Figure 3. Thus the substrate concentration added was equal to the value of K_m. Whereas the V_{max} value shows that the speed of the formation of the final product (N-acetyl-D-glucosamine) and the speed of returning to the enzyme chitinase must be the same as the speed of the breakdown of chitin that is equal to 0.066 µmol min^{-1}.

Calcium ions can form bridge complexes with enzymes and substrates according to their role in enzymatic reactions. Ca^{2+} can function as an enzyme inhibitor but can also be an enzyme activator. Enzymes that require Ca^{2+} as activators especially in extracellular enzymes (Bilecen and Yildiz, 2009; Garrison-Schilling *et al.*, 2011). It plays an important role in modifying the structure needed for their catalytic activity. With the addition of substrate concentration, chitinase activity also increases with a fairly high increase in the concentration of 2.5 % (w/v). Calcium ion acts as an activator for enzymes that work to hydrolyze a macromolecule. The Ca^{2+} ions change the conformation and orientation of the active site of the enzyme, also increase the activeness of the enzyme to bind to the substrate to form an Enzyme-Substrate complex. The added Ca^{2+} influences chitinase activity because Ca^{2+} act as cofactors so that they can increase chitinase activity. The effect of Ca^{2+} on the chitinase isolated from *Vibrio* sp. is shown in Figure 4.

The presence of Ca^{2+} ions causes an increasing number of enzymes that bind to the substrate. This causes a greater level of substrate saturation as indicated by changes in the values of K_m and V_{max}. Determination of K_m and V_{max} values was carried out by measuring chitinase activity with an optimum Ca^{2+} concentration of 0.4 % in each variation of substrate concentration (Figure 5). The value of K_m and V_{max} (Figure 6) provides information that the substrate concentration needed to reach half of the maximum speed becomes smaller (13.5 % fewer) and the enzymatic reaction becomes faster (19.7 % faster) at the optimum concentration with the addition of Ca^{2+} ions. In the other words, additional Ca^{2+} up to 0.4 % can provide benefits of larger chitinase activity and lesser required chitin.

Hydrolysis of chitin by chitinase with Ca^{2+} shows that the Calcium on the allosteric site (Asp-140) binds the substrate which can then change the active site conformation (Asp-142) to become active and bind to the substrate. When the conformation Asp-142 corresponds to the substrate and there is an interaction between those two, Ca^{2+} ions are released. The release of Ca^{2+} causes Asp-142 to rotate so that it is oriented closer to Glu-144 and hydrogen bonds occur. The interaction between Glu-144 and chitin causes the breakdown of glycosidic bonds and N-acetyl-D-glucosamine is formed. The interaction between Asp-142 and the amine group chitin and chitin with water also causes the formation of N-acetyl-D-glucosamine (Paknisa, 2014).

The presence of Ca^{2+} ions causes an increasingly enzymatic reaction which is characterized by an increase in chitinase activity after adding Ca^{2+} ions. The increase in chitinase enzyme activity is still relatively smaller compared to the research of Park *et al.* (2000) after adding Ca^{2+} ions. This is allegedly due to the concentration of the addition of Ca^{2+} ions which are relatively small and the use of chitin substrate in the form of powder, so that chitinase work is less optimal than the use of chitin substrate in the form of colloids and the addition of greater Ca^{2+} ion concentrations. The presence of Ca^{2+} causes conformation changes that make enzymes bind easier with the substrate, thereby increasing the saturation of the enzyme to the substrate as indicated by the increase in K_m and V_{max} values.

5. Conclusion

The optimum reaction parameters for the chitinase isolated from *Vibrio sp*. are pH 7.5, temperature 45 ^{o}C, and 120 min incubation time. The chitinase activity increases until the addition of Ca^{2+} 0.4 % and decreases with an increasing concentration of Ca^{2+} above 0.4 %. The value of K_m and V_{max} before adding Ca^{2+} was 7.781 µmol mL^{-1} and 0.066 µmol min^{-1}, respectively. After adding Ca^{2+}, the value of K_m and V_{max} was 6.723 µmol mL^{-1} and 0.079

µmol min^{-1}. In conclusion, chitinase kinetic parameters with the addition of Ca^{2+} affects K_m (13.5 % fewer substrate) and V_{max} (19.7 % faster), which means its reaction efficiency is improved.

6. Competing interest statement

The authors have declared that no competing interest exists in the manuscript.

Acknowledgments

Appreciation was sincerely conveyed to the Head of Laboratory for Fish Health and Environment Assessment, Muntilan, Central Java, Indonesia who has supported the place to carry out the research. We also thank the Head of the Laboratory from all related affiliations for providing the means for the implementation of this research.

Funding disclosure

The researchers would like to thank several parties who helped in this research, namely the UMM Rector and staff who have helped fund this research; Director of Directorate of Research and Community Service (DPPM) of the University of Muhammadiyah Malang (UMM), and staff (contract Number. 1322/SK-BAA/XII/2016), who facilitated the implementation of this research.

References

Adrangi S and Faramarzi MA. 2013. From bacteria to human: A journey into the world of chitinases. *Biotechnol Adv*, **31(8)**: 1786–1795.

Atalla SM, Gamal NG and Awad HM. 2020. Chitinase of marine *Penicillium chrysogenum* MH745129: isolation, identification, production and characterization as controller for citrus fruits postharvest pathogens. *Jordan J Biol Sci*, **13(1)**: 19–28.

Awad HM, El-Enshasy HA, Hanapi SZ, Hamed ER and Rosidi B. 2014. A new chitinase-producer strain *Streptomyces glauciniger* WICC-A03: isolation and identification as a biocontrol agent for plants phytopathogenic fungi. *Nat Prod Res*, **28(24)**: 2273–2277.

Bilecen K and Yildiz FH. 2009. Identification of a calcium-controlled negative regulatory system affecting *Vibrio cholerae* biofilm formation. *Environ Microbiol*, **11(8)**: 2015–2029Felix F, Nugroho TT, Silalahi S and Octavia Y. 2011. Screening of Indonesian original bacteria *Vibrio sp.* as a cause of shrimp diseases based on 16s ribosomal DNA-technique. *Jurnal Ilmu dan Teknologi Kelautan Tropis*, **3(2)**: 85–99.

Garrison-Schilling KL, Grau BL, McCarter KS, Olivier BJ, Comeaux NE and Pettis GS. 2011. Calcium promotes exopolysaccharide phase variation and biofilm formation of the resulting phase variants in the human pathogen *Vibrio vulnificus*. *Environ Microbiol*, **13(3)**: 643–654.

Hamed ER, Awad HM, Ghazi EA, El-Gamal NG and Shehata HS. 2015. *Trichoderma asperellum* isolated from salinity soil using rice straw waste as biocontrol agent for cowpea plant pathogens. *J Appl Pharm Sci*, **5(2)**: 091–098.

Harini N and Indranila TH. 2006. Purification of crude extract of kinitase enzyme from *Vibrio cumpbelli* by multilevel precipitation method with ammonium sulfate. *Prosiding Seminar Nasional Tahunan III Hasil Penelitian Perikanan dan Kelautan*. Balitbang Kelautan dan Perikanan. Yogyakarta. pp. 267–276.

He X, Yu M, Wu Y, Ran L, Liu W and Zhang XH. 2020. Two highly similar chitinases from marine Vibrio species have different enzymatic properties. *Mar Drugs*, **18(139)**: 1–14.

Jahromi ST and Barzkar N. 2018. Marine bacterial chitinase as sources of energy, eco-friendly agent, and industrial biocatalyst. *Int J Biol Macromol*, **120**: 2147–2154.

Kharisma A and Manan A. 2012. The Abundance of *Vibrio sp.* bacteria on enlargement water of Whiteleg shrimp (*Litopenaeus vannamei*) as the early detection of Vibriosis. *Jurnal Ilmiah Perikanan dan Kelautan*, **4(2)**: 129–134.

Krolicka M, Hinz SW, Koetsier MJ, Eggink G, van den Broek LA and Boeriu CG. 2018. β-N-Acetylglucosaminidase Mth NAG from *Myceliophthora thermophila* C1, a thermostable enzyme for production of N-acetylglucosamine from chitin. *Appl Microbiol Biotechnol*, **102(17)**: 7441–7454.

Kumari A, Rosenkranz T, Kayastha AM and Fitter J. 2010. The effect of calcium binding on the unfolding barrier: A kinetic study on homologous α-amylases. *Biophys Chem*, **151(1-2)**: 54–60.

Kusmarwati A, Hermana I, Yennie Y and Wibowo S. 2017. Presence of potentially human pathogenic *Vibrio parahaemolyticus* of fresh shrimp in ponds of the northern coast of Java. *Jurnal Pascapanen dan Bioteknologi Kelautan dan Perikanan*, **11(1)**: 41–54.

Nguyen PN and Nguyen TT. 2020. Effects of pH, temperature and oxygen-limited condition on the virulence of *Vibrio parahaemolyticus*. *Sci Tech Dev J*, **23(3)**: 569–575.

Paknisa S. 2014. Studies on chitinolytic enzymes from *Vibrio Harveyi*: Transglycosylation reaction and inhibition kinetics of sodium salts. Doctoral dissertation, School of Biochemistry Institute of Science, Suranaree University of Technology, Thailand.

Park SH, Lee JH and Lee HK. 2000. Purification and characterization of chitinase from a marine bacterium, *Vibrio sp.* 98CJ11027. *J Microbiol*, **38(4)**: 224–229.

Rathore AS and Gupta RD. 2015. Chitinases from bacteria to human: properties, applications, and future perspectives. *Enzyme Res*, **791907**: 1–8. Sadik MW, Zohair MM, El-Beih AA, Hamed ER and Sedik MZ. 2021. Utilization of Agro-industrial wastes as carbon source in solidstate fermentation processes for the production of value-added byproducts. *Jordan J Biol Sci*, **14(1)**: 157–161.

Shalaby HM, Abo-Sdera SA, Easa SM and Ismail AM. 2019. Biosynthesis of biologically active chitinase utilizing some Egyptian chitinaceous wastes and the properties of the synthesized enzyme. *Egypt Pharm J*, **18(4)**: 320–331.

Taqwa FH, Sasanti AD, Haramain K, Kusrini E and Gaffar AK. 2014. Addition of calcium to swamp water as a diluent for salinity media for post-larvae maintenance of giant prawns on survival,

osmotic work rate, and oxygen consumption. *Jurnal Riset Akuakultur*, **9(2)**: 229–236.

Utami W. 2016. Effect of salinity on *Vibrio harveyi* infection in Whiteleg Shrimp (*Litopenaeus vannamei*)]. *J Aqua Manag Technol*, **5(1)**: 82–90.

Van den Broek LAM, Knoop RJI, Kappen FHJ and Boeriu CG. 2015. Chitosan films and blends for packaging material. *Carbohydr Polym*, **116**: 237–242.

Veliz EA, Martínez-Hidalgo P and Hirsch AM. 2017. Chitinase-producing bacteria and their role in biocontrol. *AIMS Microbiol*, **3(3)**: 689–705.

Yang S, Fu X, Yan Q, Guo Y, Liu Z and Jiang Z. 2016. Cloning, expression, purification and application of a novel chitinase from a thermophilic marine bacterium *Paenibacillus barengoltzii*. *Food Chem*, **192**: 1041–1048.

Zafran Z, Roza D and Koesharyani I. 2017. Resistance of Vibrio isolated from infected *Penaeus monodon* to antibiotics. *Jurnal Penelitian Perikanan Indonesia*, **3(1)**: 11–15.

Zarkasi KZ, Shukri AA, Nazari TF, Abdullah AA and Daud F. 2019. Molecular characterization of microbial community diversity associated with Blood Cockles (*Anadara granosa*) in Blood Cockle Farms. *Jordan J Biol Sci*, **12(3)**: 339-344.

JJBS

Volume 14, Number 5,December 2021
ISSN 1995-6673
Pages 933 – 937

Jordan Journal of Biological Sciences

Callus-mediated Somatic Embryogenesis and Plant Regeneration in *Vanda tricolor* Lindl. var. Pallida

Popy Hartatie Hardjo[1,*] , Wina Dian Savitri[1], Ida Bagus Made Artadana[1], Sulistyo Emantoko Dwi Putra[1], Elizabeth Pio Parac[2] and Asad Jan[3]

[1]*Faculty of Biotechnology, University of Surabaya, Jalan Raya Kalirungkut, Surabaya 60292, East Java, Indonesia;* [2]*College of Agriculture and Agri-Industries, Caraga State University, Amapayon, Butuan City, 8600 Philippines;* [3]*Institute of Biotechnology and Genetic Engineering, University of Agriculture, Peshawar, Pakistan*

Received: May 20, 2021; Revised: June 18, 2021; Accepted: June22, 2021

Abstract

In this study, a protocol to induce indirect somatic embryogenesis from the basal leaf segments of *Vanda tricolor* Lindl. var. Pallida has been developed. The experiments consisted of two stages، i.e. induction of SEs from calli and regeneration of plantlet from SEs. Embryogenic calli obtained from previous experiment (0.05 mg L^{-1} NAA + 0.01 mg L^{-1} BAP) were used to induce somatic embryos (SEs) on half-strength Murashige and Skoog (MS) medium supplemented with (0.05 mg L^{-1} to 0.20 mg L^{-1}) 6-benzylaminopurine (BAP) alone or in combination with 0.01 mg L^{-1} α-naphtalene acetic acid (NAA). Embryogenic calli, those cultured on 0.05 mg L^{-1} BAP and 0.01 mg L^{-1} NAA resulted in 90 % induction of SE structures at 30 d of culture period. Histological observation exhibited development of pro-embryo to form completed embryo. The pattern of SEs development started from embryogenic callus to form pro-embryo, followed by globular phase at 10 d of culture. Globular embryo elongated to form suspensor at 20 d of incubation period, and completed embryo. Regeneration of SEs into complete plantlets was attained on the half-strength MS medium without addition of any plant growth regulator (PGR). Based on the results of the present study, it can be concluded that half-strength MS medium supplemented with NAA 0.01 mg L^{-1} and BAP 0.05 mg L^{-1} is the best medium for induction of SEs from embryogenic calli.

Keywords: Embryogenic calli, Histology, Half-strength Murashige-Skoog medium, Micropropagation, Orchid, Pro-embryo

1. Introduction

Vanda is a genus of orchids that consists of approximately 50 species. *Vanda tricolor*, just like its name, has fragrant flowers composed of three colors, i.e. white sepal, white with brown spot petal, and violet labellum. *Vanda tricolor* Lindl. in the slope of Mount Merapi located in Central Java, and *Vanda tricolor* Lindl. var. pallida in Amerta Jati Forest, Bali are local endemic species labelled endangered in Indonesia (Kurniawan *et al.*, 2020; Semiarti, 2018). These species are generally used as the parental for crossing to produce hybrids that have economic value.

The propagation of orchids, in most cases, is done by seed germination by *in vitro* culture. Thus, the result is not homogeneous and the flowers are varied. To overcome this problem, the clonal multiplication by using *in vitro* technique can be performed. Besides, *V. tricolor* as well as *V. testacea* are monopodial orchids that are not easy to be propagated vegetatively in conventional method (Sebastinraj *et al.*, 2014). It is necessary to develop a rapid and efficient micropropagation protocol in large quantities and in a short period of time. Micropropagation through callus has the potential for somaclonal variation, so it should be carried out in a shorter culture period as well as reducing costs (Melviana *et al*. 2021a).

Cardoso *et al.* (2020) stated that induction, proliferation and regeneration of protocorm-like bodies (PLBs) is one of the most advantageous methods for mass propagation of orchids. *In vitro* multiplication by direct or indirect embryogenesis through callus will result in somatic embryo(s). According to Naing *et al*. (2011) and Shen *et al*. (2018), embryogenesis in orchids, both direct and indirect, occurred through the development of protocorm-like bodies (PLBs). Thidiazuron cytokinin (< 1 μM) significantly stimulated formation and regeneration of PLBs compared to other plant growth regulators (Kundu and Gantait, 2018). Lee *et al*. (2013) stated that in early stage of PLBs development, the cells had characteristics that cytologically similar to that of the zygotic embryos. Therefore, it was concluded that PLBs were actually somatic embryos (SEs) in orchids. As reported by Jainol and Gansau (2017), embryogenic callus developed into nodular structures and progressed further formed into aggregates of PLBs. Somatic embryogenesis was a process where cells developed resemble the zygotic embryos with bipolar structure (Shen *et al*., 2018). The use of somatic embryo derived from callus tissue was chosen in this research because the produced propagules were unlimited where each somatic embryo originated from a somatic cell, i.e. callus cell.

Orchids propagation using protocorm-like bodies had been studied by Soe *et al.* (2014). In addition to that,

* Corresponding author e-mail: poppy_hardjo@staff.ubaya.ac.id.

somatic embryogenesis protocols from several orchids have been reported, for examples *Phalaenopsis bellina* (Rchb.f.) Christenson (Khoddamzadeh *et al.*, 2011), *Phalaenopsis amabilis* (L.) - Blume Orchid (Mose *et al*., 2017, Mose *et al*., 2020), *Tolumnia* Louise Elmore 'Elsa' (Shen *et al*., 2018). Concentration and combination of plant growth regulators play an important role throughout *in vitro* proliferation of different orchids. Auxins, especially α-naphtalene acetic acid (NAA) affect the process of regeneration in monopodial orchids, and act synergistically on the formation of PLBs (Jainol and Gansau, 2017). Hardjo and Savitri (2017) succeeded in callus induction from the basal part of *V. tricolor* var. pallida's leaf using half-strength MS medium (Melviana, *et al*, 2021b; Murashige and Skoog, 1962) with the addition of 0.05 mg L^{-1} NAA in collaboration with 0.01 mg L^{-1} BAP. Callus induction method which has been done by Hardjo and Savitri (2017) will be used and developed to induce somatic embryos and then to regenerate them into plantlets. The effect of NAA and BAP was studied for induction and maturation of somatic embryos. This study intended to develop a protocol to indirectly produce somatic embryo (SE) via callus, initiated from leaf basal segment of *V. tricolor* var. Pallida.

2. Materials and Method

2.1. Plant material

In vitro grown plantlets of *V. tricolor* var. Pallida were provided by Handoyo Budi Orchid, in Malang City, East Java, Indonesia. Three-month old *in vitro* plantlets, measuring 3 cm had four leaves and long roots. Leaf basal segments were used as explant source for callus induction.

2.2. 2.2 Induction and regeneration of somatic embryo

Basal segment of leaf was cultured on half-strength MS medium + 0.05 mg L^{-1} NAA + 0.01 mg L^{-1} BAP (following Hardjo and Savitri, 2017). Subculturing was carried out after 4 wk (week)s intervals. The experiments consisted of two stages, i.e. induction of SEs from calli and regeneration of plantlet from SEs. Embryogenic calli (approx. 5 mm in diameter), formed after subculturing, were transferred to half-strength MS medium added with various levels of BAP (0.05 mg L^{-1} to 0.20 mg L^{-1} and 0.01 mg L^{-1} NAA) to induce SEs.

2.3. Culture conditions

The half-strength MS basal medium contained half-strength macro- and micro-element of MS enriched with: myo-inositol (100 mg L^{-1}), niacin (0.5 mg L^{-1}), pyridoxine.HCl (0.5 mg L^{-1}), thiamine HCl (0.1 mg L^{-1}), glycine (2.0 mg L^{-1}), sucrose (10 000 mg), and phytagel (2 500 mg). Plant growth regulators as well as compulsory additives (according to the experimental objectives) were added to the media prior to autoclaving. The pH of the media was adjusted to 5.8 with 1 N KOH or HCl prior to autoclaving for 20 min at 121 °C. Explants were incubated under 16:8-h photoperiod at 24 °C to 26 °C. Subculturing was also executed every 4 wk.

2.4. Histological observation of SE

The tissue was fixed in formaldehyde-acetic acid - ethanol (FAA) solution (5 % formaldehyde: 5 % glacial acetic acid: 90 % ethanol 70 %) for 24 h, then continued with further processes (washing and gradual dehydration) until finally the tissue was covered in paraffin. The paraffin embedded tissue was cut at a thickness of 5 µm, and stained with hematoxylin-eosin. At the end, the specimen was then observed under the light microscope.

2.5. Complete plantlet regeneration and acclimatization

Regeneration of SE was performed on hormone-free MS medium and half strength MS + BAP (0 mg L^{-1} to 0.05 mg L^{-1}). The observations were recorded weekly to trace different stages of protocorm development. For stereo microscopy and histological observations, about five PLBs at every developmental stage were randomly collected from culture tubes. Plantlets with four leaves and three roots were transplanted into a 2-inch pot containing sphagnum moss and were covered with a clear plastic lid in greenhouse. Plastic lids were removed after 15 d. The moisture content of the pots was maintained by regular water spraying. Survival plantlets were recorded 2 mo after transplanting.

2.6. Experimental design and statistical analysis

The experiment was based on completely randomized design. Each experiment was composed of six treatments and 40 replications. Embryogenic callus induction from basal leaf explant was carried out as long as 4 wk. Embryogenic calli were transferred to various treatment media to promote somatic embryo formation. Observation parameters for SE induction were the initial time of SE formation, percentage of callus forming SE, and histological analysis of SE. For the observation of SE regeneration, the parameters were the initial time of emerging shoot, percentage of SE forming shoots, and percentage of SE forming plantlet. Data were analyzed with analysis of variance (ANOVA) and followed by Duncan's Multiple Range Test (DMRT) at α = 0.05 (Adinurani, 2016)

3. Results and Discussions

3.1. Embryogenic callus induction and stages of SE

Basal leaf of *V. tricolor* var pallida's explant formed callus on half-strength MS medium + NAA 0.05 mg L^{-1} + BAP 0.01 mg L^{-1} (Figure 1A). Naing *et al*. (2011) reported the same thing that high auxin and cytokinin ratio has synergistic effect to induce callus on *Coelogyne cristata* Lindl. leaf explant. Figure 1B shows that after first subculture, callus structure shaped nodule and compact, with isodiametric size and shiny green in color. According to Jainol and Gansau (2017), these characteristics are typical in embryogenic callus and will be subsequently developed into embryo. Figure 1C represents callus that develop into SE, while the nodule size is bigger than others and color is dark green.

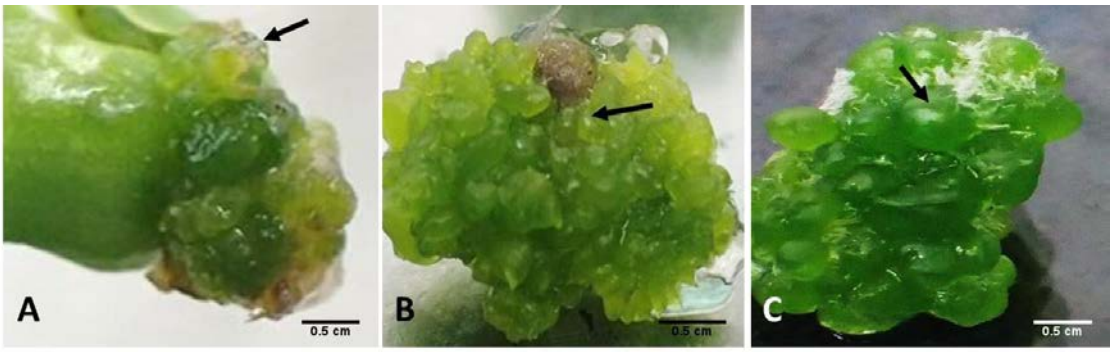

Figure 1. Callus formation on *V. tricolor* var. pallida basal leaf segment A. 8 wk of culture (½ MS medium + NAA 0.05 mg L^{-1} + BAP 0.01 mg L^{-1}); B. Embryogenic callus; C. SEs at globular phase

Treatment of 0.05 mg L^{-1} BAP and 0.01 mg L^{-1} NAA, all at once, was able to induce SE formation (90 %) in faster time rather than single BAP treatment (0.05 mg L^{-1} to 0.2 mg L^{-1}) as shown in the Table 1. Combination of NAA with cytokinin like BAP on various orchid species can increase the formation of PLBs such as Tolumnia cv. Snow Fairy (0.5 mg L^{-1} NAA with 4 mg L^{-1} BA) (Chookoh *et al*., 2019) while on leaf explant of *Phalaenopsis* 'Join Angle × Sogo Musadian' 2 mg L^{-1} 2,4-D was applied in combination with 1 mg L^{-1} TDZ but number of PLBs was less than the combination treatment of 0.5 mg L^{-1} NAA, 5 mg L^{-1} BAP, and 0.5 mg L^{-1} IAA that used root explant (Meilasari and Iriawati 2016). Furthermore, Mose *et al*. (2020) also reported combination of 3 mg L^{-1} TDZ with 1 mg L^{-1} NAA effectively induced *Phalaenopsis amabilis* L. (Blume) SEs formation from stem explants. Basal segment explants of *Dendrobium* (Sw) Sonia 'Earsakul' cultured on ½ MS medium supplemented with 1 mg L^{-1} TDZ alone could be stimulated to form PLBs (Juntada *et al*., 2015). In numerous orchids, SE induction has been completed with cytokinin alone or as a group with auxin at low concentration. The effect of various concentration is variable, depending on the type of explant and species. The decrease of auxin concentration results in inhibition of cell division and cells are encouraged to develop into embryos.

Table 1. Percentage of callus forming SE and time duration of SE maturation in *V. tricolor* var. pallida at various concentration and combination of BAP and NAA.

PGR treatment (mg L^{-1})	Time duration formed SEs (d)	Percentage of callus formed SEs after 30 d cultured (%)
BAP 0.2 + NAA 0.01	65.7 ± 0.65^{c}	60.2±8.92^{bc}
BAP 0.1 + NAA 0.01	45.3 ± 0.52^{d}	70.2±5.45^{b}
BAP 0.05 + NAA 0.01	30.8 ± 0.84^{e}	90.1±4.72^{a}
BAP 0.2	112.3 ± 0.75^{b}	60.1±7.65^{bc}
BAP 0.1	120.5 ± 0.64^{b}	55.4±9.83^{c}
BAP 0.05	130.2 ± 0.54^{a}	50.3±8.15^{c}

Note.: numbers followed by different letter in a column means that they are significantly different, tested with DMRT at α = 0.05. There were 40 explants used for every treatment.

According to histological observation of longitudinal section of *V. tricolor* var. pallida's SE, it was noticeable that there were embryogenic cells in the form of proembryo which consisted of three cells (Figure 2A), and then developed into globular shape (Figure 2B), and differentiation occurred where cells in apical area were small while they were huge in basal area (Figure 2C). Furthermore, globular structure started to elongate at basal area, forming a suspensor-like structure and at apical area it formed a curvature, consequently there were two bulges (Figure 2D). At next development, the two bulges transformed into two leaves primordial, while the curvature developed into shoot apical meristem (Figure 2E). Figure 2F, exhibits that there was cell differentiation at the center of the specimen to form vascular tissue which will connect shoot apical meristem and root apical meristem. Embryogenic calli were able to form embryos because medium contained BAP cytokinin combined with low content of NAA (0.01 mg L^{-1}).

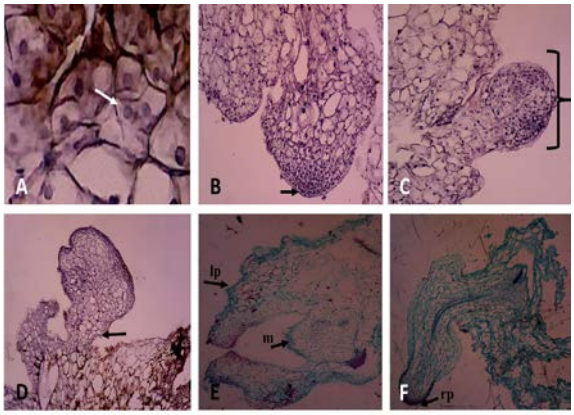

Figure 2. Histology of SE from callus of *V. tricolor* var. pallida.

A. Proembryo (three cells); B. SE on ½ MS medium supplemented with 0.05 mg L^{-1} BAP + 0.01 mg L^{-1} NAA; C. Globular stage of SE; D. Basal of SE with suspensor-like structure; E. Shoot apical meristem after 30 d on hormone-free ½ MS medium; F. Differentiation of the procambium at SE. (m = meristem; lp = leaf primordia; rp = root primordia).

3.2. Regeneration of SE to form plantlets

First and foremost, SE (Figure 3A) regenerated to form shoot (Figure 3B) occurred in a faster time on hormone-free half strength MS. Yet, it was not significantly different with half-strength MS supplemented with BAP at low concentration to 0.02 mg L^{-1} (Table 2). In line with that, there was a same report on protocorms in *Phalaenopsis* (Winarto *et al.*, 2016), regeneration of *Phalaenopsis bellina* (Rchb.f.) PLBs (Chew *et al*., 2018) and SE in *Tolumnia* Louise Elmore 'Elsa' (Shen *et al.*, 2018) which regenerated into plantlets after being transferred to hormone-free half-strength MS medium. The addition of BAP in higher concentration from 0.02 mg L^{-1} evidently had an effect to slow down germination of SE to form plantlets and caused germination time to be delayed.

High concentration of BAP actually inhibit SE germination. Morphological observation (Figure 3C) showed that the roots emerge after the first and second leaf develop. In a period of 30 d of culture (Table 2) all of SEs (100 %) form whole plantlets, while on MS medium and half-strength MS + BAP ≥ 0.03 mg L^{-1} only 80 % SEs form plantlets. Low concentration cytokinin has beneficial effect on SE germination of *V. tricolor* var. pallida. Naing *et al*. (2011) stated that BAP effectively promote regeneration on *Coelogyne cristata* (Lindl.)'s PLBs to form shoots, and it was similar to the result reported by Zhao *et al*. (2013) using *Dendrobium wangliangii* (G.W.Hu, C.L.Long & X.H.Jin). Generally, cytokinins have the effect of encouraging cell division and regeneration to form shoots, and the optimum concentration is specific for each species. Cytokinin BA are also commonly used for *in vitro* shoot multiplication of various species such as for example *Ammi visnaga* (L.) Lam. (Al-Saleh *et al*., 2019).

Table 2. Regeneration of SEs of *V. tricolor* var. Pallida forming plantlets on half-strength MS and MS supplemented with PGRs after 30 d of culture period

Medium and PGR (mg L^{-1})	SE forming shoot (d)	Percentage of SE forming shoot (%)	Percentage of SE forming plantlet (%)
MS	25.5 ± 2.27[a]	80	85
½ MS	17.8 ± 3.45[c]	100	100
½ MS + BAP 0.01	15.2 ± 2.68[c]	100	100
½ MS + BAP 0.02	16.4 ± 2.85[c]	100	100
½ MS + BAP 0.03	20.8 ± 2.85[b]	90	80
½ MS + BAP 0.05	22.4 ± 2.85[b]	80	80

Note.: numbers followed by different letter in a column means that they are significantly different, tested with DMRT at α = 0.05. There were 40 explants used for every treatment.

The percentage of plantlets (Figure. 3D) that were well acclimatized in the glasshouse with survival rate 95 %. These plantlets were grown in sphagnum moss medium and exhibited normal developmental (Figure 3E). Sphagnum moss was used to maintain the moisture.

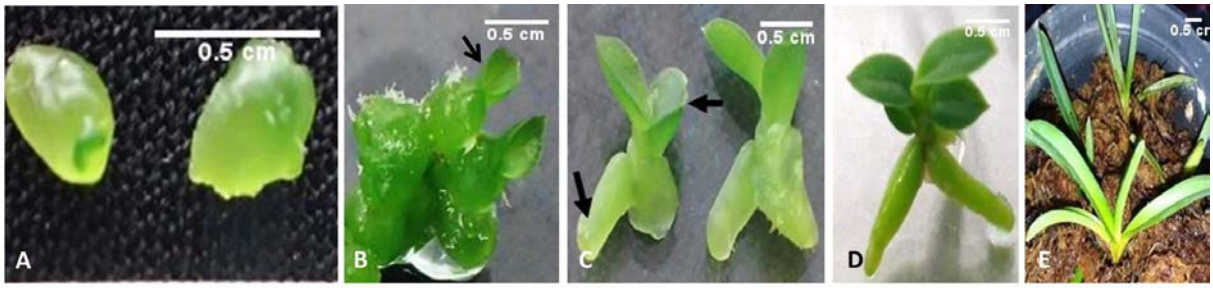

Figure 3. Mature SE of *Vanda tricolor* Lindl. var. pallida transformed into plantlet on hormone-free half-strength MS medium. A. Somatic embryo (SE); B. SE with shoot; C. SE with shoot and root; D. Plantlet; E. Acclimatized plantlets (2 mo old after planting)

4. Conclusion

Embryogenic calli formed SEs on ½ MS medium + NAA 0.01 mg L^{-1} + BAP 0.05 mg L^{-1} at 30 d of culture period. The development of embryo started with the formation of proembryo structure from embryogenic callus and then developed into globular structure with suspensor. Somatic embryo could germinate to form shoots firstly and subsequently form root on hormone-free half-strength MS medium after 30 d of culture period. Plantlets regenerated through somatic embryogenesis would be a new procedure of clonal propagation in *V. tricolor*.

The success in somatic embryo formation from callus followed by the establishment of *Vanda tricolor* Lindl. var. Pallida plantlets opened the chance to develop orchid synthetic seed and advanced plant breeding.

Acknowledgement

This research was funded by Campus Intellectual Product Business Development Program Grant [*Hibah Program Pengembangan Usaha Produk Intelektual Kampus* (PPUPIK)] Kemendikbud-Ristek 2021 with contract no. 004/SPP-PPM/LPPM-02/DRPM/FTB/IV/ 2021 (on behalf of Dr.rer.nat. Sulistyo Emantoko Dwi Putra). All experiments were conducted in Faculty of Biotechnology University of Surabaya. The authors would like to thank to our laboratory assistants and students for their intensive helped to support this research.

References

Adinurani PG. 2016. **Agro Experimental Data Design and Analysis**. Plantaxia, Yogyakarta, Indonesia

Al-Saleh MM, Shibli RA, Al-Qadiri HM, Tahtamouni RW, Darwish MM and Al-Qudah TS. 2019. Investigating the antimicrobial potential of in- vitro grown microshoots and callus cultures of Ammi visnaga (L.) Lam. *Jordan J of Biol Sci.* **12(1)**:43-48.

Cardoso JC, Zanello CA and Chen JT. 2020. An overview of orchid protocorm-like bodies: Mass propagation, biotechnology, molecular aspects, and breeding. *Int. J. of Mol Sci.,* **21 (985)**: 1–32.

Chew YC, Halim MHA, Wan Abdullah MAN, Abdullah JO and Lai KS. 2018. Highly efficient proliferation and regeneration of protocorm like-bodies (PLBs) of the threatened orchid *Phalaenopsis bellina*. *Sains Malays,* **47(6):**1093–1099.

Chookoh N, Chiu YT and Chang C. 2019. Micropropagation of *Tolumnia* orchids through induction of protocorm-like bodies from leaf segments. *Hortscience* **54(7):**1230–1236.

Hardjo PH and Savitri WD. 2017. Somatic embryo from basal leaf segments of *Vanda* tricolor Lindl. var. pallida. *KnE Life Sci* **3(5):**173–179.

Jainol JE and Gansau JA. 2017. Embryogenic callus induction from leaf tip explants and protocorm-like body formation and shoot proliferation of dimorphorchis lowii: Borneon endemic orchid. *Agrivita J of Agricultural Science*. **39(1):** 1–10.

Juntada K, Taboonmee S, Meetum P, Poomjae S and Chiangmai PN. 2015. Somatic embryogenesis induction from protocorm like-bodies and leaf segments of *Dendrobium* Sonia 'Earsakul'. *Silpakorn U. Science & Tech. J.* **9(2):**9–19.

Khoddamzadeh AA, Sinniah UR, Kadir MA, Kadzimin SB, Mahmood M and Sreeramanan S. 2011. In vitro induction and proliferation of protocorm-like bodies (PLBs) from leaf segments of *Phalaenopsis bellina* (Rchb.f.) Christenson. *Plant Growth Regul*. **65:**381–387.

Kundu S and Gantait S. 2018. Thidiazuron-induced protocorm-like bodies in orchid: progress and prospects. In: N Ahmad, M Faisal (eds.), **Thidiazuron: From Urea Derivative to Plant Growth Regulator**, Volume 1, Springer Nature, Singapore, pp. 273–287.

Kurniawan FY, Putri F, Suyoko A, Masyhuri H, Sulistianingrum MP and Semiarti E. 2020. The diversity of wild orchids in the southern slope of Mount Merapi, Yogyakarta, Indonesia eight years after the 2010 eruption. *Biodiversitas* **21(9):**4457–4465.

Lee YI, Hsu ST, and Yeung EC. 2013. Orchid protocorm-like bodies are somatic embryos. *Am. J. Bot.*, **100(11):**2121–2131.

Meilasari D and Iriawati. 2016. Regeneration of planlets through PLB (protocorm-like body) formation in *Phalaenopsis* 'Join Angle X Sogo Musadian'. *J. Math. Fundam. Sci.* **48(3):**204–212.

Melviana AC, Esyanti RR, Mel M and Setyobudi RH. 2021a. Biomass enhancement of *Stevia rebaudiana* Bertoni shoot culture in temporary immersion system (TIS) RITA® bioreactor optimized in two different immersion periods. *E3S Web Conf.* **226(00007):** 1–9.

Melviana AC, Esyanti RR, Setyobudi RH, Mel M, Adinurani PG and Burlakovs J. 2021b. Gene expression related to steviol glycoside synthesis produced in *Stevia rebaudiana* (Bert.) shoot culture induced with high Far-Red LED light in TIS RITA® bioreactor system. *Sarhad J. Agric*, **37(1)**: 1–8

Mose W, Daryono BS, Indrianto A, Purwantoro A and Semiarti E. 2020. Direct somatic embryogenesis and regeneration of an Indonesian orchid *Phalaenopsis amabilis* (L.) Blume under a variety of plant growth regulators, light regime, and organic substances. *Jordan J of Biol Sci.* **13(4):**509–518.

Mose W, Indrianto A, Purwantoro A and Semiarti E. 2017. The influence of thidiazuron on direct somatic embryo formation from various types of explant in *Phalaenopsis amabilis* (L.) Blume orchid. *Hayati* **24(4):**201–205.

Murashige T and Skoog F. 1962. A revised medium for rapid growth and bio assays with tobacco tissue cultures. *Physiol. Plant.* **15**:473-497

Naing AH, Chung JD, and Lim KB. 2011. Plant regeneration through indirect somatic embryogenesis in *Coelogyne cristata* Orchid. *Am. J. Plant Sci*., **2(2):**262–267.

Parthibhan S, Rao MV, DaSilva JAT and Kumar TS. 2018. Somatic embryogenesis from stem thin cell layers of *Dendrobium aqueum. Biol. Plant.*, **62(3):**439–450.

Sebastinraj J, Britto SJ, Kumar DV, Robinson JP, and Thangavel P. 2014. Rapid propagation of *Vanda testacea* (Lindl.) Rchb.F. -A highly medicinal value epiphytic orchid of India. *World J of Agricultural Sciences* **10(5)**:223–230.

Semiarti E. 2018. Orchid biotechnology for Indonesian orchids conservation and industry. *AIP Conf. Proc*. **2002(020022):**1–5.

Shen HJ, Chen JT, Chung HH, and Chang WC. 2018. Plant regeneration via direct somatic embryogenesis from leaf explants of *Tolumnia* Louise Elmore 'Elsa'. *Bot Stud* **59(4)**:1–7.

Soe KW, Myint KT, Naing AH, and Kim CK 2014. Optimization of efficient protocorm-like body (PLB) formation of *Phalaenopsis* and *Dendrobium* hybrids. *Curr. Res. Agric. Life Sci.* **32(4)**:179–183.

Winarto B, Atmini KD, Badriah DS and Wegadara M. 2016. In vitro embryogenesis derived from shoot tips in mass propagation of two selected-clone of *Phalaenopsis. Not Sci Biol* **8(3):**317–325.

Zhao D, Hu G, Chen Z, Shi Y, Zheng L, Tang A and Long C. 2013. Micropropagation and in vitro flowering of *Dendrobium wangliangii*: A critically endangered medicinal orchid. *J. Med. Plant Res*., **7(28)**:2098–2110.

JJBS

Volume 14, Number 5,December 2021
ISSN 1995-6673
Pages 939 – 944

Jordan Journal of Biological Sciences

Growth and Productivity of Four Cassava Cultivars on Several Levels of Mixed Fertilizers

Sri Wahyuningsih[1], Febria Cahya Indriani[1], Joko Restuono[1], Kartika Noerwijati[1,*], Abdullah Taufiq[1], Yuliantoro Baliadi[1], Rohmad Budiono[2], Nguyen Van Minh[3] and Peeyush Soni[4]

[1]*Indonesian Legumes and Tuber Crops Research Institute, Jl. Raya Kendalpayak km 8, Malang 65101, East Java, Indonesia;* [2]*East Java Assessment Institute of Agriculture Technology, Jl.Raya Karangploso km 4 PO BOX 188, Malang,65101, East Java, Indonesia;*[3]*Faculty of Agriculture and Forestry, Tay Nguyen University, 567 Le Duan, Ea Tam, Thanh pho Buon Ma Thuot, Dak Lak 630000, Vietnam;* [4]*Department of Agricultural and Food Engineering, Indian Institute of Technology Kharagpur, Kharagpur, West Bengal, India – 721302;*

Received: May, 5, 2021; Revised: August, 20, 2021; Accepted Oct, 16, 2021

Abstract

Cassava is responsive to fertilization, and it is one of the important factors for high productivity. Root formation needs sufficient Phosphorus (P) and Potassium (K) nutrients, and adequate nutrients uptake increases root weight and starch content. However, the optimum effect of P and K fertilization should be balanced with Nitrogen (N) fertilization. The objective of the study was to determine the effect of mixed (inorganic and organic) fertilizers doses on the growth and yield of several cassava cultivars grown in Pati district, Central Java, Indonesia. The experiment was carried out during planting season in 2018. Four cassava cultivars (Litbang UK 2, UK 1 Agritan, Malang 4, and UJ 5) were tested under five doses of mixed fertilization. The split-plot design with three replicates was used in this experiment, where fertilizations as the main plot and cultivars as the subplot. The results showed that mixed fertilization had no significant effect, while the cultivars had a significant effect on growth and yield parameters as well as starch content. No significant interaction effect of the two factors, except in plant height.

Keywords: Environmentally-friendly fertilization, Improving cassava production, Optimal fertilizer, Prevent nutrient loss, Rational and balanced fertilization, Root yield, Soil fertility, Starch content

1. Introduction

Central Java Province contributes 15.70 % of the cassava (*Manihot esculenta* Crantz) production in Indonesia. Pati District, Central Java, Indonesia is one of the highest cassava producers among 12 other districts with a planting area of 20.000 ha and productivity of 43.55 t ha^{-1}. In this district, cassava is a commodity that attracts many farmers, and has become the main crop in their farming. So that, cassava production in Pati District in the period of 2011 to 2015 increased by 9.7 % each year (BPS Jawa Tengah, 2016). The appeal of cassava is triggered by the increasing demand for industrial raw materials.

The majority of cassava in Indonesia is grown on dry land with marginal soil fertility, and hence fertilization plays an important role in cassava cultivation. Several Inorganic Compound (Nitrogen, Phosphorus, and Potassium — NPK) fertilizers grades commonly used for food crops are 15-15-15, 20-10-10, and 30-6-8 (Budiono *et al*. 2019). Cassava plants are known to be very responsive to fertilization (Howeler, 2017). Increasing cassava productiveness due to NPK fertilization is well reported by Biratu *et al.* (2018). In the soil with low fertility, high rate of inorganic fertilizers are reqiured (Budiono *et al*., 2021; Macaloua *et al*., 2018). Agronomic research is needed to significantly increase the cassava yield through optimal fertilizer application (Ezui *et al*., 2016).

Cassava absorbs potassium (K) nutrients in high amount, even higher than N. For producing 30 t ha^{-1}, cassava uptake 147.6 kg N, 47.4 kg P_2O_5, and 179.4 kg K_2O. Potassium (K) has an important role in synthesis and accumulation of starch in cassava root (Fernandez *et al*., 2017). However, imbalance fertilization hampered productivity and profitability (Hiironen and Riekkinen, 2016). Imbalance fertilization will also increase nutrient loss (Van der Velde *et al*., 2014), and consequently degrade soil fertility (Adinurani *et al*. 2021, Li *et al.*, 2013), as well as pollute the environment (Muhammad *et al*., 2021; Utami *et al*. 2020). Cassava more response to inorganic fertilizer when combined with organic fertilizer (Biratu *et al*., 2018). Badewa *et al*. (2020) recommend to use 100 kg N —22 kg P — 83 kg K ha^{-1} combined with 2.4 t ha^{-1} chicken manure to increase cassava yield. Optimum NPK fertilizer dosage varies among cultivar and environment. Wahyuningsih and Sutrisno (2019) found that to attain yield of 33 t ha^{-1}, Malang 4 cultivar grown under young teak stands needs fertilization of 125 kg Urea ha^{-1} + 150 kg SP36 ha^{-1} + 100 kg KCl ha^{-1}. Noerwijati and Budiono (2015) found different yield in different altitude with same fertilization at rates of 200 kg ha^{-1} Urea + 100 kg ha^{-1} SP36 + 100 kg ha^{-1} KCl, where the higher yield of

* Corresponding author e-mail: tika_iletri@yahoo.com

54.84 t ha^{-1} attained at altitude of 80 m a.s.l., followed at 530 m a.s.l. (37.08 t ha^{-1}), and 7.79 t ha^{-1} at 800 m a.s.l.

The study was aimed to determine optimum dose of mixed (inorganic and organic) fertilizers on the growth and yield of several improved-cassava cultivars grown in Pati district, Central Java, Indonesia.

2. Materials and Methods

2.1. Experiment site

The field experiment was carried out during planting season of 2018 in Pati district, Central Java, Indonesia. Soil in the study site is acidic, but contains very low Al. The soil has very low organic matter, N, and Mg content, low Ca content, and medium available P, but high exchangeable K (Table 1).

Table 1. Soil properties in the experiment site.

Soil properties	Methods	Value	Criteria[1)]
pH-H_2O	1:5 (soil : H_2O)	4.68	L
C-organic (%)	Walkley & Black	1.21	VL
N-total (%)	Kjedahl	0.06	VL
P_2O_5 (mg kg^{-1})	Bray-1	13.6	M
Exchangeable K ($cmol^+ kg^{-1}$)	1 N NH_4OAc pH 7.07	0.24	H
Exchangeable Ca ($cmol^+ kg^{-1}$)	1 N NH_4OAc pH 7.07	1.08	L
Exchangeable Mg ($cmol^+ kg^{-1}$)	1 N NH_4OAc pH 7.07	0.05	VL
Exchangeable Al ($cmol^+ kg^{-1}$)	1 N KCl	3.39	VL

[1)]L=low, VL=very low, M=medium, H=high according to Howeler (2002; 2014), Howeler *et al*. (2019).

2.2. Treatment and experimental design

The experiment consisted of two factors which were laid out in a split-plot design, three replicates. The main plot was five fertilizer levels, namely P_1: 275 N + 45 P_2O_5 + 45 K_2O kg ha^{-1} (farmer practice as check), P_2: 135 N + 60 P_2O_5 + 30 K_2O kg ha^{-1}, P_3: P_2 + manure 0 t ha^{-1}, P_4: 130 N + 60 P_2O_5 + 60 K_2O kg ha^{-1}, and P_5: P_4 + manure 10 t ha^{-1}. The subplot was four cassava cultivars consisting of Litbang UK2 (V_1), UK1 Agritan (V_2), Malang 4 (V_3), and UJ5 (V_4). Urea 46 % N, SP36 36 % P_2O_5, and KCl 60 % K_2O use as the source of N, P, and K fertilizer, respectively.

2.3. Procedure

The soil was cultivated and mounded before planting. The cutting stems of 20 cm length were planted in plot measuring of 5 m × 5 m with planting distance of 1 m × 1 m. Phosphorus (P) and K fertilizer according to the treatments were applied once at 1 mo (month) after planting (MAP), while half dose of N fertilizer was applied at 1 MAP, and the remaining at 3 MAP.

2.4. Data collection and analysis

Growth variables (plant height and biomass), fresh root yields, yield components (number and weight of fresh root per plant, and harvest index), and starch content (wet base) were recorded at harvest (10 MAP). The plant height was measured from the stem above ground up to the tallest branch of the plant (Gyau 2015; Macalau *et al*. 2018). The shoot biomass measured based on weight of three plants at 9 mo after the crop was established (Pacheco *et al.* 2020. Yield components were observed from three plants (Fukuda *et al.* 2010). Yield was calculated through destructive harvesting by uprooting and weighing cassava roots from a 25 m^2 land area in the farmer's field, and the final yield (t ha^{-1}) calculated through extrapolation (Tarawali *et al*. 2012). Harvest index was calculated as the ratio of the storage root weight to the total biomass of shoots and storage root (Adjebeng-Danquah *et al.* 2016; Adu *et al.* 2020). Starch content was measured according to Fukuda *et al.* (2010). Red mite (*Tetranychus urticae* Koch) attacks was recorded during the growth according to Bellotti and Schoonhoven (1978). Observation of mite attack was carried out by scoring on the affected leaves, by giving a score 0 to healthy leaves (no spots), score 1 if there is early yellowish spotting (about 10 %) on some lower and/or middle leaves, score 2 if there is slightly yellowish spots (11 % to 20 %) on lower and middle leaves, score 3 if there is obvious damage; a lot of yellow spots (21 % to 50 %), few areas are necrotic (< 20 %), especially the lower and middle leaves are slightly wrinkled; some leaves turn yellow and fall off, score 4 if there is severe damage (51 % to 75 %) on the lower and middle leaves, the mite population is abundant and white threads are found like spider webs, and score 5 if total leaf loss occurs; plant shoots shrink; more and more white thread; plant death.

The collected-data were subjected to statistical analysis of variance (ANOVA) and the means were compared using the *LSD* test at a 5 % level of significance (Adinurani, 2016)

3. Result and Discussions

3.1. Soil chemical properties

The soil data indicate that soil fertility is low. The acidic soil pH with very low Al might be due to Ca and Mg cations leached-out from the top soil layer. Soil pH is classified as optimum for cassava growth because it is in the optimum soil pH range for cassava, which is 4.5 to 6.5, according to Howeler *et al.* (2019). The soil pH might not become a major limiting factor for cassava because it is still in the range of the optimum value.

Available P is medium, but it might become limiting factor because of low soil pH. Under low soil pH, P nutrient become less mobile due to Al or Fe fixation. Soil organic matter content as indicated by C-organic content is below the critical levels of organic matter of 3.2 % according to Howeler (2014), or at least at the critical level of 1.3 % according to Gomes (1998). Organic matter (OM) content is very low, and so that N content is also very low because OM is a main source of N in soil. The soil data indicate that soil fertility is low, and OM, N, P, Ca, and Mg might become the main constraint for cassava growth and high yield.

3.2. Growth and yield of four cassava cultivars

The results of the analysis of variance (ANOVA) showed that the fertilizer factor did not significantly affect all parameters observed, while the cultivars significantly affected all the parameters observed. There is no significant interaction between the two factors, except for plant height (Table 2). The genetic differences among cultivars have more effect on growth, yield, and yield components than fertilizer treatment.

Table 2. Results of ANOVA on all parameters observed.

Factor	Mean square value								
	Plant height (cm)	Shoot weight plant^{-1} (kg)	Biomass plant^{-1} (kg)	Number of root plant^{-1}	Root weight plant^{-1} (kg)	Root yield (t ha^{-1})	Harvest index	Starch content (% wb)	Starch yield (t ha^{-1})
Fertilizer (F)	0.08 ns	0.004 ns	0.02 ns	3.28 ns	0.10 ns	8.37 ns	0.004 ns	2.26 ns	0.28 ns
Cultivar (V)	0.11 *	0.035 **	0.10 **	5.70 *	3.29 **	5.81 **	0.049 **	26.10 **	5.13 **
F x V	0.06 *	0.002 ns	0.04	3.34 ns	0.05 ns	4.32 ns	0.003 ns	2.43 ns	0.19 ns
CV (%)	13.7	28.88	17.70	21.5	29.50	29.50	8.43	7.53	15.71

Annotation: ns = not significant, * = significantly different at 5 %, ** = significantly different at 1 %, wb = wet basis

Soil N, P, and organic matter in the experiment site were low, but application of N-P-K fertilizer, and also addition of organic fertilizer could not improve cassava growth (Table 3), as well as root yield and yield components (Table 4). The results indicate that fertilizer applied may be ineffective. Cassava in this experiment was planted in January 2018, so that the crop received high rainfall only for 3 mo (January to March), and rainfall decreased from April 2018 (Figure 1). It means that the plants suffer from drought after 3 MAP. The age at 3 MAP to 6 MAP is critical period for cassava because fast growing, root formation, as well as root development take place during that period. Lack of water will limit water absorption, as well as nutrient uptake which reduce crop growth and yield. Under these conditions, production efficiency was low as indicated by low harvest index. Plant height at harvest averaged 175.2 cm, biomass accumulation less than 1 kg plant^{-1} (Table 3), fresh root yield (14.22 to 16.29) t ha^{-1}, harvest index about 0.6, and starch content 13.82 % to 15.17 % (Table 4). Decrease in nutrient uptake occured in cassava plants under insufficient soil water (Howeler, 2012), and also reduction of plant height of cassava by 33 % to 47 % (Vitor *et al.*, 2019). Root yield, harvest index, and starch content in this experiment is low. In acidic soil in Lampung with fertilization of 135 N + 36 P_2O_5 + 30 to 60 K_2O kg ha^{-1}, UJ3 and UJ5 cultivar at 6 MAP produced (30 to 40) t ha^{-1} of fresh root with harvest index 0.7 to 0.8 and starch content >25 % (Taufiq *et al.*, 2015), and Malang 4 cultivar in East Java produced > 40 t ha^{-1} at 10 MAP with harvest index 0.7 to 0.8 and starch content > 26 % (Taufiq *et al*., 2016).

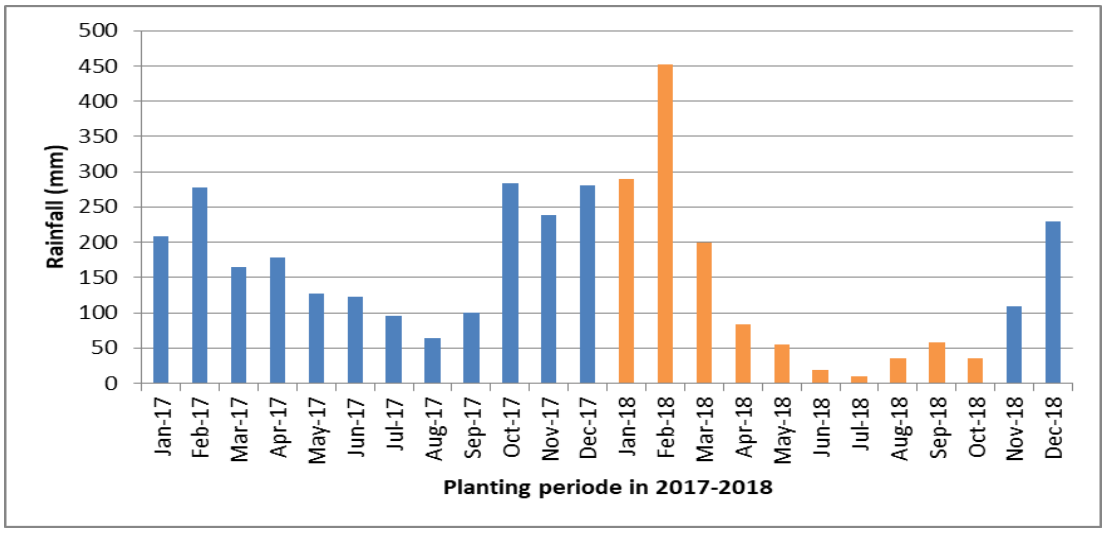

Figure 1. Rainfall in Pati District, Central Java, Indonesia during the experiment (January to October 2018).

Table 3. Effect of fertilizer doses on plant height, shoot weight, and biomass accumulation of cassava crop Pati district, Central Java, Indonesia 2018

Fertilizer doses	Plant height (cm)	Shoot weight plant^{-1} (kg)	Biomass weight plant^{-1} (kg)
P_1	185.8	0.24	0.99
P_2	165.8	0.21	0.89
P_3	168.6	0.22	0.89
P_4	180.0	0.20	0.91
P_5	175.9	0.25	0.95
Average	175.2	0.22	0.93
LSD (5 %)	0.19	0.05	0.196

Table 4. Effect of fertilizer on root number plant^{-1}, root weight plant^{-1}, root yield (t ha^{-1}), harvest index, starch content (% wb), and starch yield (t ha^{-1}), in dryland. Pati district, Central Java, Indonesia 2018

Fertilizer doses	Root number plant^{-1}	Root weight plant^{-1} (kg)	Root yield (t ha^{-1})	Harvest index	Starch content (% wb)	Starch yield (t ha^{-1})
P_1	7.11	1.59	14.32	0.61	14.32	2.44
P_2	8.11	1.59	14.22	0.64	13.82	2.29
P_3	7.44	1.68	15.15	0.65	14.62	2.48
P_4	7.99	1.64	14.76	0.63	14,69	2.46
P_5	8.33	1.81	16.29	0.65	15.17	2.72
Average	7.76	1.66	14.94	0.64	14.52	2.48
LSD (5 %)	0.93	0.252	2.27	0.025	1.08	0.44

The fertilization doses independently did not significantly affect the yield and the components of yield (Table 4). Similar to Pypers *et al*. (2011), the addition of fertilizer did not influence root yield. But reported by Cuvaca *et al.* (2017), fertilizer addition increased cassava root yield. Aplication 60 kg N ha^{-1} + 60 kg P_2O_5 ha^{-1} + 0 kg K_2O ha^{-1} increase root yield up to 27.7 t ha^{-1} compared with no fertilizer aplication. Organic matter utilization could improve root yield and soil fertility (Badewa *et al*. 2020), but in this study organic matter didn't improve the yield. Although not significantly different, it is seen that the root yield (t ha^{-1}) in the P_2 to P_5 fertilizer treatment is higher than the root yield in P_1 (farmer control) as well as the harvest index. Highest starch content and starch yield found in P_5 (130 kg N ha^{-1} + 60 kg P_2O_5 ha^{-1} + 60 kg K_2O ha^{-1} + manure 10 t.ha^{-1}) which indicate that increasing K fertilizer dose and the addition of manure could increase the starch content.

The effect of cultivars on plant height, shoot weight, and total plant weight (without root) were significantly different (Table 5). Plant height ranges from 164.3 cm to 182.9 cm. UK 1 Agritan grows tallest, while the shortest was Litbang UK 2 compared to the other cultivar. Growth parameters were more influenced by cultivar differences than fertilization treatment. According to Misganaw and Bayou (2020), variations in plant height can occur due to genetic variations. The highest shoot weight was achieved by the UK 1 Agritan variety while the lowest was the Litbang UK 2 cultivar. Likewise, the total plant biomass weight plant^{-1} (without root), the highest weight was achieved by UK 1 Agritan cultivar, and the lowest was UJ 5 cultivar. UJ 5 cultivar had a high shoot weight, but the stem was relatively small, so that the total plant biomass weight was the lowest among the other cultivars (Table 5). This indicates that UK 1 Agritan cultivar has better adaptability compared to the other cultivars.

Table 5. Effect of cultivars on plant height, shoot weight plant^{-1}, and biomass weight plant^{-1} in dryland. Pati District, Central Java, Indonesia 2018

Cultivars	Plant height (cm)	Shoot weight plant^{-1} (kg)	Biomass weight plant^{-1} (kg)
Litbang UK 2	164.3 b	0.17 b	0.88 bc
UK1 Agritan	182.9 a	0.27 a	1.01 a
Malang 4	173.1 ab	0.19 b	0.98 ab
UJ 5	180.6 a	0.26 a	0.84 c
Average	175.2	0.22	0.93
LSD (5 %)	0.13	0.05	0.12

Note : Mean values in each colum followed by different letters were significantly different ($P < 0.05$) .

The interaction between fertilizer doses and cultivar only significantly affected plant height. The highest plant height was achieved in the P_3V_2 treatment (195.0 cm), while the lowest was in the P_2V_1 treatment which was 140.7 cm (Figure 2). It can be seen that the UK 1 Agritan (V_2) variety which has good plant growth, plant height increased with the treatment P_3 (135 N + 60 P_2O_5 + 30 K_2O kg ha^{-1} + manure 10 t ha^{-1}). This indicates that the plant height of UK 1 Agritan didn't require the addition of K nutrients because the soil had high K nutrient, even the addition of K actually reduced plant height as shown in treatment P_4 and P_5.

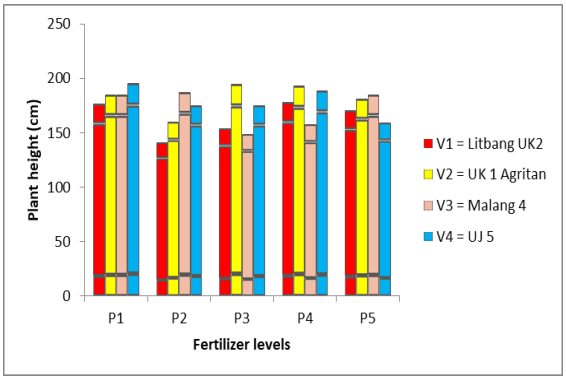

Figure 2. Effect of fertilization and cultivars on cassava plant height at 10 mo. Pati district, Central Java, Indonesia 2018. (P_1 = 275 N + 45 P_2O_5 + 45 K_2O, P_2 = 135 N + 60 P_2O_5+ 30 K_2O kg ha^{-1}, P_3 = P_2+ manure 10 t ha^{-1}, P_4 = 130 N + 60 P_2O_5+ 60 K_2O kg ha^{-1}, and P_5 = P_4 + manure 10 t ha^{-1}).

Cultivars showed significant differences in yield and yield components, namely the root number plant^{-1}, root weight plant^{-1}, root yield ha^{-1}, harvest index, starch content, and starch yield ha^{-1} (Table 6). These suggested that among varieties used, there were potential genetic differences.

The highest root number plant^{-1} was found in UJ 5 cultivar, but it was not significantly different with UK 1 Agritan cultivar. The smallest root number plant^{-1} was found in Malang 4. Likewise, the highest root weight plant^{-1} and the highest root yield ha^{-1} was in UK 1 Agritan cultivar, and the lowest was in the Litbang UK 2 cultivar. UK 1 Agritan was a cassava cultivar released in 2016 with early maturity characters. Based on farmers' information, UK 1 Agritan was quite preferred as a choice besides UJ 5 because it has not only high yield potential but also plant posture was not too large, with white root skin color. UK 1 Agritan also had a high harvest index (HI). HI is one indicator to estimate root yield. Harvest index were positively correlated (r = 0.61**) with root yield, so that the higher harvest index will have higher root yields. Karim *et al.* (2020) also found positive correlation between root yield and HI. The HI is variable to measure the efficiency of storage root production (Badewa *et al*., 2020). UJ 5 cultivar had the highest starch content followed by Malang 4 and Litbang UK 2, and the lowest was UK 1 Agritan (Table 6). Even though it has the lowest starch content, UK 1 Agritan has the highest root yield and hence the higher starch yield ha^{-1}.

Table 6. Effect of cultivar on root number, plant weight, root yield, harvest index, starch content, and starch yield in dryland. Pati district, Central Java, Indonesia 2018

Cultivars	Root number plant^{-1}	Root weight plant^{-1} (kg)	Root yield (t ha^{-1})	Harvest index	Starch content (% wb)	Starch yield (t ha^{-1})
Litbang UK 2	7.07 c	1.16 c	10.45 c	0.57 c	16.88 b	1.76 d
UK1 Agritan	8.11 ab	2.29 a	20.57 a	0.70 a	15.17 c	3.10 a
Malang 4	7.43 bc	1.53 b	13.77 b	0.61 b	16.52 b	2.29 c
UJ 5	8.41 a	1.67 b	14.99 b	0.67 a	18.38 a	2.76 b
Average	7.76	1.66	14.95	0.64	16.74	2.48
LSD (5 %)	0.97	0.18	1.66	0.036	0.95	0.29

Red mite pests commonly attack cassavas in the dry season. A red mite score, that was observed in the 3rd mo, was between 7.35 to 18.57. P_1V_3 treatment showed the lowest attack, and the highest in P_3V_3 treatment (Table 7). Fertilization treatment P_3 and P_5 had a higher mite attack score than the other treatments. It seems that the addition of organic matter can increase N nutrition, which causes plant tissue to become softer and it is easily attacked by mites. Altieri *et al* (2005) stated that an increase of N nutrient results in increased plant damage due to mites attack. Howeler *et al.* (2013) stated that application soil organic matter early in the cropping cycle, increases pest-regulating populations. To prevent more severe damage from mite attacks, spraying using Starban insecticides is carried out.

Table 7. Red mite pests population in cassava at 3 MAP.

Treatment	Mite score (%)				
	V1	V2	V3	V4	Average
P1	10.44	7.44	7.35	9.19	8.61
P2	12.57	8.36	12.03	6.93	9.97
P3	16.41	9.36	18.57	10.70	13.81
P4	11.50	11.55	11.48	9.69	11.05
P5	13.80	13.90	14.34	13.98	14.01
Average	12.94	10,12	12.75	9.50	

4. Conclusions

Reducing N fertilizer dosage from 275 kg N ha^{-1} to (130 to 135) kg N ha^{-1} and K from 45 K_2O ha^{-1} to 30 kg K_2O ha^{-1}, increasing P dosage from 45 P_2O_5 ha^{-1} to 60 P_2O_5 ha^{-1}, and application of 10 t ha^{-1} manure has no effect on both cassava growth and yield. Agronomic and yield performance of UK 1 Agritan cultivar is better than Litbang UK 2, Malang 4, and UJ 5 cultivars, and hence can be recommended as an alternative cultivar for farmers in the Pati area, Central Java, Indonesia. But the increase in N nutrient increases the attack of mite pests.

References

Adjebeng-Danquah J, Gracen VE, Offei SK, Asante IK, and Manu-Aduening J. 2016. Genetic variability in storage root bulking of cassava genotypes under irrigation and no irrigation. *Agric. Food Secur*, **5(9):**1–12.

Adinurani, P.G. 2016**. Design and Analysis of Agro Trial Data: Manual and SPSS.** Plantaxia, Yogyakarta, Indonesia.

Adinurani PG, Rahayu S, Purbajanti ED, Siskawardani DD, Stankeviča K, and Setyobudi RH. 2021. Enhanced of root nodules, uptake NPK, and yield of peanut plant (*Arachis hypogaea* L.) using rhizobium and mycorrhizae applications. *Sarhad J. Agric*. **37 (Special Issue 1)**: 16–24.

Adu MO, Asare PA, Yawson DO, Nyarko MA, Razak AA, Kusi AK, Tachie-Menson JW, Afutu E, Andoh DA, Ackah FK, Vanderpuije GC, Taah KJ, Bediako EA, and Amenorpe G. 2020. The search for yield predictors for mature field-grown plants from juvenile pot-grown cassava (*Manihot esculenta* Crantz). *PLoS One* **15(5)**e0232595:1–27.

Altieri MA, Nicholls CI, and Fritz M. 2005. **Manage Insects on Your Farm: A Guide to Ecological Strategies.** Sustainable Agriculture Research and Education - Handbook Series; bk. 7.

Badewa OD, Saba AG, Tsado EK, and Tolorunse KD. 2020. Selection of early bulking performance among pro vitamin A cassava genotypes based on selective indices of fresh storage root yield and harvest index. *International Journal of Genetics and Genomics* **8(1):**11–18.

Bellotti AC and Schoonhoven AV. 1978. **Cassava Pests and Their Control**. Centro Internacional de Agricultura Tropical (CIAT), Cali, Columbia.

Biratu GK, Elias E, Ntawuruhunga P, and Sileshi GW. 2018. Cassava response to the integrated use of manure and npk fertilizer in Zambia. *Heliyon* **4(00759)** :1–23.

BPS Jawa Tengah. 2016. Harvested area, production, and productivity of cassava by Regency / City in Central Java Province, 2012–2015. from https://jateng.bps.go.id/dynamictable/2020/01/10/653/luas-panen-produksi-dan-produktivitas-ubi-kayu-menurut-kabupaten-kota-di-provinsi-jawa-tengah-2012-2015.html (Accessed on August 19th 2020].

Budiono R, Adinurani PG, and Peeyush S. 2019. Effect of new NPK fertilizer on lowland rice (*Oryza sativa* L.) growth. *IOP Conf Ser Earth Environ Sci*., **293(012034):**1–10.

Budiono R, Aziz FN, Purbajanti ED, Turkadze T, and Adinurani PG. 2021. Effect and effectivity of granular organic fertilizer on growth and yield of lowland rice. *E3S Web Conf.*, **226(00039):**1–7.

Cuvaca IB, Eash NS, Lambert DM, Walker FR, and Rustrick W. 2017. Nitrogen, phosphorus, and potassium fertilizer effects on cassava root yield in the coastal district of Dondo, Mozambique. *Afr. J. Agric. Res* **12(42):**3112–3119.

Ezui KS, Franke AC, Mando A, Ahiabor BDK, Tetteh FM, Sogbedji J, and Giller KE. 2016. Fertilizer requirements for balanced nutrition of cassava across eight locations on West Africa. *Field Crops Res*. **185:** 69–78.

Fukuda WMG, Guevara CL, Kawuki R, and Ferguson ME. 2010. **Selected Morphological and Agronomic Descriptors for the Characterization of Cassava**. International Institute of Tropical Agriculture (IITA), Ibadan, Nigeria.

Gyau GB. 2015. Evaluation of growth, yield and root quality of four (4) cassava (*Manihot esculenta* Crantz) varieties in the semi-deciduous zone of Ghana. MSc Dissertation, Kwame Nkrumah University of Science and Technology, Kumasi, Ghana.

Hiironen J and Riekkinen K. 2016. Agricultural impact and profitability of land consolidations. *Land Use Policy* **55**:309–317.

Howeler RH. 2002. Cassava Mineral Nutrition and Fertilization. In: Hillocks RJ, Thresh JM, Bellotti AC (Eds.), **Cassava: Biology, Production and Utilization**. CAB International, pp. 115–147.

Howeler RH. 2012. Dry matter accumulation and nutrient absorption and distribution during the growth cycle of cassava. In: Howeler RH (Ed.) Chapter 14, **The Cassava Handbook: A Reference Manual Based on the Asian Regional Cassava Training Course held in Thailand**. Centro Internacional de Agricultura Tropical (CIAT) Cassava Office for Asia, Bangkok, Thailand. pp 351–410.

Howeler RH, Lutaladio NB, and Thomas G. 2013. Crop nutrition. In: Gutiérrez D (Ed.), Chapter 5- **Save and Grow: Cassava, A Guide to Sustainable Production Intensification**. Food and Agriculture Organization of the United Nations, Rome. pp 59–72.

Howeler RH. 2014. **Sustainable Soil and Crop Management of Cassava in Asia**– Cali, CO : Centro Internacional de Agricultura Tropical (CIAT). – (CIAT Publication No. 389)

Howeler RH. 2017. Does cassava cultivation degrade or improve the soild? Proc. 8th Regional Workshop A New Future for Cassava in Asia: Its Use as Food, Feed and Fuel to Benefit the Poor. Vientiane, Lao PDR. pp 320–354.

Howeler RH, Oates CG, and Allem AC. 2019. An Assessment of the impact of cassava production and processing on the environment and biodiversity. Strategic environmental assessment (fao.org).

Karim KY, Ifie B, Dzidzienyo D, Danquah EY, Blay ET, Whyte JBA, Kulakow P, Rabbi I, Parkes E, Omoigui L, Norman PE, and Iluebbey P. 2020. Genetic characterization of cassava (*Manihot esculenta* Crantz) genotypes using agro-morphological and single nucleotide polymorphism markers. *Physiol Mol Biol Plants* 26: 317–330.

Li Q, Xu M, Liu G, Zhao Y, and Tuo D. 2013. Cumulative effects of a 17-years chemical fertilization on the soil quality of cropping system in the loess hilly region China. *J. Plant. Nutr. Soil Sci* .**176(2)**:249–259.

Macaloua S, Mwongab S, and Musanduc A. 2018. Performance of two cassava (*Manihot escculenta* Crantz) genotypes to NPK fertilizer in Ultisols of Sikasso Region, *Int. J. Sci. Basic Appl. Res.* **38(2**): 189–206.

Magdoff F and van Es Harold. 2021. What is organic matter and why is it so important. In: Magdoff F and van Es Harold (Eds) Chapter 2. **Building Soils for Better Crops**. Sustainable Agriculture Research and Education. College of Agriculture and Natural Resources, University of Maryland, USA. 394p.

Misganaw CD and Bayou WD. 2020. Root yield and yield component performance of cassava (*Manihot esculenta*) varieties in Fafen Disrict, Ethiopia. *Int. J. Agron***. (5836452)**: 1–6.

Muhammad M., Umi I, Peeyush S, and Praptiningsih GA. 2021. Effectiveness of mycorrhiza, plant growth promoting rhizobacteria and inorganic fertilizer on chlorophyll content in *Glycine max* (L.) cv. Detam-4 Prida. *E3S Web Conf*., **226(00031):**1–8.

Noerwijati K and Budiono R. 2015. Yield and yield components evaluation of cassava (*Manihot esculenta* Crantz) clones in different altitudes. *Energy Procedia* **65**:155–161.

Pacheco RI, Macias MP, Campos FC, Izquierdo AJ, and Izquierdo GA. 2020. Agronomic and physiological evaluation of eight cassava clones under water deficit conditions. Revista Facultad Nacional De Agronomía Medellín, **73(1)**: 9109–9119.

Pypers P, Sanginga JM, Kasereka B, Walangululu M, and Vanlauwe B. 2011. Increased productivity through integrated soil fertility management in cassava-legume intercropping systems in the highlands of Sud-Kivu, DR Congo. *Field Crops Res*., **120(1)**: 76–85.

Tarawali G, Iyangbe C, Udensi UE, Ilona P, Osun T, Okater C, and Asumugha GN. 2012. Commercial-scale adoption of improved cassava varieties: A baseline study to highlight constraints of large-scale cassava based agro-processing industries in Southern Nigeria. Journal of Food, Agriculture & Environment, **10 (3&4):** 689–694. 2012.

Taufiq A, Subandi, and Suyamto H. 2015. Response of Cassava (*Manihot esculenta* Crantz.) to potassium application on acidic dryland in Indonesia. International Potash Institute e-ifc **42**:18–26.

Taufiq A, Subandi, and Suyamto H. 2016. Response of Cassava (*Manihot esculenta* Crantz.) to potassium application on various soil types in East and Central Java, Indonesia. International Potash Institute e-ifc **45**:19–30.

Utami SNH, Abduh AM, Hanudin E, and Purwanto BH. 2020. Study on the NPK uptake and growth of rice under two different cropping systems with different doses of organic fertilizer in the Imogiri Subdistrict, Yogyakarta province, Indonesia. *Sarhad J. Agric*. **36(4):** 1190–1202.

Van der Velde M, Folberth C, Balkovič J, Ciais P, Fritz S, Janssens IA, and Jeñuelas J. 2014. African crop yield reductions due to increasingly unbalanced Nitrogen and Phosphorus comsumption. *Glob. Change Biol*. **20(4):**1278–1288.

Vitor AB, Diniz RP, Morgante CV, Antônio RP, and de Oliveira EJ. 2019. Early prediction models for cassava root yield in different water regimes. *Field Crops Res*, **239**:149–158.

Wahyuningsih S and Sutrisno. 2019. Growth and productivity of several cassava varieties with different level of fertilizers in young teak field. *Buletin Palawija* **17(1):**40–45.

Yasmin F, Othman R, and Maziz MNH. 2020. Yield and nutrient content of sweet potato in response of plant growth-promoting rhizobacteria (PGPR) inoculation and N fertilization. *Jordan J Biol Sci*., **13(1)**:117–122**.**

JJBS

Volume 14, Number 5,December 2021
ISSN 1995-6673
Pages 945 – 951

Jordan Journal of Biological Sciences

Utilization of "Uwi" Plant (*Dioscorea* sp.*)* as a Renewable Bioenergy Resource

Wuryantoro Wuryantoro[1,*], Praptiningsih Gamawati Adinurani[1],Ratna Mustika Wardhani[1], Sutrisno Sutrisno[2],Bohari Mohammad Yamin[3] and Syukri Muhammad Nur[4,5]

[1]*Department of Agrotechnology, Faculty of Agriculture, Merdeka University of Madiun, Jl. Serayu 79 Madiun 63133, Indonesia;* [2]*Department of Mechanical Engineering, Faculty of Engineering, Merdeka University of Madiun, Jl. Serayu 79 Madiun 63133, Indonesia;* [3]*Department of Chemistry, Faculty of Science and Technology, Kebangsaan University of Malaysia, 43600 UKM, 43600 Bangi, Selangor, Malaysia;*[4]*Graduate School of Renewable Energy, Darma Persada University, Jl. Radin Inten 2, Pondok Kelapa, East Jakarta 13450, Indonesia;*[5]*Center of Renewable Energy Studies, Darma Persada University, Jl. Radin Inten 2, Pondok Kelapa, East Jakarta 13450*

Received: June, 11, 2021; Revised: Sep, 20, 2021; Accepted Oct, 16, 2021

Abstract

Many countries are currently making efforts to obtain alternative energy to reduce dependence on fossil energy resources. "Uwi" plant is a carbohydrate source that has many types and is tolerant of being planted on the upland, so it has the potential to be used as a food crop and as bioenergy. This research aims to study the potential of varieties of "uwi" (*Dioscorea* sp.) as raw material for ethanol production. The eight varieties of "uwi" were studied to assess their ethanol potential. The selected raw materials are *Dioscorea alata* L. (white yam, purple yam, and yellow yam); *Dioscorea esculenta* (Lour.) Burkill ("uwi gembili" and "uwi gembolo"); *Dioscorea bulbifera* L. ("uwi gandul"); *Dioscorea pentaphylla* L. ("uwi katak") and *Dioscorea hispida* Dennst. ("uwi gadung"). A field experiment with Randomized Block Design was used to obtain homogenous tuber raw material, followed by laboratory methods on the assessment of ethanol production potential through fermentation. The research showed that the variety, *D. hispida* had the highest ethanol content (4.94 %), followed by *D. esculenta* (4.16 %) and *D. alata* (white yam) (3.89 %). The lowest ethanol production was obtained from *D. pentaphylla* (0.36 %) and *D. bulbifera* (1.53 %). However, in terms of productivity, *D. alata* (white-yam) is the most prospective considering its high production, ease of cultivation and tolerance of forest stands.

Keywords: Alternative energy, Bioethanol, Clean energy, Diversity, Energy plant, Root tuber crop, Upland, Yam

1. Introduction

Indonesia is the country with enormous energy consumption in Southeast Asia and fifth in the Asia Pacific, after China, India, Japan and South Korea. Increasing energy demand will increase along with the high average Gross Domestic Product (GDP) growth of 6.04 % during 2017 to 2050. Indonesia's final energy consumption (without firewood) in 2016 was still dominated by fuel oil at 47 % (Anindhita *et al*., 2018). The dependency on fuel is a problem because, in future time, it will run out and give emissions that harm the environment (Adinurani *et al.* 2017). The threat of scarcity of fossil energy has implications for an increase in the price of itself. On the other hand, Indonesia has great potential in producing renewable energy, one of which is biofuels (Adinurani *et al*, 2015; Tampubolon and Fauzi, 2016).

Biofuels such as bioethanol are a form of fuel that will be dominant for the future because they are renewable (Adelabu *et al*. 2018). The production of renewable fuels, especially from starchy materials such as root crops, has great potential to meet future energy demand. The tuber group is a promising raw material for bioethanol because it has enough carbohydrates (16 % to 24 %), abundant availability and cost-effective processing (Wuryantoro *et al*., 2020). Root crops are a better choice for bioethanol because they are cheap and less competitive as food than grains, only about 45 % of the tuber plant is consumed as food, and the rest is used for feed and industrial raw materials.

"Uwi" plant, ["uwi" is a common name in Indonesian, while in English it is called "yam" (*Dioscorea* sp.)] is a tuber group with lesser attention and has not received priority as a food source. This plant has many species and varieties, about 200 varieties with colours, shapes and flavours. Types of *Dioscorea alata* L., in particular, have colour variants and forms ranging from primary colours from white, yellow and purple, along with variations in shapes such as elongated, oblong, rounded, fingering to irregular (Wuryantoro *et al*., 2021). The existence of this plant is increasingly marginalized from cultivation techniques and is even allowed to grow wild. This group of tubers has excellent potential as a source of carbohydrates to use as raw material for bioethanol without disturbing food needs. "Uwi" plants are very suitable for planting in various land conditions,

* Corresponding author e-mail: wuryantoro@unmer-madiun.ac.id.

especially in an upland that has not been optimally utilized. This upland area covers more than 60 % of the land area in Indonesia (Hakim et al., 2017) and more than 40 % in the world (UNESCO, 2020). This highlights the adaptability of "uwi" to the local climatic conditions and ability to thrive without significant climate impacts (Okongor *et al*., 2021). Some varieties can even be adapted to forest stands with higher production capacity (Wuryantoro *et al*., 2019). However, the product potential of this commodity for industrial use is still not well utilized (Andres and Adeoluwa, 2016). These plants are also crucial in socio-religious life in various countries. Research in Nigeria shows the importance of "uwi" plant in social, economic, religious and cultural fabric of society (Obidiegwu and Akbapio, 2017). In Ghana, these plants have even become an essential commodity being cultivated intensively involving men and women with various levels of education, which ultimately determines the level of productivity and farming efficiency (Tanko and Alidu, 2017). And in Cameroon, the commodity of yam is the primary buffer for food security and in overcoming poverty. There are seven species cultivated in this country, and about 17 wild species are feared for genetic erosion if there is no Gen Bank Institute to handle it immediately (Azeteh *et al*., 2019).

According to Hoover (2001) in Ulyarti (2016), the starch content of *D. alata* tubers reaches 80 % of the total dry weight (Ulyarti and Lavlinesia, 2016). The starch content in *D. alata* tubers varies greatly depending on the cultivar and growing conditions. Sahusilawane *et al.* (2011) stated that this plant produces an excellent source of carbohydrates in tropical and subtropical areas. In Indonesia, *Dioscorea* sp. is a type of tuber plant that has not been widely cultivated and even grows as wild plants on the edge of gardens, forests or abandoned land. This plant productivity is quite high if cultivated properly; it can reach (40 to 60) t ha^{-1}. Under certain types of forest stands, they still produce (3 to 5) kg $plant^{-1}$. The results of the study by Winarti and Saputro (2013) showed the starch content of *Dioscorea alata* L. (yellow yam = 83.38 %, purple yam = 86.12 %, and white yam = 86.68 %), *Dioscorea esculenta* (Lour.) Burkill ("uwi gembili" = 82.82 %), *Dioscorea pentaphylla* L. ("uwi katak" = 79.27 %), and *Dioscores bulbifera* L. ("uwi gembolo" = 84.80 %). Due to its high starch concentration, the tuber plant is considered one of the most important first-generation feedstocks for bioethanol production. Root starch can be hydrolyzed, fermented, and then refined to produce ethanol (Thatoi *et al*., 2016). Starch content is a good substrate for producing glucose as an intermediate product for making bioethanol. Variations in the starch content of *Dioscorea* sp. may depend on several environmental factors and agronomic practices, and the degree of maturity. The difference in starch content in *Dioscorea* sp. requires studying to determine the potential varieties as raw material for bioethanol. The research on tuber skin yielded 12.3 % bioethanol. It showed that the tubers could produce bioethanol, although not as good as cassava peels which grew 18.6 %, using the yeast *Gloeophylum saplarium, Pleurotus ostreatus, Zymomonas mobilis* and *Saccharomyces cerevisiae* (Adiotomre, 2015). The fermentation process has been widely used in agricultural, livestock, and fishery activities to obtain material inputs for biological productivity processes (Yasmin *et al*., 2020). Fermentative microbes are widely available in nature, which is accessible to isolated for various needs. It is reported that traditionally fermented vegetables are a good source of *Lactobacillus* probiotics (Mahasneh *et al*., 2020). Another study on fermentation resulted in ethanol yield of 13 % and 11 % from bitter yam [*Dioscorea dumetorum* (Kunth.) Pax.] and skin of water yam tubers (*Dioscorea alata* L.), respectively (Banjo *et al*., 2019).

2. Materials and Method

2.1. Time and Place

The research was carried out with field experiments in the Cepoko village's uplands, Ngrayun sub-district, Ponorogo district, East Java at an altitude of 700 m a.s.l., in the rainy season of November 2019 to June 2020. Subsequent experiments on ethanol production were carried out in the Faculty of Agriculture Laboratory, the Merdeka University of Madiun, from August 2020 to October 2020.

2.2. Materials and Tools

The materials used in the field experiment were eight varieties of "uwi" plants, compost and NPK "Mutiara" fertilizer (N:P:K = 16:16:16), from PT Meroke, Indonesia. The equipment used is a hoe, sickle, bamboo for plant propagation, and measuring equipment such as meters, scales and calipers. For laboratory experiments, using tuber materials from field experiments, distilled water, well water, "tape" yeast brand "Kencana", Indonesian product, alpha-amylase enzyme, NaOH. The equipment used is in the form of boiling equipment: gas stove, pan, peel knife and chopper, fermentation equipment in the form of closed jars, pH meters, refractometers, distillation equipment: laboratory-scale distillation, Erlenmeyer flasks, round flasks, thermometers, cooling water reservoirs, distillate containers, Bunsen heaters, gas stoves and electric stoves.

2.3. Research method

The field experiment used a Randomized Block Design consisting of eight treatments of "uwi" species *(Dioscorea* sp.), repeated three times. The treatments consisted of three sub-varities of *D. alata (*white yam, yellow yam and purple yam), two sub-varietes of *D. esculenta* ("uwi gembili" and "uwi gembolo"), *D. hispida* ("uwi gadung"), *D. bulbifera* ("uwi gandul") and *D. pentaphylla* ("uwi katak"). Observations were made on the production of tubers after going through homogeneous cultivation techniques. The experiment used a Randomized Block Design (Ramesh *et al*., 2019), and as a block, the length of fermentation time was 5 d, 7 d, and 10 d. The eight types of "uwi" tubers from field experiments as treatments were:

U1 *D. alata* type white yam
U2 *D. alata* type purple yam
U3 *D. alata* type yellow yam
U4 *D. esculenta* type "gembili"
U5 *D. esculenta* type "gembolo"
U6 *D. bulbifera* ("uwi gandul")

U7 *D. pentaphylla* (“uwi katak”)
U8 *D. hispida* (“uwi gadung”)

2.4. Practices

The study has two experimental stages. The first is a field experiment using a Randomized Block Design and soil fertility as block and repeated three times. Observations variable on the production of tubers after going through homogeneous cultivation techniques. Planting was carried out on the mounds in the treatment plot with four bunds for each treatment type and repeated in three blocks. The tuber weight for seedlings ranged from 75 g to 100 g, planted at a 75 cm × 100 cm spacing. When the bulbs sprout, a double-row model of propagation poles is given (Wuryantoro, 2020).

The second stage is the laboratory experiment using a randomized block design and a grouping according to fermentation time, namely 5 d, 7 d, and 10 d. The study used eight treatments of "uwi" tubers whose productivity had been investigated from previous field experiments. The stages of ethanol production are material preparation, stripping, cutting, boiling, administering enzymes (alpha-amylase), yeast (*Saccharomyces cerevisiae*) and NPK, fermentation, filtering, refining, ending with measuring ethanol production by distillation.

Table 1. Density conversion of ethanol at various ethanol content

Ethanol content (%)	Density (30 °C)	Ethanol content (%)	Density (30 °C)	Ethanol content (%)	Density (30 °C)	Ethanol content (%)	Density (30 °C)
0	0.995 68	13	0.974 24	26	0.954 42	39	0.929 79
1	0.993 79	14	0.972 78	27	0.952 72	40	0.927 70
2	0.991 94	15	0.971 33	28	0.950 98	41	0.925 58
3	0.990 14	16	0.969 90	29	0.949 22	42	0.923 44
4	0.988 39	17	0.968 44	30	0.947 41	43	0.921 28
5	0.986 70	18	0.966 97	31	0.945 57	44	0.919 10
6	0.985 07	19	0.965 47	32	0.943 70	45	0.916 92
7	0.983 47	20	0.963 95	33	0.941 80	46	0.914 72
8	0.981 89	21	0.962 42	34	0.939 86	47	0.912 50
9	0.980 31	22	0.960 80	35	0.937 90	48	0.910 28
10	0.978 75	23	0.959 29	36	0.935 91	49	0.908 05
11	0.977 23	24	0.957 69	37	0.933 90	50	0.905 80
12	0.975 73	25	0.956 07	38	0.931 86		

3. Result and Discussion Carbohydrate and Glucose Level

From the analysis, results of carbohydrate content of fresh tubers from eight varieties of *Dioscorea* sp. were observed to be between 18.80 % and 26.60 %, sugar content before fermentation was 1.00 % to 7.00 % and sugar content after 10 d fermentation was between 0.77 % and 4.10 % (Figure 1).

Figure 1 also shows that the varieties with higher carbohydrate content in fresh tubers do not always produce high sugar content. The highest carbohydrate content in white yam *(D. alata)* was 26.60 %, with sugar content before fermentation (0 d) was 1.2 % and 10 d as 2.00 %. On the other hand, "uwi gembili " and "uwi gembolo" (*D. esculenta*) varieties with the lowest carbohydrate content (18.80 % and 20.62 %) produced the highest sugar content during the fermentation process, which indicates that the starch from these materials were more readily hydrolyzed into sugar. This condition causes an increase in breaking the starch polymer chains in carbohydrates of "uwi gembili” and “uwi gembolo" species into sugar.

The measure of ethanol content taking 200 mL of fermented liquid samples with three repetitions, namely on the 5th d, 7th d, and 10th d of fermentation. Observations were made on pH solution by pH meter, sugar content measure by Refractometer Brix, and ethanol content by alcohol meter. The pH level is measured every day to maintain pH 5 to pH 6 with the addition of NaOH. Therefore, sugar and ethanol levels were observed on 5 d, 7 d, and 10 d, of the fermentation process. Calculation of alcohol content was made using Equation (1):

$$Ec = \frac{DE \times Vf \times 100}{Ws} \quad (1)$$

Note: Ec; Ethanol content (%)
DE: Density of alcohol at the rate of distillation (Table 1)
Vf: Volume of fermentation liquid from Ws tuber material
Ws: Sample weight of tuber material

The Density value of ethanol (DE) uses the conversion table approach in Table 1 (Perry *et al*., 2000).

Figure 1 also shows that the varieties with higher carbohydrate content in fresh tubers do not always produce high sugar content. The highest carbohydrate content in white yam *(D. alata)* was 26.60 %, with sugar content before fermentation (0 d) was 1.2 % and 10 d as 2.00 %. On the other hand, "uwi gembili " and "uwi gembolo" (*D. esculenta*) varieties with the lowest carbohydrate content (18.80 % and 20.62 %) produced the highest sugar content during the fermentation process, which indicates that the starch from these materials were more readily hydrolyzed into sugar. This condition causes an increase in breaking the starch polymer chains in carbohydrates of "uwi gembili” and “uwi gembolo" species into sugar.

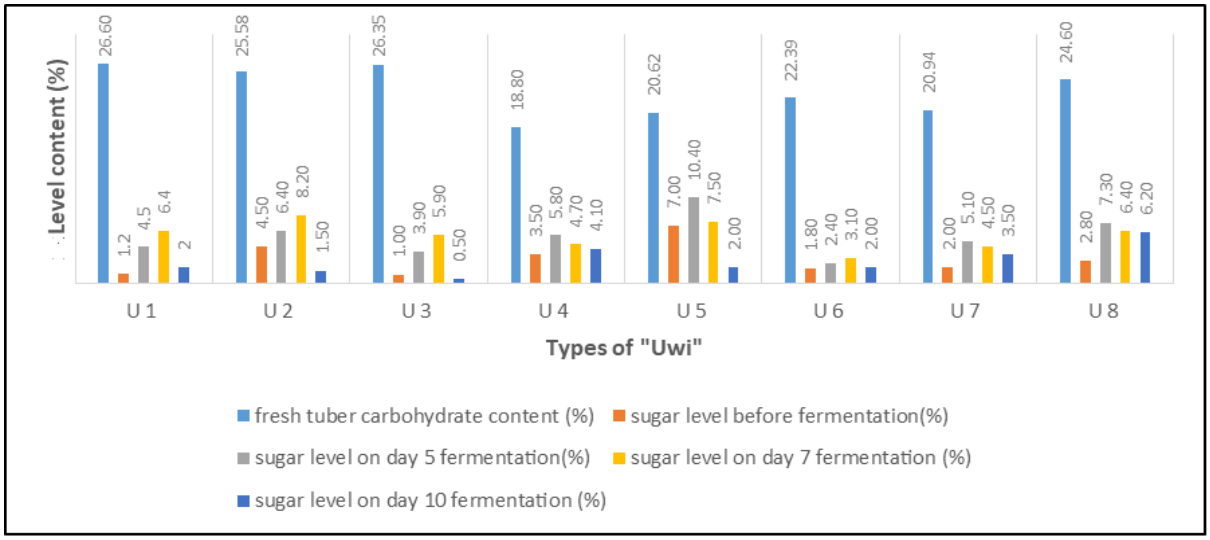

Figure 1. Carbohydrate content of fresh tubers and sugar content of various types of "uwi" at different fermentation times

The high sugar content indicates that glucose conversion to ethanol has not maximized for 10 d of fermentation. This speed of hydrolysis, in turn, yields higher ethanol (Table 2). At the same time, the enzymatic hydrolysis process of many carbohydrates in *D. alata* (white yam) needed relatively longer duration than that of "uwi gembili" to produce lower sugar levels. The α-amylase enzyme used in hydrolysis can specifically break α-1,4-glucoside bonds and quickly reduce the starch molecules size into a simple form, namely sugar (Praputri and Sundari, 2019). "uwi gadung" has a high starch content, and the amylase enzyme plays a role in the formation of high sugar until the 10th d of the fermentation process, which produces 4.94 % ethanol although not significantly different from "uwi gembili", "uwi gembolo", and white yam. This process is not the case if the hydrolysis runs faster and the hydrolyzed substrate contains enough sugar to be fermented as in the "uwi gembili" variety. High substrate concentrations can reduce energy use and overall water consumption. This is to increase the effectiveness of the fermentation process.

Based on Figure 1, the highest sugar content was in the "uwi gembolo" variety but did not show the maximum ethanol production. This may be due to the inhibition of reducing sugar fermentation (Raul *et al.* 2016). Even though the ethanol content of the "uwi gembili" variety (3.89 %) was not high, the ethanol content produced was quite a lot and not significantly different from the ethanol content of the "uwi gembolo" (4.17 %), as shown in Table 2. These results have no significant difference from the results of the research by Yuniawati *et al.* (2010), carried out for the ethanol production from white yam (3.2 %), yellow yam (2.6 %), and purple yam (2.6 %). For the "uwi gembolo" variety, the sugar content from the beginning was high (7 %), indicating that the starch was hydrolyzed into sugar, resulting in higher ethanol yield. The enzymatic and fermentation processes that run simultaneously require high energy and are generally in the early fermentation stages. In the beginning, the high amount of sugar converted a lot to ethanol during the fermentation process, so caused the amount to be lower at the end of fermentation. The amount of sugar available in the media is still tiny. In this condition, microbial growth is slow and affects ethanol production—the level of ethanol yield is determined by the yeast activity used with fermented sugar substrate. Microbial activity in yeast enters a death phase when there are enough sugar substrates. Therefore, the microbial population does not considerably impact ethanol production, but it significantly consumes the sugar content in the fermentation substrate (Selim *et al.*, 2018). In the "uwi gembili" variety, the number of microbes grows slowly. Therefore, there is no increase in the number of microbes that can convert the substrate into bioethanol, thereby reducing bioethanol production. This moment causes the ethanol content produced to be not optimal.

The fermentation process can take a long time, depending on the yeast's ability to convert sugar into alcohol. In the fermentation process, microbes change the substrate that can turn into ethanol and produce enzymes to catalyze the conversion of complex carbohydrates to simpler sugars (Thatoi *et al.*, 2016). Enzymatic and fermentation processes that run simultaneously will reduce energy input and increase the substrate (Chen-Yeon Chu *et al.*, 2012).

Table 2. The productivity tuber of "uwi" and estimation of ethanol production

Types of "uwi"	Tuber yield (t ha^{-1})	Level of ethanol (%)	Estimation of ethanol product (t ha^{-1})
U1	47.77 c	3.56 cd	1.089 cd
U2	57.57 d	3.04 bc	1.141 d
U3	56.70 d	2.76 bc	1.049 cd
U4	29.80 ab	3.89 cd	0.517 abc
U5	33.47 b	4.17 cd	0.687 bcd
U6	25.07 ab	1.53 ab	0.162 ab
U7	23.57 a	0.36 a	0.042 a
U8	30.27 ab	4.94 d	0.885 cd

Notes: The number followed by same letters, in the same column, not significant at 5 % DMRT

The research results on ethanol content in the varieties of *Dioscorea* sp. did not show linearity in the relationship of sugar content with ethanol yield. The relationship between 10th d fermentation substrate sugar content and ethanol content follows the equation y = 2.815 + 0.025x.

R2 = 0.001, which indicates that the effect of sugar content on the 10th d fermentation ethanol yield is insignificant. The results also showed that the ethanol yield on 5th d, 7th d and 10th d was not significant, with sugar content. The high sugar content on the 10th d fermentation indicates that the activity microbial was not maximum or the inhibition fermentation process. The addition of the enzyme glucoamylase seems necessary to increase sugar levels, given the relatively low glycemic index value of "uwi" plant tubers (Ramdath *et al*., 2004). Braide *et al.* (2018) showed that the maximum yield of ethanol obtained at pH (4.0 to 4.5) for *Zymomonas mobilis* and pH (4.2 to 4.5) for *Saccharomyces cerevisiae*. The optimum ethanol production at 72 h fermentation process by *Z. mobilis* was 8.36 % (v/v) and 7.39 % (v/v) by *S. cerevisiae*. The sugar concentration was reduced from (11.82 to 7.69) mg g^{-1} and (13.08 to 7.50) mg g^{-1} in the substrate fermented by *Z. mobilis* and *S. cerevisiae.* In addition, the quality of the yeast is thought to be the cause of the low ethanol content production. Another study stated that fermentation with newly isolated yeast produced more ethanol at room temperature (11.30 %) and at 80 °C (6.15 %) than fermented with baker's yeast (Olayemia *et al*., 2019). "Uwi" peels also had more ethanol at room temperature than at 80 °C using either of the two enzymes for fermentation (21.72 % and 27.08 %) (Olayemia *et al*., 2019). The research results on *D. rotundata* also revealed its potential as raw material for lactic and alcohol fermentation due to the high concentration of reducing sugars after hydrolysis. However, *Saccharomyces bayanus* is not suitable to replace *S. cerevisiae* in ethanol production via SSF due to its low ethanol productivity in the first 24 h of fermentation (Villadiego-del Villar *et al*., 2021)

3.1. Ethanol Content

The ethanol content (%) of types of "uwi" in the three fermentation stages is shown in Figure 2.

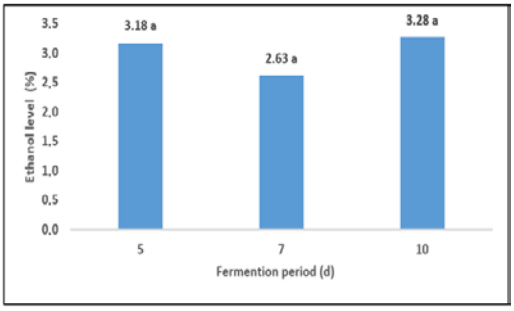

Figure 2. The average of "uwi" tuber plant ethanol content (%) in three stages of fermentation

Figure 2 shows that the fermentation time of (5 to 10) d did not show any significant changes and differences, indicating that the fermentation process of up to 5 d is sufficient to convert carbohydrates into sugar and ethanol. The ethanol content did not increase until 10 d due to the fermentation process's delay by the high level of ethanol in the fermentation liquid, which caused the yeast to become inactive.

The amount of sugar substrate produced from the hydrolysis process seems to be an obstacle in increasing the ethanol yield. The hydrolysis process is the key to an optimum ethanol recovery from starch-based materials. The use of alpha-glucosidase enzymes and variations in hydrolysis temperature affected in increasing the rate of hydrolysis (Kusmiyati, 2010). Other studies also showed that the longer the fermentation time, the greater the bioethanol content produced until the 3th d. There was a decrease in bioethanol levels the next day (Novia and Khairunnas, 2017). The research results regarding the durian (*Durio zibethinus* L.) seed bioethanol content revealed the optimal fermentation time of 72 h. The fermentation of 20 g L^{-1} reducing sugars for 72 h results in the highest ethanol concentration, viz., 9.85 g L^{-1} (Purnomo *et al*., 2016). While in the other studies on *Colocasia* Schott plants, the resulting highest bioethanol content was 19.10 % during 96 h fermentation using *S. cerevisiae* (Praputri and Sundari, 2019).

3.2. Productivity

The ethanol production process was determined by two factors, namely tuber-plant productivity and ethanol content of each type. The purple tuber of *D. alata* species produced the highest ethanol (1.141 t ha^{-1}) due to increased tuber production (57.57 t ha^{-1}), although it is not significantly different from the yellow yam. Meanwhile, "gembolo" yielded a higher ethanol yield with low tuber productivity; therefore, estimation ethanol productivity was few (0.687 t ha^{-1}). Thus, in terms of productivity, white, purple and yellow *D. alata* variety have more potential for ethanol production (Figure 3). The tuber production process determined by many factors such as climate, soil, fertilization and other cultivation techniques such as population size, seed quality, plant varieties and others. *D. alata* has more variety, differentiated based mainly on the colour and shape of the tubers. The research results of *D. alata* species revealed productivity of (5 to 7) kg $plant^{-1}$ with a spacing of 1.00 cm × 0.75 cm. However, the other varieties of *D. alata* had production of less than 2 kg per plant. The yellow yam is rarely used as food because of its unfavourable taste, which can be considered as a raw material for bioethanol.

Yellow yam White yam Purple yam

Figure 3. Three potential types of *Dioscorea alata*

4. Conclusion

The "uwi" plant species *D. alata* , namely white yam, purple yam and yellow yam, had the highest tuber and ethanol productivity even though the ethanol content was lower than the "uwi gadung" *(D. hispida)*, "uwi gembolo" and "uwi gembili" *(D. esculenta*). High levels of tuber carbohydrates, not necessarily resulting in high ethanol yield, still depend on the speed of converting carbohydrates into sugar at the beginning and during the fermentation process. The highest percentage of ethanol yield was obtained for "uwi gadung" (*D. hispida*) at 4.94 %, followed by "uwi gembolo" and "uwi gembili" at 3.89 % and 4.17 %, and the lowest was for "uwi katak" (*D. pentaphylla*) at 0.36 %. The highest ethanol productivity was obtained by the species of "uwi kelapa" (*D. alata*) with production of (1.049 to 1.141) t ha^{-1} of ethanol, considering higher tuber production.

Acknowledgment

The authors appreciate Kemenristekdikti (Ministry of Research, Technology and Higher Education of Republic of Indonesia) for funding this research, by contract number 009/KP2TJ/PTUPT/Unmer.Mdn/LPPM/III/2020, Rector of the Merdeka University of Madiun and the Dean of the Faculty of Agriculture for all facilities. Also, the entire team and students have helped get a lot of data in the field and laboratory.

References

Adelabu, BA, Kareem SO, Adeogun AI, and Ademolu KO. 2018. Direct bioconversion of sorghum straw to ethanol in a single-step process by *Candida* species. *Jordan J. Biol. Sci.* **11(1)**: 57–63.

Adinurani PG, Setyobudi RH, Nindita A, Wahono SK, Maizirwan M, Sasmito A, Nugroho YA, and Liwang T. 2015. Characterization of *Jatropha curcas* Linn. capsule husk as feedstock for anaerobic digestion. *Energy Procedia* **65**:264–273

Adinurani PG, Setyobudi RH, Wahono SK, Maizirwan M, Nindita A, Purbajanti ED, Harsono SS, Malala AR, Nelwan LO and Sasmito A. 2017. Ballast weight review of capsule husk *Jatropha curcas* Linn. on acid fermentation first stage in two-phase anaerobic digestion. *Proc. Pakistan Acad. Sci. B. Life and Environmental Sciences* **54 (1)**: 47–57

Adiotomre KO. 2015. Production of bioethanol as an alternative source of fuel using Cassava and Yam Peels as raw materials. *International Journal of Innovative Scientific & Engineering Technologies Research*, **3(2):** 28–44.

Anindhita, Rahardjo I, Fitriana I, Dewi REP, Siregar E, Niode N, Yudiartono, Sugiyono A, La Ode, Wijaya WPT, Paminto AK, Gustriani N. 2018. **Indonesia Energy Outlook 2018: Sustainable Energy for Land Transportation**, 134 (4). BPPT, Jakarta, Indonesia.

Andres C, Adeoluwa O and Bhullar GS. 2016. Yam (*Dioscorea* spp.). In : Thomas B, Murry BG and Murphy DJ (Eds.) **Encyclopedia of Applied Plant Sciences**, Vol 3, Academic Press, Waltham, MA, USA pp. 435–441.

Azeteh IN, Hanna R, Sakwe PN, Njukeng AP and Kumar PL. 2019. Yam (*Dioscorea* spp.) production trends in Cameroon. *Afr. J. Agric. Res.* **14(26)**:1097–1110

Braide W, Oji IO, Adeleye SA and Korie MC. 2018. Comparative study of bioethanol production from agricultural wastes by *Zymomonas mobilis* and *Saccharomyces cerevisiae. Int. J. Appl. Microbiol. Biotechnol. Res* **6**:50–60

Chen-Yeon Chu L, Biswarup Sen, Chyi-How Lay and Yi-Chun Lin. 2012. Direct fermentation of Sweet Potato to produce maximal hydrogen and ethanol. *Appl. Energy*, **100**: 10–18.

Green RH and Maloney DW (Eds.). 2008. **Perry's Chemical Engineers' Handbook**, Eighth Edition, McGraw-Hill, USA

Hakim, M.L., Ongki W. dan Aulia A.A. 2017. **Statistics of Agricultural Land 2012-2016**. Center for Agricultura Data and Information System Secrtariat General – Ministry of Agriculture..

Kusmiyati. 2010. Comparasion of Iles-Iles and Cassava tubers as a *Saccharomyces cerevisiae* substrate fermentation for bioethanol production. *Nusantara Bioscie*. **2(1)** : 7–13.

Mahasneh A M.,Sarah H and Sari A. M. 2015. Probiotic properties of *Lactobacillus* species isolated from local traditional fermented products. *Jordan J. Biol. Sci.* **8 (2) :** 81 – 87

Novia N, Khairunnas and Purboyo GT. 2017. Effect of sodium hydroxide concentration during pretreatment and fermentation time on bioethanol levels from Pineapple leaves. *Jurnal Teknik Kimia*, **21(30)**:16–26

Obidiegwu JE and Akpabio EM. 2017. The geography of Yam cultivation in Southern Nigeria: Exploring its social meanings and cultural functions. *J. Ethn. Foods*, **4 (1)**: 28–35

Okongor, G., C. Njoku, P. Essoka and J. Efiong. 2021. Climate variability and Yam production: Nexus and projections. *Sarhad J. Agric*, **37(2)**: 406-418.

Olayemia S, Ibikunleb A and Olayemic J. 2019. Production of ethanol from Cassava and Yam peels using acid hydrolysis. *Am Sci Res J Eng Technol Sci*. **52(1)**: 67–78

Praputri E and Sundari E. 2019. Production of bioethanol from *Colocasia esculenta* (L.) Schott (Talas Liar) by hydrolysis process. *IOP Conf. Ser. Mater. Sci. Eng.*, **543(012056)** :1–7

Purnomo A, Yulius AWY, Jindrayani NP, Adi TN, Wenny I, and Suryadi I. 2016. Subcritical water hydrolysis of Durian seeds waste for bioethanol production. *Int J Ind Chem* **7**:29–37

Ramdath DD, Isaacs RLC, Teelucksingh S and Wolever TMS. 2004. Glycaemic index of selected staples commonly eaten in the Caribbean and the effects of boiling v. crushing. *Br. J. Nutr*., **91**: 971–977

Ramesh, D, Manjunatha GR, Mishra P, Tailor, AK and. Dhekale BS. 2019. **Design Experiments in the Basic of Statistics in Agricultural Sciences**. Apple Academic Press Inc. Canada. pp 73–142.

Santos Michel Jr RJ, Canabarro NI, Alesio C, Maleski T, Laber T, Sfalcin P, Foletto EL, Mayer FD and Kuhn RC. 2016. Enzymatic saccharification and fermentation of rice processing residue for ethanol production at constant temperature. *Biosyst. Eng.*, **142**: 110–116.

Selim KA, Dina EE, Saadia ME, and Mohamed IAH. 2018. Bioethanol a microbial biofuel metabolite. *Fermentation* **4 (16)** : 1–27.

Tampubolon BI and Fauzi A. 2016. Internalization of external costs and policy analysis for the development of geothermal energy as alternative energy. *Jurnal Risalah Kebijakan Pertanian dan Lingkungan - Rumusan Kajian Strategis Bidang Pertanian dan Lingkungan*, **2(2)**: 97–104.

Tanko M and Alidu A F. 2017. Profit efficiency of small scale yam production in Northern Ghana. *Int J Dev Sustain* , **5(1):** 69–82

Thatoi H, Krishna DP and Swain MR. 2016. Bioethanol production from tuber crops using fermentation technology: A review. *Int. J. Sustain. Energy*,**35 (5)**: 443–468.

Ulyarti S and Lavlinesia DF. 2016. The study of physical properties of *Dioscorea alata* 's starch from Jambi Province. *Int J Adv Sci Eng Inf Technol*., **6(4)**: 456–459.

UNESCO. 2020. Ecological Sciences for Sustainable Development. http://www.unesco.org/new/en/natural-sciences/environment/ecological-sciences/specific-ecosystems/drylands

Villadiego-del Villar AE, Sarmiento-Zea N, León-Pulido J and Rojas-Pérez LC. 2021. Bioethanol production from Yam (*Dioscorea rotundata*) using simultaneous saccharification and fermentation (SSF). *TecnoL.* **24(50) e1724:**1–10

Winarti S and Saputro EA. 2013. Yam tuber flour prebiotic characteristic (*Dioscorea* spp.). *Jurnal Teknik Kimia* **8(1)**:17–21

Wuryantoro, Wardhani RM and Puspitawati IR. 2019. Yield test of 13 accession groups of Yam (*Dioscorea alata* L.) on three various agroecology. *IOP Conf. Ser Earth Environ. Sci*. **347 (012004):** 1–6.

Wuryantoro, Praptiningsih GA and Wardhani RM. 2020. Study of planting models on growth and yield of "Uwi" (*Dioscorea alata* L.) *Agri-Tek Journal Penelitian Ilmu-Ilmu Eksakta*, **21(1):**35–41.

Wuryantoro, Wardhani RM, Puspitawati IR, Adinurani PG and Yamin BM. 2021. Exploration and characterization of "Uwi" plant (*Dioscorea* sp.*)* in East Java uplands, Indonesia. *E3S Web Conf*. **226 (00049)**:1–8.

Yasmin F, Radziah O. and Mohammad Nazmul HM. 2020. Yield and nutrient content of Sweet Potato in response of plant growth-promoting Rhizobacteria (PGPR) inoculation and N fertilization. *Jordan J. Biol. Sci* **13 (1)** : 117–122.

JJBS

Volume 14, Number 5,December 2021
ISSN 1995-6673
Pages 953 – 958

Jordan Journal of Biological Sciences

Metabolite Profiling of Black Rice (*Oryza sativa* L.) Following *Xanthomonas oryzae* pv. *oryzae* Infection

Ema Nur Hidayah[1], Febri Adi Susanto[2,3], Tri Joko[2,4], Yekti Asih Purwestri[1,2], Tri Rini Nuringtyas[1,2,*], Manar Fayiz Mousa Atoum[5,6] , and Asad Jan[7]

[1]Department of Tropical Biology, Faculty of Biology, Universitas Gadjah Mada Jl. Teknika Selatan, Sekip Utara, Yogyakarta 55281, Indonesia;[2]Research Center for Biotechnology, Universitas Gadjah Mada;Jl. Teknika Utara, Depok, Sleman, Yogyakarta 55281, Indonesia;[3]Department of Biochemistry Molecular Biology & Molecular Plant Sciences, Michigan State University, East Lancing, MI 48824, USA;[4]Department of Crop Protection, Faculty of Agriculture, Universitas Gadjah Mada;Jl. Flora, Bulaksumur, Yogyakarta 55281, Indonesia; [5]Molecular Biology and Genetics, The Hashemite University, PO Box 330127, 13133 Zarqa, Jordan; [6]Department of Medical Laboratory Sciences, The Hashemite University, Zarqa, Jordan;[7]Institute of Biotechnology & Genetic Engineering, University of Agriculture Pesthawar, 25130, Khyber Pakhtunkhwa, Pakistan

Received: May, 10, 2021; Revised: Sep, 25, 2021; Accepted Oct, 22, 2021

Abstract

Black rice as a functional food contains a high anthocyanin content, which functions as an antioxidant. However, bacterial leaf blight (BLB) caused by *Xanthomonas oryzae* pv. *oryzae* (*Xoo*) has resulted in a reduction in yield. Black rice has been reported to have a higher resistance to BLB than white rice cultivars. This study aimed to determine the metabolite responses of two black rice cultivars, 'Melik' and 'Pari Ireng', compared to two white rice cultivars, 'IR64' and 'Java14', after infection with *Xoo* pathotype IV and mock negative control. Gas Chromatography-Mass Spectrometer (GC-MS) was used for the metabolite profiling analysis, followed by the quantification of total phenolic concentration (TPC) and total flavonoid concentration (TFC). Across all cultivars, the results revealed that following *Xoo* infection, there were significantly higher concentrations of primary metabolites including sugars, sugar alcohols, fatty acids, glycerol, and some organic acids. In 'Pari Ireng' and 'Melik' cultivars, sugars including fructose, and gluco-hexodialdose were significantly higher than the white cultivars following the infection. The infection significantly increased the TPC of all cultivars. 'Java 14' contained the highest TPC while 'Pari Ireng' was observed as cultivars with the highest TFC. These results suggested that pigmented rice cultivars possess a different chemical defense strategy from the white ones to respond to *Xoo* infection.

Keywords: Bacterial leaf blight, Disease resistance, Functional food, GC-MS, Improvements rice production, Metabolomics, Pigmented rice, *Xoo* infection

1. Introduction

Rice (*Oryza sativa* L.) is one of the most important staple foods of many Asian countries such as China, India, Bangladesh, Vietnam, the Philippines, and Indonesia. Statistical data indicate that the global consumption of rice from 2016 to 2017 was an average of 54.24 kg per capita. After China and India, Indonesia had the third-highest rice consumption of more than 50×10^6 t over this period (Shahbandeh, 2019). The increasing rice consumption in Indonesia is related to the increasing population. However, this increase in population has not been reflected in the overall rice production, resulting in increasing rice demand (Pratiwi and Purwestri, 2017).

Rice farmers aim to meet the rising demand through improvements in the rice production process (Hameed *et al*., 2021). However, biotic and abiotic factors have caused many problems, with one of them being bacterial leaf blight (BLB) in rice caused by *Xanthomonas oryzae* pv. *oryzae* (*Xoo*). The symptoms of BLB can present early in the seedling phase to maturity (Tasliah, 2012). *Xoo* has many pathotypes (i.e. strains) and is characterized by rapid changes, making its control difficult (Sudir *et al*., 2013; Susanto and Sudir, 2012). The BLB infestation from April to September 2018 was estimated at approximately 2 3055 ha, making this disease the third most devastating pest after rats and rice stem borers (Direktorat Perlindungan Tanaman Pangan, 2018). Almost all rice cultivation areas in Indonesia have experienced some levels of infection.

One of the strategies to manage BLB is planting rice varieties resistant to the pathotypes. The use of disease-resistant rice cultivars is the most economical way to combat the disease. Black rice is one of the pigmented rice types that have exhibited resistance against a range of biotic and abiotic stresses. Its consumption has begun as a functional food, i.e. food that naturally or through addition contains one or more compounds considered to possess health benefits owing to its high anthocyanin content which serves as a natural antioxidant (Kristamtini *et al*., 2014; Pratiwi and Purwestri, 2017). As a monocot, rice has been commonly used as a model organism to study defense responses in cereal crops. An integrated molecular approach combining transcriptomics, proteomics, and metabolomics is needed to study the response of rice plants to environmental changes (Ahuja *et al*., 2010).

* Corresponding author e-mail: tririni@ugm.ac.id.

Metabolites in the plant are strongly influenced by the genes present and genetic modifications. The environment also has significant effects on metabolic changes (Brunetti *et al*., 2013). Plants adapt to the changes in the environmental conditions by producing inducible metabolites or by increasing the levels of existing metabolites that may serve as stress signals or defense (Schwachtje *et al*., 2019).

Plants often apply multi strategies to defend themselves from both biotic and abiotic attacks. Pigmented rice is preferable due to its high anthocyanin content. Wijaya *et al*. (2017) suggested that black pigmented rice adjusts its metabolism to produce high anthocyanin content compared to the white and red ones. Accumulative information also showed that pigmented rice tends to have a higher resistance to *Xoo* infection (Sutrisno *et al*., 2018) with the support of phenylalanine ammonia lyase (PAL) (Solekha *et al*., 2020).

Metabolite profiling has been used as a novel tool for the comparative display of gene function. This tool not only has the potential to provide deeper insights into the complex regulatory processes of metabolite production but can also be used for direct determination of the resulting phenotype (Kumar *et al*., 2017; Pan *et al*., 2013). In this study, the objective was to observe and evaluate the metabolic changes in pigmented rice following infection by *Xoo*. This information may provide a better understanding of plant defenses in pigmented and white rice information crucial for improvement in rice production.

2. Materials and Methods

The rice seeds used in this study included two local black rice cultivars 'Pari Ireng' and 'Melik' obtained from Balai Pengkajian Teknologi Pertanian – BPTP (Institute for Agricultural Technology) Yogyakarta. The white cultivar 'Java14' was used as a resistant control (Susanto and Sudir, 2012), whereas 'IR64' cultivar was used as a susceptible control. These were obtained from Balai Besar Penelitian Tanaman Padi Sukamandi - BBPadi (Indonesian Center for Rice Research - ICRC), Subang, West Java (Sudir *et al*., 2013). The *Xoo* isolate used was pathotype IV with a concentration of 10^8 colony-forming units originally from BBPadi, Subang, West Java. The inoculum was cultured in a peptone sucrose agar medium in Petri dishes. Inoculation of plants with the *Xoo* via the leaf clipping method was performed in the late afternoon to avoid the time of the day experiencing high heat and high evaporation (Sutrisno *et al*., 2018). The negative treatments, called as mock, were done by clipping the leaves with aquadest only. Both mock and infected plants were cultivated for 4 d in the greenhouse. At the end of the treatment, leaves were harvested for chemical analysis.

2.1. Metabolite profiling using Gas Chromatography–Mass Spectrometer (GC-MS)

For metabolite profiling, rice leaf samples were collected from the plants 4 d following inoculation (Narsai *et al*., 2013). For each treatment, approximately 50 mg of the leaf material was deep-frozen at −80 °C prior to extraction. The leaf samples were refined using liquid nitrogen and then extracted by adding 1 mL of an extraction buffer (isopropanol: acetonitrile: water, 3:3:2, previously cooled at -20 °C) to the leaf material. The supernatant was stored at -20 °C for 30 min to 40 min prior to vacuuming using a cold vacuum pump and then treated by adding 10 µL methoxyamine hydrochloride solution (20 mg mL^{-1}). The derivatization process was performed by adding 90 µL MSTFA at 37 °C for 30 min (Sana *et al*., 2010). The samples were allowed to stand at room temperature for 2 hr prior to injection into a GC–MS and stored in a freezer for further analysis.

The analysis was performed using a GC–MS mass selective detector and Rxi-5MS capillary column (30 m × 0.25 mm; layer thickness of 0.25 µm). Helium was used as the carrier gas at a constant rate of 1 mL min^{-1}, and 1 µL of the gas was injected (split ratio 10:1). The temperature of the injected gas was set at 310 °C, of the column at 80 °C, and the ion at 250 °C. The temperature regime was initiated from isothermal at 80 °C (5 min), and the temperature increase was set at 10 °C min^{-1} until the final temperature of 330 °C was reached (43 min). GC–MS was performed on each leaf sample using three replications.

2.2. Sample Preparation for Total Phenolic Concentration (TPC) and Total Flavonoid Concentration (TFC) Quantification

Extracts were prepared by homogenizing 50 mg fresh leaves sample with 4 mL phosphate buffer (pH 6.5; 0.1 M), followed by centrifugation at 10 000 rpm (1 rpm = 1/60 Hz) for 15 min at 2 °C. Next, 2 mL of absolute ethanol was added to 2 mL of supernatant and boiled in water at 98 °C for 30 min. Subsequently, 5 mL of distilled water was added to the sample, and the solution was slowly mixed. The samples were divided into two equal parts to measure TPC and TFC.

2.2.1. Total Phenolic Content (TPC)

Analysis of TPC was conducted by spectrophotometry using the Folin–Ciocalteu method (Everette *et al*., 2010) with some modifications. Amount 1 mL of a sample was added to 0.5 mL Folin–Ciocalteau reagent (1:1) along with 1 mL Na_2CO_3 (7.5 %) and 2.5 mL of distilled water. The sample was incubated for 1 h prior to measuring the absorbance at 650 nm (Dahima *et al*., 2014). Gallic acid was used as a standard for the calibration curve at a concentration of 10 µg mL^{-1} to 160 µg mL^{-1} in the standard curves with intervals of 20 µg mL^{-1}. TPC was calculated in terms of gallic acid equivalents.

2.2.2. Total Flavonoid Content (TFC)

A colorimetric test with aluminum chloride was used to measure TFC. Amount 1 mL of a sample was added to 0.5 mL of 2 % $AlCl_3$ and 2.5 mL distilled water. Then, the samples were briefly shuffled and incubated for 10 min at 37 °C prior to measuring the absorbance at 425 nm (Pekal and Pyrynska, 2014). Quercetin was used as the standard. The quercetin concentration used in the standard curve was ranging from (20 to 100) µM mL^{-1} [(20, 40, 60, 80 and 100) µM mL^{-1}]. The determination of TFC was calculated in terms of equivalent quercetin in reference to the standard curve.

2.3. Data and Statistical Analysis

Metabolites were determined based on the spectrum similarity of each sample peak to the examples in the mass spectrometry library (i.e., NIST and WILEY). MS results reflected compounds derivatized using silylation.

Compounds identification was validated by checking all detected metabolites with NIST (webbook.nist.gov). Visualization of the entire area of the metabolite distribution was performed using Heat Map in Microsoft Excel 2010. The statistical analyses for metabolites levels, TPC, and TFC were performed using ANOVA with significance set at the 5 % confidence level, followed by post hoc Duncan's multiple ranges in SPSS Statistics 24 (Adinurani, 2016).

3. Results and Discussion

3.1. Metabolite profiling

GC–MS based metabolomics was used for metabolite profiling of black rice following *Xoo* infection. Eleven primary metabolites were detected in the metabolite profile of rice leaves. Metabolites found in all cultivars were mostly primary metabolites, including sugars, alcoholic sugars, fatty acids, glycerol, and some organic acids with different concentrations in each cultivar and treatment (Figure 1). These metabolites were previously reported present in the rice leaves detected using GC–MS (Kusano *et al*., 2015).

In the mock plants, the white cultivars showed higher sucrose levels and gluco-hexodialdose than the black cultivars. The higher mannitol level around 5 to 8 times was only observed on the IR64 cultivars but not the 'Java14'. The rest of the metabolites were comparable among all cultivars. Interesting shifting of metabolites profiles was observed after the plants were treated with *Xoo* (Figure 1).

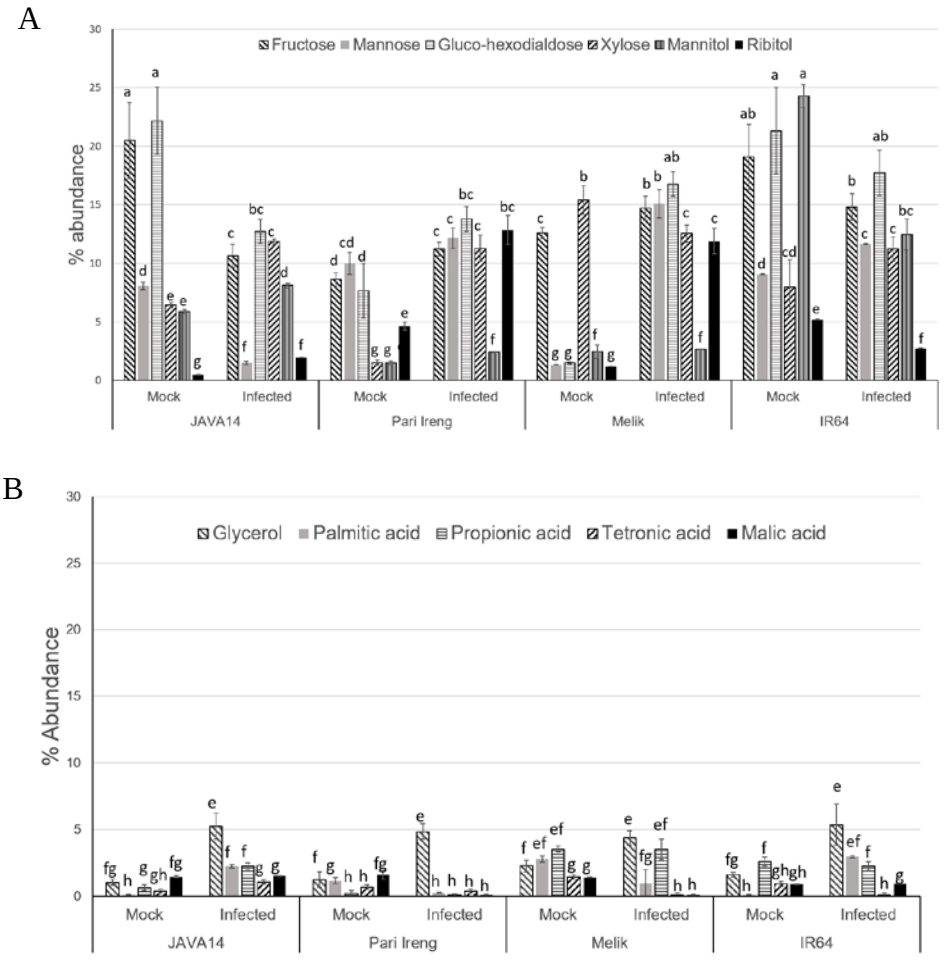

Figure 1. Metabolite contents of four rice cultivars following infection with *Xanthomonas oryzae*. A. Sugars and sugar alcohols, B. Lipids and organic acid. Data present the average and standard error of three replicates each. Different letters denote significant differences at * $P < 0.05$ analyzed using ANOVA.

The heat map of the metabolite profile revealed that metabolite profiles of all cultivars changed after infection (Figure 2). It can be observed from the change of color of several metabolites such as fructose, palmitic acid, glycerol, ribitol, and xylose in the heat map. Several responses were different between the white rice (i.e., 'Java14' and 'IR64') with pigmented rice (i.e. 'Pari Ireng' and 'Melik'). However, a similar pattern was observed in glycerol after infection. In all cultivars, increased glycerol levels were consistently observed. Fructose and gluco-hexodialdose levels were found to be higher in 'Pari Ireng' and 'Melik' following *Xoo* infection than those following the mock treatment. In contrast, the levels decreased in the white rice cultivars 'Java14' and IR64 compared with the levels in control. Sugars as a resource of carbon were also reported to be depleted in the leaves' surface upon bacterial infection (Bezrutczyk *et al*., 2018). In addition, alcoholic sugars such as mannitol demonstrated a different pattern.

Mannitol level decreased in 'IR64' following the *Xoo* infection but increased in 'Java14', 'Melik', and 'Pari Ireng'. The low content of mannitol in IR64 as the representative of susceptible cultivars suggested the role of this sugar alcohol in defense against disease. The correlation of mannitol to bacterial infection remains unclear. However, it was reported to function as antimicrobials recently (Nguyen *et al*., 2019).

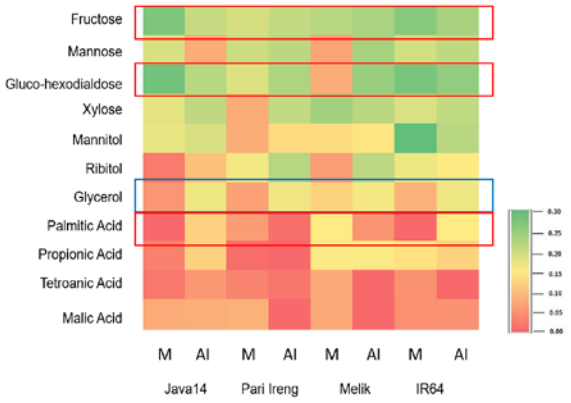

Figure 2. Heat map of metabolite profile on four rice cultivars following *Xoo* infection. M: Mock, AI: after infection. The red box indicates the different response of pigmented rice cultivars than the white cultivars. The blue box indicates the metabolites changed after infection observed in all cultivars.

The opposite response was observed for palmitic acid. A higher level of palmitic acid was observed in 'Java14' and 'IR64', while in 'Pari Ireng' and 'Melik' were lower. A group of sugars was found in all tested cultivars: xylose, glycerol, mannitol, and mannose. Glycerol levels increased across all cultivars following the infection. Remarkably, mannose levels in 'IR64', 'Melik', and 'Pari Ireng' increased following *Xoo* infection but decreased in 'Java14'. A decreased concentration of malic acid following the infection was observed only in the black rice cultivars, 'Melik' and 'Pari Ireng'. Malic acid is known to play a role in regulating pH and osmotic homeostasis in plants with pathogen infection (Figure 1.).

Sugars have been recognized as important signaling molecules that affect a variety of physiological responses. They regulate the expression of genes involved in photosynthesis, metabolism, and defense responses (Bolouri-Moghaddam *et al*., 2010; Morkunas and Ratajczak, 2014). Fructose and gluco-hexodialdose levels increased in the black rice cultivars following *Xoo* infection than the control treatment, whereas they decreased in the white rice cultivars.

Xoo infection tends to decrease sugar production and, subsequently, the energy to produce metabolites in defense response. In particular, most plant pathogens actively penetrate the plant cell wall to access the intracellular nutrients, whereas plants subsequently, strengthen cell walls and secrete antimicrobial components into the cell wall in an attempt to stop pathogen invasion as a defensive response (Malinovsky *et al*., 2014). Several studies have shown that sugar transportation plays an essential role in the rice defense response against pathogens (Chen *et al*., 2010a, 2010b, 2012; Julius *et al*., 2017). Accumulation of sucrose and gluco-hexodialdose in plants following *Xoo* infection triggers the allocation of nutrients and signals for the activation of the defense response. Remarkably, another sugar, xylose, was found in all tested cultivars. Increased xylose level in 'Java14' and 'Pari Ireng' following *Xoo* infection may trigger a defensive response against pathogens. Another compound found in the metabolite profile based on the GC–MS analysis seems to play a role against the pathogen. However, the pattern obtained by spectroscopy suggests that the compound is unlikely to be a major compound that serves in the defense mechanism. The roles of the compounds present in plants are listed in Figure 1. These are considered to play a role in the defense mechanism but not as major signaling compounds.

Metabolite profiling of black rice following *Xoo* infection demonstrated that there were more kinds of sugars than other metabolites. *Xoo*–infected rice may continue to experience changes in metabolite composition and sugar content that can affect PR protein formation and induce plant defenses (Sun *et al*., 2013). The result of metabolite profiling can be used to determine the metabolite responses and defense strategies plants use in response to BLB.

3.2. TPC following Xoo infection

Phenol, a family of compounds involved in plant defense, is considered important in plant metabolism. The TPC values of four rice cultivars were 0.45 % to 0.98 % (w/w), within the range value commonly available in grain-producing plants. The phenolic compounds in plants are usually associated with the tolerance characters against both biotic and abiotic stress due to the natural antioxidants property of phenolics (Vrancheva *et al*., 2020). 'Java 14' had the highest TPC than the other cultivars in each treatment, followed by the black rice cultivars, and 'IR64' (Figure 3). The increase in TPC indicated that there is a plant response that was a defense mechanism in response to the presence of the pathogen. 'IR64' had the lowest TPC; thus, this finding supported the fact that 'IR64' is highly susceptible to the *Xoo* pathotype (Khaeruni *et al*., 2014; Sudir *et al*., 2013). The role of phenolic compounds in the plant defense against Xoo has been reported by Khan *et al.* (2014) and Fan*Rei* (2017). High TPC was significantly detected in the resistant rice cultivars, i.e. 'Basmati-385' and 'Basmati-2000' (Khan *et al.*, 2014). More recent study using a library of phenolics compounds showed that 10 out of 45 phenolic compounds had been proven to inhibit the Xanthomonas *oryzae* pv. *oryzae* (Xoo) type III. Moreover, these ten compounds can also suppress the hypersensitive response (HR) caused by Xoo in tobacco (Fan *et al.*, 2017).

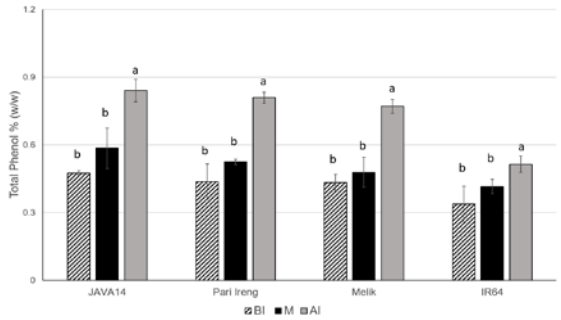

Figure 3. Total phenol content of four cultivars rice leaves after Xoo infection. BI: before infection, M: Mock, AI: after infection *** $P \leq 0.0001$. Alphabets above histograms showed significant differences between treatments in the same cultivar based on ANOVA with a 5 % confidence level.

3.3. TFC following Xoo infection

The highest TFC following *Xoo* infection was observed in the black rice cultivars. In contrast, low TFC was observed across all treatments in the white rice cultivars. Notably, the black rice showed differences in terms of TFC between the negative control and pathogen treatment groups (Figure 4). The presence of pathogens can trigger an increase in the production of flavonoids as a defense response in plants.

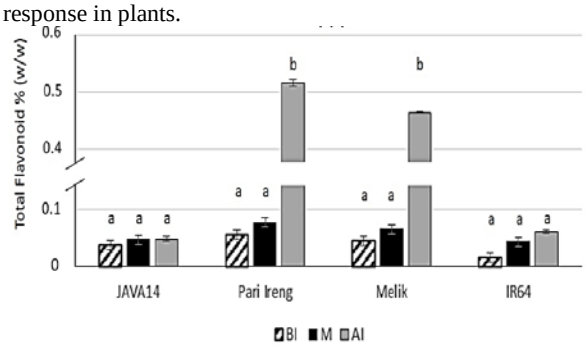

Figure 4. Total flavonoid content of four cultivars rice leaves after Xoo infection. BI: before infection, M: Mock, AI: after infection *** $P \leq 0.0001$. Alphabets above histograms showed significant differences between treatment in the same cultivar based on ANOVA with a 5 % confidence level

Pigmented rice cultivars differ from white ones because of their high anthocyanin content in their aleuron layer. Therefore, metabolism in pigmented rice is different from white rice; hence, it might affect the response of the plants to bacterial infections. In this study, the authors observed how the black rice cultivars ('Melik' and 'Pari Ireng') showed a different metabolite profile following the *Xoo* infection.

To better understand the chemical defenses utilized by black rice against *Xoo*, TPC and TFC were evaluated on all rice cultivars. The increase in TPC in 'Pari Ireng', 'Melik', and 'IR64' indicated the presence of a defensive response against pathogen infection. However, the phenolic compounds alone seem to be ineffective against *Xoo*. The black rice cultivars also showed increases in TPC following *Xoo* infection and showed similar responses against pathogen infection. This result is in line with a study by Solekha *et al.* (2020) that reported a significant increase in the phenylalanine ammonia-lyase (PAL) activity in 'Pari Ireng' and 'Melik' after *Xoo* infection. This indicated the active shikimate pathway leading to the synthesis of both phenolic and flavonoids compounds. Furthermore, specific phenolic metabolites have been investigated i.e. o-coumaric acid (OCA) and trans-3-indoleacrylic acid, for their inhibition activities against *Xoo*. The OCA specifically showed its activity on the early steps of defense by inhibiting the HR progression by *Xoo*, while the trans-3-indoleacrylic acid was proven for its high antibacterial action (Fan *et al.*, 2017). Further study of the significant phenolic and flavonoid compounds present in the black rice against *Xoo* infection may become interesting.

Based on the results, the authors found that 'Pari Ireng' has higher TPC and TFC than 'Melik', specifying a stronger defensive response in 'Pari Ireng' than in 'Melik'. Differences in terms of disease intensity observed during the second week in the black rice cultivars showed that a new main defense mechanism was activated after a week following the infection. Thus, within the first week, there were no differences in terms of the disease intensity values (data not shown). The combination of relatively high TFC, TPC, and fatty acid content in 'Java14' suggests that these compounds reduce disease intensity unlike in the other cultivars. Although TPC of 'Java14' was lower than that of the black rice cultivars, the TPC produced was believed to be more effective against BLB infection. This pattern was similar in the black rice cultivars.

4. Conclusion

The metabolite profiling of two pigmented rice cultivars and two white cultivars in response to *Xoo* infection detected primary metabolites including sugars, sugar alcohols, fatty acids, glycerol, and some organic acids observed in all cultivars following *Xoo* infection. An increase of glycerol levels was observed in all cultivars after infection. In pigmented rice, 'Melik' and 'Pari Ireng', sugars including fructose and gluco-hexodialdose were higher in concentration following *Xoo* infection. The infection significantly increased the TPC of all cultivars. 'Java14' contained the highest TPC while 'Pari Ireng' was observed as cultivars with the highest TFC. It can be concluded that pigmented rice cultivars possess a different in chemical defence strategy from the white ones to respond to *Xoo* infection.

Acknowledgment

This research was supported by PUPT Competitive Research Grant 2016, The Ministry of Research, Technology, and Higher Education Indonesia to YAP contract number 863/UN1-P.III/LT/DIT-LIT/2016. This study is part of a master's thesis research by Ema Nur Hidayah. The authors thank Ir. Sudir from Balai Besar Penelitian Tanaman Padi, Sukamandi, Subang, West Java for the valuable suggestions on the *Xoo* pathotype IV infection.

References

Adinurani, P.G. 2016. Design and analysis of agro trial data: Manual and SPSS. Plantaxia, Yogyakarta, Indonesia

Ahuja I, de Vos, RC, Bones AM and Hall RD. 2010. Plant molecular stress responses face climate change. Trends Plant Sci., **15(12):** 664–674.

Bolouri-Moghaddam MR, Roy KL, Xiang L, Rolland F and Van den Ende W. 2010. Sugar signaling and antioxidant network connections in plant cells. FEBS J., **277:** 2022–2037.

Brunetti C, George RM, Tattini M, Field K and Davey MP. 2013. Metabolomics in plant environmental physiology. J. Exp. Bot., **64(13):** 4011–4020.

Bezrutczyk M, Yang J, Eom J S, Prior M, Sosso D, Hartwig T, and Yang B. 2018. Sugar flux and signaling in plant–microbe interactions. Plant J., **93(4):** 675–685.

Chen F, Gao MJ, Miao YS, Yuan YX, Wang MY, Li Q, Mao BZ, Jiang LW and He ZH. 2010a. Plasma membrane localization and potential endocytosis of constitutively expressed *Xa21* proteins in transgenic rice. Mol. Plant., **3(5):** 917–926.

Chen LQ, Hou BH, Lalonde S, Takanaga H, Hartung ML, Qu XQ, Guo WJ, Kim JG, Underwood W, Chaudhuri B, Chermak D, Antony G, White FF, Sommerville SC, Mudgett MB, Frommer WB. 2010b. Sugar transporters for intercellular exchange and nutrition of pathogens. Nature., **468:** 527–532.

Chen LQ, Qu XQ, Hou BH, Sosso D, Osorio S, Fernie AR, Frommer WB. 2012. Sucrose efflux mediated by SWEET proteins as a key step for phloem transport. Science., **335**: 207–211.

Dahima V, Sharma SS, Khokar MK, Hooda KS. 2014. Post-infectional biochemical changes in maize leaves affected by banded leaf and sheath blight disease. Indian Phytopath., **67(4):** 370–373.

Direktorat Perlindungan Tanaman Pangan. 2018. Estimation of major pest attacks on planting period of 2018 according to each province of Indonesia

Everette JD, Bryant QM, Green AM, Abbey YA, Wangila GW and Walker RB. 2010. Thorough study of reactivity of various compound classes toward the Folin−Ciocalteu reagent. J. Agric. Food Chem., **58(14):** 8139–8144.

Fan S, Tian F, Li J, Hutchins W, Chen H, Yang F, Yuan X, Cui Z, Yang CH, and He C. 2017. Identification of phenolic compounds that suppress the virulence of *Xanthomonas oryzae* on rice via the type III secretion system. Mol. Plant. Pathol., 18(4): 555–568

Hameed, A., Padda I.U.H. and Salam A. 2021. Analysis of food and nutrition security in Pakistan: A contribution to zero hunger policies Sarhad J. Agric., **37(3)**: 1025–1042.

Julius BT, Leach KA, Tran TM, Mertz RA, and Braun DM. 2017. Sugar transporters in plants: new insights and discoveries. Plant Cell Physiol., **58**: 1442–1460.

Khaeruni A, Taufik M, Wijauanto T and Johan EA. 2014. Development of bacterial leaf blight disease inoculated on three varieties of paddy rice at various growth stage. J. Fitopatologi Indonesia., **10(4):**119–125.

Khan JA, Afroz S, Arshad HMI, Sarwar N, Anwar HS, Saleem K, Babar MM and Jamil FF. 2014. Biochemical basis of resistance in rice against Bacterial leaf blight disease caused by *Xanthomonas oryzae* pv. Oryzae. Adv. Life Sci., **1(3):** 181–190

Kristamtini K, Taryono, Basunanda P and Murti RH. 2014. Lokal genetic variability of rice pericarp color parameters and total anthocyanine content of eleven local black rice and their correlation. Ilmu Pertanian, **17(1):** 57–70.

Kumar R, Bohra A, Pandey AK, Pandey MK, Kumar A. 2017. Metabolomics for plant improvement: Status and prospects. Front. Plant Sci., **8(1302):** 1–27.

Kusano M, Yang Z, Okazaki Y, Nakabayashi R, Fukushima A and Saito K. 2015. Using metabolomic approaches to explore chemical diversity in rice. Mol. Plant., **8(1):** 58–67.

Malinovsky FG, Fangel JU and Willats WGT. 2014. The role of the cell wall in plant immunity. Front. Plant Sci., **5(178):** 1–12.

Morkunas I, and Ratajczak L. 2014. The role of sugar signaling in plant defense responses against fungal pathogens. Acta Physiol. Plantarum., **36:**1607–1619.

Narsai R, Wang C, Chen J, Wu J, Shou H and Whelan J. 2013. Antagonistic, overlapping and distinct responses to biotic stress in rice (O*ryza sativa*) and interactions with abiotic stress. BMC Genomics., **14(93)**: 1–21.

Nguyen T, Kim T, Ta HM, Ye WS, Choi J, Mizar P and Kim KK. 2019. Targeting mannitol metabolism as an alternative antimicrobial strategy based on the structure-function study of mannitol-1-phosphate dehydrogenase in *Staphylococcus aureus*. MBio., **10(4- e02660-18):** 1–23.

Pan Q, Dai Y, Nuringtyas TR, Mustafa NR, Schulte AE, Verpoorte R and Choi YH. 2014. Investigation of the chemomarkers correlated with flower colour in different organs of *Catharanthus roseus* using NMR-based metabolomics. Phytochem. Anal., **25(1)**: 66–74.

Pękal A and Pyrzynska K. 2014. Evaluation of aluminium complexation reaction for flavonoid content assay. Food Anal. Methods., **7:**1776–1782.

Pratiwi R and Purwestri YA. 2017. Black rice as a functional food in Indonesia. Functional Foods in Health and Disease. **7(3):**182–194.

Sana TR, Steve F, Wohlgemuth G, Kratekar A, Jung K and Ronald PC. 2010. Metabolomic and transcriptomic analysis of the rice response to the bacterial blight pathogen *Xanthomonas oryzae* pv. *oryzae*. Metabolomics., **6:** 451–465.

Schwachtje J, Whitcomb SJ, Firmino AAP, Zuther E, Hincha DK and Kopka J. 2019. Induced, imprinted and primed metabolic responses of plants to changing environments: Does metabolism store and process information? Front. Plant Sci., **10(106):** 1–13.

Shahbandeh M. 2019. Global rice consumpion 2018/2019, by country (in 1,000 metric tons). (https://www.statista.com/statistics/255971/top-countries-based-on-rice-consumption-2012-2013/#statisticContainer)

Solekha R, Susanto FA, Joko T, Nuringtyas TR, Purwestri YA. 2020. Phenylalanine ammonia lyase (PAL) contributes to the resistance of black rice against *Xanthomonas oryzae* pv. oryzae. . J. Plant Pathol., **102:** 359–365.

Sutrisno, Susanto FA, Wijayanti P, Retnoningrum M D, Nuringtyas TR, Joko T, Purwestri Y A. 2018. Screening of resistant Indonesian black rice cultivars against bacterial leaf blight. Euphytica., **214 (199):** 1–12**.**

Sudir S, Yogi YA. 2013. Composition and patotype distribution of *Xanthomonas oryzae* pv. oryzae in rice central production in South Sumatera. Jurnal Penelitian Pertanian Tanaman Pangan. **32(2):** 98–108.

Sun L, Yang DL, Kong Y, Chen Y, Li XZ, Zeng LJ, Li Q, Wang E and He ZH. 2014. Sugar homeostasis mediated by cell wall invertase grain in complete filling 1 (GIF1) plays a role in pre-existing and induced defense in rice. Mol. Plant Pathol., **15(2):** 161–173.

Susanto U and Sudir. 2012. Rice genotype resistance against *Xanthomonas oryzae* pv. oryzae patotype III, IV, dan VIII. .Penelitian Pertanian Tanaman Pangan, **31(2):** 108–116.

Tasliah. 2012. Resistance gene on rice to bacterial leaf blight caused by *Xanthomonas oryzae* pv. oryzae. Jurnal Penelitian dan Pengembangan Pertanian, **31(3):** 103–112.

Underwood W. 2012. The plant cell wall: A dynamic barrier against pathogen invasion. Front. Plant Sci**., 3(85):** 1–6.

Vrancheva R, Popova A, Mihaylova D and Kratanov A. 2020. Phytochemical analysis, in vitro antioxidant activity and germination capability of selected grains and seeds. Jordan J Biol Sci., **13(3):** 337–342

Wijaya DN, Susanto FA, Purwestri YA, Ismoyowati D, Nuringtyas TR. 2017. NMR metabolite comparison of local pigmented rice in Yogyakarta. Indones. J. Biotechnol., **22(2):** 68–75.

JJBS

Volume 14, Number 5,December 2021
ISSN 1995-6673
Pages 959 – 964

Jordan Journal of Biological Sciences

Evaluation of Efficiency of *Echinodorus palaefolius* (J.F. Macbr.) Involved in the *Clarias gariepinus* (Burchell, 1822) Culture for Water Quality Recovery and Fish Growth Support

Hany Handajani[1,*], Ganjar Adhywirawan[1], Soni Andriawan[1], Dony Prasetyo[1] and Boy Ronald Mavuso[2]

[1] *Department of Aquaculture, Faculty of Agriculture and Animal Science, University ofMuhammadiyah Malang, Jl Raya Tlogomas No. 246, Malang 65144, Indonesia;*[2] *Ministry of Agriculture, P.O Box 162, Mbabane H100, Eswatini, Africa*

Received: May, 15, 2021; Revised: Oct, 16, 2021; Accepted Nov, 11, 2021

ABSTRACT

Intensive catfish [*Clarias gariepinus*(Burchell, 1822)] cultivation produces organic waste that decreases water quality. The aquaponics system utilizes fish waste for plant growth to produce useful and economical products. This study aims to analyze and evaluate the best density of Mexican sword plant/water Jasmine [*Echinodorus palaefolius* (J. F. Macbr.)] in reducing waste from intensive catfish aquaculture. The research method used a completely randomized design (CRD) with four treatments with three replications. A plastic tub with a size of 38 cm × 12 cm × 30 cm filled with sand was used for plant media, while for catfish rearing containers, a 70 L tub with a water volume of 40 L was used. The fish used in this experiment were catfish fry with a size of 7 cm ± 0.8 cm, a weight of 5.14 g ± 0.45 g, with a stocking density of one fry per liter. Catfish fry were fed with floating pellet feed of 30 % protein content, and the feeding was done at satiation. The treatments were T1 = without plants, T2 = 150 g m^{-2} plants, T3 = 250 g m^{-2} plants, and T4 = 350 g m^{-2} plants. Furthermore, all data were analyzed through ANOVA (One-way analysis of variance) and the Duncan's multiple range test to measure significant variations among the treatments using SPSS (version 17, USA). The results revealed that T4 was the best treatment in terms of nutrient removal efficiency of TAN, NO_2, NO_3, and PO_4 at the rate of 23.80 %, 48.19 %, 52.99 % and 26.11 %, respectively. Moreover, growth performances of fish fry fed diet in T4 also were significantly ($P < 0.05$) higher than other fishes of different treatments. Regarding these findings, *E. palaefolius* could work well to maintain water quality during *C. gariepinus* cultivation and even accelerated *C. gariepinus* growth at the end of the period.

Keywords: Aquaponics technology, Catfish, Economically valuable, Intensive culture, Mexican sword plant, Phytoremediation, Utilization waste, Water Jasmine

1. Introduction

Catfish [*Clarias gariepinus* (Burchell, 1822)] is a very popular commodity for cultivation in Africa, Indonesia, and several other countries in the world because of its fast growth, disease resistance, and wide geographical spread (Elesho *et al.*, 2021). Consequently, catfish production in Indonesia has increased rapidly, accounting for 55 691 t in 2004 and climbed dramatically in 2014, reached 543 774 t (Zahidah *et al.*, 2018). In addition, catfish production from 2017 to 2018 increased from 841.75 × 10^3 t to 1.81 × 10^6 t (114.82 %) (FAO, 2018).

In intensive fish cultivation, only about 80 % of the feed given is consumed, while the remaining 20 % will be wasted (not eaten), and of the 80 % consumed, only about 25 % will be retained. In comparison, the remaining 10% will be wasted through faeces, and 65 % will be excreted as urine (Bureau and Hua, 2010). According to El-Shafai *et al.* (2007), in the intensive cultivation system of tilapia, the nutrients released are around 62 % to 73 % of the total nitrogen and 55 % to 70 % of the total phosphorus divided into particles dissolved. Furthermore, N and P waste can affect water quality parameters such as a decrease in the concentration of dissolved oxygen content and an increase in the concentration of carbon dioxide, ammonia, nitrite, and nitrate (Hlordzi *et al.*, 2020). According to Keramat (2011), the resulting waste could increase dissolved and suspended organic matter in the feed residue, faeces and urine, negatively affecting fish growth even at specific toxic doses. Therefore, the deterioration of water quality leads to retard fish growth (Makori *et al.*, 2017). In a review by Yavuzcan *et al.* (2017), water quality deterioration has a detrimental effect on fish physiology, growth rate, and feed efficiency, resulting in various diseases and even death. Based on those obstacles, it is necessary to find a solution to maintain water quality suitable for *C. gariepinus*, such as applying an aquaponics system.

Aquaponics is the process of maintaining aquatic organisms and plants in symbiosis into one system or several sub-systems (Goddek *et al.*, 2019; Monsees *et al.*, 2017; Pedersen *et al.*, 2012), whereas treated water is circulated freely between aquaculture and hydroponic units in a single loop system (Goddek *et al.*, 2019). The

* Corresponding author e-mail: handajani@umm.ac.id.

principle of the aquaponics system is to utilize fish cultivation waste for plant growth and produce useful and economically valuable by-products (Somerville *et al.*, 2014). The advantages of aquaponics technology compared to conventional fish cultivation technologies are to control water quality, high fish growth and production, and additional income from plants. Plants in aquaponics technology absorb nutrients from waste of fish culture system for their development (Goddek *et al.*, 2019).

The types of plants used in the aquaponics system can be vegetable plants, fruit plants, aquatic plants (aquascape), flower plants or other aquatic plants. Ghaly *et al.* (2005) reported that five types of plants, including *Medicago sativa* L., *Trifolium repens* L., *Avena sativa* L., *Secale cereale* L. and *Hordeum vulgare* L. were able to reduce total solids, COD, NO_3-N, NO_2-N, phosphate and potassium ranging from 54.7 % to 91.0 %, 56.0 % to 91.5 %, 82.9 % to 98.1 %, 95.9 % to 99.5 %, 54.5 % to 93.6 % and 99.6 % to 99.8 %. Handajani *et al.* (2018) also postulated that *Echinodorus palaefolius* (J. F. Macbr) could utilize N and P in *Anguilla bicolor* culture. Water remediation with *E. amazonicus* and *E. palaefolius* significantly reduced TAN, NO_2, NO_3, and PO_4 concentrations in effluent of fish culture system. Unfortunately, no one has used *E. palaefolius* as a phytoremediator agent in the aquaponic system of catfish culture. Thus, that system is expected to improve the performance of fish production.

The purpose of this study was to evaluate the capacity of water Jasmine/Mexican Sword [*Echinodorus palaefolius* (J. F. Macbr.)] plants as phytoremediation agents in aquaponics systems in reducing waste of catfish culture system.

2. Materials and Methods

2.1. Preparation of containers, fish, and plants

Two types of containers were used in this experiment for catfish fry and *E. palaefolius* cultivation. Twelve catfish fries were reared in containers filled with 40 L of water, while *E. palaefolius* was maintained in a tub with volume of 38 cm × 12 cm × 30 cm in length, completed with sand as a planting medium at the bottom of the tub. Meanwhile, this experiment used catfish fries (5.14 g ± 0.45 g) obtained from a group of fish farmers in Malang Regency, with a stocking density of one fish per liter. The placement of fish in the experimental unit was carried out randomly. Before the treatment, catfish was conditioned for 5 d, fed diet of 30 % of protein with a feeding rate of 3 % of the biomass. The frequency of feeding was conducted in the morning (06.00), afternoon (12.00) and evening (18.00) for 30 d. During the conditioning period, the health and vitality of catfish were controlled so that they were still suitable as a sample. Moreover, the aquatic plants obtained from ornamental aquatic plant cultivators were adapted in a fibre bath for 5 d before use.

2.2. Experimental design and data analysis

This study used a completely randomized design with four treatments with three replications. These treatments differed among teach other in the stocking density of *E. palaefolius*: 0 g m^{-2} (T1), 150 g m^{-2} (T2), 250 g m^{-2} (T3) and 350 g m^{-2} (T4). Each treatment was repeated three times.ANOVA and F test used the SPSS version 21 with 95 % confidence level, then further tested using the Duncan's multiple range test to determine whether significant variation among treatment means the treatment effect on each tested variable (Adinurani, 2016).

2.3. Measurements

Water quality measurements were carried out for 30 d (day) after introducing water plants. Water quality parameters were measured every day including temperature, pH, dissolved oxygen (DO), while total amoniacal nitrogen (TAN), nitrate nitrogen (NO_3-N), nitrite nitrogen (NO_2), phosphate phosphorus (PO_4-P), total suspended solids (TSS), once a week (1 wk=7 d) following Enduta *et al.*, 2011. Measurement of TAN, nitrite, nitrate, and orthophosphate was carried out using a spectrophotometer referring to Rice *et al.* (2017). The following measures were taken: survival rate (SR), total feed consumption, specific growth rate (SGR), absolute length (Al), and feed conversion ratio (FCR) to determine the growth performance of catfish (Liu *et al.*, 2016; Nhan *et al.*, 2019) using Equation (1) to Equation (4):

$$\text{SGR (\% d}^{-1}) = \frac{W0 - Wt}{t} \quad (1)$$

$$\text{Al (cm)} = Lt - L0 \quad (2)$$

$$\text{FCR} = \frac{F}{Wt - W0} \quad (3)$$

Note:SGR = Specific growth rate (% d^{-1}); FCR = Feed conversion ratio; Al= Absolute lenght (cm); F= Feed consumption during cultivation (kg);W0 = Initial weight (g); Wt = Final weight (g); W0 = Initial lenght (cm)

Wt = Final lenght (cm);t = Time (day)

$$\text{SR (\%)} = \frac{Nt}{No} \times 100 \quad (4)$$

Note:SR = Survival rate (%);No= Initial number of fish; Nt = Final number of fish

The calculation of nutrient removal was carried out every 7 d, such as TAN, NO_3, NO_2 and PO_4 (Enduta *et al.*, 2011). The water plant parameters, including wet biomass, were measured at the beginning and end of the experiment. At the beginning and end of the investigation, the total N and PO_4-P in plant tissue were analyzed (Amalia *et al.*, 2014).

2.4. Nutrient removal efficiency

During the experiment, there was a loss of nutrients in the water. The amount of nutrient reduction could be calculated by the following Equation (5) (Zhou *et al.*, 2006).

$$NR = \frac{(Ca - Cb)}{Ca} \times 100 \quad (5)$$

Note:NR = nutrient removal (%); Ca= nutrient concentration of influent (mg L^{-1}); Cb = nutrient concentration of effluent (mg L^{-1})

3. Result and discussion

3.1. Result

3.1.1. Water quality and nutrient removal efficiency

Measurement of water quality parameters, including temperature, pH, dissolved oxygen (DO), total suspended solids (TSS), total ammonia nitrogen (TAN), ammonia (NH_3), ammonium (NH_4), nitrate nitrogen (NO_3-N),

nitrite nitrogen (NO_2-N), orthophosphate (PO_4-P) were examined for 30 d of catfish rearing (Table 1).

Tabel 1. Water quality in catfish media during 30 d observation

Variable	T1	T2	T3	T4	Optimum Reference
Temperature (°C)	26.50 to 29.30	26.30 to 28.70	26.80 to 28.92	26.30 to 27.68	25 to 30 °C (Siqwepu *et al*., 2020)
DO (mg L^{-1})	4.75 to 5.13	4.65 to 5.60	4.75 to 5.60	4.27 to 5.53	> 3 mg L^{-1} (Siqwepu *et al*., 2020)
pH	7.37 to 7.52	7.90 to 8.10	7.95 to 8.10	7.85 to 8.03	6.5 to 8 (Siqwepu *et al*., 2020)
TSS (mg L^{-1})	4.67 to 5.44	4.40 to4.56	4.06to 4.45	4.00to 4.56	< 80 (Siqwepu *et al*., 2020)
TAN (mg L^{-1})	0.15 to 0.47	0.15 to 0.27	0.15 to 0.27	0.15 to 0.25	< 0.27 (Elesho *et al*., 2021)
NO_2-N (mg L^{-1})	0.05 to 0.35	0.05 to 0.31	0.05 to 0.27	0.05 to 0.24	< 0.21 (Elesho *et al*., 2021)
NO_3-N (mg L^{-1})	14.64 to 49.67	14.64 to 47.60	14.64 to 43.28	14.64 to 45.27	< 53 (Elesho *et al*., 2021)
PO_4-P (mg L^{-1})	0.65 to 9.96	0.65 to 8.85	0.65 to 8.63	0.65 to 8.51	< 10 (Elesho *et al*., 2021)

Figure 1 shows the trend of nutrient removal efficiency every 7 d for each treatment. The removal efficiency of NO_3 and PO_4 in all treatments tended to increase every week, except at T3 (250 g m^{-2}) that the removal of phosphate decreased at 2nd wk and nitrate at 4th wk. The TAN removal efficiency for all treatments was almost the same level at week two, and then in the following week, it tended to increase. On the other hand, NO_2 removal efficiency fluctuated for all treatments.

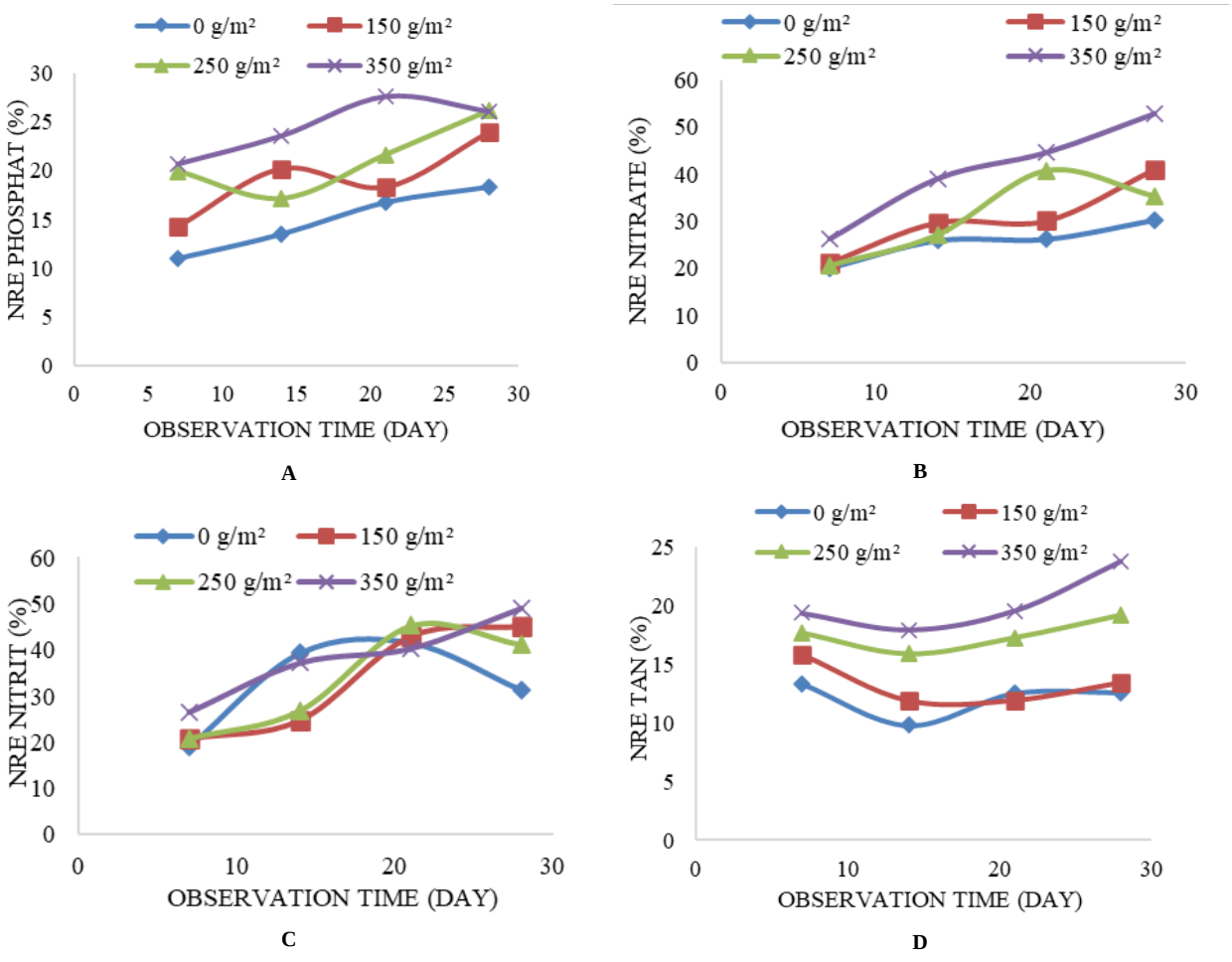

PHOSPHATE-P NITRATE-N

Figure 1. Nutrient Removal efficiency (%) Phosphate-P (A), Nitrate-N (B), Nitrite-N (C) and Total Ammonia Nitrogen TAN (D)

3.1.2. Catfish growth performance

The growth performance of catfish fry consisting of survival, specific growth rate, absolute length, total feed consumption, and feed conversion on maintenance for 30 d is presented in Table 2. The statistical analysis of results showed that Treatments, T3 and T4 almost significantly differences between treatments ($P < 0.05$) varied from other treatments, except for survival, which was not significantly different. But only absolute length of fishes of T4, T3 and T2 had significant ($P < 0.05$) difference from that of T1. (*E. palaefolius*, 350 g m^{-2}) showed the

highest value for specific growth and absolute length and the lowest feed conversion rate.

Table 2. Growth performance of catfish cultured under aquaponics system

Variable	T1	T2	T3	T4
Specific growth rate (%)	2.53±3.74[b]	3.18±5.54[b]	3.84±4.93[a]	4.00±2.73[a]
Absolute length (cm)	3.06±0.46[b]	4.57±0.16[a]	4.66±0.16[a]	4.72±0.15[a]
Feed consumption (g)	106.53±4.23	173.63±2.63	158.40±6.39	165.83±5.06
Feed conversion ratio	0.54±0.8[b]	0.43±0.02[b]	0.39±0.02[a]	0.35±0.01[a]
Survival rate (%)	100.00±0.00	100.00±0.00	100.00±0.00	100±0.00

The different letters in each row showed significant differences ($P < 0.05$)

3.1.3. Plant growth performance

The statistical analysis results showed significant differences of plant growth parameters of T4 and T3 had significant ($P < 0.05$) differences from the same of T1 but not in the case of plant height. The T4 (350 g m^{-2}) had the highest biomass gain, daily growth, nitrogen retention and phosphorus retention. Meanwhile, plant height was not significantly different.

Table 3.Plant growth performance (*E. palaefolius*)

Variable	T2	T3	T4
Δ biomass (g)	84.67±5.25[a]	109.67±2.60[b]	112.67±2.89[c]
Daily growth (g)	2.07±0.07[a]	3.37±0.49[b]	4.97±0.83[c]
Plant height (cm)	20.48±3.56	29.25±1.79	48.97±4.53
Nitrogen retention (g)	99.87±4.39[a]	143.84±0.74[b]	178.11±6.53[c]
Phosphorus retention (g)	68.23±3.62[a]	121.43±0.39[b]	149.12±1.64[c]

The different letters in each row showed significant differences ($P <0.05$)

3.2. Discussion

The maintenance of catfish fry by applying aquaponics technology was greatly influenced by environmental factors, including temperature, pH, and dissolved oxygen. The higher the temperature of the media was, the higher the metabolic rate of the fish was so that the fish appetite increased, which means an increase in the toxicity of excreted metabolic waste. The range of temperatures in this study was still in good condition for catfish growth (26.30 ºC to 28.92 ºC). According to Siqwepu *et al.* (2020), the optimal temperature ranged for catfish is 25 ºC to 30 ºC. Elesho *et al*. (2021) support that catfish can grow well at 25 ºC to 31 ºC.

The pH value during the observation period ranged from 7.37 to 8.10. This pH value was in the optimum range of catfish growth, accounting for 6.5 to 9 (Ajiboye *et al.*, 2015; Hasan *et al.*, 2020). Moreover, dissolved oxygen in this study ranged from 3.8 mg L^{-1}until 7.8 mg L^{-1} (Ekawati *et al.*, 2021), and this value was in the tolerance range for catfish growth, namely > 3 mg L^{-1} (Siqwepu *et al.*, 2020). Meanwhile, according to Elesho *et al.* (2021), dissolved oxygen for catfish must be above 4 mg L^{-1} which has the similarity with the present findings.

During the present study, it was found that TSS remained still in the optimal range, supporting catfish survival and plant growth. The optimal range of TSS values was 25 mg L^{-1} to 80 mg L^{-1} (Oseni *et al.*, 2018). The high TSS value could inhibit the growth of aquatic plants because it interferes with the plant's photosynthetic process. According to Sanjoto *et al.* (2020), suspended and dissolved materials in the water are not toxic. However, if they are in excessive amount, they can increase the turbidity value, further inhibiting sunlight penetration into the water column and ultimately affecting the photosynthetic process in the water (Oseni *et al.*, 2018).

In this study, the measured ammonia was one of the part of total ammonia nitrogen (TAN). The TAN value ranged from 0.15 mg L^{-1} to 0.47 mg L^{-1} (Table 1), lower than the research of (Akinbile and Yusoff, 2012), which used *Eichhornia crassipes* Martand, *Pistia stratiotes* L. as remediating agents. The results of TAN, NH_3 and NH_4 shown ranged from 1.34 mg L^{-1}, to 1.79 mg L^{-1}; 0.14 mg L^{-1}, to 0.2 mg L^{-1} and 0.13 mg L^{-1}, and 0.22 mg L^{-1}, respectively.

The water quality in the phytoremediation-based recirculation system was optimal because plants could utilize fish culture waste as nutrients for their growth. According to Effendi *et al.* (2015), water spinach can reduce TAN by 84.6 %, 34.8 % of NO_3 and 44.4 % of PO_4. On the other hand, Delis *et al.* (2015) reported that Vetiver grass [*Chrysopogon zizanioides* (L.) Roberty] could reduce TAN by 48.36 % and PO_4 by 19.94 %. In this study, the ability of *E. palaefolius* was the highest in reducing TAN, NO_2, NO_3, and PO_4 by of T4. The percentage of removal of TAN, NO_2, NO_3, and PO_4 on 28th d was 23.80 %; 48.91 %; 52.99 %; and 27.63 %, respectively. Meanwhile, the lowest nutrient removal by of T1, were TAN on 14th d was 9.8 %; while NO_2 on 7th d was 19.07 %; NO_3 on 7th d was 19.97 %, and PO_4 was 11.05 % on 7th d. Plants as phytoremediators utilize ammonium and nitrate, where the primary source of inorganic nutrients came through plant roots (Enduta *et al.*, 2011), while it is not toxic for fish. When the water conditions are sufficiently oxidized, ammonia will be converted into an intermediate product, namely nitrite (NO_2).

Nitrite is a relatively unstable compound because, with sufficient oxygen, it will be easily oxidized to nitrate by *Nitrobacter*. The nitrite concentration in this research could still be within tolerable levels by fish, although it increased because this compound is unstable. Their changes in the system could be overcomed with sufficient oxygen supply so that the eels can still grow well. According to Van Rijn (2013), in the circulating system, the nitrite concentration should not exceed 10 mg L^{-1} for an extended period, and in most cases it should remain below 1 mg L^{-1}. According to Elesho *et al.* (2021), nitrite concentration must be < 0.21 mg L^{-1} in water media. The *Nitrobacter* bacteria then oxidizes nitrite (NO_2) to produce nitrate (NO_3).

Furthermore, nitrate is the end product of the nitrogen cycle and a compound that is not harmful to fish and a source of nutrients for plants other than NH_4. The nitrate

concentration in this study was still supportive for catfish life because it ranged from 14.64 mg L^{-1} to 49.67 mg L^{-1}. The research results by Elesho *et al.* (2021) on the rearing system of catfish, NO_3 was 53 mg L^{-1}, while Jaeger *et al.* (2019) recommended that the NO_3 concentration not exceed 50 mg L^{-1} in waters used for fish farming. High concentrations of NO_3 can result in algae blooms which cause a decrease in pH (Ebeling *et al.*, 2006; Nuwansi *et al.*, 2019). Morning glory (*Ipomoea aquatica* Forssk.) can reduce total ammonia - nitrogen N, nitrite-N, nitrate-N and orthophosphate significantly from 78.32 % to 85.48 %, 82.93 % to 92.22 %, and 79.17 % to 87.10 %, respectively, and 75.36 % to 84.94 %, whereas by using Chinese broccoli (*Brassica oleracea* var. *alboglabra* L.), total ammonia nitrogen could be reduced from 75.85 % to 69.0 %, 79.34 % to 72.49 % for nitrite-N, 80.65 % to 66.67 % for nitrate-N and 77.87 % to 66.79 % for orthophosphate (Enduta *et al.*, 2011).

The survival rate in this study was 100 %. This result was higher when compared to the study by Okomoda *et al.* (2020) where catfish maintained in a settling tank and aerobic tank as filters gave a survival rate of 82.78 %. According to Enduta *et al.* (2011), the survival rates of African catfish (*C. gariepinus*) treated with aquaponics technology using kale (*Brassica oleracea* var. *sabellica* L.) and caisim (*Brassica rapa* L. Cv. group Caisin) plants were 94.5 % and 94.2 %, respectively. Based on the growth performance data of catfish (Table 2), the density of *E. palaefolius*plants as a phytoremediation agent in catfish culture with recirculatory aquaponics affected the growth performance of catfish significantly ($P < 0.05$). The T4 showed the highest growth performance for catfish, including a specific growth rate of 4.00 %, an absolute length of 4.72 cm, and feed conversion of 0.4. This was due to utilizing nutrients from the highest level of catfish culture waste at T4. Therefore, the water quality conditions for catfish rearing were still in good condition to utilize feed more efficiently. According to Pedersen *et al.* (2012), recirculation application of recirculatory system with water plants, duck weeds (*Lemna gibba* L), dropped FCR value, increased protein efficiency ratio, and tilapia growth. The FCR in fish farming must be considered because it would affect the cost of feed. Small changes in FCR would have a big effect on the profitability of cultured fish (Liu *et al.*, 2016).

The success of the aquaponics system was inseparable from the growth of *E. palaefolius*. During the observation period, the development of aquatic ornamental plants showed a positive response to the aquaponics system. That indicated an increase in biomass growth in all treatments and nitrogen retention in plant tissues (Table 3). Freshwater ornamental plants could utilize waste of catfish cultivation waste as a sources of nutrients for their growth. This was evidenced by an increase in the percentage of nutrient removal by plants every 7 d (Figure 1). The results of biomass growth, daily growth, plant height, nitrogen retention, and phosphorus retention were the highest in T4 with successive values: 112.67 g, 4.97 %, 48.97 cm, 178.11 g, and 149.12 g, respectively.

4. Conclusion

Based on our findings, *E. palaefolius*has a high potential as a water remediator, proved in *C. gariepinus* growth performance, nutrient removal capabilities and water quality data. The highest value of those measurements was obtained at 350 g m^{-2} density of *E. palaefolius*. Moreover, the present results indicated that the higher density of *E. palaefolius* showed a better impact on *C. gariepinus* development, nutrient removal, and water quality. Hence, further research is still needed for investigating the optimum density of *E.* palaefolius before it can be used in *C. gariepinus* culture or other fish commodities.

Acknowledgement

The author would like to thank the Faculty of Agriculture and Animal Science, the University of Muhammadiyah Malang, for the funding given to the Research Blockgrant Program with No SK: E.2.a / 131 / FPP-UMM / II / 2020.

References

Adinurani PG. Design and Analysis of Agro Trial Data: Manual and SPSS. Plantaxia, Yogyakarta, Indonesia

Ajiboye AO, Awogbade AA, and Babalola OA. 2015. Effects of water exchange on water quality parameters, nutrient utilization and growth of African catfish (*Clarias gariepinus*). *Int. J. Phytoremediation.*,**6(5)**:57-60.

Akinbile CO, and Yusoff MS. 2012. Assessing water hyacinth (*Eichhornia crassopes*) and lettuce (*Pistia stratiotes*) effectiveness in aquaculture wastewater treatment. *Int. J. Phytoremediation.*,**14(3)**:201-211.

Amalia F, Nirmala K, Harris E, and Widiyanto T. 2014. The ability of Lemna (*Lemna perpusilla* Torr.) as a phytoremediator to absorb nitrogen waste in the cultivation of catfish (*Clarias gariepinus*) in the recirculation system. *Jurnal Limnotek*,**21(2)**:185-192.

Bureau DP, and Hua K. 2010. Towards effective nutritional management of waste outputs in aquaculture, with particular reference to salmonid aquaculture operations. *Aquac. Res.*,**41(5)**:777-792.

Delis PC, Effendi H, Krisanti M, and Hariyadi S. 2015. Treatment of aquaculture wastewater using Vetiveria zizanioides (*Liliopsida, Poaceae*). *Aquacult. Aquarium Conserv. Legis.*, **8(4)**:616-625.

Ebeling JM, Timmons MB, and Bisogni J. 2006. Engineering analysis of the stoichiometry of photoautotrophic, autotrophic, and heterotrophic removal of ammonia–nitrogen in aquaculture systems. *Aquaculture*,**257(1-4)**:346-358.

Effendi H, Amalrullah Utomo B, Maruto Darmawangsa G, and Sulaeman N. 2015. Combination of water spinach (*Ipomea aquatica*) and bacteria for freshwater cryfish red claw (*Cherax quadricarinatus*) culture wastewater treatment in aquaponic system. *J. Adv. Biology*,**6(3)**:1072-1078.

Ekawati AW, Ulfa SM, Dewi CSU, Aziz A, Amin LNmS, Yanuar AT, and Kurniawan A. 2021. Analysis of aquaponic-recirculation aquaculture system (A-Ras) application in the catfish (*Clarias gariepinus*) aquaculture in Indonesia. *Aquaculture*,**21(3)**:93-100.

El-Shafai SA, El-Gohary FA, Naser FA, van der Steen P, and Gijzen HJ. 2007. Nitrogen recovery in an integrated system for wastewater treatment and tilapia production. *Environmentalist*, **27(2)**:287-302.

Elesho FE, Sutter DAH, Swinkels MAC, Verreth JAJ, Kröckel S, and Schrama JW. 2021. Quantifying methionine requirement of juvenile African catfish (*Clarias gariepinus*). *Aquaculture*, **532:(736020)**: 1–11.

Enduta A, Jusoh A, Ali Na, and Wan Nik W. 2011. Nutrient removal from aquaculture wastewater by vegetable production in aquaponics recirculation system. *Desalin Water Treat.*, **32(1-3)**:422-430.

FAO. 2018. **FAO Yearbook. Fishery and Aquaculture Statistics 2018**, Rome.

Ghaly A, Kamal M, and Mahmoud N. 2005. Phytoremediation of aquaculture wastewater for water recycling and production of fish feed.*Environ Int.*, **31(1)**:1-13.

Goddek S, Joyce A, Wuertz S, Körner O, Bläser I, Reuter M and Keesman KJ. 2019. Decoupled aquaponics systems. In: Goddek S, Joyce A, Kotzen B and Burnell GM (Eds.) **Aquaponics Food Production Systems: Combined Aquaculture and Hydroponic Production Technologies for the Future**. Springer International Publishing, Cham, Switzerland pp 201-229.

Handajani H, Widanarni W, Budiardi T, Setiawati M, and Sujono S. 2018. Phytoremediation of Eel (*Anguilla bicolor bicolor*) rearing wastewater using amazon sword (*Echinodorus amazonicus*) and water jasmine (*Echinodorus palaefolius*). *Omni-Akuatika*, **14(2)**:43-51.

Hasan M, Mawa Z, Ul-Hassan H, Rahman M, Tanjin S, Ahmed Abro N, Gabol K, Bashar M, Jasmine S, and Ohtomi J. 2020. Impact of eco-hydrological factors on growth of the Asian stinging catfish *Heteropneustus fossli*s (Bloch, 1794) in a Wetland Ecosystem. *Egypt. J. Aquat. Biol. Fish*, **24(5)**:77-94.

Hlordzi V, Kuebutornye FKA, Afriyie G, Abarike ED, Lu Y, Chi S, and Anokyewaa MA. 2020. The use of Bacillus species in maintenance of water quality in aquaculture: A review.*Aquac. Rep*,**18(100503)**:1-12.

Jaeger C, Foucard P, Tocqueville A, Nahon S, and Aubin J. 2019. Mass balanced based LCA of a common carp-lettuce aquaponics system. *Aquac Eng*., **84:**29-41.

Keramat A. 2011. Reduction in the environmental impact of waste discharged by fish farms through feed and feeding. *Rev Aquac*, **3:**19-26.

Liu H, Zhu X, Yang Y, Han D, Jin J, and Xie S. 2016. Effect of substitution of dietary fishmeal by Soya Bean meal on different sizes of Gibel Carp (*Carassius auratus* gibelio): nutrient digestibility, growth performance, body composition and morphometry.*Aquac. Nutr* .**22(1)**:142-157.

Makori AJ, Abuom PO, Kapiyo R, Anyona DN, and Dida GO. 2017. Effects of water physico-chemical parameters on Tilapia (*Oreochromis niloticus*) growth in earthen ponds in Teso North Sub-County, Busia County.*Fish Aquatic Sci*, **20(1)**:20-30.

Monsees H, Keitel J, Paul M, Kloas W, and Wuertz S. 2017. Potential of aquacultural sludge treatment for aquaponics: evaluation of nutrient mobilization under aerobic and anaerobic conditions. *Aquac. Environ. Interact*., **9(1)**:9-18.

Nhan HT, Tai NT, Liem PT, Ut VN, and Ako H. 2019. Effects of different stocking densities on growth performance of Asian swamp eel *Monopterus albus*, water quality and plant growth of watercress *Nasturtium officinale* in an aquaponic recirculating system. *Aquaculture*, **503**:96-104.

Nuwansi KKT, Verma AK, Rathore G, Prakash C, Chandrakant MH, and Prabhath GPWA. 2019. Utilization of phytoremediated aquaculture wastewater for production of koi carp (*Cyprinus carpio* var. koi) and gotukola (*Centella asiatica*) in an aquaponics. *Aquaculture*, **507**:361-369.

Okomoda VT, Musa SO, Tiamiyu LO, Solomon SG, Oladimeji AS, Hassan A, Alabi KI, and Abol-Munafi AB. 2020. Fermentation of hydrothermal processed *Jatropha curcas* Kernel: Effects on the performance of *Clarias gariepinus* (Burchell, 1822) fingerlings. *Aquac. Rep.*, **18(100428)**: 1–7

Oseni OM, Dada OE, Okunlola GO, and Ajao AA. 2018. Phytoremediation potential of *Chromolaena odorata* (L.) king and robinson (Asteraceae) and *Sida acuta* Burm. f. (Malvaceae) grown in lead-polluted soils. *Jordan J. Biol. Sci*., **11(4)**:355–360.

Pedersen L-F, Suhr KI, Dalsgaard J, Pedersen PB, and Arvin E. 2012. Effects of feed loading on nitrogen balances and fish performance in replicated recirculating aquaculture systems. *Aquaculture*, **338-341**:237-245.

Rice EW, Baird RB, and Eaton AD. 2017. **Standard Methods for the Examination of the Water and Wastewater,** 23rd ed., Washington DC (US).

Sanjoto TB, Elwafa AH, Tjahjono H, and Sidiq WABN. 2020. Study of total suspended solid concentration based on Doxaran algorithm using Landsat 8 image in coastal water between Bodri River estuary up to east flood canal Semarang City. *IOP Conf. Ser. Earth Environ. Sci.*, **561(012053)**:1-7.

Siqwepu O, Salie K, and Goosen N. 2020. Evaluation of chelated iron and iron sulfate in the diet of African catfish, *Clarias gariepinus* to enhance iron excretion for application in integrated aquaponics systems.*J World Aquac Soc*, **51(4)**:1034-1053.

Somerville C, Cohen M, Pantanella E, Stankus A, and Lovatelli A. 2014. **Small-Scale Aquaponic Food Production. Integrated Fish and Plant Farming**, Rome.

Van Rijn J. 2013. Waste treatment in recirculating aquaculture systems. *Aquac Eng*., **53:**49-56.

Yavuzcan YH, Robaina L, Pirhonen J, Mente E, Domínguez D, and Parisi G. 2017. Fish welfare in aquaponic systems: Its relation to water quality with an emphasis on feed and faeces—A Review. *Water*, **9(1)**13:1-17

Zahidah Z, Andriani Y, Dhahiyat Y, Nurruhwati I, Sahidin A, Hamdani H, and Victoria SM. 2018. Inorganic nitrogen absorption in the aquaponics farming of Sangkuriang Catfish (*Clarias gariepinus*) at uneven retention periods. *Jurnal Akuakultur Indonesia*, **17(2)**:130-136.

Zhou Q, He SL, He X, Huang XF, Picot B, Li XD, and Chen G. 2006. Nutrients removal mechanisms in high rate algal pond treating rural domestic sewage in East China.*Water Sci Technol Water Supply*, **6(6)**:43-50.

JJBS

Volume 14, Number 5,December 2021
ISSN 1995-6673
Pages 965 – 968

Jordan Journal of Biological Sciences

Effect of Bioagent-added Organo-mineral Nitrogen Fertilizer on Total Nitrogen, pH, and Chrome Content in Lowland Paddy

Rija Sudirja[1,*], Indra Oktavianus Lubis[1], Nadia Nuraniya Kamaluddin[1], Santi Rosniawaty[2]

[1]*Department of Soil Science and Land Resource, Faculty of Agriculture, Universitas Padjadjaran, Bandung, Indonesia;* [2]*Department of Crop Science, Faculty of Agriculture, Universitas Padjadjaran, Bandung, Indonesia*

Received: February 27, 2021; Revised: June 22, 2021; Accepted: October 16, 2021

Abstract

Rice field soil quality in Rancaekek decreases gradually due to textile waste water to irrigation source. One of the heavy metal contaminant is chrome (Cr). As an effort to reduce Cr residue, bioagent-added organomineral nitrogen (abbreviated as BaON) fertilizer consisted of the mixture of urea, zeolite, activated charcoal, and plant compost enriched with bioagent (*Bacillus subtilis*) was added as a slow release fertilizer. This paper studied the effect of BaON fertilizer formulation towards total nitrogen content, pH and total Cr content in Rancaekek paddy soil. The experiment was designed in Randomized Block Design with six treatments and five replicates, consisted of: 0 (control), 150; 200; 250; 300; and 350 kg ha^{-1}. The result showed that the application of BaON fertilizer increased soil total nitrogen content and pH, and decrease Cr residue in Rancaekek paddy field soils. Application of 350 kg ha^{-1} of BaON fertilizer gave the highest increase of total nitrogen in 60 days after transplant (0.11%), while 300 kg ha^{-1} of BaON gave the highest increase in pH (6.18), and the application of 250 kg ha^{-1} of BaON gave the highest reduction of chrome (16.15 mg kg^{-1}) in Rancaekek soils. This study suggests that application of Urea-zeolite-activated charcoal and bio-agent inoculated compost application could minimize Cr contaminated waste in the long-run.

Keywords: *Bacillus subtilis*, heavy metal, soil ameliorant, bioremediation

1. Introduction

The quality of productive agriculture system in Indonesia has been steadily decreasing due to environmental pollution. The pollution source also varies, ranging from agrochemical inputs such as synthetic pesticide, fertilizers, plant growth hormone, to heavy metals used in the manufacturing process of neighboring industrial areas. The discharge became a problem particularly because it was untreated prior to its release to the environment (Yaseen and Scholz, 2019).

Rancaekek was a well-known rice producer in the 1980s (Komarawidjadja, 2017), but after the land use conversion in the area, the quality of soil and water utilized for agricultural irrigation has depleted. Rancaekek experienced massive land use conversion from agriculture production area with rice as a main commodity,into textile production area. This shift has lead copious amount of pollutant to be discharged to the environment. The amounts of documented heavy metals detected in Rancaekek riverbank soil in 2017 were 174.7 mg l^{-1} of chrome, 92.2 mg l^{-1} of elemental mercury, and 4.0 mg l^{-1} of arsenic above the environmental safety level of industrial waste. Cikijing river is one of the polluted rivers used as agricultural irrigation source in four villages in Rancaekek areas: Linggar, Jelegong, Sukamulya, and Bojongloa village (Sutono and Kurnia, 2013). Trace level of heavy metal is present in water and may be essential for living organisms (Benamar and Zitouni, 2013), but high concentration may adversely impact the environment.

One of the heavy metals contained in the polluted wastewater is chrome (Cr). Cr came from fabric dyes (Chavan, 2011) and harmful for human health. Poisoning symptoms includes nausea, abdominal pain, respiratory problems, kidney and liver damage, accumulation of this metal can lead to death. In plants, Cr inhibits the availability of nitrogen, phosphate, potassium, and other primary nutrients. High Cr concentration can decrease the germination percentage of paddy up to 60% (Nagarajan and Ganesh, 2014).

Immobilization is one of the ways to reduce heavy metal availability in the environment. A method that could be used is through the addition of biological and chemical agents to bind or reduce heavy metals availability in the soil. Bio-agent added organomineral nitrogen (BaON) fertilizer is a modification of urea-based nitrogen fertilizer, zeolite, activated charcoal, and compost with a bio-agent that has a role as a slow release fertilizer and heavy metals absorbent. Zeolite addition in nitrogen fertilizer made the ammonium released by the fertilizer entrapped in by zeolite structure (Ippolito, Tarkalson and Lehrsch, 2011) and will be discharged back to the soils when the availability of nitrogen is low. Addition of activated charcoal is known as heavy metals adsorbent, due to the characteristics of charcoal that could selectively adsorb ions (Larasati et al., 2016). Addition of bio-agent on the fertilizer can improve the effectiveness of nutrient supply

* Corresponding author e-mail: rija.sudirja@unpad.ac.id.

and reduce heavy metals in soils. This research aims to find out the effect of BaON in various doses on total nitrogen value, pH value, and degradation of heavy metal Cr on polluted soils.

2. Materials and Methods

Paddy field soil were obtained from Jelegong Village, Rancaekek (6°57'41.67"-6°58'52.29"S, 107°46'54.41-107°48'10.13"E). Paddy variety used in this study was Inpara 9 Agritan variety, product of Indonesian Ministry of Agriculture. Urea (Pupuk Kujang, Cikampek, Indonesia), Zeolite, and Technical Grade Activated Charcoal were ground and sieved through 30 mesh pass to obtain 0.6 mm particle size. Compost used were plant compost with 26:1 C/N Ratio and 22% relative humidity level, and were finely ground and sieved through 70 mesh pass to obtain 0.210 mm particle size. Prior to fertilizer formulation, *Bacillus subtilis* was inoculated in Nutrient Broth (Himedia, Mumbai, India), and kept under ambient temperature (25-28ºC) on 125 rpm rotary shaker for 72 hours and reached 10^7 cfu population density. Urea, zeolite, activated charcoal, compost, and bioagent inoculant (*B. subtilis*) were mixed with 50:20:20:10 rations, respectively.

The experiment was conducted from January to July 2019 at Faculty of Agriculture, Universitas Padjadjaran experimental greenhouse, Ciparanje village, Jatinangor (6°54'59.0"S, 107°46'18.2"E). An Inpara 9 seedling were transplanted in a polybag contained 20 kg of Jelegong village paddy field soil and fertilizer were added in accordance to the treatment doses. Paddy soil were watered once daily. The experimental design used was Randomized Block Design, with one control and five doses of treatments; A= 0 (control), B = 150 kg BaON, C = 200 kg BaON, D = 250 kg BaON, E = 300 kg BaON, F = 350 kg BaON, each treatment was replicated five times.

At 20, 40, and 60 days after BaON fertilizer treatment, soil quality parameters such as total nitrogen content, soil pH, and chrome content were analyzed. Obtained data were analyzed with Analysis of Variance (ANOVA). Differences detected will be analyzed further by Tukey's post test with 5% confidence level. Data were processed by SPSS version 22 software.

3. Results and discussions

3.1. Initial Soils Analysis

Jelegong village soil was analyzed to obtain the information of total nitrogen value, pH value, Cation Exchange Capacity (CEC), and heavy metals content. The analysis revealed that total nitrogen content was 0.09% (very low), medium-high CEC (39.89 cmol kg^{-1}) and neutral pH (7.05). Heavy metals analysis showed that the chrome content was 38.84 ppm (polluted), and lead content was below the threshold (17.58 ppm).

3.2. Total Nitrogen

Nitrogen is one of the nutrients needed by plants in a large quantity. Nitrogen in soil is very mobile and could be easily lost by leaching or volatilization. BaON fertilizer application is one of the ways to supply nitrogen in soil continuously. Application of BaON fertilizer notably increased soil total nitrogen and continuously supplied nitrogen up until 60 days after application in the polluted paddy soil (Table 1). At 20 days after transplant (DAT), Treatment C (dosage 200 kg ha^{-1}) gave significant difference compared to Treatment B (dosage 150 kg ha^{-1}) and Treatment E (dosage 300 kg ha^{-1}). There was a significant difference between BaON on treatments compared to the control in 60 days after transplant (DAT).

Table 1. Bio-agent Added Organomineral Nitrogen (BaON) Fertilizer Effect on Total Nitrogen on Soils

Treatment	Total Nitrogen (%)		
	20 DAT*	40 DAT	60 DAT
A	0.12ab	0.09a	0.08a
B	0.11a	0.09a	0.10ab
C	0.14b	0.11a	0.09ab
D	0.12ab	0.10a	0.09ab
E	0.12a	0.10a	0.09ab
F	0.12ab	0.11a	0.11b

*DAT: Day after transplant

In Table 1, in 40 DAT observation all treatments show non-significant differences and lower nitrogen content compared to 20 DAT. This could be caused by the slow release trait from the fertilizer, therefore on 40 DAT, the nitrogen was released at lower rate in longer time. At 60 DAT, treatment F (350 kg ha^{-1}) with a total nitrogen of 0.11% displayed the highest amonium content at the end of vegetative phase.

The zeolite addition on fertilizer can minimize nitrogen loss in ammonium form. Zeolite has high absorbency power on ammonium. Released ammonium in soil will be reabsorbed by zeolites and released again in low ammonium conditions, which allows preservation of nitrogen in soils (Larasati et al., 2016). Zeolites and activated charcoal addition on the formulation could provide nitrogen slowly. Zeolites with 75-80% dosage of N could produce rice with the same amount as conventional fertilizer, therefore it could reduce the usage of synthetic fertilizer up to 25% (Jufri and Rosjidi, 2012).

3.3. Soil pH

There was a significant difference between the control and BaON treatments on 20 and 60 days after transplant (Table 2)

Table 2. Bio-agent Added Organomineral Nitrogen (BaON) Fertilizer Effect on pH on Soils

Treatment	pH		
	20 DAT	40 DAT	60 DAT
A	5.86ab	5.61a	5.43a
B	5.89ab	5.54a	6.13bc
C	5.73a	5.65a	5.98b
D	5.71a	5.75a	6.18c
E	5.93b	5.60a	6.12bc
F	5.94b	5.77a	5.98b

On 20 DAT, Treatment E (300 kg ha^{-1}) and Treatment F (350 kg ha^{-1}) was significantly different to Treatment C (150 kg ha^{-1}) and Treatment D (200 kg ha^{-1}), but was not significantly different to control and Treatment B (150 kg ha^{-1}). The highest value found on Treatment F (dosage 350 kg ha^{-1}) with 5.94 and categorized as slightly acidic.

All treatments were not significantly different to each other at 40 days after transplanting. The highest pH value was found on treatment F with 5.77 and categorized as slightly acidic. All treatments, except treatment D pH decreased at 20 DAT. This is very likely due to the increased nitrification in soil due to the release of hydrogen ions post nitrogen fertilization (Lu *et al*., 2012). At 60 DAT, soil pH value on BaON treatments gave significant effect compared to control. Treatment D increased pH value at 60 DAT. This allows less application of the fertilizer if the case of soil pH enhancement, as the pH value of Treatment D was not significantly different compared to treatments with higher dose (E and F). BaON contain urea that may trigger nitrification, which produce H^+ ions. Soil acidity value is affected by the existence of hydrogen ions (H^+). The higher H^+ ions on the soils, the higher the acidity of the soils.

Zeolite and activated charcoal addition on the fertilizer can amend soils pH value, as zeolite contains alkaline bases such as K^+, Na^+, and Mg^{2+} that could replace H^+ in adsorption complex, which led to the rise of pH value. In higher pH, metal ions react spontaneously and form metals-hydroxide bonds (Maulana et al., 2017). BaON application increased and maintained soil pH, which eventually impacted the nutrient availability on soils.

3.4. Heavy Metals Solubility on Soils

Statistical analysis showed BaON treatment reduced Cr availability in soil (Table 3). Treatment C displayed the highest chrome immobilization in soil compared to other treatments. Urea application in soil increases nitrate content, an important product used in the nitrification process (Shetty et al., 2019). Chrome solubility reduced due to the reaction between Cr^{3+} and NO_3^{-}.

Table 3. Bio-agent Added Organomineral Nitrogen (BaON) Fertilizer on Cr Reduction

Treatment	Heavy Metals Cr (mg kg^{-1})		
	20 DAT	40 DAT	60 DAT
A	19.61b	21.85b	21.00b
B	13.10a	17.03a	16.99ab
C	13.55a	18.73ab	16.15a
D	20.15b	20.58ab	19.32ab
E	15.41ab	17.53ab	18.30ab
F	17.59ab	18.27ab	17.36ab

Charcoal and zeolite mixture content can also reduce heavy metals content on polluted soils because of its ability to bind and maintain ions inside its complex. Adsorption by activated charcoal is an effective way to reduce heavy metals (Atmono et al., 2017). This was caused by decreased competition between H^+ and metal ions when the pH value is high, so that heavy metals adsorption process will increase rapidly if compared in lower pH conditions (Akaninwor et al., 2007).

The addition of organic matter in the form of compost may have the primary role in chrome reduction. Compost contains essential nutrient for plants and improves soil health. Compost addition could reduce the availability of heavy metals and improve plant growth and development (Angelova et al., 2010). The utilization of compost (thermophilic or vermicompost) can reduce heavy metal solubility, increasing soil pH value, electrical conductivity, and nutrients in soils (Shreshta et al., 2019).

Bacillus subtillis the microbial strain inoculated in the compost was known for its ability to absorb heavy metals. Several researches showed that *Bacillus subtilis* can reduce heavy metals contamination in a more environmentally friendly manner and as affective as 87% absorption rate towards chrome contaminants (Syed and Chintala, 2015). Besides its chrome-adsorbing abilities, genus Bacillus is also widely known as phosphate solubilizer (Bhakthavatchalu and Shivakumar, 2017).

4. Conclusion

Bioagent-added organo-mineral nitrogen fertilizer application in various concentration has improved the chemical properties of lowland paddy soil. The application improved the total nitrogen, pH, and reduced Cr residue, after 20, 40, and 60 day after treatment. Treatment F was the best treatment to increase total nitrogen, meanwhile treatment D was the best treatment to increase pH value

References

Chavan, R. B. 2011. 'Environmentally friendly dyes', in *Handbook of Textile and Industrial Dyeing: Principles, Processes and Types of Dyes*. doi: 10.1533/9780857093974.2.515.

Komarawidjadja, W. 2017. Paparan limbah cair industri mengandung logam berat pada lahan sawah di desa Jelegong, kecamatan Rancaekek kabupaten Bandung *J Teknologi Lingkungan* **18(2)** 173-181

Sutono S and Kurnia U. 2013. Identifikasi kerusakan lahan sawah di Rancaekek kabupaten Bandung, Jawa Barat *Prosiding Seminar Nasional Pertanian Ramah Lingkungan* pp 283-296

Benamar N, and Zitouni B. 2013. Levels of Chromium and copper in liver and muscle tissues of the round Sardinella sardinella AURITA (valenciennes) from the Oran coastline , *Jordan J of Biol Sci.*, 6(4), 252-256. doi:10.12816/0001622

Nagarajan M, and Ganesh KS. 2014. Effect of chromium on growth, biochemicals and nutrient accumulation of paddy (Oryza sativa L.) *Intl Letters of Nat Sci.* **23** 63-71

Ippolito, JA, Tarkalson DD, and Lehrsch GA. 2011 'Zeolite soil application method affects inorganic nitrogen, moisture, and corn growth', *Soil Sci.*. doi: 10.1097/SS.0b013e31820e4063.

Larasati, A. I., Susanawati, L. D., and Suharto, B. 2016. Efektivitas adsorpsi logam berat pada air lindi menggunakan media karbon aktif, zeolit, dan silika gel di TPA Tlekung, Batu . *J Sumberdaya Alam dan Lingkungan* **2(1)** 44-8

Jin, Q and Kirk MF 2018 pH as a primary control in environmental microbiology: 1. thermodynamic perspective *Front Environ Sci* **6(21)** 15

Jiwan S and Kalamdhad AS. 2014 Effects on heavy metals on soil, plants, human health and aquatic life I*nt Res Chem Environ* **1(2)** 15-21

Jufri A, and Rosjidi M. 2012. Pengaruh zeolit dalam pupuk terhadap pertumbuhan dan produksi padi sawah di kabupaten Badung provinsi Bali. *J Sains dan Teknologi Indonesia* **14(3)** 161-6

Li Y, Chapman SJ, Nicol GW, and Yao H. 2018. Nitrification and nitrifiers in acidic soils. *Soil Biology and Biochemistry* **116** 290-301

Lu L, Han W, and Zhang J 2012. Nitrification of archaeal ammonia oxidizers in acid soils is supported by hydrolysis of urea. *ISME Journal*. doi: 10.1038/ismej.2012.45.

Maulana A, Supartono, and Mursiti S. 2017. Biroremediasi logam Pb pada limbah tekstil dengan Staphylococcus aureus dan Bacillus subtilis *Indonesian J Chem Sci***6(3)** 2-7

Shetty P, Acharya C, and Veeresh N. 2019. Effect of urea fertilizer on the biochemical characteristics of soil *Int J Appl Sci Biotech* **7(4)** 414-420

Atmono, Natalina, and Mukti AD. 2017. Pengaruh arang aktif dan zeolit sebagai media adsorben dalam penurunan kadar logam krom pada air limbah cair penyablonan pakaian *J Rekayasa, Teknologi, dan Sains* **1(1)** 21-8

Akaninwor JO, Wegwu MO, and Iba IU. 2007. Removal of iron, zinc and magnesium from polluted water samples using thioglycolic modified oil-palm fibre. *African J BiochemRes* **1(2)** 11-3

Angelova V, Ivanova R, Pevicharova G, and Ivanov K. 2010. Effect of organic amendments on heavy metals uptake by potato plants *19th World Congress of Soil Science, Soil Solutions for a Changing World* pp 84-7

Shrestha P, Belliturk K, and Gorres JH. 2019. Phytoremediation of heavy metal contaminated soil by switchgrass: a comparative study utilizing different composts and coir fiber on pollution remediation, plant productivity, and nutrient leaching *J Environ Res Public Health* **16(1261)** 1-16

Syed S and Chinthala P. 2015. Heavy metal detoxification by different Bacillus species isolated from solar salterns *Scentifica* 2015 1-8

Bhakthavatchalu S and Shivakumar S. 2017. The Influence of Physicochemical Parameters on Phosphate Solubilization and the Biocontrol Traits of *Pseudomonas aeruginosa* FP6 in Phosphate-Deficient Conditions. *Jordan J Biol Sci* 11(2) pp 215-221.

JJBS

Volume 14, Number 5,December 2021
ISSN 1995-6673
Pages 969 – 974

Jordan Journal of Biological Sciences

The Effect of Bathing Length Time to Axillary Temperature and Dry Heat Loss on Newborns; A Comparative Analysis

Hotma Sauhur Hutagaol*

Midwifery Study Program of Padangsidimpuan, Poltekkes Kemenkes Medan, Sigulang, Padangsidimpuan, Indonesia.

Received: February 27, 2021; Revised: June 21, 2021; Accepted: August 24, 2021

Abstract

Hypothermia often occurs at the transition stage of a newborn. Transition stage is a critical stage for newborns to survive. Bathing with improper techniques can cause cold and heat loss even hypothermia in newborns. The purpose of this study was to analyzed the comparison of the length time of first time bathing for normal newborns with axillary temperature and dry heat loss with seven minutes and thirteen minutes respectively. Bathing was held on the six hours postbirth. This study was a quasi-experimental study with a pre and post test group design. Data were analyzed using Mann-Whitney test, and p value <0.05 was considered statistically significant. Sample size were two groups with 24 newborns each. This research showed that the average of axillary temperature of newborn in intervention group A (IGA, 7 Min) was higher than in intervention group B (IGB, 13 Min), and statistically with Mann-whitney test significant with p value < 0.05. The average of dry heat loss (conductive, convective and radiative heat loss) was higher in intervention group A (IGA, 7 Min) than in intervention group B (IGB, 13 Min) but statistically with Mann-whitney test not significant with p value > 0.05.

Keywords: Bathing, Newborn, Temperature, Dry Heat Loss

1. Introduction

Bathing a newborn for the first time with improper length of bath time and techniques can cause cold and heat loss to the newborn, even hypothermia. For this reason, based on WHO recommendations, bathing should be delayed for 24 hours after the newborn is born, or 48 hours for better and effective preserving of the body temperature, and if it is not possible due to cultural reasons or customs in an area, bathing should be delayed until 6 hours after the baby is born, with the condition that the baby's body temperature is normal around 36.5^0C -37.5^0C. Appropriate clothing to maintain temperature stability in newborns is also recommended, which is 1-2 layers more than adults and wearing a hat. But the literature about the length time of first time bathing newborns is rather limite (OLCHC, 2015; WHO, 2017; Chamberlain *et al.*, 2019; Duygu *et al.*, 2019; Susan *et al.*, 2019).

Hypothermia tends to occur during the transition period in newborns. Adaptation to extra-uterine life is a very critical period for the baby in an effort to survive, newborn babies must adapt the sudden change in thermal homeostatis to life outside the uterus whose temperature is much cooler when compared to temperatures in the mother's womb that are relatively warmer around 37^0C. With a normal room temperature of 25^0C – 27^0C means there is a decrease of around 10^0C. Maintenance of thermal homeostasis is crucial for the success of postnatal transition, even for the aterm and healthy newborn baby. Thus, the control of the core and the surface body temperature needs to be managed carefully to prevent heat loss (WHO, 2013; Morton *et al.*, 2016; Perlman and Kjaer, 2016; Lubkowska *et al.*, 2019).

Newborn lose heat four times more than adults, which results in a decrease in temperature. Newborns can have a temperature drop of 3-4^0C in the first 30 minutes of labor. And their skin temperature will drop by about 0.3^0C if placed in a room with a temperature of 20-25^0C. The decrease in temperature is caused by heat loss (conduction, convection, evaporation and radiation). Loss of heat by conduction, convection and radiation is also called dry heat loss, whereas heat loss by evaporation is also called wet heat loss. With the infant's immature thermoregulation ability to produce heat, the baby is very susceptible to the experience of hypothermia (Kliegman, 2012; Namnabati *et al.*, 2017; Khaled and Mohammed, 2019).

Therefore, essential care is needed in newborns to prevent complications and can save the lives of babies such as drying the newborn's body immediately, breastfeeding and delaying bathing the baby for 6 hours after delivery or after the body temperature of the newborn is normal 36.5^0C-37.5^0C (Bergstrom *et al.*, 2000; Heinig, 2001; Moore *et al.*, 2012; Farhana *et al.*, 2013; WHO, 2013; Lund, 2016).

Association of Women's Health, Obstetrics and Neonatal Nurses recommends delaying bathing the baby for up to 8 hours of labor because the body temperature of the newborn is stable after 2-4 hours of labor. Delaying bathing the newborn when the body temperature is stable will help the baby go through the transition period, reducing the incidence of hypoglycemia and hypothermia (AWHONN, 2015).

* Corresponding author e-mail: rutandsteven@gmail.com..

This contradicts the results of research that bathing a newborn in one hour postbirth will maintain newborn body temperature if the newborn has a normal body temperature (Karen and Rita, 2000; Lund, 2014).

World Health Organization recommends bathing babies with a water temperature of 38^0C but Puspita in her study obtained a safe bath water temperature for bathing a baby 6 hours of labor was 35^0C. She also got the result that bathing a newborn was better done in the afternoon than in the morning (Puspita *et al.*, 2007).

The data above shows that the implementation of bathing a newborn still needs more research to obtain better benefits, so that it can prevent hypothermia and improve the health of newborns, because of the greatly benefits of bathing when done properly.

Previous studies found that after bathing newborns for 7.6 minutes length, at one hour, two hours and 4 hours of labor, there was no difference in axillary temperature on 10, 20, 60 minutes each. But it has not been seen how much heat loss is in newborns after being bathed (Karen and Rita, 2000).

Because the pilot study revealed no significant difference in postbath temperatures between newborns bathed at one hour and two hours of age with the same length time of bath, the purpose of the current study was to see if the length time of bathing could be done even longer to see the difference change of axillary temperature and the dry heat loss of the newborn after bathed at 24 hours of birth. It was hypothesized that there would be a significant difference in postbath temperatures between newborns length time of bath at 7 minutes and 13 minutes; the purpose of the current study was to see if the length time of bath could be done even longer at the transition period in newborns.

Therefore, this study aimed to analyze the comparison of newborns bath length of time to axillary temperature and dry heat loss.

2. Materials and Methods

The Health Research Ethics Committee of Polytechnic Health Ministry of Health Medan Indonesia approved the current study (approval number 367/KEPK POLTEKKES KEMENKES MEDAN/2019). The objectives and methodologies were explained to all participants, and verbal consent had been taken. The research was conducted for six months. The population in this study were all newborns in Padangsidimpuan City Hospital. Sample was all populations that meet the inclusion and exclusion criteria. The sample chosen for the study was newborn who fullfilled inclusion criteria; normal newborn, six hours postbirth, normal body temperature of 36.5°C – 37.5°C. Exclusion criteria were hyperthermia and congenital abormalities; there was meconium in the amniotic fluid with head presentation.

This research was a quasi-experiment study with a pre and post control group design, and the aim was to analyze the comparison of the length of bathing time for newborns with body temperature and heat loss. The length time of bathing was seven minutes in intervention group A (IGA) and 13 minutes in intervention group B (IBG) respectively. The length of bath time is calculated starting from preparing toiletries then bathing the baby and finally wearing clothes. The design approach in this study can be described as follows:

01 ⟶ (A) ⟶ 02
03 ⟶ (B) ⟶ 04

01 IGA before bathing ; **02** IGA after bathing
03 IGB before bathing; **04** IGB after bathing
(A) Intervention group A bathing in 7 minutes; **(B)** Intervention group B bathing in 13 minutes

Operational Definitions of Independent Variables and Dependent Variables:

a) Newborn Bathing

Defenition : Bathing newborn at six hours after birth.

How to measure : Bathing newborns in 7 minutes and 13 minutes respectively.

Measuring instrument : Newborn Bathing Guideline from Module of Text Book Practice of Midwifery Care of Neonates, Babies, Toddler and Children, Indonesian Health Ministry 2016.

Measuring results : If the bath duration is 7 minutes then it is given a value of 1, and if the bath duration is 13 minutes then it is given a value of 0.

Measuring scale : nominal

b) Temperature

Defenition : Newborn Axilla temperature

How to measure : measuring axilla temperature before and after bathed

Measuring instrumen : digital thermometer

Measure results : temperature in ^{0}C

Measuring scale : interval

c) Dry Heat Loss

Defenition : Dry heat loss in newborn (convective, radiative and conductive heat loss).

How to measure : using equation (Gabriel, 1996; Celcar, 2013)

Measuring Scale : Equality (Gabriel, 1996, Celcar, 2013)

1) Convective Heat Loss:

$Jq_{convective} = 8{,}3\ V^{0,5}(T_s - T_a)$

$Jq_{convective}$ = convective heat loss between newborn skin and environment (J)

V = air flow velocity (m/s)

8,3 = a constant where a person stands facing the blowing air

Ts = skin temperature (^{0}C)

Equation Mean skin temperature:

$0{,}07T_{Forehead} + 0{,}175T_{Trunk} + 0{,}175T_{Chest} + 0{,}07\ T_{Arm} + 0{,}07\ T_{Shoulder} + 0{,}05T_{Hand} + 0{,}2T_{Calf} + 0{,}19T_{thigh}$

Ta = air temperature (^{0}C)

2) Radiative Heat Loss :

$Jq_{radiative} = e\sigma Ar\ (T_s^4 - T_w^4)$

$Jq_{radiative}$ = radiative heat loss (J)

Ar = the efective surface area of the body that releases radiation (Du bois) which is $W^{0.5378}$ x $L^{0.3964}$ x 0.024265 (weight in kg (W) , and length in cm (L). (Haycock, 1978)

ϵ = skin surface emissivity, 0,99 (Alexandra, 2000)

σ = Stefan – Boltzmann constant ($5{,}67 \times 10^{-8} W/m^2K^4$)

Ts = skin temperature in absolute degree (K)

Tw = wall temperature in absolute degree (K)

3) Conductive Heat Loss

$$Jq_{conductive} = \frac{ks\ ka}{ks+ka}\ \frac{(T_2-T_1)}{\Delta X}$$

. Jq $c_{onductive}$ = conductive heat loss (J) ; ks = skin conductivity coefficient (0,2 J/sm^{0}C); Ka = air conductivity coefficient (0,023 J/sm^{0}C); $T_2 - T_1$ = different temperature between air and skin (^{0}C); ∧x = the distance between air and skin

4) Total Dry Heat Loss

$$J_{total} = J_{q\ convective} + J_{q\ konduksi} + J_{q\ radiasi}$$

Measuring Instrument: Digital Infra red Thermometer, anemometer, nomogram duBois, body length measuring board, baby weight scales.

Measuring Result: Total Dry Heat Loss in J (joule).

Measuring Scale : Interval.

a. Normal newborn is newborn with 2500 – 4000 gr, body length of 44 – 53 cm, gestation 37 – 42 weeks, APGAR Score 7-10.

The number of samples taken must be the same between the two groups so that the results of the study are more significant.

The sample Equations used was Sastroasmoro formula (Sastroasmoro, 2011):

$$n_1 = n_2 = 2\left[\frac{(z\alpha + z\beta)S}{x_1 - x_2}\right] \quad 2$$

zα = 1,96 ; zβ = 1,282 ; S = Standar deviation of the two groups 1,1^{0}C ;X_1-X_2 = Clinical differences = 1^{0}C

$$n_1 = n_2 = 2\ \frac{[(1,96+1,282)1,1]^2}{1}$$

$n_1 = n_2 = 24$.

a) Measurements taken in both groups of newborns were heart rate, axillary temperature, skin temperature, air temperature, wall temperature and wind speed before and after bathing. Measurements of weight and body length were also taken.
b) Room temperature set arround 27°C - 30°C.
c) Water temperature from 37°C - 38,5°C.
d) Time of bathing about 03.00 pm.
e) Both of groups will be given clothes with the same material which is 1 layer of cloth and 1 hat.
f) After bathing, babies were immediately measured for skin and body temperature (axillary temperature) and immediately breastfed to avoid cold.
g) The health workers who bathe the baby are two midwives who have been given counseling about hypothermia. The first midwife bathed the newborns in the intervention group A (IGA) while the second midwife bathed the newborns in the intervention group B (IGB).
h) Then the differences between the pre-test and post-test in each intervention group were examined and the differences were analyzed

Data were analyzed by Mann-Whitney test to compare pre-test and post test data.

3. Results

The study was conducted in the city of Padangsidimpuan from March 2019 to October 2019. After observing, 48 newborns were found who met the inclusion criteria. 24 newborns will be bathed for seven minutes and will be called the Intervention A (IGA) group and 24 newborns will be bathed for 13 minutes and will be called the intervention group B (IGB). The average room temperature was 30.3 (° C), water temperature was 38.3 (° C) and air flow velocity in the room was 0.1m / s.

The results of this study can be seen in the following table.

Table 1: Characteristics of Respondents.

Characteristics of Respondents	Intervention Group A Mean ± SD	Intervention Group B Mean ± SD	Sig
Body Weight (BW) Kg	3216 ± 286	3100 ± 408	*p>0.05*
Body Surface Area (BSA)	0.21 ± 0.01	0.20 ± 0.01	*p>0.05*
Axillary Temperatur (AT) (^{0}C)	36.98 ± 0.42	36.99 ± 0.36	*p>0.05*
Skin Temperature (ST) (^{0}C)	36.72 ± 0.44	36.72 ± 0.51	*p>0.05*

Source : Primary data, 2019.

Table 1 showed the characteristics of respondents. Based on its characteristics, the mean respondent's body weight of respondents was 3216 ± 286 gr for IGA and 3100 ± 408 for IGB. The mean respondent's body surface area (BSA) was 0.21 ± 0.01 for IGA and 0.20 ± 0.01 for IGB. The mean respondent's systolic was 147,7 ± 9,0 mmHg for intervention group and 153,3 ± 10,1 mmHg for the control group. The mean respondent's axillary temperature was 36.98 ± 0.42 ^{0}C for IGA and 36.99 ± 0.36 ^{0}C for IGB. The mean respondent's skin temperature was 36.72± 0.44 ^{0}C for IGA and 37.72± 0.51 ^{0}C for IGB. Statistically with the Mann-Whitney technique, there was no significant difference between the two groups with a value of p> 0.05.

Table 2: The Comparison Between the Length Time of bathing on Average ± SD to Axillary Temperature in Newborn, Difference in Axillary Temperature in Newborn after The Bathing, Dry heat Loss of Newborn and Skin Temperature of Newborn

Axillary Temperature			
	Mean ± SD (^{0}C) Before The Bath	Mean ± SD (^{0}C) after the bath	Sig
IGA (7 Min)	36.98 ± 0.42	36.32 ± 0.49	0.001
IGB (13 Min)	36.99 ± 0.36	36.04 ± 0.39	
Difference in Axillary Temperature in Newborn after The Bathing			
	Mean ± SD (0C) After The Bath	Sig	
IGA (7 Min)	0.66 ± 0.30	0.001	
IGB (13 Min)	0.95 ± 0.31		
Dry Heat Loss in Newborn.			
	Mean ± SD (J) Dry Heat Loss	Sig	
Conductive Heat Loss	11.14 ± 2.48	0.54	
IGA (7 Min)	10.85 ±		
IGB (13 Min)	1.99		
Convective Heat Loss	14.36 ± 3.20	0.54	
IGA (7 Min)	14.00 ± 2.56		
IGB (13 Min)			
Radiative Heat Loss	7.26 ± 1.50	0.65	
IGA (7 Min)	7.17 ± 1.14		
IBG (13 Min)			
Skin Temperature in Newborn			
	Mean ± SD (^{0}C) After The Bath	Sig	
IGA (7 Min)	36.01 ± 0.39	0.001	
IGB (13 Min)	35.87 ± 0.36		

Table 2 showed that the mean axillary temperature after being bathed for seven minutes in IGA decreased by 0.66

± 0.30. Statistically with the Wilcoxon test, there were significant differences with p value <0.05.

The mean axillary temperature after bathing for 13 minutes in the IGB decreased by 0.95 ± 0.31. Statistically with the Wilcoxon test there are significant differences with p value <0.05.

Table 2 also showed the mean difference in axillary temperature after being bathed 7 minutes in the IGA lower than in the IGB which was bathed for 13 minutes. The mean difference in axillary temperature in the IGA was 0.66 ± 0.40, and the average axillary temperature in the IGB was 0.95 ± 0.31. Statistically with the Mann-Whitney test, there were significant differences with p value 0.001 (<0.05).

Table 2 also showed that the mean convective heat loss after being bathed for 7 minutes in the IGA was higher than in the IGB which was bathed for 13 minutes. The mean convective heat loss in the IGA was 14.36 ± 3.20, and the mean convective heat loss in the IGB was 14.00 ± 2.56. Statistically with the Mann-Whitney technique, there was no significant difference with p value> 0.05.

The mean radiative heat loss after being bathed for 7 minutes in the IGA was higher than in the IGB which was bathed for 13 minutes. The mean radiative heat loss in the IGA was 7.26 ± 1.50, and the mean radiative heat loss in the IGB was 7.17 ± 1.14. Statistically with the Mann-Whitney technique, there was no significant difference with p value> 0.05

Table 2 also showed that the mean skin temperature of newborns in the IGA after bathing for seven minutes is 36.01 ± 0.39 ℃; the mean temperature of newborn skin in the IGB after being bathed for 13 minutes was 35.87 ± 0.36 ℃ . Statistically, there was no significant difference between Mann Whitney with p value> 0.05.

4. Discussion

This study compared the axillary temperature and dry heat loss of newborns bathed in seven minutes and 13 minutes respectively for the first time. The findings showed significant statistical difference between both bathing length time in axillary temperature. The maximum variation in the pre- and postbath temperature averages were -0.6 and -0.9℃ respectively, in the IGA and IGB, indicating that the length of time for the first bath had a significant effect on the decrease in axillary temperature of newborns, but all of them experienced mild hypothermia. This might be due to the direct exposure of a newborn baby to a cold environment such as being put into warm water naked. For that, proper care is recommended after bathing a newborn baby, such as immediately wearing clothes and hats, and immediately handing over to the mother for immediate breastfeeding. On this study, almost all newborns in both intervention groups experienced axillary temperature recovery to be normal again after 15 minutes of breastfeeding by mother.

This study was in line with research that examined the comparison of conventional methods of bathing premature babies with the method of wrapping a baby in a bath or swaddled immersion bath which got the results of both treatment groups experienced a decrease in axillary temperature of the newborn; this study also got results that the axillary temperature of the newborn remains below normal or hypothermia after 20 minutes the baby is bathed. The temperature of new infants is in the range of 36.0 - 36.5°C or mild hypothermia (Alexandra *et al.*, 2000; Freitas *et al.*, 2018).

Gozen (2019) also found that there was significant difference in body temperature in newborns who were bathed at 48 hours. He also found that after 24 hours of delivery, there was a decrease in axillary temperature after bathing on the first day of the newborn, and recommended delaying bathing for up to 48 hours of labor (Gozen *et al.*, 2019).

In line with Gozen's research (2019), it was also found that axillary temperature decreased after bathing on the first day of the baby. The same was obtained by experimental studies in Iran that compared axillary temperature in 50 premature newborns with the usual bathing method and the bathing method by being wrapped. The mean axillary temperature after 10 minutes of bathing with the wrapped method was higher than that of the baby group bathed by the conventional or conventional method (36.42 ° C versus 35.96 ° C). The mean axillary temperature reduction was 0.59 ° C in the wrapped method and 0.08 ° C in infants bathed by conventional methods, whereas in this study the mean decrease in axillary temperature in the IGA bathed for seven minutes was 0.66 ± 0.30 ° C lower when compared to the mean decrease in axillary body temperature in the IGB which was bathed for 13 minutes which was 0.95 ± 0.31 ° C (Edraki *et al.*, 2014).

Clasen found no difference in axillary temperature of newborns who were bathed for 2 hours, 6 hours, 9 hours after delivery, and all newborns who were bathed at these three times experienced a decrease in axillary temperature (Clasen and Kellie, 2019).

Decreased axillary temperature in newborns after bathing can be related to the removal of vernix caseosa. The function of vernix caseosa, which prevents heat loss, no longer functions and a decrease in axillary temperature becomes unavoidable (Jhonson and Taylor, 2005; Thilo and Rossenberg, 2011; Sukesi *et al.*, 2016; Turney *et al*, 2019).

According to this study, it states that newborns who bathed after six hours of labor had an axillary temperature in the mild hypothermia range after a 7 - 13 minutes bath. Therefore, it is recommended that the newborns bathe for less than 7-13 minutes.

Efforts to maintain a constant body temperature are very important in newborns with low thermoregulatory abilities. The use of energy by newborns to produce heat comes from thermoregulation without shivering, one of three adults' ability to produce heat through metabolism, shivering thermoregulation and non-shivering thermoregulation. The heat source of thermoregulation without chills in newborns comes from brown fat tissue that is stored from the age of 26-28 weeks of pregnancy and contributes to 10% of newborn body weight. Brown fat tissue is filled with blood vessels and is located mostly in the shoulder area, armpits, around the waist and adrenal glands. If the baby experiences a cold which will increase the increase in the work of the hormone nor adrenaline which will stimulate the breakdown of brown fat tissue to produce heat, unfortunately this brown fat tissue can no longer form. Body surface area is also one of the causes of babies experiencing heat loss, lack of muscle movement and also the ability to regulate blood flow through the skin.

The lack of optimal circulation and respiratory system development is also a factor in the lack of thermoregulation in newborns. This ability will only develop in the first week of infancy (McHugh, 2008; Fraser and Cooper, 2009; WNHS, 2018; Lubkowska *et al.*, 2019).

Newborns have not been able to maintain their own body temperature without protection from the outside, especially when placed in a cold environment that can reduce the core temperature around 0.2 - 1.0°C per minute and can eventually result in death. World Health Oorganization recommends maintaining body temperature as a main principle when providing care for newborns (WHO, 2012).

Some research results showed that after 15 minutes of birth the skin temperature of the newborn will drop to 4°C, after the first hour of birth the skin temperature can drop to around 33 ° C if placed in a room with a temperature of around 25 ° C. After 15 minutes, the skin temperature can decrease around 2.5 - 3 ° C, and in the first 15 minutes this attempt to produce heat by shivering does not occur in newborns (Lubkowska *et al.*, 2019).

In this study, the average skin temperature of participants before bathing in the IGA was 36.72 ± 0.44 °C and after bathing the skin temperature decreased by an average of 36.01 ± 0.29 ° C while the mean temperature of newborns before bathing in the IGB was 36.72 ± 0.51 ° C and after the bath also decreased by an average of 35.87 ± 0.36 ° C. After bathing for seven minutes there was a decrease in the average skin temperature of around 0.71 ° C in the IGA, whereas in the IGB, there was a decrease in the average skin temperature of 0.9 ° C after bathing for 13 minutes. However, this wasn't statistically significant. If the body temperature changes to 10^{o}C, there will be a change of 10% from the metabolic rate and oxygen consumption. So by measuring the oxygen consumed by the body, we can estimate the energy or heat produced. If the IGA experienced a decrease in skin temperature after being bathed at around 0.71 ° C, there would be a change of 7% from the metabolic rate and oxygen consumption. While in the IGB the skin temperature after being bathed was around 0.9 ° C, therefore there will be a change of 9% of the metabolic rate and oxygen consumption. This certainly will aggravate the work of newborn metabolism and increase the need for oxygen consumption. If the decrease in body temperature continues without any effort to help prevent heat loss it will have an adverse effect on newborns. They'll have to depend on unrenewable brown adipose tissue to increase metabolism which will generate heat (Karlsson, 1996; Sherwood, 2012; Girsjesh and Shefali, 2019).

Heat loss in newborns can occur by conduction, convection, radiation called dry heat loss, and evaporation called wet heat loss. In the IGA and IGB groups, there was little difference in dry heat loss. However, IGA showed more signs of heat loss through conducting, convection, and radiation. There was also difference in skin temperature and axillary temperature, IGA showed lower decrease of skin temperature and axillary temperature. This situation may be influenced by several factors such as gender or maternal factors. These factors were not examined in this study, and are a weakness of this study; it is hoped that in the future further research will be conducted that will pay attention to the sex factors of newborns and maternal factors.

After being bathed, clothes and hats were immediately attached and newborns immediately given to mothers for breastfeeding for 15 minutes in both of intervention group in this study. Axillary temperature and skin temperature return to normal after that. Therefore, it was recommended that newborns be breastfed for 15 minutes after bathing.

5. Conclusion

The results indicate that bathing in 7 minutes or 13 minutes significantly differ regarding their effect on axilla temperature and skin temperature of healthy newborns for the first time. Dry heat loss was higher in newborns when bathing in 7 minutes compared to 13 minutes but not statistically significant. However, future studies addressing the suitable length time of bathing newborns are necessary, as well as studies investigating more indicators of the length time of bathing newborns such as the gender factor, the types of labour, and physiological indicators of stability.

Acknowledgment

The authors are grateful to all participants who contributed this study and to Poltekkes Kemenkes Medan who funded this study.

Funding

This study was funded by Poltekkes Kemenkes Medan.

References

Alexandra AK, Nelson RA, Bell ER and Cesar AE. 2000. Use of infrared thermographic calorimetry to determine energy expenditure in preterm infants. Am J Clin Nutr., **71**:969. http//ajcn.nutrition.org.

AWHONN (Association of Women's Health, Obstetrics and Neonatal Nurses). 2015. Improving Newborn Clinical Outcomes With Delayed Bathing. AWHON.

Bergstrom A, Okong P and Arvdson RAB. 2007. Immediate maternal thermal respons to skin to skin care of newborn. Acta Paediatr., **96(5)**:655-8.

Chamberlain J, McCarty S, Sorce J, Lesman B, Schmidt S and Meyrick E., at al. 2019. Impact on delayed newborn bathing on exclusive breastfeeding rates, glucose and temperature stability, and weight loss. J Neonatal Nurs, **25(2)**:74-77. https://doi.org/10.1016/j.jnn.2018.11.001.

Classen and Kellie. Effect of timing of the first bath on a healthy newborn's temperature**.** J Obstetric Gynecologic Neonatal Nurs, **48(3):** S148 - S149.

Duygu G, Sinem YC, Selda AB and Yildiz P. 2019. First bathing time of newborn infants after birth: A comparative analysis. J Specialists Pediatric Nurs, **24(2)**. https://doi.org/10.1111/jspn.12239.

Edraki M, Paran M, Montaseri S, Razavi Nejad M and Montaseri Z. 2014. Comparing the effects of swaddled and conventional bathing methods on body temperature and crying duration in premature infants: a randomized clinical trial. J Caring Sci. **13(2)**:83-91.

Elabbassi EB, Bach V, Makki M, Delanaud S, Telliez F, Leke A, et al. 2001. Assessment of dryheat exchanges in newborns: influence of body position andclothing in SIDS. J Appl Physiol.

Farhana SD, Khondoker MH, Azim MA and Moinul H. 2013. Isolation, characterization and determination of antimicrobial properties of lactic acid bacteria from human milk. Jordan J Biol Sci, **6(2):** 111- 116.

Fraser DM and Cooper MA. 2009. **Text Book Midwifery Myles**. Ed 14. Jakarta: EGC.

Freitas P, Munhoz MMB, Costa P and Kimura AF. 2018. Effect of two immersion bathing techniques on the axillary temperature of preterm newborns: a pilot study. Texto Contexto Enferm, 2018; **27(1)**: e0580016.

Gözen D, **Çaka SY**, **Beşirik SA** and **Perk, Y**. 2019. First bathing time of newborn infants after birth: A comparative analysis. *J Spec Pediatr Nurs*. **24**:12239. https://doi.org/10.1111/jspn.12239.

Haycock GB, Schwartz GJ and Wisotsky DH. 1978. Geometric method for measuring body surface area: A height-weight formula validated in infants, children, and adults. J Pediatr, **93**:62-6.

Heinig MJ. 2001. Host defense benefit of breatfeeding for the infant, effect of breastfeeding duration and exclusivity. Pediatr Clin North Am, **48**:105-123.

Johnson R and Taylor W. 2005. **Buku Ajar Praktik Kebidanan**. Editor bahasa Indonesia: Kurnianingsih S, Ester M. Jakarta; EGC, Hal.29-45.

Khaled MS and Mohammad BAZ. 2019. Thermal manipulation during broiler chicken embryogenesis modulates the splenic cytokines' mrna expression. Jordan J Biol Sci., **12(5):** 595 – 601.

Karen EV and Rita SB. 2000. The effect of timing of initial bath on newborn's temperature. J Obstetric Gynecologic Neonatatal Nurs., **29(1):** 27-32. AWHONN. DOI: https://doi.org/10.1111/j.1552-6909.2000.tb02753.x.

Karlsson H. 1996. Skin to skin care: heat balance. Sweden: Archives if disease in childhood, **75(1)**: F130-F132.

Kliegman RM. 2012. Janin dan bayi neonatus. In: Wahab AS (Ed). **Ilmu Kesehatan Anak Nelson**. EGC, Jakarta, pp. 535-541.

Girjesh K and Shefali S. 2019. Effect of Temperature Constraints on Morphological and Cytogenetical Attributes in Cluster bean [Cyamopsis tetragonoloba (L.) Taub.]. Jordan J Biol Sci., **12(2):** 229 – 235.

Lubkowska A, Szymański S, Chudecka M. 2019. Surface body temperature of full-term healthy newborns immediately after birth—Pilot Study. Int J Env Res Pub Health, **16(1)**:1312. Available from: http://dx.doi.org/10.3390/ijerph16081312.

Lund C. 2014. Bathing and beyond; new data to guide newborn skin care. UOSF.

Lund, C. 2016. Bathing and beyond, advances in neonatal care.,**16(1)** : S13-S20, doi: 10.1097/ANC.0000000000000336.

McHugh MK. 2008. Transisi fisiologis ke kehidupan ekstrauteri. In: Varney H, Kriebs JM and Gegor CL (Eds). **Buku Ajar Asuhan Kebidanan**. Ed 4. EGC, Jakarta, pp.878-888.

Morton, Sarah U and Dara Brodsky. 2016. Fetal physiology and the transition to extrauterine life. *Clinics in Perinatology*., **43(3):** 395-407. doi:10.1016/j.clp.2016.04.001

Moore ER, Anderson GC, Bergman N and Dowswell T. 2012. Early skin-to-skin contact for mothers and their healthy newborn infants (Review). The Cochrane Library., **1(5)**. Diunduh dari: http:// www. thecochranelibrary.com.

Namnabati M, Zamanzadeh V, Valizadeh L, Tazakori Z and Nyqvist KH. 2017. Theory of infants' transition management from the neonatal intensive care unit to home: a qualitative study. Int J Pediatr, **5(1):**4151-62. DOI:10.22038/ijp.2016.7887.

OLCHC. 2015. Guideline of bathing an infant. OLCHC.

Perlman J and Kjaer K. 2016. Neonatal and maternal temperature regulation during and after delivery. Journals.lww.com/anesthesia-analgesia, **123(1):**168–72. DOI: 10.1213/ANE.0000000000001256.

Puspita IR, Suradi R and Munasir Z. 2007. Insidens dan faktor risiko hipotermia akibat memandikan bayi baru lahir cukup bulan. Sari Pediatri, **8(2)**.

Sastroasmoro S. 2011. **Dasar-Dasar Metodologi Penelitian Klinis**. CV Sagung seto, Jakarta, pp.31-63.

Sherwood L. 2012. **Fisiologi Manusia**, sixth ed. EGC, Jakarta.

Sukesi A, Setiyani A and Esyuananik. 2016. **Modul Bahan Ajar Cetak Kebidanan; Praktikum Asuhan Kebidanan Neonatus, Bayi Balita dan Anak Prasekolah. Kemenkes RI**.

Susan W, William KM, Leigh AAN, Phil M and Laurie T. 2019. Effects of delayed newborn bathing on breastfeeding, hypothermia, and hypoglycemia. J Obstetric Gynecologic Neonatal Nurs, **10(1):** 1016/j.jogn.

Thilo EH and Rosenberg AA. 2011. The newborn infant. In: Hay WW, Levin JM, Sondheimer JM and Deterding RR (Eds). **Current Diagnosis & Treatment**: Pediatrics. 21th ed. Lange, USA, pp.30-31.

Turney J, Lowther, Pyka J, Mollon D and Fields W. 2019. Delayed newborn first bath and exclusive breastfeeding rates. AWHONN; doi: 10.1016/j.nwh.2018.**12(3)**.

WHO. 2013. WHO Recommendation on postnatal care of the mother and newborn. WHO.

WHO. 2017. WHO Recommendation on newborn health: guidelines approve by The WHO guidelines review committee. Geneva: World Health Organization; (WHO/MCA/17.07). License: CC-BY-NC-SA 3.0 IGO.

WNHS. 2018. NEO thermoregulation. Clinical practice guideline

JJBS

Volume 14, Number 5,December 2021
ISSN 1995-6673
Pages 975 – 981

Jordan Journal of Biological Sciences

Identification of Consumers' Motives in Buying Organic Luwak Coffee in terms of Agri-Touirism

Yosini Deliana[1,*], Lucyana Trimo[1], Sri Fatimah[1], Mai Fernando N[1] and Mohamad Djali[2]

[1]*Department of Agricultural Social Economics, Faculty of Agriculture, Padjadjaran University, Jatinango- 45363 Indonesia;* [2] *Department of Food Industry Technogy- , Padjadjaran University, Jatinangor 45363 Indonesia*

Received: February 27, 2021; Revised: June 10, 2021; Accepted: October 16, 2021

Abstract.

Cikole luwak (civet) coffee began to be produced in 1990 and is now well-known in about 45 countries. Unfortunately, it is suspected that the civet coffee sold in bulk and retail is just ordinary or plain coffee. The motivation to buy for consumers, the level of consumer interest in civet coffee agrotourism, marketing strategies for loyal consumers to consume civet coffee are the objectives of this study. Questionnaire interviews involving 186 respondents (by means of systematic random sampling) were used as data collection methods in this study. Furthermore, the recorded data were analyzed by Confirmatory Factor Analysis. **The results show that the primary factors of Luwak coffee, such as freshness, taste, and aroma, can identify consumer appearance as the dominant factor. The dominant usability factors were habits, leisure; and health; while the dominant promotional factors were website availability, agrotourism, and discounts.** The Luwak coffee marketing strategy must be holistic and synergize between government, companies, communities, academics and media.

Keywords: Consumer's motive, luwak coffee, external and internal factors , agrotourism, and confirmatory factor analysis

1. Introduction

One of the countries that produce the largest coffee in the world is Indonesia which ranks fourth (World Bank, 2015). There are several provinces in Indonesia that produce coffee, one of which is West Java province and Bandung Regency is the largest coffee production center, contributing 70% of West Java's total coffee production (Coffee Production by Province in Indonesia, 2017-2021). Thus, to maintain coffee production, it is necessary to develop the sustainability of coffee farming which is pioneered by young farmers (Nainggolan, *et al*., 2020). Cikole Village, Lembang sub-district, was chosen as research area because it has a uniqueness in the market of civet coffee. The uniqueness of this agro-tourism is that visitors can see the whole process from civet coffee cultivation, maintenance, harvest, post-harvest, processing, to marketing. In addition, visitors can also see the behavior of ferrets (Paradoxurus hermaphrodites) when choosing ripe coffee cherries. In addition, the location is also supported by beautiful views so that visitors can relax while drinking civet coffee.

Due to the high price of civet coffee, it is categorized as a luxury product or more specifically the specialty coffee category, although not all luxury products are expensive (depending on the perception of each consumer). According to Wiedmann et al. (2009), the four values of luxury are financial (i.e. price), functional (i.e. usability), individual (i.e. materialism) and social such as conspicuous consumption. A brand is created by adding a core product with distinctive value that distinguishes it from other products (Jobber and Fiona, 2019). Meanwhile, Heine (2021) explains that product appearance, promotion and usability are often considered characteristics of luxury brands. Luwak coffee is one of the luxury coffee products because it has many differences with other coffees including the price which is quite expensive. Consumers tend to feel prestigious every time they consume them, so they are often used as gifts for family, friends or business associates. Those who give and receive civet coffee will get their own satisfaction that cannot be valued in money so that it becomes part of the respect. On the other hand, coffee contains an antioxidant compounds**, that showed antibacterial and antibiofilm activities against *P. aeruginosa* and *S. Pyogenes* (Al Kafaween *et al.,* 2020). The crude methanol extract of *A. paniculata* leaf and its fractions demonstrated considerable antimicrobial and antioxidant properties (Banji *et al.,* 2018). This is the reason why Luwak Coffee has become a specialty coffee.**

Consumers who use luxury products or brands can convey certain social and cultural meanings (Becker et al., 2018). Personal and social relationships in society can be described by certain brands and positions. Promotion is one of the determining factors in the success of a marketing program. A product that consumers have never or rarely heard of and believe to be useless will never be purchased by consumers. One form of marketing communication carried out by a company is promotion.

* Corresponding author e-mail: y.deliana@gmail.com.

The activities carried out include disseminating information, influencing and being willing to persuade consumers; the target market must always be reminded to be willing to accept, buy, and be loyal to the products offered (Yuliawati et al, 2917). A consumer will usually buy a product based on the appearance, promotion and usability of the product itself. After determining consumer motives, producers will more easily understand consumers and find strategies to improve product quality and expand markets. There is a tendency for consumers to buy Luwak coffee because of taste, unique aroma, good facilities, unique packaging, low price, habit, leisure, and health. The purpose of this study was to determine consumer motivation in buying civet coffee, consumer interest in civet coffee agrotourism, and the marketing strategy that must be chosen. One of the novelties in this research is to identify consumer motives related to luxury products and agro-tourism using factor analysis.

Research that discusses consumer motivation in buying civet coffee is still rarely found (because civet coffee only exists in Indonesia). So far, the research that has been done has only been limited to discussing the efficiency of the civet coffee business (Niken et al, 2018) and the potential and development strategies of civet coffee (Bayunitri, 2017; Pranoto and Rajamin, 2012; Ribek and Rihayana, 2019; Satim and Puput, 2020).

2. Method

2.1. Data

The primary data recording process was carried out in a cross section through observation and questionnaire instruments based on previous literature reviews. Secondary data were obtained from the Central Bureau of Statistics, Ministry of Agriculture and related agencies. The primary survey was conducted from April – June2020 in Lembang -West Java Province- Indonesia.

2.2. Sampling

Lembang was chosen as the research location because it is famous for its civet coffee agrotourism. Systematic random sampling technique was used to collect customer data, by taking 200 samples from a population averaging one thousand consumers per month. The sample was taken from 5 percent of the population, and only 186 were matched with the research variables. Respondents are visitors who come to Luwak coffee for recreation, local tourists and foreign tourists for agro-tourism purposes. The research framework is as follows:

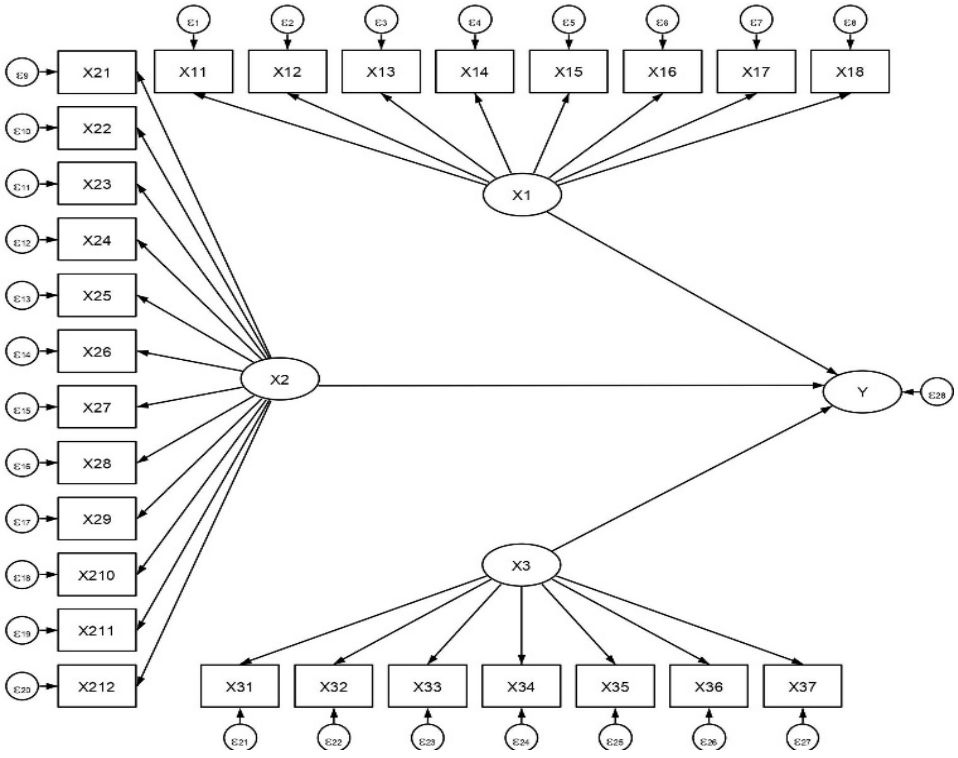

Figure 1. Research Framework

Note: Endogenous Latent Variable

Y= Consumer motivation Exogenous Latent Variables

X_1= Appearance ; X_2= Promotion; X_3= Usability

γi= Path coefficient for *i*th exogenous latent variables to endogenous latent variable (*i*=1,2,3); λi = Standardized Loading Factors for *j*th *k*th manifest variables/indicators (*i*=1,2,…;*j*=1,2,3; *k*=1,2,…) ; εi= Error term for for *j*th *k*th manifest variables/indicators (*i*=1,2,…;*j*=1,2,3; *k*=1,2,…)

2.3. Measurement

There are three factors that influence a brand to be luxurious, including appearance, promotion and product usability. The following table shows the value of the standard loading factor and measurement error for the measurement model on a variable using confirmatory

factor analysis (CFA). The validity criteria are said to be good if the load factor value of 1.96 is obtained from the t arithmetic value which is greater than t table. Respondents who came to the Luwak coffee area were asked questions by the questioners. Each respondent was given several questions and asked to fill out a form with a choice of a Likert scale, namely the answers strongly agree (5), agree (4), neutral (3) disagree (2) and strongly disagree.

3. Results

3.1. Respondent Profile

Respondents involved in this study consisted of men (54.84%) and women (45.16%). Respondents generally tend to return to buy Kopi Luwak (87.72%) and the rest do not return (12.28%) due to unsuitable taste. The survey results show that those who buy Kopi Luwak are between 20-29 years old, including the millennial generation (Deliana and Rum, 2019). This is in accordance with their work as fresh graduates at the Diploma and Postgraduate levels. What is interesting is that the income of consumers who buy civet coffee is between 5 - 10 million. This is very reasonable since the luwak coffee price is expensive.

Table 1. Respondent Characteristics

Variable	Description	(%)	Variable	Description	(%
Age (Year)	< 20	9.68	Education	High School	13
	20 - 29	82.26		Diploma	42.4
	30 - 39	4.84		Graduate	37.8
	> 40	3.23		Post Graduate	6.5
Occupation	Private sector	17.74	Income (IDR/month)	< 5 million	30.3
	Entrepreneur	27.42		5- 10	58.7
	Fresh graduate	33.87		11-15	10.4
	Others	22.57		> 15	0.5

Usually, the X-Generation (39 – 54 years) and Baby Boomer Generation (>55 years) visit the Luwak coffee place just to see the beautiful scenery and recreation. This is because those generations are generally already working, have a large income, and want to enjoy life. Meanwhile, millennials (23-38 years old), especially fresh graduates, tend to visit to enjoy the sensation of drinking Luwak coffee and edu-entertainment.

A Luwak coffee has a special characteristic, namely the natural fermentation process that distinguishes the taste/aroma from other coffees. The fermentation process becomes the selling point of Luwak coffee; besides, the volume of Luwak coffee production is not much due to the limited number of captive civets. A civet produces 600 grams/day or about 12 kg/head/month (Satim and Pupung, 2020). However, for consumers who like to drink coffee, price is not an issue but quality must be reliable (Wróblewsk et al., 2017; Wann et al., 2018).

3.2. The Consumer's Motive in Buying Luxury Brand of Luwak Coffee

Internal and external factors are indicated as consumer preferences (Y) which are depicted for identification of *luwak* coffee consumers. Appearance (X_1) and usefulness (X_3) are internal factors, while promotion (X_2) is external factor. The factors such as taste (X_{11}), aroma (X_{12}), and freshness (X_{14}) are the dominant factors of appearance. The dominant factor usability includes Habit (X_{33}), leisure (X_{34}) and Health ($X_{.35}$). The dominant factor promotion is website available (X_{25}), agrotourism (X_{26}) and discount (X_{30}).

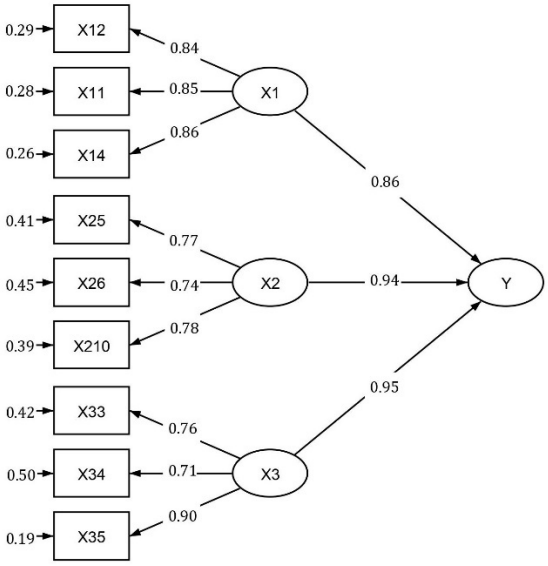

Figure 2. Dominant Factors Influence Consumer Motivation in Buying Luwak Coffee

Note: Y= Consumer motivation, X_1= Appearance, X_{11}= Taste, X_{12}= Aroma, X_{14}= Freshness, X_2=Promotion, X_{25} = Website available , X_{26}= Agrotourism , X_{210} = Discount , X_3= Usability , X_{33}= Habit , X_{34}= Leisure , X_{35}= Health

On consumer expertise and sensory skills, preference for different intrinsic qualities is dependent (Quintao *et al*, 2017). The taste, aroma, and freshness of this distinctive Luwak coffee is the main attraction for the proliferation of coffee shops. Several factors can affect the success of a coffee shop business, including taste, facilities and speed of service, and others (Humiras *et al* , 2017). If the assumption of linearity is not modeled, internal factors can be used as predictors of consumer loyalty (Deliana and Rum., 2017). Coffee users expect more satisfaction in their social experience than to pursue a taste and enjoy the service of coffee. To meet the punctuality of drinking coffee, the take-out service can meet the demands of the community, besides that there are also many social coffee drinking places that are made in several areas (Zhengyu *et al*., 2019).

Some consumers buy coffee for health reasons and concerns for the environment. Consumers have high knowledge, but buying environmentally friendly products is not necessarily good behavior (Deliana et al., 2017). This is the case between consumer subjective norms and purchase intentions, even though consumers believe the product is environmentally friendly, consumers do not necessarily buy (Phuah *et al*., 2018). Even so, prices remain a consideration for consumers in buying green products (Balathandayutham and Anandanatarajan., 2019; Hashim *et al*., 2019). **If their customers are satisfied**

and it meets their expectations, they are willing to pay more. Consumers' wants and expectations include communications, products, and marketing promotions that appeal to the heart, attract all senses, stimulate thoughts, and make it into their lifestyle (Kim *et al*., 2018; Rather, 2020).

3.3. The consumer interest in Luwak coffee agro-tourism

This research revealed that agro-tourism is one consumer motivation to buy Luwak coffee in CikoleLembang. Consumer interest in Luwak coffee was calculated by respondent (n) divided total respondent (186 person).39.78 % consumer who very interested in agrotourism, 31.11% respondents interest, 16.13% respondent ordinary, 11.29 % less interested, and 2.68% respondent not very interested. While the reason respondents visited the location of Luwak coffee in Cikole Lembang are 9 % enjoying the sensation of drinking Luwak coffee, 34% enjoy the beautiful view of the location, 28 % for leisure, 17 % buying Luwak coffee for souvenirs and 12 % for edu-entertainment to know how the initial process of ripe coffee beans eaten by the civet till the coffee ready for consumption. For the millennial generation this experience is very interesting and memorable. Thus, in general, respondents are interested in visiting Luwak coffee just to see the natural scenery there, not to enjoy the beverage which is luwak coffee. Respondents normally buy the coffee only as a gift for family and friends.

4. Discussions

From the research model, it is stated that the most influential factors on consumer motivation in purchasing luwak coffee were freshness, taste, aroma, discount, website availability, agrotourism, health, habit, and leisure. **The experience of drinking coffee involves factors that are important to create a multisensory effect. This can be used to enhance the coffee drinking experience by considering the consumer's sensory properties (Fabiana and Charles, 2019), including the freshness, taste and aroma.** Drinking coffee while looking at the beautiful scenery is a memorable experience for visitors. This is related to experiential marketing, namely sensory experience (sense), affective experience (feel), creative cognitive experience (think), physical experience, behavior and lifestyle (act), and the experience of social identity resulting from relating to a reference group, culture or relate (Etkin and Sela, 2016; Liu and Ping, 2017). Memorable place is a value created by agrorourism that makes visitors satisfied and ultimately loyal (Lewis, 2015; Lin, 2019). This experience is a novelty feeling, fun and aesthetic perception after consumers' consumption (Katherine and Peter, 2016).

The research results by Rauniyar *et al.* (2020) on coffee agrotourism is the importance of researching the use of information and communication technology. Based on the research, it was revealed that wi-fi facilities are important for visitors. Nowadays, consuming hot coffee outside the home has become a lifestyle (Kanjanakom and Lee, 2017); of course with the availability of wi-fi provided by coffee shops, it has attracted many consumers (Wu., 2017). Free Wi- Fi, low price and the attractiveness of **Luwak** coffee agrotourism become typical visitor expectations. The research also revealed that the motivation of visitors to choose **Luwak** coffee was for reasons of health, habit, leisure, eventually becoming a habit and a lifestyle. This is in line with the results of research by Susanty and Kenny (2015) and Samoggia et al (2018).

Agritourism is visiting an active agricultural holding (a farm or ranch) for leisure, recreation or even educational programs (Gil Arroyo, Barbieri, & Rozier Rich, 2013; McGehee & Kim, 2004; Tew & Barbieri, 2012). There are several issues and challenges of **agritourism**, small size of the farm lands, lack of necessary skills, poor level of product development, and poor publicity and promotion (Putra *et al* , 2019). The marketing strategy of luwak coffee must be holistic and synergize between government, companies, communities, academician and media. The undevepelopment of **Agrotourism** normally caused by the poor government and planning, (Anbalagan and Brebt, 2021). Hence the government should supervise the monopoly of tour operators, infrastructure development towards **Luwak** coffee **agritourism**, environmental pollution, provide supervision on the cleanliness and comfort of visitors. The government should also create a new-style tourism pattern different from traditional recreational activities and combining ecological conservation, environmental education, and cultural experience (Mike., 2019; Sawe., 2019).

For developing the marketing of civet coffee, a company must adapt the Starbucks marketing strategy by involving customers in all its activities (value co creation). That is, they should develop new products and product differentiation based on customers' expectations and suggestions. The step starts with the customer writing down what requests, suggestions, and complaints have been felt so far (Asli Qztopcu., 2017). The strategy that must be considered, the promise strategy, must be right on target and must be honest. In sales promotions carried out by service providers, consumers actually know this information, but are reluctant to participate. So, then, to stay afloat and compete with other brands, sales promotions must be made carefully and transparently so as to make consumers interested and have an influence on purchases. In addition, this can create a sense of trust in consumers (Eleboda., 2017).

In terms of the local community, they must be able to introduce the local culture, art and unique products that are related to coffee. The role of academics is to empower and enlighten the community in terms of increasing the added value of civet coffee. **Meanwhile, the mass media plays a role in promoting civet coffee business opportunities so that many millennial farmers become interested. Entrepreneurship in the field of agro-tourism can be developed, and this can create added value for the local community** (Stanovčić *et al*., 2018).

5. Conclusion

The results showed that the identification of luwak coffee consumers can be seen from the appearance, promotion, and usability. Freshness, taste and aroma are the main factors of appearance. Discounts, website availability and agro-tourism are the dominant factors in

promotion. Health, habits and leisure are the dominant factors for the usefulness of civet coffee products. Discounts, accessibility and agro-tourism are the dominant factors in promotion. Health, habits, and leisure are the dominant factors in the use of civet coffee products. The reason most consumers visit the luwak coffee location is just to see the surrounding natural scenery, not to enjoy the drink of luwak coffee. The luwak coffee marketing strategy must be holistic and synergize between government, companies, communities, academics and media.

Acknowledgement

We would like to thank Padjadjaran University for the research funds provided in the Academic Leadership Program 2020 with contract number 1427 / UN6.3.1/ LT / 2020. Thank you for the anonymous reviewers who provided helpful suggestions.

References

Anbalagan, K., & Lovelock, B. 2014. The potential for coffee tourism development in Rwanda–Neither black nor white. *Tour.Hosp. Res.*, **14,** 81-96

Al-kafaween Mohammad A , Abu Bakar M. Hilmi , Norzawani Jaffar, Hamid A. N. Al-Jamal, Mohd K. Zahri and Fatima I. Jibril. 2020. Antibacterial and Antibiofilm activities of Malaysian Trigona honey against Pseudomonas aeruginosa ATCC 10145 and Streptococcus pyogenes ATCC 19615. *Jordan J Biol Sci*., **13(1)**: 69 - 76

Asli Q. 2017. Evaluation of competitive strategies of coffee retailing in aspect of market economy. *Int. J. Bus. Manag.,* **5(2)**: 246- 267.

Balathandayutham P and Anandanatarajan K. 2019. Price and green attitude towards environmental friendly product in Chidambaram. *Rev. Res*., **1** :226-231

Becker Kip, Jung Wan Lee and Helena M. Nobre. 2018. The concept of luxury brands and the relationship between consumer and luxury brands. *J. Asian Finance Econ. Bus*. 51-63

Bayunitri, B. I. 2017. Customer perceptions of product Luwak Coffee based on marketing mix elements perspective (Customer Survey In Bandung). *International Conference on Organizational Innovation (ICOI 2017).* 194-198. Atlantis Press

Banji Adaramola , Benjamin Goodluck , Otuneme Oluchi and Fapohunda Stephen . 2018. Antimicrobial and Antioxidant Activities of Crude Methanol Extract and Fractions of Andrographis paniculata leaf (Family: Acanthaceae) (Burm. f.) Wall. Ex Nees. *Jordan J Biol Sci*., **11(1)** : 23 – 30.

Central Bureau of Statistics Coffee. 2018. Production by Province in Indonesia, 2017-2021

Deliana Y and Rum I A. 2017.Understanding consumer loyalty using Neural Network. *Pol. J. Manag Stud*.**16(2):**17512.

Deliana, Y and Rum I A. 2019. How does perception on green environmrnt across generations affect consumer behavior? A neural network process. *Int J Consum Stud.*, **10 (111):** 1-10.

Deliana, Y, Endah D, Engkus K and Tuhpawana P S. 2017. The perception of green marketing (A Case in Jatinnagor, West Java Province, Indonesia). *Int. J. Econ*., **14**: 201- 215.

Eleboda S S. 2017. Sales promotion as a strategy in service marketing exploring the believability dilemma and consumer purchase decision. *J. Mark. Res*., **3(2)**: 8-15.

Etkin J, Sela A. 2016. How experience variety shapes postpurchase product Evaluation. *J. Mark. Res*., **53(1)**: 77-90.

Fabiana M C and Charles S. 2019. Cup colour influences consumers expectations and experience on tasting specialty coffee. *Food Qual. Prefer*., **75**: 157–169.

Gil Arroyo, C., Barbieri, C., & Rozier Rich, S. 2013. Defining agritourism: A comparative study of stakeholders' perceptions in Missouri and North Carolina. *Tour. Manag.*, **37:**39–47.

Hashim M, Baig S A, Abrar M, Afzal A and Mohsin, M. 2019. Effects of Green Marketing on Green Purchase Intentions. *Dialogue*., **14(2)**:1819-6462.

Heine Klaus. 2012. **The Concept of Luxuary,** second ed. Emlyon Business School, France

Jobber David and Fiona Ellis Chad Wick. 2019. **The Principles and Practice of Marketing,** ninth ed. Mc. Graw Hill Education. London

Kanjanakom A and Lee J. 2017. Examining emotions and comparing the essense profile and the coffee drinking experience in coffee drinkers in the natural environment. *Food Qual. Prefer.*, **56**:69–79.

Katherine NL, Peter CV. 2016. Understanding customer experience throughout the customer journey. *J. Mark.*, **80(6)**: 69-96.

Lewis S. 2015. Qualitative inquiry and research design: Choosing among five approaches. *Health Promot. Pract.*, **16(4)**: 473-475.

Liu, Yajuan & Ping Gui. 2017. An analysis of the problems and countermeasures in the Application of Experiential Marketing - A Case Study of Starbucks. Proceedings of the seventh International Conference on Education, Management, Information and Mechanical Engineering (EMIM 2017), Hainan Tropical Ocean University, Shenyang, China.

Mbango, Phineas . 2019. The role of perceived value in promoting customer satisfaction: Antecedents and consequences**.** *Cogent Soc. Sci*., (pp. 1-16).

McGehee, N. G. 2007. An agritourism systems model: A weberian perspective. *J. Sustain. Tour.*, ***15*(2)** :111–124.

Mike T Y L . 2019. Effects of experiential marketing on experience value and customer satisfaction in ecotourism. *Ekoloji Dergisi*., **107**: 3151-3156.

Nainggolan, MF and Nugraha, A Turnip. 2020. Empowering of young farmer for Arabica Coffee Farming Business in Simalungun. IOP Conference Series: *Environ. Earth Sci.*, **466 (012034)**: 1-9.

Phuah K T, Mun W O, Sukjeet K S and Umi K K . 2018. Green attitude and purchase intention towards environmental friendly product. *Journal of Emerging Economies & Islamic Research* (JEEIR). **6 (1)**: 17–25.

Putra A, Amalia F R and Utami S W. 2019. Community based Agro-Tourism development strategy for Sumber Arum Village, Songgon, Banyuwangi. *Int. j. appl. sci. tourism events.*, **3(1)**: 68-80.

Pratono, A. H., & Radjamin, I. P. 2012. Kopy Luwak: a conservation strategy for global market. *Emerald Emerging Markets Case Studies.*

Z , Mei-Ling L , Hui L , Min L and Jian-Guo Zhou. 2015. Coffee consumption and risk of endometrial cancer a doseresponse meta-analysis of prospective cohort studies. *Sci. Rep.*, **5**: 13410.

Quintão R T, Brito E P Z and Belk R W. 2017. The taste transformation ritual in the specialty coffee market. *Rev. Adm. Empresas.*, **57(5)**: 483-494.

Rather R A. 2020. Customer experience and engagement in tourism destinations: the experiential marketing perspective. *J. Travel Tour*. Mark., **37(1)**:15-32.

Rauniyar, S., Awasthi, M. K., Kapoor, S., & Mishra, A. K. 2021. Agritourism: structured literature review and bibliometric analysis. *Tour. Recreat. Res.*, **46(1)**:52-70.

Ribek, P. K., & Rihayana, I. G. (2019). Innovation as a strategy of Agrowical competition advantage in improving marketing performance of Luwak Coffee products in Gianyar Bali. *Int. J. Appl. Business Int. Manag*., **4(2)**: 41-48.

Satim Hamid and Pupung Purnamasari. 2020. Analysis marketing strategy of Coffee Luwak Cikole A Case Study. *Int. J. Entrepreneurship Innov*., ***2*(4)**:205-211.

Sawe B J. 2019. Influence of cultural heritage dimension on potential Agro-Tourism development in Nandi County, Kenya. *African J. Sci. Technol. Innov. Dev*., ***5*(2)**:141-154.

Stanovčić T, Peković S, Vukčević J and Perović D. 2018. Going entrepreneurial: Agro-tourism and rural development in Northern Montenegro. *Bus. Syst. Res.*, **9(1)**:107-117.

Susanty, A and Kenny E. 2015. The relationship between brand equity, customer satisfaction, and brand loyalty on coffee shop: Study of Excelso and Starbucks. *AMJ*., **14**:27.

World Bank. 2015. Toward a more competitive dynamic value chain for Indonesian Coffee. World Bank Working Paper No. 7.

Tew, C., & Barbieri, C. (2012). The perceived benefits of agritourism: The provider's perspective. *Tour. Manag.*, ***33*(1)**, 215–224. https://doi.org/10.1016/j.tourman.2011.02.005

Wann, Jong W, Kao, C Y and Yang Y C. 2018. Consumer preferences of locally Grown Specialty Crop. *The Case of Taiwan Coffee Sustainability*., ***10* (7)**: 2396.

Wiedmann, K. P., Hennigs, N., & Siebels, A. 2009. Value-based segmentation of luxury consumption behavior. *Psychol Mar.*, ***26*(7)**, 625-651

Wu H C. 2017. What drives experiential loyalty? A case study of starbucks coffee chain in Taiwan. *Br. Food J*., **119 (3):** 1–51

Wróblewski Ł and Mokrysz S. 2017. Consumer preferences for coffee types and coffee bean brands available on the Polish market. *J. adv. humanit.*, ***3*(10):** 36352-36362.

Yuliawati, A., Budiman, A. and Hadian, M. 2017. Geoheritage and brand awareness of Batur Geopark through e-promotion. Increasing Management Relevance and Competitiveness. Proceedings of the Second Global Conference on Business, Management and Entrepreneurship (GCBME 2017). Bandung Institute Technology, West Java, Indonesia

Zhengyu Wang, Meiyu Zhou and Xiangyu Liu. 2019. Research on the effectiveness of service design based on the Quantitative Method of Kansei Engineering. Taking the LANNA coffee service process as an example. IOP Conf. Ser.: Mater. Sci. Eng. 616 012035 . DOI : 10.1088/1757-899X/616/1/012035

Table2. Parameter estimates the Loading Factor and t_{value} Model measurements on variable Brand

Variabel		**λ**	**t hitung**	**Error**	**Explanation**
Appearance (X_1)					
X_{11}	There is a sweet taste in coffee	0,85	-	0,28	Valid
X_{12}	Aroma	0,84	14,06	0,29	Valid
X_{13}	Brand of coffee	0,50	7,02	0,75	Valid
X_{14}	Freshness	0,86	14,60	0,26	Valid
X_{15}	Color	0,55	7,91	0,70	Valid
X_{16}	Variety of product	0,77	12,41	0,41	Valid
X_{17}	Price suitability	-0,1	-1,25	0,99	Not Valid
X_{18}	Brand trust	0,47	6,57	0,78	Valid
Promotion (X2)					
X_{21}	Unique Packaging	0,28	-	0,92	Valid
X_{22}	Packaging material	0,49	3,34	0,76	Valid
X_{23}	Tourist Guidance	0,42	3,18	0,82	Valid
X_{24}	Facility	0,55	3,44	0,70	Valid
X_{25}	Website available	0,77	3,65	0,41	Valid
X_{26}	Agrotourism	0,74	3,62	0,45	Valid
X_{27}	Free Delivery	0,44	3,24	0,81	Valid
X_{28}	Country of Labeling	0,08	1,04	0,99	Not Valid
X_{29}	Green packaging	0,65	3,56	0,58	Valid
X_{210}	discount	0,78	3,65	0,39	Valid
X_{211}	Welcome drink	0,68	3,58	0,54	Valid
X_{212}	Product knowledge	0,55	3,44	0,70	Valid
Usability (X3)					
X_{31}	Concern of enviromentaly friendly	0,62	-	0,62	Valid
X_{32}	Prestige	0,69	7,96	0,52	Valid
X_{33}	Habit	0,76	8,57	0,42	Valid
X_{34}	Leisure	0,71	8,12	0,50	Valid
X_{35}	Health	0,90	9,6	0,19	Valid
X_{36}	Experience in watching coffee luwak was produced	0,61	7,21	0,63	Valid
X_{37}	Sensation	0,58	6,91	0,66	Valid

JJBS

Volume 14, Number 5,December 2021
ISSN 1995-6673
Pages 983 – 989

Jordan Journal of Biological Sciences

Combination of Hyaluronic Acid with *Advance*-Platelet Rich Fibrin to Reduce Chronic Inflammation: a study in IL-6 and Granulation Index

Ronald W. Kartika[1], Idrus Alwi[2], *Mirta Hediyati Reksodiputro* [3], Em Yunir[2], Sarwono Waspadji[2], Suzzana Immanuel[4,] Todung Silalahi [5], Saleha Sungkar[6], Jusuf Rachmat[7], Saptawati Bardosono [8], Franciscus D. Suyatna [9,*]

[1]Department of Surgery, Faculty of Medical and Health Science, Krida Wacana Christian University, Jakarta, Indonesia; Doctoral Program in Medical Science Faculty of Medicine Universitas Indonesia; [2]Department of Internal Medicine, Faculty of Medicine Universitas Indonesia – Cipto Mangunkusumo Hospital, Jakarta, Indonesia ; [3] Facial Plastic Reconstructive Division, Department of Otorhinolaryngology, Faculty of Medicine, Universitas Indonesia, Cipto Mangunkusumo Hospital, Jakarta, Indonesia; *[4]Department of Clinical Pathology, Faculty of Medicine Universitas Indonesia – Cipto Mangunkusumo Hospital, Jakarta, Indonesia; [5]Department of Internal Medicine, Krida Wacana Christian University, Jakarta, Indonesia ; [6]Department of Clinical Parasitology, Faculty of Medicine Universitas Indonesia, Jakarta, Indonesia; [7]Department of Thoracic Cardiac and Vascular Surgery, Faculty of Medicine Universitas Indonesia, Jakarta, Indonesia ; [8]Department of Nutrition, Faculty of Medicine Universitas Indonesia, Jakarta, Indonesia; [9] Department of Clinical Pharmacology, Faculty of Medicine Universitas Indonesia, Jakarta, Indonesia (Corresponding author)*

Received: March 3, 2021; Revised: May 3, 2021; Accepted: September 21, 2021

Abstract

BACKGROUND: Type-2 Diabetes mellitus patients have risk of diabetic foot ulcers (DFUs) ranging from 15% to 25% with morbidity of 5% in the first 12 months, and the mortality rate at 5 years is around 42%.

AIM: This research was conducted to study the novelty of a combining Hyaluronic Acid (HA) with Advanced Platelet Rich Fibrin (A-PRF) to reduce inflammation in DFUs healing through raising granulation index.

METHODS : The study used a randomized control trial design, done from July 2019−March 2020 at Gatot Soebroto Army Hospital and Koja District Hospital, Jakarta. Subjects were DFU wound area < 40 cm^2. At the start of the study all subjects received the same treatment, debridement and standard wound care. Twenty subjects were recruited according to the rule of thumb and were randomly divided into two groups namely topical A-PRF + HA (n = 10) and NaCl 0.9% (control) groups (n = 10). A part of the sample was processed into lysate and stored in -80^oC. The rest is applied as a topical therapy in DFU base on intervention (A-PRF+HA or NaCl as a control). We analyzed the inflammation use swab sampling in DFU and analyze use ELISA on day- 3 and day-7. We also measured the wound area by a digital photograph and analyzed using ImageJ at the same time.

RESULT: From this research, it was obtained 20 DFU subjects with Wagner 2 classification. We also performed analysis of IL-6 from swab topical DFU. A-PRF+HA group was significantly lower than NaCl (control) from swab DFU on day -3 (p = 0,,049) and day-7 (p = 0.041). In A-PRF+HA group affected on increase epithelialization process/ decrease wound area on day-3 (p = 0.016), day-7 (p = 0.048), and day-14 (p= 0.03

CONSLUSION: With the homogeneous gel formation of A-PRF + HA, it will accelerate the formation of granulation tissue compared to conventional NaCl therapy through reduce inflammation by decrease IL-6 levels. In addition, the combination A-PRF + HA has the effect of accelerating the formation of epithelialization shown by decreasing wound area in intervention group.

Keywords: Diabetic Foot Ulcer- Advanced Platetelet Rich Fibrin- Hyaluronic Acid-Granulation

1.1. Background

One of the common complications of Diabetes mellitus has the most common complication in the form of Diabetic Foot Ulcer (DFU) with significant morbidity and mortality and requires intensive care. It is estimated that 19% -34% of diabetic patients have diabetic foot ulcers. According to a report by the International Diabetes Federation, 9.1–26.1 million people with diabetes develop DFU each year (Cho NH,2018). A cohort study in the United States showed that DFU patients increased risk of death by 2.5 times risk of death Heydar 2009).

DFU treatment options vary widely, so no single dressing is ideal for all types of wounds. The goal of the dressing should be to create a moist environment that supports granulation, autolytic processes, angiogenesis, and faster engineering of epidermal cells at the wound bed. A wide variety of dressings are available from standard treatment to adjuvant therapy. In addition, it requires

* Corresponding author e-mail: fransdsuyatna@yahoo.com.

weight bearing loading, vascular assessment, control of infection and blood glucose (Everett E, 2018)

The standard care is described by Caroline C, 2016 as DFU wound care, namely local wound care with sharp debridement, daily care that increase the humidity of the wound environment.[4] In standard practice in DFU care, a wide variety of agents are available and developed as adjuvant therapies. Adjuvant therapies that are developed include negative pressure wound therapy, supplement oxygen therapy, acellular bioproducts, growth factors, biologically tissue engineered (Grazul-Bilska AT, 2003).

Several growth factors have been developed for the management of DFU, including epidermal growth factors, fibroblast growth factors, endothelial vascular growth factors, granulocyte colony stimulating factors, and platelet-derived growth factors (Doulton AJM, 2018).

There is limited data on the benefits of growth factor on wound healing in DFU, but studies evaluating platelet-derived growth factor may show some benefits. Several products derived from platelets, including autologous platelet-rich plasma (PRP), used for wound healing, have been widely used by using centrifuged blood samples from patients Platelets that are processed into high concentrated suspensions will contain growth factors. Growth factors cannot be released from blood clotting by several techniques, including clotting, clotting, or clotting (Schär MO, 2015). The 2016 Cochrane Review reviewed 11 RCTs using PRP in patients with chronic wounds, although there are some drawbacks to chronic inflammatory wounds. Another developing platelet product is the leukocyte- and platelet-rich fibrin combination, which can augment growth factor and matrix protein release (Carolline 2014). In control inflammation in DFU, a combination of A-PRF and Hyaluronic Acid is used to control inflammation (Dhurat R, 2014).

Hyaluronic acid (HA) is the main component of the extracellular matrix which plays a role in tissue regeneration (Ilio K, 2016). Specific HA receptor modulation can influence inflammation, cell migration, and angiogenesis, which are the main phases of wound healing. Other studies have revealed that combining HA with platelet-rich plasma exhibits anti-inflammatory properties in cases of knee osteoarthritis. In this review, the authors discuss the role of combined A-PRF + HA in reducing inflammation and regeneration of DFU tissue through the role of the major cellular receptors involved in HA signaling. The role of HA addition to A-PRF for healing DFU is proven by inflammation reduction, angiogenesis process, and the antioxidant properties of HA (Park D 2012)

Hyaluronic acid has anti-inflammatory properties. Likewise, A-PRF also has properties in reducing inflammation. It is hoped that A-PRF + HA can work together to reduce inflammation which is marked by a decrease in IL-6 (Ulcers DF, 2012). During chronic inflammatory process in DFU, preparation of HA can also protect and stabilize the alpha platelet granules membrane from protease enzymes so as might prevent damage to growth factors inside them.(Kartika 2021).

Until now there have been no studies comparing the combination of A-PRF + HA with A-PRF alone in reducing inflammation which affects the healing of DFU. Assessment granulation improvement can be done by using image (A. Suarez, 2020)

2. Methods

2.1. Research Design and Sample

This study has been approved by The Ethics Committee of the Faculty of Medicine Universitas Indonesia (ID 0855/UN2.F1/ETIK/2018). This open-label randomized controlled trial was conducted at Koja District Hospital and Gatot Soebroto Hospital from July 2019 to April 2020. DFU patients with wound duration of three months, Wagner-2, and ulcer size < 40 cm^2 were recruited and randomly assigned into A-PRF + AH and control group. On day-0, day-3 and day -7, samples and photographs were taken. Samples were analyzed with ELISA and photographs were analyzed with ImageJ to calculate wound area (WA). Statistical analysis was performed using SPSS version 20.

2.2. Material and Sample Measurement Techniques

Measurement of IL-6 from wound surface use cotton swabs on days 0, 3 and 7 using the ELISA technique (kit) and obtained numerical data in units of pg / mL. The examination was carried out at the FKUI Integrated Laboratory. The ELISA reagent used was the Human IL-6 / ELISA Kit with the Insert Kit from LifesSpan BioSciences, Inch.Cat:LS-F4604. ELISA was done according to the manufacturer's instruction. In addition, the wounds reduction was recorded with a digital camera (Cannon Camera 48 mega pixel, China) with an accuracy of 0.1% on the 0, 3, 7 and 14 days. The results of the wound photographs were processed using Image-J (Java software program) by evaluating the granulation index

2.3. Topical A-PRF + HA preparation

To make A-PRF, 20-40 mL of peripheral blood was taken without anticoagulant tube (RegetKit tube), then centrifuged (RegenLab centrifuge, Le Mont, Switzerland) at about 200 G for 8 minutes. Fibrin and buffy coat are separated from erythrocytes. For the A-PRF + HA (intervention group); the process was continued by making A-PRF and HA homogenate with a ratio of 1 cc: 0.6 cc with vortex for 20 seconds. The preparation of A-PRF + HA was repeated on day-3 and day-7 and applied as a DFU topical therapy.

2.4. Application of A-PRF + HA in DFU

Prior to intervention, the wound was cleaned and debridement. Topical therapy was carried out by giving 1 mL of material for an area of 10 cm^2 according to the group (group 1 A-PRF + AH, group 2 NaCl soaked gauze). The wound is covered with sterile gauze as a secondary dressing to maintain moisture.

2.5. Evaluation of Inflammation Signs in DFU Intervention

To assess changes in inflammation after intervention, an evaluation was carried out by looking at changes in IL-6 levels (swab) on baseline, day-3 and day-7. Meanwhile, for clinical assessment, measurements of reduction of wound area from day-0, day-3, day-7 and day-14 were accompanied by pain response with numeric pain score at the same time.

3. Result

We recruited 20 subjects, consisting of 12 men and 8 women. The median age was 64 years in women and 61 years in men. The subjects were randomly divided into three groups (A-PRF + HA and NaCl) comprised of 10 subjects per group (Table 1)

Table 1. Subjects baseline characteristics

Subject Characteristic	A-PRF+AH (n=10)	Control (n=10)	p-value
Age (year)	59,8 (SB 12,7)	66 (SB 12.3)	0,626
Sex			
man	5	3	
woman	5	7	
Body Mass Index	28,9 (SD 2,7)	28,4 (SD 2.5)	0,337
Hemoglobin (g/dL)	12,7 (SD 1.2)	12,05 (SD 1.4)	0.224
Hematocrit (%)	34.1 (SD 4.3)	33,8 (SD 4.5)	0,145
Leucocyte (10^3/µl)	13,30 (SD 1,08)	9,23 (SD 1,66)	0,985
Platelet (10^3/µl)	354,9 (SD 167,5)	319,9 (SD 128,4)	0,880
Random Blood Glucose, mg/dL	286,0 (SD 67.5)	254,7 (SD 58,6)	0,104
HbA1C (%)	11,34 (SD 1,30)	8,5 (SD 0,72)	0,950
Total Cholesterol (mg/dL)	214,5 (SD16,9)	202,3 (SD 38,6)	0,096
Albumin (mg/dL)	3,3 (SD 0,4)	3,2 (SD 0,4)	0,662
Anti Platelet Medication	4	3	
Statin Medication	3	4	

[a] Mean,SD, Independent t test

3.1. Evaluation of IL-6 Swab DFU Receiving Intervention

Level of IL-6 was analyzed to see the pathway of healing DFU through inflammation. The baseline IL-6 levels in the two groups were not significantly different. After two interventions, changes in levels of IL-6 (Δ IL-6) in the A-PRF + AH group, there was a significant decrease on day(-10.9 pg/mg protein) and day-7 of (-18.3 pg/mg protein), while Δ IL-6, group NaCl increased on day 3 of 4,3 pg/mg protein and day-7 by 35,6 pg/mg protein. The A-PRF + AH group showed a significant reduction in Δ IL-6 compared to the NaCl (Control) group on day 0−7 (p = 0.015), according to Table 2.

Table 2. IL-6 Levels Swab DFU Based on Intervention

Intervention	A-PRF+HA (n = 10)	Control (n = 10)	p-value
Before treatment	106.4 (83.1−407.6)	125,3 (20,3−287.0)	0.337
Day-3	99.5 (76.3-302.2)	131,1 (5,3−337,5)	0.049
Day-7	88.7 (44.3−217.9)	167,9 (27,7−156,2)	0.041*
Δ day- 0–3	-10.9 (-105.4−17.7)	4,3 (-47.8−50,5)	0.046
Δ day- 0−7	-18.3 (-189.7 –44.6)	35,6 (-160,6−108,4)	0.015

* Median (min-max), Mann Whitney test

Figrue 1 show in DFU which use topical A-PRF+HA has decrease of IL-6 swab significantly on day-3 (p =0.049*) and day-7 (p= 0.041**), signiificantly

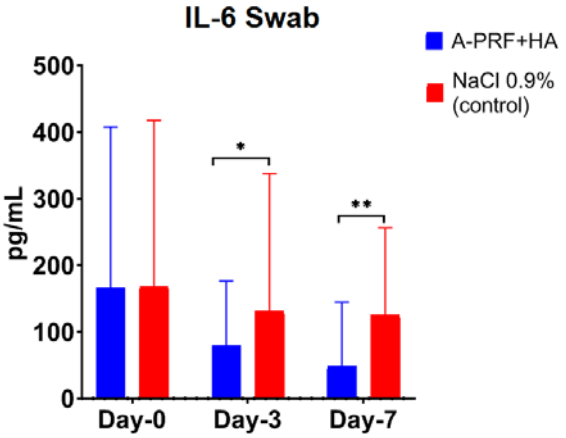

Figure 1. A-PRF +HA group decrease of IL-6 level compare with control on day-3 (p =0.049*) and day-7 (p= 0.041**)

3.2. Evaluation of Wound Area (WA) of DFU in A-PRF + HA Fibrin versus NaCl

To see the correlation between angiogenesis and clinical conditions, an analysis of wound area and granulation tissue growth was performed as measured by ImageJ software. The measurement of increase of epithelialization tissue changes, can be done by evaluating the woundrea (WA). The average wound area was shown in Table 3

\\

Table 3.Evaluation of Wound Area base on Intervention

Intervention	A-PRF + HA (n = 10)	Control (n = 10)	p value
Baseline	7,0 (1,9–31,9)	5,2 (2,0–20,6)	0,848
Day-3*	6,3 (1,4–26,1)	3,2 (1,9–18,4)	0,016
Day-7*	5,5 (1,1–25,4)	2,6 (1,1–17,1)	0,048
Day -14*	5,0 (0,9–18,6)	2,3 (0,3–16,2)	0,030
Δ Day- 0−3	-0,5 (-0,1−-5,8)	-1,1(-0,1−-2,3)	0,036
Δ Day -0−7	-1,1(-0,3−-5,9)	-1,5(-0,2−-3,9)	
Δ Day-0−14	-1,5(-0,7−-13,3)	-2,5(-0,5−-4,4)	0,045 0,003

* median (min-max), Mann Whitney test

Figure 2. shows the measurement, clinical evaluation and clinical photographs taken at baseline, day-3, day-7 and day-14 on different treatment groups. Here, we observed different rates of wound closure and healing, especially at day-14 compared to control group**.**

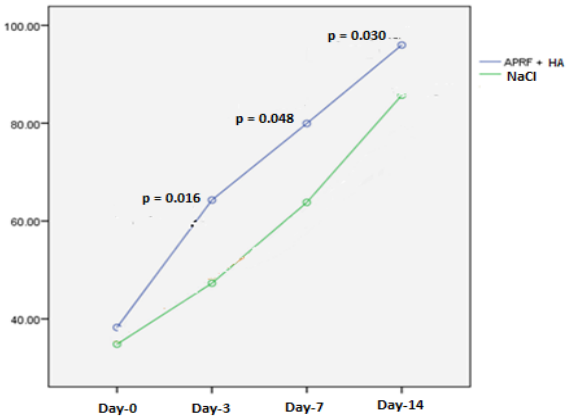

Figure 2 Wound Area of DFU at day-0, day-3, day-7 and day-14

3.3. Evaluation of Inflammation Clinical Symptoms DFU Subjects

We analyzed clinical symptoms such as Numeric Pain Score (NPS) and Inflammation sign in DFU. At baseline examination of the two groups in NPS evaluation was 7-8 (severe pain). After the intervention, pain scores decreased in both groups. However, there was a significant decrease of NPS on day-3 and day-7 in the A-PRF + HA group compared to NaCl (contro) groups (Table 4).

Table 4. Different Numeric Pain Score (NPS) in DFU Base on Intervention

Intervention	A-PRF + HA (n = 10)	Control (n = 10)	p-value
Baseline	8 (8−9)	8 (7−8)	0.164
Day-3	4 (3−5)	5 (5−6)	0.021*
Day-7	2.5 (1−3)	3 (3−5)	0.019*
Day-14	2.1 (2−4)	2 (2−3)	0.047*

Median (min−max), Mann Whitney test 0: none, 1−3= Mild , 4−6 : moderate : 7-9 = severe

Figure 3. show an evaluation of NPS in A-PRF + AH group compare with A-PRF group on day -3 (p - 0.021)[a], day-7 (p=0.019) [b], and day-7 (p = 0.047)

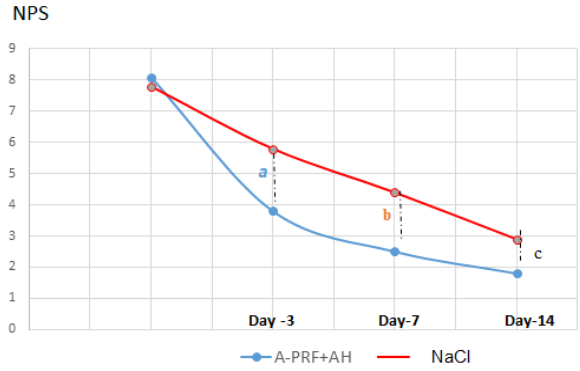

Figure 3. Numeric Pain Scale (NPS) in LKD after Intervention

We aimed to quantify the inflammatory state using an Inflammatory Score inspired by an additive effect of inflammatory sign on diabetic foot ulcers, such as redness, heat, swelling, pain, and functio laesa before and after treatment. Compared to baseline condition, the inflammation score in DFU on day-7 in A-PRF+HA showed a significant decrease in redness, heat, swelling, and pain compared to A-PRF alone. Data for these inflammation sign of DFU are shown in Table 5.

Table 5 Inflammation Sign of DFU Base on Intervention

Sign Of Inflammation	A-PRF+HA (n=10)	Control (n=10)	p-value
Redness			
Day-0	2.9 ± 0.5	2.5 ± 1.1	0.890
Day-7	0.1 ± 0.03	1.0± 0.2	0.028
Heat			
Day-0	2.8 ± 0.1	2.4 ± 0.5	0.707
Day-7	0.3 ± 0.1	0.9 ± 0.1	0.032
Swelling			
Day-0	2.9 ± 0.2	2.5 ± 0.3	0.179
Day-7	0.1 ± 0.05	0.7 ± 0.2	0.021
Pain			
Day-0	2.9 ± 0.5	2.7 ± 0.6	0.328
Day-7	0.2 ± 0.4	0.8 ± 0.1	0.032
Functio Laesa			
Day-0	2.5± 0.3	2.6 ± 0.2	0.978
Day-7	0.3 ± 0.1	0.5± 0.1	0.043

Mean (SD), independent t test 0= none, 1= mild, 2=moderate, 3 =severe

4. Discussions

Treatment of diabetic foot ulcer therapy with supplementary growth factor therapy has begun to be developed in the late decades. Growth factors are needed in new cell growth and wound healing.[14] change style Treatment of diabetic foot ulcers with growth factors can accelerate ulcer healing characterized by granulation tissue formation. Several growth factors influenced by the healing of DFU i.e. TGF-β1 and β2, IGF, and VEGF, have been used in orthopaedics, maxillofacial, periodontal fields, plastic surgery, and sports medicine because of their anti-inflammatory and antimicrobial properties (Geerlings SE et al , 2019).

In this study, 20 DFU subjects were found with almost homogeneous basic characteristics. The use of A-PRF + HA group compared with NaCl (control), there was significant reduction in delta inflammation in local swabs (Δ IL-6) in DFU on day 0−3 (p= 0.046) and on day 0−7 (0 = 0.015).

In diabetics, there is a prolongation of the inflammatory phase in the wound healing process (Amanulla, 2020).

Several biomarkers play a role in the inflammatory process such as TGF-β which is a pluropotent cytokine of the three isoforms in mammals such as TGF-β 1, TGF-β -2, and TGF-β -3, with TGF-β 1 dominant in tissue healing, including skin. Otherwise, interleuking family also influence in inflammation in woud healing such as IL-6 and IL-1β (Hasan 2019).

Interleukin (IL) -6 is produced by fibroblasts, keratinocytes and macrophages of cells at the site of inflammation. IL-6 biomarkers play a role in acute to chronic inflammation by changing the nature of leukocyte infiltrates (from polymorphonuclear neutrophils to monocytes / macrophages). Additionally, IL-6 stimulates T and B cells, which support a chronic inflammatory response. Strategies that target IL-6 signaling are useful for the prevention and treatment of an effective model of diabetic foot ulcers and other chronic inflammatory diseases. IL-6 has a dual effect; to some extent, it acts as a defense mechanism but in chronic inflammation it acts as a pro-inflammatory (Gabay Cem, 2016).

In assessesment the inflammatory status of DFU, it can be both locally and systemically. In this study, a swab of DFU was carried out using a cotton swab to check for a decrease in inflammatory mediators such as IL-6. This examination is a new method that has been done for the first time. Research by Liu et al, 2002a tried to perform an MMP examination of the wound fluid Ref. Other methods used to examine biomarkers in DFU are using invasive techniques such as tissue biopsy or patch skin biopsy Ref. Research by Michael et al, 2017 has used swab examination in cases of DNA abnormalities examination in cerebral palsy cases in infants and cases of Alzheimer's Ref. The cells were obtained by means of swab or smear using a cotton bud or small brush for further analysis using the PCR technique. This method has a fairly good accuracy with a sensitivity of 93%. To increase the sensitivity of the examination of other researchers, replacement of the stick swab with a soft brush is recommended (isohelix DNA / RNA buccal swab). This method can replace DNA examination with PCR of blood or hair materials. Another study at UGM used fine needle biopsy with paraffin block for detection of TGF-β for the evaluation of biomarkers in DFU (Yang P, 2016)

5. The use of Advance PRF in DFU healing

In wound healing, PRF plays a crucial role in the proliferation phase by continuously releasing growth factors at the wound site and inducing viability, proliferation and differentiation of cells. PRF stimulation releases growth factors TGF-β1 and PDGF-AA on day 5 of wound healing. A part from playing a role in accelerating wound healing through the induction of growth factors, PRF also plays an active role in inducing the proliferation and migration of skin cells through increased expression of MMP-1 and MMP-9. Platelet-rich fibrin elicited the anti-inflammatory response of macrophages in in-vitro studies. In addition, PRF has anti-inflammatory activity and shifts the polarization of macrophages from M1 to the M2 phenotype (Mussano F, 2016).

Advanced platelet-rich fibrin (A-PRF) was first described in 2014 as a new concept using cell-based tissue engineering by lowering rpm while increasing the standard PRF time Ref. To obtain PRF, venous blood is drawn without adding anticoagulants. The protocol for the standard PRF (S-PRF) utilized a 2700 rpm or 360 x g centrifuge, for 12 minutes. In contrast to standard PRF, the APRF manufacturing technique uses a low-speed centrifuge (1500 rpm or 200 x g for 8 minutes) because centrifugal force in speed and time which affects the distribution of growth factor cells suitable for wound healing and tissue regeneration (Nasirzade, 2020) .

Immunohistochemistry of monocytes, T and B lymphocytes, neutrophilic granulocytes, CD34, were detected around the buffy coat. Decreasing rpm while shortening the centrifugation time of A-PRF can increase the neutrophilic granulocytes in platelet fibrin concentrates more in APRF than in standard PRF, whereas in the Standard PRF (S-PRF) group, neutrophils were found on the surface of erythrocytes. Neutrophilic granulocytes play a role in the differentiation of monocytes into macrophages so that A-PRF can affect tissue regeneration, especially through monocytes / macrophages and growth factors (Gardiner E,2014).

6. The use of Hyaluronic Acid in Wound Healing

Isolated glycoaminoglycans has been done from the vitreous humor of a cow's eye as a hyaluronan. Hyaluronic acid is a polysaccharide with extracellular matrix components synthesized in the plasma membrane of fibroblast cells which activates many inflammatory mediators and growth factors (Greco, 1998). Hyaluronic acid recruits macrophages and modulates the inflammatory response (Ilio , 2016).

The mechanism of reducing inflammation of A-PRF + AH is through the pathway of changes in macrophage polarization by accelerating the polarization of M1, which has strong pro-inflammatory properties (IL-1β, IL-6, and TNF-α) to M2 (IL-10, Arginase, TGF-β1, VEGF), which is anti-inflammatory. M1 activation was associated with inflammation, tumor resistance, and graft rejection. Conversely, M2 cell activation results in immune system regulation, cellular matrix deposition and tissue remodeling. Hyaluronic acid through the CD44 receptor in synergy with A-PRF strengthens the shift of macrophage polarization from M1 as a pro-inflammatory) to M2 phenotype as an anti-inflammatory. (Fujisaka, 2009)

Another advantage of HA is that it has antioxidant properties and reduces inflammation so it is widely used to treat osteoarthritis (OA). The structure of Hyaluronic acid which is contain disaccharide polymer, consisting of N-acetyl-D-glucosamine and D-glucuronic acid, linked via β-glycosidic bonds. Hyaluronic acid inhibits the collagenase enzyme, which is the proteolysis enzyme of collagen (Wu, 2016). Hyaluronic acid affects cell migration, cell adhesion and angiogenesis. Fibroblasts play a major role in wound healing by forming extracellular matrix components such as collagen, elastin and proteoglycans.

Fibroblasts also play an essential role in the migration of keratinocytes from the wound edges to achieve wound closure and matrix reconstruction resulting in the maximal wound healing force of contraction (Afat et al, 2017).

7. Combination of HA with A-PRF to Accelerate Epithelialisation

In this study show in intervention group (Topical A-PRF+HA) had decrease of wound area and increase granulation tissue significantly on day-3 and day-7.

Regarding the effect of HA on tissue regeneration, it is related to the interaction of HA with CD44 which drive the maintenance and establishment of collagen synthesis and normal skin function. Hyaluronic acid is present in the extracellular matrix of basal keratinocytes and the structural integrity of dermal collagen fragments and fibroblast penetration. Decreased levels of HA correlate to impaired local inflammatory response and reduced tissue repair due to degeneration of the granular tissue matrix (Fischer 2008). The combination of HA and PRP reduces pro-inflammatory cytokines and increases articular chondrocyte proliferation and chondrogenic differentiation via the HA-dependent Erk1 / 2 pathway and the PRP-dependent Smad 2 / 3 pathway (Ilio , 2016). The clinical application of the combination of PRP and AH is more effective than PRP or HA alone; both are therapeutic options for osteoarthritis and chronic tendinopathy. The combined effect of PRP and AH is not fully understood. It is thought that PRP stimulates the healing process of new tissue by producing growth factors and cytokines released by platelets. The addition of HA to PRP can increase the release of growth factor on day 5 (Gardiner, 2014).

Combination of AH with PRF stimulated growth factors such as TGF-β, significantly increasing the proliferation index and collagen deposition (Ilio, 2016). AH also interacts with the TGF-ß1 transformation of PRF thereby protecting growth factors from degradation of tryptic and collagen by protease enzymes (Afat, 2017).Combination of AH with L-PRF reduced edema after oral surgery of the 3rd molar although through HA linking wih ICAM, VCAM receptor. This link will reduce vascular leakage of neutrophil and reduce edema. (Fathi, 2012)

Hyaluronic acid affects three main receptors in tissue regeneration's modulation, namely migration, proliferation and activation of keratinocyte cells (CD44). This is done to restore the epidermis, fibroblast migration (RHAMM), control of inflammation and neoangiogenesis (ICAM-1), as well as promotion of ECM deposits such as collagen fibers that contribute to wound healing (Park, 2012). Wound healing begins with a complex integration process through cellular, physiological, and biochemical processes, such as inflammation, cell migration, and proliferation. Interleukin-6 is a multifunctional cytokine that regulates the inflammatory response of the wound healing process in a timely manner. Hyaluronic acid is an important component of ECM contributing significantly to cell proliferation and migration. The combination of PRF and AH provides a synergistic effect on wound healing cell migration with ERK (extracellular signal) activation (Wu, 2016).

In this study, A-PRF corresponded to high concentrations of platelets in liquid fibrinogen which contains growth factors required for soft tissue regeneration. The low speed and low time centrifugation protocol (200 G, 8 minutes) lead to enhance the healing of chronic diabetic foot wounds. The addition of HA to A-PRF will further induce the release of growth factors (Kartika RW, 2020).

Here is the proposed mechanism of A-PRF + HA in reducing inflammation and increase granulation in wound healing (Figure 4).

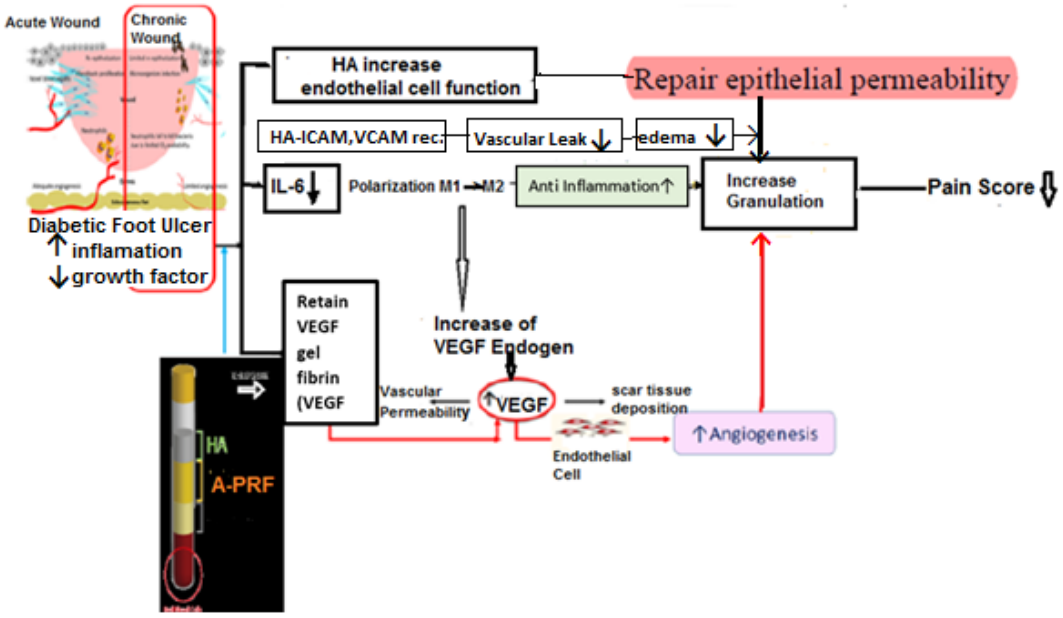

Figure 4. Proposed mechanism of A-PRF HA increase Granulation in DFU healing

8. Conclusion

The combination of A-PRF and HA increases the granulation and epithelialization in DFU healing by reducing the inflammation state which will induce the angiogenesis process. Clinically, the application of A-PRF and HA combination showed to reduce pain better than the control NaCl in DFU patients.

9. Limitation Study

The subject in this study only 20 patient and the evaluation of inflammation was only the use of Interleukin -6 and clinical inflammation preview. We need more subjects for evaluation with more variants of inflammation biomarker.

Acknowledge

This study was a dissertation of Program Doctoral Medical Science Universitas Indonesia.

Conflict of Interest

This study was funded by Universitas Indonesia, Jakarta.

References

Cho NH. 2018. IDF Diabetes Atlas : Global estimates of diabetes prevalence for 2017 and projections for 2045. Diabetes Res Clin Pract, **138**:271−81. doi:10.1016/j.diabres.2018.02.023

Heydari I. 2010. International Journal of Diabetes Mellitus Chronic complications of diabetes mellitus in newly diagnosed patients. Int J Diabetes Mellit, **2(1):**61−3. doi:10.1016/j.ijdm.2009.08.001

Everett E and Mathioudakis N. 2018. Update on management of diabetic foot ulcers. Ann N Y Acad Sci, **11(1):**153−65. doi:10.1111/nyas.13569

Caroline C.L.M and Naves .2016, The Diabetic Foot: A Historical Overview and Gaps in Current Treatment, Adv.W Care, **5 (5),**1−7

Grazul-Bilska AT. 2003. Wound healing: The role of growthfactors.DrugsToday,**39(10):**787−800. doi:10.1358/dot2003.39

Doulton AJM. 2018. Diagnosis and management of diabetic foot complications.Current Diabetes Update, **(2):**1−20. doi:10.2337/DB20182-1

Schär M. 2015. Platelet-rich Concentrates Differentially Release Growth Factors and Induce Cell Migration In Vitro. Clin Orthop Relat Res, **473(5):**1635−43. doi:10.1007/s11999-015-4192−9

Dhurat R and Sukesh M, 2104. Principles and methods of preparation of platelet-rich plasma: A review and author′s perspective. J Cutan Aesthet Surg,**7(4):**189−95. doi:10.4103/0974-2077.150734

Vokurka J, 2016. Concentrations of growth factors in platelet-rich plasma and platelet-rich fibrin in a rabbit model. Vet Med (Praha), **61(10):**567−70. doi:10.17221/24/2016-VETMED

Iio K. 2016. Hyaluronic acid induces the release of growth factors from platelet-rich plasma. Asia-Pacific J Sport Med Arthrosc Rehabil Technol, **4(3)** : 17−32 doi:10.1016/j.asmart.2016.01.001

Fathi WK. 2012. The Effect of Hyaluronic Acid and Platelet - Rich Plasma on Soft Tissue Wound Healing : An Experimental Studyon Rabbits. Al-Rafidain Dent J, **12(3):**115−25.

Ulcers DF. 2012.Role of Interleukin-6 (IL-6) and Indicators of Inflammation in the Pathogenesis of. Aust. J. Basic & Appl. Sci., **6(6):**430−5.

Suarez. 2020, An image J plugin for the high throughput image analysis of in vitro scratch wound healing assays,Plos One, **15(7):**1−14, doi. org/10.1371 /journal.pone.0232565

Geerlings SE and Hoepelman AI. 2019. Immune dysfunction in patients with diabetes mellitus (DM). FEMS Immunol Med Microbiol, **26(3):**259− 65. doi:10.1111/j.1574-695X.1999.tb01397.x

Harris M.2008. Challenges in diabetes management. Aust Fam Physician **37(9):**716−20. doi:10.1186/1744-8603-9-63

Agrawal M .2015. Platelet Rich Fibrin and its Applications in Dentistry- A Review Article. Int J Clin Exp Med, **8(5):** 7922–9

Gabay Cem.2006. Interleukin-6 and chronic inflammation, Arthritis Res Ther, **8(2):**3−8 doi: 10.1186/ar1917

Liu RAN .2002. Ratios of activated matrix metalloproteinase-9 to tissue inhibitor of matrix metalloproteinase-1 in wound fluids are inversely correlated with healing of pressure ulcers.. Wound Repair Regen , **1(2):**26−37. doi 10.1046/j.1524-475x.2002.10903.x

Michael GL .2017. Difference of DNA Quantity Extracted from Buccal Swab with Different Amount of Swab. J Kedokt Diponegoro, **6(2):**443−50.

Yang P.2016. Compromised wound healing in ischemic type 2 diabetic rats. PLoS One , **11(3):**1−19 doi:10.1371. /journal pone.0152068

Gill SE and Parks WC . 2009. Metalloproteinases and Their Inhibitors: Regulators of Wound Healing, **40(206):**1334−47. doi:10.1016/j.biocel.2007.10.024

Mussano F.2016. Cytokine , chemokine , and growth factor profile of platelet-rich plasma. Platelets , **27(5):**467−71. doi :10.3109. /09537104.2016.1143922

Nasirzade J.2020. Platelet-Rich Fibrin Elicits an Anti-Inflammatory Response in Macrophages In Vitro. J Periodontol, **91(2):**244−52. doi: 10.1002/JPER.19-0216.

Gardiner E. 2014.A Systems Biology Approach to Blood. Exp Hematol,**12(844):**201−25 doi:10.1007/978-1-4939-2095-2

Afat IM.2017. Effects of leukocyte- and platelet-rich fibrin alone and combined with hyaluronic acid on pain, edema, and trismus after surgical extraction of impacted mandibular third molars. J Oral Maxillofac Surg, **76(5):**926−32 doi: 10.1016/j.joms.2017.12.005.

Park D. 2012.Hyaluronic acid promotes angiogenesis by inducing RHAMM-TGFβ receptor interaction via CD44-PKCδ. Mol Cells, **33(6):**563−74. doi:10.1007/s10059-012-2294-1

Wu X.2016. Src promotes cutaneous wound healing by regulating MMP-2 through the ERK pathway.International J of Molecular Med, **(37)3**: 639−48. doi:10.3892/ijmm.2016.2472

Amanulla A.2020. Assosiation of hs-CRP with Diabetic and non-Diabetic Individuals,JJBS, **2(1):**1-17

Snur Muhammaed Amir Hassan.2019. Anti-inflammatory and Anti-proliferative Activity of Coconut Oil against Adverse Effects of UVB on Skin of Albino Mice, JJBS, **13(3):**295−302

Greco RM, Iocono JA, Ehrlich HP. Hyaluronic acid would stimulates human fibroblast proliferation within a collagen matrix. J Cell Physiol. 1998;**177(3):**465−73. doi:10.1002/(SICI)1097-4652

Fujisaka S, Usui I, Bukhari A, Ikutani M, Oya T, Kanatani Y et al (2009). Regulatory Mechanisms for Adipose Tissue M1 and M2 Macrophages in Diet-Induced Obese Mice.;**58**:2574–82

Fisher GJ, Varani J, Voorhees JJ, 2008) . Looking older: Fibroblast Collapse and Therapeutic Implication . Arch Dermatol.; 144(5): 666-672.

Kartika RW, Alwi I, Yunir EM,Waspadji S, Suyatna F,Bardosono S, Immanuel S, Rachmat J, Silallahi T, Reksodiputro M, Sungkar S (2011) Efficacy of Combining Hyaluronic Acid and Platelet-Rich Fibrin in Diabetic Foot Ulcer, JJBS ; 14(3):607−611.

JJBS

Volume 14, Number 5,December 2021
ISSN 1995-6673
Pages 991 – 997

Jordan Journal of Biological Sciences

Value Chain Model for Straw Mushroom (*Volvariella volvacea*) Agribusiness Performance in Karawang, Indonesia

Suhaeni[1,*], Winda Rianti[2] and Yuyun Umaidah[3]

[1]*Department of Agribusiness,* [2]*Department of Agrotechnology,* [3]*Department of Information Technology, Universitas Singaperbangsa Karawang, Indonesia*

Received: March 3,2021; Revised: May 31, 2021; Accepted: September 16, 2021

Abstract

Straw mushroom is one of the potential commodities in Indonesia with consumption growth always increasing every year. This commodity has great potential to be developed but must be accompanied by the right value chain performance. In this study, the mapping and value chain performance of straw mushroom quality were analyzed. This research was conducted using a descriptive survey method to 56 respondents through interviews and questionnaires. Data were collected and analyzed using the value chain analysis model and the Analytical Hierarchy Process (AHP). The results showed that there were 6 patterns of the straw mushroom value chain. The actors involved consisted of farmers, traders, wholesalers, retailers, and consumers. The performance element that needs great attention is reliability (37.4%), followed by cost (22.6%), agility (20.1%) and responsiveness (19.9%). The results of this study are then used to facilitate decision making in improving value chain performance.

Keywords: value chain, performance, agribusiness, straw mushroom

1. Introduction

Mushroom production has increased rapidly and is expected to further increase in the future (Grimm & Wösten, 2018a) with its consumption growth always increasing every year (Grimm & Wösten, 2018b). Mushrooms is not only used as a delicious food or flavour but also for health (Pop et al., 2018) since they are enriched with proteins, phenolics, vitamins, antioxidants, and microelements (Kora, 2020). Plants that contain phenolics and antioxidants can be used as medicine (Al-Ghamdi et al., 2020) and treatment goals (Abdel-Mawgoud et al., 2019). So, apart from being food, mushrooms can also be used as a medicine (Ashraf et al., 2020); and they are good for diet because they are low in calories, carbohydrates, fat and cholesterol (Fontes et al., 2019).

Straw mushroom is one of the most widely cultivated food types in tropical and subtropical regions (Liu, 2020). Apart from being a source of food and good for health, this product has an environmentally friendly production process and can be a source of income for the community (Datta, 2019). Straw mushroom cultivation has economic and environmental feasibility (Atila, 2019), but there are still obstacles in the procurement of seeds, limited technical information, and lack of agricultural extension role. In addition, farmers also have constraints in marketing and pest control, climate or weather inconsistencies (Robinson et al., 2019), water quality (Sakinah, 2019), and there is no added value for straw mushrooms.

Straw mushroom is one of the leading commodities in Karawang Regency, Indonesia with an increase in consumption that always increases every year. Demand per day reaches 4-10 tons, while the supply is only around 4-7 tons. This condition shows that straw mushroom agribusiness has the potential to be developed, but the performance of the value chain (starting from the planning process, procurement of agro-input facilities, production, distribution, to returns) needs to be improved. These activities are very important for the development and competitiveness of the company as well as the company's supply chain management strategy (Florescu et al., 2019). Therefore, this study aims to determine the structure of the value chain and measure the performance of the mushroom value chain. It is important to select performance attributes to improve the mushroom value chain. This study uses the Analytical Hierarchy Process (AHP) methodological approach with its ability to make decisions from various criteria (Bunyan Unel & Yalpir, 2019). This approach is also able to measure supplier performance which can help organizations to optimize costs and quality of functions (Touil et al., 2019). The AHP method developed by Saaty (saaty, 1990) is an effective and easy-to-apply tool to assess criteria that influence intuitive decision-making problems through a multi-level hierarchical structure (Sevinç et al., 2018).

2. Methodology

The method used in this study is a descriptive method by surveying, interviewing, and distributing questionnaires to respondents, namely 40 mushroom farmers by

* Corresponding author e-mail: didikdidikindradewa@gmail.com.

purposive sampling and 16 sellers by snowball sampling. Surveys and interviews were conducted to find out the main actors involved in the performance of the value chain and to get an overview of the straw mushroom business process. The research location is in the center of straw mushrooms in Jatisari District, Karawang Regency. The location determination was carried out by purposive sampling, with the consideration that the location of this study was the center of straw mushrooms. This research was conducted from January to August 2020. Furthermore, the measurement data was processed by value chain analysis and the Analytical Hierarchy Process (AHP) method.

2.1. Value Chain Analysis.

Value chain analysis refers to a series of activities required to present a product or service starting from the conceptual stage, the production stage, to delivery to the final consumer and destruction after use. The stages in value chain analysis are as follows:

1. Entry point

The entry point is to determine the point where the research will begin. The selected entry point is a mushroom farmer, then tracing with snowball sampling to get a sample at the next point to the consumer, as in the cotton industry value chain research (Mapanga et al., 2018).

2. Value chain mapping

Market mapping is very much needed in value chain mapping analysis. It is used to determine the contribution of the actors involved and the relationship between the actors. Identification of factors that affect value chain performance can be obtained from the interaction information (Muloi et al., 2018).

3. Improve the value chain

Value chain improvements are carried out to identify possible improvements, by optimizing the performance of the edible mushroom value chain.

2.2. Model Analytical Hierarchy Process (AHP).

The AHP method was developed by Thomas Saaty (Saaty, 1990). This method is used to update the value chain performance by making decisions and determining the best alternative by considering various criteria (Improta, 2018). This method is also used for decision making by making pairwise comparisons of the available criteria options (Leśniak et al., 2018). The AHP model software expert choice 11 can be used to select the performance criteria of the mushroom value chain based on priority. Data to measure performance are obtained from literature studies and in-depth interviews with several experts / actors who are directly involved in the mushroom value chain. AHP working principle stages are as follows (Susanawati & Fauzan, 2019):

1. Problem Identification

The first step is to identify the problem in depth. The next process is the identification and selection of elements that will be included in the system components, such as goals (target), objectives, criteria, sub criteria and alternatives in the AHP structure. AHP method is able to break down complex problems into sub-problems, classify these sub-problems based on domination relations, and build an orderly hierarchy (Beiragh, 2020). The hierarchical structure of the mushroom value chain performance is shown in the Figure 1.

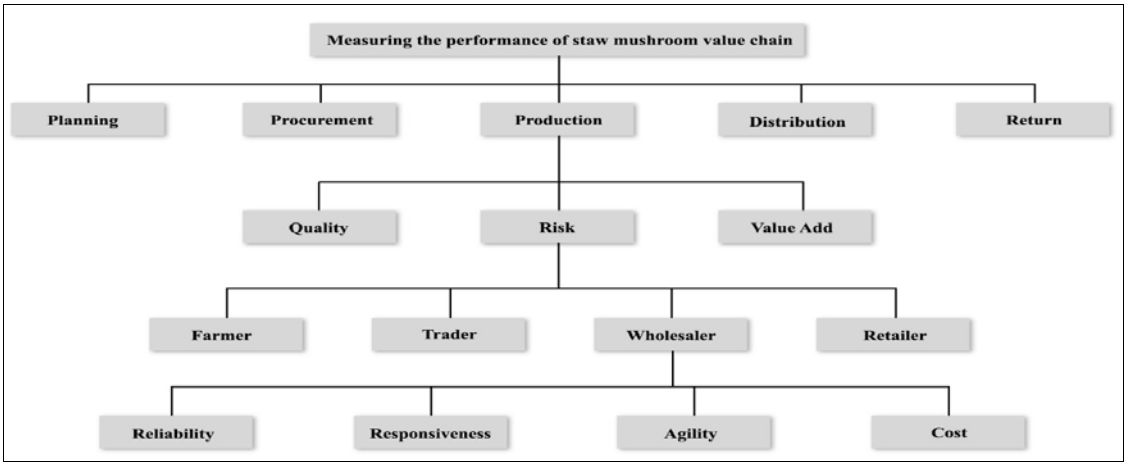

Figure 1. Hierarchy Structure of Value Chain Model for Performance of Straw Mushroom AgribusinessCreating a hierarchical structure

The AHP process method involves consideration of a hierarchical structure in the form of goals (targets), criteria, sub criteria and alternatives (Improta, 2018). The goals is to measure the performance of the mushroom commodity value chain, the criteria consist of planning, procurement, production, distribution and return. Sub criteria consist of quality, risk and value-added (Setyabudi, 2018), actors consist of farmers, traders, wholesalers and retailers (Sachan, 2020). While the alternatives are reliability, responsiveness, agility and cost.

2. Assessment of each level of the hierarchy

The assessment process is carried out to find the elements that most influence the overall objectives. The initial step is to make an assessment of the importance of the two elements at a given level in relation to the higher-level hierarchy. The results of the assessment are presented in a paired matrix of size nxn. Saaty gives a rating of 1 to 9 to assess the comparison of the importance of one element to another (Susanawati & Fauzan, 2019).

Table 1. Comparison Scale.

Comparison Scale	Definition	Description
1	Both elements are equally important	Two elements have the same influence greatly to the goals
3	Elements of a little more important than other elements	Experience and judgement slightly favor one element compared to other elements
5	Elements which one is more important than other elements	Experience and strong vote supporting one element compared to the other elements
7	One element is obviously more important than other elements	One very powerful element supported, and the domain has been in practice
9	One absolutely essential element than other elements	The evidence that supports one element against another element has the highest possible degree of confirmation strengthens
2,4,6,8	The values between two adjacent values	Values considerations is given when there are two compromises between two options

3. Determination of element priority

Each level of the hierarchy needs to be compared in pairs to determine priority. Paired elements must be compared based on certain standards and considerations. Relationships between elements from each level of the hierarchy are established by comparing them in pairs. This relationship describes the relative influence of an element at a hierarchical level to each element at a higher level. Elements at this higher level function as criteria and are called properties. The result of this differentiation process is the priority vector or the relative importance of an element to each trait. Pairwise comparisons are repeated for each element in each level. Then the next step is to give weight to each vector with its priority properties. The first comparison is performed starting at the top of the hierarchy in the comparison process. The second comparison is performed by comparing the elements at the lower level.

Table 2. Random index Value (R1).

Matrix Size	RI	Matrix Size	RI
1	0	9	1,45
2	0	10	1,49
3	0,58	11	1,51
4	0,90	12	1,48
5	1,12	13	1,56
6	1,24	14	1,57
7	1,32	15	1,59
8	1,41		

4. Logical Consistency

In making decisions, an assessment that has high consistency is needed so that the results are accurate. Authentic results can be obtained by applying an overall consistent assessment by considering a consistency ratio of 10% which is measured using the AHP method in equation (1). If the consistency is > 10% then the assessment must be increased because it is still considered random.

$$CI = \frac{\lambda\, max - n}{n-1} \quad \text{and CR} = \frac{CI}{RI} \qquad (1)$$

where, Ci is consistency index, CR is Ration consistency, RI is random index, and n is size of the matrix.

3. Results and Discussion

3.1. Value Chain Mapping

In the straw mushroom value chain pattern, there are four main components that form the value chain, namely products, actors, activities and inputs (Figure 2). The product referred in the picture is a straw mushroom that is produced to be delivered to consumers. Straw Mushrooms have perishability and low durability while product freshness is a measure of marketing quality. Therefore, the longer the marketing pattern, the lower the freshness quality. The straw mushroom value chain structure consists of six value chain patterns involving five actors, namely farmers, traders, wholesalers, retailers and consumers. These services/institutions are supporting actors of the straw mushroom value chain.

Explanation of the functions and roles of actors in the value chain of hay mushroom commodities, namely:

1. Farmers or producers

Farmers are the parties who carry out the cultivation of the straw mushrooms. The productivity of the mushrooms in one crop averages 200-250 kg per mushroom house. The process of cultivating straw mushrooms to harvest takes 23 days, with details: the composting process about 7 days, the planting period until ready to harvest about 9 days and the length of harvest from beginning to end about 12 days. Straw mushrooms produced are sold to traders, wholesalers, or retailers.

2. Traders

Traders play a role in buying crops from farmers and also carry out collection, packaging, and delivery to wholesalers and retailers as well as selling directly to consumers. The trader purchases straw mushrooms in one growing season as much as 100-1,000 kg depending on the capital and availability of the mushrooms. Next, the merchant will sell the product to wholesalers and retailers.

3. Wholesaler

Wholesaler play a role in buying straw mushrooms from traders and farmers in a large volumes. The average purchase is normally in about 2,000-3,000 kg in one harvest season. Wholesalers usually market this product also to retailers in local markets and outside Karawang, for example Jakarta, Bogor, Tangerang and other cities.

4. Retailers

Retailers play a role in buying straw mushrooms from traders, wholesalers or directly from farmers to be sold to local consumers for small volume sizes of around 20-30 kg per one harvest season.

Among the actors in the value chain pattern, usually traders are the most influential parties. This is because traders have a big role in marketing and providing capital. In marketing straw mushrooms, farmers rely heavily on traders. More than 50% of farmers sell their crops to traders. The selling price of straw mushrooms tends to be around 20-30 percent cheaper than other middlemen. Even in the procurement of capital, farmers are still very dependent on traders. This is because the majority of farmers do not have sufficient capital, so they are forced to

borrow from traders to get raw materials whose prices are around 20-30% higher than the cash price.

Activities carried out by value chain actors along the marketing pattern include production, collection, sorting, packaging, transportation, and sales. Input is an instrument needed to carry out every activity in the value chain pattern, from product manufacturing to distribution to final consumers. Some of these inputs include labor, information, skills, knowledge, and capital. The quantity and quality of products, performance of actors, activities and value chain inputs are influenced by business processes, from planning, procurement, production (processing), distribution and returns. Based on field observations, business processes need to be improved in line with value chain performance.

Figure 2. The Straw Mushroom Value Chain Pattern.

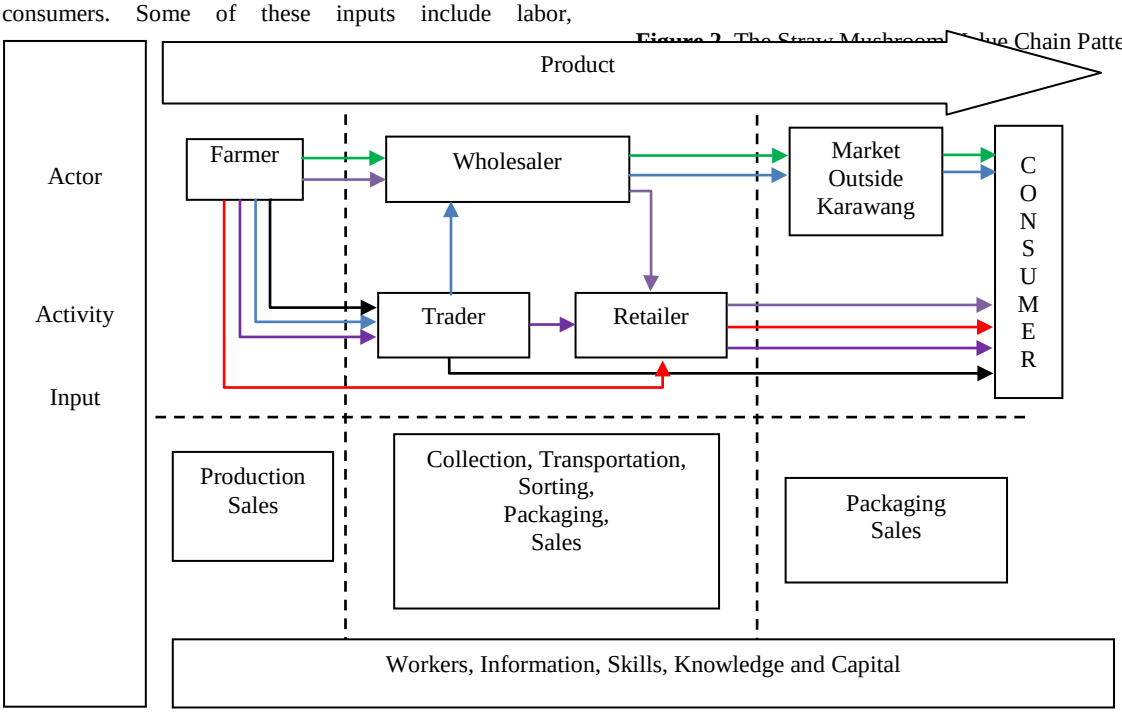

3.2. Performance Measurement of the Straw Mushroom Value Chain

The measurement of the performance of the straw mushroom value chain consists of objectives, criteria, sub-criteria, actors and alternatives. The aim is to measure the performance of the hay mushroom value chain as shown in Figure 1. The criteria contained in the hierarchical structure are the hay mushroom business processes, which consist of planning, procurement, production, distribution and returns, while the sub-criteria are performance parameters in the form of quality, risk and added value. The actors directly involved in the performance of the straw mushroom value chain are farmers (producers), traders, wholesalers and retailers.

Based on the comparison of pairs between criteria, the measurement results show that the production business process with a value of 0.386 is the most important process compared to other business processes (Figure 3). This is because the production process is the main process in determining the success of the straw mushroom business. Things that can affect the production process or straw mushroom cultivation are weather, water quality, seed quality, pests and diseases and flooding. So far, farmers get mushroom seeds directly from nurseries outside the city, or through seed stalls in the city. Farmers have not been able to cultivate straw mushrooms independently; this is due to the lack of farmers' abilities. In addition to production, the next business process is procurement, distribution, planning and returns.

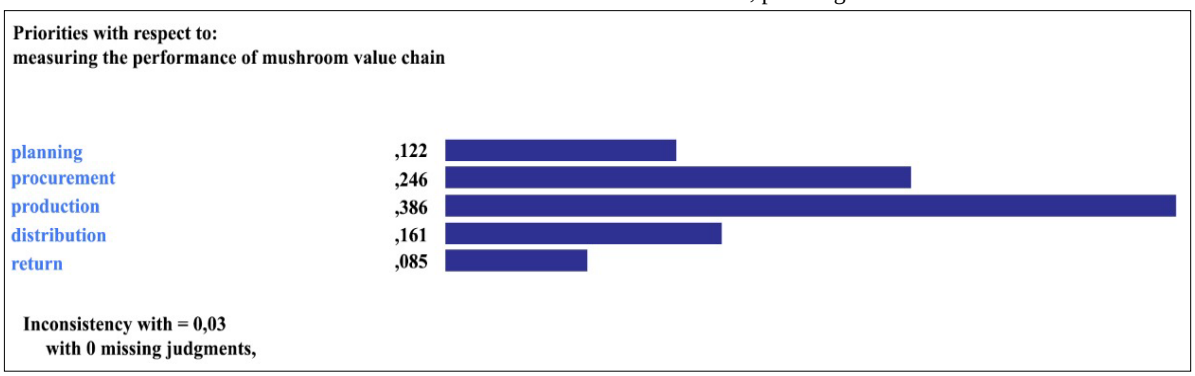

Figure 3. Comparison of Inter-Criteria Pairings

The comparison of pairs of criteria in measuring the performance of the straw mushroom value chain can be seen in Table 3. In terms of performance parameters, the most important element in the planning process is quality followed by added value, then risk. In the procurement process, the most important element is quality, followed by risk and finally added value. In the production process, the most important element is risk, the second element is

added value, and the last element is quality. An important element in the distribution business process is quality, followed by value added and finally risk. Meanwhile, in the return business process, the most important element is risk, followed by quality and added value. In general, quality performance parameters are considered as the most important element when compared to other performance parameter elements; this is because quality greatly affects the quality of mushroom products that will be distributed to consumers and can be a measure of consumer confidence.

Table 3. Pairwise Comparisons Between Criteria in Value Chain Performance Measurement.

Performance Parameters	Planning	Procurement	Production	Distribution	Return
Quality	0,493	0,540	0,196	0,594	0,311
Risk	0,196	0,297	0,493	0,157	0,493
Value-Added	0,311	0,163	0,311	0,249	0,196
Consistency Index	0,05	0,01	0,05	0,05	0,05

Assessment of performance parameters based on value chain actors can be seen in Table 4. Farmers are very interested parties in the production and return process, both in terms of quality, risk and value-added parameters. Meanwhile, traders are very interested in quality parameters in the procurement process. This is because quality is closely related to the quality of the final product that will be distributed to consumers and becomes a measure of consumer confidence.

Wholesalers have a strong interest in the parameters of quality, risk and value-added in the distribution process. In the product procurement process, wholesalers have a strong interest in quality and value-added. This is because the quality of the product and the value-added of the product are the benchmarks in the success of the mushroom business. Moreover, large traders usually buy products in large quantities and distribute them to other regions. In addition, straw mushroom is a product that is not durable and easily damaged. Product durability is only up to 1-2 days. It is very necessary to handle efficiently and effectively in the distribution process. Thus, the parameters of quality, risk and value-added are very important. Based on research conducted by Sakinah (2020), the straw mushroom can last up to 6 days if stored with PVC film packaging at the temperature of 15 degrees Celcius. Therefore, it might reduce business losses.

Meanwhile, retailers are a party that has less interest than other value chain actors. Retailers are the value chain actors with the lowest risk compared to other actors. Moreover, the number of product purchases is not as many as other intermediary traders and product marketing is only carried out in traditional markets, which do not demand high quality. The consistency index value of all assessments between sub criteria is below 10%, so it is consistent.

Table 4. Pairwise Comparisons Between Sub Criteria in Value Chain Performance Measurement

Value Chain Actor	Quality	Risk	Value Add
Planning			
Farmer	0,124	0,276	0,138
Trader	0,389	0,195	0,276
Wholesaler	0,299	0,391	0,391
Retailer	0,188	0,138	0,138
Consistency Index	0,05	0,05	0,05
Procurement			
Farmer	0,276	0,391	0,138
Trader	0,195	0,276	0,276
Wholesaler	0,391	0,195	0,391
Retailer	0,138	0,138	0,195
Consistency Index	0,05	0,05	0,05
Production			
Farmer	0,391	0,461	0,391
Trader	0,276	0,236	0,195
Wholesaler	0,195	0,168	0,276
Retailer	0,138	0,135	0,138
Consistency Index	0,05	0,08	0,05
Distribution			
Farmer	0,138	0,124	0,107
Trader	0,276	0,299	0,293
Wholesaler	0,391	0,389	0,415
Retailer	0,195	0,188	0,185
Consistency Index	0,05	0,05	0,03
Return			
Farmer	0,391	0,395	0,395
Trader	0,276	0,278	0,239
Wholesaler	0,195	0,163	0,198
Retailer	0,138	0,163	0,168
Consistency Index	0,05	0,02	0,02

In alternative elements, the performance attribute shows the reliability value which is considered the most important element compared to other elements. This shows that the level of consumer trust in the mushroom value chain actors in meeting consumer demand on time and in perfect condition needs to be carefully considered. This is because reliability is necessary to ensure successful sustainable value chain performance. The value chain performance assessment can be seen in Table 5.

The combined assessment of the edible mushroom value chain performance measurement is shown in Figure 4. The most important performance attribute was reliability (37.4%), followed by cost (22.6%), agility (20.1%) and lastly responsiveness (19.9%). Reliability should receive greater attention where the delivery of ordered products must be delivered in full, delivery accuracy and products delivered must be perfect both in quality and quantity.

In cost performance, it is necessary to pay attention to all expenses such as production and labor costs. In agility performance, what needs to be considered is the response to changes, including the fulfilment of production capacity and product stock inventory. Meanwhile, on responsiveness performance, things that need to be considered are the cycle time to obtain seeds and other input facilities, as well as the production cycle time.

Table 5. Performance Assessment of Straw Mushroom Value Chain in Karawang Regency.

Performance Attributes	Planning	Procurement	Production	Distribution	Return
Reliability	0,397	0,392	0,357	0,402	0,319
Responsiveness	0,195	0,224	0,201	0,188	0,143
Agility	0,182	0,179	0,197	0,251	0,216
Cost	0,226	0,205	0,245	0,158	0,322
Consistency Index	0,005	0,04	0,06	0,05	0,004

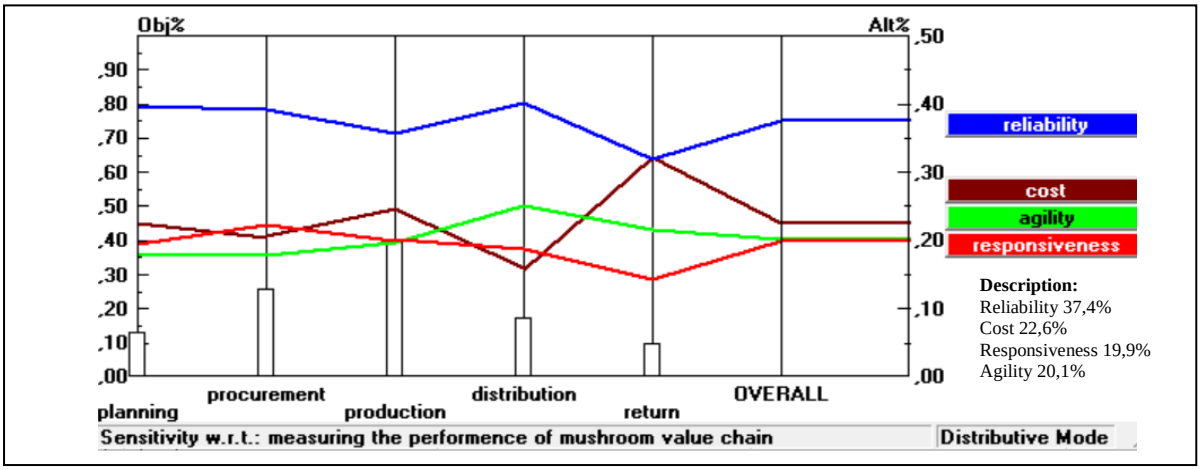

Figure 4. Combined Measurement of Straw Mushroom Value Chain Performance.

4. Conclusion

The actors of the straw mushroom value chain in Karawang consist of 5 actors, namely farmers, traders, wholesalers, retailers and consumers. The pairwise comparison results show that the production process (0.386) was the most important business process compared to procurement (0.246), distribution (0.161), planning (0.122) and return (0.085). From the results of measuring the performance of the mushroom value chain, the attributes that need great attention are reliability performance attributes (37.4%), followed by cost (22.6%), agility (20.1%) and responsiveness (19.9%). The essential things that must be considered in the performance of the reliability element are the delivery of product orders that must be sent as the consumer's demand, the accuracy of delivery, and the delivery of the product must be in perfect condition, both in quality and quantity.

Acknowledgments

The author would like to thank the Faculty of Agriculture, Computer Science and Research & Community Service (LPPM) Universitas Singaperbangsa Karawang, West Java, Indonesia, for their support for the implementation of this research.

References

Abdel-Mawgoud M, Khedr FG and Mohammed EI. 2019. Phenolic Compounds, Antioxidant and Antibacterial Activities of Rhus flexicaulis Baker. In *Jordan J Biol Sci.*, **12 (1)**: 17-21.

Al-Ghamdi, AY, Fadlelmula AA and Abdalla MOM. 2020. Total Phenolic Content, Antioxidant and Antimicrobial Activity of Ruta chalepensis L. Leaf Extract in Al-Baha Area, Saudi Arabia. In *Jordan J Biol Sci*., **13**: 675-680.

Ashraf SA, Elkhalifa AEO, Siddiqui AJ, Patel M, Awadelkareem AM, Snoussi M, Snoussi M, Ashraf MS, Adnan M and Hadi S. 2020. Cordycepin for Health and Wellbeing: A Potent Bioactive Metabolite of an Entomopathogenic Medicinal Fungus Cordyceps with Its Nutraceutical and Therapeutic Potential. *Molecules.*, **25(12)**:1-21.

Atila F. 2019. A Useful Way to Dispose of Phenolic-rich Agro-industrial Wastes: Mushroom Cultivation. *Journal EJENS - Eur J Eng Nat Sci*, **3(2)**: 32-41.

Beiragh RG. 2020. An integrated multi-criteria decision making model for sustainability performance assessment for insurance companies. *Sustainability (Switzerland).*, **12(3)**: 1-24.

Bunyan Unel F and Yalpir S. 2019. Valuations of building plots using the AHP method. *Int J Strategic Prop Manag*, **23(3)**: 197–212.

Datta P. 2019. Model-based strategic planning for strengthening mushroom entrepreneurship: insights from a sub-Himalayan Region of West Bengal, India. *GeoJournal*., **86**: 145-148.

Florescu MS, Ceptureanu EG, Cruceru AF and Ceptureanu SI. 2019. Sustainable supply chain management strategy influence on supply chain management functions in the oil and gas distribution industry. *Energies*., **12(9)**: 1-16 .

Fontes A, Alemany-Pagès M, Oliveira PJ, Ramalho-Santos J, Zischka H and Azul AM. 2019. Antioxidant versus pro-apoptotic effects of mushroom-enriched diets on mitochondria in liver disease. In *Int J Mol Sci*., **20(16)**: 1-35.

Grimm D and Wösten HAB. 2018a. Mushroom cultivation in the circular economy. *Appl Microbiol Biotechnol.*, **102(18)**: 7795–7803.

Grimm D and Wösten HAB. 2018b. Mushroom cultivation in the circular economy. In *Appl Microbiol Biotechnol*., **102(18)**: 7795–7803.

Improta G. 2018. Use of the AHP methodology in system dynamics: Modelling and simulation for health technology assessments to determine the correct prosthesis choice for hernia diseases. *Math Biosc*, **299**: 19–27.

Kora AJ. 2020. Nutritional and antioxidant significance of selenium-enriched mushrooms. *Bulletin Nat Res Centre*, **44(1)**: 1-9.

Leśniak A, Kubek D, Plebankiewicz E, Zima K and Belniak S. 2018. Fuzzy AHP application for supporting contractors' bidding decision. *Symmetry*., **10(11)**: 1-14.

Liu M. 2020. A comparative transcriptome analysis of volvariella volvacea identified the candidate genes involved in fast growth at the mycelial growth stage. *Genes.*, **11(2)**: 1-14.

Mapanga A, Miruka CO and Mavetera N. 2018. Barriers to effective value chain management in developing countries: New insights from the cotton industrial value chain. *Prob Perspectives Manag*, **16(1)**: 22–35.

Muloi D, Alarcon P, Ombui J, Ngeiywa KJ, Abdullahi B, Muinde P, Karani MK, Rushton J and Fèvre EM. 2018. Value chain analysis and sanitary risks of the camel milk system supplying Nairobi city, Kenya. *Pre Vet Med.*, **159:** 203–210.

Pop RM, Puia IC, Puia A, Chedea VS, Leopold N, Bocsan IC and Buzoianu AD. 2018. Characterization of Trametes versicolor: Medicinal mushroom with important health benefits. *Not Bot Horti Agrobo.*, **46(2)**: 343–349.

Robinson B, Winans K, Kendall A, Dlott J and Dlott F. 2019. A life cycle assessment of Agaricus bisporus mushroom production in the USA. *Int J Life Cycle Assess.*, **24(3)**: 456–467.

Saaty TL. 1990. How to make a decision: The analytic hierarchy process. *Eur J Oper Res.*, **48(1)**: 9–26.

Sachan S. 2020. Cost benefit analysis and marketing of mushroom in Uttar Pradesh. *Plant Arch*, **20**: 2532–2536.

Sakinah MJN. 2019. A review: Production and postharvest management of Volvariella volvacea. *Int Food Res J*, **26 (2)**: 367–376.

Sakinah MJN. 2020. Evaluation of storage temperature, packaging system and storage duration on postharvest quality of straw mushroom (Volvariella volvacea). *Food Res*, **4(3):** 679–689.

Setyabudi AG. 2018. *Smart Decision Support System Risk Management of Starfruit Commodity Supply Chain Risk.* Dissertation. Bogor Agriculture University (IPB), Bogor, Indonesia.

Sevinç A, Gür Ş and Eren T. 2018. Analysis of the difficulties of SMEs in industry 4.0 applications by analytical hierarchy process and analytical network process. *Processes.*, **6(12)**: 1-16.

Susanawati SP and Fauzan M. 2019. Risk of shallot supply chain: An Analytical Hierarchy Process (AHP) model in Brebes Java, Indonesia. *Int J Sup Chain Mgt.*, **8(1)**: 124–131.

Touil A, Echchatbi A and Charkaoui A. 2019. International Journal of Supply and Operations Management. *Int J Supply and Oper Manage.*, **6(1)**: 30–50.

JJBS

Volume 14, Number 5,December 2021
ISSN 1995-6673
Pages 999 – 1008

Jordan Journal of Biological Sciences

Integrative survey for ant diversity: exhaustive deployment of several ant collection methods in Biological Education and Research Forest of Universitas Andalas, Indonesia

Henny Herwina[1,*] , Rijal Satria[2], Yaherwandi[3], Yositaka Sakamaki[4], Mairawita[1], Diyona Putri[5], Ahmad Efendi[1], Yusuke Kusuhata[4], Muhammad N. Janra[2]

[1]Animal Taxonomy Laboratory, Biology Department, Faculty of Mathematics and Sciences, Universitas Andalas, Indonesia, [2]Department of Biology, Faculty of Mathematics and Natural Sciences, Universitas Negeri Padang, Padang 25131, West Sumatra, Indonesia; [3]Department of Pests and Plant Diseases, Faculty of Agriculture, Universitas Andalas, 25163 West Sumatra, Indonesia, [4]Entomological Laboratory, Faculty of Agriculture, Kagoshima University, Korimoto 1-12-24 Kagoshima, 890-0065, Japan ; [5]Department of Biological Sciences, Graduate School of Science and Engineering, Tokyo Metropolitan University, Tokyo, Japan

Received: March 8, 2021; Revised: June 21, 2021; Accepted: September 16, 2021

Abstract

A long period of ant sampling has been conducted in Biological Education and Research Forest (BERF), Universitas Andalas, West Sumatra, Indonesia by deploying several methods i.e. direct hand collection in rotten logs, at flowering plants and at bird nests, Quadra Protocol for sampling diurnal and nocturnal ground ants and subterranean trap for soil ants. A total of 100 ant species which taxonomically grouped into 41 genera, 15 tribes and eight subfamilies resulted from this study. Myrmicinae became subfamily with the most species recorded (46 species), after the Formicinae with 28 species and Ponerinae with 11 species. On the other hand, the rest subfamilies were represented with less species e.g. Dolichoderinae (6 species), Dorylinae (3 species), Pseudomyrmicinae (3 species), Ectatommine (2 species) and Ambliponinae (1 species). *Pheidole* was genus with the most species recorded (17 species) followed by *Crematogaster* (7 species) and *Polyrhachis* (6 species). Quadra Protocol became the most effective method to record ant species in this study (42 species), subsequently followed by purposive hand collection method (40 species), subterranean trap (10 species), direct collection in rotten logs (8 species), observation at flowering plants (8 species) or collection from within bird nests (4 species). Despite the robustness of inventory produced from this study, it is indicated that BERF area still holds more ant species that are not recorded by research done so far.

Keywords: Ant diversity, Biology Education and Research Forest, ground ants, subterranean ants, arboreal ants

1. Introduction

Ants are estimated to comprise around 30% of terrestrial faunal biomass in the world (Hölldobler and Wilson, 1990). Ants are essential ecological components as they have direct interaction with plants (Putri *et al.* 2016), soil organisms (Meer, 2012) and other organisms in the most of trophic levels. Their roles usually relate to seed consumption (Andersen, 1990; Majer, 1990) and dispersal (Majer, 1990). Acting as predators for pest insects (Choate and Drummond, 2011), ants retain equal value with other predators such as lady beetles, lacewings and mantis (Saleh et al., 2010; Sanda and Sunusi, 2014).

Ants have been recognized as a useful ecological indicator as similar as with bees, as they exist in abundant numbers and ubiquitously, even at a disturbed area (Andersen, 1990; Schreven at al., 2018; Munyuli, 2012). Ants are very sensitive to environmental disturbances, hence they rapidly respond to any change in their habitat (Van Der Woude *et al*., 1997; Andersen, 1990). On the other hand, ants build stationary nests with limited foraging range, which helps with avoiding competition among species and colonies (Agosti *et al.*, 2000).

Ants have become long-standing research objects. They are reported to have high diversity in tropical rainforest of Southeast Asia (Yamane, 1996; Chung and Maryati, 1996; Brühl *et al*, 1998; Idris *et al*., 2002). In Indonesia, ant diversity was studied from various locations in Java, such as at Bogor Botanical Garden, West Java, where 216 ant species inventoried (Ito *et al*., (2001); 48 species were recorded from conservation area in Kepulauan Seribu, Jakarta (Rizali *et al*., 2008); 37 species were reported from around Mount Krakatou in Sunda Strait (Asfiya *et al*., 2010. Meanwhile in Sumatra, 76 ant species were recorded from oil palm plantation in West Sumatra and Riau (Herwina *et al*., 2020), 27 ant species were collectively observed across altitudinal gradients in Mt. Talang, West Sumatra (Herwina *et al*., 2020), in addition to 18 species

* Corresponding author. e-mail: hennyherwina@sci.unand.ac.id.

that were found associated with white germ in potato plantation of highland agricultural area (Herwina, 2020).

Universitas Andalas is located in Limau Manis, Pauh Subdistrict, approximately 15 km from the downtown of Padang City, West Sumatra Province. Universitas Andalas covers 500-hectare area, where its forested surrounding is considerably representative to hold various topics of field research, including those in entomology. The prominent forested area is situated within the Biological Education and Research Forest of approximate 150-hectare area. The BERF site harbors lowland tropical rainforest connected with the Bukit Barisan Range (Rizaldi *et al*., 2018). It has been the ground for ant research since more than two decades ago (Herwina *et al*, 2018). This study aimed to trackback the progress of works on ants in Universitas Andalas campus complex, as well as to analyze the ecological aspects of ants, such as species diversity and composition.

2. Materials and Methods

2.1. Study area and sampling methods

The data used in this study was synthesized from published and unpublished works mainly conducted within Biological Education and Research Forest (hereinafter BERF), Universitas Andalas, Indonesia (GPS coordinates 1°00'S, 100°30'E; Figure 1). The samplings were undertaken at ten sites established between 250 to 450 m elevation in BERF, with measured temperature between 28 to 32°C. Sampling sites can be detailed as Site 1 (permanent plots for plant ecological study, dominated by secondary vegetation and medium trees), Site 2 (water dam 1, located at forest edge with early successive vegetation), Site 3 (camping ground with grasses and tall trees), Site 4 (water dam 2 inside forested area of BERF), Site 5 (bushy area in the border of BERF), Site 6 (Puncak Ixora, a peak of small hill with big trees and other primary vegetation), and Site 7 (bushy area in adjacent to Site 1). Site 8 to 11 are located on the borderline between BERF and campus area, separated by concrete road and each marked with field station or research lodge. Methodology applied in preceding and recent works conducted at those sites can be summarized as follow (also see Table 1): at Site 1 to 6, quadra protocol for ant collection (Hashimoto *et al*., 2001), which repeated between 2013 to 2016 (*unpublished*); Site 7, subterranean trap and probe (Herwina *et al*., 2018); Site 8, rotten log ant collection (*unpublished*); Site 9, ant collection in bird nests (Herwina *et al*., 2021); Site 10, hand collection method (ongoing since 2010; *unpublished*); and Site 11, hand collection and recording ant visitation at flowering plants (2019, *unpublished*). The exact position of sampling sites in BERF can be seen in Figure 1 below.

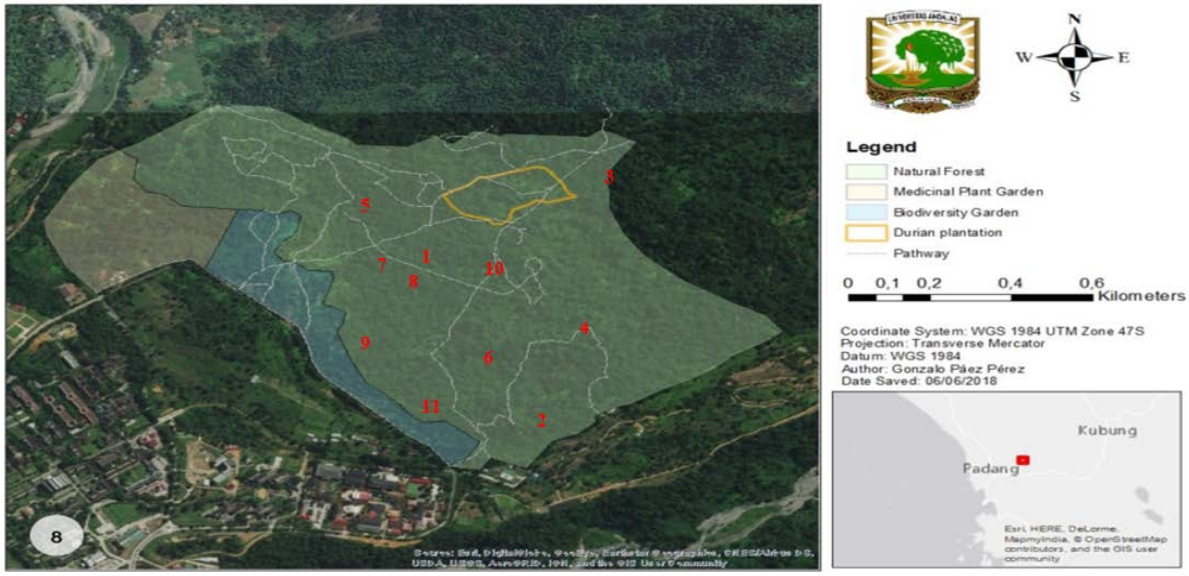

Figure 1. Sampling sites for ant collection at Biological Education and Research Forest (BERF), Universitas Andalas. No 1-11 = sites numbers.

2.2. Species Species Identification

Sampled ants were sorted to morphospecies and genus level before prepared according to the standard preparation for ant specimen. Identification process was guided by appropriate literatures (Hashimoto, 2003; Jaitrong, 2011; Bolton, 2014) in addition to being compared with specimen housed at the Animal Taxonomy Laboratory of Biology Department, Universitas Andalas. Any specimen resulted from the works listed here was also stored in this place.

2.3. Data Analysis

Ants were grouped into their taxonomic orders as follows; species, genus and subfamily. Individual and species number were counted and tabulated. The Shannon-Wiener formula (Magurran, 2004) was used to calculate species diversity, while Estimate S Veers. 9.0 was for calculating the rarefaction curves of observed and estimated number of ant species. The formula for species diversity is below:

$$H' = -\sum_{i=1}^{n} pi \ln pi$$

H'= Species diversity index
pi = Total proportion of sample from the i^{th} species

3. Results and Discussion

This study recorded a total of 100 ant species from 43 genera and eight subfamilies. They were identified from overall sampling efforts within BERF that spanned from 2010 to 2019 (Table 1, Apendix 1). The subfamily Myrmicinae was observed with the highest species number (46 species), followed by 28 species of Formicinae, 11 species of Ponerinae, 3 species each for Dorylinae and Pseudomirmicinae, two species of Ectatomminae and one species of Ambliponinae (Appendix 1). Myrmicinae was frequently reported as family with the highest species number observed in many previous studies (such as Shattuck, 1999; Herwina *et al*., 2013). *Pheidole* was genus with the most species recorded (17 species) in this study, followed by *Crematogaster* (7 species) and *Polyrhachis* (6 species). *Pheidole* was reported as genus with the highest species number in previous studies, including among subterranean ants (Herwina *et al*., 2018), within the species inventory from conservation forest and oil palm plantation in West Sumatra (Herwina *et al*., 2020) or from the protected forest in Riau (Putri *et al*., 2021). *Crematogaster* and *Polyrhachis* were also previously recorded as genera with high species number (Herwina *et al*., 2020).

Table 1. Sampling times, sites, methods, total number of species (S), total number of individuals (N), species increment (SI), and species accumulation (SA) synthesized from works on ants in BERF, Universitas Andalas

Site #	Time	Site remark	Methodology	S	N	SI	SA
1	2013	Permanent plots inside primary forest	Quadra protocol	25	336	0	25
2	2014	Water dam 1, secondary forest	Quadra protocol	34	1289	12	37
3	2014	Camping ground, open grassland with trees	Quadra protocol	35	1510	12	49
4	2014	Water dam 2, secondary forest	Quadra protocol	19	1121	0	49
5	2016	Bushes	Quadra protocol	32	931	13	62
6	2016	Hilly forested area	Quadra protocol	42	2316	16	78
7	2017	Bushes and thickets	Subteranean ant collection	10	369	3	81
8	2018	Primary forest interior	Rotten log ant collection	8	62	4	85
9	2018	Forest edge	Collection from bird nests	4	19	1	86
10	2010, 2012, 2018	Primary forest interior	Hand collection applied purposively	40	-	14	100
11	2019	Forest edge	Hand collection, photography documentation	8	-	0	100
Diversity Index (H')			3.25				

The inventory of ant species and subfamilies recorded in this study exceeded any previous study from other locations in West Sumatra, which included natural reserves, agricultural and household area. The BERF, in overall, can be considered as good habitat for ants, as high species diversity observed in this study (H'=3.25, Table 1) . The ants recorded here were more diverse than those observed at white germ and potato plantation in Sumatran highland agricultural area (Herwina *et al*., 2020c), at oil-palm plantations and its conservation forest in Solok Selatan, West Sumatra (Herwina *et al*., 2020d), at some altitudes of Mount Talang, West Sumatra (Herwina *et al*., 2020e), or at several islands offshore of Sulawesi (Asfiya *et al*., 2010).

Site six contributed the highest among other sites, in terms of collecting 2,316 ant individuals that identified into 42 species recorded and increased 16 new records into the species accumulation record (Table 1). Site 3 (1,510 individuals, 35 total species, 12 new records), Site 2 (1,280 individuals, 34 total species, 12 new records) and Site 5 (931 individuals, 32 total species, 13 new records) were also significantly increasing species inventory to BERF area. The works on Site 10 and 11 were majority based on sporadic rapid assessment on ant species without paying much attention on collecting individual, hence no exact number provided for collected individual. The work on Site 10, however, recorded total 40 species with additional 14 new records to the BERF's ant species inventory. In addition to sampling efforts and methodology applied in collecting ants, physical-ecological factors were also thought to play role in having high sampling result. Sites with high individual number, total species and/or species increment (Site 2, 3, 4, 5, 6 and 10) were with denser secondary or primary cover, thicker leaf litter coverage on ground surface and more organic resources needed by ants than the other sites. The abundance of organic materials within the tropical vegetated area are useful for food, nesting site or other purposes for ants; hence the high ant diversity and population found in this type of habitat (Rizali *et al*., 2008; Sabu *et al*., 2008; Souza-Campana *et al*., 2017).

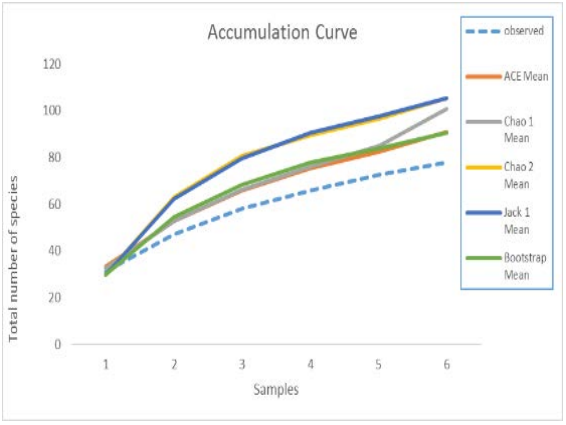

Figure 2. Accumulation curve of ant species collected by using quadra protocol at BERF

When counting the result method-wise, there was difference observed on the number of species resulted from each sampling method. Quadra protocol singly and remarkably accumulated a total of 78 ant species from six sites within the BERF area (Figure 2). Moreover, the

computerized calculation performed using the data from quadra protocol provided estimation curve that predicted the possibility of actual number of 85-100 ant species could be recorded at BERF if this method continuously applied. Quadra protocol involved thorough sampling procedure by simultaneously applying four collection techniques (hand collection, leaf litter sifting, soil core sampling and honey bait trap) within three sections of a 180 m transect. Hence, the techniques can be complimentary in collecting various ants with different life habits, instead of single technique or method that focus on one specific life habit. Given the species increasing trend that showed in Figure 2, indicated that further sampling efforts will potentially enrich the inventory of ant species in BERF.

Lophomyrmex bedoti was frequently collected in BERF (82%), along with *Pheidole aristotelis* and *Pheidole* sp 3. of HH (73% each), tailed by *Diacamma holosericum* and *Acanthomyrmex ferox* (64%). *Lophomyrmex* was reported as generalist foragers and tropical climate specialist, which explain their successfulness in adapting to various habitats (Brown, 2000). Genus *Pheidole* was recorded with many species in this study, while *D. holosericum* and *A. feroxs* were the two species with prominent frequency. All of these taxa were collected using quadra protocol, which may emphasize the effectiveness of this sampling method to detect common and abundant ant species.

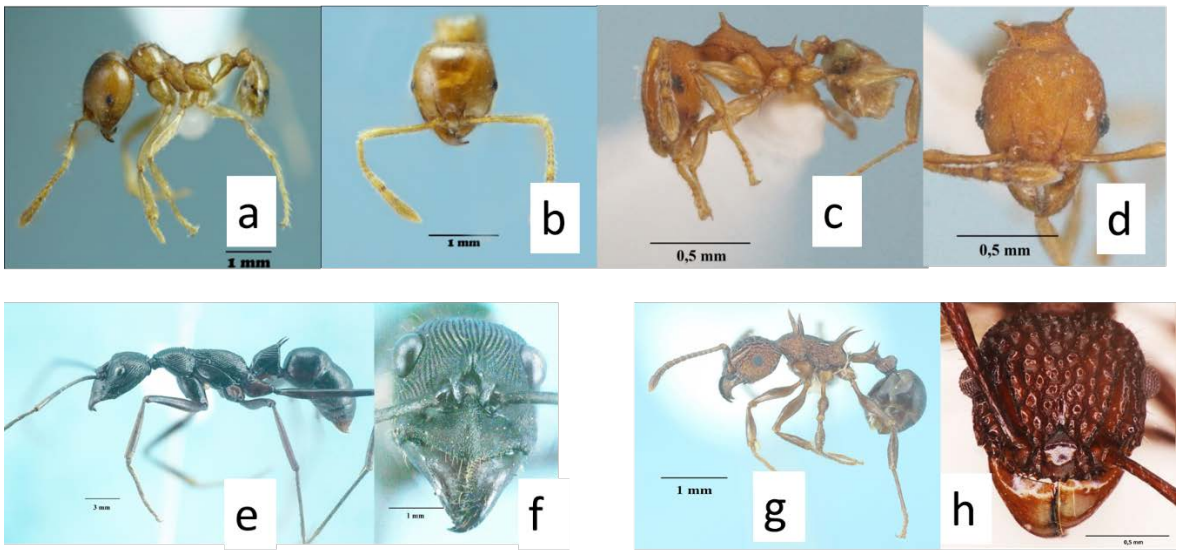

Figure 3. Abundant ant species in BERF (lateral and anterior-rostral aspect). A,b = *Lophomyrmex bedoti*. C,d = *Pheidole aristotelis*, e,f = *Diacamma holocericum*, g,h = *Acanthomyrmex ferox.*

Diacamma ants were observed to prefer the secondary portion of BERF, similarly with *A. ferox*. It is thought to be related with their feeding habit and in connection to the resource available in such secondary habitat. The first taxon mainly consists of predatory species, while the later more of seed harvester (Brown, 2000). Some species were infrequently observed at one or a few sites with a handful individuals collected. These included *Dolichoderus* spp., *Aenictus* spp., *Gnamptogenys coxalis*, *Camponatus* spp., *Odontomachus minangkabau*, *O. rixoxus*, *Carebara* cf. *affinis*, *Meranoplus mucronatus*, *Crematogaster medigmiani*, *Paratrechina* sp. 1 or *Anoplolepis gracilipes* (Appendix 1).

The current study also recognized the existence of alien, tramp and invasive ant species from sites in BERF, i.e. *Tapinoma melanocephalum*, *Anoplolepis gracilipes*, and *Paratrechina longicornis*. These categories are attached to species that extend their distribution outside their original range by adapting and invading new territory (Pfeiffer *et al*., 2008). The presence of alien, tramp and invasive ant species in BERF gave strong indication of interference incurred from high human activities, which in many cases, negatively impacts the habitat for wildlife. The movement and distribution of alien, tramp and invasive species have been thought to be mediated by human activities (Pfeffer et al., 2008; Wetterer 2009, 2010). Since these alien, tramp and invasive species have good adaptability to new or disturbed habitats, they can also negatively influence the native communities (Pfeffer et al., 2008). Hence, from the ecological standpoint of ants, this study can provide further recommendation to reduce human interference within the BERF area in order to maintain better habitats therein.

4. Conclusion

Combining some collection methods for sampling ant show significant species number can be recorded at Biological Education and Research Forest of Universitas Andalas. The total species number accumulated in this study was the highest among other studies reported from Sumatra. Quadra Protocol, a standardized method for rapid assessment of ants, collected prominent number of species among other methods listed in this study as well as effective to detect frequent and abundant ant species. The analysis on the procured data indicates the possibility to record more ant species given the field exploration continued. Alien, tramp and invasive ant species were also observed during the study, indicated existing interference incurred from human activities within BERF.

Acknowledgements

We would like to express our gratitude to Seiki Yamane (Kagoshima University) for his valuable assistance in identifying ant specimens. This research was

funded by Universitas Andalas' Research Funding Scheme with contract number T/16/UN.16.17/PP.OK-KRP2GB/LPPM/2019 on behalf Henny Herwina.

References

Agosti D, Majer JD, Alonso LE and Schultz TR. 2000. **Ants: standard methods for measuring and monitoring biodiversity. Biological diversity hand book series**. Washington & London, 280 pp.

Andersen AN. 1995. Measuring more of biodiversity: genus richness as a surrogate for species richness in Australia ant faunas. *Biol Conserv*, **73**: 39-43.

Andersen AN. 1990. The use of ant communities to evaluate change in Australian terrestrial ecosystems: a review and a recipe. *Proc. Ecol. Soc. Aust.,* **16**: 347–357.

Asfiya W, Ubaidillah R and Yamane S. 2010. Ant (Hymenoptera: Formicidae) of The Krakataus and Sebesi and Sebuku Islands. *Treubia*, **36**: 1 - 9.

Bestelmeyer BT and Wiens JA. 2001. Ant biodiversity in semiarid landscape mosaics: the consequences of grazing vs. natural heterogeneity. *Ecol Appl*, **11**: 117-126.

Bolton B. 1994. **Identification Guide to The Genera of the World**. Hardvard University Press. London.

Bolton B. 2014. **New General Catalogue of the Ants of The World**. Harvard University Press. London.

Brown Jr WL. 2000. Diversity of Ants. In: D. Agosti, J. Majer, L. E. Alonso & T. R. Schultz (Eds), **Ants: standard methods for measuring and monitoring biodiversity**. Biological diversity hand book series. Washington & London.

Bruhl CA, Gunsalam G and Linsemair KE. 1998. Stratification of ants (Hymenoptera, Formicidae) in primary rain forest in Sabah, Borneo. *J Tropical Ecol*, **14**: 285-297.

Cadotte MW, Carscadden K and Mirotchnick N. 2011. Beyond species: functional diversity and the maintenance of ecological processes and services. *J App Ecol*, **48**: 1079-1087.

Chapin FS, Zavaleta ES, Eviner VT, Naylor RL, Vitousek PM, Reynolds HL, Hooper DU, Lavorel S, Sala OE, Hobbie SE, Mack MC and Diaz S. 2000. Consequences of changing biodiversity. *Nature*, 405.

Choate B and Drummond F. 2011. Ants as biological control agents in agricultural cropping systems. *Terr Arthropod Rev*, **4**:157-180

Chung AY and Maryati M. 1996. A comparative study of the ant fauna in primary and secondary forest in Sabah, Malaysia. In: Edward DS, Booth WE, Choy SC (eds). **Tropical Rainforest Research-Current Issues**. Kluwer Academic, Dodrecht.

Colwell RK. 2013. Estimates: Statistical estimation of species richness and shared species from samples. Version 9. User's Guide and application published at: http://purl.oclc.org/estimates.

Fittkau EJ and Klinge H. 1973. On biomass and trophic structure of the central Amazonian rain forest ecosystem. *Biotropica*, **5**: 2–14.

Hashimoto Y. 2003. **Identification Guide to the Ant Subfamili of Borneo**. Tools for Monitoring Soil Biodiversity in The ASEAN Region. DarwinInitiaive.

Herwina H, Nasir N, Jumjunidang and Yaherwandi. 2013. The composition of ant species on banana plants with Banana Bunchy-top virus (BBTV) symptoms in West Sumatera, Indonesia. *Jurnal Asian Myrmicology*, **5**: 151-161.

Herwina H, Satria R, Yaherwandi and Sakamaki Y. 2018. Subterranean ant species diversity (Hymenoptera: Formicidae) in Educational and Biological Research Forest of UniversitasAndalas. *J Ent Zool Studies*, **6 (1) 1**: 720-1724.

Herwina H, Satria R and Mairawita. 2021. **Wajah-wajah Semut Eksotis di Hutan HPPB**. Rajawali Pers. Depok.

Herwina H, Mairawita, Yulvita L, Putri P, Satria R, Janra MN, Yaherwandi and Sakamaki Y. 2020 Ant Species Composition (Hymenoptera: Formicidae) at a Highland Agricultural Area for Wheat and Potato in Alahan Panjang, West Sumatra. IOP Conf. Series: Earth and Environmental Science, **515**: 012018.

Herwina H, Sakamaki Y, Satria S and Janra MN. 2020. Ground-dwelling ants species diversity (Hymenoptera: Formicidae) at conservation forest and oil-palm plantation in Sumatra, Indonesia. *J Ent Res*, **44** (1): 113-120.

Herwina H, Dari MW, Yaherwandi and Kojima J. 2020. Altitudinal gradients of ant species diversity (Hymenoptera: Formicidae) in Mount Talang, West Sumatra, Indonesia. *J Ent Res*, **44** (3): 469-474.

Herwina H, Janra MN, Anita F, Mairawita, Yaherwandi. 2021. Are Bird Nest the habitat for Ants? Implication from Ant Inventory (Hymenoptera: Formicidae) across Various Bird Nests. IOP Conf. Series: Earth and Environmental Science, **748**: 012036.

Hölldobler B and Wilson EO. 1990. **The Ants**. Belknap Press. Harvard University Cambridge.

Idris AB, Nor SM and Rohaida R. 2002. Study on Diversity of Insect Communities at Different Altitudes of Gunung Nuang in Selangor, Malaysia. *J Biol Sci*, **2**: 505-507.

Ito F, Yamane S, Eguchi K, Noerdjito W A, Kahono S, Tsuji K, Ohkawara K, Yamauchi K, Nishida T and Nakamura K. 2001. Ant Species Diversity in Bogor Botanic Garden, West Java, Indonesia, with Descriptions of Two New Species of the Genus Laptanilla (Hymenoptera, Formicidae). *Tropics*, **10** (3): 379-404.

Jaitrong W. 2011. **Identification Guide to The Ant Genera of Thailand.** Thailand National Science Museum Press. PathumThani. 115 pp.

Janra MN, Herwina H, Febria FA Darras K and Mulyani Y A. 2019. Knemidokoptiasis in a Wild Bird, the Little Spiderhunter (Arachnotheralongirostracinireicollis), in Sumatra, Indonesia. *J Wildlife Dis*, 55(2).

Kalif KAB, Azevedo-Ramos C, Moutingio P and Malcher SAO. 2001. The effect of logging on the ground-foraging ant community of eastern Amazonia. *Stud Neotropical Fauna Env*, **36**: 215-219.

Magguran AE. 2004. **Measuring Biological Diversity**. Blackwell Science Ltd., UK.

Majer JD. 1990. Rehabilitation of disturbed land: long term prospects for the recolonization of fauna. – Proceedings of the Ecological Society of Australia, **16**: 509-519.

Meer RV. 2012. Ant interactions with soil organisms and associated semichemicals. *J Chem Eco.,l* **38**: 728-745.

Munyuli, TMB. 2012. Diversity of life-history traits, functional groups and indicator species of bee communities from farmlands of central Uganda. ***Jordan J Biol Sci***, **5 (1)**: 1-14

Pfeiffer M, Tuck HC and Lay CT. 2008. Exploring arboreal ant community composition and cooccurrence patterns in plantations of oil palm *Elaeis guineensis* in Borneo and Peninsular Malaysia. *Ecography,* **31 (1)**: 21-32

Putri D, Herwina H, Arbain A and Handru A. 2016. Ant species compositions in *Macaranga*spp trees at a conservation forest of palm oil plantation in West Sumatra, Indonesia. *J Ent Zool Stud*, **4 (1)**: 342-348.

Putri FA, Yulminarti, Herwina H, Janra MN, Satria R. 2021. Ant Community (Hymenoptera: Formicidae) at the Forest Park of Sultan Syarif Hasyim, Riau. IOP Conf. Ser.: Earth Environ. Sci. 757 012079

Rizaldi, Novarino W, Nurainas, Idris M, Nurdin J and Mairawita. 2018. An Introduction to the Biology Education and Research Forest of Andalas University. *www.repo.unand.ac.id*.

Rizali A, Bos MM, Buchori D, Yamane S and Schulze CH. 2008. Ants in tropical urban habitats: the myrmecofauna in a densely populated area of Bogor, West Java, Indonesia. Hayati *Biosci*, **15**: 77-84.

Sabu TK, Vineesh PJ and Vinod KV. 2008. Diversity of forest litter-inhabiting ants along elevations in the Wayanad region of the Western Ghats. *J Insect Sci*, **8**: 1-14.

Saleh A, Ghabeish I, Al-Zyoud F, Ateyyat M and Swais M. 2010. Functional response of the predator *Hippodamia variegate* (Goeze) (Coleoptera: Coccinellidae) feeding on the aphid *Brachycaudus helichrysi* (Kaltenbach) infesting chrysanthemum in the laboratory. ***Jordan J Biol Sci* 3 (1)**: 17-20

Sanda, NB and Sanusi M. 2014. Fundamental of Biological Control of Pest. *IJCBS Review Paper*, **1 (6)**: 1-11

Satria R, Kurushima H, Herwina H, Yamane S and Eguchi K. 2015. The trap-jaw ant genus *Odontomachus Latreille* (Hymenoptera: Formicidae) from Sumatra, with a new species description. *Zootaxa*, **4048 (1)**: 001-036.

Schreven SJJ, Perlett ED, Jarrett BJM, Marchanti NC, Harsanto FA, Purwanto A, Sykora KV and Harrison ME. 2018. Forest gaps, edge and interior support different ant communities in a tropical peat-swamp forest in Borneo, *Asian Myrmecology*, **10**: 1-14

Shattuck .SO. 1999. **Australian Ants: Their Biology and Identification**. CSIRO Publishing, Australia.

Souza-Campana DR, Silva RR, Fernandes TT, Silva OGM, Saad LP and Morini MSC. 2017. Twigs in the litter as ant habitats in different vegetation habitats in Southeastern Brazil. *Tropical Cons Sci*, **10**: 1-12.

Van Der Woude C, Andersen AN and Houswe APN. 1997 Ant communities as bioindicators in relation to fire management of spotted gum (*Eucalyptus maculate* Hook.) forest in south-east Queensland. *Memoirs Museum Victoria*, **56**: 671-675.

Yamane S. 1997. A list of Bornean ants. In Inoue, T. and Hamid, A.A. (eds). **General flowering of tropical rainforest in Sarawak. Canopy Biology Program in Sarawak (CBPS): series II**. Center for Ecological Research, Kyoto University

Wetterer JK. 2009. Worldwide spread of the ghost ant, *Tapinoma melanocephalum* (Hymenoptera: Formicidae). M*yrmecological News*, **12**: 23-33.

Wetterer JK. 2010. Worldwide spread of the tropical fire ant, *Solenopsis geminata* (Hymenoptera: Formicidae). *Myrmecological News*, **14**: 21-35.

.

Appendix 1. List of Subfamily, Tribe and Species of ants collected by using several methods in HPPB Universitas Andalas.

Sampling sites along with collection method as follows: site 1 = Permanent Plot inside BERF in 2014 (daytime Quadra Protocol), site 2 = Water Dam site point 1 in 2014 (daytime Quadra Protocol), site 3 = Camping ground, on 2014 (daytime Quadra Protocol), site 4 = Water Dam site point 2, in 2014 (Night Quadra Protocol), site 5 = bushy area, in 2016 (daytime Quadra Protocol), site 6 = Puncak Ixora, in 2017 (daytime Quadra Protocol), site 7 = bushy area and permanent plot, in 2017 (subterranean ant collection), site 8 = BERF area, purposive sampling, in 2018 (rotten log ant collection), site 9 = BERF area, purposive sampling, in 2018 (bird nest ant collection), site 10 = BERF area, purposive sampling, between 2010-2018 (hand collection), site 11 = BERF area (ants as pollinator); T = total, F = ant frequency at sampling sites. asterisk (*) indicate individual number for that species unavailable.

No.	Sp Code	Subfamily	Species	Total number of individuals at each Sites											T	F
				1	2	3	4	5	6	7	8	9	10*	11		
1	421	Amblyponinae	*Mystrium camillae* Emery, 1889										1		1	1
2	219	Dolichoderinae	*Dolichoderus* sp. 1 of HH					2							2	1
3	346		*Dolichoderus* sp. 2 of HH					1							1	1
4	81		*Dolichoderus thoracicus* (F. Smith, 1860)						17					1	18	2
5	42		*Tapinoma melanocephalum* (Fabricius, 1793)			3	6								9	2
6	36		*Technomyrmex horni* Forel, 1912		15	3	19								37	3
7	48		*Technomyrmex kraepelini* Forel, 1905			11	397		27					1	436	4
8	424	Dorylinae	*Aenictus gracilis* Emery, 1893										1		1	1
9	437		*Aenictus laeviceps* (F. Smith, 1857)										1		1	1
10	251		*Iridomyrmex anceps* (Roger, 1863)						1						1	1
11	425	Ectatomminae	*Gnamptogenys coxalis* (Roger, 1860)										1		1	1
12	28		*Gnamptogenys menadensis* (Mayr, 1887)	16		7		18					1		42	4
13	46	Formicinae	*Camponotus (Tanaemyrmex) arrogans* (F. Smith, 1858)			10	43	9						1	63	4
14	11		*Camponotus (Tanaemyrmex) odiosus* Forel, 1886	1	1	1									3	3
15	153		*Camponotus (Tanaemyrmex)* sp. 12 of SKY					2							2	1
16	426		*Camponatus* sp. 4 of HH								5				5	1
17	101		*Colobopsis leonardii* Emery, 1889						1				1		2	2
18	53		*Colobopsis* cf. *saundersi* Emery, 1889			6							1		7	2
19	39		*Dinomyrmex gigas* (Latreille, 1802)		1			1	1				1		4	4
20	6		*Polyrhachis (Myrma) hosei* Donisthorpe, 1942	2	2										4	2
21	196		*Polyrhachis (Myrma)* cf. *vindex* F. Smith, 1857		3										3	1
22	18		*Polyrhachis (Myrmatopa) phalerata* Menozzi, 1926	4	3										7	2
23	201		*Polyrhachis (Myrmhopla) armata* (Le Guillou, 1842)						1						1	1
24	158		*Polyrhachis (Polyrhachis) bihamata* (Drury, 1773)						5						5	1

No.	Sp Code	Subfamily	Species	Total number of individuals at each Sites											T	F
				1	2	3	4	5	6	7	8	9	10*	11		
25	19		*Polyrhachis (Polyrhachis) olybria* Forel, 1912	4	12			1							17	3
26	427		*Myrmoteras bakeri* Wheeler, 1919										1		1	1
27	55		*Myrmoteras* sp. 1 of HH			1									1	1
28	51		*Myrmoteras* sp. 2 of HH			1									1	1
29	57		*Oechophylla smaragdina* (Fabricius, 1775)						1					1	2	2
30	2		*Anoplolepis gracilipes* (F. Smith, 1857)	16	535		244	17	2				1		815	6
31	8		*Euprenolepis procera* (Emery, 1900)	4		6		240	3			1			254	5
32	410		*Nylanderia obscura* (Mayr, 1862)						16			`			16	1
33	43		*Nylanderia* sp. 1 of HH			10	13	2	20					1	46	5
34	13		*Nylanderia* sp. 2 of HH	4	132		43		2						181	4
35	44		*Nylanderia* sp. 3 of HH			8	40		5						53	3
36	421		*Paraparatrechina butteli* (Forel, 1913)						3						3	1
37	26		*Paraparatrechina* sp. 1 of HH	4	7	5		2	56		1				75	6
38	38		*Paraparatrechina* sp. 2 of HH		2	8									10	2
39	198		*Paratrechina longicornis* (Latreille, 1802)						4						4	1
40	10		*Pseudolasius* sp. 1 of HH		4										4	1
41	428	Myrmicinae	*Pheidole acantha* Eguchi, 2001								12				12	1
42	16		*Pheidole aristotelis* Forel, 1911	8	4	6	1		32	37	22		1		111	8
43	12		*Pheidole longipes* (Latreille, 1802)	52	24	15			434				1		526	5
44	103		*Pheidole plagiaria* Smith, 1860					3							3	1
45	307		*Pheidole quadrensis* Forel, 1900					59	2			2			63	3
46	429		*Pheidole* cf. *sauberi* Forel, 1905										1		1	1
47	7		*Pheidole* sp. 1 of HH	1		809			124	131			1		1066	5
48	14		*Pheidole* sp. 2 of HH		78	81	2	33							194	4
49	29		*Pheidole* sp. 3 of HH	22	74	38	5	5	20	1			1		166	8
50	4		*Pheidole* sp. 4 (major worker) of HH	6	8	2		6							22	4
51	197		*Pheidole* sp. 5 of HH			39			79						118	2
52	171		*Pheidole* sp. 8 of HH					264	421						685	2
53	174		*Pheidole* sp 11 of HH			4									4	1
54	192		*Pheidole* sp. 12 of HH							2			1		3	2
55	193		*Pheidole* sp. 13 of HH					1							1	1
56	240		*Pheidole* sp. 14 of HH					1							1	1
57	396		*Pheidole* sp. 17 of HH						1						1	1
58	430		*Strumigenys chimaera* Bolton, 2000										1		1	1
59	21		*Strumigenys koningsbergeri* Forel, 1905	1	2								1		4	3
60	275		*Srtumigenys* sp. 2 of HH						1						1	1
61	17		*Acanthomyrmex ferox* Emery, 1893	16	1	15	10	4	37				1		84	7

No.	Sp Code	Subfamily	Species	Total number of individuals at each Sites											T	F
				1	2	3	4	5	6	7	8	9	10*	11		
62	168		*Acanthomyrmex padanensis* Terayama, Ito & Gobin, 1998					3	16				1		20	3
63	23		*Carebara* cf. *affinis* (Jerdon, 1851)	26	56	78		6			8		1		175	6
64	314		*Carebara* cf. *pygmaea* (Emery, 1887)						11						11	1
65	291		*Cataulacus horridus* F. Smith, 1857										1		1	1
66	253		*Crematogaster (Crematogaster)* cf. *rogenhoferi* Mayr, 1879					13					1	1	15	3
67	22		*Crematogaster (Decacrema) borneensis* Andre, 1896	8	28		39								75	3
68	252		*Crematogaster (Orthocrema) longipilosa* Forel, 1907					34	412						446	2
69	409		*Crematogaster (Paracrema) coriaria* Mayr, 1872						7						7	1
70	24		*Crematogaster (Paracrema) modiglianii* Emery, 1990	33	99	29	142	29	24						356	6
71	431		*Crematogaster (Physocrema) inflata* F. Smith, 1857										1		1	1
72	228		*Crematogaster (Physocrema) sewardi* Forel, 1901						6				1	1	8	3
73	5		*Lophomyrmex bedoti* Emery, 1893	55	22	77	62	1	16	179	1		1		414	9
74	122		*Lordomyrma* sp. queen of HH		1										1	1
75	25		*Meranoplus mucronatus* F. Smith, 1857		30	4	27	2	21				1		85	6
76	**423**		*Pristomyrmex bicolor* Emery, 1900							1			1		2	2
77	175		*Recurvidris browni* Bolton, 1992					26	451						477	2
78	27		*Tetramorium kheperra* (Bolton, 1976)		6	57									63	2
79	177		*Tetramorium pacificum* Mayr, 1870						1						1	1
80	**420**		*Tetramorium smithi* Mayr, 1879						6						6	1
81	**432**		*Tetramorium* sp. 2 of HH								1				1	1
82	33		*Aphaenogaster (Deromyrma)* cf. *feae* Emery, 1889	2	1			95	6				1		105	5
83	195		*Monomorium* cf. *chinense* (Santchi, 1925)		17										17	1
84	37		*Monomorium floricola* (Jerdon, 1851)		23				1			16		1	41	4
85	45		*Monomorium* sp. of HH			99	23								122	2
86	54		*Solenopsis geminata* (Fabricius, 1804)			2				1			1		4	3
87	230	Ponerinae	*Anochetus rugosus* Donisthorpe, 1941										1		1	1
88	34		*Brachyponera* sp. 28 of SKY		46	12									58	2
89	3		*Diacamma holosericum* (Roger, 1860)	25	11	17	1	37	15				1		107	7
90	422		*Hypoponera truncata* (Smith, F. 1860)							8			1		9	2

No.	Sp Code	Subfamily	Species	Total number of individuals at each Sites											T	F
				1	2	3	4	5	6	7	8	9	10*	11		
91	434		*Hypoponera* sp. 5 of HH								12				12	1
92	231		*Leptogenys parvula* Emery, 1900										1		1	1
93	185		*Odontomachus minangkabau* Satria *et al*., 2015	1	1	3			7	8			1		21	6
94	20		*Odontomachus rixosus* F. Smith, 1857	4	12	21	4	13					1		55	6
95	191		*Odontoponera denticulata* (F. Smith, 1858)					1		1					2	2
96	1		*Odontoponera transversa* (F. Smith, 1857)	21	28	22							1		72	4
97	435		*Pseudoneoponera tridentata* F. Smith, 1858										1		1	1
98	113	Pseudomyrmecinae	*Tetraponera attenuata* F. Smith, 1887										1		1	1
99	436		*Tetraponera crassiuscula* (Emery, 1900)										1		1	1
100	437		*Tetraponera allaborans* (Walker, 1859)									1			1	1
Total number of individual				336	1289	1510	1121	931	2316	369	62	19	40	8		
Total number of species				25	34	35	19	32	42	10	8	4	40	8		

JJBS

Volume 14, Number 5,December 2021
ISSN 1995-6673
Pages 1009 – 1014

Jordan Journal of Biological Sciences

Combined Test of Jatropha Biodiesel Based on Altitude Towards Arbuscular Mycorrhizal Fungi (AMF) Combination with Cultivars and Cytokinins

R. Budiasih[1,*], Kovertina Rakhmi Indriana[1,2,*], Reni Nurhayatini[1], Roni Assafaat Hadi[1], Noertjahyani[1], Karyana K.S.[3]

[1]Department of Agriculture, Winaya Mukti University, Jl. Raya Bandung – Sumedang Km.29 Tanjungsari 45362, Sumedang Regency, West Java, Indonesia; [2]Department of Agriculture, Padjadjaran University, Jl. Raya Bandung – Sumedang Km.21 Jatinangor 45363, Sumedang Regency, West Java, Indonesia; [3]Department of Agribusiness, Winaya Mukti University, Jl. Raya Bandung – Sumedang Km.29 Tanjungsari 45362, Sumedang Regency, West Java, Indonesia

Received: March 9, 2021; Revised: June 17, 2021; Accepted: November 9, 2021

Abstract

The increase in Government policy from B20 to B30 towards Jatropha biodiesel tends to increase every year but the current condition is constrained by low yields both in quality and quantity, so that improvement efforts are needed to increase the yield of Jatropha biodiesel. The dosing of Arbuscular Mycorrhizal Fungi (AMF) with Jatropha cultivar and cytokinin concentrations is expected to increase the yield of Jatropha biodiesel in two different locations based on altitude, where the research was verificatived. The experiment starts from January to August 2019 at an altitude of 0-50 masl (lowland) and an altitude of 750-850 masl (medium land). The combination trial evaluated the Jatropha cultivar and the best AMF dosage and cytokinin concentrations that were repeated 3 times. The results of the experiment showed that there was an effect of the best interaction between AMF, cultivars, and cytokinin concentrations on the increased yield of fruit per plant (55.33 g), number of seeds per plant (124.17 g), fruit fresh weight per plant (208.55 g), Fresh weight of 100 seeds (70.22 g), seed fresh weight per plant (39.28 g) and biodiesel oil yield that was increased in Cirebon (42.66% - 47.50%) compared to Jatinangor (35.44% -44.10%).

Keywords : Combined test, Jatropha biodiesel, Arbuscular Mycorrhizal Fungi, Cytokinins.

1. Introduction

One of the government programs in 2016 is the declaration of the use of B20 (a substitute for diesel with a composition of 20% biodiesel and 80% diesel). There are 2 types of viable development opportunities for biofuels, namely biodiesel and bioethanol. Esspecifically to make biodiesel, Jatropha can be chosen because this plant does not compete with food-producing plants, it is not eaten by animals as it is toxic, environmentally friendly, easy to adapt in tropical and subtropical climates in marginal and non-marginal areas, even though the environmental conditions are not good, but showed better crop performance and productivity. This plant has the advantage of fast growth and ease of propagation (Meher, *et al.,* 2013). Jatropha biodiesel has competitive economic value because it is an alternative energy material from fossil fuels, where the price is relatively cheaper, environmentally friendly and renewable.The availability of fertile land decreases due to the higher land use change to settlement, along with the increasing number of people. Therefore, marginal land use is one of the important solutions to do. One type of marginal soil is the order inceptisol, with limiting factors for low soil chemical fertility, especially elemental phosphate (P). Elemental P can become available to plants with the help of arbuscular mycorrhizal fungi (AMF) because AMF is able to extract phosphate from its bonds with Al^{+}, Fe^{2+}, Ca^{+}, and Mg^{2+} by removing organic acids and phosphatase enzymes where the activity of the enzymes formed depends on the activity of the enzymes that interact with them. active microbial cells (AMF) (Nannipieri *et. al*., 2002). The benefits of AMF can also play a role in nutrient cycling, improve soil structure and transfer carbohydrates from plant roots to other soil organisms (Novriani and Madjid, 2010).

In some plants such as jatropha, stem tip growth often dominates the growth of other parts so that the formation of lateral branches is inhibited. This phenomenon is referred to as apical dominance. The addition of 6-benzyl aminopurine (BAP) further enhances the regeneration of leaf branches where the differential response of the genotype is influenced by cytokinins (Singh, 2017). In plants, especially jatropha, there are lateral shoots which then form lateral branches. The addition of cytokinins is one of the cultivation techniques that can be employed to enhance the growing branches aiming to obtain the maximum number of branches, so that the maximum fruit is produced. The symbiosis of arbuscular mycorrhizal fungi (CMA) with terrestrial plants is regulated by plant

* Corresponding author e-mail: entybudiasih@gmail.com ; kovertina.rakhmi.indriana@gmail.com.

hormones, stimulation of cytokinins (CK) plays a role in the development of symbiosis of CMA with peanut plants; and confirm the effect of CMA inoculation on plant CK homeostasis. Most of these hormones have a role in this interrelationship; however, there are still reported contradictions for the hormone cytokinin (CK) (Dane M. Goh, *et al.*, 2019).

The elements of climate and altitude greatly influence the plant growth process (Hasibuan., *et al.*, 2017). The altitude of different places will vary with the physiological processes of plants. This difference will affect plant growth. Biodiesel grown in lowland areas has a higher quantity of biofuel oil than that grown in mediumland areas, but the quality of biodiesel produced is not better than that grown in midland areas, so the two locations have different oil yields, with biotic and abiotic environmental conditions that affect the ecophysiological process of plants.

2. Materials and Methods

The materials used in this experiment were Jatropha seed cultivar IP-3P (Improve Population 3 Pakuwon), IP-3A (Improve Population 3 Asembagus), IP-3M (Improve Population 3 Muktiharjo), AMF Consortium (Glomus sp., Gigaspora sp., Acaulospora sp.) (Cucu Suherman, 2011), cytokinins (BAP), manure, chemical fertilizers used are Urea (45% N), SP-36 (36% P2O5), KCl (60% K2O), and Dithane fungicide M-45. Experiments were carried out in the lowlands of Cirebon (0-50 m asl) and in the medium plains of Jatinangor (800-859 m asl), having an inceptisol soil order and rainfall types including C (Schmidt and Ferguson, 1951). The trial period starts from January to June 2019.

The experimental design used was a factorial randomized block design (RBD) consisting of two factors, namely the first factor, three levels of dose combination of AMF with cultivar IP-3P : 5 g, IP- 3A : 5 g, IP-3M : 10 g for lowland location; IP-3P : 10 g, IP-3A : 5 g, IP-3M : 10 g for medium land locations and the second factor is five levels of cytokinin concentrations, namely 0 mg L^{-1}, 100 mg L^{-1}, 200 mg L^{-1}, 300 mg L^{-1}, 400 mg L^{-1}. The number of treatment combinations was repeated 3 times, so the number of plots in this experiment was 45. Placement of the treatments in each replication was done randomly. Yield data (number of fruits per plant, number of seeds per plant, fresh weight of fruit per plant, fresh weight of 100 seeds, and fresh weight of seeds per plant) were calculated manually and weighed using digital scales and oil yield was obtained by the transesterification method using the Soxlet tool then all test data were analyzed statistically to determine the level of variance homogenity, by using the Bartlet test.

3. Results and Discussion

Before testing the combining power of the two experimental locations, it is necessary to first test the homogeneity of the variance. The level of data homogeneity between the two locations was tested using the Bartlet Test. Johnson and Winchern (2007) explain that the Bartlet test is used to test the homogeneity of the data in different populations. Test data on different populations can be analyzed in a combined manner if it has

$$\chi^2_{hitung} = -\left(n - 1 - \frac{1}{6}(2p+5)\right)\ln|\hat{\rho}|$$

homogeneous data variance. The Bartlet test formula according to Sudjana (2005) is as follows:

Information : n = number of samples; p = number of variables; | Ṕ | = the determinant value of the correlation matrix of each variable.

Data in different populations are declared homogeneous if the count X2 is greater than X2 Table at the 5% level, it is necessary to test the combining power of the two locations (Gomez and Gomez, 1995) (Table 1). Thus, it can be concluded that the characters of the number of fruits per plant, number of seeds per plant, fresh weight of fruit per plant, fresh weight of 100 seeds, fresh weight of seeds per plant and oil yield can be tested by combined ANOVA.

Table 1. Results of the Bartlet Character Test for Character Component Results and Results

Character	Location	db	X^2_{Count}		X^2_{Table}
Number of Fruits in Plant	2	1	40.89	*	3.84
Number of seeds in plant	2	1	19.88	*	3.84
Fruit Fresh Weight in Plant	2	1	8.92	*	3.84
Fresh Weight 100 Seeds	2	1	23.09	*	3.84
Fresh Seed Weight in Plant	2	1	27.60	*	3.84
Oil Yield	2	1	13.94	*	3.84

Combined linear model analysis of two locations was carried out using the Freeman and Perkins analysis model as described by Singh and Chaudhary (1979) as follows :

$$Y_{ijkr} = m + d_i + e_j + g_{ij} + \varepsilon_{ijr}$$

Information : Yijr = the result of observing a variable in the ith result, the jth location, the r repeat; m = general average value; di = the effect of the first treatment; ej = effect of jth location; gij = the effect of the interaction of the i-th treatment and j-location; εijr = the combined effect of other factors in the i-th, j-th place, and r-th test results.

3.1. Number of Fruits in Plants

For the variable number of fruits per plant, the coefficient of diversity (kk) on the variable number of fruits per plant, number of seeds per plant, fresh weight of fruit per plant, fresh weight of seeds per plant ranged from 23.21% -29.74% while for the variable fresh weight 100 seeds (0.95 %) and oil yield (5.21%). According to Gomez and Gomez (1995), a good kk value is below 20%, although there are exceptions for quantitative characters such as outcome variables which are highly influenced by the environment (Baihaki and Wicaksana, 2005).

The number of fruits is influenced by the pollination process. Jatropha has fewer female flowers than male flowers, which will affect fruit formation. The ratio of male and female flowers is 1: 29 to 1: 13 (Pan and Zeng, 2010), so the possibility of pollination does not exist.

Table 2. Average Number of Fruits in Plant (Fruit) of Each Treatment Planted in Different Regions Based on Altitude at Different Places

Cytokinins	Cirebon			Average Cytokinins(Lokasi 1)	Jatinangor			Average Cytokinins(Lokasi 2)	Average Cytokinins(M1+M2)
	x1	x2	x3		x1	x2	x3		
s0	3.67	9.00	4.67	5.78[f]	6.67	14.67	11.33	10.89 ef	8.33[d]
s1	6.33	13.33	4.67	8.11[ef]	7	16.67	13.33	19.22 de	13.67[d]
s2	0	18.0	8.67	15.67 def	7	30.67	27.33	31.22 c	23.44[c]
s3	7	35.6	25.6	26.22 cd	3	49.33	45.03	45.56 b	35.89[b]
s4	7	37.6	25.6	36.11 bc	0	53.07	52.67	57.11 a	46.61[a]
Two Locations Combined									
s0	5.17 i	11.8 3ghi	8.00 hi						
s1	11.5 0ghi	20.5 0efgh	9.00 hi						
s2	24.3 3defg	28.0 0cdef	18.0 0fghi						
s3	42.5 0abc	33.1 7bcde	32.0 0bcdef						
s4	45.3 3ab	55.3 3a	39.1 7bcd						

Based on the results of the combined test of the two treatment locations, the concentration of cytokinin S4 showed the best performance in the variable number of fruits per plant (46.61). The test results showed an interaction between cytokinin concentration and location. The variable appearance of the number of fruits per plant at the Jatinangor location was the highest based on the tuckey further test (57,11). In addition, there was also an interaction between cytokinin concentrations and the application of Jatropha cultivar with the best AMF dose. Further test results showed that the treatment of cytokinin S4 concentration (400 mg L-1) in the Jatropha cultivar application with a dose of AMF X2 (IP-3A + dose of AMF 5 grams) had the highest average number of fruits per plant (55.33), which is also influenced by the presence of AMF which is useful for increasing nutrient uptake, especially P phosphate (Nur Fitriani *et al*., 2019).

The slow fruit formation in Jatinangor can be caused by a slower metabolic process than in Cirebon. This slow excess metabolism can increase oil yield, because less photosynthate is used for respiration. Mengel and Kirkby (2001) suggest that 80% of photosynthate is transferred to seeds in wheat plants, so it can be assumed that even in jatropha most of the photosynthate is transferred to seeds.

3.2. Number of seeds in plant

In the variable number of seeds per plant, the results of further tests showed that the treatment of cytokinin S4 concentration had the best performance (109.06) compared to other cytokinin hormone treatments. The test results showed that there was no interaction between cytokinin concentrations and location, although there was an interaction between cytokinin concentrations and Jatropha cultivar application with the best AMF dose. This is due to the fact that the size of the seeds is more influenced by genetic factors and there are striking environmental changes. The large flow of photosynthate from the source to the reproductive organs does not increase the capacity of the container, but is used for the process of seed growth, so that the number of seeds that reach normal size can be increased. Seeds that have been able to pass the critical limit of the seed filling period will effectively be able to reach the perfect size. The seeds that are harvested must meet the requirements of one of the agronomic characters, namely seeds that have reached normal size.

Table 3. Average Number of Seeds in Plant (Fruit) of Each Treatment Planted in Different Regions Based on Altitude at DifferentPlaces

Cytokinins	Cirebon			Average Cytokinins (Location1)	Jatinangor			Average Cytokinins (Location 2)	Average Cytokinins (M1+M2)
	x1	x2	x3		x1	x2	x3		
s0	16.33	30.67	21.67	22.89	26.33	40.67	31.67	32.89	27.89 d
s1	23.33	58.33	42.00	41.22	34.00	67.67	51.67	51.11	46.17 c
s2	54.33	59.00	38.00	50.44	65.00	70.67	49.67	61.78	56.11 c
s3	82.67	99.33	62.00	81.33	97.33	113.33	74.33	95.00	88.17b
s4	114.67	103.67	86.33	101.56	133.67	114.67	101.33	116.56	109.06[a]
Two Locations Combined									
s0	21.33[f]	35.67[def]	26.67[ef]						
s1	28.67 def	63.00[cde]	46.83[def]						
s2	59.67 cdef	64.83[cde]	43.83[def]						
s3	90.00 abc	106.33[ab]	68.17[bcd]						
s4	124.17[a]	109.17[a]	93.83[abc]						

Further test results showed that the treatment of cytokinin S4 concentration with Jatropha cultivar application with the best AMF dose X1 had the highest number of seeds per plant (124.17). The interaction between cytokinins and AMF with low levels of cytokinins affects the rate of plant development so that it stimulates the growth of AMF hyphae in the roots to continue to grow (Marco cosme and Susane Wurst, 2013) which in turn increases the number of fruits. According to Bago *et. al*. (2003), plants that have a high rate of photosynthesis will have high food reserves and are stored in seeds in the form of fatty acids.

Fresh weight of fruit per plant, fresh weight of 100 seeds, fresh weight of seeds per plant, and oil yield on fresh fruit weight per plant there was no interaction between cytokinin concentrations and location; cytokinin concentrations and applications of Jatropha cultivar with the best AMF dose; and cytokinin concentrations, application of Jatropha cultivar with the best AMF dose and location.

Table 4. Average of fresh fruit weights in plant, fresh weight of 100 seeds, fresh weight of seeds in plant, and yield of oil for each of the treatments planted in the two regions are different based on altitude

Treatments	Mean Cytokinins at Two Locations(M1+M2)			
	Fruit Fresh Weight in Plant (g)	Fresh Weight 100 Seeds (g)	Fresh Seed Weight in Plant (g)	Oil Yield (%)
s0x1 ; s0x2 ; s0x3	141.94[c]	66.24[e]	39.28[c]	42.22[ab]
s1x1 ; s1x2 ; s1x3	135.16[c]	67.26[d]	42.83[c]	41.66[b]
s2x1 ; s2x2 ; s2x3	154.68[bc]	67.96[c]	54.72[bc]	43.45[ab]
s3x1 ; s3x2 ; s3x3	185.02[ab]	68.71[b]	59.39[b]	43.78[ab]
s4x1 ; s4x2 ; s4x3	208.55[a]	70.22[a]	75.54[a]	43.88[a]

In the variable fruit fresh weight per plant, the test results showed that there was a significant difference in the application of cytokinin concentrations as a whole. The results of further tests using the tuckey test showed that the S4 application had the highest fruit fresh weight per plant reaching

208.55 grams. From Table 4, it can be concluded that the amount of photosynthate allocation in the seeds is in line with the plant biomass due to the ZPT application. High cytokinin concentrations can increase the strength of the reproductive container to attract photosynthate, so that the growth of reproductive organs is better (Sumadi, 2000).

Variable fresh fruit weight per plant (Table 4) there was no interaction between cytokinin concentrations and location; cytokinin concentrations and the application of Jatropha cultivar with the best AMF dose; as well as cytokinin concentrations, Jatropha cultivar application with the best AMF dose, and location. The test results using the tuckey test showed that there was a significant difference in the application of the overall cytokinin concentration. Further test results showed that the S4 application with the best AMF dose in each location had the highest fresh weight of 100 seeds reaching 70.22 grams. It is thought that AMF can help absorb water and nutrients, including P nutrient which plays an important role in seed formation. Musfal (2008) states that the increase in dry shelled yield of maize is closely related to the increase in P uptake byplants.

Variable seed fresh weight per plant (Table 4) did not have an interaction between cytokinin concentration and location; BAP cytokinin concentration and Jatropha cultivar application with the best AMF dose; as well as cytokinin concentrations, Jatropha cultivar application with the best AMF dose, and location. Further analysis using the tuckey test showed that there were significant differences in the application of the overall cytokinin

concentration. The results of further tests showed that the S4 application with the best AMF dosage in each location had the highest seed fresh weight per plant, reaching 75.54 grams. According to Selamet and Suyatmo (2000), during their growth from germination to production, plants have needs that must be fulfilled such as solar radiation, CO_2 for photosynthesis, O_2 for respiration, water, and nutrients in certain amounts in order to grow normally to reach their potential results. The two different locations are thought to have different effects on each individual plant so that the variations that occur are quite large. Plants with mycorrhizal are more efficient in water use, then water is translocated to the top of the plant which supports the opening of the stomata, and plays a role in the process of foosynthesis which in turn will increase the production of dry matter that will be used for seed formation, so that the number of seeds formed is greater (Nuraini, 2002). The increase due to AMF administration is possible because the P- available and P from mycorrhizal secretion play a role in the preparation of phospholipids, cell nuclei and protein and increase the percentage of flower formation into fruit and seeds. P is also a constituent component of ATP, as an energy source for metabolic processes in plants. In plants deficient in P, P in the cytoplasm decreases and to compensate for this so that P in the cytoplasm remains constant, transfer is required from the vacuole via the P-aseenzyme.

Oil yield is the ratio of the amount (quantity) of oil produced from the extraction of aromatic plants. The higher the yield value, the more oil is produced. Increasing the yield or comparison of the amount of oil produced can be done with two approaches, namely the cultivation process and the oil-

making process. From the results of the analysis showed that, treatment with additional plant AMF doses could increase the oil content significantly compared to without the addition of AMF, the more spores applied, the higher the oil content detected. The results of photosynthesis, NADPH2 and ATP can also be obtained from cellular respiration with the pentose phosphate pathway (Taiz & Zeiger, 2006). Both of these energies are highly dependent on inorganic phosphate compounds, especially pyrophosphoric acid. Pyrophosphate is a form of inorganic phosphate molecule that can be absorbed directly by plants from the soil. According to Schacmat et al. (1998), the association between plant roots and AMF will increase pyrophosphate molecules in the soil and can increase the intensity of pyrophosphate absorption by plant roots. Thus, the more pyrophosphate compounds that plants can absorb, the more NADPH2 and ATP molecules that plants can form for fatty acid synthesis.

The basic ingredient in the formation of jatropha oil biodiesel is in the form of triglycerides which are produced from the seeds. Triglycerides are synthesized from fatty acids, glucose and glycerol. Fatty acids are derived from acetyl CoA, which occurs in the endoplasmic reticulum. Glucose is produced from photosynthesis and glycerol is produced from fructolysis. Fatty acids are important in the synthesis of triglycerides. This fatty acid formation occurs in the cytoplasm. The main basic ingredient of fatty acids is acetyl CoA which is derived from pyruvic acid in mitochondria (Salisbury and Ross, 1995). Dihydroxy acetone P is synthesized from glucose which occurs in the glycolysis process. Dihydroxy acetone P can also be obtained from the fructolysis reaction. Dihydroxy acetone P can be converted into 3 P glycerol with the help of the enimglycero 1 3 dehydrogenase. The 3 P glycerol will then react with fatty acids to form triglycerides. Fatty acids react with ATP and enzymes to form enzyme-acyladenylate complexes. The ATP molecules in this reaction are converted into acyl-AMP and pyroP. Then acyl-AMP reacts with coenzyme A to form acetyl CoA. This acetyl CoA will react with glycero P to form speech acid. Furthermore, the pidic acid is hydrolyzed to produce 1.2 diglycerides. The assimilation reaction in 1.2 diglycerides, namely the acetyl CoA molecule will bond to the C number 3 atom to form triglycerides. Each process of the triglyceride synthesis sequence always requires energy and enzymes involving P elements, therefore giving AMF will ultimately increase the yield of castor oil seed oil. In this study it was detected that there was an increase in phosphate, presumably this element caused the oil content in the seeds of the AMF inoculated plants to increase. This study is in accordance with the study by Bago *et. al.* (2003), who reported that Canola plants inoculated with AMF showed a higher fatty acid content than non-inoculatedplants.

The oil yield in Cirebon (42.66% - 47.50%) was higher than that in Jatinangor (35.44% - 44.10%), because the lipid / oil formation process in Cirebon is more perfect, without being divided for respiration (Rosniawaty, 2011). Fat formation requires a lot of energy, because almost 2 pairs of electrons (2 NADPH) and one ATP are needed for each acetyl group present (Salisbury and Ross, 1995), here is a summary of fatty acid synthesis with the example of palmitic acid (as an ester of co- enzyme A):

$$8 \text{ asetil CoA} + 7 \text{ ATP}^{3} + 14 \text{ NADPH} + 14\text{H}^{+} \longrightarrow \text{palmitil CoA} + 7 \text{ CoA} + 7 \text{ ADP}^{2-} + 7 \text{ H}_2\text{PO}^{4-} + 14 \text{ NADP}^{+} + 7 \text{ H}_2\text{O}$$

4. Conclusion

The results showed that there was an effect of the best AMF interaction with cultivars and cytokinin concentrations, where the best combination of AMF and cultivar and the best concentration of 400 mg L-1 cytokinins was able to increase the yield of fruit number per plant (55.33 g), number of seeds per plant (124, 17 g), fresh weight of fruit per plant (208.55 g), fresh weight of 100 seeds (70.22 g), fresh weight of seeds per plant (39.28 g) and increased yield of biodiesel oil in Cirebon (42.66%) - 47.50%) higher than in Jatinangor (35.44% - 44.10%).

Acknowledgments

LPDP (Education Fund Management Institute) which has provided an opportunity for writers to obtain a 2016 BUDI – DN doctoral education scholarship and has provided a Dissertation Research Fund; Faculty of Agriculture, Padjadjaran University (UNPAD), which has facilitated this research; and the Academic Community of Winaya Mukti University who has supported the author to continue her studies.

References

Aneesha Singh. 2017. **N-(2-chloro-4-pyridyl)-N-Phenylurea Enhanced Regeneration of Jatropha Curcas Leaf Explants by High Mineral Acquisition**. *J Biologia*. 72 (3) : 300-304.

Bago, B., Zipfel, W., Williams, R., Jun, J., and Arreola, R. 2003. **Translocation and Utilization of Fungal Lipid in the Arbuskular Mycorrhizal Symbiosis**. *J Plant Physiol*, 128:331-340.

Baihaki, A., and N. Wicaksana. 2005. **Genotype x Environment Interaction, Adaptability, and Yield Stability, in the Development of Superior Varieties in Indonesia**. *Zuriat* 16 (1):1-5.

Dane M. Goh, Marco Cosme, Anna B. Kisiala, Samantha Mulholland, Zakaria M. F. Said, Lukáš Spíchal, R. J. Neil Emery, Stéphane Declerck and Frédérique C. Guinel. 2019. **A Stimulatory Role for Cytokinin in the Arbuscular Mycorrhizal Symbiosis of Pea**. *Frontiers in Plant Science* 10 : 268.

Gomez, K. A., and A.A Gomez. 1995. **Statistical Procedures for Agricultural Research**. Translation : E. Sjamsuddin and J. S Baharsyah. University of Indonesia, Jakarta.

Hasibuan, S., R. Mawarni and R. Hendriadi. 2017. **The Response of Giving Bagasse Bokashi Fertilizer and Water Hyacinth Bokashi Fertilizer to the Growth and Production of Soybean (*Glycine max (L) Merril.*)**. *BERNAS Agr Res J* (BARJ) 13 (2) : 59-64.

Johnson, R. A., and Winchern, D. W. 2007. **Applied Multivariate Statistical Analysis (six edition)**. United State of America : Prentice.

Meher L.C., C.P. Churamania, Md. Arifb, Z. Ahmedb, and S.N. Naikc. 2013. **Jatropha Curcasas a Renewable Source for Bio-Fuels**. *Renew Sust Energy Rev*, 26 : 397-407.

Marco Cosme and Susanne Wurst. 2013. **Interactions Between Arbuscular Mycorrhizal Fungi, Rhizobacteria, Soil Phosphorusand Plant Cytokinin Deficiency Change the Root Morphology, Yield and Quality of Tobacco**. *Soil Biol Biochem*, 57 : 436-443.

Mengel, K and E. Kirkby. 2001. **Principles of Plant Nutrition**. International Potash Institute, Switzerland. 4-655 hal.

Musfal. 2008. **Effectiveness of Arbuscular Mycorrhizal Fungi (AMF) on Location-Specific Fertilizer for Corn on Inceptisol Soil**. Thesis. University of North Sumatra.79p.

Nannipieri P, Kandeler E, and Ruggiero P. 2002. **Enzyme Activities and Microbiological and Biochemical processes**. In : Burns RG, Dick RP (eds) Enzymes in the environment. Activity, Ecology and Applications. Marcel Dekker, New York, pp1–3.

Novriani and Madjid. 2010. **Role and Prospects of Mycorrhizae**. Sriwijaya University, Palembang.

http://www.scribd.com/doc/22391846/**Peran-Dan-Prospek-Mikoriza**. accessed on April 10,2017.

Nuraini, A. 2002. **Response of Soybean (Glycine max (L.)Merr.) to Potassium and Arbuscular Mycorrhizal Fungi in Drought-Triggered Conditions During the Pod Forming Period to Seed Filling**. *Dissertation*. Padjadjaran University Graduate Program. Not Published, Bandung.

Nur Fitriani Litta, Rachmawati Hasid, and Laode Afa. 2019. **Effectiveness of Arbuscular Mycorrhizae and Sago Dregs in Increasing the Yield of Okra (*Abelmochusesculentus* L.) Plants on Dry Land**. *Int J Agr*, 7 (1) : 23-31.

Salisbury, F.B. and C.W. Ross. 1995. **Plant physiology. 3rd Editio**. Wadsworth Publishing Co. Inc.

Santi Rosniawaty. 2011. **Response of *Jatropha carcass* L. to Organic Fertilizer, Nitrogen and Phosphorus in Two Different Locations**. *Dissertation*. Unpad Postgraduate Program, Bandung.

Schachmat, D.P., Reid, J. R., and Ayling, S.M. 1998. **Phosphorus Uptake by Plants From Soil to Cell, University of Adelaide, Australia**. *J Plant Physiol* 166 :447-453.

Schmidt, F.H. and J.H.A. Ferguson. 1951. **Rainfall Types Based on Wet and Dry Period Ration for Indonesia with Western New Guinea**. Verhandelingen No. 42. Ministry of Transportation. Department of Meteorology and Geophysics, Djakarta.

Slamet and Suyamto. 2000. **Preliminary Yield Test of Drought Tolerant Soybeans**. Technique Report of Research Results, Research Institute for Legumes and Tubers.

Suherman, C. 2011. **Increased Growth, Results and Oil Yield (Jatropha curcas Linn) Through the Application of Mycorrhizal Fungi and Phosphate Fertilizer in Inceptisol Jatinangor**. *Dissertation*. Unpad Postgraduate Program, Bandung.

Sudjana. 2005. **Statistical Methods**. Bandung : Tarsito.

Sumadi. 2000. **Responses of Soybeans That are Stricken With Drought During The Pod Forming Period to Seed Development to the Application of Cytokinins and Gibberellins**. *Dissertation*. Unpad Postgraduate Program, Bandung.

Taiz, L., and E. Zeiger. 2006. **Plant Physiology, 3rd Ed**. Sinauer Associates.Sunderland.

Pan, BZ and Zeng-Fu Xu. 2010. **Benzyladenin Treatment Significantly Increase the Seed Yield of the Biofuel Plant Jatropha curcass**. *J Plant Growth Regul*. DOI 10.007/S003.44-010-9179-3.
www.jatropha.de/journal.(24/12/2019).

Sidiq, Yasir., Subiastuti, Aprilia Sufi., Wibowo, Wiko Arif, Daryono, and Budi Setiadi. 2020. **Development of SCAR Marker Linked to Begomovirus Resistance in Melon *(Cucumis melo L.)***. *Jordan J Biol Sci*, **13 (2)** : 145-151.

Purnobasuki, Hery., Hariyanto, Sucipto and Purnama, and Putut Rakhmad. 2021. **Genetic Diversity of Seagrass *Thalassiahemprichii* and *Enhalusacoroides* in Coastal Area of East Java**. *Jordan J Biol Sci*. **14 (1)**: 111-119.

JJBS

Volume 14, Number 5,December 2021
ISSN 1995-6673
Pages 1015 – 1020

Jordan Journal of Biological Sciences

Effect of Mangosteen Peel Extract (Garcinia mangostana l.) with Supplemental Zinc and Copper on Performance and Egg Quality of Sentul Laying Chicken

Tuti Widjastuti[1,*], Lovita Adriani[2], Indrawati Yuda Asmara[1], Iwan Setiawan[1], Abun[2], Leni Nurlaeni[2]

[1] Departemen of Production, Faculty of Animal Husbandry, Universitas Padjadjaran, 45363, Indonesia, [2]Department of Animal Nutrition and Feed Technology, Faculty of Animal Husbandry, Universitas Padjadjaran, 45363, Indonesia

Received: March 12, 2021; Revised: May 17, 2021; Accepted: September 21, 2021

Abstract

Mangosteen peel extract is a medicinal plant that can be used as an herbal supplement, containing xanthone compounds that function as antioxidants and antimicrobials. The research was conducted to determine the effect of Mangosteen Peel Extract with mineral (MPEm) as a feed supplement to the production and egg quality of Sentul Chicken. Sentul Chicken is a local chicken of west java which have potential as dual-purpose chickens. This study used 40 female chickens. The method used was a completely random design with five treatments namely, P0 (basal ration), P1 (basal ration with 60 mg/kg MPEm), P2 (basal ration with 120 mg/MPEm, P3 (basal ration with 180 mg/kg MPEm, P4 (basal ration with 240 mg/kg MPEm) and repeated four times. The result showed that the use of MPEm in the ration was significant ($p<0.05$) on conversion ration, hen-day, egg weight, egg cholesterol, the color of egg yolk, and the thickness of eggshell but not significant on consumption ration, haugh unit, and yolk index score. It can be concluded that MPEm can be used as a feed supplement until 180 ml/kg ration to give the best on performance production and eggs quality of Sentul chicken.

Keywords: Mangosteen peel extract with mineral, performance production, egg quality, Sentul chicken

1. Introduction

Sentul chicken is a local Indonesian chicken family that has been cultivated from generation to generation, and so it becomes a wealth of genetic resources of local Indonesian livestock. Sentul chicken is a dual-use chicken that has relatively fast growth and high egg production compared to ordinary local chickens. Sentul chickens can lay eggs around 150 eggs/year (Baktiningsih et al., 2013). The spur production, farmers usually add synthetic antibiotics. Currently, synthetic antibiotics have been banned because they can cause meat and eggs produced to be unsafe for consumption. Therefore, the use of synthetic antibiotics needs to be replaced with natural ingredients which can simultaneously improve performance such as mangosteen peel. Mangosteen is an annual plant whose life span reaches tens of years. The mangosteen tree is evergreen with a height of 6-20 meters. Mangosteen Peel contains 68 types of xantone compounds Aizat et al., (2019) which have many pharmacological functions, especially as natural antioxidants (S Melia, et al., 2019), antibacterial (A Saepudin et al., 2018) and antihyperlipidemic (Alkilany, 2017). Mangosteen Peel contains xanthone compounds at 107.76 mg per 100 g (Fabiola Gutierrez-Orozco and Mark L Failla,, 2013). Besides, mangosteen functions as an antitumoral, anti-inflammatory, antiallergic, antibacterial, antifungal, and antiviral agent. Xantone has many pharmacological functions such as antioxidant, anti-inflammatory and antibacterial, antihyperlipidemic (Alkilany, 2017), and is able to improve blood lipid profile. Xantone compounds can be isolated and taken advantage of by the appropriate extraction methods (Do. Q. D., et al., 2014), one of which is maceration. Mangosteen peel extracted using the maceration method produced total xanton levels of 27.7% (Andayani et al., 2015).

However, Mangosteen Peel Extract (MPE) contains unsaturated organic acid compounds that have short-chain bonds and have characteristics that are unstable, sensitive, easy to react, and oxidized (Boots AW. Et al., 2008). The way to stabilize it is by supplementing minerals that function as metal catalysts. Supplementation of Cu and Zn minerals in the form of $CuCl_2.2H_2O$ and ZnO mineral salts is intended for two purposes, first for the function of the Mangosteen Peel Extract itself, which is to stabilize its active compounds which are easily ionized and the second purpose of supplementation of Cu and Zn minerals as inorganic minerals can form bonding with a protein or carbohydrate group, where minerals can be bound to become organic minerals in the form of Cu proteinate and Zn proteinate so that they are easily absorbed by the small intestine, besides, Zn supplementation can also increase the activity of protease enzymes that are regulated by the pancreas (Supriyati, et al., 1999).

* Corresponding author e-mail: tuti.widjastuti@unpad.ac.id.

Mangosteen peel extract can be implemented as a feed supplement and then formulated into the ration as a feed supplement in Sentul chicken rations. Xanthone active compounds in MPEm function as antioxidants can change free radical compounds into more stable compounds and can prevent chain reactions from damage caused by free radicals that will have an impact on chicken production (Zaboli, et al., 2013). Besides, xanthones in MPEm can assist in the digestion process by improving the structure of the small intestine villi in the process of absorption of nutrients and suppress the growth of bacteria pathogens inside the intestines (Vemurugan, and Citarasu, 2010). This condition causes the surface area of the intestinal villi to become wider so that the absorption of nutrients can be more and can increase egg production. MPEm also contains flavonoids, anthocyanins, which are water-soluble color pigments. The color produced by anthocyanins ranges from red, blue, to purple, including yellow. Besides that, in mangosteen peel also contains minerals including magnesium 3.3%, copper 0.7%, manganese 1.3%, calcium 1.1 mg, Phosphorus 1.7 mg, and iron 0.09 mg (Setiawan, D. et al., 2011).

Agung (2014) that MPE administration with a level of 120 mg/kg body weight/day in broiler chicken rations was able to improve growth performance and increase feed efficiency and carcass percentage. While Widjastuti et al., (2020) the addition of 133 ml/kg ration MPE without minerals gave a positive response to the production of Sentul chicken eggs. Therefore, the research aims to determine the use of MPE (*Garcinia mangostana l*) with supplement mineral Zinc and Copper on performan production and eggs quality of sentul chicken.

2. Material and Methode

2.1. Experiment Chicken

Chicken used in the experiment were 40 Sentul chickens, kept in cages for 12 weeks. Chickens were divided into five treatments and repeated times, each replication containing 2 chickens. The average body weight was 1244.1 grams, with the coefficient of variation in body weight 7.03 %.

2.2. Cage

Cages used were cage system cages of bamboo as many as 40 units, each unit measuring 40 cm x 21 cm x 30 cm for one chicken.

2.3. Experiment ration

The ration was arranged based on the needs of sentul chicken for the phase layer, namely protein and metabolic energy, 17% protein and 2750 kcal/kg (Widjastuti T, 1996). The treatment consisted of the use of extract of mangosteen peel (MPEm), namely: P0 = 0 mg MPEm/kg ration; P1 = 60 mg MPEm/kg ration; P2 = 120 mgMPEm/kg ration; P3 = 180 mg MPEm/kg ration and P4 240 mg MPEm/kg. Mangosteen extraction obtained by maceration (Rismana et al., 2014). The macerate (maceration result) of mangosteen peel obtained was temporarily filtered and concentrated using a rotary evaporator to obtain a thick extract. Furthermore, the thick extract of mangosteen peel was dried using a spray and freeze dryer to obtain mangosteen peel extract powder. The addition of 5 ppm $CuSO_4$ and 40 ppm ZnO was carried out with a ratio of mangosteen fruit extract and catalyst, respectively 1:10.

Table 1. Nutrient Composition Of Basal Diet

Ingredients	%
Yellow corn	51.85
Rice bran	18.52
fish meal	6.48
soybean meal	13.89
bone meal	5.56
Ca CO3	3.70
Chemical composition (Calculated)	
Crude Protein (%)	15.63
Crude Fat (%)	5.14
Crude Fiber (%)	4.16
Calcium (%)	3.28
Phosphorus (%)	1.39
Lysine (%)	1.06
Methionine (%)	0.35
Metabolizable energy, kcal/kg	2757

2.4. Experiment Design and Data Analysis

The study was conducted experimentally with 5 ration treatments containing MPEm with 4 replications. The data were analyzed statistically using a completely randomized design and if there were differences, it was tested by the Duncan test.

2.5. Observed variables and how they are measured

- Feed intake was recorded in each 7-day interval.
- Hen day was calculated by dividing number of eggs produced weekly by number of birds and multiplying by 100%.
- Feed conversion is obtained by dividing the amount of feed consumption by weekly total weight of eggs.
- The egg weight produced is weighed and recorded
- Egg Yolk color, as a measure of egg quality, was determined using a Roche colorimetric fan, with scores varying between 1 and 15.
- Eggshell thickness was measured in three points at the egg equator using a pachymeter and calculating the average among the three points.
- Haugh units were calculated based on the height of the albumen and egg weight. Haugh unit= 100 log HA+7.57-1.7WE 0.37 Where, HA = albumen height, and WE = egg weight
- Yolk index was calculated by dividing the yolk height by the yolk weight.
- Cholesterol levels of meat were analyzed using the Enzymatic Photometric Test method

3. Result and discussions

3.1. Effect of MPEm treatment in ration on sentul chicken production performance

The effect of MPEm addition in the ration on Sentul chicken production performance was seen in Table 2.

Table 2. Average the Ration on Sentul Chicken of Laying Phase

Variable	P0	P1	P2	P3	P4
Consumption ration (g)	78.85 ± 3.35a	78.06 ± 3.05a	77.34 ± 2.98a	77.05± 3.07 a	77.00 ± 3.02 a
Hen- day (%)	45.13 ± 4.03b	50.85 ± 4.09a	55.38 ± 5.09a	51.78 ± 5.08 b	47.37 ± 4.9ab
Convertion ration	5.32 ± 0.07 b	4.41 ± 0.09b	3.63 ± 0.13c	3.66 ± 0.08 c	3.96 ± 0.07c

Description: The same letter in the direction of the rows shows no significant difference (P>0.05)
*Duncan test, P0 = without MPEm ; P1 = 60 mg MPEm/kg ration ; P2 = 120 mg MPEm/kg ration; P3 = 180 mg MPEm/kg ration; P4 =240 MPEm/kg ration

Table 1. shows the average ration consumption in various treatments has decreased from the control treatment (P0) until P4. The decrease in feed consumption from each treatment was due to the mangosteen peel extract having a distinctive odor that can affect the delicacy of the chicken. Table 1. and Figure 1. shows that the addition of MPEm does not affect feed consumption. These results that feed consumption in each treatment are in the same range. And this gives an idea that the use of MPEm until level 240 mg/kg, did not give a negative effect on the consumption of ration. The mangosteen peel contains a fairly high tannin and can affect the palatability rate of the ration (Ngamsaeng et al., 2006). But in this study the addition of MPEm did not reduce palatability, which could be due to the extraction process with ethanol solvents which could reduce tannin levels to reduce the bitter taste and odor that is typical of mangosteen peel.

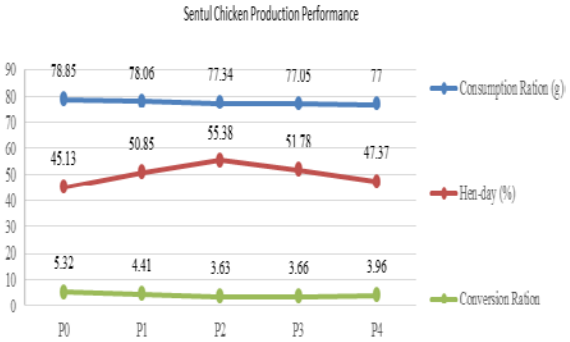

Figure 1. The effect of MPEm addition in the ration on Sentul chicken production performance

The average egg production (Hen-Day) in various treatments has increased, the addition of MPEm in the ration gives a positive response to egg production. Due to the active substance in the MPEm in the form of xanthones functioning as an antioxidant. These antioxidants can prevent free radicals that can cause a decrease in the immune system. Kusumasari et al., (2013) state that antioxidants have an important role to prevent damage caused by free radicals. Xanthones are considered capable of improving the structure of the intestinal villi in the process of absorption of nutrients and suppress the growth of bacteria pathogens inside the intestines. The more xanthones in the body, the more nutrients are absorbed in the body, so that production needs can be met. According Sreedam Chandra Das (2012) that xanthone derivatives like mangostin, isomangostin and mangostin triacetate are known to possess significant anti-inflammatory activities. However, MPE contains methyl esters of unsaturated organic acids that are easily oxidized. Therefore, Cu and Zn supplementation will play a role in activating bioactive compounds contained in MPE which is reactive, thus making the ionization in the digestive tract higher and can be utilized optimally resulting in egg production.

The average value of feed conversion with the addition of MPEm has decreased. FCR values in the MPEm treatment ranged from 3.63 to 4.41 lower than the control ration without the addition of MPEm. The addition of MPEm at doses of 120-240 mg indicates a better and more efficient quality of ration which is indicated by the lower FCR value. Xanthone compounds can inhibit the growth of pathogenic microbes that cause disease so that the digestive system of Sentul chickens can work optimally and the utilization of rations will be more efficient. According Toghyani (2010) the addition of bioactive compounds to herbs can increase appetite stimulation and food intake, increase endogenous digestive enzmes, immune response activities, anti-oxidants, and antimicrobials. With this role, the nutrients can be utilized to produce eggs more effectively. Xanthone compounds in MPEm at optimal doses have an effective role in improving the structure of intestinal villi in the absorption of feed nutrients (Adriani et al., 2018). Increased absorption of nutrients by intestinal villi increases egg production and decreases the value of feed conversion.

3.2. Effect of MPEm treatment in ration on Sentul Chicken egg quality

Data on the effect of adding MPEm in the ration to the variables of the quality sentul chicken eggs can be seen in Table 3.

Table 3. Effect MPEm in The Ration On Egg Quality

Variable	P0	P1	P2	P3	P4
Egg weight (g)	40.87±8.07 a	43.89 ± 9.08 b	44.00 ±10.04 b	44.37± 9.07 b	44.23 ± 9.04 b
Shell Thickness (mn)	0.26± 0.09 a	0.31 ±0.1b	0.32 ±0.12b	0.32 ±0.19b	0.30 ± 0.99 b
Haugh Unit Value	78.47±10.08 a	78.66± 9.08 a	78.88 ±8.09a	79.73 ±7.09 a	79.22± 8.09 a
Yolk index	0.44 ±0.12a	0.41 ±0.14a	0.41 ±0.18a	0.44 ± 0.19 a	0.42± 0.19 a
Color Yolk score	9 ± 2.8 a	10 ± 2.9 a	11 ±2.4 b	11 ±3.0b	11±2.9 b
Egg yolk cholesterol (mg/100g)	122.25 ±10.9a	125.62 ±11.9a	109.49 +11b	102.46 ±12.06b	102.24 ±11.03 b

Description: The same letter in the direction of the rows shows no significant difference (P>0.05)
*Duncan test, P0 = without MPEm ; P1 = 60 mg MPEm/kg ration ; P2 = 120 mg MPEm/kg ration; P3 = 180mg MPEm/kg ration; P4 =240 MPEm/kg ration

Egg quality measurements are summarized in Table 3 after 4 weeks of treatment. Analysis of variance showed that MPEm in real ration increased the egg weight compared to control. These results indicate that a higher dose of MPEM can increase egg weight. This is due to mangosteen peel containing xanthones, 6.45% protein, and 3.02% fat. Xanthones function as an antibacterial that can suppress the growth of pathogenic bacteria in the intestine, and can improve the structure of intestinal villi in the process of absorption of nutrients (Vemurugan and Citarasu, 2010). Thus, the presence of xanthones makes the condition of the digestive tract better and the process of absorption of nutrients in feed, especially protein and fat, which are the most important food factors that affect egg weight more optimally. This was supported by Argo and Mangisah, (2013) that egg weight was influenced by protein, fat, and essential amino acids contained in the ration. Another factor that leads to increased egg weight is the presence of antioxidants contained in the MPE. Antioxidants can capture free radicals in the body so that the presence of an antioxidant can suppress the emergence of free radicals. In line with Kusumasari et al., (2013) that free radical damage can be prevented by antioxidants. Increased free radicals cause the body's defense ability to decrease so that it can trigger stress on livestock that has an impact on decreasing egg production, especially egg weight. This condition shows that the xanthone compound at optimal dosage has the potential as a natural antibiotic in poultry through antibacterial and antioxidant mechanisms so that it will improve the immune system of Sentul chickens, eventually the maximum nutrient intake and an increase in egg weight.

The average range of shell thickness is 0.26 – 0.32. The range is in the range of chicken eggshell thickness in general. MPEm administration up to 240 mg/kg in the diet significantly (P <0.05) on the shell thickness. This can be caused by mangosteen extract containing 11 mg Ca minerals, and 17 mg Phosphorus, with the supplementation of Cu and Zn minerals in the form of $CuCl_2.2H_2O$ and ZnO mineral salts, will play a role to activate the bioactive contained in the mangosteen peel extract which is reactive, so that makes ionization in the digestive tract higher and can be optimally utilized right on target, and will increase the thickness of Sentul.

The average value of HU is between 78.47–79.22 and the average yolk index is 0.41 – 0.44. The effect of adding MPEm on the ration did not significantly affect the HU value and egg yolk index. Yolk index and albumen are influenced by protein content in feed. Based on the research results, levels of protein (15%) in feed and feed intake (unpublished data) were not significantly different between treatments. So, the protein consumption for each treatment is the same, which causes the amino acid content in the egg to be the same, which in turn produces an egg with the same freshness. This condition will produce egg yolk index and haugh unit value, relatively the same between treatments. Following the opinion of Lengkey et al., (2012) that the Yolk Index and Haught Unit values are used to determine the freshness of eggs.

Figure 2. Effect of Adding MPEm in The Ration to The

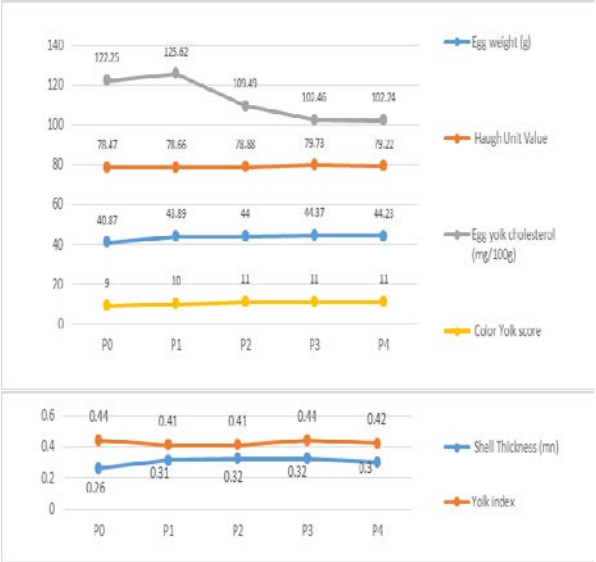

Variables of The Quality Sentul Chicken Eggs

Table 3 and Figure 2. shows that results of the Kruskal-Wallis test showed that MPEm in the ration significantly improved color of the yolk of Sentul chicken. The content of xanthones and xanthophyll contained in the feed able to improve the structure of the intestinal villi in the process of absorption of nutrients (Vemurugan and Citarasu, 2010). Thus, the existence of xanthones will make the digestive tract conditions better and the process of absorption of nutrients in the feed, especially xanthophyll which is a colorant in egg yolks, becomes more optimal. The color pigment will be absorbed by the small intestine digestive organs and transported in the blood circulation and then circulated to the target that needs, namely the egg yolk. Color pigments will be absorbed by the digestive organs of the small intestine and transported.

The current study shows that MPEm reduced the level of yolk egg cholesterol. Following Mangisah (2003) that normal chicken egg cholesterol levels range from 125-200 mg/dL. The process of cholesterol synthesis. The process of cholesterol synthesis starts from acetyl CoA which is the result of carbohydrate or fat metabolism. Xanthones in MPEm work through the mechanism of inhibiting the

activity of HMG CoA reductase enzymes, which can cause inhibition of cholesterol biosynthesis (Botham et al., 2015). Among phenolic compounds found in MPEm are flavonoids which have been studied extensively because of their capability to moderate some metabolic process such carbohydrate and lipid metabolism. Mohamed et al (2019) that phenolic compounds could be a major determinant of antioxidant potentials of foods and could, therefore, be a natural source of antioxidants.

Flavonoids are antioxidants that can reduce blood cholesterol levels, the mechanism by which flavonoids inhibit cholesterol synthesis through HMG CoA reductase inhibitors (Metwally, 2009). In addition to xanthones, MPEm also contains lipophilic saponins that can dissolve fats and emulsions that can reduce blood cholesterol levels due to hypercholesterolemia (Francis et al., 2002 ; Adriani et al., 2018).

4. Conclusions

It can be concluded that:

1. The use of MPEm in ration was significant ($p<0.05$) on conversion ration, hen-day, egg weight, the thickness of eggshell, the color of egg yolk and egg cholesterol but not significant on yolk index score, consumption ration and haugh unit.
2. MPEm can be used as a feed supplement until 180 mg/kg ration to give the best on performance production and egg quality of Sentul chicken.

Acknowledgements

This research was funded by the Grand Research Academic Leadership project from Universitas Padjadjaran to Tuti Widjastuti. I would like to thank Lovita Adriani, Indrawati Yudha Asmara, Iwan Setiawan, Abun, Leni Nurlaeni who helped write this paper.

References

Adriani L, Widjastuti T, Nurdianti, RR, Wiradimadja R. 2018. Effects of mangosteen peel extract (garcinia mangostana l.) on blood lipid of sentul chicken growth phase. The 3rd International Conference of Integrated Intellectual Community (ICONIC). Jerman.

Agung AC. 2014. Comparison of the activity of mangosteen peel extract and various antioxidants on broiler performance.*JPPT*., **15 (1)**: 68-74.

Aizat WM, Jamil IN, Ahmad HFH, Noor NM. 2019. Recent updates on metabolite composition and medicinal benefits of mangosteen plant. *Peer J.,* **7**: e6324.

Alkilany SA, Elin YN, Neng FK and Ketut AI. 2017. Antihyperlidemic effects of mangosteen (garcinia mangostana l.) pericarp ethanolic extract in high-carbohydrate wistar rats. *Journal Of Natural Remedies*., **17 (4)** : 165-173

Andayani R, Novita R and Verawati. 2015. Effect of extraction methods on total xanthones in mangosteen (garcinia mangostana l.) fruit rind extract by ultraviolet spectrophotometry. Prosiciding Conference & *Workshop*. Universitas Andalas, Padang.

Argo LB. dan Mangisah I. 2013. Physical quality of phase i laying arab chicken eggs with various levels of azolla microphylla. *Animal Agricultural Journal*., **2(1)**: 445-457.

Baktiningsih S, Mugiyono S and Saleh DM. 2013. Egg production of various types of Sentul chickens at the Ciung Wanara Livestock Group Association, Ciamis District, Ciamis Regency. *JIPT.,* **1(3)**: 993-1000.

Boots AW, Haenen GRMM, Bast A. 2008. Health effects of quercetin: From antioxidant to nutraceutical. *Eur J Pharmacol*., **585**: 325–327.

Botham KM, Mayes PA. Cholesterol synthesis, transport, & excretion. dalam Murray RK, Bender DA, Botham KM, Kennelly PJ, Rodwell VW, Weil PA. 2015. **Harper's illustrated biochemistry**. 30th ed. The Mc Graw-Hill education. 266-72.

Do QD, Angkawijaya AE, Tran NPL, Huynh LH. Soetarredjo. FE, Ismadji. S, Ju. YH. 2014. Effect of extraction solvent on total phenol content, total flavonoid content and antioxidant activity of Limnophila aromatic. J. *Food Drug Anal*., **22(3).** 296 – 302.

Fabiola GO, Mark LF. 2013. Biological activities and bioavailability of mangosteen xanthones: a critical review of the current evidence. *Nutrients:*13., **5(8)** : 3163.

Francis G. Kerem Z, Makkar HPS, Becker K, 2002. The biological action of saponins in animal systems: a review. *Br. J. Nutr*., **88**: 587-605.

Kusumasari DP, Mangisah I, dan Estiningdriati I. 2013. Effect of Addition Vitamin A and Vitamin E in Diet on Egg Weight and Embryo Mortality in Kedu Black Hens. *Anim. Agric. J.,* **2(1)**: 191-200.

Lengkey HAW, Widjastuti T, Darana S, 2012, the effect of storage time in different temperature on native chicken egg haugh unit and yolk index. *Scientific Papers. Series D. Animal Science*., **Vol. LV**, ISSN-L 2285-5750, 173-175.

Mangisah I. 2003. Use of C. domestica and C. xanthorrhiza in BroilerDiet as Agent for Decrease of Meat Cholesterol. *JLITBANG.,* **1(2)**: 96-101.

Marisca EG, Bambang P, Sutiman BS, Wahyu W, Kusworini H. 2019. Xanthones Analysis and Antioxidant Activity Analysis (Applying ESR) of Six Different Maturity Levels of Mangosteen Rind Extract (Garcinia mangostana Linn.). *Pharmacogn J.,* **11(2):** 369-373

Metwally MAA. 2016. Effects of Garlic (Allium sativum) on Some Antioxidant Activities in Tilapia Nilotica (*Oreochromis niloticus*). *World J. Fish Mar. Sci.,* **1** : 56-64.

Mohamed AM, Fawzy G. K and Enas I. M. 2019. Phenolic Compounds, Antioxidant and Antibacterial Activities of Rhus flexicaulis Baker. *Jordan Journal of Biological Sciences.,* **12 (1)** : 17-21

Ngamsaeng, M. Wanapat and S. Khampa. 2006. Effects of Mangosteen Peel (*Garcinia mangostana*) Supplementation on Rumen Ecology, Microbial Protein Synthesis, Digestibility and Voluntary Feed Intake in Cattle. *Pakistan Journal of Nutrition., 5: 445-452*.

Rismana, Eriawan, Kusumaningrum, Susi, Bunga, Olivia, Nizar, Marhamah. 2014. Determination Of Antiacnes Activity Of Chitosan - Garcinia Mangostana Extract Nanoparticles. *Media of Health research & Development*., **24 (1)** : 19-27

S Melia, D Novia, I Juliyarsi, and E Purwat. 2019. The characteristics of the pericarp of garcinia mangostana (mangosteen) extract as natural antioxidants in rendang. International Conference on Animal Production for Food Sustainability. *IOP Conf. Series*: Earth and Environmental Science. **287**.

Saepudin A, Natawijaya D, Hartini E and Iskandar R. 2018. Evaluation of antibacterial activity of mangosteen (Garcinia mangostana L.) pericarp extract against rice leaf blight bacteria (Xanthomonas oryzae pv. oryzae) at various temperatures and durations of fruit storage. IOP Conference Series: Earth and Environmental Science. **250**.

Setiawan DV, Djunaedi, dan Sudjarwo. 2011. Effect Of Addition Mangosteen Peel Powder (Garcinia Mangostana L.) As Feed Additive To The Production Performance Of Male Mojosari Duck. Article of Universitas Brawijaya. Malang. Indonesia.

Sreedam CD, Subrata B, Sumon Roy, Sajal KS, Md. Saiful Islam and Sitesh CB. 2012. Analgesic and Anti-inflammatory Activities of Ethanolic Root Extract of Swertia chirata (Gentianaceae) *Jordan Journal of Biological Sciences*. **5 (1)** : 31 – 36.

Supriyati D, Yulistiani, Wina dan Haryanto. 1999. Micro mineral supplementation in an effort to increase sheep productivity. Indonesian Journal of Animal and Veterinary Sciences., 11-30.

Toghyani M, Toghyani, Gheisari, Ghalamkari, and Mohammad R. 2010. Growth performance, serum biochemistry and blood hematology of broiler chicks fed different levels of black seed (Nigella sativa) and peppermint (Mentha piperita). *Livestock Science*., **129 (1)**:173–178.

Vemurugan S. And T. Citarasu. 2010. Effect of herbal antibacterial extracts on the gut floral changes in indian white shrimp Fenneropenaeus indicus. *Rom. Biotech. Lett*., 5709-5717.

Widjastuti T, Setiawan I, Abun, Asmara IY, Roostita LB. 2020. application of mangosteen peel extract (*Garcinia mangostana l*) as feed additive in ration for performance production and egg quality of sentul chicken. *Internasional Journal on Anvenced Science, Enginering and Information Technology*., **10 (2)** : 789-794.

Widjastuti T. 1996. Determination of Efficiency of Protein Use, Protein Energy Needs for Growth and Production of Sentul Chicken Eggs on Cage System and Litter System. *[Dissertation]*. Postgraduate Program, Universitas Padjadjaran, Bandung.

Zaboli GZ, Bilondi and Miri. 2013. The effect of dietary antioxidant supplements on abdominal fat deposition in broilers. *Life Sci. J.,* **10** : 328-333.

JJBS

Volume 14, Number 5,December 2021
ISSN 1995-6673
Pages 1021 – 1024

Jordan Journal of Biological Sciences

Improving Blood Protein and Albumin Level Using Dried Probiotic Yogurt in Broiler Chicken

Lovita Adriani[1,*] , Andi Mushawwir[1], Chitra Kumalasari[1], Leni Nurlaeni[1] Ronny Lesmana[2], Urip Rosani[1]

[1]*Department of Animal Nutrition and Feed Technology, Faculty of Animal Husbandry, Universitas Padjadjaran, 45363, Indonesia;*
[2]*Departement of Biomedical Science, Faculty of Medicine, Universitas Padjadjaran , 45363, Indonesia*

Received: March 12, 2021; Revised: May 17, 2021; Accepted: September 28, 2021

Abstract

Dried probiotics have a good effect on the digestive tract in inhibiting the growth of pathogenic bacteria and increasing the blood protein content. This study aims to identify the effect of dry probiotics on protein and blood albumin levels in broiler chickens. In the experiment, a Completely Randomized Design (CRD) consisting of five treatments and 4 replications was applied. The probiotic treatments included T0: basal ration (BR); T1: basal ration with dry probiotic A (100% fermented cow's milk/FCM); T2 : basal ration with dry probiotic B (fermented cow's milk/FCM and fermented mung bean milk/FMBM, with a composition of 75% : 25%), T3: basal ration with dry probiotic C (fermented cow's milk/FCM and fermented soy milk/ FCM, with a composition of 75% and 24%); and T4: basal ration with dry probiotic D (consisting of fermented cow's milk/FCM, fermented mung bean milk/FMBM and fermented soy milk/FSM, with compositions: 50%, 25% and 25%, respectively). The results showed that the difference in blood protein and albumin levels ($P>0.05$) was not significant. Dried probiotics tend to increase blood protein and albumin and have the potential to correlate with protein anabolism and broiler performance.

Keywords: dried probiotic, oven-dry, blood protein, albumin, broiler chicken

1. Introduction

Broilers in the form of poultry are used as meat producers and are widely consumed. The quality and consumer expectations of good broiler meat are weight and muscle contours. Weight gain is influenced by the amount of protein contained in the ration (high protein content plays a role in weight gain) (Saleh and Dwi, 2005). Broiler chicken feed must pay attention to the balance of energy and protein contained in the ration. Broiler chicken ration is an additional feed to optimize shelf life and increase efficiency during rearing. However, the side effects of feed additives can bring some health problems. Thus, probiotics are alternative feed additives that can improve livestock health, especially improving the digestive tract ecosystem through microflora balance. Administration of probiotics from an early period improves the balance of intestinal microbes (Adriani et al., 2019).

Blood proteins in plasma are albumin, globulin, and fibrinogen (Ganong, 2000). Total protein examination serves as an examination of health status by looking at changes in protein levels that occur. The protein profile in blood serum shows protein deposition, because if protein and albumin are high, the probability of protein deposition in meat is higher. Albumin is the main protein contained in blood plasma which is responsible for osmotic pressure and as a transport agent for various small molecules in the blood such as fatty acids and bile pigments (Mushawwir and Latipudin, 2011). Probiotics increase ration efficiency, egg production, and lower egg cholesterol and serum cholesterol levels. In addition, probiotics are also able to reduce non-protein nitrogen in the blood, concentrations of uric acid, ammonia and urea in the blood (Rusmana, and Adriani, 2020).

The experiment in this study was conducted to assess the impact of dry probiotics on several blood biochemical parameters, including blood protein and broiler albumin. The use of probiotics in combination with mung bean milk, FCM, and FSM has not been widely reported by previous researchers; therefore, this study studied the biochemical profile of broiler blood given dry probiotics. Previous studies have shown that the phenol content and antioxidant activity of fermented products appear to increase. This phenomenon is caused by the mobilization of the phenolic conjugate form during the fermentation activity (Xiao et al., 2015). Another study reported that microbes belonging to the lactate group were able to produce enzymes. One type of enzyme that is synthesized during the fermentation process is an enzyme that breaks down carbohydrates. This phenomenon is characterized by the release of phenolic compounds (Razak et al., 2015). In addition, it can reduce anti-nutrition (Susi, 2012).

Some researchers use liquid or dry yogurt with the dry fries method. However, in this study, drying was carried out using a simple technology at a very low cost to reduce

* Corresponding author e-mail: teddyhidayatconf@gmail.com.

feed prices. The result of drying probiotics produces low microbiota than liquid form. However, dried probiotics have beneficial because produce high lactic acid, bacteriocin, and several compounds from soybeans and mung beans (Lengkey and Adriani, 2009; Adriani et.al., 2015).

2. Materials and Methods

2.1. Materials

The materials used in this study consisted of Cow's milk (CM), soybean, mung bean, and the starter contains several types of bacteria, namely *Streptococcus thermophilus, Lactobacillus bulgaricus, Bifidobacterium bifidum, Lactobacillus acidophilus*, maltodextrin DE 10-12, spectrophotometer, and several blood biochemical kits. (Biolabo, Bandung).

2.2. Methods

2.2.1. Experiment method

A total of 100 broiler DOC, 5 days old used in this investigation. This feeding treatment was carried out for 30 days study, accompanied by the physical recording of the environment and blood sampling. Giving dry probiotics was done by adding them to the ration. The dose of dry probiotics mixed into the ration was 2% of the total basal ration. A completely randomized design was used in this experiment, consisting of four treatments and five replications. The treatments include T0: BR; T1: BR with dried probiotic A (100% FCM); T2: BR with dried probiotic B (FCM and FMBM, with composition 75%: 25%), T3: BR with dried probiotic C (FCM and FSM, with composition 75% and 24%); and T4: BR with dried probiotics D (consisting of FCM, FMBM and FSM, with a composition, each: 50%; 25% and 25%).

2.2.2. Processing of probiotics

The basic ingredients used for fermentation in this experiment have been soy milk, CM, and green bean milk. The microbes that have been added to this fermentation process are Streptococcus thermophilus, Lactobacillus bulgaricus, Bifidobacterium bifidum and Lactobacillus acidophilus. Fermented milk mixed with 10-12 5% DE maltodextrin, serves as a nutritional supplement for microorganisms. Furthermore, probiotics were dried for 25 hours using an oven (simple method) at a temperature of 40^{o}C.

2.2.3. Detection Method

Blood sampling through the external pectoralis vein using a 5 mL EDTA tube was performed randomly on 20 broilers (consisting of 5 birds per replication, and treatment of 4 birds per replication). Blood plasma samples were analyzed according to the kit protocol (Biolabo, France). The absorbance of the sample was determined using a spectrophotometer at the Laboratory of Animal Physiology and Biochemistry, University of Padjadjaran. The blood biochemistry observed included total protein and albumin in blood plasma. Blood samples were taken when the chickens were 2 and 4 weeks old as much as 3 ml. using a syringe containing EDTA, then the plasma is separated for further analysis. Analysis of total protein and albumin used a spectrophotometer.

2.2.4. Data Statistical analysis

The data of plasma protein and albumin were analyzed using the variance of one-way analysis method. The significant difference between feed treatments was determined by Tukey's analysis with the degree of significant difference at P <0.05. As a basis for statistical analysis, the hypothesis has been established that dry probiotic levels can increase blood protein and albumin levels in broiler chickens.

3. Results and Discussion

Table 1. Effect Dried Probiotic on Blood Protein and Albumin Broiler Chicken

Variable	T0	T1	T2	T3	T4	p-value
Blood Protein (g/dl)	2.52 ± 0.20	2.59 ± 0.85	3.22 ± 0.47	2.60 ± 2-0.12	2.81 ± 0.51	0.074; n=100
Albumin (g/dl)	1.30 ± 0.36	1.36 ± 0.66	1.44 ± 0.91	1.32 ± 0.35	1.38 ± 0.51	0.062; n=100

The results showed that the administration of dry probiotics had no significant effect on increasing blood protein and albumin (P>0.05). Although there was no significant difference, blood protein and albumin levels increased by 21.74% and 10.77% at T2 (FCM + FMBM dry probiotic mixture, with a ratio of 75%: 25%). Sugiharto et al. (2017) showed that the normal range of blood protein ranges from 2.14 to 3.12 g/dl. Analysis of variance showed that dry probiotic feeding showed no significant difference (P>0.05). The results of the current investigation seem to agree with the findings of Djouvinov et al. (2005), and Aluwong et al. (2012) who found that probiotic supplementation did not affect protein and total albumin levels in chickens. Although not significantly different, there is a tendency to increase protein levels in the blood. Based on previous research, Arslan and Saatci (2004) and El-Rahman et al. (2012) showed an increase in plasma protein concentration with the addition of probiotics in the diet. The high protein content in the blood indicates that the protein deposition in the meat is also high; on the contrary, the low protein value in the blood or below the standard indicates that the chicken lacks nutrition. Optimal liver function will be followed by an increase in plasma protein because most plasma proteins are synthesized in the liver (Widhyari., et al. 2014). Previous studies have also shown that plasma protein can be a valid indicator in determining the status of tissue function (Mushawwir, A et al, 2020; Tanuwiria and Mushawhir, 2020. This is related to the function of liver tissue as a producer of albumin protein. It is known that 75% of plasma protein blood is albumin.

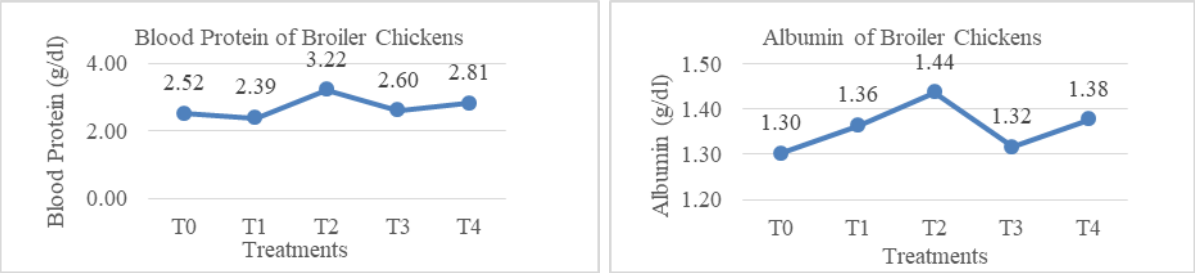

Figure 1. Effect Dried Probiotic on Blood Protein and Albumin Broiler Chicken

The average albumin for each treatment (Table 1) ranges from 1.30-1.44 g/dl. Blood albumin levels from lowest to highest include T0: 1.30 g/dl, T3: 1.32 g/dl, T2: 1.36 g/dl, T4: 1.38 g/dl, and T2: 1.44 g/dl. Blood albumin in the study is in the normal range about 1.06 - 1.39 g/dl (Owo Sibo *et al*., 2013). The variance analysis results showed that supplementation of dry probiotics did not show a significant difference (P> 0.05). However, there is a tendency to increase blood albumin levels.

Albumin and blood protein plays a major role in the deposition of protein into the meat. In accordance with Liu et al. (2015) which states that albumin affects the growth rate of broiler chicken. It means low albumin will have an effect on total protein. Consumption of less protein causes reduced blood albumin so that protein deposition into the meat will also decrease. Parmentier *et al*. (2009) and Savary-Auzeloux *et al*., (2010) reported that blood albumin produced in the liver forms the majority of all plasma proteins (consisting of 60% albumin). The content of blood protein values is normally used for weight gain (Saleh and Dwi, 2005). Blood protein and albumin were highest in T2 with dry probiotics combined with 75% FCM and 25% FSM. Probiotics in the ration increase the content of lysine analogue and aminoethyl cysteine in the digestive tract which is converted to amino acid lysine and cysteine so as to increase the retention of proteins that play a role in meat formation (Candrasih and Bidura. 2001; Farhana *et al*., 2012; Saikat *et al*., 2017).

One of the causes of weight gain in living things is the activity of probiotic bacteria. Previous researchers reported that the increase in digestive efficiency is caused by the use of nutrients and absorption of nutrients by absorptive cells (Lengkey and Adriani, 2011; Sheval et al., 2020). The results of previous studies showed that an increase in digestive enzyme activity and an increase in the morphometric surface of intestinal villi occurred due to the presence of probiotic bacteria (Muhannad et al., 2019). This physiological condition also has an impact on increasing digestibility, absorption of nutrients, as well as the formation and increase in the size of new tissues (Lengkey and Adriani, 2011; Priastoto et al., 2016; Adriani et al., 2019). The results of the same study have also been reported by other researchers (Hernawan et al., 2017; Mushawwir et al., 2018; Adriani and Mushawwir, 2020). An increase in the number and width of the jejunal villi from feed plus probiotics that affect the final body weight of broilers has also been reported by Adriani et al. (2019). In addition, several researchers, including Toghyani et al., (2015), Astuti (2015), Jin et al., (2000) emphasized that increasing the population of microbes that are beneficial to livestock will prevent the development of pathogenic microbes in the digestive tract of food.

4. Conclusion

Dried probiotics can increase protein in the blood by 27.77%, and albumin by 10.76% compared to control, in the FCM + FMBM mixture treatment by 75% and 25%, respectively. Although all treatments were able to increase blood protein and albumin, the results of increasing levels were not significantly different in broiler chickens. Interestingly, the increase in plasma protein and albumin may be a valid indication of increased protein anabolism and overall broiler performance.

5. Significant statement

This study found that the application of FCM, FMBM and FSM as probiotics added to broiler feed was beneficial for increasing blood protein and albumin in plasma. The results of this study have helped researchers to explore more deeply the effect of various combinations of FCM, FSM, and FMBM as probiotics to increase protein metabolism in supporting the immune and performance of broiler chickens. Thus, the new theory about the application technique and the impact of using FCM, FMBM and FSM in broiler rations can be accepted.

Acknowledgments

This work is supported by the PTUPT project from the Ministry of RISTEK-DIKTI Grant 2020, as well as the Academic Leadership Grant from Padjadjaran University for Lovita Adriani (2020). Therefore, we give the award to both parties.

References

Adriani L, Widjastuti T, and Dermawan R. 2015. The effect of probiotic supplemented ration on broiler abdominal fatty content and final weight. *Lucrari Stiintifice Zeria Sohteniee*., **53 (2)**: 22-25.

Adriani, L., Latipudin D, Balia RL, and Widjastuti T. 2019. Improvement of Small Intestine Morphometry in Broiler Chicken Using Fermented Cow and Soymilk as Probiotic. *International J Pakistan Sci*., **18 (8)**: 255-259.

Adriani L, and Mushawwir A. 2020. Correlation Between Blood Parameters, Physiological and Liver Gene Expression Levels in Native Laying Hens Under Heat Stress. *IOP Conf. Series: Earth Env Sci*, 466:1-7

Aluwong, T, MA. Raji, BF. Hassan, MU. Kawu, P. Kobo, JO. Iaand Ayo. 2012. Effect of Different Levels of Supplemental Yeast on Performance Indices and Serum Biochemistry of Broiler Chickens. *The Open Conference Proceedings Journal.*, **3**: 41-45.

Arslan C, and Saatci M. 2004. Effects of probiotic administration either as feed additive or by drinking water on performance and blood parameters of Japanese quail. *Arch Geflügelkd.,* **68**: 160–163.

Astuti. 2015. Utilization of Lactic Acid Bacteria Probiotics from Fish Digestion Channels on Growth and Cholesterol Levels of Broiler Chicken Meat. *J Sci Technol Res*, ***20*** : 2.

Candrasih NNK, and Bidura IGNG. 2001. The Effect of Use of Cocoa Shells Supplemented with Yeast Tape in the Ration on the Appearance of Bali Ducks. *Animal Husb Sci Mag.*, **4 (3)**: 67-72.

Djouvinov D, Svetlana B, Tsvetomira S, and Tatiana V. 2005. Effect of Feeding Lactina Probiotic on Performance, Some Blood Parameters and Caecalmicroflora of Mule Ducklings. *Trakia J Sci*, **3**: 22–28.

El-Rahman, AHA., HH. Kamel, WM. Ahmed, OSH. Mogoda, and AH. Mohamed. 2012. Effect of Bactocell® and Revitilyteplustm as probiotic food supplements on the growth performance, hematological, biochemical parameters and humoral immune response of broiler chickens. *World Appl Sci J*, **18 (12)**: 305–316.

Farhana SD, Khondoker MH, Azim MA, and Moinul HMd. 2012. Isolation, Characterization and Determination of Antimicrobial Properties of Lactic Acid Bacteria from Human Milk. *Jordan J Biol Sci*, 6 **(2)** : 111- 116

Ganong WF. 2000. **Medical Physiology**, Medical Book Publisher EGC, Jakarta.

Hernawan, E, Adriani L, Mushawwir A, Cahyani C, and Darwis D. 2017. Effect of dietary supplementation of chitosan on blood biochemical profile of laying hens. *Pakistan J Nut,***16 (9)**:696-699.

Jin, LZ, Ho YW, Abdullah N, and Jalaludin S. 2000. Digestive and bacterial enzyme activities in broilers fed diets supplemented with Lactobacillus cultures. *Poul. Sci*, **79**: 886–891.

Massadehd IM, and Mhmoud S. 2019. Antibacterial Activities of Soil Bacteria Isolated from Hashemite University Area in Jordan. *Jordan J Biol Sci*, 12 (4) : 503 – 511.

Mushawwir A, and Latipudin D. 2011. Some biochemical parameters of the laying hens of grower and layer layers in the "upper zonathermoneutral" environment. *J Indonesian Animal Husb*, 13 (3): 191 - 198.

Mushawwir A, Tanuwiria UH, Kurnia AK, Adriani L, Wiradimadja R, and Suwarno N. 2018. Evaluation of Haematological Responses and Blood Biochemical Parameters of Heat-stressed Broilers with Dietary Supplementation of Javanese Ginger Powder (Curcuma xanthorrhiza) and Garlic Extract (Allium sativum). *Int J Poultry Sci.*, **17**:452-458.

Mushawwir, A, Arifin J, Darwis D, Puspitasari T, Pengerteni DS, NuryanthiN, and Permana R. 2020. Liver metabolic activities of Pasundan cattle induced by irradiated chitosan. *Biodiversitas*., **21 (12)**:5571-5578.

Lelamurni LAR, Nur YAR, Anisah J, Shaiful AS, Kamariah L, 2015. Enhancement of phenolic acid content and antioxidant activity of rice bran fermented with Rhizopus oligosporus and Monascus purpureus. *Biocatalysis and Agricultural Biotechnology*., 4 (1): 33-38.

Lengkey HAW and Adriani L. 2009. Effects of milk fermented with Lactobacillus acidophilus and Bifidobacterium spp., on lactic acid and acetic acid content and on Staphylococcus aureus and Pseudomonas aeruginosa. *Biotechnology in Animal Husbandry.*, **25**: 719-724

Lengkey HAW and Adriani L. 2011. The Effect of Lactobacillus bulgaricus and Streptococcus thermophilus as Ration Supplement on Broiler Carcass Weight, Carcass Fat Content and The Serum Cholesterol Carcass Content. *Int Sem Biotechnol.*

Liu B, Pang Y, Bouhenni R, Duah E, Paruchuri S, and McDonald L. 2015. A Step Toward Simplified Detection of Serum Albumin on SDS-PAGE Using an Environment-Sensitive Flavone Sensor. *Chem Comm*, **51 (55)** :11060-11063.

Owo sibo, AO., OM. Odetola, O. Odunsi, OO. Adejinmi, and OO. Lawrence-Azua. 2013. Growth, haematology and serum biochemistry of broilers fed probiotics based diets. *J Academic*., **8 (41)**: 5076 – 5081.

Parmentier HK, Rodenburg B, Reilingh GDV, Beerda B, and Kemp B. 2009. Does Enhancement of Spesific Immune Responses Predipose Laying Hens For Feater Pecking. *Poultry Sci*, **88**: 536-542.

Priastoto D, Kurtini T, and Sumardi. 2016. The Effect of Probiotics from Local Microbes on Performance of Layer. *Jurnal Ilmiah Peternakan Terpadu.*, **4(1):** 80-85.

Rusmana D. and Adriani L, 2020. Effect of Fermented Cow and Soymilk as Probiotic on Energy Metabolism and Nutrient Retention in Broiler Chicken. *Int J Poultry Sci*, **19**: 277-281.

Saleh, E. and J. Dwi. 2005. The Effect of Katuk Leaf Flour on Broiler Chicken Performance. *Jurnal Agribisnis Peternakan.*, **1(1)**:14-16.

Saikat RP, Raad SMD, and Lukman HMD. 2017. Antibacterial Different Solvents. *Jordan J Bio Sci*, **10 (3)** : 213 – 217**.**

Savary- Auzeloux, I., G. Kraft, BJ. Bequette, I. Papet, D. Remond, and I. Ortigues-Marty. 2010. Dietary Nitrogen-to-Energy Ratio Alters Amino Acid Partition in the Whole Body and Among The Splanchnic Tissues of Growing Rams. *J Animal Sci*, **88**: 2122-2131.

Sheval FM , Qerim IS, Kasum RrL, and Isa RE. 2020. Chronic Effects of Lead Exposure on Oxidative Stress Biomarkers in Feral Pigeon (Columba livia) from Smelter Area in Kosovo. *Jordan J Biol Sci*, **13 (3) :** 589 - 595.

Sugiharto S, Isroli Y, Endang W, and Fatan DP. 2017. Intestinal microbial ecology and hematological parameters of broiler fed cassava waste pulp fermented with Acremonium charticola. *J Vet World.*, **10 (3)**: 324 – 330.

Susi, S. 2012. Chemical Composition and Amino Acid Composition of Nagara Bean Tempe ((Vigna unguiculata ssp. cylindrica). *Agroscientiae.*, **19(1)**: 28-36.

Tanuwiria, U.H. and Mushawwir A. 2020. Hematological and antioxidants responses of dairy cow fed with a combination of feed and duckweed (Lemna minor) as a mixture for improving milk biosynthesis. *Biodiversitas.*, **21 (10)** :4741-4746.

Toghyani, M, Mosavi SK, Modaresi M, and Landy N. 2015. Evaluation of kefir as a potential probiotic on growth performance, blood biochemistry and immune responses in broiler chicks. *Animal Nut.*, **1(3)** : 305–309.

Widhyari SD, Esfandiari A, dan Herlina. 2014. Profile of Total Protein, Albumin, and Globulin on Broiler were Given Turmeric, Garlic, and Zn. *Indonesian Agr Sci J*, **10(3)**:179-184.

Yu XL, Wang XW, Li X, Chen MJ, and Mingsheng D. 2015. Enhancement of the antioxidant capacity of soywhey by fermentation with Lactobacillus plantarum B1–6. *J functional foods.*, **12(2)** : 33–44.

JJBS

Volume 14, Number 5,December 2021
ISSN 1995-6673
Pages 1025 – 1029

Jordan Journal of Biological Sciences

Physiological Analysis of Orchid Chlorophyll against *Odontoglossum ringspot virus* Infection

Mahfut[1,*], Irni Yuni Minarni[2], Sri Wahyuningsih[1], Tundjung Tripeni Handayani[1]

[1]*Department of Biology, Faculty of Mathematics and Natural Sciences, Universitas Lampung, Indonesia;* [2]*Undergraduate Student, Department of Biology, Faculty of Mathematics and Natural Sciences, Universitas Lampung, Indonesia*

Received: July 21, 2021; Revised: October 23, 2021; Accepted: November 6, 2021

Abstract

Orchids (Orchidaceae) are one of the most popular ornamental plants having diverse flower shapes and colors. They are vastly applied as cut flowers, potted plants, and garden elements. Infectious diseases are still a major obstacle in the cultivation of orchids in Indonesia. *Odontoglossum ringspot virus* (ORSV) is one of the most widely reported viruses that infect orchids worldwide, including Indonesia. This research was done by mechanically injecting the virus on *Phalaenopsis amabilis* and *Dendrobium* Salaya Fancy. This study aimed to determine the symptoms of the disease, plant resistance, and chlorophyll content. The results showed that each orchid had severe disease symptoms, the incidence of both orchids was 80%, and *Phalaenopsis amabilis* reaction was more susceptible than *Dendrobium* Salaya Fancy that showed tolerant response to ORSV. Physiological response analysis also showed that the content of chlorophyll A,B, and total *Dendrobium* Salaya Fancy was higher (0.35 ± 0.02; 0.29 ± 0.05; 0.63 ± 0.05) than *Phalaenopsis amabilis* (0, 18 ± 0.0; 0.31 ± 0.06; 0.48 ± 0.04) respectively, after viral infection. This proves that *Phalaenopsis* is the most susceptible type of orchid virus compared to *Dendrobium*.

Keywords: selection of resistance; analysis of chlorophyll; orchid; ORSV

1. Introduction

Orchidaceae are ornamental plants that have a high aesthetic value (Mose et al., 2020), because they have a variety of colors and flower shapes. For that, high demands of markets on orchids have been raised in the form of cut flowers and potted plants (Mahfut et al., 2016). One of the obstacles in cultivating orchids is infectious diseases that affect flower quality. Orchids can be infected with 50 types of viruses (He et al., 2019), including *Odontoglossum ringspot virus* (ORSV) (Pai et al., 2019). The virus is an important type that attacks orchids and is popular in the world.

ORSV, also known as *Tobacco mosaic virus* orchid strain (TMV-O), belongs to the genus *Tobamovirus* and the family Virgaviridae (Forterre et al., 2017). There is very little information about ORSV infection in Indonesia. The virus is reported to be able to infect *Phalaenopsis* and *Dendrobium* orchids in West Java, Central Java, East Java, Banten, Yogyakarta, and Bali (Mahfut et al., 2016). ORSV infection causes damage to chlorophyll and affects the growth and development of orchids.

Efforts to protect orchids against viral infections need to be carried out to reduce the spread and preserve orchids in Indonesia. The initial stage of protection is considered through observing symptoms to determine the type and nature of a disease (He et al., 2017; Ko et al., 2020). This data is then used in determining plant resistance. In addition, chlorophyll analysis was also carried out, and so the physiological response of plants due to viral infection was collected.

This study was conducted to distinguish plant responses in the form of disease symptoms, plant resistance, and chlorophyll content between *Phalaenopsis amabilis* and *Dendrobium* Salaya Fancy against ORSV infection. The results of this study are expected to provide information about the response and level of resistance of orchids to ORSV infection, and it could be used as a reference for the right type of orchid to be cultivated in disease endemic areas or there has been a history of previous ORSV infection.

2. Materials and Methods

2.1. Plantlet Acclimatization

This study used two orchid species, *Phalaenopsis amabilis* and *Dendrobium* Salaya Fancy on six replicates. Plantlets were immersed in a fungicide Benlate solution, with active ingredient Benomyl (2 grams/l water) for 20 minutes and then planted in plastic pots containing sterile of moss media (Mahfut et al., 2021). Orchids were well cared for before treatment in a green house.

2.2. Virus Inoculation

The inoculum used was prepared from inoculation of the Magelang isolate virus on tobacco plants that had been previously analyzed (Mahfut et al., 2016). The inoculum was then mechanically inoculated. The initial stage of inoculation is to weigh 1 gram of viral inoculum, then

* Corresponding author e-mail: mahfut.mipa@fmipa.unila.ac.id.

grind in a sterile mortar by adding 10 ml of 0.01 M phosphate buffer solution (pH 7) (w : v = 1 : 10). Before being inoculated, 100 mess of carborundum powder was sprinkled on the upper surface of the leaves, then the virus was applied to the two youngest leaf surfaces that were fully opened. After the virus sap dries, the carborundum that remains attached to the leaf surface of the test plant was cleaned by spraying sterile water (Mahfut et al., 2016).

2.3. Observation of Infection Symptoms

The results of the inoculation test on plants were noted for variations in symptoms and incubation time. Observations were made every three days for one month to determine the response among host plants that were more quickly infected with symptoms of the disease. ORSV inoculation on each host plant was carried out at different times depending on the fast or slow growth of the plant and indicated whether or not the number of leaves was sufficient.

2.4. Plant Resistance

Determination of disease resistance criteria for various types of plants against ORSV infection was based on several factors, including symptoms of viral infection and the percentage of disease incidence. Analysis of plant resistance was used to determine the development of the observed disease, namely disease incidence. The incidence of disease is carried out by calculating the scale of damage (%) of the disease that appears on the host plant. Plant resistance was grouped into very resistant, resistant, moderately resistant, tolerant, susceptible, and very susceptible, following the method of Dwipa et al. (2018).

2.5. Chlorophyll Content Test

This test was carried out following Sedjati et al. (2020) using a spectrophotometer. For measuring chlorophyll content, the sample was applied an orchid leaf that had been identified as infected with ORSV. In the first step, 1 gram of treated orchid leaves were weighed, the leaves had been removed, then crushed with a mortar and added 10 ml of ethanol. The solution was filtered with Whatman paper no. 1 and put into a flakon, then tightly closed. Sample solution and standard solution (ethanol) 1 ml were put into different cuvettes. Furthermore, absorption readings were carried out with a UV spectrophotometer at wavelengths (λ) 648 nm and 664 nm, the measurements were carried out three times for sample replication.

3. Results

3.1. Observation of Infection Symptoms

The response of plants after virus inoculation showed that ORSV could infect all types of host plants with variations in symptoms and different incubation times. The results showed that in general the response began to appear about 2-3 weeks after inoculation. The symptoms showed necrotic *Phalaenopsis amabilis*, while *Dendrobium* Salaya Fancy showed necrotic and mosaic symptoms. Variations in response to symptoms of viral infection in both host plants are shown on (Figure 1).

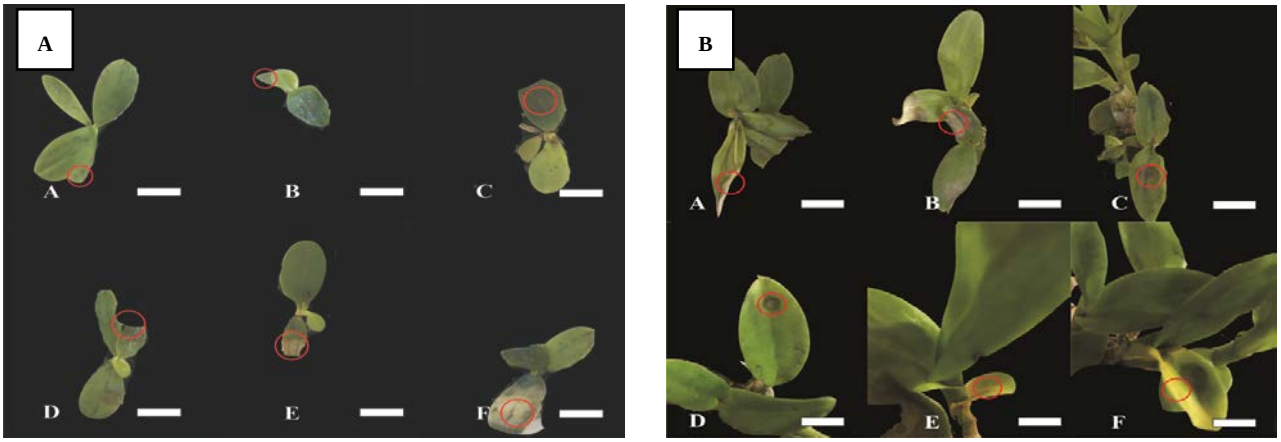

Figure 1. Symptoms of virus infection on (A) *Phalaenopsis amabilis* and (B) *Dendrobium* Salaya Fancy. Bar= 1cm

3.2. Plant Resistance Analysis

The results of the analysis of plant resistance to ORSV infection were based on variations in symptoms, incubation times, and disease incidence. The results of the analysis showed that the level of resistance is very susceptible to symptoms of very severe infection. Meanwhile, *Dendrobium* Salaya Fancy showed a level of resistance that was tolerant to a fairly severe variety of symptoms, but not as severe as the symptoms of infection in *Phalaenopsis amabilis*.

3.3. Chlorophyll Content Test

The results of the physiological response analysis showed that the chlorophyll A, chlorophyll B, and chlorophyll total content of *Dendrobium* Salaya Fancy was higher than *Phalaenopsis amabilis* after being infected with the virus. The complete test results for the content of chlorophyll on both types of host plants for 30 days after ORSV inoculation are shown in Table 1.

Table 1. Tukey's test of chlorophyll A, B, total content of two types of host plants 30 days after inoculation

Treatment	Type of Chlorophyll	Species of Host Plant	
		Phalaenopsis amabilis	*Dendrobium* Salaya Fancy
Control	Chlorophyll A	0,17 ± 0	0,37 ± 0
	Chlorophyll B	0,24 ± 0,01	0,28 ± 0
	Chlorophyll Total	0,41 ± 0,01	13,9 ± 13,27
Virus Inoculated	Chlorophyll A	0,18 ± 0,01	0,35 ± 0,02
	Chlorophyll B	0,31 ± 0,06	0,29 ± 0,05
	Chlorophyll Total	0,48 ± 0,04	0,63 ± 0,05
Total of Average	Chlorophyll A	$0,18^{a}$ ± 0,05	$0,36^{b}$ ± 0,01
	Chlorophyll B	0,28 ± 0,04	0,29 ± 0,03
	Chlorophyll Total	0,45 ± 0,025	7,27 ± 6,66

Note: The values followed by the same letter are not significantly different at the 5% level. Chlorophyll A: HSD Cell [.05] = 0.05. HSD Columns [.05]= 0.02. Chlorophyll B: Values followed by the same letter are not significantly different at the 5% level. HSD Cell [0.05] = 0.12. HSD Columns [.05]= 0.06. Total Chlorophyll: HSD Cell [0.05] = 26.86. HSD Columns [.05]= 14.5

The homogeneity of Levene's test variance at 5% significance level showed that the variance of the samples of the two host plants was homogeneous (P=0.201>0.05). Analysis of variance at the 5% level of significance showed that the virus treatment had no significant effect on the chlorophyll a content of the host plant (P=1>0.05), but the type of plant had a significant effect on the chlorophyll a content (P<0.0001). Thus, the interaction between virus inoculation and plant species did not significantly affect the chlorophyll a content (P=1>0.05). The content of chlorophyll A after virus inoculation with two types of host plants is shown in (Figure 2).

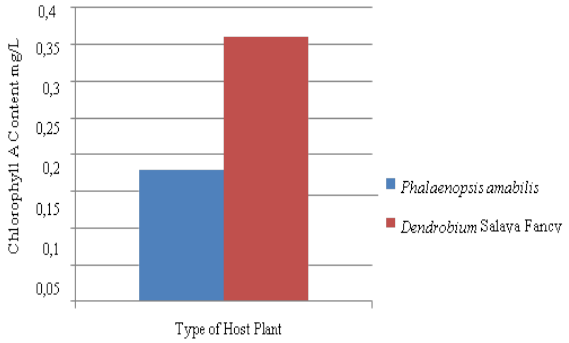

Figure 2. Curves of chlorophyll A content after virus inoculation in two types of host plants

Chlorophyll B is one of the parameters that affect plant metabolism through photosynthesis. The homogeneity of Levene's test variance at 5% significance level showed that the variance of the samples of the two host plants was homogeneous (P= 0.076>0.05). Analysis of variance at 5% significance level showed that the virus treatment (P=0.15>0.05) and plant species (P>0.05) had no significant effect on chlorophyll B levels, respectively. Likewise, the interaction between virus inoculation and plant species did not significantly affect the chlorophyll B content (P>0.05). Virus inoculation and plant species did not significantly affect chlorophyll B. ORSV inoculation on chlorophyll B content on *Phalaenopsis amabilis* and *Dendrobium* Salaya Fancy is shown in (Figure 3).

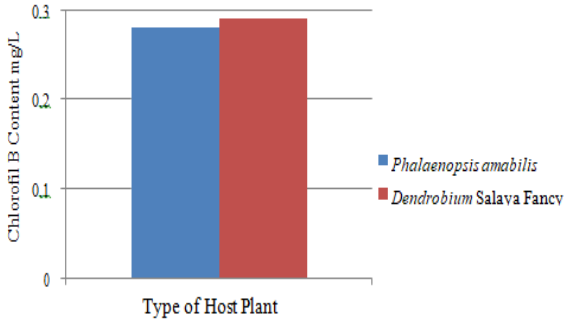

Figure 3. Curves of chlorophyll B content after virus inoculation in two types of host plants

The results of the total chlorophyll content test in both host plant samples also showed homogeneity of the Levene test variance at the level of significance 5 (P=0.224). The results showed that the virus treatment had no significant effect (P=0.34) and the type of plant also had no significant effect on the total chlorophyll content (P=0.32) in the analysis of variance at 5% significance level.

Likewise, the interaction between virus inoculation and plant species did not significantly affect the total chlorophyll content (P=0.33). ORSV virus inoculation, plant species and interactions on host plants did not significantly affect total chlorophyll. ORSV virus inoculation on total chlorophyll content in *Phalaenopsis amabilis* and *Dendrobium* Salaya Fancy is presented in (Figure 4).

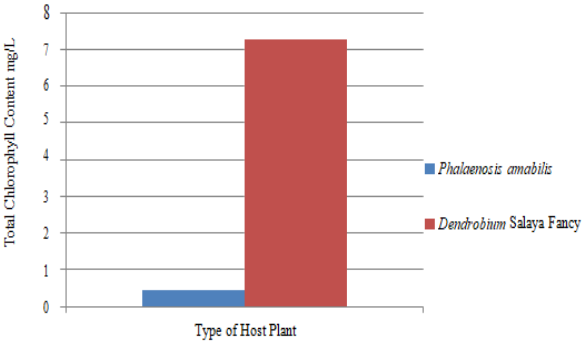

Figure 4. Curves of total chlorophyll content after virus inoculation in two types of host plants

4. Discussion

The symptomatic response of ORSV in host plants shows a wide range of symptoms on the examined host plants *Phalaenopsis amabilis* and *Dendrobium* Salaya Fancy. Based on the results of the virus inoculation on the two orchids did not show symptoms until the 30th day, so reinoculation was necessary. Then, reinoculation is performed and observed again until symptoms can be seen. *Phalaenopsis amabilis* showed necrotic symptoms on the 18th day. Observations continued until day 30 and showed worsening necrotic symptoms. In a previous study of Mahfut et al. (2020[a]), it was also known that ORSV infection in *Phalaenopsis* sp. showed necrotic symptoms on 23rd day.

Dendrobium Salaya Fancy also showed necrotic symptoms on the 15th day. Necrotic symptoms in *Dendrobium* were shown more rapidly than *Phalaenopsis*. Based on the observation of symptoms up to day 25, necrotic symptoms turned into a mosaic indicating that

ORSV infection in *Dendrobium* was getting worse. In previous studies, it was known that ORSV infection in *Dendrobium* sp. also appeared necrotic and mosaic symptoms on 15th and 23rd day (Mahfut, 2020; Mahfut et al., 2020[a]; Mahfut et al., 2020[b]; Mahfut et al., 2021).

The results of disease incidence analysis showed that each host plant had the same response that the disease incidence was > 40% and disease infection was found. This proves that the inoculation of ORSV on the whole host plant was successful. In previous research (Mahfut, 2020), it is also known that ORSV inoculation in *Phalaenopsis* sp. and *Dendrobium* sp. showed an incidence of disease > 40% and found the presence of disease infection.

Based on the results of the study, it is known that the host plant *Phalaenopsis amabilis* which shows a very susceptible level of resistance with very severe symptoms of infection. Meanwhile, *Dendrobium* Salaya Fancy orchid showed a tolerant level of resistance with a fairly severe variation of symptoms, but not as severe as the symptoms of infection in *Phalaenopsis amabilis*. This means that *Phalaenopsis amabilis* orchids are more susceptible to ORSV than *Dendrobium* Salaya Fancy.

Previous research (Mahfut, 2020) reported that *Phalaenopsis* is a highly susceptible host orchid plant and most susceptible to ORSV. In other research (Mahfut et al., 2020[a]; Mahfut et al., 2020[b]; Mahfut et al., 2021), it was also known that the plants *Phalaenopsis amabilis, P. small* Red White Lips x, *D. nindii*, *D. kyosimori*, *D. liniae*, *D. schulerii* had a response, i.e. are susceptible to ORSV.

Chlorophyll content analysis aims to determine the chlorophyll content in the host plant (Jaelani et al., 2016; Alananbeh et al., 2018; Saeed, 2019). Result of Tukey's test at the 5% significance level showed that two host plants, namely *Phalaenopsis amabilis* and *Dendrobium* Salaya Fancy, had a significant effect only on plant species but had no significant influence on viral treatment on chlorophyll A. The content of chlorophyll B in the leaves of *Dendrobium* Salaya Fancy was not much different from the content of chlorophyll B on *Phalaenopsis amabilis* leaves. This shows that the plants *Dendrobium* Salaya Fancy and *Phalaenopsis amabilis* have the same level of resistance, which is very susceptible to diseases not only caused by ORSV virus but can be caused by other factors such as fungi, bacteria, nutrients found in the media.

Total chlorophyll content in *Dendrobium* Salaya Fancy orchid leaves is relatively higher than the total chlorophyll content in *Phalaenopsis amabilis* orchid leaves. This indicates that the *Dendrobium* Salaya Fancy orchid is more resistant than the *Phalaenopsis amabilis* orchid to disease. Chlorophyll is a green pigment found in chloroplastide. In general, chlorophyll is found in leaf mesophyll cell chloroplasts, i.e. in palisade parenchyma cells and parenchyma sponge cells. In chloroplasts, chlorophyll is present in the gamma thylakoid membrane. In higher plants, the types of chlorophyll are chlorophyll A and chlorophyll B. Under normal circumstances, the proportion of chlorophyll A is much greater than that of chlorophyll B (Sedjati et al., 2020).

According to the chlorophyll data in this study, it was found that the chlorophyll data on *Dendrobium* Salaya Fancy plants are more than *Phalaenopsis amabilis* plants because seen morphologically, *Phalaenopsis amabilis* orchid plants have more severe symptoms than *Dendrobium* Salaya Fancy. It is possible that the leaf mesophyll tissue in *Dendrobium* Salaya Fancy is not damaged by the virus, and can produce more chlorophyll for photosynthesis. Therefore, it can be concluded that *Dendrobium* Salaya Fancy is more resistant to ORSV virus or other viruses than *Phalaenopsis amabilis*. Data on chlorophyll B and total chlorophyll in both host crops are stated to be statistically similar because usually the amount of chlorophyll B is less than that of chlorophyll A (Jaelani et al., 2016; Sedjati et al., 2020). Virus treatment and plant species interactions did not significantly affect the two host plants, so further testing was not performed. Therefore, it can be concluded that *Dendrobium* Salaya Fancy have a higher level of resistance than *Phalaenopsis amabilis*.

5. Conclusion

The results showed that the indicator crops and the host crops had quite severe disease with various symptoms. Each crop had the same response, the indicator crop had a disease incidence of > 40% i.e. 75% while the host crop with a disease incidence of > 40% i.e. 80%. Indicator and host plant responses to ORSV are highly susceptible, except that *Dendrobium* Salaya Fancy orchid host plants have a tolerant response to ORSV. The results of physiological response analysis showed that the content of chlorophyll A, B, and total *Dendrobium* Salaya Fancy were higher (0.35 ± 0.02; 0.29 ± 0.05; 0.63 ± 0.05) than *Phalaenopsis amabilis* (0.18) ± 0.0; 0.31 ± 0.06; 0.48 ± 0.04) respectively, after being infected with the virus. This proves that *Phalaenopsis* is the most susceptible type of orchid virus compared to *Dendrobium.*

References

Alananbeh KM, Bouqellah NA, Harbi MRA and Ouf SA. 2018. The Efficacy of Photosensitizers on Mycelium Growth, Mycotoxin and Enzyme Activity of *Alternaria* spp. *Jordan J Biol Sci.,* **11(5):** 499-510.

Dwipa I, Syarif A, Suliansyah I, Swasti E. 2018. West Sumatra Brown Rice resistance to Brown Planthopper and Blast Disease. *Biodivers J.,* **19(3):** 893-898.

He J, Lim RMP, Dass SHJ and Yam TW. 2017. Photosynthetic acclimation of *Grammatophyllum* speciosum to growth irradiance under natural conditions in Singapore. *Bot Stud.*, **58(1):** 58.

He Z, Dong T, Wu W, Chen W, Liu X and Li L. 2019. Evolutionary Rates and Phylogeographical Analysis of *Odontoglossum ringspot virus* Based on the 166 Coat Protein Gene Sequences. *Plant Pathol J*., **35(5):** 498-507.

Jaelani LM, Limehuwey R, Jurniadin N, Pamungkas A, Koenhardono ES, and Sulisetyono A. Estimation of Total Suspended Sediment and Chlorophyll-A Concentration from Landsat 8-Oli: The Effect of Atmospher and Retrieval Algorithm. *J Technol Sci Educ.,* **27(1):** 9-16.

Ko SS, Jhong CM and Shih MC. 2020. Blue Light Acclimation Reduces the Photoinhibition of *Phalaenopsis aphrodite* (Moth Orchid). *Int J Mol Sci.*, **21(17):** 61-67.

Mahfut. 2020. Identification and Detection *Odontoglossum ringspot virus* on Native Orchids Collection of Nurserys in Java, Indonesia. Proceedings of ICAISD Conference. University of Bina Sarana Informatika. West Java, Indonesia.

Mahfut, Anggreiny A, Wahyuningsih S, Handayani TT and Sukimin. 2020[b]. Identification of Disease and Efforts to Protect Native Orchid Plants Against Bacteria Infection in Liwa Botanical Garden. Proceedings of ICAISD Conference. University of Bina Sarana Informatika. West Java, Indonesia.

Mahfut, Indrianto A, Somowiyarjo S and Daryono BS. 2020[b]. Molecular phylogeny of orchids mycorrhiza isolated from native tropical orchids in Indonesia. *Malays J Microbiol.,* **16(1):** 68-72.

Mahfut, Joko T and Daryono BS. 2016. Molecular Characterization of *Odontoglossum ringspot virus* (ORSV) in Java and Bali, Indonesia. *Asian J Plant Pathol.*, **10(1-2):** 9-14.

Mahfut, Shafira H, Wahyuningsih S, Handayani TT and Sukimin. 2021. Identification of Virus Infection on Native Orchid in Liwa Botanical Garden. Proceedings of ICASMI Conference. University of Lampung. Lampung, Indonesia.

Mose W, Daryono BS, Indrianto A, Purwantoro A and Semiarti E. 2020. Direct Somatic Embryogenesis and Regeneration of an Indonesian orchid *Phalaenopsis amabilis* (L.) Blume under a Variety of Plant Growth Regulators, Light Regime, and Organic Substances. *Jordan J Biol Sci.,* **13(4):** 509-518.

Pai H, Jean WH, Lee YS, Chang YCA and Lin SL. 2019. Genome-wide analysis of small RNAs from *Odontoglossum ringspot virus* and *Cymbidium mosaic virus* synergistically infecting *Phalaenopsis*. *Mol Plant Pathol.,* **21(2):**188-205.

Saeed AK. 2019. Photo-protective Measurements of Almond Oil on UVB Irradiated Mouse's Skin and Cyclin D1 Expression. *Jordan J Biol Sci*., **12(4):** 395-401.

Sedjati S, Pringgenies D and Fajri M. 2020. Determination of the Pigment Content and Antioxidant Activity of the Marine Microalga *Tetraselmis suecica*. *Jordan J Biol Sci.,* **13(1):** 55-58.

JJBS

Volume 14, Number 5,December 2021
ISSN 1995-6673
Pages 1031 – 1034

Jordan Journal of Biological Sciences

Morphological Identification of Mycorrhizal Fungi Isolated from Native Orchid in Indonesia

Mahfut*

Department of Biology, Faculty of Mathematics and Natural Sciences, Universitas Lampung, Indonesia

Received: February 27, 2021; Revised: May 2, 2021; Accepted: November 28, 2021

Abstract

Moth orchid [*Phalaenopsis amabilis* (L.) Blume] is a species of native orchid from Indonesia. The association of this orchid with mycorrhizal fungi in nature is as a biocontrol agent. In a previous study, one *Ceratobasidium* isolate from Yogyakarta, Indonesia was successfully identified based on rDNA-ITS molecular analysis. This study aimed to identify these isolates based on morphological analysis to complement other identification data, namely anatomy and molecular. Verification morphological analysis is carried out by observing macroscopic and microscopic characteristics, as well as observing peloton. The results of showed that the characterization of Yogyakarta isolates had similarities with *Ceratobasidium*. These character equations include colony color, cell length, core number, and cell width. The examination of orchid roots also showed the presence of pelotons in the cortical cells. This study confirms that the fungal isolates of orchid mycorrhiza from Yogyakarta, Indonesia were *Ceratobasidium* based on morphological and molecular analysis. This research is one of the efforts to preserve native orchids in Indonesia using myccorhiza fungi as a biocontrol agent. This study is the first to report regarding *Ceratobasidium* isolated from native orchids in Indonesia based on morphological analysis.

Keywords: *Ceratobasidium*; mycorrhiza; morphological analysis; *Phalaenopsis*; Indonesia

1. Introduction

Orchid is a type of ornamental plant that has a high aesthetic value and is most in demand by the community (Mose et al., 2020). The moth orchid [*Phalaenopsis amabilis* (L.) Blume] is one of Indonesia's national flowers, namely the charm that was set through Presidential Indonesia Decree Number 4/1993. Diseases are still the main obstacle in the cultivation and development of natural orchids (Mahfut et al., 2019; Mahfut, 2020; Mahfut et al., 2020[b]; Mahfut et al., 2021).

Endophytic mycorrhiza is a form of symbiosis between fungi and plant roots during a certain period of their life cycle, forming colonies in plant tissues without endangering their hosts. In general, mycorrhizal fungi help germination of orchid seeds in the presence of ethylene and various vitamins. Another role is to support efforts to provide nutrition for plant growth and development (Haro and Benito, 2019), and to assist in the formation of more buds and flowers. In plant resistance, mycorrhiza fungi serve as a biological agent of control in plant protection against pathogenic infections (Safarini et al., 2020; Song et al., 2020).

In a previous study, Mahfut et al. (2020) reported one *Ceratobasidium* isolate from Yogyakarta, Indonesia based on rDNA-ITS molecular analysis. The results show sequences measuring 600-750 bp DNA products located on the ITS1-5.8S-ITS4 region. Reconstruction of phylogenetic trees resulted in Indonesian isolates having undergone speciation and separated from C*eratobasidium* isolates from other countries. This research is a follow-up study which aims to clarify the identification of these isolates as *Ceratobasidium* based on morphological analysis. Furthermore, this research can be used as a benchmark in developing strategy for conserving moth orchid through protection against plant diseases.

2. Materials and Methods

2.1. Collection of Healthy Orchid Root Samples and Endophytic Mycorrhizal Isolation

Healthy root of *P. amabilis* collected from Yogyakarta, Indonesia on coordinates 8º 30' - 7º 20' LS 109º 40' - 111º 0' BT. The sample was taken to the Biotechnology Laboratory of the Faculty of Biology UGM to isolate endophytic mycorrhiza following the Chand et al. (2020) method. Isolation of endophytic fungi was then carried out by cutting the roots and culturing on PDA medium. The fungal colonies obtained from the isolation were then purified by sub-culturing aseptically and incubating for 7 days at room temperature (20-25℃). It is possible that the isolates obtained are pure and single isolates that are not contaminated by other fungi.

2.2. Macroscopic Characteristic Observation

To observe the macroscopic characteristics of the isolated fungi, small portion of isolates (± 1 mm^2) were placed in the middle of the PDA medium. Furthermore, the growth of the isolates was observed and measured every day for 7 days. Furthermore, observations of colony morphological characteristics such as colony color, colony

* Corresponding author e-mail: mahfut.mipa@fmipa.unila.ac.id.

base color, the surface color of young colonies, the appearance of colonies, and the growth rate of the colony were carried out.

2.3. Making Slide Culture Preparations

Observation of microscopic characteristics was also carried out using the slide culture method (Stoian et al. 2019) with a slight modification. This method was carried out to monitor microscopic characteristics such as the color of hyphae, bulk in hyphae, angle of branching of hyphae, and number of cell nuclei. The number of nuclei was observed after treating with safranin and 3% KOH.

2.4. Observation of Pelotons in roots

Observation of peloton was carried out by making squash preparations on root samples which had been treated with previous endophytic fungal inoculations. Root samples are sliced and soaked in trypan blue dye for 15 minutes. Observations were carried out using a light microscope at 100 x magnification.

3. Results

3.1. Collection of Healthy Orchid Root Samples and Endophytic Mycorrhizal Isolation

One endophytic fungus, namely Yogyakarta was isolated from root samples of *P. amabilis* in Yogyakarta, Indonesia in Figure 1.

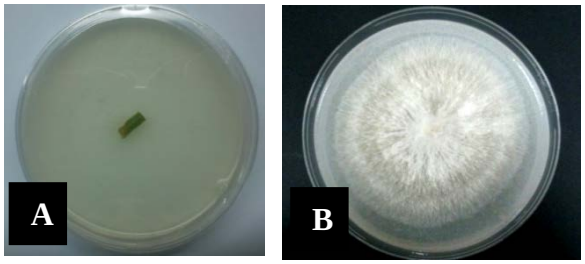

Figure 1. A) Root samples of MP1 cultured on PDA medium, B) Colonies of fungi that grow on 7 days old orchid roots

Identification results based on macroscopic, microscopic, and molecular characteristics showed that the isolate was *Ceratorhiza* which is one of the types of *Rhizoctonia* endophytic mycorrhiza. According to Chand et al. (2020), *Ceratorhiza* is *Rhizoctonia* grouped by cell hyphae and moniloid, and many are found to be associated with orchid roots.

3.2. Macroscopic Characteristics

Special characteristics of Yogyakarta isolate were identified as having branching types that formed elbows or 90º angles and hyphae cells with a cell nucleus 2 (binucleate). These two characteristics are special characteristics of endophytic mycorrhiza. Endophytic fungi have 1-3 nuclei (binucleate) nuclei, whereas pathogenic fungi have more than 3 nuclei (multinucleates). This is in accordance with the opinion of Pannecoucque & Hofie (2009) that in addition to binucleates, the characteristics of endophytic fungi are branching which forms a 90ºC or T-shaped branches.

Overall, the results of identification of Yogyakarta isolates showed similarities with the types of *Ceratorhiza* mycorrhiza. The following characteristics of Yogyakarta isolates compared to supporting references are presented in Tables 1 and 2.

Table 1. Comparison of the characteristics of Yogyakarta isolates and *Cerathoriza* isolates according to Shan et al. (2002)

Characteristics	**Yogyakarta Isolate**	***Cerathoriza* Isolate**
The surface color of young colonies	White to yellow	Yellow to white
The appearance of colonies	Like cotton	Like cotton
Hyphae color	Hyaline	Hyaline
Hyphae diameter (µm)	6.20-6.72	3.8-7.5
Monilioid cell form	Elongated, barrel shaped	Ellipsoidal or elongate barrel shape
Monilioid cell size (µm)	(12.22-14.56) × (2.39-2.91)	(7.5-15.0) × (10.0-25.0)
The growth rate of the colony (mm / hr)	0.72	0.42-0.52
Number of cell nuclei	Binucleate	Binucleate

Table 2. Comparison of the characteristics of Yogyakarta isolate and *Cerathoriza* isolates according to Currah and Zelmer (1992)

Characteristics	**Yogyakarta Isolate**	***Cerathoriza* Isolate**
Colony color	White to yellow	Cream, yellow, or brown
The appearance of colonies	Like cotton	Like cotton
The form of branching hyphae	90 º	90º
Air hyphae diameter	<3 µm	<4 µm
Number of nuclei per cell	Binucleate	Binucleate
Clamp connection	-	-
Surface of the colony	Like cotton	*Flat and waxy*
Monilioid cells	*Elongate barrel shaped*	-
Monilioid cell length	12.22-14.56	-
Monilioid cell width	2.39-2.91	-

Based on observations of hyphae and cells using safranin O-KOH dye **(**Figure 2**)**, it was found that Yogyakarta isolates were endophytic fungi of *Ceratorhiza* with specific characteristics having branching types that form elbows or 90° angles, the color of vegetative hyphae is hyaline, with diameters of 6.20-6.72 µm, fungal colonies form cell monilioids with elongate barrel shape and monilioid size (12,22-14,56) µm x (2.39-2.91) µm.

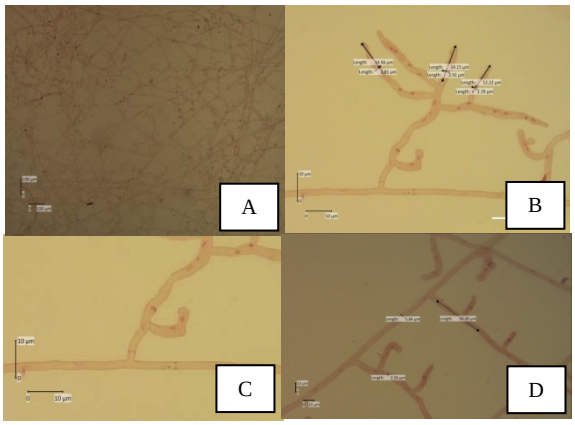

Figure 2. Microscopic observation of hyphae cells and moniliod cells *Ceratorhiza* from Yogyakarta isolates on the 7-day PDA medium using safranin O-KOH staining; (A) Colony, (B) Monilioid cell nucleus, (C) Binucleate, (D) Branching of hyphae 90º. Magnification (A) 10 x, (B, C, D) 40 x. Bar = 10 µm

3.3. *Observation of Endophytic Mycorrhizal Hyphae (Peloton)*

Observation of the cross section of the root sample indicated the presence of pelotons in the root cortex (Figure 3). Currah & Zelmer (1992) explain that the characteristic of endophytic fungal hyphae colonizing plants will form a mass of dense hyphae in cortical cells called pelotons.

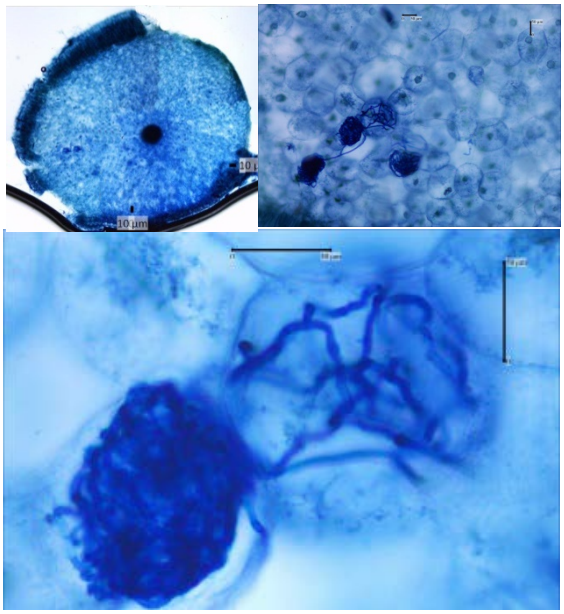

Figure 3. Peloton structure in the anatomy of the root cortex cells of MP1 with Tryphan Blue staining. Magnification (A) 4 x, (B) 10 x, (C) 40 x. Bar = 10 µm

4. Discussion

Characteristics of endophytic mycorrhizal analysis were obtained and compared with the reference characteristics (Shan et al., 2002; Currah and Zelmer, 1992); it was found that Yogyakarta isolates were *Ceratorhiza* isolates. *Ceratorhiza* is an anamorphic phase of *Ceratobasidium.* According to Athipunyakom et al. (2004), the genus *Ceratorhiza* is a mycorrhizal isolate which is commonly found associated with orchids, where endophytic fungi of this type are *Rhizoctonia* which are grouped according to cell hyphae and moniloid. Growth of *Ceratorhiza* reached a diameter of 9 cm after 4 days of incubation by forming a symmetrical zone. The colony turned yellowish after 7 days, and the colony surface appeared as cottony clumps. The lumps are aerial hyphae; this is known from the hyphae that grow on the surface of the agar media. These hyphae are fertile hyphae which play a role for reproduction. The length of moniloid cells is 12.22-14.56 µm, width 2.39-2.91µm and lancet-shaped. If the ratio of length and width is 3.5-4: 1 then it is called the lancet type. The number of nuclei in binucleic cells, according to the characteristics reported by Shan et al. (2002) and Currah and Zelmer (1992).

The peloton structure is evident in the roots of *P. amabilis* which are associated with endophytic fungi (Figure 3). One of the parameters for the mechanism of resistance induction can be the formation of a peloton structure which shows that endophytic fungi penetrate the epidermal finger and into the cortex. In the cortex, the pulp will enter the cell space (intracellular) and form a peloton.

The presence of peloton proves that the endophytic fungi can penetrate into the root tissue of *P. amabilis*. According to Currah and Zelmer (1992), the stage of infection with endophytic fungi begins with the formation of appressorium which is an inflated hyphae. These hyphae originate from spores that germinate or externally hyphae at the root surface of infected host plants. Hyphae will then penetrate the root surface mechanically and enzymatically into the space between the root epidermal cells and into the cortex and beyond. Hyphae develop without destroying the cells of the root cortex. In cortex cells, hyphae form a peloton in the form of dense hyphae. In the platoon, the accumulation of organic materials includes protein, glycogen, fat, and nutrients produced by absorption from the soil.

5. Conclusion

The results showed that the characterization of endophytic mycorrhizae from the roots of *P. amabilis* from Yogyakarta, Indonesia had similarities with the type of endophytic mycorrhizal *Ceratorhiza*. These character equations include colony surface color, colony appearance, hyphae color, hyphae diameter (µm), cell monilioid shape, monilioid cell size (µm), colony growth rate (mm / hour), core number, hyphae branching shape, and clamp connection. The results of mycorrhizal induction also produce a peloton structure in orchid root cortex cells. The peloton structure is evident in the roots of *P. amabilis* which are associated with endophytic fungi. The presence of peloton proves that endophytic fungi can penetrate into the root tissue.

References

Chand K, Shah S, Sharma J, Paudel RM and Pant B. 2020. Isolation, characterization, and plant growth-promoting activities of endophytic fungi from a wild orchid *Vanda cristata. Plant Sig Behavior*, **15(5):** 1744294.

Currah RS and Zelmer C. 1992. A Key and Notes for the Genera of Fungi Mycorrhizal with Orchids and A New Species in the Genus Epulorhiza. *Rept Tottori Mycol Institution*, **30:** 43-59.

Haro R and Benito B. 2019. The Role of Soil Fungi in K^+ Plant Nutrition. *Int J mol Sci*, **20(13):** 3169.

Mahfut. 2020. Identification and Detection Odontoglossum ringspot virus on Native Orchids Collection of Nurserys in Java, Indonesia. Proceeding of International Conference on Advanced Information Scientific Development (ICAISD). West Java, Indonesia. **1641:** 1-8.

Mahfut, Anggreiny A, Wahyuningsih S, Handayani TT and Sukimin. 2020[b]. Identification of Disease and Efforts to Protect Native Orchid Plants Against Bacteria Infection in Liwa Botanical Garden. Proceedings of ICAISD Conference. University of Bina Sarana Informatika. West Java, Indonesia.

Mahfut, Daryono BS, Indrianto A and Somowiyarjo S. 2019. Effectiveness Test of Orchid Mycorrhizal Isolate (*Ceratorhiza* and *Trichoderma*) Indonesia and Its Role as a Biofertilizer. *Ann Res Review Biol*, **33(4):** 1-7.

Mahfut, Indrianto A, Somowiyarjo S and Daryono BS. 2020. Molecular phylogeny of orchids mycorrhiza isolated from native tropical orchids in Indonesia. *Malaysian J Microbiol*, **16(1):** 68-72.

Mahfut, Shafira H, Wahyuningsih S, Handayani TT and Sukimin. 2021. Identification of Virus Infection on Native Orchid in Liwa Botanical Garden. Proceedings of ICASMI Conference. University of Lampung. Lampung, Indonesia.

Mose W, Daryono BS, Indrianto A, Purwantoro A and Semiarti E. 2020. Direct Somatic Embryogenesis and Regeneration of an Indonesian orchid Phalaenopsis amabilis (L.) Blume under a Variety of Plant Growth Regulators, Light Regime, and Organic Substances. *Jordan J Biol Sci.* **13(4):** 509-518.

Pannecoucque J and Hofie M. 2009. Interaction Between Cauliflower and *Rhizoctonia* Anastomosis Groups with Different Levels of Aggreeiveness. *BMC Plant Biol,* **9(95):** 1-12.

Safarini M, Rosyidah IH, Mertaniasih NM, Hamzah MNSB, Novianti KA, Primaharinastiti R, Rahmawaty D and Isnaeni I. 2020. In vitro Antibacterial Activity of Cell Free Fermentation Supernatant of *Passiflora edulis* forma flavicarpa Sims. Fruit Fermented by de Man, Rogosa and Sharp Media. *Jordan J Biol Sci.* **13(4):** 469-475.

Shan XC, Liew ECY, Weatherhead MA and Hodgkiss IJ. 2002. Characterization and Taxonomic Placement of *Rhizoctonia*-like Endophytes from Orchids Roots. *Mycologia*, **94(2):** 230-239.

Song Z, Bi Y, Zhang J, Gong Y and Yang H. 2020. Arbuscular mycorrhizal fungi promote the growth of plants in the mining associated clay. *Sci Reports,* **10:** 2663.

Stoian V, Vidican R, Crisan I, Puia C, Sandor M, Stoian VA, Pacurar F and Vaida I. 2019. Sensitive approach and future perspectives in microscopic patterns of mycorrhizal roots. *Sci Reports***, 9:** 10233.

JJBS

Volume 14, Number 5,December 2021
ISSN 1995-6673
Pages 1035 – 1043

Jordan Journal of Biological Sciences

Transcriptional Impact of E-cadherin Loss on Embryonic Stem Cells

Hani Alotaibi[1,2,*]

[1] Izmir Biomedicine and Genome Center, Izmir, Turkey; [2] Izmir International Biomedicine and Genome Institute, Dokuz Eylül University, Izmir, Turkey

Received: April 22, 2021; Revised: August 15, 2021; Accepted: August 24, 2021

Abstract

In embryonic stem cells, E-cadherin plays a crucial role in sustaining the pluripotent state; this is achieved by the simultaneous presence of active core pluripotency transcriptional network, proper cell-cell adhesion, and an undifferentiated-state chromatin signature. In contrast, N-cadherin is linked to a more differentiated cell state but can support pluripotency if expressed as a knock-in allele from the E-cadherin locus. This study describes the N-cadherin ki/ki embryonic stem cells, which lack E-cadherin expression, to identify transcriptional changes distinct from the known changes observed in E-cadherin knockout embryonic stem cells. As a result, a remarkable similarity in the expression profiles of N-cadherin ki/ki and wild-type embryonic stem cells was observed. Further analysis of the slight differences revealed significant alterations in several biological processes such as chromatin organization and epithelial-mesenchymal transition. The findings presented here shed light on a new aspect of E-cadherin biology in embryonic stem cells and lay the foundations for comprehensive understanding of E-cadherin's functional relevance beyond the prominent role in maintaining pluripotency.

Keywords: E-cadherin, Epithelial to Mesenchymal Transition, EMT, Embryonic Stem Cells, Gene replacement.

1. Introduction

Embryonic stem (ES) cells can self-renew, maintain an undifferentiated state of pluripotency, and generate cells that can differentiate into the various cell types of the body (Niwa, 2007). The pluripotent state's maintenance requires the function of a core transcriptional network comprised of three main transcription factors, Nanog, Sox2, and Oct4 (Ying *et al.*, 2008). The functions of these transcription factors keep the cells in an undifferentiated state distinguished by growth in compact colonies, an active pluripotency transcriptional network, and the presence of bivalent histone modifications on the promoters of several essential genes (Mikkelsen *et al.*, 2007). The transcription factors Sox2 and Oct4, Klf4, and c-Myc induce the pluripotent state in mouse somatic cells by establishing ES-like cells called induced pluripotent stem cells (iPSCs) (Takahashi and Yamanaka, 2006). *Nanog*'s activation is an essential step in establishing the pluripotent state (Silva *et al.*, 2009). The reprogramming to the pluripotent state requires completing a well-orchestrated series of events, including changes in the chromatin landscape and DNA methylation states (Boyer *et al.*, 2006, Maherali *et al.*, 2007). These events coincide with the initiation of the mesenchymal to epithelial transition (MET), during which the somatic cells lose their fibroblast-specific mesenchymal morphology and gradually establish polarization and gain the ES cell-like appearance (Li *et al.*, 2010). This MET event is a crucial step and depends on E-cadherin's (E-cad) activation, a calcium-dependent adhesion molecule. E-cad is essential for maintaining stemness and the pluripotent state since its loss can cause alterations in homophilic adhesion, causing a scattered cell growth of ES cells in culture (Larue *et al.*, 1996, Soncin *et al.*, 2009). Moreover, exogenous E-cad expression can substitute *Oct4* in the mixture of reprogramming factors, which results in effective iPSC reprogramming (Redmer *et al.*, 2011).

ES cell homeostasis fundamentally requires the E-cad-mediated adhesion, an indispensable event for cell-cell communication and signaling (Chen *et al.*, 2010). On the other hand, in mesenchymal cells, such as fibroblasts, cell-cell adhesion is achieved by N-cadherin (N-cad). The protein sequences of both cadherins show striking conservation; thus, they have a similar role in mediating homophilic adhesion and even interact with similar intracellular proteins such as beta-catenin. However, they are primarily present in a mutually exclusive fashion. These molecules also promote contrasting phenotypes; E-cad expression will result in a polarized epithelial form; in contrast, N-cad expression correlates with a depolarized motile state (Wheelock *et al.*, 2008). Several studies addressed the functional redundancy of the two cadherins, their impact on critical developmental stages, and their impact on the pluripotent state in ES cells. One report investigated the impact of replacing E-cad by N-cad during trophectoderm formation and concluded that E-cad functions could not be restored by N-cad (Kan *et al.*, 2007). Besides, the expression of N-cad from the E-cad

* Corresponding author e-mail: hani.alotaibi@ibg.edu.tr

** **Abbreviations:** Embryonic stem (ES), induced pluripotent stem cells (iPSCs), E-cadherin (E-cad), N-cadherin (N-cad), knockout (ko), knock-in (ki), Gene Expression Omnibus (GEO).

locus was sufficient to maintain the pluripotent state and was also suitable for reprogramming fibroblasts into iPSCs (Bedzhov *et al.*, 2013). The maintenance of adhesion was enough for the preservation of pluripotency. Maintaining the pluripotent state by N-cad in ES cells provided a unique opportunity to study the impact of E-cad loss on ES cells that retain the pluripotent state. In recent years, a great deal of research has been dedicated to studying ES cells and iPSCs, notably for their potential use in personalized medicine (Yamanaka, 2020). So, it is of interest to have a better understanding of stem cell biology in general, and a better understanding of the outcomes of potential gene expression signature changes would be of utmost importance for the design and planning of such therapies. The current study reveals the changes in ES cells' gene expression profiles expressing N-cad instead of E-cad. This is addressed by performing in silico analyses and then comparing the expression profiles of E-cad knockout (ko) cells and N-cad knock-in (ki) cells to the wild-type ES cells.

2. Materials and Methods

2.1. ES cell culture

ES cells used in this work were described previously; in summary, N-cad ki/ki, E-cad ko/ko, and wt ES cells were prepared from E2.5 embryos as described in (Bedzhov *et al.*, 2013). ES cells were grown on feeder cells (mitotically inactivated mouse embryonic fibroblasts) in ES cell medium prepared with DMEM (Biochrom) and supplemented with 15% FCS (PAN), 10 U/ml Penicillin and Streptomycin, 0.1 mM non-essential amino acids, two mM L-glutamine (Gibco), 0.15 mM β-mercaptoethanol (Sigma), and 500 U/ml Lif (Millipore). ES cells were grown at 37°C in the presence of 10% CO_2. The medium was changed every two days, and the cells were sub-cultured or processed at sub-confluence.

2.2. RNA isolation and gene expression analysis

Cells were seeded in 6-well plates (10^5 cells per well), incubated to sub-confluence, and collected for RNA isolation. For gene expression analysis, RNA extraction and preparation of cDNA were performed using the methods and reagents described previously (Bedzhov *et al.*, 2013). Primers used in this study and their corresponding UPL probes are presented in Table 1. Relative expression was calculated using the $2^{-\Delta\Delta Ct}$ method (Livak and Schmittgen, 2001) relative to the wt control and normalized to the housekeeping gene *Gapdh*. Data represent at least three biological replicates. One-way ANOVA, followed by Tukey's multiple comparison tests, was performed for statistical analysis of group comparisons.

Table 1: Primers and corresponding UPL probes used in qPCR experiments.

Gene Name	Primer Sequence	UPL probe ID
Cdh1	F: atcctcgccctgctgatt R: accaccgttctcctccgta	UPL No: 18
Cdh2	F: tccctgagatacagcgtcact R: ataatgaagatgcccgttgg	UPL No: 17
Eomes	F: accggcaccaaactgaga R: aagctcaagaaaggaaacatgc	UPL No: 9
Klf4	F: cgggaagggagaagacact R: gagttcctcacgccaacg	UPL No: 62
Neurod1	F: cgcagaaggcaaggtgtc R: tttggtcatgtttccacttcc	UPL No: 1
Vim	F: ccaacctttttcttccctgaa R: ccaacctttttcttccctgaa	UPL No: 109
Snai1	F: gtctgcacgacctgtggaa R: caggagaatggcttctcacc	UPL No: 71
Zeb1	F: gccagcagtcatgatgaaaa R: tatcacaatacgggcaggtg	UPL No: 48
Gapdh	F: agcttgtcatcaacgggaag R: tttgatgttagtggggtctcg	UPL No: 9

2.3. Microarray analysis

Microarray analysis for the ki/ki and wt2 cells was described before (Bedzhov *et al.*, 2013). In short, RNA from two independent samples per genotype was hybridized to the GeneChip Mouse Genome 430 v2.0 array (Affymetrix, Inc.). The raw data can be downloaded from the NCBI GEO database (Barrett *et al.*, 2013) (GEO accession number GSE42008). Raw data for the E-cad knockout and the corresponding wild-type cells (wt1) are publicly available and were obtained from the ArrayExpress, accession number E-MEXP-2836 (Soncin *et al.*, 2011). Data analysis was performed in R v4.0.3. The data set's quality was examined with the simpleaffy package v2.66.0 (Wilson and Miller, 2005), and expression values and normalization were performed by the GCRMA function, with quantile normalization and excluding features with expression values of < 4 in all samples. Differential expression analysis was performed with the limma package v 3.46.0 (Ritchie *et al.*, 2015), applying the eBayes function. Heatmaps were plotted using the Heatmap.2 function of the gplots package v3.1.1 (https://cran.r-project.org/web/packages/gplots/index.html). Using Log2-transformed and normalized expression values, heatmap images were generated, applying Pearson's correlation to calculate hierarchical clustering. Significant genes were calculated by measuring the standard deviation for each row, then subsetting the shortest interval covering half of the values in the data set using the shorth function of the genefilter package v1.72.0 (https://bioconductor.org/packages/release/bioc/html/genefilter.html), and then calculating the adjusted p-value according to FDR. PCA plots were generated using the stats package's prcomp command and plotted using the autoplot command of the ggplot2 package v3.3.2 (Wickham, 2009). GO enrichment analysis was performed using the GOexpress package v1.24.0 (Rue-Albrecht *et al.*, 2016) with the following parameters: seed = 4543, permutations = 1000, and random forest method was selected.

3. Results

In order to understand the impact of E-cad deletion in ES cells, the previously generated mouse models and ES cells where E-cad was replaced for N-cad as a knock-in allele were used (Bedzhov *et al.*, 2013). In the presence of N-cad (either as ki/wt or ki/ki), ES cells retained the pluripotency state as opposed to the E-cad ko/ko cells, which lose the pluripotency. The functional loss of E-cad expression in ES cells is not limited to loss of pluripotency; this is why the N-cad knock-in (ki/ki) ES cells present a unique model for studying the consequences of E-cad depletion beyond pluripotency.

3.1. High correlation between wt and N-cad ki/ki ES cells

We have previously shown that the N-cad ki/ki cells resembled wt cells morphologically; they grow as compact colonies on feeder cells and express key pluripotency-specific genes (Bedzhov *et al.*, 2013). This is a continuation of the previous analysis to shed light on the global changes in ki/ki and ko/ko cells. The first analysis revealed that ki/ki cells were closely related to wt cells rather than ko/ko cells (Figure 1A). This remarkable similarity is, of course, reflected by the previous findings regarding pluripotency genes and is also reflected by the morphological features mentioned earlier. Moreover, correlation analysis revealed a remarkable 97% correlation (Figure 1B). As expected, there was no statistically significant correlation between the ko/ko cells compared to either ki/ki or wt cells. These results confirmed once more the functional redundancy of E-cad and N-cad in ES cells. The global resemblance of gene expression profiles can also be recognized by looking at a heatmap comparing the three cellular models (Figure 1C). The three-way analysis of samples highlighted the similarities and differences between the three cell lines. However, careful examination of the heatmap also unveils the slight differences between ki/ki and wt ES cells (Figure 1C). This analysis was followed by qPCR experiments to validate the expression profiling results. Accordingly, the status of *Cdh1* and *Cdh2* (The official gene symbols for E-cad and N-cad, respectively) expression was confirmed and reflected the genotypic changes in both cell lines (Figure 1D)

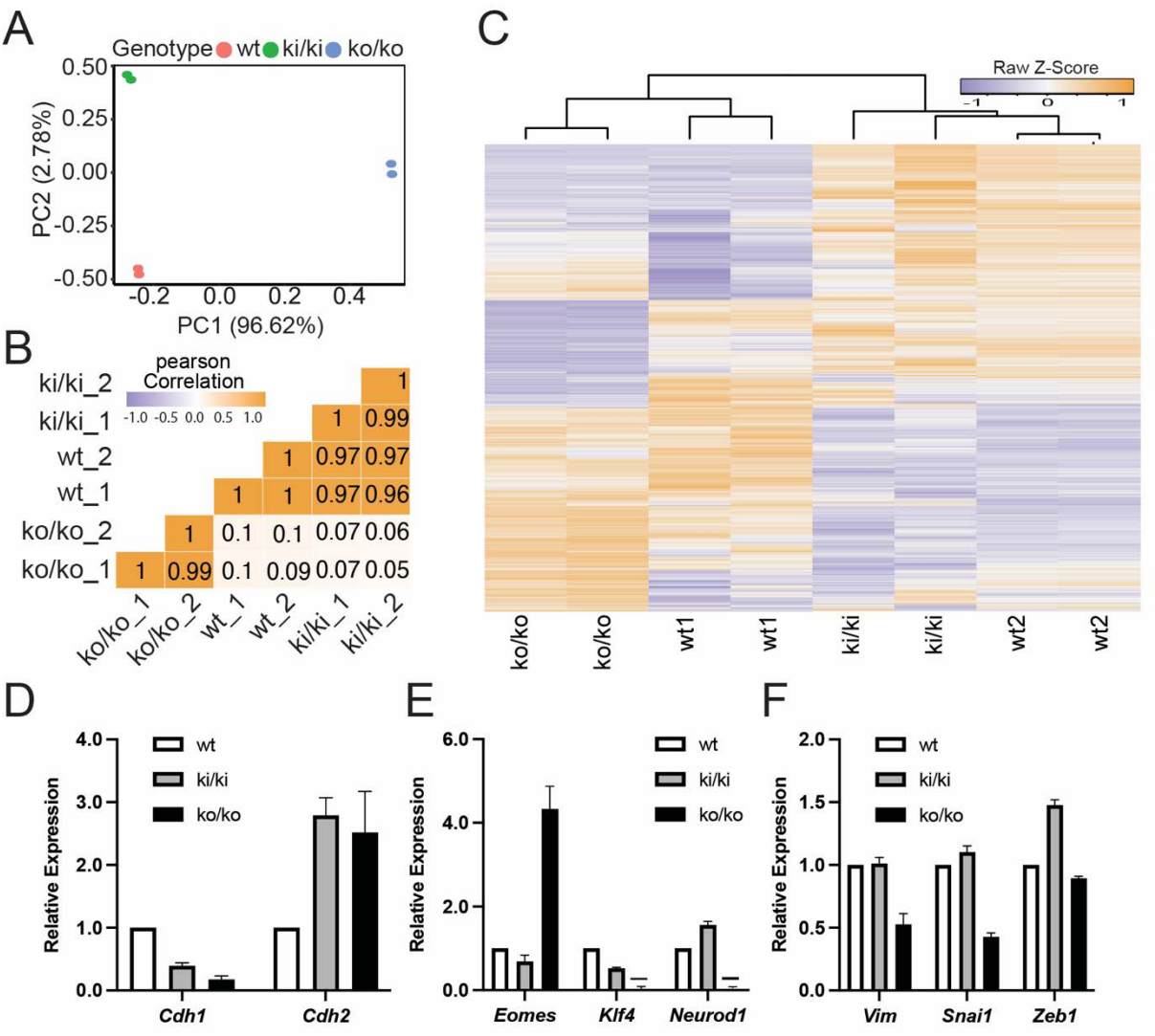

Figure 1. The N-cad ki/ki ES cells are highly similar to the wt ES cells. A) Principal component analysis showing the high similarity between ki/ki and wt cells. PC2 corresponds to less than 3% difference, while PC1 corresponds to more than 95% difference. B) Correlation matrix indicating the percentages of similarity between the samples. C) Heatmap drawing of the expression values of all samples used in this study, D-F) qPCR analysis of genes selected to verify the expression data obtained from microarray analysis. Experiments were performed at least 3 times in triplicates. Error bars correspond to the standard error of the mean. Significant values were labeled with the asterisk.

We have previously studied the expression levels of pluripotency-related genes (Bedzhov *et al.*, 2013). Here, other developmentally relevant genes, such as *Eomes*, *Klf4*, and *Neurod1* (Figure 1E), as well as genes relevant to the cadherin switching, were selected (Figure 1F). Overall, the expression levels detected using qPCR confirmed the signals obtained from microarray experiments' expression profiles.

3.2. Common genes differentially expressed in ki/ki and ko/ko ES cells

Studying the differentially expressed genes in ko/ko cells compared to wt ES cells will reveal the impact of E-cad deletion on gene expression, which is reflected by changes in ES physiology. These changes include the known impact on pluripotency. Similarly, examining differentially expressed genes between ki/ki and wt cells will show the impact of the forced N-cad expression on ES cells. Differential expression analyses of ko/ko-wt and ki/ki-wt ES cells were performed using the R-package limma with a cutoff of log2 0.6. The number of differentially expressed genes in ko/ko ES cells was 3527 (Figure 2A), and in ki/ki ES cells, it was 1976 (Figure 2B). To better understand E-cad's impact on ES cells, the differentially expressed genes of ko/ko-wt and ki/ki-wt ES cells were compared first. The common genes were categorized into different groups, as illustrated in Figure 2.

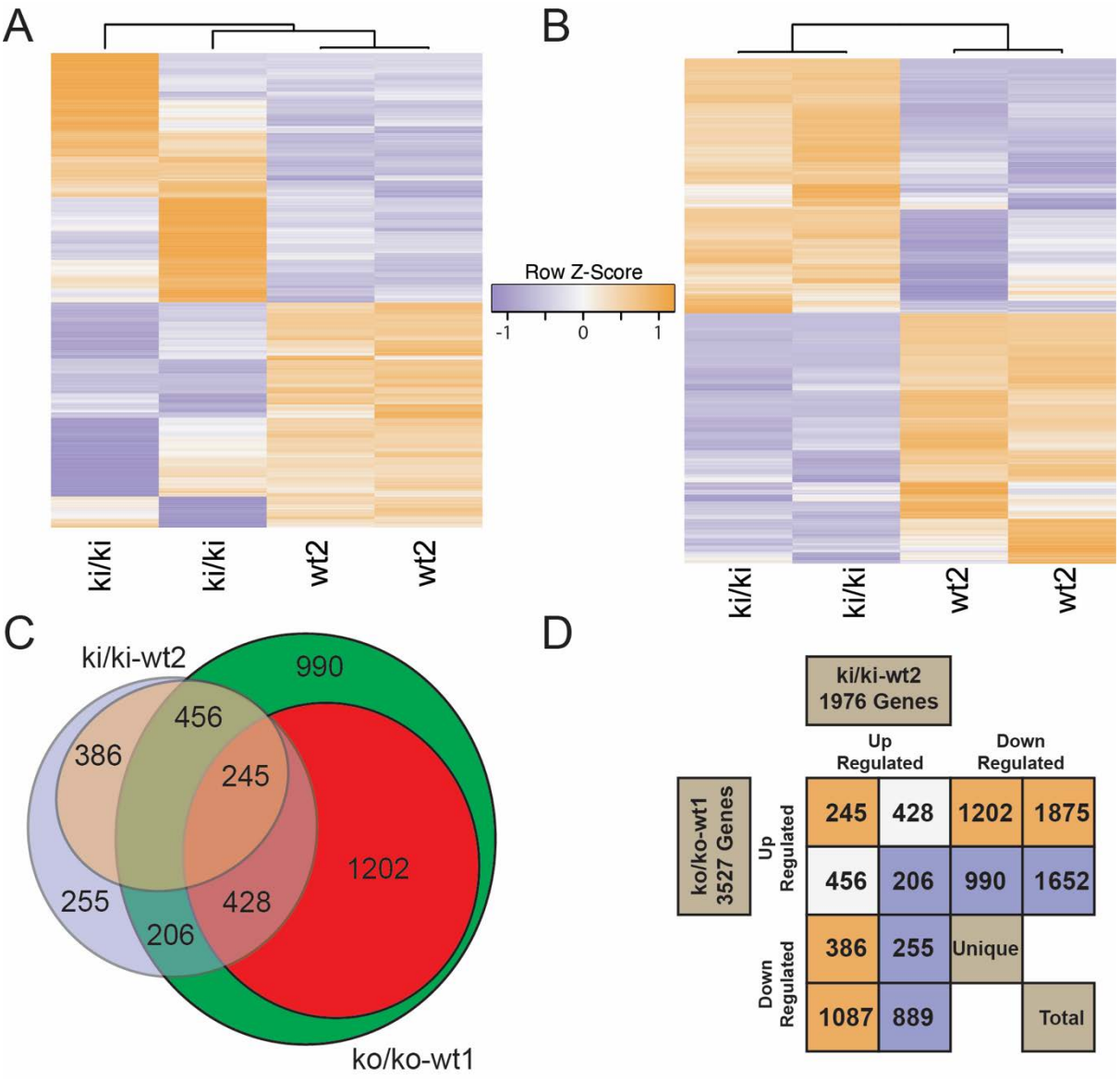

Figure 2. Common differentially expressed genes. A-B) Heatmaps show 1335 differentially expressed genes in ki/ki and ko/ko ES cells. C-D) Numeric representation of commonly expressed genes.

In total, 1335 genes differentially expressed in both ki/ki-wt and ko/ko-wt comparisons are common. The number of commonly upregulated genes was 245, while 206 genes were found downregulated. The Venn diagram in Figure 2C shows the common and unique areas with the number of genes depicted; the complete data is also summarized as a matrix in Figure 2C. Of note here is the difference in differentially expressed genes in both comparisons. The number of differentially expressed genes in ko/ko cells was about two times higher than in ki/ki cells, attesting to the similarities between ki/ki and wt cells (Figure 2C). As described in materials and methods,

common genes differentially expressed were subjected to sequential filtering to find significant genes. The number of remaining genes that remained after applying the adjusted p-value of 0.01 filter was 280 (Supplementary Table S1). These genes were also plotted in the heatmap in supplementary Figure S1 and revealed the remarkable resemblance of ki/ki ES cells to their wt counterparts. The heatmap view also revealed the subtle differences between ki/ki ES cells and wt cells. To better understand these differences, subsetting the common differentially expressed genes for the ki/ki and wt samples from the dataset was performed and followed by applying the filtering as done in the previous analysis. As a result, 179 differentially expressed genes in the ki/ki ES cells with an adjusted p-value of < 0.05 were found (Figure 3A and Supplementary Table S2).

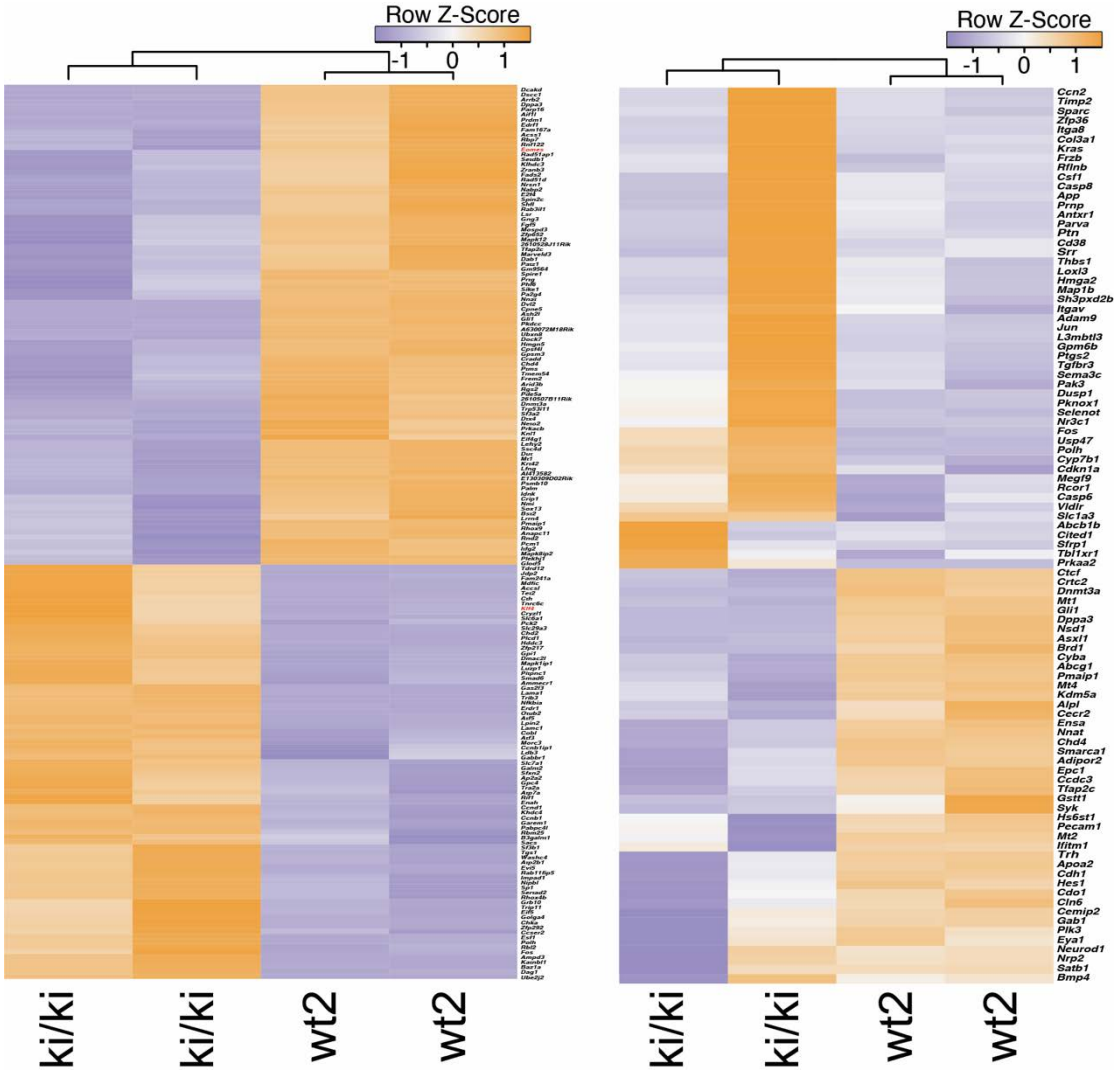

Figure 3. Commonly upregulated and downregulated genes in the ki/ki ES cells. A) Heatmap of the common differentially expressed genes in ki/ki cells. One hundred seventy-nine genes with an adjusted p-value of 0.05 or less were plotted here. Upregulated or downregulated genes in both genotypes were subjected to GO enrichment analysis. The heatmap in B represents 95 genes that were found as enriched.

3.3. GO enrichment analysis of common genes differentially expressed in ki/ki and ko/ko ES cells

To determine the relevance of the differentially expressed genes in ki/ki cells, commonly expressed up- and downregulated genes were included in the GO enrichment analysis. A total of 451 genes (245 upregulated and 206 downregulated) were subjected to GO enrichment analysis using the R-package GOexpress. This analysis revealed significant enrichment in 95 genes belonging to 19 different biological processes. The expression pattern of these genes is presented in the heatmap in Figure 3B. The GO enrichment analysis revealed significant changes in genes within the response to the drug biological process (20 genes: ~14%).

Moreover, chromatin organization (18 genes: ~12%) related genes and genes related to angiogenesis (14 genes: ~ 10%) were also significantly represented. A summary of the GO enrichment analysis results is depicted in the pie chart in figure 4A. Eighteen genes belonging to the chromatin organization biological process were mainly downregulated in response to *Cdh1* depletion in the ki/ki cells (Figure 4B), suggesting a positive correlation between these biological processes and E-cad function. On the other hand, genes related to EMT were found to be upregulated in the ki/ki cells, suggesting a tendency to shift to a mesenchymal state in the absence of E-cad (Figure 4C).

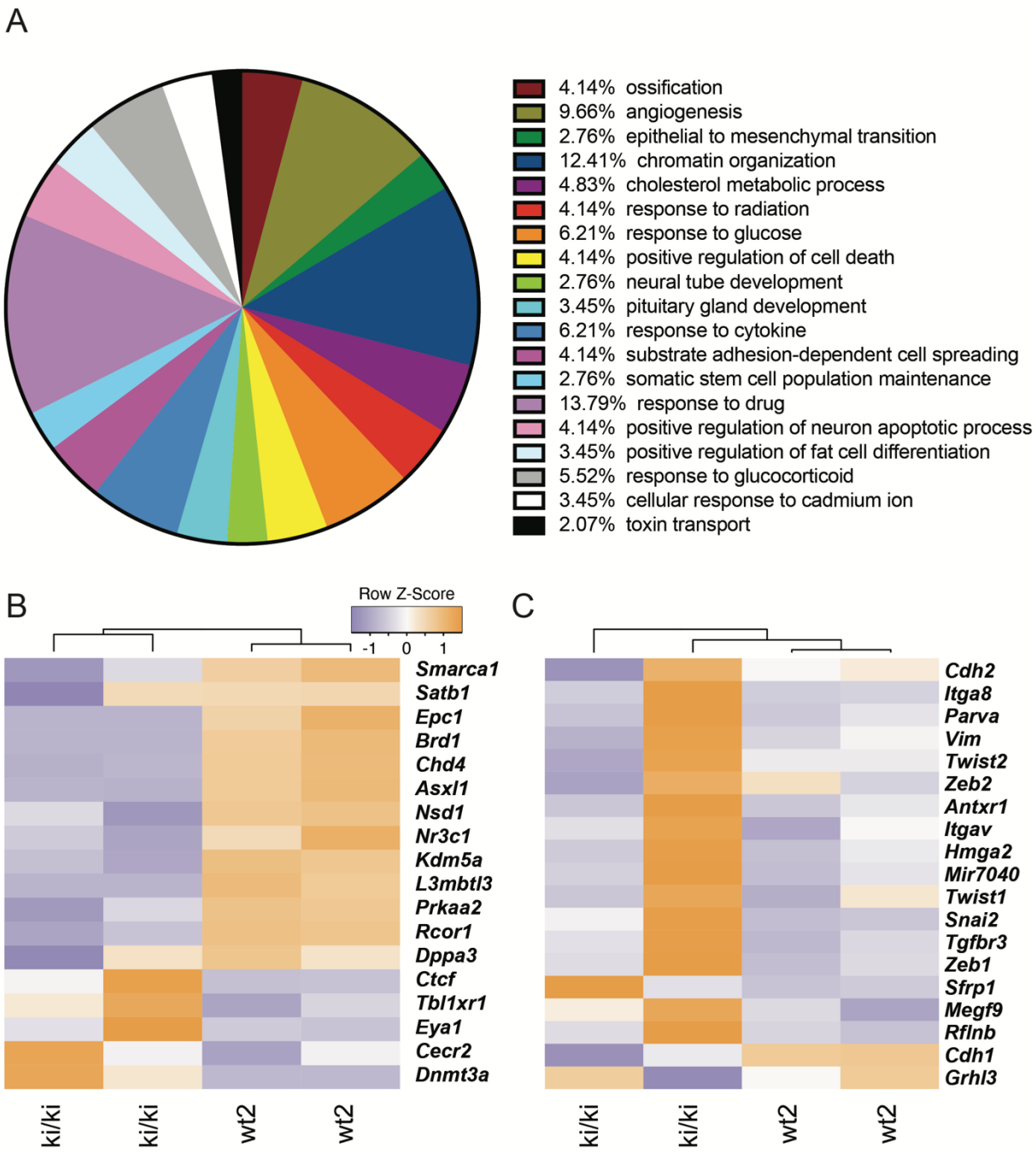

Figure 4. GO enrichment analysis identifies significant biological processes affected by E-cad depletion. A) Nineteen biological process GO terms were enriched in ki/ki ES cells, and their percentage is represented in the pie chart. B) Chromatin organization genes were mostly downregulated in ki/ki ES cells. C) EMT-related genes were upregulated ki/ki ES 1 cells.

Other gene groups are also presented in Supplemental Figure 2. Of note, genes belonging to three developmental processes were mapped in supplementary Figure S2; the ossification gene group was mainly upregulated in the absence of E-cad. In contrast, genes belonging to the pituitary gland development were mainly downregulated in the ki/ki cells. The neural tube development genes were mixed (Figure S2A). Genes in the angiogenesis (Figure S2B), apoptosis (Figure S2C), and response to drugs (Figure S2D) were mainly upregulated as a result of E-cad absence. A detailed description of all biological processes represented by the 95 enriched genes is displayed in Table 2.

Table 2: Detailed descriptions of the identified GO enrichment analysis showing significant biological process terms and corresponding genes.

GO ID	GO Name	Gene ID	Total count	Data count	p.val
GO:0001503	ossification	*Sparc, Bmp4, Gpm6b, Ifitm1, Ptn, Csf1*	177	6	0.009
GO:0001525	angiogenesis	*Ccn2, Ptgs2, Hs6st1, Jun, Syk, Itgav, Pecam1, Bmp4, Casp8, Cemip2, Parva, Gab1, Pknox1, Nrp2*	459	14	0.009
GO:0001837	epithelial to mesenchymal transition	*Mir7040, Tgfbr3, Hmga2, Rflnb*	84	4	0.001
GO:0006325	chromatin organization	*Satb1, Epc1, Dnmt3a, Dppa3, Prkaa2, Cecr2, Asxl1, Kdm5a, Rcor1, Chd4, Brd1, Nsd1, Tbl1xr1, Ctcf, L3mbtl3, Eya1, Smarca1, Nr3c1*	610	18	0.001
GO:0008203	cholesterol metabolic process	*Apoa2, App, Cyp7b1, Abcg1, Prkaa2, Vldlr, Cln6*	170	7	0
GO:0009314	response to radiation	*Ptgs2, Jun, App, Polh, Col3a1, Plk3*	65	6	0.001
GO:0009749	response to glucose	*Casp6, Ccn2, Apoa2, Trh, Fos, Nnat, Neurod1, Selenot, Thbs1*	143	9	0.002
GO:0010942	positive regulation of cell death	*Prnp, Ccn2, Ptgs2, Cdkn1a, Bmp4, Dnmt3a*	106	6	0.002
GO:0021915	neural tube development	*Hes1, Sema3c, Cecr2, Sfrp1*	94	4	0.006
GO:0021983	pituitary gland development	*Hes1, Bmp4, Cdh1, Gli1, Hmga2*	67	5	0
GO:0034097	response to cytokine	*Casp6, Sparc, Ptgs2, Jun, Fos, Col3a1, Timp2, Cited1, Cd38*	141	9	0.006
GO:0034446	substrate adhesion-dependent cell spreading	*Itgav, Parva, Megf9, Antxr1, Itga8, Sfrp1*	107	6	0.002
GO:0035019	somatic stem cell population maintenance	*Hes1, Tfap2c, Hmga2, Sfrp1*	78	4	0.007
GO:0042493	response to drug	*Ptgs2, Jun, Gstt1, Abcb1b, Cdkn1a, Map1b, Dnmt3a, Fos, Slc1a3, Neurod1, Usp47, Timp2, Adipor2, Srr, Ptn, Cdh1, Cd38, Cyba, Sfrp1, Thbs1*	619	20	0.008
GO:0043525	positive regulation of neuron apoptotic process	*Casp6, PrnpvJun, Pmaip1, App, Pak3*	153	6	0.007
GO:0045600	positive regulation of fat cell differentiation	*Frzb, Ccdc3, Sh3pxd2b, Zfp36, Sfrp1*	90	5	0.007
GO:0051384	response to glucocorticoid	*Adam9, Sparc, Ptgs2, Cdkn1a, Alpl, Kras, Dusp1, Cdo1*	126	8	0.01
GO:0071276	cellular response to cadmium ion	*Jun, Mt1, Fos, Mt2, Mt4*	68	5	0.004
GO:1901998	toxin transport	*Abcg1, Crtc2, Antxr1*	78	3	0.009

4. Discussion

This manuscript addresses the impact of E-cad deletion in ES cells while retaining the pluripotency state, taking advantage of our previously published cellular model in which the expression of N-cad as a knock-in allele in the E-cad locus was performed. The expression profiles of ES cells with deleted E-cad (the ko/ko cells) or N-cad as a knock-in allele in the E-cad locus (the ki/ki cells) were compared to the wild type ES cells using an in silico approach. The analysis revealed a slight shift to the mesenchymal gene signature by upregulating EMT-related genes. On the other hand, a decrease in the expression of chromatin organization-related genes was observed in the absence of E-cad. The gene replacement model analyzed here proved to be a powerful tool to study aspects of E-cad biology. The first studies of replacing E-cad with N-cad revealed that N-cad could not replace E-cad function during the formation of the trophectoderm (Kan *et al.*, 2007); this was illustrated by the specific crosstalk between E-cad and Igf1r signaling providing a survival signal that cannot be reproduced when N-cad is expressed instead of E-cad (Bedzhov *et al.*, 2012). Several reports described the essential role E-cad plays in defining the identity of ES cells and the maintenance of stemness (Chen *et al.*, 2010, Soncin *et al.*, 2011).

Furthermore, E-cad was also described as an essential facilitator of the reprogramming of iPSCs; it could even replace members of the Yamanaka cocktail used in iPSC derivation (Li *et al.*, 2010, Redmer *et al.*, 2011). The high homology between E-cad and N-cad results in a significant redundancy in ES cells' pluripotency. As opposed to trophectoderm development, ki/ki ES cells injected in blastocysts can develop up to embryonic day E8.5, showing that N-cad could replace E-cad in these chimeric embryos (Bedzhov *et al.*, 2013). Notably, the N-cad ki/ki ES cells maintained pluripotency, and the resemblance of the gene expression profile to the wild-type ES cells was distinctive. Despite the global comparability of gene expression profiles of N-cad ki/ki ES cells and the wild-type ES cells, subtle differences were observed. These differences are evident when looking at subsetted heatmaps encompassing genes within the biological processes enriched using the GO enrichment analysis.

The results presented here suggest that the loss of E-cad in ES cells results in the foundation of a partial EMT-like state; while cells retain adhesive characteristics, due to N-cad expression, they upregulate specific EMT associated genes such as *Zeb1* and *Tgfbr3* and downregulate essential epithelial genes such as *Grhl3*.

Loss of *Grhl3* was previously shown to result in a robust mesenchymal phenotype during MET initiation (Alotaibi *et al.*, 2015). The effects of E-cad depletion have been studied in the non-tumorigenic MCF10A cells. The cells presented significant changes associated with tissue remodeling and cell-substrate attachment proteins such as ITGA1. On the other hand, they did not show a similar increase in EMT-related genes (Chen *et al.*, 2014). The observed increase in *Itga8* and *Itgav* gene expression is in agreement with their findings. E-cad deletion also affected several developmental genes, particularly the ossification genes, and some of the neural tube development-related genes were mainly upregulated. This was associated with changes in differentiation genes and suggested a link between the changes in the EMT-associated genes and the development-related or differentiation-related genes. Cellular reprogramming is known to include EMT and MET (Li *et al.*, 2010), and the differentiation state of cells is also expressed in terms of epithelial-like or mesenchymal-like. A recent report showed that a sequential EMT/MET is required to differentiate hESCs to the hepatic lineage. This process involves an autocrine TGFβ signaling loop resulting in an upregulation of EMT inducers and downregulation of E-cad expression (Li *et al.*, 2017). Concerning reprogramming, the observed downregulation in the chromatin organization gene signature was profound, except for *Ctcf* and *Dnmt3a*, which regulate chromatin architecture and DNA methylation. Epigenetic reprogramming is closely associated with fate determination, differentiation, and cellular reprogramming. Previous studies indicated a critical role for E-cad in reprogramming MEFs into iPSCs (Li *et al.*, 2010, Redmer *et al.*, 2011).

Furthermore, genetic ablation of E-cad prevented iPSC reprogramming (Redmer *et al.*, 2011, Bedzhov *et al.*, 2013). This reprogramming is associated with global epigenetic reorganization, resetting the chromatin infrastructure from a differentiated somatic state to an undifferentiated pluripotent state (Hochedlinger and Jaenisch, 2015). E-cad's importance to ES cells in terms of pluripotency is well known, and its essential role in the reprogramming to the pluripotent state is central to the establishment of MET that precedes the pluripotency network activation. In the absence of E-cad, the tendency to shift to a more differentiated state as illustrated by changes in chromatin organization genes and EMT-associated genes shed light onto new aspects of E-cad functions in ES cells. It will be of great interest to experimentally corroborate these novel findings, which will significantly benefit the field of stem cell biology and eventually personalized medicine. Stem cell therapy and personalized medicine are considered the future of medicine (Strauer and Kornowski, 2003). The scope of personalized medicine goes beyond common diseases such as cancer and is considered for developmental disorders or rare diseases as well (Garcia-Castro and Singec, 2017). Hematopoietic stem cells are used to treat leukemia (Tian *et al.*, 2016), and recent examples can also be seen in studies related to Parkinson's disease (Parmar *et al.*, 2020). With this in mind, it is imperative to acknowledge the importance of understanding changes in molecular pathways and gene signatures when planning novel therapeutics.

Acknowledgments

We would like to thank Dr. Gökhan Karakülah and Prof. Uygar Tazebay for carefully reading the manuscript. This study was financed by İzmir Biomedicine and Genome Center institutional funds. The author discloses no conflict of interest that may have influenced either the conduct or the presentation of the research.

Supplementary Data

Supplementary Data is available online at the Mendeley data website (http://dx.doi.org/10.17632/wd66b4gb4d.2).

References

Alotaibi H, Basilicata MF, Shehwana H, Kosowan T, Schreck I, Braeutigam C, Konu O, Brabletz T and Stemmler MP. 2015. Enhancer cooperativity as a novel mechanism underlying the transcriptional regulation of E-cadherin during mesenchymal to epithelial transition. *Biochimica Et Biophysica Acta-Gene Regulatory Mechanisms*, **1849(6)**: 731-742.

Barrett T, Wilhite SE, Ledoux P, Evangelista C, Kim IF, Tomashevsky M, Marshall KA, Phillippy KH, Sherman PM, Holko M, Yefanov A, Lee H, Zhang N, Robertson CL, Serova N, Davis S and Soboleva A. 2013. NCBI GEO: archive for functional genomics data sets--update. *Nucleic Acids Res*, **41(Database issue)**: D991-995.

Bedzhov I, Alotaibi H, Basilicata MF, Ahlborn K, Liszewska E, Brabletz T and Stemmler MP. 2013. Adhesion, but not a specific cadherin code, is indispensable for ES cell and induced pluripotency. *Stem Cell Res*, **11(3)**: 1250-1263.

Bedzhov I, Liszewska E, Kanzler B and Stemmler MP. 2012. Igf1r signaling is indispensable for preimplantation development and is activated via a novel function of E-cadherin. *PLoS Genet*, **8(3)**: e1002609.

Boyer LA, Plath K, Zeitlinger J, Brambrink T, Medeiros LA, Lee TI, Levine SS, Wernig M, Tajonar A, Ray MK, Bell GW, Otte AP, Vidal M, Gifford DK, Young RA and Jaenisch R. 2006. Polycomb complexes repress developmental regulators in murine embryonic stem cells. *Nature*, **441(7091)**: 349-353.

Chen A, Beetham H, Black MA, Priya R, Telford BJ, Guest J, Wiggins GA, Godwin TD, Yap AS and Guilford PJ. 2014. E-cadherin loss alters cytoskeletal organization and adhesion in non-malignant breast cells but is insufficient to induce an epithelial-mesenchymal transition. *BMC Cancer*, **14**: 552.

Chen T, Yuan D, Wei B, Jiang J, Kang J, Ling K, Gu Y, Li J, Xiao L and Pei G. 2010. E-cadherin-mediated cell-cell contact is critical for induced pluripotent stem cell generation. *Stem Cells*, **28(8)**: 1315-1325.

Garcia-Castro J and Singec I. 2017. Prospects of Pluripotent and Adult Stem Cells for Rare Diseases. *Adv Exp Med Biol*, **1031**: 371-386.

Hochedlinger K and Jaenisch R. 2015. Induced Pluripotency and Epigenetic Reprogramming. *Cold Spring Harb Perspect Biol*, **7(12)**.

Kan NG, Stemmler MP, Junghans D, Kanzler B, de Vries WN, Dominis M and Kemler R. 2007. Gene replacement reveals a specific role for E-cadherin in the formation of a functional trophectoderm. *Development*, **134(1)**: 31-41.

Larue L, Antos C, Butz S, Huber O, Delmas V, Dominis M and Kemler R. 1996. A role for cadherins in tissue formation. *Development*, **122(10)**: 3185-3194.

Li Q, Hutchins AP, Chen Y, Li S, Shan Y, Liao B, Zheng D, Shi X, Li Y, Chan WY, Pan G, Wei S, Shu X and Pei D. 2017. A sequential EMT-MET mechanism drives the differentiation of human embryonic stem cells towards hepatocytes. *Nat Commun*, **8**: 15166.

Li R, Liang J, Ni S, Zhou T, Qing X, Li H, He W, Chen J, Li F, Zhuang Q, Qin B, Xu J, Li W, Yang J, Gan Y, Qin D, Feng S, Song H, Yang D, Zhang B, Zeng L, Lai L, Esteban MA and Pei D. 2010. A mesenchymal-to-epithelial transition initiates and is required for the nuclear reprogramming of mouse fibroblasts. *Cell Stem Cell*, **7(1)**: 51-63.

Livak KJ and Schmittgen TD. 2001. Analysis of relative gene expression data using real-time quantitative PCR and the 2(-Delta Delta C(T)) Method. *Methods*, **25(4)**: 402-408.

Maherali N, Sridharan R, Xie W, Utikal J, Eminli S, Arnold K, Stadtfeld M, Yachechko R, Tchieu J, Jaenisch R, Plath K and Hochedlinger K. 2007. Directly reprogrammed fibroblasts show global epigenetic remodeling and widespread tissue contribution. *Cell Stem Cell*, **1(1)**: 55-70.

Mikkelsen TS, Ku M, Jaffe DB, Issac B, Lieberman E, Giannoukos G, Alvarez P, Brockman W, Kim TK, Koche RP, Lee W, Mendenhall E, O'Donovan A, Presser A, Russ C, Xie X, Meissner A, Wernig M, Jaenisch R, Nusbaum C, Lander ES and Bernstein BE. 2007. Genome-wide maps of chromatin state in pluripotent and lineage-committed cells. *Nature*, **448(7153)**: 553-560.

Niwa H. 2007. How is pluripotency determined and maintained? *Development*, **134(4)**: 635-646.

Parmar M, Grealish S and Henchcliffe C. 2020. The future of stem cell therapies for Parkinson disease. *Nat Rev Neurosci*, **21(2)**: 103-115.

Redmer T, Diecke S, Grigoryan T, Quiroga-Negreira A, Birchmeier W and Besser D. 2011. E-cadherin is crucial for embryonic stem cell pluripotency and can replace OCT4 during somatic cell reprogramming. *EMBO Rep*, **12(7)**: 720-726.

Ritchie ME, Phipson B, Wu D, Hu Y, Law CW, Shi W and Smyth GK. 2015. limma powers differential expression analyses for RNA-sequencing and microarray studies. *Nucleic Acids Res*, **43(7)**: e47.

Rue-Albrecht K, McGettigan PA, Hernandez B, Nalpas NC, Magee DA, Parnell AC, Gordon SV and MacHugh DE. 2016. GOexpress: an R/Bioconductor package for the identification and visualisation of robust gene ontology signatures through supervised learning of gene expression data. *BMC Bioinformatics*, **17**: 126.

Silva J, Nichols J, Theunissen TW, Guo G, van Oosten AL, Barrandon O, Wray J, Yamanaka S, Chambers I and Smith A. 2009. Nanog is the gateway to the pluripotent ground state. *Cell*, **138(4)**: 722-737.

Soncin F, Mohamet L, Eckardt D, Ritson S, Eastham AM, Bobola N, Russell A, Davies S, Kemler R, Merry CL and Ward CM. 2009. Abrogation of E-cadherin-mediated cell-cell contact in mouse embryonic stem cells results in reversible LIF-independent self-renewal. *Stem Cells*, **27(9)**: 2069-2080.

Soncin F, Mohamet L, Ritson S, Hawkins K, Bobola N, Zeef L, Merry CL and Ward CM. 2011. E-cadherin acts as a regulator of transcripts associated with a wide range of cellular processes in mouse embryonic stem cells. *PLoS One*, **6(7)**: e21463.

Strauer BE and Kornowski R. 2003. Stem cell therapy in perspective. *Circulation*, **107(7)**: 929-934.

Takahashi K and Yamanaka S. 2006. Induction of pluripotent stem cells from mouse embryonic and adult fibroblast cultures by defined factors. *Cell*, **126(4)**: 663-676.

Tian H, Qu Q, Liu L and Wu D. 2016. Advances in Stem Cell Therapy for Leukemia. *Curr Stem Cell Res Ther*, **11(2)**: 158-165.

Wheelock MJ, Shintani Y, Maeda M, Fukumoto Y and Johnson KR. 2008. Cadherin switching. *J Cell Sci*, **121(Pt 6)**: 727-735.

Wickham H (2009). *ggplot2* City.

Wilson CL and Miller CJ. 2005. Simpleaffy: a BioConductor package for Affymetrix Quality Control and data analysis. *Bioinformatics*, **21(18)**: 3683-3685.

Yamanaka S. 2020. Pluripotent Stem Cell-Based Cell Therapy-Promise and Challenges. *Cell Stem Cell*, **27(4)**: 523-531.

Ying QL, Wray J, Nichols J, Batlle-Morera L, Doble B, Woodgett J, Cohen P and Smith A. 2008. The ground state of embryonic stem cell self-renewal. *Nature*, **453(7194)**: 519-523.

JJBS

Volume 14, Number 5,December 2021
ISSN 1995-6673
Pages 1045 – 1050

Jordan Journal of Biological Sciences

Mathematical evaluation of chromosomal anomalies induced by xylol in *Vicia faba* L. regarding application time and concentration

Ali Özdemir[1] and Canan Özdemir[2,*]

[1]*Celal Bayar University, Science and Art Faculty, Mathematics Department, Manisa, Turkey;* [2]*Celal Bayar University, Science and Art Faculty, Biology Department, Manisa, Turkey.*

Received: June 12, 2021; Revised: August 4, 2021; Accepted: September 4, 2021

Abstact

This study investigates how xylol acts on chromosomes of broad bean (*Vicia faba* L.) according to the time and concentration parameters. Xylol has the chemical formula C_6H_4 $(CH_3)_2$, which is also called dimethylbenzene. This chemical is evaluated as a basic substance or a supplementary basic substance in many industrial products such as farming chemicals. Xylol is used as a typical solvent in solvent-based formulations and serves as the carrier solution for the pesticide ingredient in farming chemicals.

The present study investigates the chromosomal changes induced by xylol in the meristematic cells of the root tips of *V. faba*, which is widely used as food by humans. The root tips were treated with xylol solutions which are prepared in various concentrations (5,20,40 and 80 ml/L) for different treatment duration periods (8 and 72 h). The aim of the microscopic examination was to clarify chromosomal anomalies of cell division. The microscopic examination showed that various anomalies occurred in cells of the root tip meristems such as chromosome breaking, dispersion, adherence, bridge chromosome and ring chromosomes. The data obtained from microscopic analysis in the study were evaluated statistically.

We have tried to demonstrate and assess the effects obtained from laboratory studies numerically. The Pearson's correlation and variance analysis were applied to data to reveal the similarities and the differences of the chromosomal features. The statistical analyses used in the study also serve the purpose of reliability, concreteness and the comparison of the results. The study also sheds light on the possible harms of xylol on chromosomes transferring genetic codes of living beings to forthcoming generations.

Keywords: Chromosome Anomalies, Mathematically Evaluation, Xylol, *Vicia faba*.

1. Introduction

Xylol is uncoloured, characteristical dissolvent, fragrant and fluid form crude substance with a chemical formula of C_6H_4 $(CH_3)_2$. It was first isolated and named in 1850 by the French chemist Auguste Cahours, having been discovered as a constituent of wood tar (Cahours, 1850). It has industrial value and medical technology as a solvent, but concerns about its safety have raised questioned from time to time. In addition, the areas of application of xylol include the printing, rubber, and leather industries. It can be used where slower drying is desired (Jenifer, 1994). For similar reasons, it is often the active ingredient in commercial products for ear wax removal (Fabri *et al.*, 2000). Xylol easily penetrates most ordinary clothing and can become trapped in ordinary gloves and boots. Xylol trapped in the clothing can cause burns and blistering. Long-term exposure to xylol may lead to headaches, irritability, depression, insomnia, agitation, extreme tiredness, tremors, impaired concentration and short-term memory loss. This condition is sometimes generally referred to as "organic solvent syndrome." Unfortunately, there is very little information available that isolates xylol from other solvent exposures in the examination of these effects. The type and severity of health effects depends on several factors, including the amount of xylol you are exposed to and the exposure time (Vijayakumar, 2015). In the literature, some researchers made investigations on cytogenetic effects of especially heavy metal pollution on plants and other living things (Shraideh, 2010; Özdemir *et al*., 2015; Şutan *et al*., 2018; Osama *et al*., 2020; Tengjaroenkul & Neeratanaphan, 2020). In the literature, the studies on the effects of solvents on plants have mostly been evaluated in terms of agricultural productivity (Barchan *et al.*, 2014; Ghasemzadeh *et al.*, 2011). Studies on the effects of solvents on plant chromosomes are very limited. Recently, Alaca *et al.*, (2020) have investigated the effect of xylol solvent on *Vicia faba* plant chromosomes for different concentration and time.

In this study, we investigated the effects of xylol used as raw materials in many industrial products especially agrochemicals on the *V. faba* plant as a model system for plant cytogenetic studies to configure its mode of action on mitotic chromosomes

The new aspect here is to evaluate the data observed from the research mathematically, in particular

* Corresponding author e-mail: cozdemir13@gmail.com.

statistically. Statistical analysis was performed using Pearson's correlation and analysis of variance methods, which are widely used in similar studies.

2. Material and Methods

The study was carried out in Manisa Celal Bayar University, Botanical Research Laboratory in 2020. Ten number plump and equal-sized seeds of *V. faba* were used for each treatment and as a control group. The seeds were soaked with distilled water for 10 -15 minutes then germinated at 20-25 º C in petri dish. When the root tips reached 10-15 mm in length, germinated seeds were treated with different concentrations (5,20,40 and 80 ml/L) of xylol for 8 and 72 hours. The root tips of the control group were grown in water only. Then, the root tips obtained, were fixed with carnoy's fixative (60 ml ethanol absolute+30 ml chloroform+10 ml acetic acid glacial) for 2 hours. Then, preserved in 70 % ethyl alcohol (Puchtler *et al.*, 1968). For microscopic observation the root tips were stained by Feulgen method (Darlington and La Cour, 1976). Homologous areas were chosen on the preparations for cytogenetic examination. The cells were counted in selected areas, and the number of mitotic cells was also detected. The mitotic index was calculated based on the frequency of division in cell images obtained under a microscope. The preparation was prepared using 5 root tips for each xylol application. Twenty image fields were chosen on these preparations for cytogenetic examination, and chromosome abnormalities were detected. Approximately, 600 cells were evaluated for each application. The occurrence and frequency of chromosomal anomalies in the cells were established by hand counting from the microscope images. Chromosomel anomalies were tried to detected in the cells counted. Preparates were photographed with motorized Leica DM 3000 microscope. For statistical analyses, chromosome anomalies detected in the study were coded as A-G and the concentrations/times of treatment as 1-8 (Table 1-6). Statistical analyses were performed using the Pearson's correlation and analysis of variance method with MINITAB software package.

3. Results

It was observed that the different concentrations of xylol treatment on the root tips at different time periods increased mitotic cell division compared to the the control group. Mitotic cell division was observed the highest level at 40 ml/L -72h treatment. Mitotic cell division was observed high levels at all 72th hours of treatment times according to the 8th hour of treatment times. It was observed that the mitotic index increased in parallel with the increase in concentration with only one exception after 80ml/L treatment (Table 1).

Table 1. The effect of xylol treatment on mitosis index and chromosome abnormalitiea of Vicia faba root tip meristems.

	Control	Total counted cells	5 ml/L 8h (1)	5 ml/L 72h (2)	20 ml/L 8h (3)	20 ml/L 72h (4)	40 ml/L 8h (5)	40 ml/L 72h (6)	80 ml/L 8h (7)	80 ml/L 72h (8)
Mitotic indeks (%) ± SD	10 ± 4.1	600	11 ± 4.1	25 ± 7.1	12± 6.1	27 ± 7.3	14 ± 8.5	30 ± 7.8	10 ± 8.4	11± 9.1
Total anomalies (%)	00.00	600	02.35	08.20	10.03	14.05	12.31	18.13	13.02	17.00
Number of different anomalies	00.00	600	3	5	3	5	4	6	3	2

S.D.- Standart Deviation Time (h): hour

Some chromosome anomalies were caused by xylol on the root tips of *V. faba* such as bridge chromosome, fish bone chromosome, sticky chromosome, ring chromosome, scattered anaphase, C- chromosome at different stages of mitotic division as shown in (Figures 1-7). The percentage of anomaly was highest after (40 ml/L -72h). Bridge, fish bone, sticky and ring chromosomes were the common types of anomalies in percentage after all treatments. The most frequently observed anomaly was bridge chromosome in all treatments. Treatment with 40 ml/L -8h mainly induced the highest percentage of chromosome anomalies, chromosome bridge (3%) and highest percentage of sticky chromosome (2.9 %). The highest percentage of fish bone chromosome anomaly (2.50%) was observed after (80 ml / L -72h) treatment. Ring chromosome was recorded after all treatments except (80 ml/L -8h) and (80 ml/L -72h). C- chromosome anomaly was observed in only 4 treatment (Table 2). The lowest total percentage of different chromosome anomalies were observed at (80 ml/L -72h) treatment. When all treatments were considered, the most common type anomaly was the fish bone chromosome.

The results of statistical analysis were obtained based on the Pearson's correlation and analysis of variance method. According to the statistical results, there is a considerable positive relation between the treatment concentrations and the percentage chromosome anomaly except after (80 ml/L -72h) treatment (Table 2, Figures 1-7). Statistical analysis based on Pearson's correlation pointed to the important correlations among the anomaly's types (A-E, A-G, D-F, E-F and F-G) (Table 3). Also, the variance statistical analysis pointed to the important correlations among (A-G, D-F, E-F and F-G) at levels of 0.01 and 0.05 (Table 5). It was shown that the correlations between the treatment time and concentrations in Table (4) are based on the Pearson's correlation method, while the correlations in Table (6) are based on the analysis of variance method. The collected data revealed that there are highly significant correlations among the following (2-3; 2-4; 2-5;2-7;3-4;3-5;4-5) concentrations /times of treatment at levels of 0.01 and 0.05 (Table 4 and 6).

Table 2. The percentage of chromosome anomalies in *Vicia faba* root – tip meristems after treatment with xylol.

		Xylol concentation/time of treatment							
		5 ml/L		20 ml/L		40 ml/L		80 ml/L	
Chromosome anomaly's type		8h	72h	8h	72h	8h	72h	8h	72h
		(1)	(2)	(3)	(4)	(5)	(6)	(7)	(8)
Bridge chromosome	A	1.10	1.50	1.60	2.10	3.00	2.50	0.10	0.20
Fish bone chromosome	B	1.30	1.20	1.30	1.90	1.70	1.80	1.40	2.50
Sticky chromosome	C	1.90	0.70	1.20	1.60	2.90	1.10	1.80	0.80
Ring chromosome	D	0.50	0.24	1.10	1.20	1.70	2.10	2.00	1.10
Chromosome breaking	E	0.70	1.00	1.30	1.80	2.10	1.20	0.00	0.00
Scattered anaphase	F	1.10	0.00	1.00	0.80	1.15	0.50	0.00	0.00
C- chromosome	G	0.00	0.00	0.00	0.80	0.50	0.50	0.00	0.80

Treatment time (h): hour; Abbreviations: A-G: Codes of chromosome anomalies; Abbreviations: 1-8: Codes of Treatment (5 ml/L -8h): 1, (5 ml/L -72h): 2, (20 ml/L -8h): 3, (20 ml/L -72h): 4, (40 ml/L -8h): 5, (40 ml/L -72h): 6, (80 ml/L -8h):7, (80 ml/L -72h):8.

Table 3. Pearson's correlation based on chromosome anomalies.

	A	B	C	D	E	F
B	0,087 0,837					
C	0,398	0,142				
	0,328	0,737				
D	0,192	0,292	0,349			
	0,648	0,483	0,397			
E	0,942	0,133	0,453	0,060		
	0,001 **	0,753	0,259	0,888		
F	0,624	0,223	0,635	0,018**	0,700	
	0,099	0,595	0,090	0,967	0,050*	
G	0,702	0,397	0,331	0,411	0,705	0,349
	0,048*	0,330	0,423	0,312	0,041*	0,397

* Significant at the level of $P< 0.05$. ** Significant at the level of $P< 0.01$. Abbreviations: A-G : Codes of chromosome anomalies

Table 4. Pearson's correlation based on treatment (concentration / time).

	1	2	3	4	5	6	7
2	0,446						
	0,316						
3	0,650	0,760					
	0,114	0,048*					
4	0,485 0,269	0,985 0,010**	0,795				
			0,033*				
5	0,698 0,081	0,748 0,050*	0,824 0,023*	0,805			
				0,029*			
6	0,165 0,724	0,698 0,081	0,692 0,085	0,722 0,067	0,617 0,140		
7	0,395	0,010**	0,229	0,142	0,280	0,368	
	0,381	0,984	0,621	0,761	0,542	0,417	
8	0,337	0,308	0,261	0,350	0,071	0,409 0,363	0,706
	0,460	0,501	0,572	0,442	0,879		0,076

* Significant at the level of $P< 0.05$. ** Significant at the level of $P< 0.01$ Abbreviations: 1-8 : Codes of Treatment

Table 5. Correlation between the investigated chromosome anomalies (Analysis of Variance).

	MS	F-value	Probability	Significance
A-B	0.057	0.05	0.837	NS
A-G	3.66	5.83	0.052	*
C-G	0.38	0.74	0.423	NS
D-F	3.15	6.22	0.010	**
D-G	0.52	1.22	0.312	NS
E-F	1.97	5.78	0.050	*
E-G	2.01	5.95	0.049	*

MS: Mean Square *P<.05 **P<.01 A-G: Codes anomalies NS: Not Significant

Table 6. Correlation between treatment time and concentrations (Analysis of Variance).

	MS	F-value	Probability	Significance
1-4	0.522	1.54	0.269	NS
1-3	0.346	0.92	0.381	NS
1-8	0.251	0.64	0.460	NS
2-3	1.232	6.83	0.048	*
2-4	2.071	7.47	0.010	**
2-5	1.196	6.37	0.050	*
2-7	1.067	4.87	0.045	*
3-4	0.969	8.59	0.033	*
3-5	1.039	10.54	0.023	*
4-5	1.086	9.20	0.029	*
4-7	0.033	0.10	0.761	NS

MS: Mean Square **P<.01 Abbreviations: 1-8 : Codes of Treatment NS: Not Significant

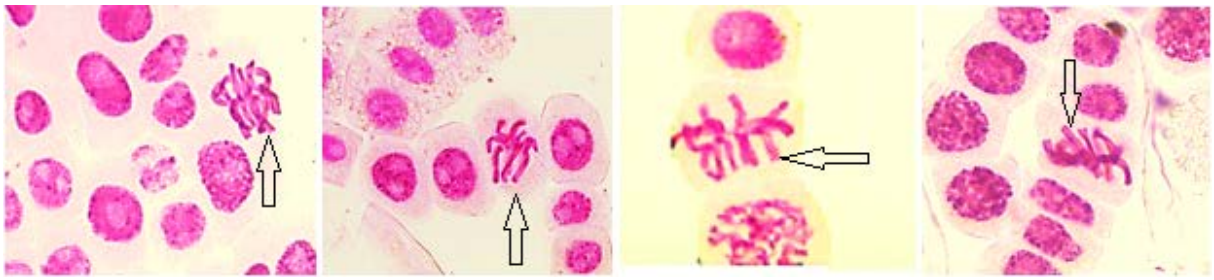

Figure 1. Metaphase stages with fish bone chromosomes after treatment with 80 ml/L concentration xylol for 8 and 72 hours.

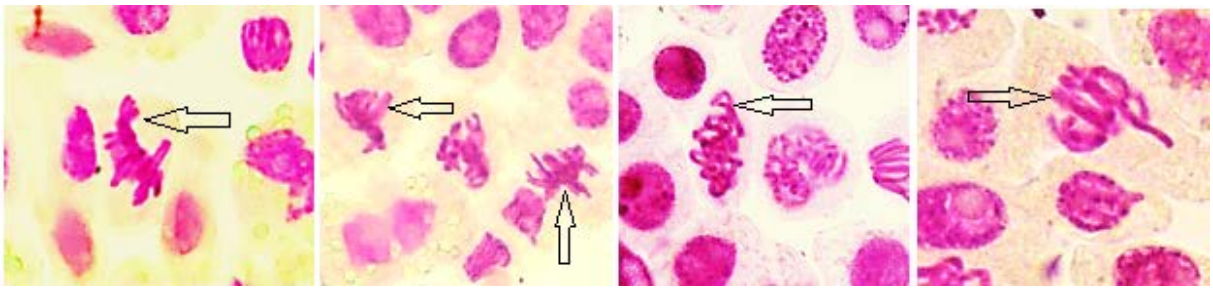

Figure 2. The stage of mitosis with sticky chromosomes after treatment with 40 and 80ml/L concentrations xylol for 8 and 72 hours. The first image shows that ever stickiness at late metaphase stage preventing it from entry to anaphase. The third image shows stickiness at prophase stage, the other two images represent metaphases.

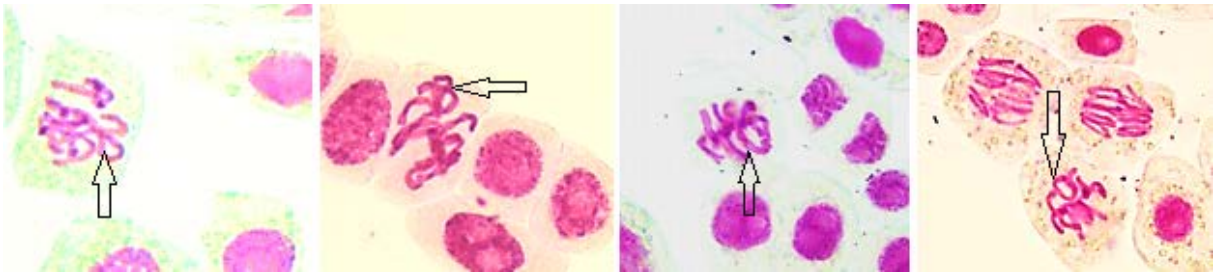

Figure 3. Metaphase stages with ring chromosomes after treatment with 40ml/L concentration xylol for 8 and 72 hours.

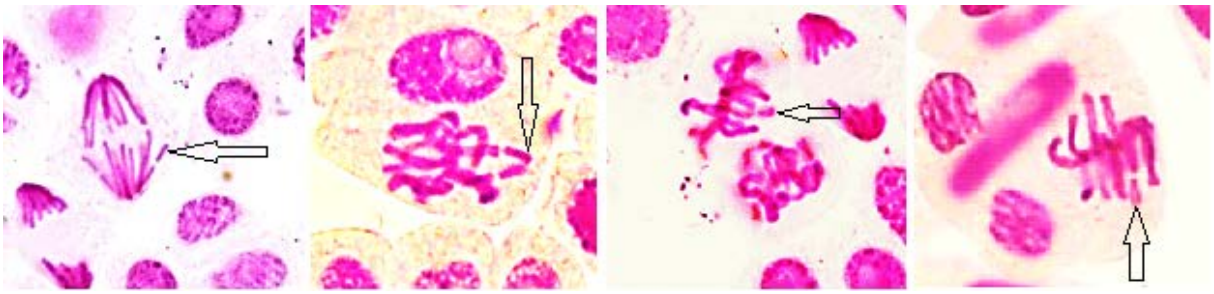

Figure 4. The stage of mitosis with chromosome breaking after treatment with 40ml/L concentration xylol for 8 and 72 hours. First image: anaphase stage, the other three images represent metaphases.

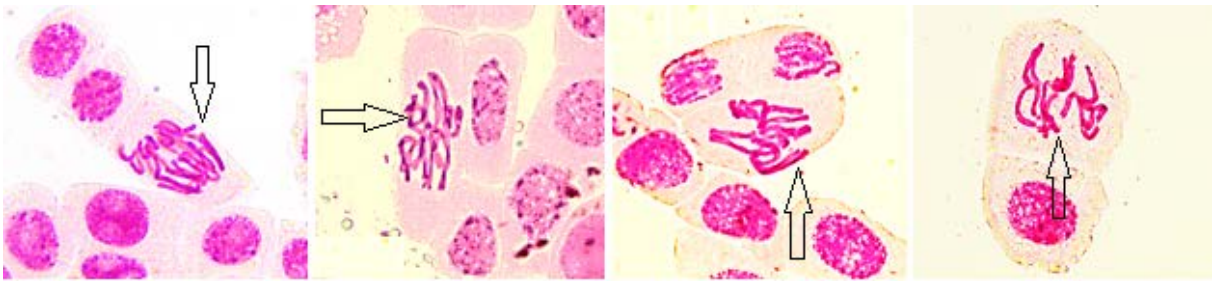

Figure 5. The first and fourth images anaphase stage with scattered anaphase chromosomes after treatment with 40 ml/L concentration xylol for 8 hour, the other two images represent meta-phase with fish bone chromosomes after treatment with 40 ml/L concentration xylol for 8 hours.

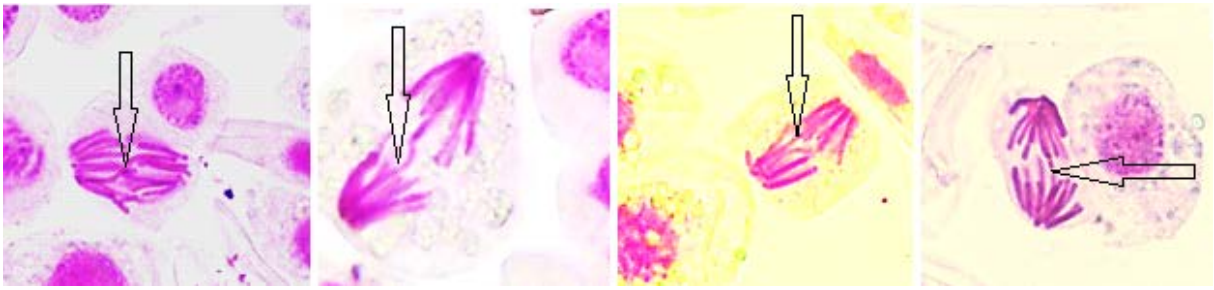

Figure 6. Anaphase stage with anaphase bridges after treatment with 40 ml/L concentrations xylol for 8 and 72 hours.

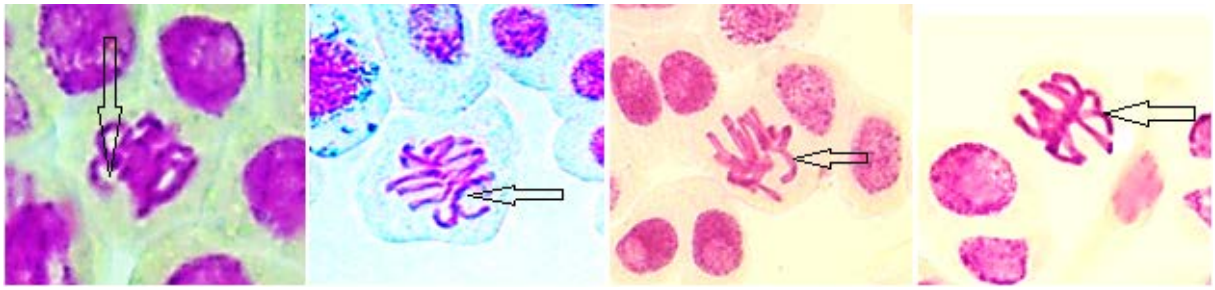

Figure 7. Metaphase stage with chromosome C after treatment with 40 and 80 ml/L concentrations xylol for 8 and 72 hours.

4. Discussion

In the current study, cytogenetic effects of xylol on meristematic cells of root tips belonging to *V. faba* (widely used as food by humans) have been investigated. We determined that xylol stress affects mitotic cell division and causes various types of chromosome anomalies. The obtained results of chromosome anomalies were mostly on the same track with (Alaca *et.al.*, 2020) after treatment the *Vicia faba* seeds with xylol in different concentrations (10 and 100 ml/L) for different times (12 and 24 hours) of treatment. Similarly, Barbhuiya *et al.* (2018) investigated the effect of benzene and thinner solvents, which are used as materials in many industrial products as in the case of xylol, on the root tip cells of *Allium cepa*. They observed that the solvents enhanced the mitosis index and caused chromosomal anomalies. Similar to our results, they observed that the solvents caused abnormalities such as bridge, sticky and scattered chromosomes and increased the mitosis index.

In another study, it has been determined that the chromosome adherence and the bridge chromosomes were the most frequently observed anomalies in cells of lettuce after exposure to glyphosate (Silva *et al.*, 2018). In our study, the mitotic division of the root tip treated with xylol gradually increased in comparison to the control group except to 80ml/L treatment. Parween *et al.*, (2011) obtained similar results examining the effect of cadmium chloride in pure germ line in broad beans (*V. faba*) in relation to chromosome anomalies and cell division rate. However, in another study, the seeds of *Lens culinaris* Medik.were kept at different concentrations of Sr (stronsiyum) (0.05, 0.1, 0.25, 0.5 and 1.0 M) for 12 hours; those anomalies showed no regular distribution (Sepet and Çanlı, 2020). Thus, it is not in agreement with the previous reference and our work.

As an example of similar results with non-solvent treatment, we refer to Özdemir *et al.*, (2008), where the effects of uranium exposure on *V. faba* cells are investigated. They found a concentration dependent increase in mitotic index.

The statistical analysis therein was also performed using the Pearson's correlation and analysis of variance method. The results were taken into account in the significance evaluations at $P<0.05$ and $P<0.01$ levels. Similarly, we tried to prove and evaluate the results obtained from laboratory studies numerically. According to the statistical results derived, different concentrations of xylol treatment on root tip increased the mitotic cell division at the different periods of time, compared to the control group. However, mitotic division was decreased at (80 ml/L -72h) treatment. At the same time, the least number of different anomalies was seen in this application.

We refer to this concentration with sever damage on the cell cycle and delay the mitotic division. On the contrary, the different anomalies were mainly observed at the application level (80 ml / L -8h), where the mitosis was at its highest frequency. This result shows that the concentration and the time periods of the treatment in mitotic division is important. As shown in the tables 3-6 according to Pearson's correlation and analysis of variance method, it has been found that there have been statistically important differences at levels of 0.01P between ring chromosome and scattered anaphase. At the same time, there have been statistically important differences at levels of 0.05P between chromosome breaking and C-chromosome (Tables 3,5). We can say that these chromosomal anomalies are inter-related and trigger each other. Studies on the effect of xylol on chromosomes in the literature have mostly been done on animal cells. Donner *et al.*, (1980) exposed rats to technical grade xylol by inhalation at 300 ppm, 6 h/day, 5 days/week for up to 18 weeks. The chromosome damage has been detected in animals examined after 9, 14 or 18 weeks exposure. Thus, these researchers stated that that xylol administered to rats for different periods of time, similar to our findings, caused chromosomal abnormalities in the cells. Lebowitz *et al*. (1979) observed the damage of chromosome in bone marrow cells of rats after dosing with xylol.

We think that, based on our finding results, xylol as an ingredient in many industrial products such as farming products should be reconsidered as it caused sever anomalies in chromosomes for various concentrations (5,20,40 and 80 ml/L) and different treatment durations (8 and 72 h), which may cause plant growth disorder and deformations.

5. References

Alaca C, Özdemir A, Bozdağ B and Özdemir C. 2020. Cytogenetic effects of C_6H_4 $(CH_3)_2$ (xylol) on meristematic cells of root tips of *Vicia faba* L. and mathematical analysis. *Caryologia* **73**: 27-35.

Barbhuiya SN, Barhoi D, Datta S.K, and Giri1 S. 2018. Two Major Components of Steel Fabrication Industry, Benzene and Thinner Induce Cytotoxicity in Allium cepa L. Root Cells. *Cytologia* **83(2):** 155–158.

Barchan A, Bakkali M, Arakrak A, Pagán R and Laglaoui A. 2014. The effects of solvents polaritiy on the phenolic contents and antioxidant activity of three Mentha species extracts. *Int J Curr Microbiol App Sci*. **3(11):**399-412.

Cahours A. 1850. Recherches sur les huiles légéres obtenues dans la distillation du bois. *Compte rendus* **3**: 319-323.

Darlington CD and La Cour L.F. 1976. The handling of chromosomes, Sixth Edition, George Allen and Unwin Ltd., London, 0-04-574014-3.

Donner M, Maki-Paakkanen J, Norppa H, Sorsa M and Vainio H. 1980. Genetic toxicology of xylols. *Mutat Res* **74**:171-172.

Fabri J, Graeser U and Simo T. 2000. "Xylols". Ullmann's Encyclopedia of Industrial Chemistry. doi:10.1002/14356007.a28_433. ISBN 978-3527306732.

Ghasemzadeh A, Jaafar HZ and Rahmat A. 2011. Effects of solvent type on phenolics and flavonoids content and antioxidant activities in two varieties of young ginger (Zingiber officinale Roscoe) extracts. *J Med Plants Res.* **5(7):**1147-1154.

Jenifer M. 1994. Xylol: Its toxicity, measurement of exposure levels, absorption, metabolism and clearance, *Journal Pathology* **26**: 301-309.

Lebowitz H, Brusick D, Matheson D, Jagannath DR, Reed M, Goode S and Roy G. 1979. Commonly used fuels and solvents evaluated in a battery of short-term bioassays, *Environmental Mutagen* **1**: 172-173.

Osama H, Elhamalawy and Aida I. El Makawy. 2020. Estimation of Grape Seed Oil Alleviative Role on Cadmium Toxicity in Male Mice. *Jordan Journal of Biological Sciences* **13**: 77 – 83.

Özdemir A, Bozdağ B, Sepet H, Parlak Y, Kocabaş O, Serap E and Özdemir C. 2015. Cytogenetic effects of technetium on meristematic cells of root tips of *Vicia faba* L. and statistical comparison. *Caryologia* **68**: 200-206.

Özdemir C, Ereeş S and Çam S. 2008. Cytogenetic Effects of Uranium On Root Tip Cells Of *Vicia faba* L. *Botanica Lithuanica* **14**: 155-158.

Parween T, Jan S, Mahmooduzzafar MP, Mujib A and Fatma T. 2011. Genotoxic impact of cadmium on root meristem of *Vicia faba* L. *Russ Agric Sci.* **37**: 115–119.

Puchtler H, Sweat Waldrop F, Conner HM and Terry MS. 1968. Carnoy fixation: practical and theoretical considerations. *Histochemie* **16**: 361–371.

Shraideh ZA. 2010. Toxicity of triethyllead chloride (TriEL) on cytoplasmic shuttle streaming, structure, growth and migration of the plasmodial slime mold Physarum polycephalum, *Jordan Journal of Biological Sciences*, **3**: 33 – 40.

Sepet H and Çanlı M. 2020. Concentration- and time-dependent effects of strontium on *Lens culinaris* Medik. *Botanica Serbica* **44**: 175-182.

Silva AC, Gonçalves CG, Scarano MC, Pereira MR and Martins R. 2018. Effect of glyphosate on guineagrass submitted to different soil waterpotential. *Planta Daninha* **36**:1–12.

Şutan NA, Uta G and Barbucean D. 2018. Oxidative stress and cytogenetic effects in root tip cells of *Allium cepa* L. induced by alcoholic extracts of *Leptinotarsa decemlineata* (Say). *Caryologia* **71**: 1–9.

Tengjaroenkul B and Neeratanaphan L. 2020. Acute Effect of Cadmium Chloride on Chromosomal Abnormalities in the Nile Tilapia Fish In Vivo, *Jordan Journal of Biological Sciences*, **13**: 127 – 132.

Vijayakumar Y, Ganesh KM, Ramana MV and Bosco BR. 2015. Nanostructured flower like V2O5 thin films and its room temperature sensing characteristics. *Ceramics International* **41**: 2221-2227.

Subscription

Jordan Journal of Biological Sciences

An International Peer – Reviewed Research Journal

Published by the Deanship of Scientific Research, The Hashemite University, Zarqa, Jordan

Name: ..... الاسم:

Specialty: ..... التخصص:

Address: ..... العنوان:

P.O. Box: ..... صندوق البريد:

City &Postal Code:..... المدينة: الرمز البريدي:

Country: ..... الدولة:

Phone: ..... رقم الهاتف

Fax No.: ..... رقم الفاكس:

E-mail: ..... البريد الإلكتروني:

Method of payment: ..... طريقة الدفع:

Amount Enclosed: ..... المبلغ المرفق:

Signature: ..... التوقيع:

Cheque should be paid to Deanship of Research and Graduate Studies – The Hashemite University.

I would like to subscribe to the Journal

For

- ☐ One year
- ☐ Two years
- ☐ Three years

One Year Subscription Rates

	Inside Jordan	Outside Jordan
Individuals	JD10	$70
Students	JD5	$35
Institutions	JD 20	$90

Correspondence

Subscriptions and sales:

The Hashemite University
P.O. Box 330127-Zarqa 13115 – Jordan
Telephone: 00 962 5 3903333
Fax no. : 0096253903349
E. mail: jjbs@hu.edu.jo

المجلة الأردنية للعلوم الحياتية
Jordan Journal of Biological Sciences (JJBS)

http://jjbs.hu.edu.jo

المجلة الأردنية للعلوم الحياتية: مجلة علمية عالمية محكمة ومفهرسة ومصنفة، تصدرعن الجامعة الهاشمية وبدعم من صندوق دعم البحث العلمي والإبتكار – وزراة التعليم العالي والبحث العلمي.

ترسل البحوث الى العنوان التالي:

رئيس تحرير المجلة الأردنية للعلوم الحياتية
الجامعة الهاشمية
ص.ب , 330127 , الزرقاء, 13115 , الأردن
هاتف: 0096253903333
E-mail: jjbs@hu.edu.jo, Website: www.jjbs.hu.edu.jo

المملكة الأردنية الهاشمية

المجلة الأردنية

للعلوم الحياتية

مجلة علمية عالمية محكمة

تصدر بدعم من صندوق دعم البحث العلمي و الابتكار

http://jjbs.hu.edu.jo/